

UNIVERSITÀ DEGLI STUDI DI MILANO
PhD School in Industrial Chemistry - XXX Cycle
Department of Chemistry



**SYNTHESIS OF METAL COMPLEXES WITH BIO-INSPIRED
NITROGEN-CONTAINING MACROCYCLIC LIGANDS
AND THEIR USE IN CATALYSIS**

PhD THESIS OF:
Giorgio Tseberlidis
R10866

TUTOR: Prof. Alessandro Caselli
COORDINATOR: Prof. Maddalena Pizzotti

ACADEMIC YEAR 2016-2017

General Index

1. INTRODUCTION	5
1.1 HISTORY OF MACROCYCLES.....	5
1.2 MACROCYCLIC VERSUS ACYCLIC CHELATORS	6
1.3 AZA-MACROCYCLES	6
1.4 PORPHYRINS.....	9
1.5 TETRA-AZA MACROCYCLES	11
1.6 STRUCTURAL MODIFICATIONS.....	19
1.7 LIGANDS DERIVED FROM AMINOACIDS	19
1.8 CATALYTIC APPLICATIONS	21
1.8.1 <i>Cyclopropanation</i>	21
1.8.2 <i>X-H carbene insertion</i>	25
1.8.3 <i>Henry reaction</i>	26
1.8.4 <i>Isochromene cycloisomerization</i>	27
1.8.5 <i>Iron catalyzed alkene oxidation</i>	28
2. RESULTS AND DISCUSSION	31
2.1 SYNTHESIS OF AMINOALCOHOLS	31
2.2 SYNTHESIS OF AZIRIDINES	32
2.2.1 Synthesis of tosyl protected aziridines.....	32
2.2.2 Synthesis of o-nosyl protected aziridines	33
2.3 SYNTHESIS OF BISULFONAMIDES.....	33
2.3.1 Synthesis of "Disubstituted" bisulfonamides.....	34
2.3.2 Synthesis of "Monosubstituted" bisulfonamides.....	36
2.4 SYNTHESIS OF THE MACROCYCLES.....	37
2.4.1 Synthesis of deprotected ligands	40
2.4.2 Functionalizations of deprotected ligands	43
2.5 COPPER COMPLEXES.....	47
2.5.1 <i>Synthesis</i>	47
2.5.2 <i>Cu(I) catalysis: cyclopropanation</i>	49
2.5.3 <i>Cu(I) catalysis: X-H bond insertion</i>	58
2.6 SILVER COMPLEXES.....	63
2.6.1 <i>Synthesis</i>	63
2.6.2 <i>Ag(I) catalysis: Henry reaction</i>	64
2.6.3 <i>Ag(I) catalysis: isochromene cycloisomerization vs Henry reaction</i>	72
2.7 IRON COMPLEXES.....	78
2.7.1 <i>Synthesis</i>	78
2.7.2 <i>Fe(III) catalysis: highly selective alkene oxidation</i>	79
2.8 OTHER METALS	89
2.8.1 Zinc complexes.....	89
2.8.2 Cadmium complexes.....	95
2.8.3 Cobalt complexes.....	96
2.8.4 Ruthenium complexes	98
2.8.5 Group 10 complexes	99
3. CONCLUSIONS	101
4. EXPERIMENTAL PART	102
4.A SYNTHESIS.....	103
4.1 <i>Aminoalcohols</i>	104
4.2 <i>Tosyl protected aziridines</i>	105
4.2.1 2-tosyl ammine ethyl toluene sulfonate	105
4.2.2 N-tosyl ariziridine	105
4.2.3 2-substituted N-tosyl ariziridine 2b-c.....	106

4.2.4	Aziridines 2d-e	107
4.3	<i>Nosyl protected aziridines</i>	108
4.3.1	o-Nosyl Aziridine 2f	108
4.3.2	Nosyl protected (S)-isopropyl aziridine 2g	109
4.4	<i>Bis-sulfonamides</i>	110
4.4.1	Bis-sulfonamides 3a-i	110
4.4.2	Synthesis of bis-sulfonamides 3j-k-l	115
4.5	<i>Mono-sulfonamides</i>	117
4.5.1	Synthesis of monosulfonamides 4a-c	117
4.5.2	Monosubstituted bis-sulfonamides	119
4.5.3	Synthesis of Ns-protected bis-sulfonamides	122
4.5.4	Synthesis of Ns-protected mono-sulfonamide 4d	125
4.5.5	Synthesis of Ns-protected mono-substituted bisulfonamide 5d	125
4.6	<i>Synthesis of macrocycles</i>	126
4.6.1	Synthesis of 2,6-bis (OMs-methyl)-pyridine	126
4.6.2	Synthesis of macrocycles 6a-q	127
4.6.3	Synthesis of macrocycles 6r-u	140
4.6.4	Synthesis of macrocycle 6v	143
4.6.5	Synthesis of macrocycle 6w	144
4.6.6	Synthesis of macrocycle 6x	145
4.7	<i>Deprotection of macrocycles</i>	146
4.7.1	Deprotection of Nosyls	146
4.7.2	Deprotection of Tosyls	150
4.7.3	Other deprotections	152
4.8	<i>Functionalized ligands</i>	154
4.8.1	Synthesis of ligand 8a	154
4.8.2	Synthesis of ligand 8b	155
4.8.3	Synthesis of ligand 8c	156
4.8.4	Synthesis of ligand 8d	157
4.8.5	Synthesis of ligand 8e	158
4.9	<i>Copper complexes</i>	160
4.9.1	Method 1:	160
4.9.2	Method 2:	163
4.10	<i>Silver complexes</i>	167
4.10.1	Synthesis of silver BF ₄ complexes	167
4.10.2	Synthesis of silver OTf complexes	177
4.11	<i>Iron complexes</i>	181
4.12	<i>Zinc complexes</i>	184
4.13	<i>Other transition metal complexes</i>	191
4.B	CATALYSIS	197
4.14	<i>X-H carbene insertion</i>	197
	Copper-catalyzed Si-H bond carbene insertion using diazo compounds	197
	Copper-catalyzed Si-H bond carbene insertion using enynes	208
	Copper-catalyzed O-H/N-H bond carbene insertion using diazo compounds	210
4.15	<i>Silver catalysed Henry reaction</i>	215
4.16	<i>One-pot isochromene cycloisomerization vs Henry reaction</i>	222
4.17	<i>Fe(III) catalysed alkene oxidation</i>	225
4.18	NMR-SPECTRA OF SELECTED LIGANDS AND COMPLEXES	256
5.	REFERENCES	318

Abbreviation List:

Å	Ångström	EW	Electron-withdrawing
br	Broad signal	FAB	Fast atom bombardment
°C	Celsius degree	h	Hours
cat	Catalyst	HPLC	High Performance Liquid Chromatography
COD	1,5-Cyclooctadiene	HSQC	Heteronuclear Correlation
COSY	Correlation spectrometry	Hz	Hertz
CDMT	2-Chloro-4,6-dimethoxy-1,3,5- triazine	J	Coupling constant
δ	Chemical shift	L	Ligand
d	Doublet	m	Multiplet
dd	Double doublet	[M+]	Molecular ion peak
ddd	Double double doublet	MS	Mass spectrometry
DIC	<i>N,N'</i> -Diisopropylcarbodiimide	m/z	Mass/Charge
DiPEA	<i>N,N</i> -Diisopropylethylamine	NMR	Nuclear Magnetic Resonance
DMAP	4-Dimethylaminopyridine	PcL	Pyridine-containing macrocyclic ligand
DME	1,2-Dimethoxyethan	q	Quartet
DCE	1,2-Dichloroethane	rt	Room temperature
DCM	Dichloromethane	s	Singlet
DMF	Dimethylformamide	T	Temperature
DMSO	Dimethylsufoxide	t	Triplet
dt	Double triplet	td	Triplet doublet
ED	Electron-donating	TFA	Trifluoroacetate
EDA	Ethyl-diazoacetate	THF	Tetrahydrofuran
EI	Electron collision ionization	TLC	Thin layer chromatography
Eq.	Equivalents		
ESI	Electrospray ionization		

1. INTRODUCTION

1.1 History of Macrocycles

The history of macrocyclic compounds dates back a long time; we could say they are as ancient as life. We know several examples such as porphyrins, corrins and chlorins that are natural compounds with biological and vital roles in the animal (haemoglobin) and plant worlds (chlorophyll). The great role played by the biologically occurring macrocycles directed most early synthetic studies to the imitation of those species. Natural ligands were taken as models in the synthesis, resulting in an evident predominance of nitrogen-containing ligands over ligands containing other heteroatoms. Fisher, considered the pioneer of the chemistry of porphyrins, reported the first total synthesis of etioporphyrin-III and octamethylporphyrin in 1926,¹ but the first “artificial” macrocycle came on the scene only in 1960,² when Curtis synthesized a nickel(II) complex from tris(ethylenediamine) nickel(II) perchlorate and acetone. Polyazamacrocycles are a common class of macrocyclic compounds, that find application across a great number of fields including (but not limited to) catalysis, selective metal recovery and recycling, medical therapy, materials and sensors. Worthy of note is their ability to form stable complexes with a considerable number of transition metal cations. Alternative geometries of the resulting complex, deviating from planarity, often leads to uncommon oxidation states of the coordinated metal atom. Both the thermodynamic properties and the complexation kinetics are affected by the introduction of a pyridine moiety into the backbone of a ligand by increasing the conformational rigidity and tuning the basicity. Pyridinecontaining ligands have attracted great interest due to various potential fields of applications and have been successfully employed in biology, magnetic resonance imaging and molecular recognition. Much effort in the use of macrocyclic pyridine-containing ligands has been devoted to the study of catalytic oxidation reactions. The first studies were inspired by nature and the understanding of metalloenzymes, which use molecular oxygen from air as the main oxidant and the final goal of these class of studies would be to find a cheap alternative to the use of heme-like catalysts.

1.2 Macrocyclic versus acyclic chelators

Even if the first macrocycles were synthesized in 1960, it was only in 1969 that in literature was introduced the concept of “macrocyclic effect”.³ Under this name undergoes the notable enhancement of the complex stability constants of ligands with cyclic structure compared to the acyclic analogues. The thermodynamic stabilities of macrocycles and acyclic compounds have been demonstrated to be approximately the same, but there is a great difference for what regards the kinetic stability, since macrocycles are by far more inert than acyclic ligands. It is well known that the stability of the complexes is enhanced by the presence of one, or more, coordinating atoms and this phenomenon is called “chelating effect”. At the same time, the cyclic structure imposes a reduced structural freedom to the ligands, determining a pre-organized geometry. On the contrary, acyclic chelators, must undergo to a heavy change of geometry to organize the binding atoms in the right orientation to coordinate the metal ion: for this reason, the entropy drastically decreases, making the coordination unfavorable compared to macrocyclic ligands.⁴

1.3 Aza-Macrocycles

As mentioned above, the polyaza macrocycles are a common class of macrocyclic compounds, thanks to their similarity with natural molecules and to their ability to form stable complexes with metals from the later transition, more than with alkali or alkaline earth metal ions. This important difference with respect to other ligands makes polyaza macrocycles more suitable for application in organometallic chemistry.

The similarity to other natural macrocycles like porphyrins and corrins made **Cyclam** (1, 4, 8, 11-tetraazacyclotetradecane) and related ligands, the most investigated among the polyaza compounds. They have been mainly applied in stabilizing high oxidation state metals and in formation of chelators with more than one function. This kind of molecules is also used for the binding of radioisotopes to biological targets.

Tetramethylcyclam is frequently employed as stabilizer of reactive high valent iron oxo compounds, since it forms stable iron(IV)-oxo complexes with a wide range of anions coordinated.⁵

Delgado and co-workers reported the monopicolate cyclam derivatives (**Figure 1.1**); they formed stable copper(II) complexes demonstrating preference for Cu(II) coordination over other metal ions.⁶

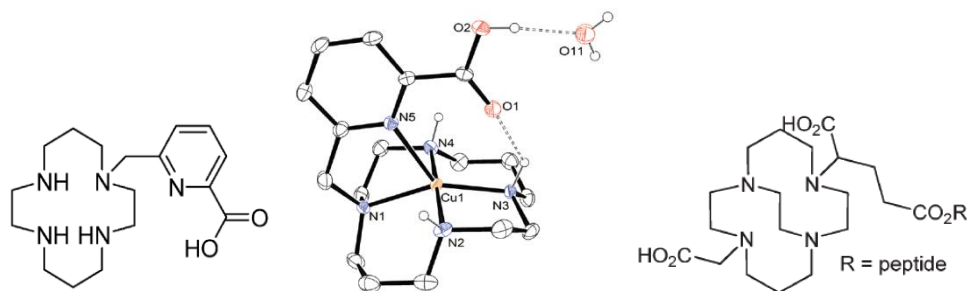


Figure 1.1 – Cyclam derivatives.

As analogue of the crown ether 12-crown-4, also the **Cyclen** (1,4,7,10-tetraazacyclododecane) and its derivatives were studied since a long time. One of the most important applications of such compounds was in the biological NMR field, like the paramagnetic lanthanide(III) chelating protein probe (**Figure 1.2**), that shows different properties depending on the pH.⁷

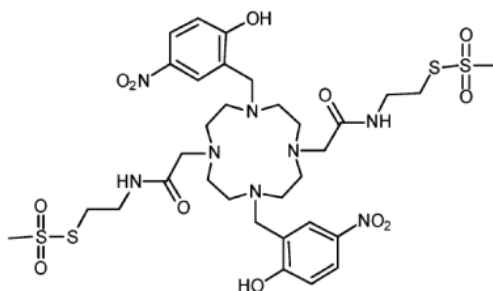


Figure 1.2 – Lanthanide (III) chelating protein probe.

Delgado and coworkers developed also several other cyclen analogues, like ligands with pinacolate arms, and tested their reactivity toward copper(II).⁵ The coordination of the cyclen derivative switched between the carboxylate and the nitrogen donors depending on the pH. They reported also an example of a macrocycle with two *trans*-*N*-acetate arms, very selective for Cu(II).⁸ In the literature, it is frequent to find some tetraaza macrocycles described as “cyclen derivatives”, especially in the last years, due to their ability to form very stable complexes with a wide range of metal cations. In 2012 were reported twelve-membered pyridine-based macrocycles with quinoline as pendant arms (compound **C**, **Figure 1.3**). The copper(II) complexes of these ligands showed that the reaction kinetics and the stability of the complexes are affected by the *N*-substituent of the quinoline.⁹

These macrocycles give to the relative complexes with relevant isotopes a wide range of important chemical properties as thermodynamic stability and mild complex formation. These features, together with the possibility of coupling with targeting biomolecules, are necessary to make

complexes usable in medical and pharmaceutical field.¹⁰ For these reasons, Cooper and co-workers (as well as Ferreira) employed this pyridine-based twelve-membered pattern for ⁶⁴Cu complexes for labeling of antibodies (compound **A** and **B**, **Figure 1.3**).¹¹

In order to coordinate a bulkier ion as iron(IV), also the fourteen-membered pyridine containing cyclam derivatives were synthesized and studied as mediator for catalytic epoxidations of cyclooctene and other olefins (compound **D**, **Figure 1.3**).¹²

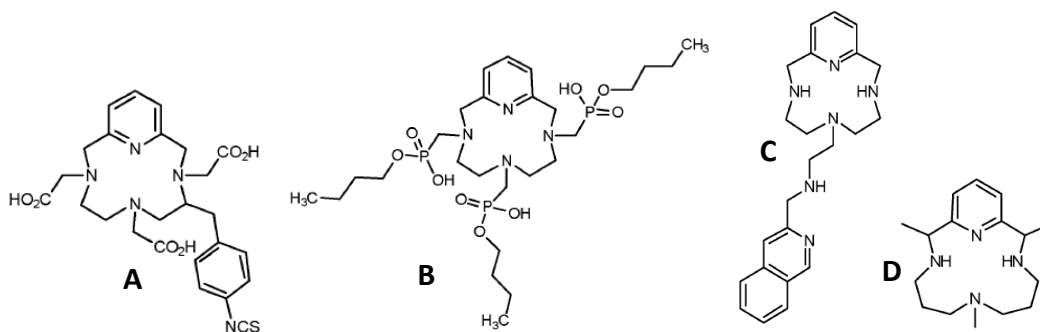


Figure 1.3 – Some examples of twelve- and fourteen-membered pyridine containing ligands.

The ligands studied and synthesized in our group are part of this category, since they are twelve-membered tetraaza macrocycles and they include a pyridine moiety in their backbone.

Another important class of polyaza macrocycles are **Cyclidenes** (1,4,7-triazacyclononane). They are ligands with a cavity synthesized and extensively studied by D. H. Busch. They can coordinate a single metal ion and maintain a cavity, which allows access to small molecules. For this reason, they are still studied and their complexes are applied in many different fields as for example catalysis.¹³

This kind of compounds were also employed in building metallorganic framework structures for the absorption of CO₂.¹⁴ The zinc(II) complexes of the ligands shown below (**figure 1.4**) are able to form a framework with a surface area of 1350 m²/g and shows a good selectivity for CO₂ over other gases similar in dimension as CO, CH₄ and N₂.¹⁵

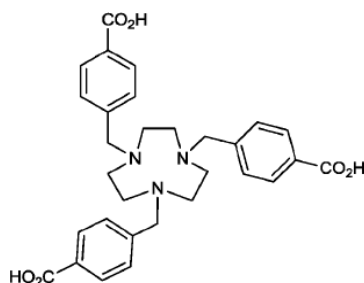


Figure 1.4 – Structural formulae of symmetrical cyclidene.

Finally, it is important to cite also larger polyaza macrocycles. They can be classified by increasing macrocyclic ring size and number of donor atoms. The application for this kind of compounds is often the chelation of metal ions, as for what concern the macrocyclic pentaaza ligands that were synthesized and evaluated as novel chelating agents in copper(II) and nickel(II).¹⁶

1.4 Porphyrins

As particular class of tetraaza macrocycles is represented by porphyrins. The general structure of this molecule is made by four pyrrolic units, connected by methinic bonds (**Figure 1.5**). In dependence of the position, carbon atoms could be known as meso-carbon (5, 10, 15 and 20) or β -pyrrolic. Meso-carbons are the ones involved in methinic bonds.

The importance of porphyrins is due mainly to their natural abundance, where they play crucial roles in the metabolism of living beings, often associated to metal ions coordinated in porphyrins. After the deprotonation of the two N-H of the pyrroles, porphyrins act as tetradentate dianionic ligand and they can coordinate nearly every metal ion in their cavity. Porphyrin complexes for all the transition metals, all the lanthanides, several of the actinides and even some of the main group metals are known. The reason of such a kind of versatility is due to the high electron density and to the high electron stabilization of the porphyrin ring.

Among the metalloporphyrins, one of the most known is iron protoporphyrin IX, also known as heme, that is the cofactor of the hemoglobin, responsive of the O₂/CO₂ transportation in blood and also stated as pigment of the red blood cells (**Figure 1.5**)

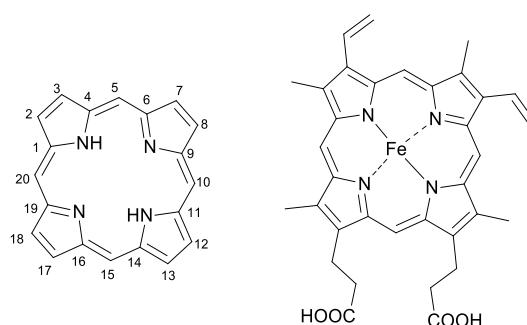
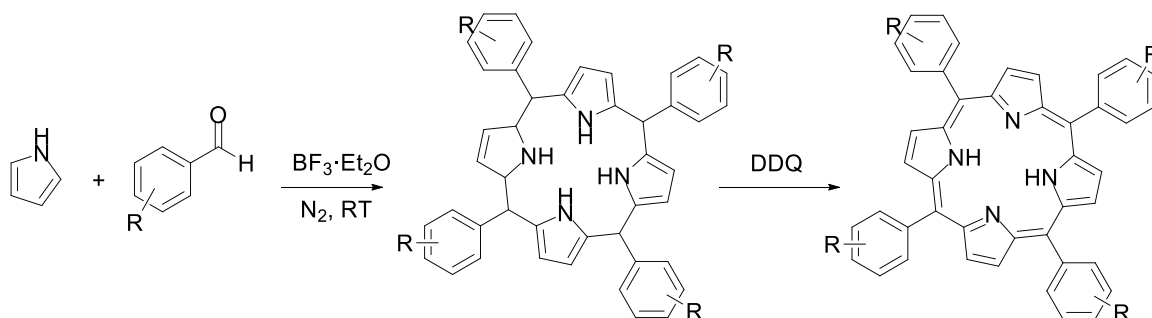


Figure 1.5 – Porphirine with numbering scheme adopted; Heme B.

In 1926 Hans Fisher and Bruno Walach described the first synthesis of a porphyrin¹ and laid the first stone for the different and increasingly optimized routes reported between 1930s and 1950s, in particular by Rothermund.¹⁷ These new works, despite the limitations in the number of aldehydes

used and the low yields, paved the way for the studies by Adler and Longo, who published a one pot procedure for the reaction of different benzaldehydes and pyrrole in presence of propionic acid. The yield of this synthetic pathway is up to 20-25%.¹⁸ This method is still used nowadays, when large amounts of non-symmetrical porphyrins are needed. Higher yields (50%) and milder conditions are reported in the work of Lindsey and co-workers, who proposed a way of synthesis via porphyrinogen (Scheme 1.1).¹⁹



Scheme 1.1 – Synthetic method reported by Lindsey. The porphyrinogen intermediate can be directly aromatized by 2,3-dichloro-5,6-dicyano-1,4-benzoquinone (DDQ).

Synthetic chiral porphyrin derivatives have been developed over the years, to extend the application of metalloporphyrins also to enantioselective applications. Chiral derivatives have been mainly prepared by the approach of Groves and Meyers that involves the attachment of chiral units to preformed porphyrins.²⁰ Then O'Malley and Kodadek demonstrated that it is possible to insert chiral substituent on the porphyrin by using the classical Lindsey procedure with chiral aldehydes.²¹ Since then, the number of chiral porphyrins appeared in literature is still growing.

A significant example of chiral porphyrin is the single-face protected picket fence and picnic basked compounds (**Figure 1.6**), synthesized by Collman in 1993 and used as ligands for iron(III)-chloride complexes in enantioselective epoxidation of styrene by Rose and colleagues.²² Important works in asymmetric catalysis mediated by chiral porphyrins are those by Che and Berkessel, who employed ruthenium and manganese complexes of the simplest D_4 -symmetric double-faced porphyrins for stoichiometric and catalytic oxidation,²³ cyclopropanation,²⁴ and amination²⁵ reactions of unfunctionalized hydrocarbons, always reaching good to very good results in term of yields.

It is important to mention also the family of the “bis-strapped” porphyrins, characterized by the presence of a chiral binaphthyl (BINAP) moiety, which produces a significant steric hindrance in the proximity of the active cavity. In this way, the catalytic activity and, in particular, the selectivity are drastically enhanced. Collman and Rose reported the synthesis of C_2 -symmetric bis-binaphthyl chiral

porphyrin and the corresponding Fe(III) complex that gave TON of 16000 in the epoxidation of some terminal olefins (**Figure 1.7**).²⁶

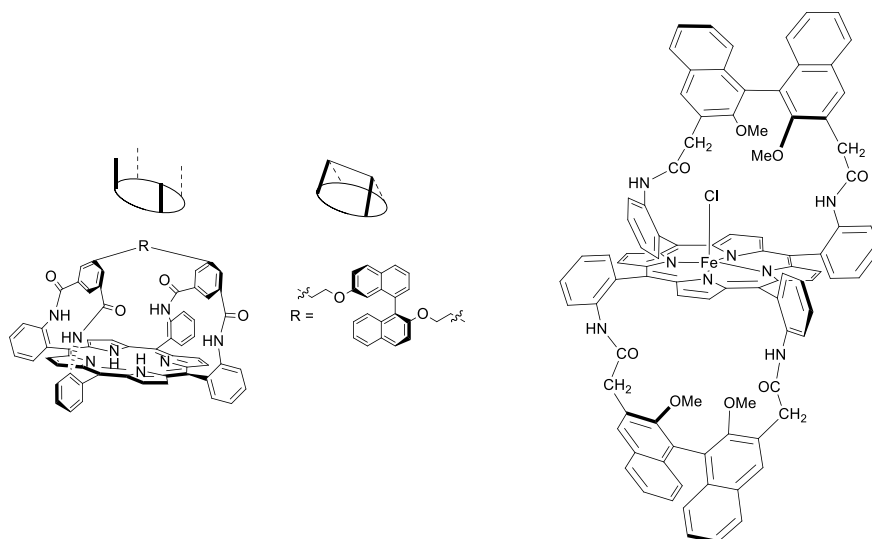
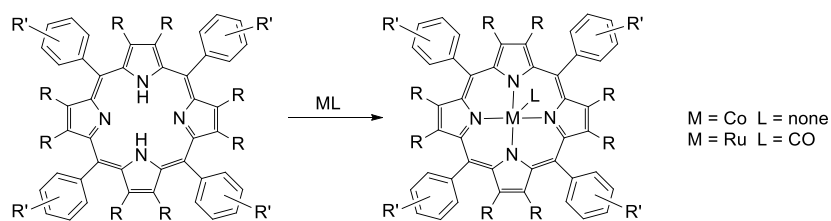


Figure 1.7 – Schematic representation of the single-face protected picket fence and picnic basket; picnic basket porphyrin bearing isophthalate amide loops and a binaphthyl diether linkers; iron (II) complex of the C₂ bis-strapped porphyrin.

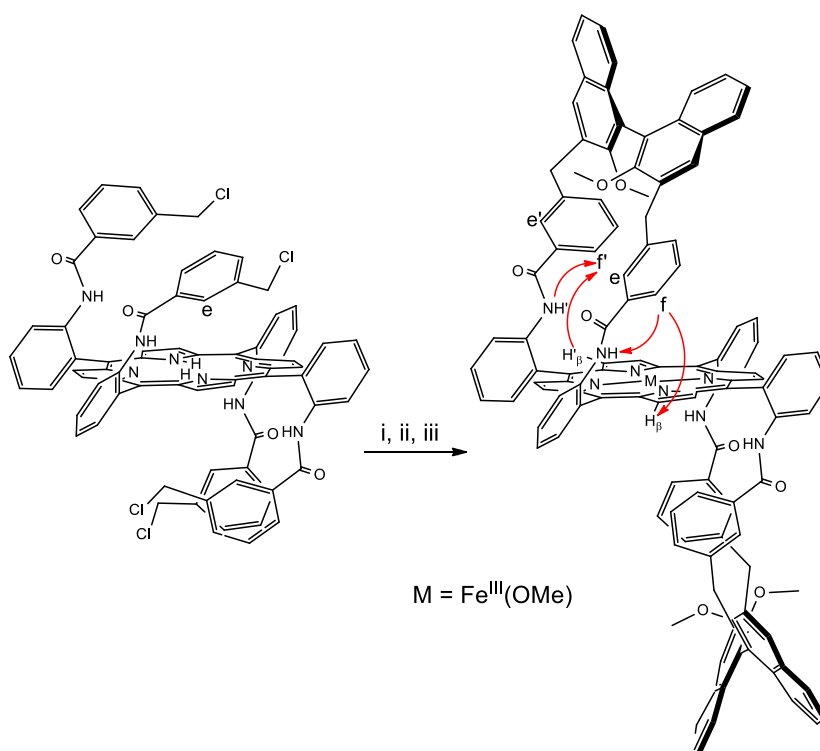
1.5 Tetra-aza macrocycles

The group in which I conducted my PhD thesis is interested in the use of nitrogen containing ligands, in particular tetra-aza macrocyclic compounds, and on the studies of their reactivity and their catalytic activity as metal complexes. Several years ago, Cenini and co-workers reported the synthesis of Co^{II}-porphyrin complexes that catalyzed the amination of benzyl compounds²⁷ and the cyclopropanation of alkenes.²⁸ Since then, other interesting reactions were exploited, such as the amination of 1,2-dihydronaphthalene derivatives, demonstrating an unusual reactivity of dihydronaphthalene towards several aryl azides.²⁹ Using another porphyrin [Ru-(CO)(TPP)] (TPP = dianion of tetraphenylporphyrin) as catalyst we catalyzed the aziridination of olefins using aryl azides as nitrogen source.³⁰ This ruthenium complex has been found to catalyze the direct aziridination of conjugated dienes by aryl azides with high chemoselectivity, to provide *N*-aryl-2-vinylaziridines.³¹ More recently, our research group discovered that [Ru-(CO)(TPP)] promoted the amination of both exocyclic and endocyclic benzylic C-H bonds (**Scheme 1.2**).³²



Scheme 1.2 – General scheme for the synthesis of cobalt and ruthenium complexes.

Finally, we have explored cyclopropanation reactions employing a new chiral iron porphyrin (**Scheme 1.3**), obtaining cyclopropanes with excellent yields (up to 99%), enantio- and diastereoselectivities (ee_{trans} up to 87%, $trans/cis$ ratios up to 99:1) and outstanding TON and TOF values (up to 20,000 and 120,000/h respectively).³³



Scheme 1.3 – Porphyrin complex highly active in carbene transfer reactions.

Porphyrin complexes have shown excellent catalysts turnovers and unusual selectivities, thanks to the high versatility of the porphyrin ligand and to its ability to coordinate the metal in one way only. For example, chiral porphyrin complexes of cobalt(II) and ruthenium(II) were tested in catalytic cyclopropanation³⁴ and amination reactions.³⁵

From another point of view the synthesis of this class of compound generates several problems, especially if some functional groups are introduced on the framework or if the optical pure form is synthesized. Moreover, the synthetic methodologies reported in literature concerning chiral

porphyrins require difficult and long procedures, expensive reagents and lead to very low overall yields. For this reason, our attention turned to the development of synthetic pathways that allow to obtain a class of tetraaza macrocyclic ligands that we could functionalize easily and in few synthetic steps, in good yield and with economic and commercially available starting materials. In collaboration with Prof. Sisti of Università dell'Insubria, we synthesized a new type of tetraaza macrocycle containing a pyridinic ring. Sisti and co-workers studied these classes of compounds and their use as ligand for gadolinium(III) since their complexes are useful contrast agents for magnetic-resonance images (MRI) (**Figure 1.8**).³⁶

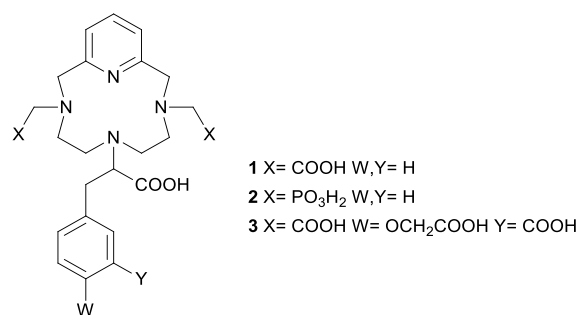
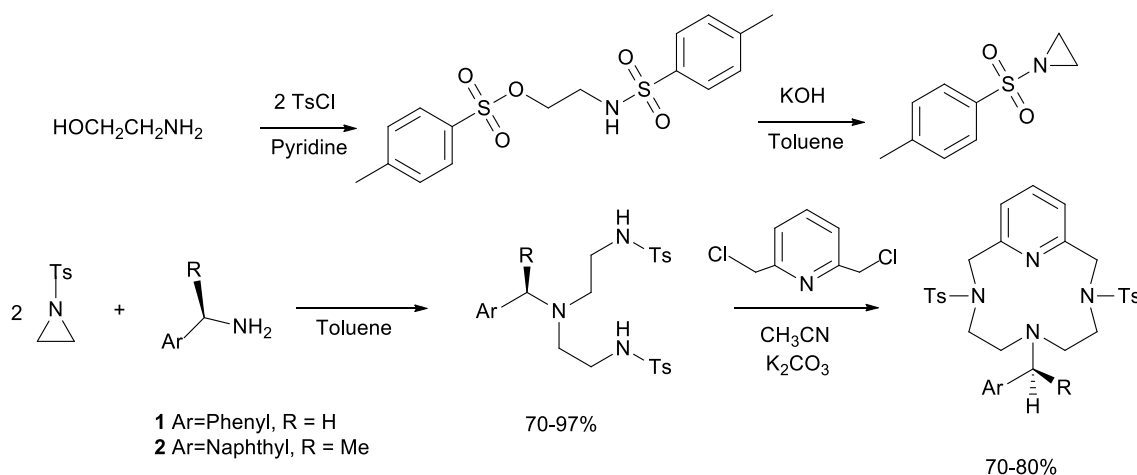


Figure 1.8 – Structure of the PC-type ligand.

We decided to modify this kind of ligands making them suitable for catalytic purpose. In 2008 the new pyridine based 12-membered tetraaza-macrocyclic ligands, named Pyridine containing Ligands (**PcL**) were obtained. The synthetic approach employed to synthesize these macrocyclic ligands, is reported in **scheme 1.4**.³⁷



Scheme 1.4 – Synthesis of macrocyclic molecules **PcL**.

The synthesis of the macrocycle is simple and it involves three main steps. Firstly ethanolamine is reacted with tosyl chloride and the obtained *N,O*-ditosylethanolamine undergoes a ring closure

reaction after treatment with a base to obtain the tosyl-aziridine. Then a solution of the tosyl-aziridine (2 equivalents) is added to a commercially available chiral aryl-amine to yield a substituted *bis*-sulfonamide. Finally, the *bis*-sulfonamide is reacted with 2,6-*bis*(chloromethyl)pyridine, yielding the desired macrocycle. It should be underlined that the crucial step of the macrocyclization, is conducted under heterogeneous conditions as a modification of the Richman-Atkins protocol (NaH/DMF). This synthetic strategy allows to avoid high dilution techniques and to obtain the 12-membered macrocycles in 80–99% yields, without any racemization at the asymmetric carbon. Moreover, it is worth of note that, even conducting this step in concentrated condition, we never observed any polymerization side-reaction. The presence of different types of variously substituted nitrogen atoms (one sp^2 and three sp^3) makes this class of compounds of great interest.

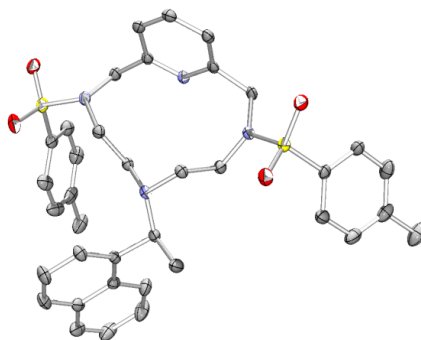
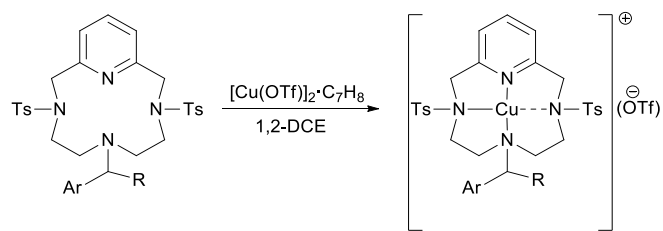


Figure 1.9 – Ortep view of a PcL. The ORTEP view shows the good conformational degree of freedom of the macrocyclic cavity.

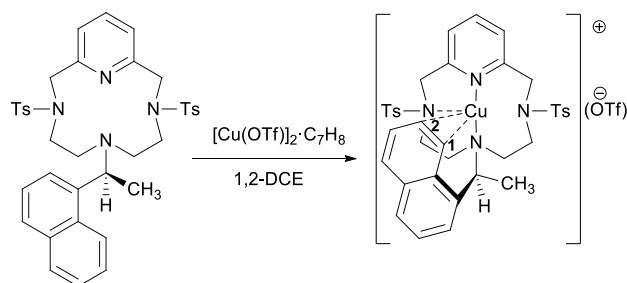
This synthetic methodology is simple and to apply different functionalizations on the macrocyclic framework, in order to change the steric hindrance and to create stereocenters on the backbone. It is possible to develop a modular design of the ligand by varying – for example – the structure of the amine nucleophile, starting from different commercially available chiral or non-chiral amines. Moreover, the tosyl groups can be removed and/or replaced with others protecting groups.

Metal complex formation with PcL was investigated with copper(I) triflate toluene complex ($[\text{Cu}(\text{OTf})]_2 \cdot \text{C}_7\text{H}_8$) as copper(I) source (**Scheme 1.5**).³⁷



Scheme 1.5 – Synthesis of the copper(I) complex.

Treating the ligand with $[\text{Cu}(\text{OTf})]_2 \cdot \text{C}_7\text{H}_8$, a pale-yellow Cu(I) complex, quite sensitive to air and moisture, was obtained. On the other hand, by layering with benzene a 1,2-dichloroethane (DCE) solution of the ligand, after treatment of the ligand with an equimolar amount of $[\text{Cu}(\text{OTf})]_2 \cdot \text{C}_7\text{H}_8$, a colorless crystalline solid was obtained (**Scheme 1.6**).



Scheme 1.6 – Cu(I) complex formation from the ligand, highlighting the η^2 coordination mode of naphthyl moiety.

All the analytical data confirmed the formation of a *mono*-metallic Cu(I) complex (45% yield) which did not readily oxidize to Cu(II). This complex has been isolated and fully characterized. The ^1H NMR spectrum of the complex in CDCl_3 displays a very low symmetry: particularly, in the ^1H NMR (**figure 1.10**) spectrum, the proton directly bound to carbon **1** shifted to higher frequencies, 8.93 ppm compared to 8.16 ppm for the free ligand.

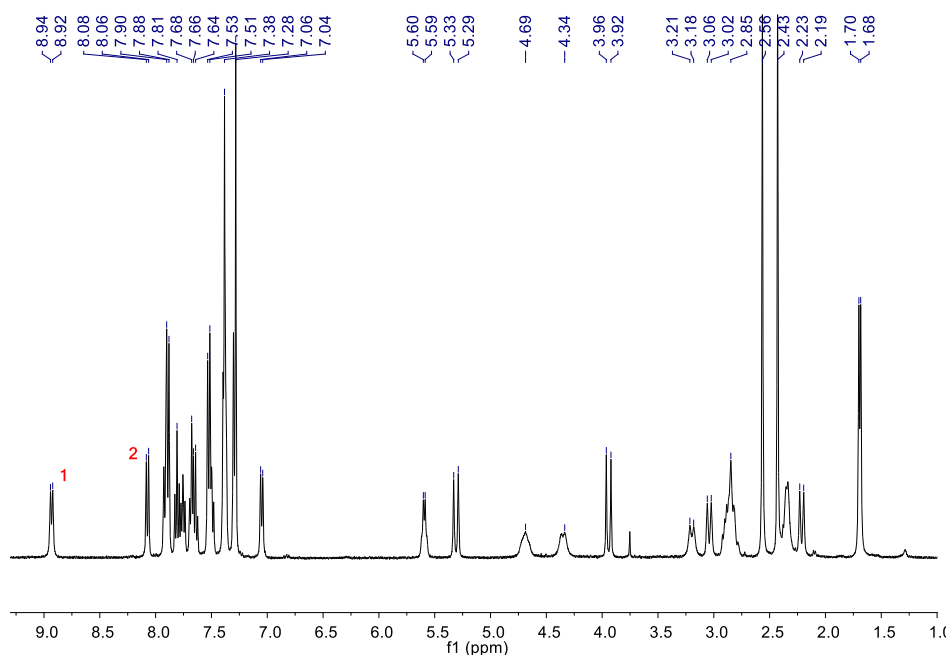


Figure 1.10 – ^1H NMR spectrum of complex **XXXI 2** in CDCl_3 .

Moreover, two sets of signals are observed for the sulfonamide moieties and this can be due only to very low symmetry of the molecule, retained also in solution. Indeed, the solid-state structure of the complex shows that the copper atom is placed in the large macrocyclic cavity of the ligand, which has five potential coordination sites (the four nitrogens and the naphthyl moiety) in a strongly distorted trigonal bipyramidal geometry (**figure 1.11**).

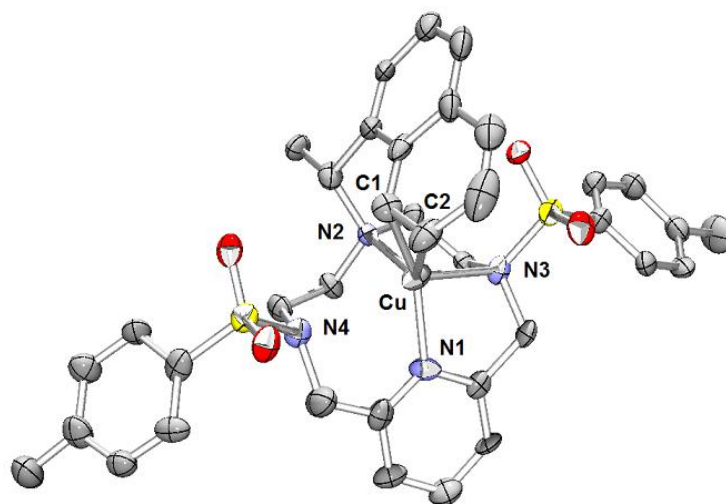


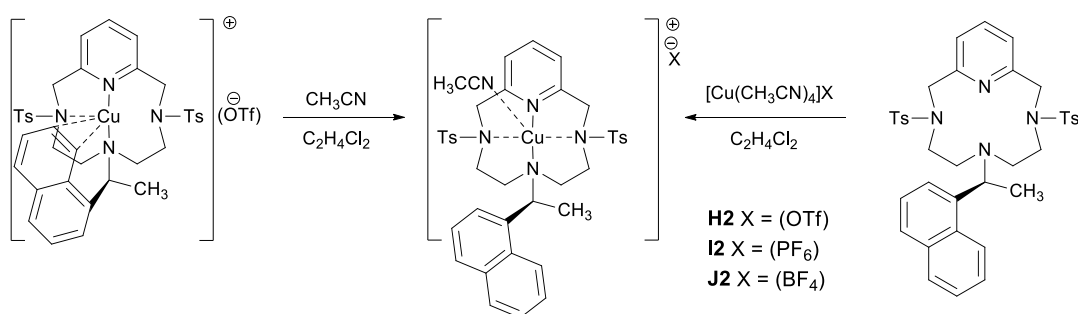
Figure 1.11 – Selected bond distances: Cu–N1 1.980 Å, Cu–N2 2.151 Å, Cu–N3 2.346 Å, Cu–N4 2.820 Å, Cu–C1 2.017 Å, Cu–C2 2.428 Å.

To be precise, in this complex the copper is tetra-coordinated since for steric reasons it is shifted toward one side of the cavity, away from N4 (at a distance in excess of 2.8 Å, well above a regular

Cu–N bond). The η^2 coordination mode of the naphthyl on copper(I) in solution has been also observed by ^{13}C NMR studies in CDCl_3 solution. The signal of naphthyl carbon **1** involved in the η^2 bond with copper shifts from 124.5 ppm in the free ligand, to 94.2 ppm in the complex (see **figure 1.11** for labeling of the carbon atoms **1** and **2**). Conversely, carbon **2** is affected to a lower extent (low frequency shift from 124.6 to 118.2 ppm). The observed coupling constant 1J (^{13}C , ^1H) of 149 Hz for carbon **1** provides hints of a partial re-hybridization state from sp^2 to sp^3 . Since carbon **2**, instead, is less affected a predictable 1J (^{13}C , ^1H) of 163 Hz is observed.³⁸

The effect of the copper complexation to the ligand was also evidenced by the ^{15}N NMR chemical shifts observed in CDCl_3 solution. The ^{15}N NMR spectrum shows a marked shift for the pyridinic nitrogen atom (from 313 to 245 ppm), while the sp^3 nitrogen atom bonded to the asymmetric carbon is affected to a lesser extent (from 39 to 51 ppm).

The η^2 coordination mode of the naphthyl on copper(I) can explain not only the better stability of the copper complex but also the higher performances in term of enantioselection observed in the catalysis.³⁷ The reactivity of the complex was then tested with acetonitrile (**scheme 1.7**).



Scheme 1.7 – Synthesis of the acetonitrile Cu(I) complexes of PCL.

The ^1H NMR spectrum discloses a marked shift of all the signals, especially in the aliphatic region. The ^{15}N NMR spectrum shows that the position of the pyridine nitrogen signal is unaffected while the sp^3 nitrogen atom bonded to the stereogenic carbon is located at 38 ppm.

All the obtained complexes were fully characterized and in some cases crystals suitable for an X-ray structural determination were obtained by crystallization from dichloroethane/*n*-hexane (**figure 1.11**), showing the coordination of the incoming acetonitrile molecule and the displacement of the naphthyl pendant arm.

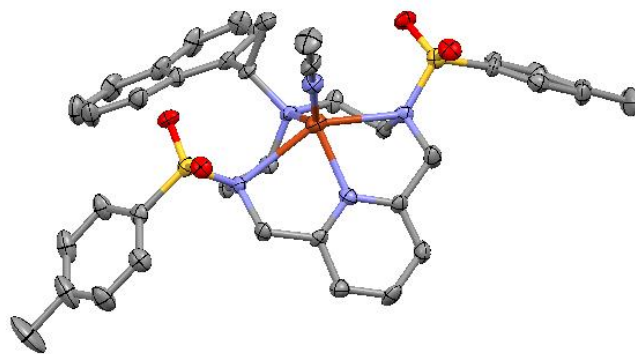


Figure 1.12 – Crystal structures of the acetonitrile Cu(I) complexes of PCL ligands, showing the displacement of the naphthyl moiety.

1.6 Structural modifications

As it will be discussed in the next chapter (result and discussion), it is easy to insert new substituents, and hence new stereocenters, on the backbone of the ligand, just by changing one or more of the starting reagents. The easiest and cheapest way to modify the final outlook of the ligands is to use an enantiomerically pure aminoalcohol instead of the 1,2 – ethanolamine. Since 1,2 aminoalcohols are derivatives of naturally available aminoacids, these latter compounds are perfect to be used as starting material in the synthesis of our ligands. As first test, we used L-valinol for the synthesis of a chiral ligand, bearing two isopropyl substituents on the backbone. While the synthesis of the corresponding aziridine is simple and quite fast, the ring opening reaction is slower and it could be stopped after the addition of 1 equiv. of the aziridine. Hence, the *mono*-adducts could be isolated, although in moderate yields (13-50%).

1.7 Ligands derived from aminoacids

In the last years, several new classes of ligands, containing chiral, biologically inspired, building blocks such as proteins and/or peptides as well as synthetic ligands structurally modified by introducing natural-derived compounds able to act as coordination sites for metal cations, have been reported in the literature.

The use of small peptides able to mimic the activity of natural metalloenzymes presents important advantages like an easy synthetic protocol and the possibility to modify the sequence in order to finely tune the catalytic activity and the coordination kinetics.³⁹ Finally, thanks to the ability of the peptide to adopt several different conformations and to form complex supramolecular structures, it is possible to influence also the second coordination sphere of the metal cation.⁴⁰

In the case of the synthetic modified ligands, the most recent examples are represented by synthetic dipeptides, such as small peptidic chains characterized by the presence of β -turns and by modified aminoacids containing phosphorous atoms (**Figure 1.13**).⁴¹

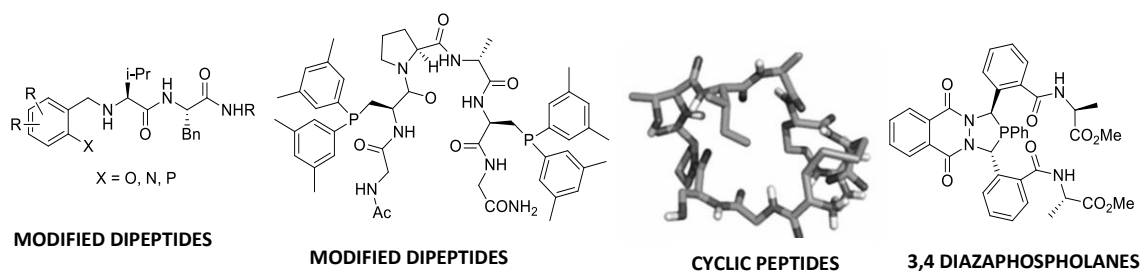


Figure 1.13 – Example of modified synthetic peptides.

The presence of building blocks with natural origin allows the development of catalysts able to induce more selectivity thanks to the local chirality of a single amino acid and to the global chirality generated by the entire system.

This new class of ligands could have affinity for macromolecules, such as proteins, and can be able to form artificial metalloenzymes.⁴² In the last years this class of catalysts became a valid alternative to the traditional ones due to their unique features that couples the characteristics of homogeneous catalysis with those of natural metalloenzymes.

Important examples are the artificial metalloenzymes based on the interaction between biotine and streptavidine.⁴³ Biotine is known especially for its role as cofactor of several carboxylases and is essential due to its ability to act as carrier of CO₂, that binds on the nitrogen of the imidazole ring opposite to the chain of valerianic acid.

In the second half of the last century, the study of the interaction between biotine and streptavidine has been explored in detail and nowadays their interaction is considered the strongest non-covalent bond ever known (**Figure 1.14**).

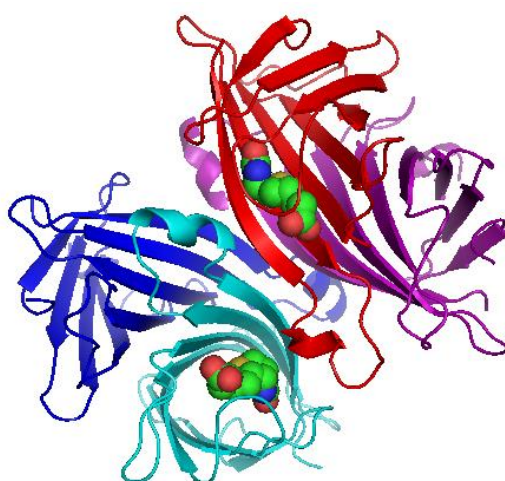


Figure 1.14 – Biotin-streptavidine interaction.

Inspired by these works, we developed a structurally modified PCL containing an aminoacid pendant arm of alanine or lysine in order to further functionalise the macrocycle by implementing a dipeptide or a biotine moiety. In this way the resulting metal complex could be incorporated in streptavidine (in the case of lysine) or in a peptide chain (in the case of alanine) leading potentially to enantioselective and/or diastereoselective catalytic activities.

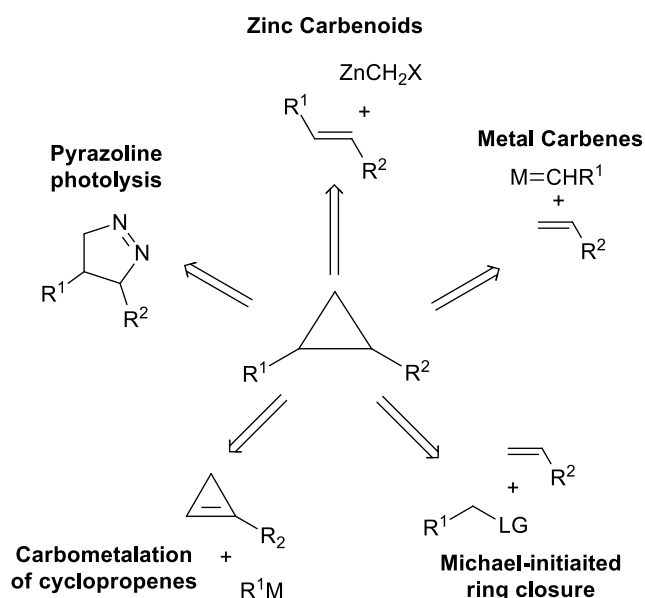
1.8 Catalytic applications

1.8.1 Cyclopropanation

Among the simplest compounds in organic chemistry, we find cyclopropanes and, for this reason, they are very common in nature. Thanks to their importance in natural – and also biological and pharmaceutical – products,⁴⁴ they continue to gain interest in the last years. They are versatile and useful intermediates in the synthesis of more complex molecules. They have been found to show a wide range of biological proprieties and applications encompassing enzyme inhibitions to insecticidal,⁴⁵ antibacterial,⁴⁶ antimicrobial,⁴⁷ antibiotic and antitumor activities.

The cyclopropane rings are present also in industrially relevant and largely produced pharmaceuticals such as antidepressants⁴⁸ and drugs for the treatment of sleep disorders.⁴⁹

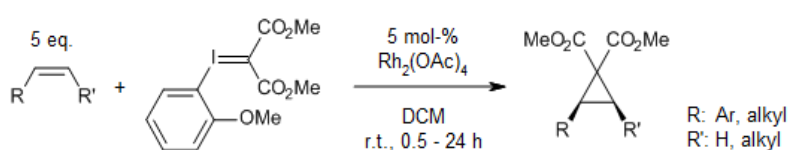
Many different methods have been reported up to now for the synthesis of cyclopropane derivatives from various achiral substrates (**scheme 1.8**).



Scheme 1.8 – Various approaches to cyclopropane derivatives

After the pioneering work of Emschwiller in 1929,⁵⁰ the conversion of alkenes to cyclopropane derivatives was officially attributed to Simmons and Smith in 1958, using zinc-derived carbenoids⁵¹ and, up to now, this method remains one of the most important for the synthesis of this class of molecules. Several zinc carbenoid reagents have been synthesized after Simmons and Smith, Wittig,⁵² and Furukawa publications.⁵³

Different and alternative routes have been reported to obtain more highly functionalized substrates. Zhu and co-workers in 2012 proposed a methodology based on a highly soluble iodonium ylides in the Rh-catalyzed cyclopropanation under homogeneous conditions (**Scheme 1.9**).⁵⁴



Scheme 1.9 – Synthesis of functionalized cyclopropane molecules proposed by Zhu and co-workers.

One of the most useful methods for cyclopropanation reaction is based on the transition metal catalyzed decomposition of a carbene precursor, such as a diazoalkane, or iodonium ylide, or a triazole, leading to the real reactive species (**Figure 1.15**).

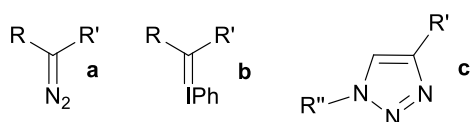
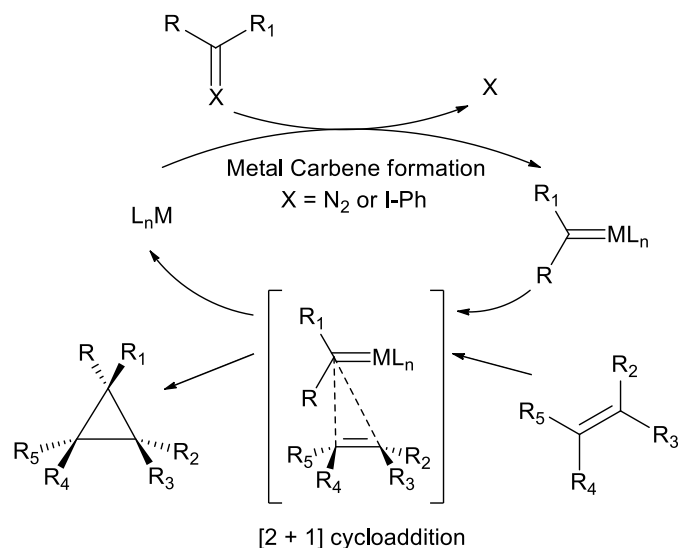


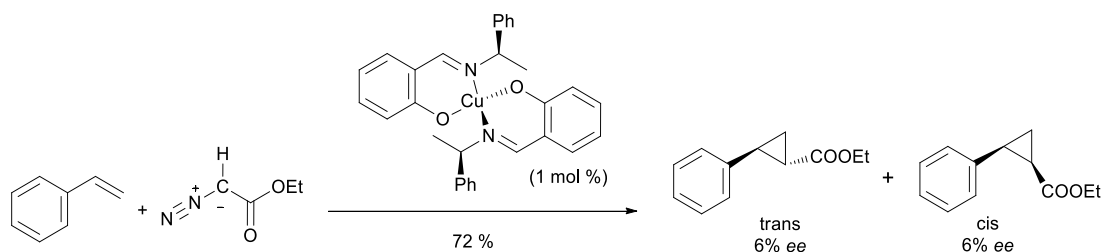
Figure 1.15 – Most commonly used types of carbene precursors in asymmetric cyclopropanation.

The formed metallo-carbene is then able to react with an alkene to produce a cyclopropane derivative in a concerted, [2+1] cycloaddition (**Scheme 1.10**).



Scheme 1.10 – General mechanism of the intermolecular cyclopropanation using metal carbenes.

Up to now, even if a great variety of transition metal catalysts has been used for this transformation, only rhodium(II), copper(I/II), ruthenium(II), iridium(III), iron(III) and cobalt(II) have found to be active with a reasonable stereoselection, but only with the metal center surrounded by the appropriate chiral environment. With these transition metals, the formed carbene has an electrophilic character (Fischer-type carbene) and instantly reacts with electron-rich substrates. The electronic nature of the substituents on the carbene influences its reactivity and, thus, the stereoselectivity of the reaction. The cyclopropanation of olefins using the transition metal-catalyzed decomposition of diazoalkanes is one of the most extensively studied reaction. Both inter- and intramolecular versions of this reaction have been developed and exploited in synthesis. The first example of an enantioselective copper based intermolecular cyclopropanation reaction was reported by Nozaki in 1966.⁵⁵



Scheme 1.11 – Nozaki's copper catalyzed cyclopropanation.

Although the enantiomeric ratios were modest, this catalyst defined the basis for further ligand optimization. In particular, the copper-catalyzed enantioselective version of the reaction is now well

established, and chiral C_2 symmetric bidentate ligands such as bisoxazolines are⁵⁶ are the most widely used, generally employing EDA⁵⁷ as carbene source. As an example, very recently Kellehan *et al.* described copper complexes of chiral BOX ligands applied as catalysts for the asymmetric cyclopropanation reaction of styrene with ethyldiazoacetate and enantioselectivities of up to 70% were obtained. (Figure 1.16).⁵⁸

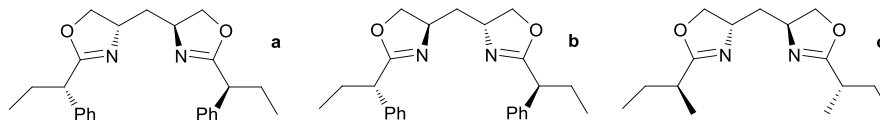


Figure 1.16 – Two different PhPrAraBOX (a and b) and MePrArBOX (c) synthesized by Kellehan *et al.*

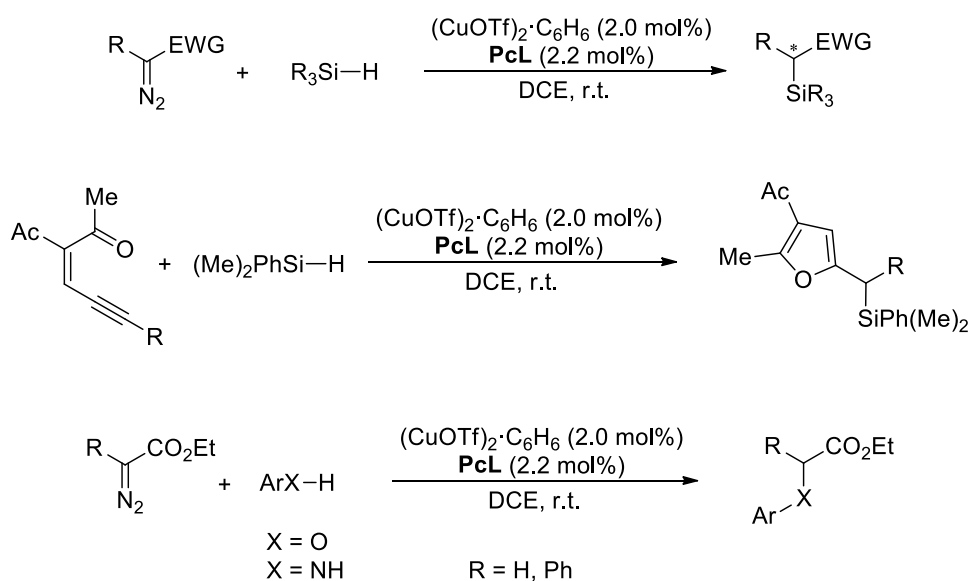
Also porphyrines are widely employed as ligands in cyclopropanation reactions.⁵⁹ For example very recently, S. Gharaati *et al.* described tin(IV) tetraphenylporphyrinato trifluoromethanesulfonate, $[\text{Sn}^{\text{IV}}(\text{TPP})(\text{OTf})_2]$, and tin(IV)tetraphenylporphyrinato tetrafluoroborate, $[\text{Sn}^{\text{IV}}(\text{TPP})(\text{BF}_4)_2]$ as catalysts for cyclopropanation of styrene derivatives with EDA.⁶⁰ These electron-deficient catalysts catalyzed the cyclopropanation of styrene derivatives in high yields, with very high diastereoselectivity and under mild conditions.

The literature concerning the cyclopropanation reaction is continuously expanding:⁶¹ new and more efficient methods for the preparation of these functionalities in enantiomerically pure form are still evolving. Few years ago, our group reported the synthesis and characterization of copper(I) complexes of the previously described ligands (PcL) and very promising results on their use as catalysts in asymmetric cyclopropanation reactions.⁶² Here we report our new findings concerning the extremely challenging diastereoselective cyclopropanation reaction of 2- and 3-vinylindoles exploring the catalytic performances of copper(I) complexes derived from our coordinated PcLs.

1.8.2 X-H carbene insertion

Seen the catalytic competence of our Cu(I) catalysts in alkene cyclopropanation reactions⁶²⁻⁶³ and knowing that Cu(I)-PcL complexes showed to be able to promote cyclopropanations even on vinyl indoles in good yields and high diastereoselectivity, we decided to explore also the field of the X-H bond insertion of carbenes.

The selective functionalization of X-H bonds, particularly those with high bonding energies, constitutes appealing transformations with interest from synthetic and theoretical perspectives. Electrophilic metal-carbene intermediates generated from diazocompounds enable the functionalization of strong X-H bonds under very mild reaction conditions.⁶⁴ With the aim to expand the scope and selectivity of Cu(I)-PcL complexes in carbene transfer reactions, we decide to evaluate them in archetypal X-H bond functionalization reactions. Considering the relevance of silicon-containing compounds,⁶⁵ which can be used as versatile synthetic intermediates, we selected the metal-promoted carbene insertion into Si-H bonds⁶⁶ to test the activity and selectivity of the Cu(I)-PcL catalytic system. After that, we expanded our investigation by testing the Cu(I)-PcL catalytic activity also in O-H and N-H bond insertion⁶⁴ of carbene deriving from diazo-compounds as well as the X-H insertion of furyl-carbenes deriving from relative precursors called enynones (**Scheme 1.12**).⁶⁷ Our findings, despite the modest enantioselectivity, showed to be very interesting in terms of stability and activity of the catalyst as well as in terms of generality of the reaction and of turnover number (TON).



Scheme 1.12 – Cu(I) PcL catalyzed X-H bond insertion of carbenes.

1.8.3 Henry reaction

Carbon–carbon bond forming reactions, thanks to their unique capability of generating molecular complexity, represent a very strong tool for synthetic chemist.⁶⁸ In the last decade considerable advances in the catalytic generation and enantioselective addition of carbon nucleophiles to different types of electrophiles were made. In this context, nitroalkanes are remarkable reagents not only due to their propensity to undergo easy dehydrogenation but also for their easy and direct interconversion to other organic functional groups.⁶⁹

Even weak bases are able to deprotonate the α -position of a nitro group ($pK_a = 10$) and the nucleophilic attack of the generated nitronate anion on a carbonyl to give the corresponding β -nitro alcohol is commonly called Henry (or nitroaldol) reaction.⁷⁰ Even though more than one century old, this reaction is still to be considered one of the most important examples of an atom-economical transformation.⁷¹ No need for a stoichiometric amount of a base, metal catalysts,⁷² enzymes⁷³ or organocatalysts⁷⁴ can efficiently promote the Henry reaction. Among the metal complexes commonly employed as catalysts, copper(I)⁷⁵ and copper(II)⁷⁶ complexes play a huge role but to the best of our knowledge the activity of silver salts and complexes have not been tested. In several cases reported in the literature, the replacement of Cu with Zn gave comparable results but in some of them a reversed enantioselectivity was observed. Surprisingly, such a correlation in reactivity with silver has never been made and the few examples appeared in the literature report that silver salts either failed in promoting the reaction, or gave very poor yields.

In the last years, several studies on the Henry reaction were made in our research group. The copper(I) complexes of the 12-membered pyridine-containing ligands (PcL) have been successfully employed as catalysts in the Henry reaction.^{75b} Among transition metals, reports on the catalytic activity of silver complexes are relatively sparse when compared to the more extensively studied copper and gold. We have recently reported the full characterization of [silver(I)(PcL)] complexes and their organometallic reactivity,⁷⁷ and we have demonstrated their catalytic activity in the regiospecific domino synthesis of 1-alkoxyisochromenes under mild conditions⁷⁸ and in the microwave enhanced A^3 -coupling multicomponent reaction.⁷⁹ Compared

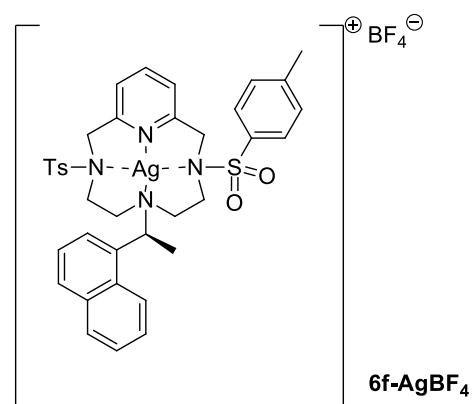


Figure 1.17

with simple silver salts, the great advantages of [Ag(I)(PcL)] complexes are their solubility, their enhanced stability and the easy way of handling (**Figure 1.17**).

Prompted by the interesting results above mentioned, we were intrigued to check if our well-defined silver(I) complexes were suitable catalysts also for the Henry reaction. Thanks to this study, we were pleased to find that [Ag(I)(Pc-L)] complexes can actually activate the aldehyde toward the nitronate nucleophilic attack, in the first example of a silver mediated Henry reaction.⁸⁰

Since the Henry reaction has provided a good platform for testing the dual activation of metal/base catalysts, we have modified our ligands by attaching in the proper position a suitable internal base in order to drive the reaction without the need of any basic cocatalyst.

1.8.4 Isochromene cycloisomerization

Encouraged by the promising results in the nitroaldol reaction mentioned above (see section 1.7.3) and in connection with our ongoing interest in the study of domino nucleophilic addition/cyclization reaction involving alkynes characterized by the presence of a proximate nucleophile (see also section 1.7.3) we decided to test the reaction on proper bifunctional substrates.

Based on our experience, we chose the *o*-alkynylarylaldehydes with the ambition to join the Ag catalyzed Henry reaction (by activation of the aldehyde moiety) to the Ag catalyzed cycloisomerisation (by activation of the triple bond). In this manner we can obtain, in a cascade fashion, new interesting *O*-heterocycles such as isochromenes carrying a -NO₂ substituent making them extremely useful for further functionalizations. A two-step process that takes advantage of a Cu(II) catalyzed Henry reaction followed by an Au(I) mediated cycloisomerisation⁸¹ has recently been reported by Y. Gong and coworkers (**Figure 1.18**).⁸²

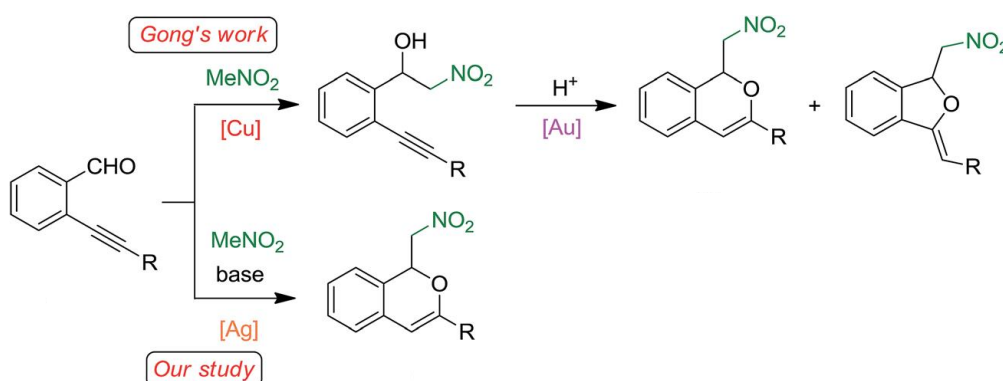


Figure 1.18 – Two steps approach for the synthesis of nitro functionalized *O*-heterocycles by Gong, compared with our domino sequence.

1.8.5 Iron catalyzed alkene oxidation

Much efforts in the use of macrocyclic pyridine-containing ligands have been devoted to the study of catalytic oxidation reactions. Early studies were inspired by Nature and the understanding of metalloenzymes, which use molecular oxygen from air as the primary oxidant. Copper proteins such as haemocyanin, the enzymes tyrosinase and catechol oxidase and nonhaem iron enzymes are very sophisticated catalysts and their reactions are fast and highly selective under mild experimental conditions. The prospect of using model compounds for such metalloenzymes as industrial oxygenation catalysts⁸³ has driven efforts to synthesise molecules capable of mimicking the oxygen binding and activation in natural systems.⁸⁴

The interest in understanding the structures and properties of iron complexes containing coordinated dioxygen has led the scientific community to explore ligands capable of stabilizing superoxo and/or μ -peroxo intermediates before their rapid autoxidation to Fe(III)–oxo species, due either to the presence of water or to oxidative dehydration of the ligands.⁸⁵

In a pioneering paper that appeared in 1982, Kimura and co-workers reported a new pyridine-containing pentaaza macrocyclic ligand (Pyan) capable of stabilising the O₂ adduct of its iron(II) complex in aqueous solutions at room temperature (**Figure 1.19**).⁸⁶

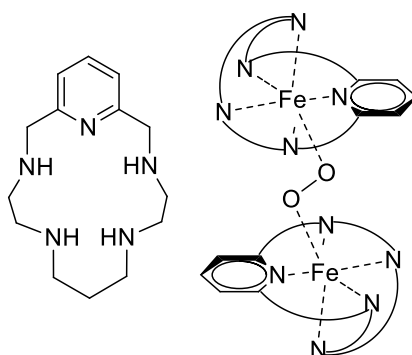


Figure 1.19 – Pyan ligand and its O₂ iron adduct.

The presence of the pyridine ring in the macrocycleskeleton, altering both the electronic and steric properties, was of fundamental importance in the stabilisation of the dioxygen adduct. The more rigid configuration imposed on the macrocycle by the presence of the pyridine ring in the diiron(III)– μ -peroxo complex rendered the complex kinetically inert by preventing ligand dissociation.

Some years later, in the course of modelling the intradiol cleavage of catechol dioxygenase, Koch and Krüger reported the structure and the catalytic reactivity of an Fe(III) catecholate complex of a pyridinophane ligand (**Figure 1.20**).⁸⁷

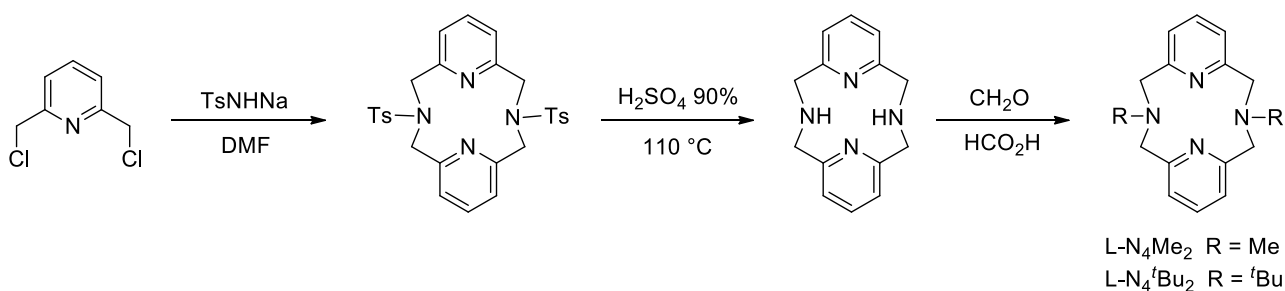


Figure 1.20 – Synthetic scheme for the preparation of different pyridinophane ligands.

One attractive feature of pyridine containing macrocycles is represented by the different synthetic paths to their synthesis, allowing easy modulation of the substitution pattern of the macrocyclic skeleton. Another feature is the presence of inequivalent nitrogen donor atoms, which can be used to introduce coordinating groups on the pendant arm.⁸⁸ In the search for non-haem iron complexes that are active as catalysts for oxygen and peroxide activation, it is important to prepare ligands that can fix the donor atoms in a square-pyramidal (or square-planar) geometry around the metal ion.

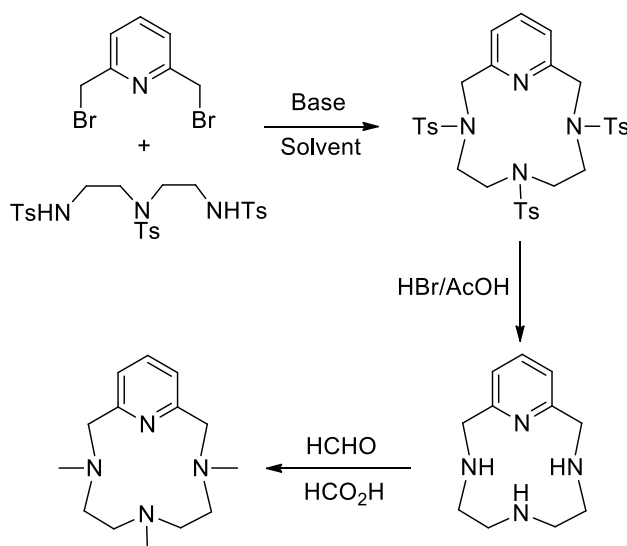


Figure 1.21 – Synthesis of 12-membered tetraazamacrocycles following the modified Richman-Atkins procedure.

Another approach to the synthesis of pyridine-containing macrocyclic ligands consists of the modified Richman–Atkins procedure,⁸⁹ by treatment of an N-tosyl-protected polyamine with 2,6-bis(bromomethyl)pyridine, in the presence of K_2CO_3 as a base under heterogeneous conditions (**Figure 1.21**).⁹⁰ After the hydrolysis, promoted by HBr, of the Ts protecting group, the free-base ligand could be further functionalized. This synthetic scheme was mainly applied to obtain 12-membered macrocycles. The iron(II) complex obtained by treating the final ligand of **Figure 1.21** with $[Fe^{II}(CF_3SO_3)_2(CH_3CN)_2]$, upon treatment with peracetic acid gave rise to the fastest non-heme

oxo-iron complex for cyclohexane oxidation ever, that also proved to be a competent catalyst in alkene epoxidation with peracetic acid.⁹¹

In this work we developed a new tetraaza macrocyclic pyridine containing ligand (PcL) starting by the modified Richman–Atkins procedure, by treatment of an *N*-tritosyl-diethylenetriamine with pyridine-2,6-diylbis(methylene) dimethanesulfonate, in the presence of K₂CO₃ as a base under heterogeneous conditions. After the hydrolysis in HBr of the Ts protecting groups, the free-base ligand has been perbenzylated on the three sp³ nitrogens. The resulting product has been coordinated with different sources of iron(III) and tested as catalyst in the oxidation of alkenes showing a surprisingly good and complementary activity in epoxidation and diol formation in mild conditions and strictly dependent on the counteranion.

2. RESULTS AND DISCUSSION

The first aim of this work was the development of a synthetic strategy for obtaining an increased number of ligands with several different substituents and protecting groups. This class of ligands has the general structure reported below (**Figure 2.1**) and a lot of attention has been paid to the optimization of all the synthetic steps, in order to increase yields and to reduce reaction times.

We choose the tosyl (Ts) moieties as protecting groups thanks to the easy synthesis of the starting materials, their excellent general stability, their ability in forming stable complexes with coinage metals in +1 oxidation state (the presence of two less basic nitrogen in the ligand, in fact is useful for the catalytic properties of the corresponding metal complexes) and the low cost of tosyl chloride compared to other protecting groups. Finally, since the tosyl groups require harsh conditions for the deprotection reaction (use of HBr 47%), we developed a new class of *ortho*-nosyl protected ligands. We used them to obtain unprotected macrocycles bearing -NH moieties.

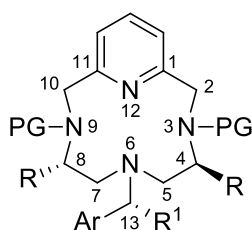
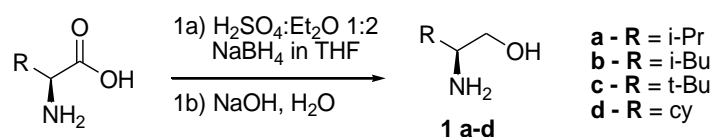


Figure 2.1 – General structure of the PCL ligands.

2.1 Synthesis of aminoalcohols

As detailed in the introduction, one of the easiest modification that can be made to the skeleton of the ligands, is the change of the starting aminoalcohol in order to provide substituents and stereogenic carbons on the backbone of the molecule. Enantiomerically pure aminoalcohols are available on commerce with accessible prices. However, the cost of the direct synthesis from the corresponding aminoacids is much lower.

The classical procedure starts with the esterification of the carboxylic group, followed by the reduction of the ester. This pathway allowed us to obtain the products in good yields (75-90%), but it was very time-expensive. We found in literature only one direct synthesis of aminoalcohols from aminoacids, reported by Cozzi et al., involving NaBH_4 and H_2SO_4 (**Scheme 2.1**). The procedure worked well with all the tested substrates and led us to obtain the aminoalcohols **1a-d** in excellent yields (90-99%) with complete retention of configuration.

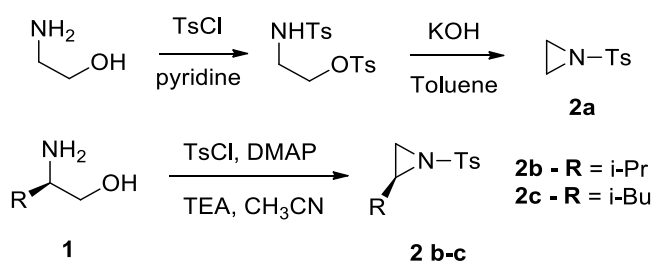


Scheme 2.1 – Reduction of aminoacids.

2.2 Synthesis of aziridines

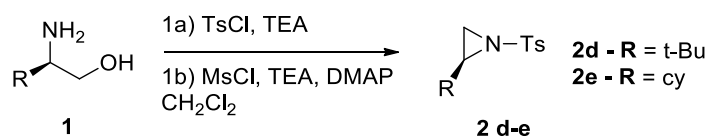
2.2.1 Synthesis of tosyl protected aziridines

The synthetic path that we used to convert aminoalcohols into tosyl protected aziridines depended on the nature of the substituents. The easiest reaction is the one with ethanolamine, L-valinol and L-*t*-leucinol that involves a first tosylation of both nitrogen and oxygen atoms and the subsequent ring closure driven by a strong base (**Scheme 2.2**).



Scheme 2.2 – Synthesis of *N*-Ts-aziridines.

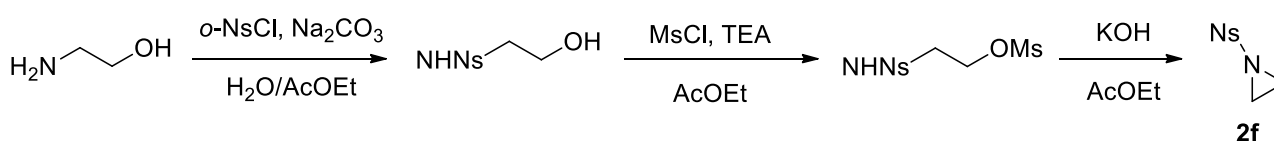
For others, more sterically hindered aminoalcohols, we searched in literature for a different pathway involving the tosylation of the nitrogen atom, followed by the mesylation of the oxygen and the final ring closure.⁹² We were pleased to find that these two steps one pot reaction allowed us to obtain the product in high yields (about 80%) without further chromatographic purifications (**Scheme 2.3**).



Scheme 2.3 – Synthesis of substituted *N*-Ts-aziridines.

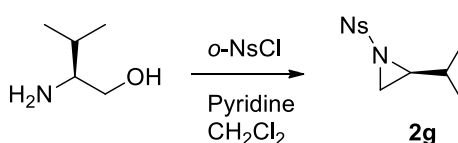
2.2.2 Synthesis of *o*-nosyl protected aziridines

The synthesis of *o*-nosyl (Ns) protected aziridines was easy and fast. For aminoethanol, the pathway consists in a three-step reaction, where the first two steps are the protection of the nitrogen and oxygen atoms respectively with *o*-nosyl and mesyl groups. The last step is the base-catalyzed ring-closure reaction that leads to the formation of the *ortho*-nosyl protected aziridine (**Scheme 2.4**). The aziridine, if needed, is purified by precipitation of the impurities, and the overall yield of the three steps is high (>90%).



Scheme 2.4 – Synthesis of *N*-Ns-aziridine.

The pathway for L-valinol is much simpler and it involves a one pot reaction (**Scheme 2.5**).⁹³ This reaction allowed us to obtain the aziridine with a reasonable 65% of yield after mandatory chromatographic purification.



Scheme 2.5 – Synthesis of 2-isopropyl-*N*-Ns-aziridine.

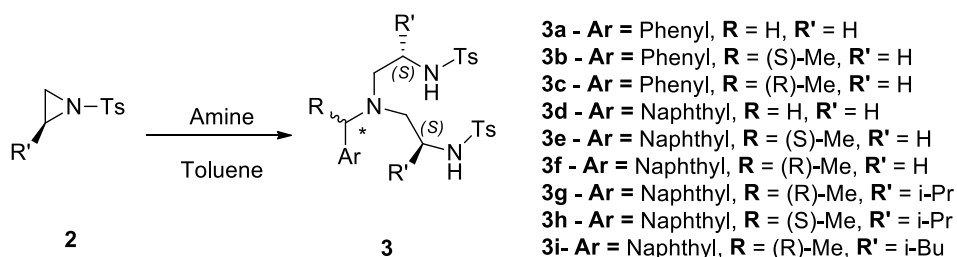
2.3 Synthesis of bisulfonamides

The general procedure for this step involves the ring opening reaction of two aziridines by a primary aromatic amine: the ones used in this work are benzylamine, 1-*R*- and 1-*S*-methyl benzylamine, naphthylmethylamine and both the isomers of 1-naphthylethylamine. In addition to the low price of these compounds, we chose them because of the availability of the pure enantiomers and their stability towards racemization. An important feature that needs to be highlighted is that, for every amine used, the attack at the terminal position of the aziridines is highly regioselective and we never observed a competing ring opening reaction at the more substituted carbon atom. Moreover, the absolute configuration of the stereocenters was always maintained.

2.3.1 Synthesis of “Disubstituted” bisulfonamides

The procedure for this step consisted in refluxing two equivalents of aziridine and one of amine in the appropriate solvent until the reaction was complete. In some more challenging cases more than two equivalents of aziridine are required to drive the reaction to completion. In some much more challenging cases a mixture of bisulfonamide and monosulfonamide was obtained, thus requiring a separation of the two products by flash chromatography. The so-recovered monosulfonamide can be reacted with further aziridine in order to provide again the corresponding bisulfonamide.

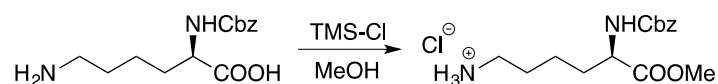
For tosyl protected aziridines, the solvent chosen is a mixture of toluene and acetonitrile. The first one allows higher temperatures and avoids the formation of byproducts and the second one being polar helps the S_N2 reaction of this step. Anyway, while the reaction takes only few hours for unsubstituted aziridines, it requires prolonged times (more than one week) for substituted aziridines (**Scheme 2.6**).



Scheme 2.6 – Synthesis of tosyl protected sulfonamides.

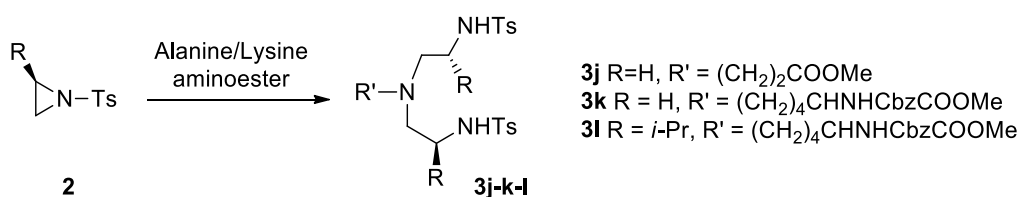
With the aim to synthesize macrocycles bearing an amino acid moiety, we applied this last procedure also in the case in which, instead of using one of the organic amines already described, the amine function of natural amino acids such as β -alanine and $N(\alpha)$ -Cbz-lysine were employed as nucleophiles for the aziridine ring-opening. In this way, the resulting ligand could be employed in peptidic chains as a new synthetic macrocyclic amino acid capable to coordinate different metals. The number of fields of possible applications is extremely high and heterogeneous (from catalytic to biomedical applications).

First, we had to protect the acid function of the amino acids as esters in order to avoid side reactions and to increase the compound solubility. The reaction between the amino acid and TMS-Cl (TMS = trimethylsilyl) in the presence of methanol provided the resulting methyl ester in quantitative yields (**Scheme 2.7**).



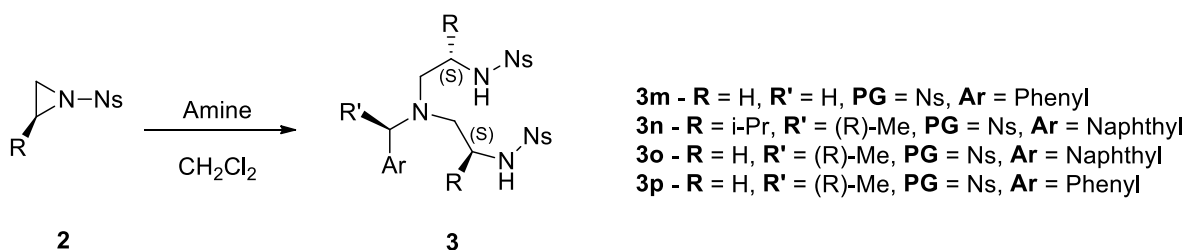
Scheme 2.7 – Aminoacid protection.

Using the aminoacids, a mixture of monosulfonamide and bisulfonamide has always been observed, probably due to the higher polarity of the species. Nevertheless, bisulfonamides **3j-k-l** were obtained in more than reasonable yields, especially after the recovery of the monosulfonamides and their subsequent conversion to bisulfonamides with a further aziridine equivalent (**Scheme 2.8**).



Scheme 2.8 – Bisulfonamides derived from aminoacids.

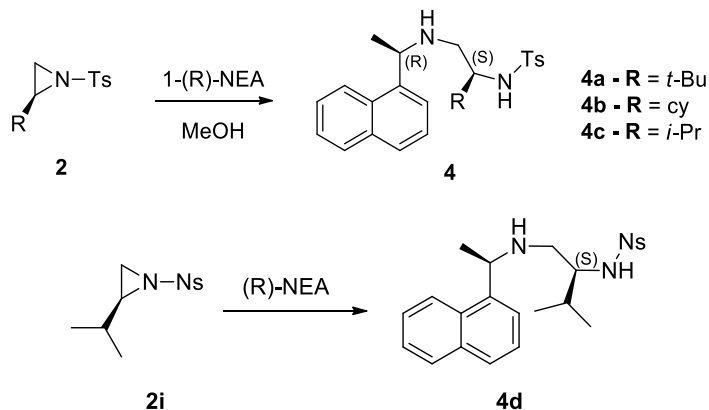
On the other hand, the reactions between the nosyl protected aziridines and the amines were by far shorter thanks to the activating effect of the protecting groups. For this reason, milder conditions have been employed (**Scheme 2.9**).



Scheme 2.9 – Ns-protected bisulfonamides.

2.3.2 Synthesis of “Monosubstituted” bisulfonamides

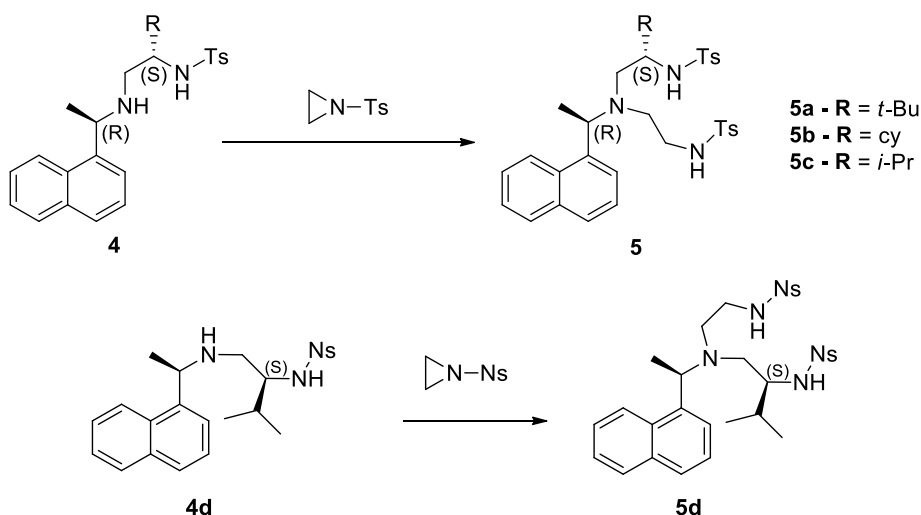
The monosulfonamides products **4a-d** obtained as by-products in the synthesis of the bisulfonamides precedently described, were subsequently employed as starting material for the preparation of completely un-symmetric bisulfonamides (**Scheme 2.10**).



Scheme 2.10 – Ts and Ns-protected monosulfonamides **4a-d**.

To the scope, we conducted a step by step reaction, using a substituted aziridine in the first part and a different aziridine in the second step. In this case, MeOH was the best solvent concerning the yield, while a mixture of toluene and acetonitrile avoided the formation of by-products (**Scheme 2.11**).

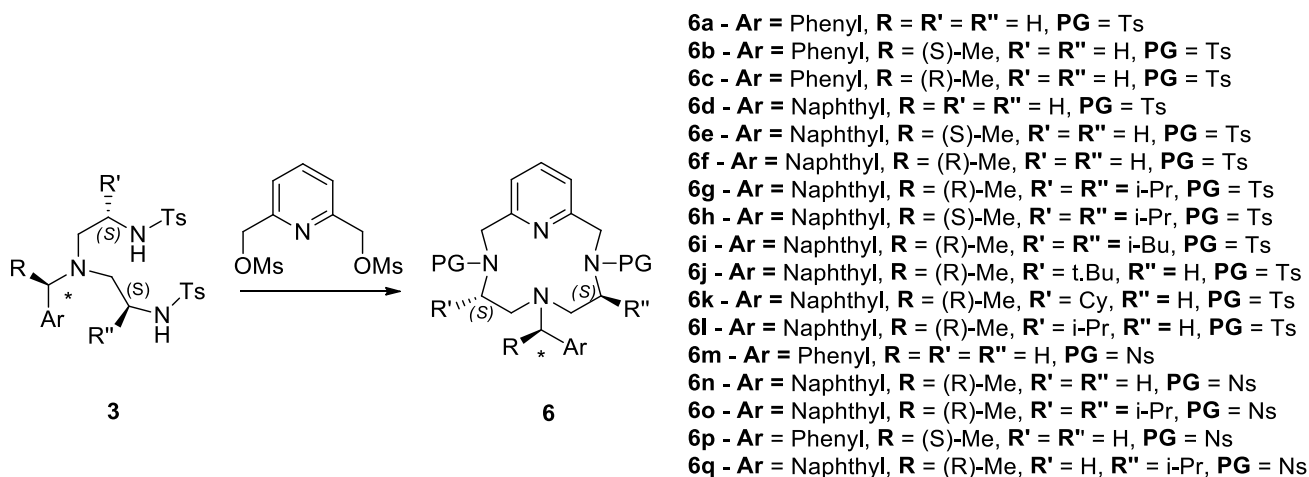
We easily obtained in this way the bisulfonamides **5a-d**, in high yields (80-85%) after chromatographic purification.



Scheme 2.11 – Synthesis of monosubstituted bisulfonamides **5a-d**.

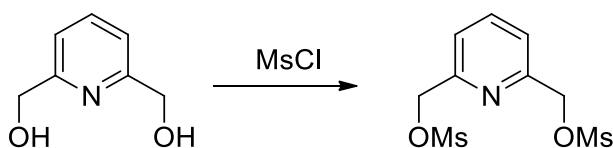
2.4 Synthesis of the macrocycles

All the bisulfonamides obtained were used to synthesize the corresponding macrocycles, by reaction with 2,6-bis(mesyilmethyl)pyridine. This step was conducted in heterogeneous conditions, employing K_2CO_3 as base, in order to avoid high dilution techniques and to prevent the formation of polymeric byproducts. The reaction allows to obtain the desired macrocycles in yields ranging from 50 to 99% after chromatographic purification (**Scheme 2.12**).



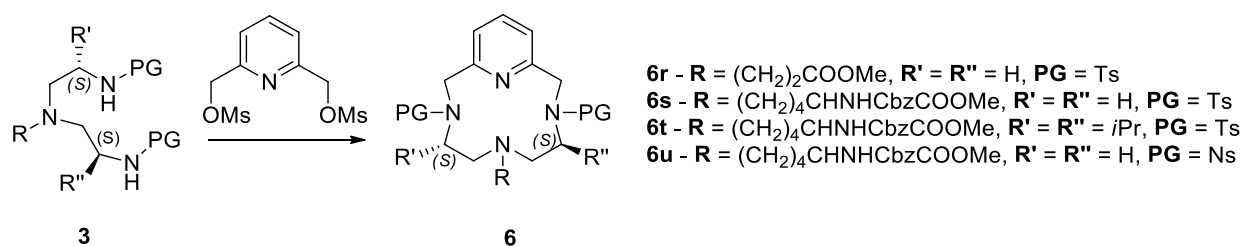
Scheme 2.12 – Synthesis of the macrocycles **6a-q**.

In fact, in the research group it was discovered that 2,6-bis(mesyilmethyl)pyridine is more reactive (and cheap) with respect to the commercially available 2,6-bis(chloromethyl)pyridine. It is synthesized in almost quantitative yields by reacting 2,6-bis(hydroxymethyl)pyridine with mesylchloride (**Scheme 2.13**).⁹⁴



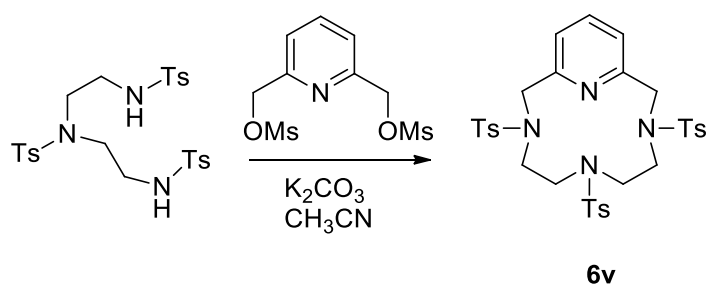
Scheme 2.13 – Synthesis of 2,6-bis(mesyilmethyl)-pyridine.

With the same procedure already described, we have also synthesized the aminoacid-derived macrocycles **6r-u** in quantitative yields (**scheme 2.14**). This new class of bio-inspired ligands was fully characterized and employed directly in coordination of metals, in deprotection and further functionalization.



Scheme 2.14 – Synthesis of aminoacid-derived ligands **6r-u**.

In the same way we have also prepared other three macrocycles with different electronic features and properties with the aim to test different coordination environments for other metals. The first one is ligand **6v**, already known in literature and obtained by the reaction of *N,N',N''*-tritosyldiethylenetriamine with the already mentioned 2,6-*bis*(mesylmethyl)pyridine (**Scheme 2.15**). Despite the fact that this ligand is already reported in the literature, its structure is not known. We have thus grown crystals suitable for an X-Ray structural determination in order to have insights into the distances of the coordination pocket (**Figure 2.2**). The most relevant feature of the structure is the parallel arrangement of the lateral tosyl substituents, which is in contrast to what we observed for ligands **6f** and **6h**, where the conformation of the cycle brings the two tosyl aromatic rings far from each other in antiparallel arrangement.⁶² This ligand has been subsequently deprotected and further functionalized as described in the next subchapter.



Scheme 2.15 – Synthesis of ligand **6v**.

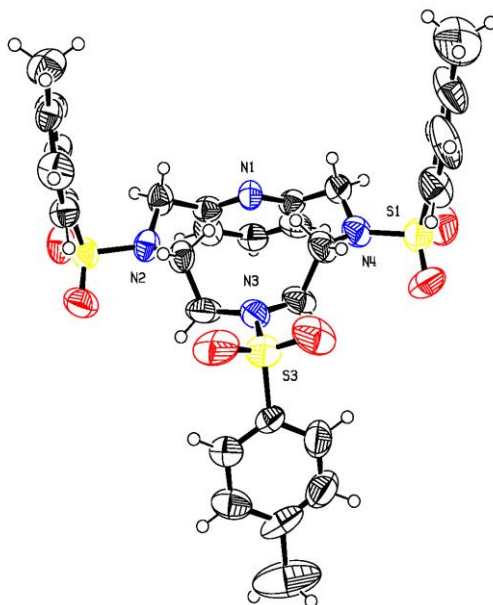
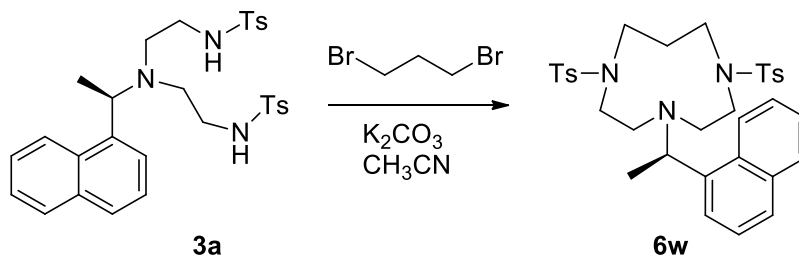


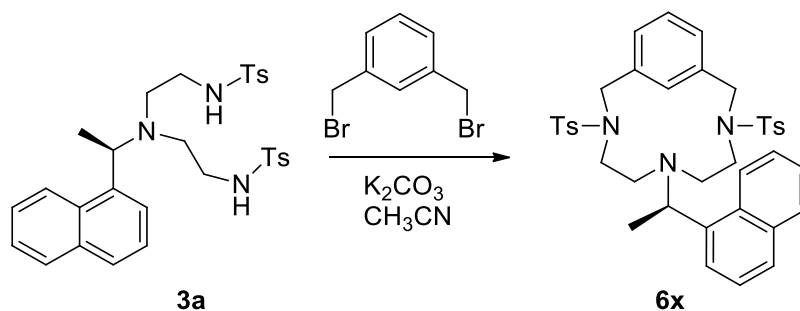
Figure 2.2 – Structure of compound **6v** (thermal ellipsoids are shown at 50% probability level). To give an idea of the size available for coordination inside the cycle, the distances N1...N3 and N2...N4 are 3.968 Å and 5.607 Å, respectively.

The second one, product **6w**, was obtained by the reaction between 1,3-dibromopropane and bisulfonamide **3a** and have been synthesized in order to test the coordination activity of a 10-membered tridentate macrocyclic ligand (**Scheme 2.16**).



Scheme 2.16 – Synthesis of ligand **6v**.

Finally, ligand **6x**, was obtained by the reaction between α,α' -dibromo-*m*-xylene and bisulfonamide **3a** and it has been synthesized in order to test the coordination activity of a 12-membered tridentate macrocyclic ligand (**Scheme 2.17**).



Scheme 2.17 – Synthesis of ligand **6x**.

2.4.1 Synthesis of deprotected ligands

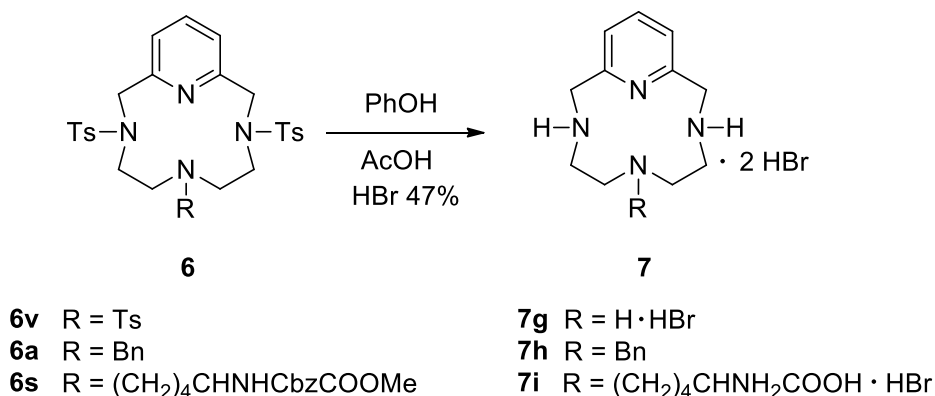
In the previous years, our research group have studied the coordinative behavior of the PCL ligands with the coinage metals copper and silver in +1 oxidation state. Some trials made up to now with gold(I) salts met with failure, probably due to the size and electronics of the macrocyclic ligands. The good catalytic activities observed in the previous works for Cu(I) and Ag(I) complexes are due to the weak coordinative ability of the sulfonyl protected nitrogen atoms, possessing a very low basicity, and to the much more pronounced basicity of the other two nitrogen atoms, which results in the formation of very stable complexes. In order to extend the range of metals suitable for complexation, we decided to deprotect the *N*-sulfonylated atoms. This transformation should increase the basicity of the two nitrogens and give access to dianionic complexes with different catalytic features. Moreover, the two -NH moieties could be further functionalized.

First, we tried to remove the tosyl moieties from the ligand **6a**. The classical procedures involve the use of strong acids, strong bases or powerful reactants.⁹⁵ Aime et al.⁹⁶ used concentrated sulphuric acid to deprotect similar ligands. An alternative method involves the use of SmI_2 under various condition; Anker and Hilmersson optimized this reaction for many tosylamides, tosylaziridines and tosyl esters.⁹⁷

The route that we chose involves the use of an HBr solution (47% w/w in water). The reaction worked well and we obtained the product in 60% of yield.

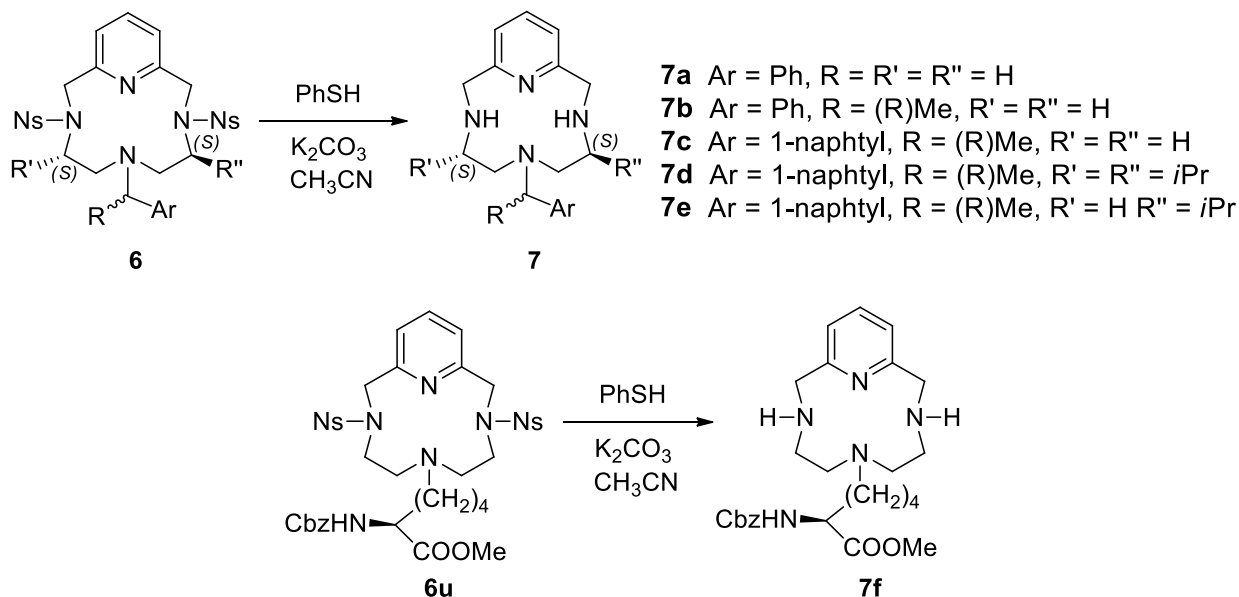
However, the same method turned out to be effective just on macrocycles bearing substituents that cannot undergo to *beta*-elimination reaction. In fact, the simplest macrocycle **6a**, bearing a benzyl substituent and **6s** bearing the six-carbon lysine-derived chain, have demonstrated to be suitable for this deprotection reaction. In particular, product **6s** was completely deprotected also from *Cbz*-

and methyl ester protecting groups resulting in a tri-hydrobromide salt. On the contrary, employing the macrocycles with a chiral aryl pendant arm or alanine-derived pendant, the same conditions caused also the cleavage of the aryl/alkyl moiety probably due to a *beta*-elimination favoured cleavage. The same result was obviously obtained by applying this deprotection procedure also on ligand **6v** leading to the formation of the *tri*-hydrobromide salt (**Scheme 2.18**).



Scheme 2.18 – Deprotected ligands from tosyls.

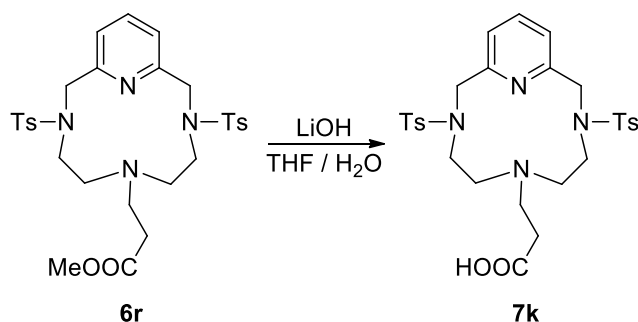
These problems prompted us to develop a new class of *ortho*-nosyl protected macrocycles as previously described. We successfully deprotected the *o*-Ns protected ligands providing the free-base products **7a-f** with good yields (**Scheme 2.19**).⁹⁸



Scheme 2.19 – Deprotected ligands from *o*-nosyls.

Concerning the deprotection of these ligands, we successfully employed the conditions reported by Fukayama: we allowed our ligands to react with thiophenol in acetonitrile in the presence of K_2CO_3 as base.⁹⁸ The base generates a thiolate anion that attacks the nosyl aromatic ring, forming a thioether and SO_2 as byproducts. It is important to note that both the base and the solvent employed for this step are the same used for the macrocyclization reaction, meaning that it could be ideally possible to conduct the two steps in one pot.

Other deprotection strategies have been applied for the selective deprotection of the groups present on the aminoacid-derived macrocycles **6r** and **6s**. In fact, for the alanine-derived product **6r**, a methyl ester hydrolysis with LiOH has been performed leading to the formation of the free acid product **7k** with a yield of 90% (**Scheme 2.20**). Single crystals for X-ray diffraction studies for ligand **7k** were obtained from slow diffusion of THF in a water solution of ligand **7k** (**Figure 2.3**). The high symmetry of the crystals, (triclinic crystal system with space group P-1) allowed locating the acidic proton atom. Ligand **7k** crystallizes as zwitterion, with the H^+ coordinate into the catalytic pocket, more closely bound to N4 (Distance N4-H = 1.03(5) Å).



Scheme 2.20 – Deprotected ligand **7k**.

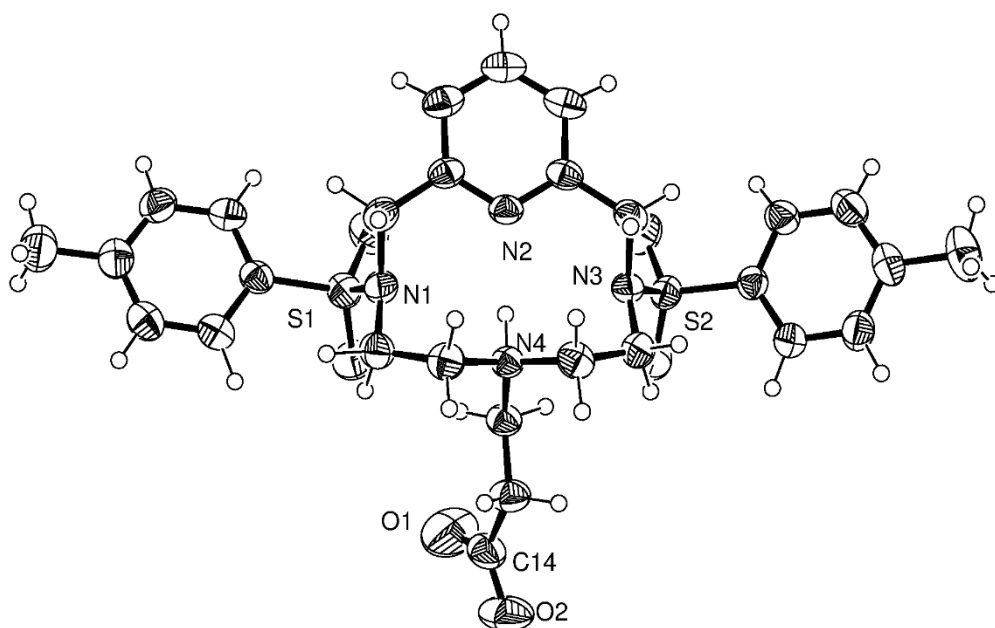
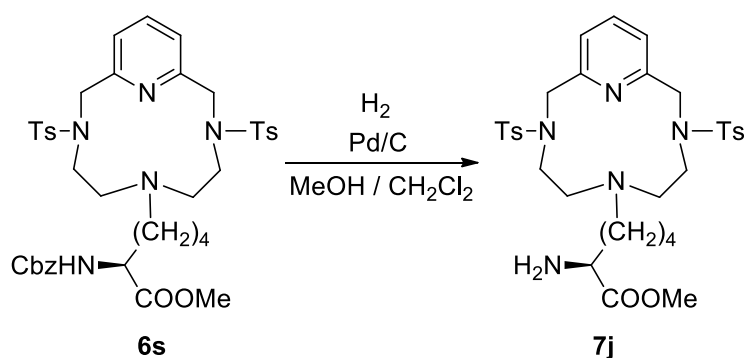


Figure 2.3 – Structure of compound **7k** (thermal ellipsoids are shown at 50% probability level).

On the other hand, *Cbz*-lysine derived ligand **6s** has been treated with Pd/C in H₂ atmosphere leading to the formation of the free -NH₂ product **7j** in very good yields (90%). (**Scheme 2.21**).

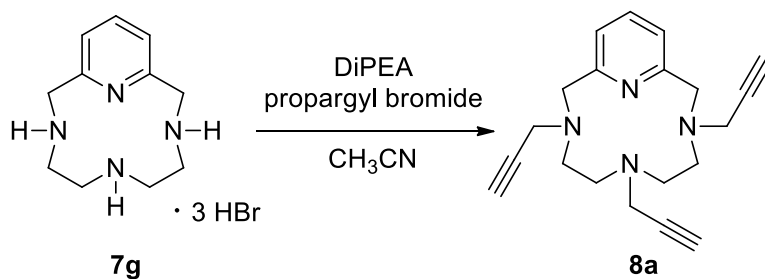


Scheme 2.21 – Deprotected ligand **7j**.

2.4.2 Functionalizations of deprotected ligands

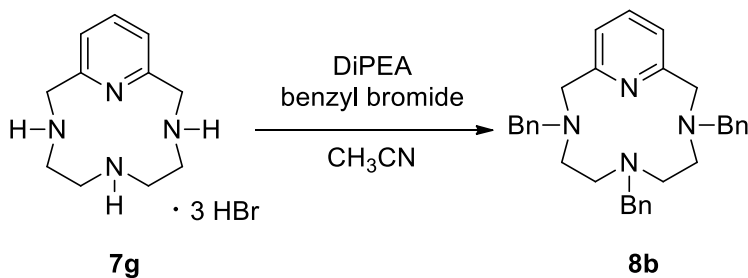
Generally, all of the deprotected ligands were used as synthesized for the study of the coordination activity towards transition metals. In some cases, they were further functionalized with the aim to use them in a specific field of application. We chose three specific deprotected ligands to perform these studies, namely **7g-j-k**.

Ligand **7g** has been chosen for studies of direct alkylation of the three -NH functionalities. For this reason it was treated with one to three equivalents of propargyl bromide in presence of DiPEA (diisopropylethylamine) in order to verify the rate of the direct alkylation and the final symmetry of the alkylated macrocycle (**Scheme 2.22**). The reaction proceeds easily and without formation of byproducts. Moreover, the so-obtained product **8a** was selectively the trisubstituted one. Propargyl bromide was chosen as model alkylating agent, since it can be easily functionalized further. In fact, propargyl can undergo to a 3+2 condensation with an azide in the Huysgen's reaction, also known as "click" chemistry. In this way, any kind of compound bearing an azide can be bound to the macrocycle in an easy way (i.e. chiral moieties, biocompatible molecules, polar compounds enhancing the hydrophilicity of the final ligand, etc).



Scheme 2.22 – Synthesis of trifunctionalized ligand **8a**.

With the same protocol, ligand **7g** was treated also with benzyl bromide leading to the formation of the desired trisubstituted compound **8b** with the encouraging yields of 70% (**Scheme 2.23**). This new macrocycle was originally designed with the aim to promote π -stacking interactions in a possible aromatic catalytic reaction media. Moreover, the resulting product showed increased solubility in non-polar solvents.



Scheme 2.23 – Synthesis of trifunctionalized ligand **8a**.

The second deprotected ligand chosen for functionalization was **7j**. This compound, thanks to the -NH₂ pental and the potential free acidic function, can be employed in peptidic bonds with the aim to implement the macrocyclic monomer in a peptide chain. Ideally, more than one unit can be

inserted in such a chain, leading to a non-natural peptide suitable for the coordination of different metals (**Figure 2.2**).

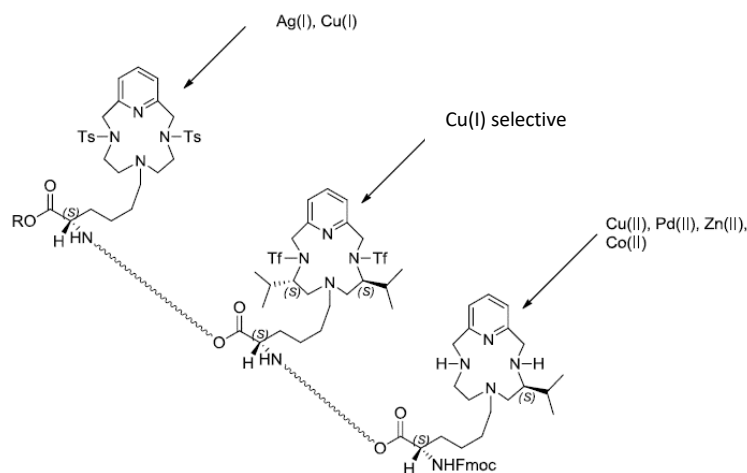
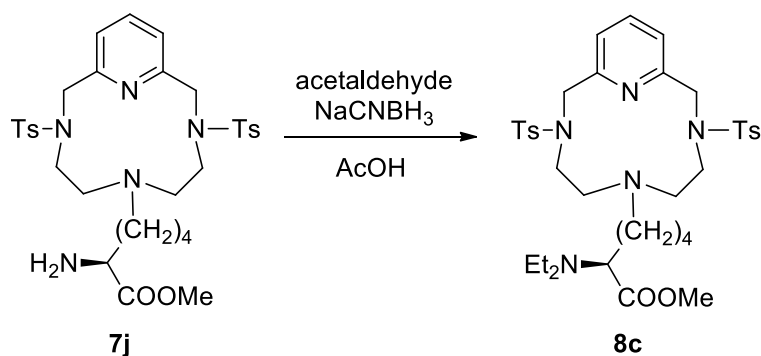


Figure 2.4 – Non-natural peptide with several macrocyclic pendals.

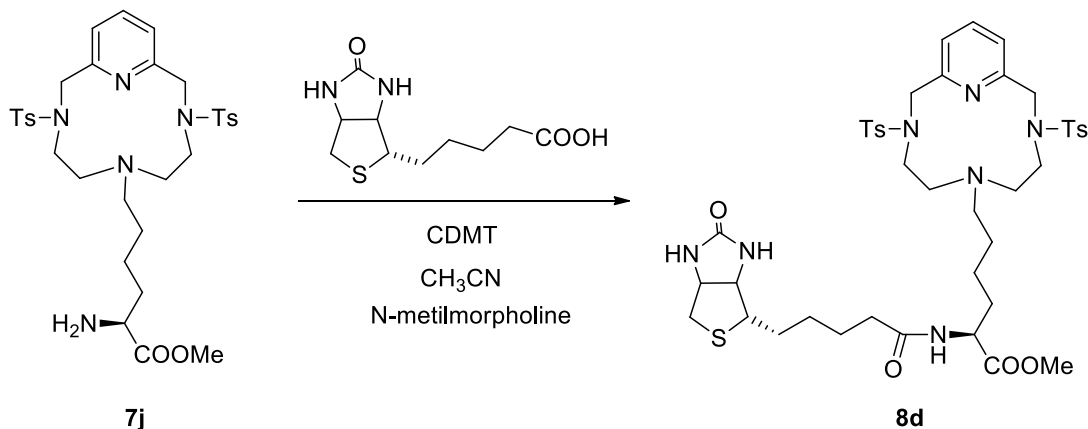
Moreover, **7j** can be also used for double alkylation of -NH₂ in order to provide a macrocycle bearing an internal non-nucleophilic base. Such a bifunctional compound was successfully employed as Ag(I) catalyst in the study of the nitroaldol reaction without the addition of external bases (see catalysis subchapter). To do so, **7j** was treated with NaCNBH₃ in presence of acetaldehyde resulting in a reductive amination that lead us to obtain the macrocycle **8c** in 61% yield (**Scheme 2.24**).



Scheme 2.24 – Synthesis of diethylated ligand **8c**.

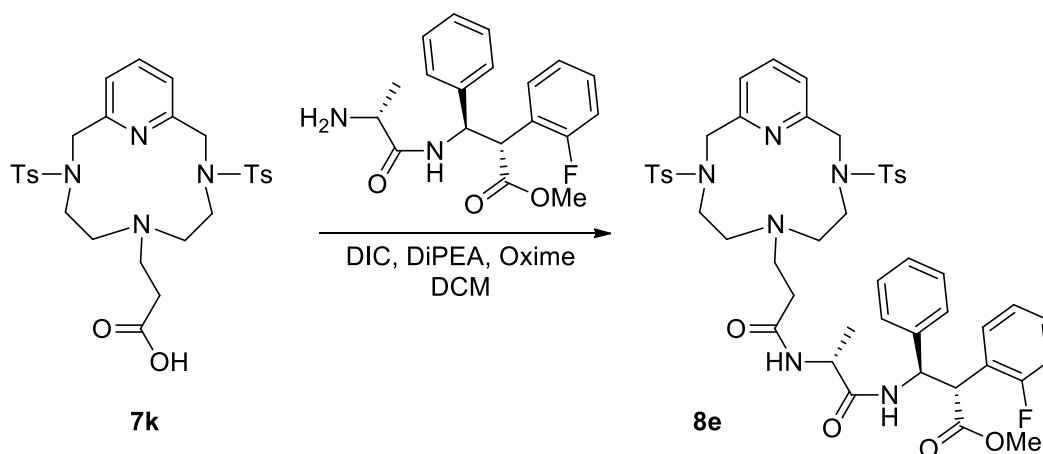
Another reaction performed on **7j** involved the water-soluble vitamin B₇ also known as biotin. In collaboration with Dr. Rimoldi of our Univeristy (DISFARM), the starting material was treated with biotin in presence of CDMT (2-Chloro-4,6-dimethoxy-1,3,5-triazine) and *N*-methylmorpholine leading to the formation of the peptide bond (**Scheme 2.25**). The so-obtained ligand **8d**, thanks to the biotin arm, showed a great affinity for the protein substructure called streptavidine (*as*

explained in the introduction) and the resulting complex can be used in asymmetric catalytic applications in water media with chiral information induced by the protein substructure itself.



Scheme 2.25 – Synthesis of biotin ligand **8d**.

An analogous treatment was the one to which underwent the alanine-derived deprotected macrocycle **7k**, but in this case was the free acidic function of the molecule that was involved in a peptidic bond with the synthetic dipeptide “**D2**” synthesized in the laboratories of Prof. Gelmi of our University (DISFARM). The reaction was performed in DCM (dichloromethane) in the presence of one equivalent of DIC (*N,N'*-Diisopropylcarbodiimide), ethylene cyano oxime and DiPEA and led to the final product **8e** with acceptable yields (**Scheme 2.26**).



Scheme 2.26 – Synthesis of ligand **8e**.

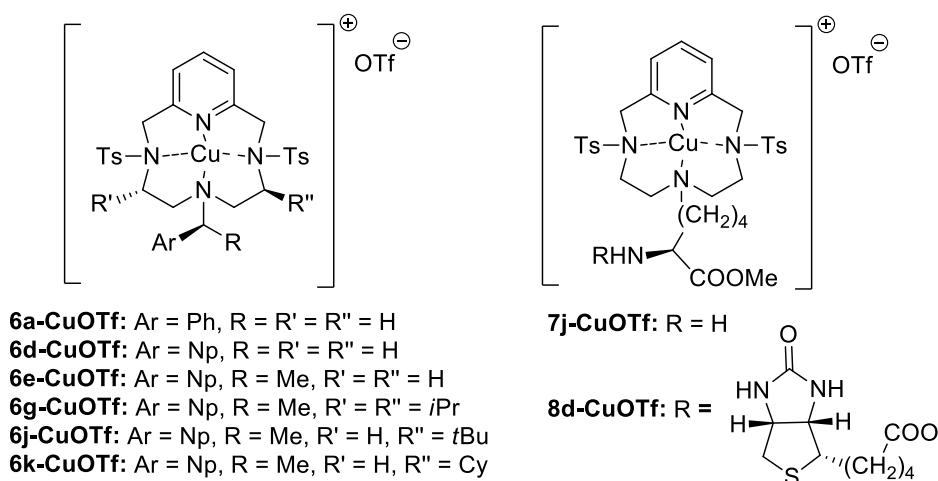
The resulting product **8e** can be coordinated with Ag(I) or Cu(I) metal salts and used as catalyst in many organic transformations, performed in water media, leading to high added value products and using conditions in agreement with the principles of the green chemistry.

2.5 Copper complexes

2.5.1 Synthesis

Having discovered in the previous years that our PCLs can coordinate in excellent way Cu(I) salts, providing complexes with remarkable catalytic activity in many organic transformations, we decided to focus our initial attention on Cu(I) coordination on our new macrocycles.

The coordination of Cu(I) salts to our ligands is straightforward and just by treating a solution of the copper salt and our ligand (1:1 ratio) in 1,2-dichloroethane (DCE) at room temperature followed by layering of *n*-hexane under inert atmosphere yielded the desired metal complexes. The complex precipitated as a white powder, in quantitative yields. The copper(I) complexes shown in **scheme 2.27** were isolated and fully characterized.



Scheme 2.27 – Synthesis of Cu complexes.

As reported in previous works of the research group, the effect of the copper complexation to the ligands is evident by the shift of the signals in ^1H , ^{13}C and ^{15}N NMR spectra. Moreover, although the synthesis is better performed under protecting atmosphere to maximize the yield, many of the final complexes can be manipulated in air without oxidation or decomposition. The reason of this greater stability is due to the presence of the naphthyl group that acts as a further coordination site for the metal. In these cases, low symmetry is retained in solution, as shown by NMR studies (**Figure 2.3**). Again, the ^{15}N NMR spectrum shows a marked shift for the pyridinic nitrogen atom (from 313 to 245 ppm), while the *N*-6 atom bonded to the stereogenic carbon, is affected to a lower extent (from 39 to 51 ppm). All these complexes were isolated in good yields and fully characterized.

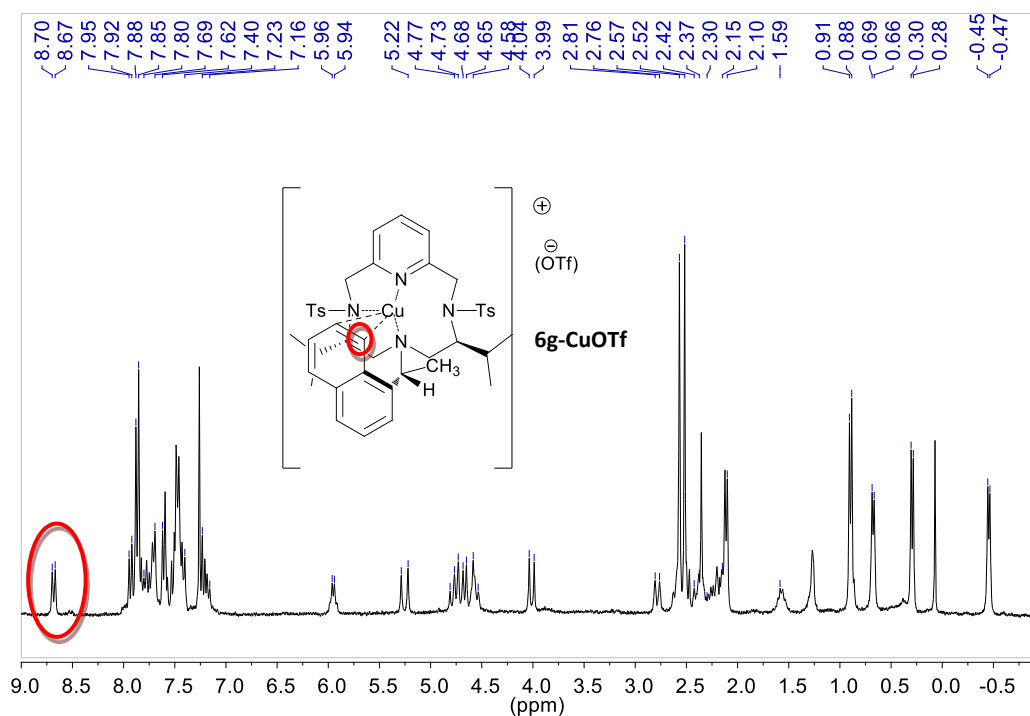
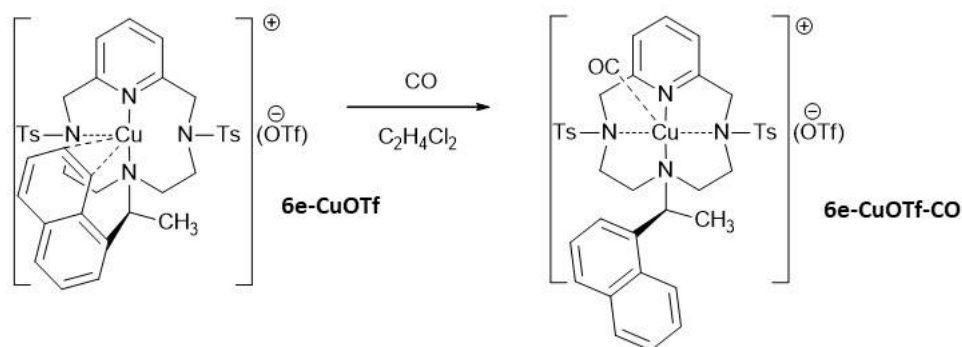


Figure 2.5 – ^1H NMR relative to complex **6g-CuOTf**. In the ^1H NMR the proton directly bound to the highlighted carbon shifted to higher frequencies 8.68 ppm compared to 8.58 ppm for the free ligand **6g**.

To better understand the behavior of the naphthyl group, in the past were studied the coordination of these complexes in the presence of added ligands such as CO and acetonitrile showing a displacement of the η^2 -coordinated naphthyl operated by the incoming new ligand (**Scheme 2.28**). This displacement is visible via ^1H NMR in which the highlighted signal shown before shifts once again to lower ppm.



Scheme 2.28 – Reaction of complex **6e-CuOTf** with carbon monoxide.

2.5.2 Cu(I) catalysis: cyclopropanation

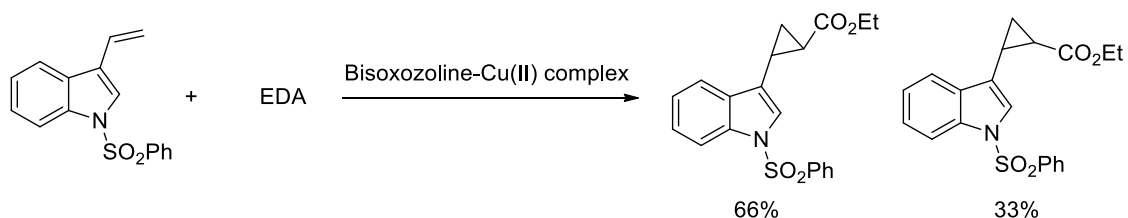
As described in the introduction, cyclopropanes are one of the simplest cyclic compounds in organic chemistry and, probably for this reason, they are very common in nature. Thanks to their importance in natural, biological and pharmaceutical products, they are attracting a lot of interest in the recent years. They are versatile building-blocks in the synthesis of complex molecules in any field of application.

In particular, the copper-catalyzed enantioselective version of cyclopropanation is now well known and chiral C_2 symmetric bidentate ligands such as bisoxazolines are widely used, normally employing diazo-compounds as carbene source.

In recent years, our research group studied in detail the catalytic activity of our Cu(I) PCL complexes in the reaction of cyclopropanation of styrenes using EDA as the carbene source.^{62, 75b} The enantioselective version of this reaction was also developed, providing extremely good results in terms of enantiomeric excess, reaching up to 99% *ee* in some cases. Moreover, the scope of the reaction was demonstrated to be quite general but, despite the excellent *ee*%, poor diastereoselection was observed.⁶³

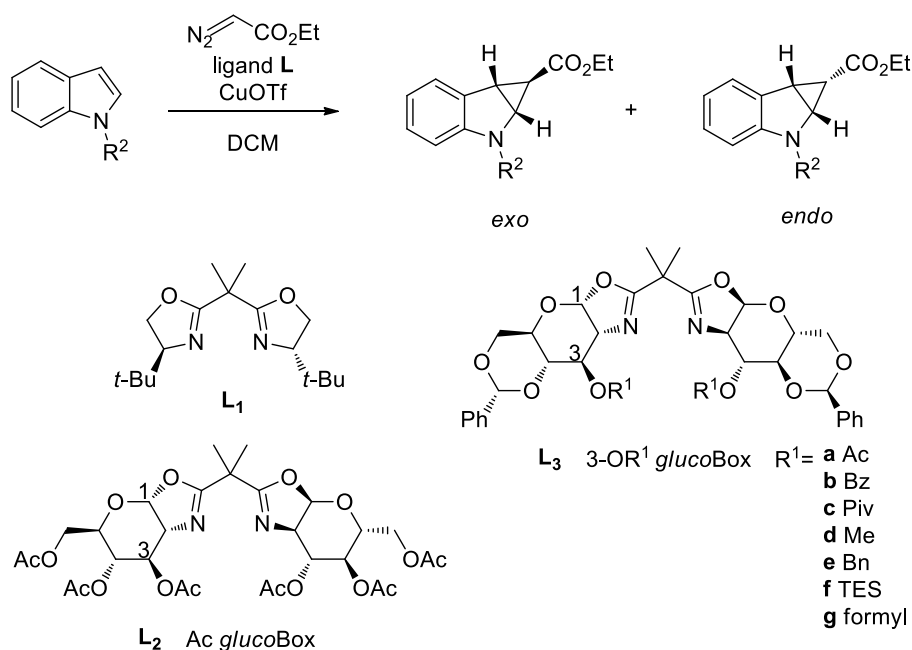
Encouraged by these exciting results, we decided to push the research activity towards much more challenging targets, such as the Cu(I)PCL catalyzed cyclopropanation of 2- and 3-vinylindoles in collaboration with Dr. Valentina Pirovano of our University (DISFARM).

One of the first examples of cyclopropanation of an indole derivative date back to 1998. Raj and coworkers presented in this work the synthesis of indol-3-cyclopropyl derivatives from 3-vinylindole protected with benzensulfonyl group, EDA and bisoxazoline copper(II) as catalyst.⁹⁹ They obtained a mixture of *trans* and *cis* stereoisomers with a good overall yield. Using this method, they obtained preferentially the *trans* stereoisomer (**Scheme 2.29**).



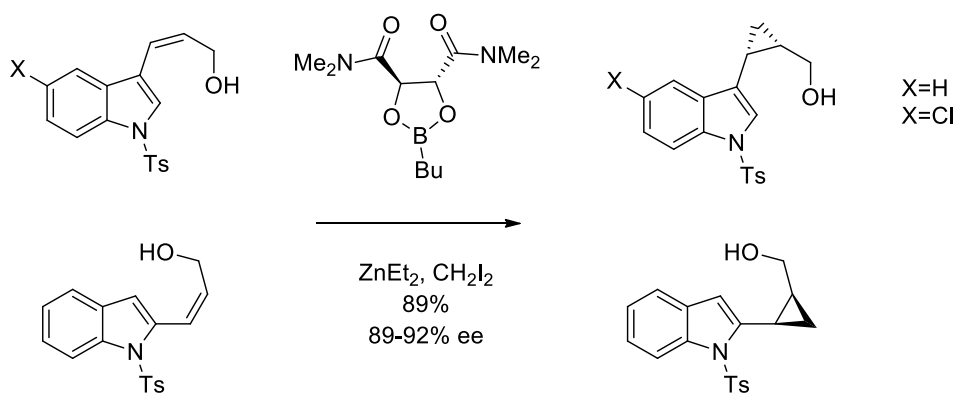
Scheme 2.29 – Raj and coworkers first examples of cyclopropanation of vinylindoles.

Recently, Boysen and coworkers investigated the cyclopropanation of *N*-Boc 3-methyl indole for the synthesis of a product with an all-carbon quaternary stereocenter, useful as precursor of indole alkaloids.¹⁰⁰ In order to obtain a good enantioselectivity, CuOTf and particular bisoxazolines bearing D-glucosamine moiety were employed as catalytic system (**scheme 2.30**).



Scheme 2.30 – Boysen and coworkers cyclopropanation of vinylindoles using BOX ligands.

In 2013, Gaich and coworkers proposed an enantioselective cyclopropanation of *Z* 2- and 3-vinylindoles using zinc as catalyst in Simmons-Smith type reaction.¹⁰¹ In this case, the cyclopropane ring was formed only at the vinylic double bond in high yield and with good enantioselection (**Scheme 2.31**). No remarkable difference was observed between substituent in 2- or 3-position.



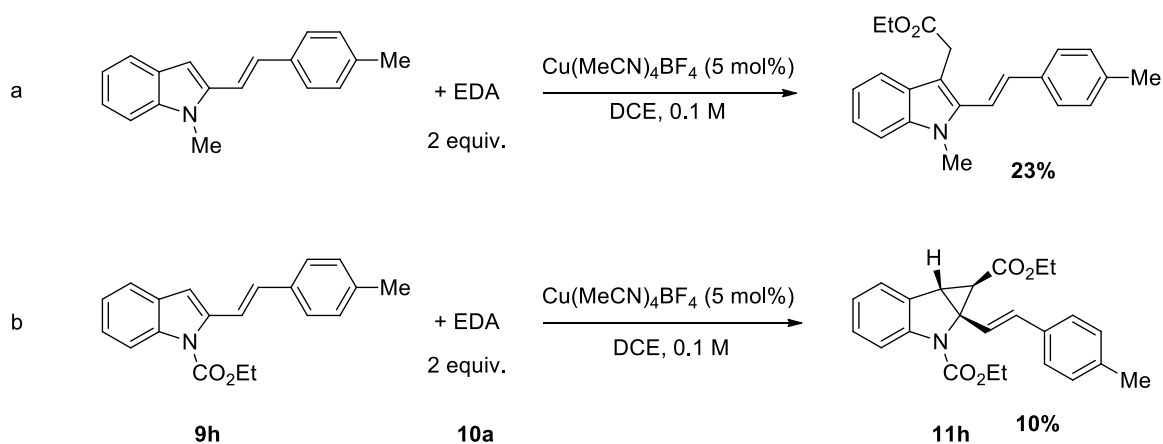
Scheme 2.31 – Gaich and coworkers Simmons-Smith cyclopropanation of vinylindoles.

Taking into account these last results, and the previous literature reports, it is clear that the selectivity of the formation of cyclopropane on C2-C3 position of the indole or on the vinyl moiety relies principally on the catalytic system that is employed.

Considering the experience of our collaborating research group on indole functionalization and the literature reports on cyclopropanation of indoles and vinylindoles, our main objective was to test the feasibility of the reaction between 2-vinylindoles and diazoesters catalyzed by Cu(I) PCL complexes.

The preliminary results demonstrated that our catalysts were not only active, but also very chemoselective and diastereoselective, especially if compared with Cu(I) complexes of BOX ligands (previously described) that were almost inactive and inefficient towards a so challenging application.

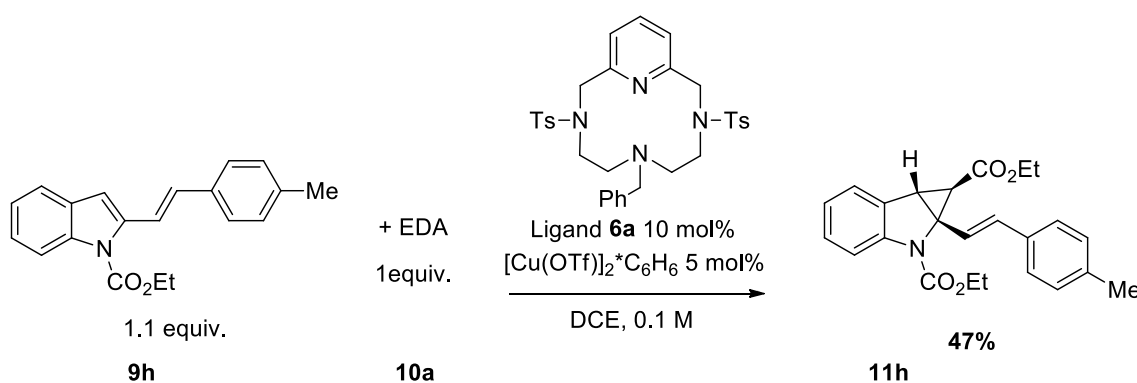
To start our investigations, we decided to test two different *N*-substituted 2-vinylindoles in a reaction with EDA. As metal to form the carbene, we employed a Cu(I) species by considering previous reports on cyclopropanation with vinylindoles. Using *N*-methyl 2-vinylindole, EDA and Cu(MeCN)₄BF₄, the principal product was the one arising from carbene insertion on nucleophilic C3 position (Scheme 2.32). Instead, using the same 2-vinylindole but with ethyl carbamate as protecting group, we were able to isolate a cyclopropyl indoline **11a** as single product besides unreacted starting material (Scheme 2.32). Thus, it was clear that the different electronic properties of the protecting group had a strong influence on the reactivity of 2- and 3-position of the 2-vinylindole.



Scheme 2.32 – Our preliminary tests of cyclopropanation of vinylindoles.

Starting from these results, we decided to focus our research on the synthesis of product **11h** bearing a cyclopropyl group. In fact, despite of the very low yield, the reaction was totally regio- and diastereoselective, affording an interesting dearomatized tricyclic indoline.

As first step to improve the yield, we consider necessary to use a more reactive copper(I) salt as catalyst and to this scope copper(I) triflate (CuOTf) appeared as the best choice. However, this salt is characterized by low solubility in some organic solvents and by low stability to oxidation. As consequence, we tested our Cu(I) complex of PcL **6a**. Thus, when the reaction was conducted in the presence of **6a-CuOTf**, generated *in situ* from CuOTf and the corresponding ligand **6a**, the yield was significantly increased to 47% (**Scheme 2.33**).



Scheme 2.33 – Cu(I)PcL catalyzed cyclopropanation of vinylindoles.

Subsequently, for the screening of the reaction conditions, we selected a 2-vinylindole having a methyl group instead than a *p*-tolyl on the vinyl moiety, in order to avoid any possible interference due to the conjugated aromatic ring. Moreover, the reduced steric hindrance of the methyl group could have beneficial effects in increasing the yield.

The model reaction previously described was used to test the activity of different Cu(I) catalysts.

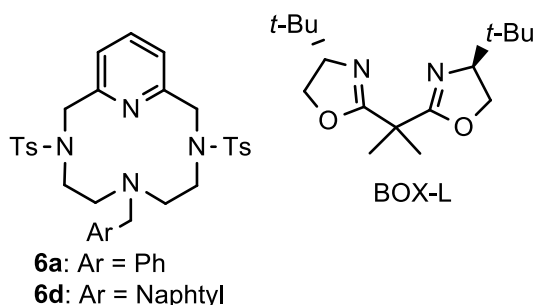
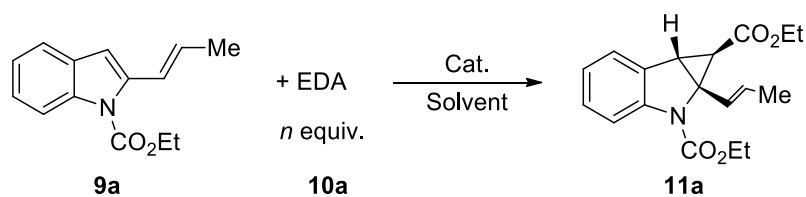


Figure 2.6 – Ligands used for the optimization of cyclopropanation of 2-vinylindoles.



Entry	Cat.	Time, h	equiv EDA	Solvent	Yield, % ^a
1	[Cu(OTf) ₂]*C ₆ H ₆ (2.5 mol%) Ligand 6a (5 mol%)	3	1.5	DCE (0.1M)	43 ^b
2	[Cu(OTf) ₂]*C ₆ H ₆ (2.5 mol%)	3	1.5	DCE (0.1M)	6 ^b
3	[Cu(OTf) ₂]*C ₆ H ₆ (2.5 mol%) Ligand 6d (5 mol%)	3	1.5	DCE (0.1M)	19 ^b
4	[Cu(OTf) ₂]*C ₆ H ₆ (2.5 mol%) Ligand 6a (5 mol%)	3	2.5	DCE (0.1M)	48 ^b
5	[Cu(OTf) ₂]*C ₆ H ₆ (2.5 mol%) Ligand 6a (5 mol%)	3	1.5 ^c	DCE (0.1M)	33 ^d
6	6a -(Cu)BAR _F (5 mol%)	3	1.5	DCE (0.1M)	27 ^b
7	[Cu(OTf) ₂]*C ₆ H ₆ (2.5 mol%) Ligand 6a (5 mol%)	3	1.5	DCE (0.1M) ^e	32 ^b
8	[Cu(OTf) ₂]*C ₆ H ₆ (2.5 mol%) Ligand 6a (5 mol%)	12	2.5	DCE (0.07 M)	32 ^d
9	[Cu(OTf) ₂]*C ₆ H ₆ (5 mol%) Ligand 6a (10 mol%)	12	2.5	DCE (0.07 M) ^f	68 ^b
10	[Cu(OTf) ₂]*C ₆ H ₆ (5 mol%) Ligand 6a (10 mol%)	12	2.5	Toluene (0.07 M) ^f	27 ^b
11	[Cu(OTf) ₂]*C ₆ H ₆ (5 mol%) BOX-L (10 mol%)	12	2.5	DCE (0.07 M) ^f	19 ^d
12	IPrCuCl (5 mol%) NaBAR _F (5 mol%)	3	1.5	DCE (0.1 M)	n.r. ^b
13	Rh ₂ OAc ₄ (2.5 mol%)	3	1.5	DCE (0.1M)	traces ^b
14	Pd(CH ₃ CN) ₂ Cl ₂ (5 mol%) NaBAR _F (12 mol%)	3	1.5	DCE (0.1M)	n.r. ^g
15	(ArO) ₃ PAuCl (5 mol%) AgSbF ₆ (4.5 mol)	3	1.5	DCE (0.1M)	n.r. ^g
16	Ph ₃ PAuCl (5 mol%) AgSbF ₆ (4.5 mol)	3	1.5	DCE (0.1M)	n.r. ^g

Procedure: To a solution of the catalyst in 1 ml DCE, vinylindole was added under N₂. A solution of EDA in 1 or 2 mL of DCE was added with a syringe pump at 0.5 or 0.17 mL/h.

^a: Isolated yield. ^b: besides unreacted vinylindole. ^c: added in a single portion. ^d: besides unreacted vinylindole and unidentified sideproducts. ^e: at 60 °C. ^f: 200 mg 4A MS added. ^g: vinylindole was completely converted in its dimer.

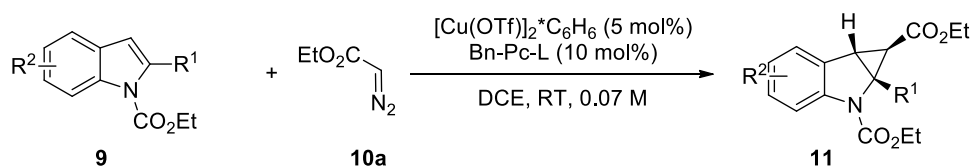
Table 2.1 – Cu(I)PcL catalyzed cyclopropanation of vinylindoles.

The screening of the reaction conditions was performed by modifying the equivalents and the addition time of EDA and the catalytic system.

We firstly tested the reaction using 2-vinylindole **9a**, instead of **9h**, [Cu(OTf)]₂*C₆H₆ (2.5 mol%), ligand **6a** (5 mol%) in anhydrous DCE at room temperature, according to the procedure described in **table 2.1**. Then 1.5 equivalents of EDA were added in 2 h using a syringe pump. The desired product was isolated in 43% yield (entry 1). To compare the activity of the Cu complex to the one of CuOTf, the salt was used alone with a strong decrease of the yield (entry 2). Then, we tried a different PCL **6d** (entry 3), an increase of temperature (entry 7) and a lower concentration of the reaction (entry 8). However, we did not obtain any progresses, while increasing the equivalent of EDA (2.5 equiv) the yield was higher (entry 4). We decided to try a different anion than triflate, for example BARF⁻ known as one of the lesser coordinating counteranion. However, this change (entry 6) did not improve the results. Nevertheless, when the speed of addition of EDA was reduced and molecular sieves were used to maintain anhydrous conditions, we reached a satisfying yield of 68% (entry 9). The use of toluene as reaction solvent was not tolerated by the system and yield decreased (entry 10). Worth to note the fact that the use of a ligand commonly used in combination with copper(I) for the cyclopropanation reaction such as BOX-L did not improve the results (entry 11).

In literature, different types of transition metals are employed for generating a carbene from EDA. In order to verify the ability of different metals to obtain our product of interest, we employed Rh, Au, Pd and another Cu(I) complex, but none of these showed to be active in this transformation.

Using the best reaction condition (**Table 2.2**, entry 9), 2-vinylindoles **9a-o** with different electronic and steric characteristics and diazo-compounds **10a-d** were tested. In particular, the influence of the substituents on 2-vinylindoles was investigated. Moreover, diazo-compounds with diverse degree of hindrance were tested. The entire scope of this transformation was studied by Dr. Valentina Pirovano in the laboratories of DISFARM (Department of Pharmacy of Università degli Studi di Milano) and the results have been just accepted for publication in *Org. Lett.*



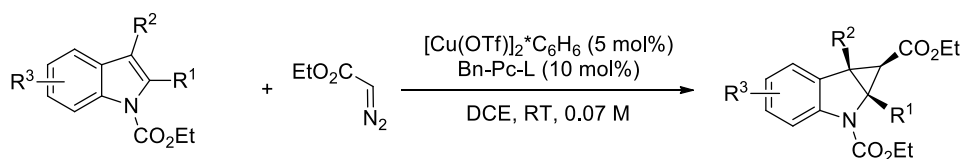
Entry	9	R ¹	R ³	11	Yield
1	9b	<i>n</i> -Pr	H	11b	64%
2	9c		H	11c	54%
3	9d		H	11d	60%
4	9e		H	11e	42%
5	9f		5-Me	11f	59%
6	9g		5-Br	11g	61%
7	9h		H	11h	61%
8	9i		H	11i	55%
9	9l		H	11l	63%

Table 2.2 – Scope of Cu(I)PcL catalyzed cyclopropanation of vinylindoles.

The results demonstrated that the reaction tolerated a wide substituent pattern on vinylindole and the formation of products **11a-o** was successful in all the cases. In particular, three alkyl substituted 2-vinylindoles (**9b-d**), with different steric hindrances, were tested (entries 1-3). Longer alkyl chain than methyl (entry 1) as well as secondary cyclic alkyl groups (entry 2-3) led to products **11b-d** with good yields. Also, **9e**, having an endocyclic vinyl moiety, reacted with EDA forming the product even if with a lower yield (entry 4), probably because of the steric hindrance of the lateral chain. Also the use of 2-vinylindoles with ED moiety **9f** (entry 5) or EW moiety **9g** (entry 6) in 5-position did not show any significant difference.

Moreover, we decided to use also aryl substituted 2-vinylindoles and we verified that the presence of an aromatic ring did not influence the reaction outcome. Apart from 4-Me (entry 7), also ED 4-OMe (entry 8) and EW 3-F (entry 9) aryl substituted ring could be employed with formation of products **11h-l** in good yields.

Considering the good results obtained with vinylindoles **9a-l**, we decided to verify the possibility of forming the product using more challenging substrates **9m-o**.

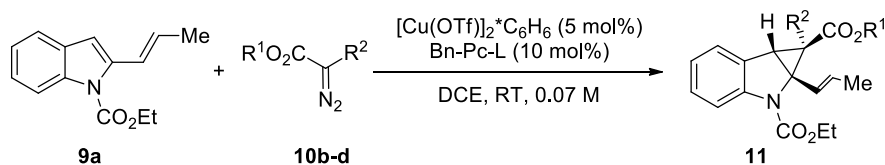


Entry	9	R ¹	R ²	R ³	11	Yield
1	9m		H	H	11m	22% ^a
2	9n		Me	H	11n	n.r.
3	9o		H	H	11o	61%

^abesides 23% of allylic cyclopropanation product

Table 2.3 – Cyclopropanation of challenging substrates.

The use of 2-allylindole **9m** showed a low yield (**Table 2.3**, entry 1) for the desired product because part of the activated diazo-compound reacted on the allylic double bond. In fact, these double bonds presented approximately the same reactivity. 2-vinylindole **9n** did not react with EDA (entry 2) probably because of the reduced reactivity of C-3 due to the methyl group also the use of 2-alkynyl indole **9o** was tolerated affording **11o** in 61% yield (entry 3).



Entry	10	R ¹	R ²	11	Yield
1	10b	<i>t</i> -Bu	H	11p	51%
3	10c	Bn	H	11q	traces
2	10d	Et	Ph	11r	72%

Table 2.4 – Different diazo-compounds tested.

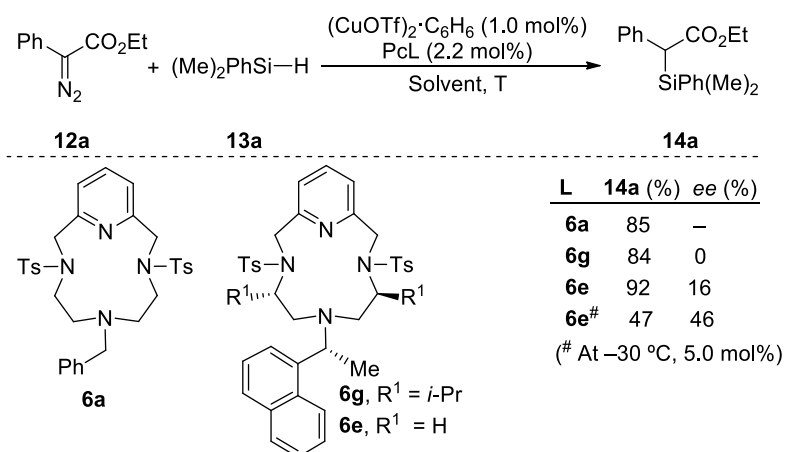
We tried also three others diazo-compounds in addition to EDA. In the first two examples, we used diazo-compounds with a different ester moiety. In entry 1, the reaction was conducted with *t*-butyldiazo acetate and the desired product **11p** was obtained in a yield lower than with EDA. Using the diazo-compound with benzyl ester the product was found only in traces probably because of steric hindrance (**Table 2.4**, entry 2). Besides, we decided to try the α -disubstituted diazo compound. In this case, the yield was higher than in the standard conditions, with a surprising formation of **11r** as single isomer also in this case (entry 3).

Considering the obtained results with the non-chiral P_CL, we decided also to explore the possibility of having an enantioselective version of this reaction and this will be a certain future study of our research group.

2.5.3 Cu(I) catalysis: X-H bond insertion

Encouraged by the results obtained until now in cyclopropanations catalyzed by Cu(I) PCL complexes, we decided to move towards the challenging X-H bond insertion of carbenes. Considering the relevance of silicon-containing compounds, which can be used as versatile synthetic intermediates, we selected the metal-promoted carbene insertion into Si-H bonds to test the activity and selectivity of the Cu(I)-PcL catalytic system.

In our study, ethyl 2-diazo-2-phenylacetate (**12a**) and dimethyl(phenyl)silane (**13a**, 3.0 equiv.) were used as benchmark substrates for the study of the reaction (**Scheme 2.34**).

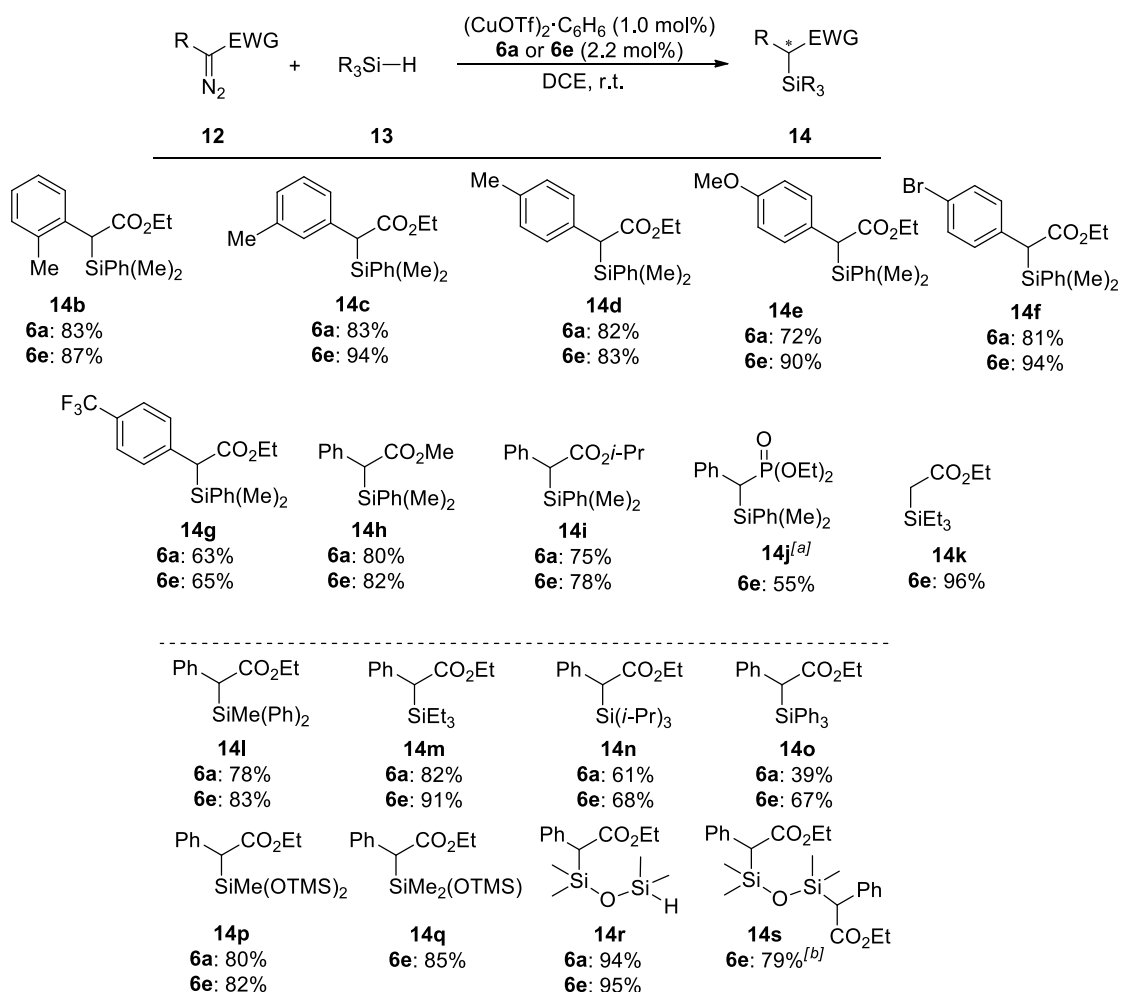


Scheme 2.34 – Cu(I)/PcL-catalyzed Si-H bond carbene insertion.

The catalytic system based on $(\text{CuOTf})_2 \cdot \text{C}_6\text{H}_6$ and ligand **6a** promoted efficiently the Si-H bond insertion under mild reaction conditions (r.t, DCE, 18 h, slow addition of **12a** in 1.5 h), affording compound **14a** in 85% isolated yield and with a remarkably high product selectivity, since only residual amounts of alkenes arising from homo-coupling of the carbene were detected. Heterogeneous system employing $(\text{CuOTf})_2 \cdot \text{C}_6\text{H}_6$ in the absence of the ligand led to the formation of **14a** (75% yield) along with alkenes by-products derived from diazo homocoupling (ca. 25%). It should be noticed that the formation of these by-products influences dramatically the usefulness of the reaction since product isolation and purification by standard techniques becomes difficult to perform. With this result in hands and based on our previous studies, pseudo- C_2 -symmetric ligand **6g** was used to promote a stereoselective Si-H insertion. Even though **6g** showed similar yields, **14a** was unfortunately obtained as a racemate. As explained in previous works regarding cyclopropanation reactions, we believe that the chiral information is provided preferentially by the presence of the stereogenic carbon of the amine pendal. Moreover, an overcrowded and hindered environment around the metal probably influences negatively the selectivity of the carbene

transfer. In fact, unsubstituted enantiopure ligand **6e** provided **14a** as a single reaction product in excellent yield (92%) and with a promising preliminary 16% of *ee*. Moreover, ligand **6e** provides complete product selectivity since dimers arising from diazo compounds **12a** were not detected in the reaction crude. Anyway, despite various modifications on the reaction conditions, the asymmetric version of the reaction could be obtained only with 46% *ee* at low temperatures with a 5.0 mol% catalyst loading.

Despite the modest values of *ee* obtained, we explored the scope of the transformation using ligands **6a** and **6e**. Thus, various diazo compounds were subsequently tested, as shown in **table 2.5**.



^a T = 70 °C. ^b Diazo/silane ratio 5:1. **14s** was obtained as a mixture of diastereoisomers

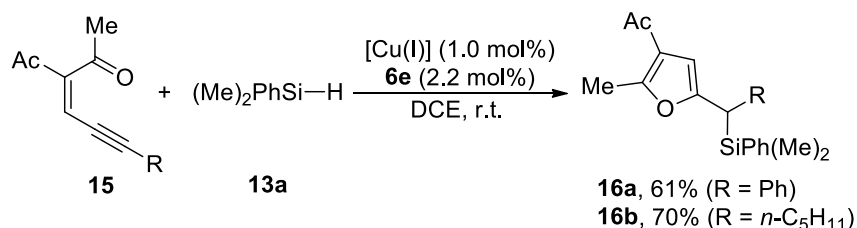
Table 2.5 – Scope of Cu(I)/PCL-catalyzed Si-H bond carbene insertion.

We can see how several 2-aryl diazo compounds could be employed to provide the corresponding functionalized silanes in good to excellent yields. Neither the electronic properties nor the steric hindrance of the arene influenced the yields. Modification on the ester of the diazo could be also

done as demonstrated in the scope. Remarkably, a diazo phosphonate could also be employed, yet higher temperature was required to reach a satisfying yield. Unfortunately, the use of alkyl- or vinylsubstituted diazo compounds seemed not to be compatible with this protocol. Commercially available ethyl diazoacetate was also employed in the reaction with triethylsilane, leading to compound **14k** almost quantitatively (96% yield) and, more important, avoiding the undesired maleate and fumarate homo-coupling products.

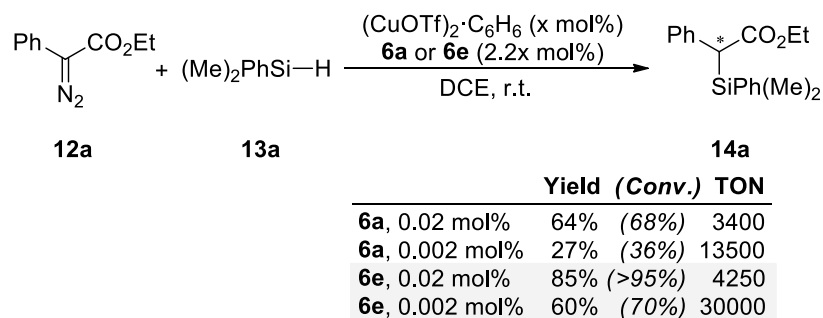
With respect to the silane, commonly employed silanes, such as diphenylmethylsilane or triethylsilane underwent the insertion in generally good yields. It should be noticed that sterically hindered silanes, as triphenylsilane or triisopropylsilane were well tolerated from our system (**14n,e,o**). The preparation in good yields of **14p,e,q**, which can be further modified, demonstrated the broad scope of the transformation. Interestingly, by tuning the stoichiometry of diazocompound and 1,1,3,3-tetramethyldisiloxane (TMDS, **13h**) we have been able to prepare mono and difunctionalized silanes **14r** and **14s** with very good overall yield and complete product selectivity. As already noted before, copper(I) triflate in the absence of the ligand is a competent catalyst for the diazoalkane activation but, especially with more hindered substrates such as triphenylsilane, the carbene dimerization side-products are formed preferentially.

In the recent years, the use of conjugated enynones as precursors of furyl carbene intermediates has been fruitfully exploited in metal-catalyzed carbene transfer.^{67b, 67c} We wondered if the Cu(I)-PcL catalytic system could be used with this type of carbenes for the Si-H insertion reaction. Indeed, when enynones were treated with silane under our standard conditions, the corresponding 2-furylmethylsilanes **16a,b** were obtained in good yields, confirming the activity of the catalyst (**Scheme 2.35**). Noteworthy, despite the absence of stereoselection, the formation of furyl-carbene dimerization products was also minimized by using our catalytic system.



Scheme 2.35 – Cu(I)/PcL-catalyzed Si-H bond carbene insertions using conjugated enynones as the carbene source.

In addition to the scope in Si-H bond insertion reactions, we also tested the robustness of the catalytic system Cu(I)-PcL using **6a** and **6e** by performing the model reaction at lower catalyst loadings (**Scheme 2.36**).



Scheme 2.36 – Robustness of the catalytic system Cu(I)/PcL in Si-H bond carbene insertions at low catalyst loadings.

Interestingly, a 100-fold decrease in the catalyst loading with **6a** under identical reaction conditions (r.t, DCE, 18 h, slow addition of **1a** in 1.5 h), led to the formation of **14a** in a useful 64% yield (68% conversion of **1a** by ^1H NMR, 94% selectivity). It should be pointed out that the same reaction in the absence of added ligand resulted in a lower conversion (35% ^1H NMR yield) and product selectivity (a 3:1 ratio of **14a** with respect to dimers arising from carbene homo-coupling). A slow addition of the diazocompound was still required in order to avoid the formation of dimerization products. A one order of magnitude diminution of the catalyst loading revealed the formation of **14a** in lower yield (27% yield, 36% conv.). Moreover, the use of **6e** at low catalyst loadings was also feasible. Indeed, silane **14a** was obtained in 85% yield by using 0.02 mol% of catalyst loading after 48 h (>95% conv.). A decrease in the loading to 0.002 mol%, resulted in a slower reaction, nevertheless, a remarkable 60% yield of **14a** was obtained after 84 h (70% conv.), meaning a respectable TON number of 30000. Further decrease in the catalyst loading (0.0002 mol%) led to the formation of only carbene dimerization products (20% NMR yield; 24% conv.). It is important to highlight the high product selectivity of both catalytic systems.

Finally, we wondered if the present catalytic system could be able to promote other typical X-H bond insertion reactions (**Table 2.6**).

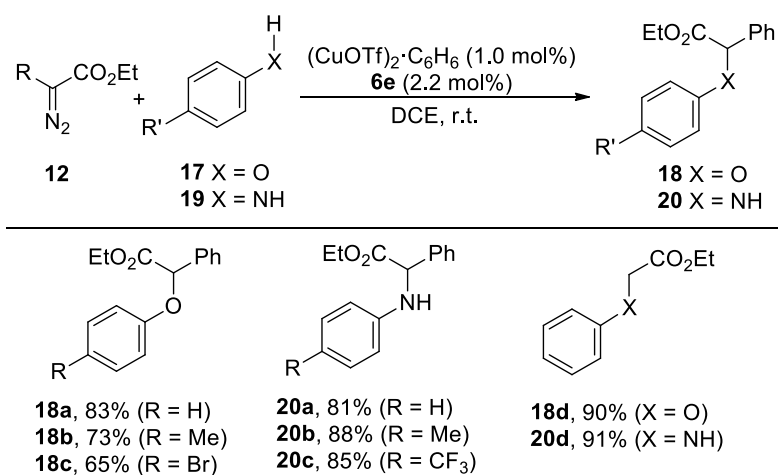


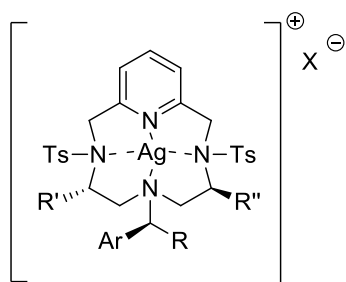
Table 2.6 – X-H insertion catalyzed by Cu(I)/PcL complexes.

For instance, under the standard reaction conditions (with **6e**), the reaction of diazo compound **12a** with phenol afforded the corresponding insertion product **18a** in a good isolated yield of 83% as racemic mixture. The catalytic system was active with both electron rich and electron poor phenols, leading to the corresponding ethers in reasonable yields. Additionally, the analogous transformation using aniline led to the formation of secondary amine **20a** in 81% isolated yield. In this case, also EDG- or EWG-substituted anilines were used.

2.6 Silver complexes

2.6.1 Synthesis

As already reported, our ligands are capable to complex and stabilize copper (I) salts; for this reason we decided to extend our research on the complexation of another metal of the group: silver. We have prepared silver(I) complexes of our macrocycle from different sources, such as silver tetrafluoroborate and silver triflate.



6a-AgBF₄: Ar = Ph, R = R' = R'' = H, X = BF₄

6a-AgOTf: Ar = Ph, R = R' = R'' = H, X = OTf

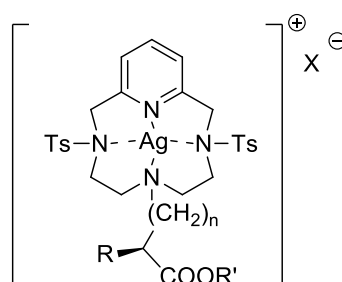
6b-AgBF₄: Ar = Ph, R = Me, R' = R'' = H, X = BF₄

6b-AgOTf: Ar = Ph, R = Me, R' = R'' = H, X = OTf

6d-AgBF₄: Ar = Np, R = R' = R'' = H, X = BF₄

6d-AgOTf: Ar = Np, R = R' = R'' = H, X = OTf

6f-AgBF₄: Ar = Np, R = Me, R' = R'' = H, X = BF₄



6r-AgBF₄: n = 1, R = H, R' = Me, X = BF₄

6r-AgOTf: n = 1, R = H, R' = Me, X = OTf

6s-AgBF₄: n = 4, R = NHCbz, R' = Me, X = BF₄

6s-AgOTf: n = 4, R = NHCbz, R' = Me, X = OTf

7j-AgBF₄: n = 4, R = NH₂, R' = Me, X = BF₄

7k-AgBF₄: n = 1, R = H, R' = Me, X = BF₄

8c-AgOTf: n = 4, R = NEt₂, R' = Me, X = BF₄

8d-AgOTf: n = 4, R' = Me, X = BF₄, R =

8e-AgBF₄: n = 1, R = H, X = BF₄, R' =

Scheme 2.37 – Synthesis of silver(I) PCL complexes.

We added the silver salt to the solution of the ligand in DCE and we stirred the solution for one hour, keeping the mixture in the dark until we isolated the final product. Silver complexes were easily obtained by precipitation, concentrating the solvent and layering *n*-hexane. We filtered and collected the white precipitated in yields up to 91%.

Ag(I) complexes demonstrated to be very stable and could be used under open-air atmosphere without any problem. Anyway, they are more sensitive to the atmospheric moisture and tend to form monoquo species.

As reported in previous works of our research group, for silver(I) complexes the effect of the metal complexation to the ligand could be easily followed in solution by the ^1H and ^{13}C NMR spectra. Moreover, the stability of these Ag(I) PCL complexes resulted comparable with the Cu(I) ones, and when a naphthyl moiety was present on the backbone an η^2 -coordination mode was observed in solution, as well as the displacement of this last one by an incoming external ligand such as acetonitrile or carbon monoxide.

2.6.2 Ag(I) catalysis: Henry reaction

Our research group has recently reported the full characterization of [silver(I)(pyridinecontaining ligand)] complexes and their organometallic reactivity.⁷⁷ Their catalytic activity has been demonstrated in the regioselective domino synthesis of 1-alkoxy-isochromenes under mild conditions⁷⁸ and in the microwave enhanced A^3 -coupling multicomponent reaction.⁷⁹ Compared with simple silver salts, the great advantages of Ag(I) PCL complexes are their solubility, their enhanced stability and the easiness of handling.

Encouraged by the interesting results above mentioned, we wanted to check if our Ag(I)-PCL complexes were suitable catalysts also for the Henry reaction. As a result of this study, we were pleased to find that our complexes can actually activate the aldehyde toward the nitronate nucleophilic attack, in the first example of a silver mediated Henry reaction.⁸⁰

At first, we decided to test the ability of silver to promote the Henry reaction by using simple silver(I) salts such as Ag(OTf) or Ag(BF₄) and the PCL silver(I) complex (already used in the A^3 -coupling study). We compared then their reactivity with those of the corresponding PCL copper(I) complex (**Figure 2.5**).

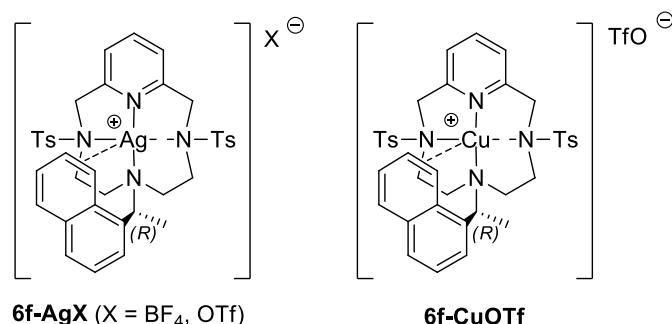
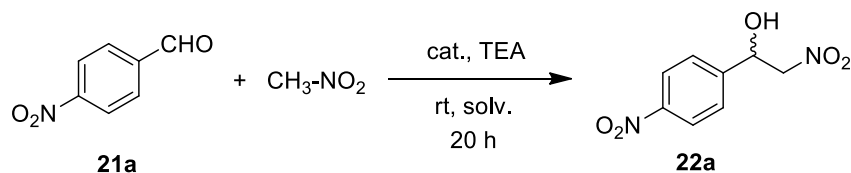


Figure 2.7 – Silver(I) and copper(I) PCL complexes used.

As model reaction, we chose the condensation between 4-nitrobenzaldehyde and nitromethane (**Table 2.7**). To promote the generation of the nitronate anion, a catalytic amount of triethylamine (TEA) – equal to the catalyst loading – was added to the reaction mixture.



Entry	Cat.	X	Solv.	Base	Yield (%) ^b
1	Ag(OTf)		CH ₂ Cl ₂	TEA	21
2 ^c	Ag(BF ₄)		CH ₂ Cl ₂	Cs ₂ CO ₃	25
3 ^d	-		CH ₂ Cl ₂	TEA	35
4	6f-Ag	OTf	CH ₂ Cl ₂	TEA	84
5	6f-Ag	BF₄	CH ₂ Cl ₂	TEA	75
6 ^e	6f-Ag	BF₄	CH ₂ Cl ₂	TEA	85
7	6f-Ag	OTf	CH ₃ NO ₂	TEA	84
8	6f-Ag	OTf	Tol	TEA	60
9	6f-Cu	OTf	CH ₂ Cl ₂	TEA	85

^a Reactions were performed with [Ag(I)] (3.2 × 10⁻² mmol) in the solvent (5 mL) at a cat./base/aldehyde/nitromethane ratio of 1:1:10:50 at rt for 20 h; lower catalyst loadings (1 mol%), resulted in very slow reactions. ^b Isolated yields based on initial 4-nitrobenzaldehyde; unreacted aldehyde accounted for the rest of the reaction mass balance. ^c T = 30 °C, t = 6 h. ^d Reaction conditions in the absence of metal catalyst: TEA/aldehyde/nitromethane ratio of 1:10:500 at rt for 20 h. Unreacted 4-nitrobenzaldehyde did not account for the rest of the reaction mass balance and some unidentified by-products derived from competitive side reactions were observed. ^e In the presence of molecular sieves (4 Å).

Table 2.7 – Preliminary study of the silver(I) PCL catalyzed Henry reaction.

Simple silver(I) salts gave results comparable with those observed just in the presence of the base, the only difference being that in the last case several byproducts were observed. On the other hand, complex **6f-AgOTf**, which is fully soluble in chlorinated solvents, gave results comparable to those obtained with the related copper complex **6f-CuOTf** (**Table 2.7**, entries 4 and 9). Under these conditions, the reaction gave identical results either employing the preformed complex **6f-AgOTf** or the in situ formed 1:1 ligand/Ag(I) complex. We also investigated the role of the counteranion, by changing from OTf to BF₄, obtaining a slightly lower yield with the latter (**Table 2.7**, entry 5). However, when the same reaction was repeated in the presence of molecular sieves, a comparable conversion was again obtained (**Table 2.7**, entry 6). The use of a large excess of nitromethane (**Table**

2.7, entry 7) did not affect the reaction yield. We previously observed that the copper PCL complexes failed to catalyse the Henry reaction when it was performed in aromatic hydrocarbons and that PCL ligands alone, in the absence of any metal, are not active catalysts.

On the contrary, our complex **6f-AgOTf** demonstrated to be active also in toluene, giving the desired nitroalcohol **22a** in 60% yield (**Table 2.7**, entry 8). Finally, despite the presence of a defined stereocentre on the ligand, under all conditions tested we always obtained the nitroalcohol **22a** as a racemic mixture.

Having in hand a quite active catalytic system, we decided to further optimize the ligand characteristics and then to explore the scope and the limitations of the Henry reaction. In order to extend our method to the synthesis of PCL's bearing a noninnocent pendant arm we thought that natural amino acids (i.e., β -alanine and lysine) could be perfect nucleophilic partners for the ring opening reaction of the aziridine.

The main advantage of this synthetic approach is that a modification of a key moiety of the macrocycle can be done easily by exploiting both chiral and functional properties of the natural amino acids. The new Ag(I) complexes shown in **Figure 2.6** were tested as catalysts in the model nitroaldol reaction between 4-nitrobenzaldehyde and nitromethane.

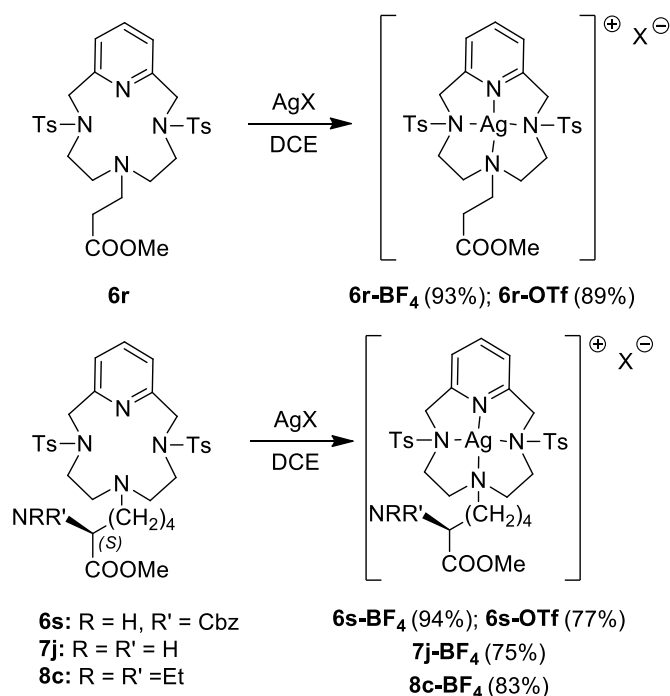


Figure 2.8 – Silver(I) PCL complexes derived from aminoacids.

With the exception of complex **7j-AgBF₄**, which is the only one not soluble in dichloromethane, all other silver complexes gave the nitroalcohol **22a** from moderate to very good yields in the model reaction. Together with the desired nitroalcohol **22a**, the starting aldehyde **21a** was the only product recovered from the reaction crude, meaning that the reported yields are coincident with conversions and that a selectivity >99% was observed. Silver complex **6r-AgOTf/BF₄** (Table 2.8, entries 1–8), characterised by the presence of a slightly coordinating lysine-derived pendant arm, gave results comparable to those observed by using complex **6f-AgOTf**.

Entry	Cat.	X	Base	Solv.	t (h)	T (°C)	Yield 22a (%) ^b
1	6r-Ag	OTf	TEA	CH ₂ Cl ₂	20	rt	60
2	6r-Ag	OTf	TEA	Tol	40	rt	15
3	6r-Ag	OTf	DiPEA	CH ₂ Cl ₂	20	rt	53
4	6r-Ag	OTf	DMAP	CH ₂ Cl ₂	20	rt	53
5	6r-Ag	OTf	Morfoline	CH ₂ Cl ₂	20	rt	50
6	6r-Ag	OTf	K ₂ CO ₃	CH ₂ Cl ₂	20	rt	45
7	6r-Ag	OTf	Cs ₂ CO ₃	CH ₂ Cl ₂	20	rt	70
8	6r-Ag	BF₄	Cs ₂ CO ₃	CH ₂ Cl ₂	20	rt	70
9	6s-Ag	OTf	TEA	CH ₂ Cl ₂	20	rt	67
10	6s-Ag	BF₄	TEA	CH ₂ Cl ₂	20	rt	65
11	6s-Ag	BF₄	DiPEA	CH ₂ Cl ₂	20	rt	75
12	6s-Ag	BF₄	Cs ₂ CO ₃	CH ₂ Cl ₂	20	rt	90
13	6s-Ag	BF₄	Cs ₂ CO ₃	CH ₂ Cl ₂	20	30	95
14	6s-Ag	BF₄	Cs ₂ CO ₃	CH ₂ Cl ₂	12	30	92
15	6s-Ag	BF₄	Cs ₂ CO ₃	CH ₂ Cl ₂	6	30	75
16	6s-Ag	BF₄	Cs ₂ CO ₃	CH ₂ Cl ₂	3	30	45
17	6s-Ag	OTf	-	CH ₂ Cl ₂	20	rt	25
18	-	-	Cs ₂ CO ₃	CH ₂ Cl ₂	20	30	55
19 ^c	7j-Ag	BF₄	-	CH ₂ Cl ₂	20	rt	-
20 ^c	7j-Ag	BF₄	-	MeNO ₂	20	rt	-
21	7j-Ag	BF₄	-	MeOH	20	rt	- ^d
22	8c-Ag	BF₄	Cs ₂ CO ₃	CH ₂ Cl ₂	12	30	90
23	8c-Ag	BF₄	-	CH ₂ Cl ₂	12	30	64

^a Reactions were performed with [Ag(I)] (3.2 x 10⁻² mmol) in the solvent (5 mL) at a cat./base/aldehyde/nitromethane ratio of 1:1:10:50 in the presence of molecular sieves (4 Å). ^b Yields based on initial 4-nitrobenzaldehyde calculated via ¹H NMR using 2,4-dinitrotoluene (DNT) as internal standard; unreacted aldehyde accounted for the rest of the reaction mass balance. ^c The metal complex **8c** is not soluble in the reaction medium: no reaction after 20 h as judged by TLC analysis. ^d Dimethyl acetal derived from the nucleophilic attack of MeO⁻ on the 4-nitrobenzaldehyde was recovered in 25% yield (see SI).

Table 2.8 – Screening of the catalysts and of the reaction conditions.

Several bases were tested (**Table 2.8**, entries 3–7), and best results were obtained with cesium carbonate (**Table 2.8**, entry 7). The counter anion do not seem to influence the reaction yields (**Table 2.8**, entry 8).

Complex **6s-AgOTf/BF₄**, characterised by the presence of a Cbz protecting group on the pendant arm, displayed a similar behaviour regarding counter anion (**Table 2.8**, entries 9 and 10) and base (**Table 2.8**, entries 10–12), but the yields were higher. Raising the temperature to 30 °C resulted in increasing the yield to 95% (**Table 2.8**, entry 13). In the absence of a base, poor results were obtained (**Table 2.8**, entry 17). It should be pointed out that Cs₂CO₃ alone is able to promote the Henry reaction, but under the same reaction conditions only a 55% of nitroalcohol **22a** was formed (**Table 2.8**, entry 18).

In order to avoid the addition of the base as co-catalyst, we tested complexes **7j-AgBF₄** and **8c-AgBF₄**, both containing a basic amine functionality on the pendant arm. As above pointed out, complex **7j-AgBF₄** is insoluble in dichloromethane, as well as in nitromethane and failed to give any reaction in such heterogeneous system (**Table 2.8**, entries 19 and 20). When methanol was used as solvent, we observed the formation of the dimethyl acetal derived from the nucleophilic attack of MeO⁻ on the 4-nitrobenzaldehyde in 25% yield (**Table 2.8**, entry 21).

Under standard conditions, complex **8c-AgBF₄**, which is fully soluble in dichloromethane, gave the Henry product **22a** in excellent yields (**Table 2.8**, entry 22). Moreover, we were pleased to observe that the presence of a tertiary amino group on the active-pendant made this complex able to promote the formation of **22a** in 64% yields without any basic co-catalyst in just 12 h at 30 °C (**Table 2.8**, entry 23).

We next explored scope and limitation of the approach (**Table 2.9**), employing complex **6s-AgBF₄** under the best reaction conditions (**Table 2.8**, entries 13 and 14). In particular, our interest was to verify the activity of our catalytic system in the promotion of the reaction of aldehydes of different nature (aryl, heteroaryl and cycloalkyl) also in the presence of EW or ED groups on the aromatic ring. We decide to perform all reactions in CH₂Cl₂ at 30 °C and stop them after 12 h with the aim to compare the results obtained by changing the electronic properties of the aldehyde at fixed reaction time and temperature.

It is well known that the Henry reaction is an equilibrium reaction and temperature plays an important role. The 12 h reaction time was decided based on a simple kinetic study performed on the model reaction (**Table 2.9**, entries 13–16), which displayed that a plateau in terms of % of conversion of the starting aldehyde is reached after 12 h (**Fig. 2.7**).

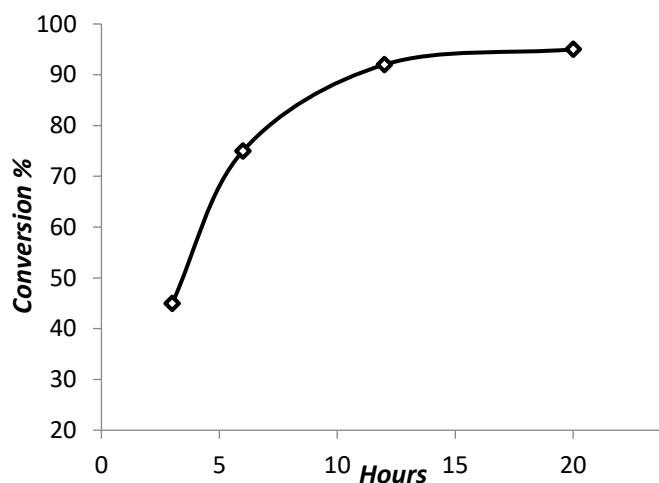
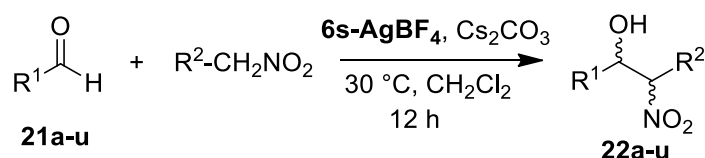


Figure 2.9 – Kinetic study of conversion vs time.

Good results in terms of yields were obtained when one or more EWGs were present on the aryl ring (**Table 2.9**, entries 1–6 and 12–16). Although not linearly correlated with σ -*para* Hammett constants, yields between 83% and 93% were obtained with aromatic aldehydes having high positive values of *para* substituent constant (**Table 2.9**, entries 1–5). Slightly lower yields have been observed for *para*- and *per*-fluorobenzaldehydes (**Table 2.9**, entries 6 and 12), and neutral benzaldehyde (**Table 2.9**, entry 7). On the other hand, electron-rich aromatic aldehydes failed to give the Henry products (**Table 2.9**, entries 8–11). These latter results can be easily rationalised based on the less pronounced electrophilic character of the aldehyde. The presence of EW groups is well tolerated also in *meta* and *ortho* positions (**Table 2.9**, entries 13–16), suggesting that steric hindrance does not limit the transformation.



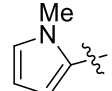
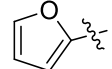
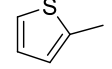
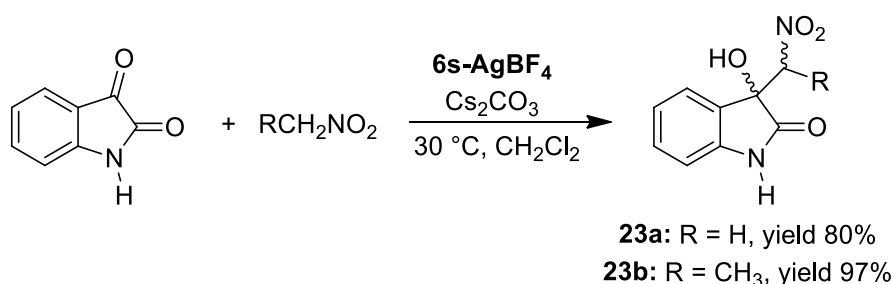
Entry	R ¹	R ²	Product	<i>syn/anti</i> ^b	Yield ^c (%)						
1	4-NO ₂ C ₆ H ₄	H	22a	-	92 (90)	17	2- MeOC ₆ H ₄	H	22n	-	10
2	4-CNC ₆ H ₄	H	22b	-	83 (80)	18	3- MeOC ₆ H ₄	H	-	-	n.d.
3	4-CF ₃ C ₆ H ₄	H	22c	-	93 (92)	19	Cy	H	-	-	n.d.
4	4-BrC ₆ H ₄	H	22d	-	85 (82)	20	Ph-CH=CH-	H	-	-	n.d.
5	4-ClC ₆ H ₄	H	22e	-	83 (80)	21		H	-	-	n.d.
6	4-FC ₆ H ₄	H	22f	-	70 (64)	22		H	22o	-	65 (62)
7	C ₆ H ₅	H	22g	-	60 (55)	23		H	22p	-	10
8 ^d	4-MeC ₆ H ₄	H	22h	-	15	24	4-NO ₂ C ₆ H ₄	CH ₃	22q	60:40	95 (90)
9	4-Bu ^t C ₆ H ₄	H	-	-	n.d.	25 ^e	4-NO ₂ C ₆ H ₄	CH ₃	22q	60:40	90
10	4-MeOC ₆ H ₄	H	-	-	n.d.	26	2-NO ₂ C ₆ H ₄	CH ₃	22r	45:55	96 (93)
11	4-Et ₂ NC ₆ H ₄	H	-	-	n.d.	27	4-CF ₃ C ₆ H ₄	CH ₃	22s	51:49	93 (89)
12	C ₆ F ₅	H	22i	-	72 (68)	28	4-ClC ₆ H ₄	CH ₃	22t	61:39	80 (75)
13	3,5-(CF ₃) ₂ C ₆ H ₄	H	22j	-	70 (66)	29	C ₆ H ₅	CH ₃	22u	55:45	75 (60)
14	2-NO ₂ C ₆ H ₄	H	22k	-	97 (95)	^a Reactions were performed with [Ag(I)] (3.2 x 10 ⁻² mmol) in CH ₂ Cl ₂ (5 mL) at a cat./Cs ₂ CO ₃ /aldehyde/nitromethane ratio of 1:1:10:50 in the presence of molecular sieves (4 Å) at 30 °C for 12 h. ^b <i>Syn/anti</i> ratio determined by ¹ H NMR. ^c Yields based on initial aldehyde calculated via ¹ H NMR using 2,4-dinitrotoluene (DNT) as internal standard (isolated yields); unreacted aldehyde accounted for the rest of the reaction mass balance. ^d Reaction performed with complex 6r-AgBF₄ as catalyst. ^e Reaction performed with complex 8c-AgBF₄ as catalyst and in the absence of Cs ₂ CO ₃ .					
15	2-BrC ₆ H ₄	H	22l	-	72 (65)						
16	2,6-Cl ₂ C ₆ H ₄	H	22m	-	70 (68)						

Table 2.9 – Scope of the Ag(I) PCl catalyzed Henry reaction.

As for electron-rich benzaldehydes, no reaction was observed with aliphatic aldehydes (**Table 2.9**, entry 19) and with cinnamaldehyde (**Table 2.9**, entry 20). Among furan, thiophene and pyrrole carbaldehydes, a good reactivity was observed only in the case of furfural (**Table 2.9**, entry 22). Next,

we briefly explored the reactivity of some aromatic aldehydes with nitroethane. In all cases, almost identical results were obtained switching from nitromethane to nitroethane, and all the reactions with electron poor aromatic aldehydes gave the corresponding Henry product in very good yields, but with very modest *syn/anti* ratio (**Table 2.9**, entries 24–29). Again, we were pleased to verify that complex **8c-AgBF₄** was able to catalyse the reaction between 4-nitrobenzaldehyde and nitroethane without the need of any additional base, yielding **22q** in a very satisfying 90% yield (**Table 2.9**, entry 25).

Taking into account that the indole nucleus is present in a large number of compounds of biological and/or pharmaceutical interest, we tested our approach also on isatin (**Scheme 2.38**).

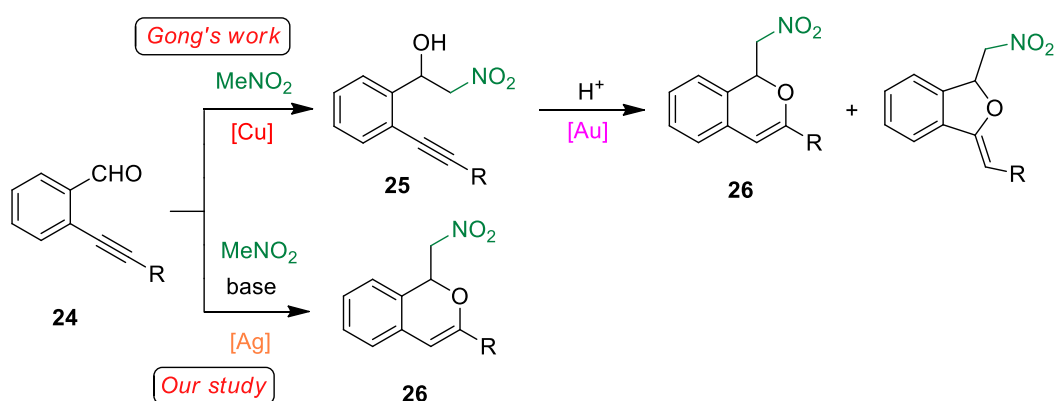


Scheme 2.38 – **6s-AgBF₄** catalyzed reaction of nitromethane and nitroethane with isatin.

The reaction with nitromethane gave the desired 3-hydroxy- 3-(nitromethyl)-1,3-dihydro-2H-indol-2-one **23a** in 80% isolated yield whereas the reaction with nitroethane gave a 6:4 diastereoisomeric mixture of **23b** with an overall yield of 97% (yield based on initial isatine calculated via ¹H NMR using 2,4-dinitrotoluene as internal standard). It should be emphasized that this transformation on isatin opens up new routes for the synthesis of a plethora of interesting oxindole alkaloids related molecules.

2.6.3 Ag(I) catalysis: isochromene cycloisomerization vs Henry reaction

As mentioned above, our research group has recently reported that [silver(I)(Pc-L)] complexes are competent catalysts for the regioselective synthesis of 3-substituted-1-alkoxyisochromenes starting from 2-alkynylbenzaldehydes in the presence of alcohols as nucleophiles.⁷⁸ Having seen their ability in promoting the Henry reaction, we were thus intrigued to see if it was possible to combine in a single domino sequence the Henry reaction of 2-alkynylbenzaldehydes and the cycloisomerisation step to yield isochromenes **26**. A two-step process that take advantage of a Cu(II) catalysed Henry reaction followed by an Au(I) mediated cycloisomerisation has recently been reported by Y. Gong and co-workers (**Scheme 2.39**).⁸²



Scheme 2.39 – Alternative domino silver(I) catalysed synthesis of 1-isochromenes.

The reaction between 2-[(4-methoxyphenyl)-ethynyl]benzaldehyde **24a** and nitromethane was selected as model reaction for the optimization of reaction conditions. Firstly, we compared the activity copper(I) catalyst **6f-CuOTf** and silver(I) catalyst **6f-AgOTf** (10 mol%) in dichloromethane in the presence of 5 equiv. of nitromethane and 10 mol% of TEA (**Table 2.10**, entries 1 and 2). This preliminary test interestingly revealed that while the copper complex **6f-CuOTf** gave selectively the Henry reaction product **25a** in 56% yield, the silver complex **6f-AgOTf** was able to promote the domino sequence, although with low selectivity, yielding the desired 1-isochromene **26a** and the nitroalcohol **25a** in equal amount, beside a 12% of unreacted aldehyde **24a** and a complex mixture of unidentified by-products. An increase of the reaction temperature resulted in lower yields and selectivity, with an increase of by-products formation (**Table 2.10**, entries 3 and 4). The addition of an excess of TEA resulted in the selective formation of the Henry product in 45% yield, but was detrimental for the formation of the desired product **26a** (**Table 2.10**, entry 5). As already stated above, while the Henry product can be formed also in the absence of the silver catalyst (although in

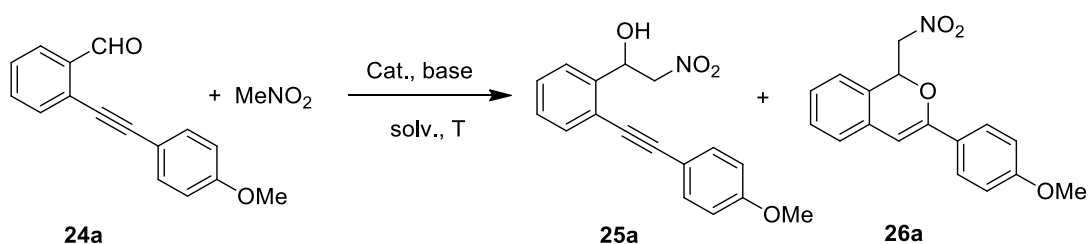
poor yields), the presence of the metal is essential for the formation of the isochromene **26**. In fact, in the presence of 1 equiv. of TEA and without the metal catalyst, the nitroalcohol **25a** was selectively obtained in 77% yield (**Table 2.10**, entry 6).

The screening of solvent effect (**Table 2.10**, entries 7-9) revealed that polar aprotic solvents favor the formation of the nitroalcohol **25a**. The reduction of the equivalent of nitromethane was detrimental to the reaction outcome (**Table 2.10**, entry 10), whereas, when CH₃NO₂ was employed as a reagent/solvent, the formation of **25a** (39%) was accompanied by the formation of a discrete amount of isochromene **26a** (29%, **Table 2.10**, entry 11). This last result suggests that an excess of nitroalkane is able to promote both isochromene and nitroalcohol formation. Interestingly, when simple AgOTf salt was used no trace of Henry product **25a** was observed, and only a little amount of **26a** was obtained (**Table 2.10**, entry 12).

Thus, a 50 fold excess of the nitromethane (with respect to aldehyde **24a**) was used and this seems to favor the formation of the isochromene product, especially when freshly distilled nitromethane was used (**Table 2.10**, entries 13 and 14).

Among the counter anion tested, BF₄⁻ and OTf⁻ displayed very close results, while NTf₂⁻ led to slightly lower overall yields (**Table 2.10**, entries 14-16). It is interesting to note that the presence of 4 Å molecular sieves as water scavenger seems to speed up the formation of the Henry product at the expense of the isochromene (**Table 2.10**, entry 17). Complete selectivity in favour of the Henry product **25a** was observed when the reaction was performed in acetonitrile (**Table 2.10**, entry 18). We tried to improve the formation of the isochromene **26a** by using bases with different pK_b, ranging from organic to inorganic ones (**Table 2.10** entries 19-24), but the more acceptable results remained those obtained with TEA or with the more sterically demanding diisopropylethyl amine (DiPEA) (**Table 2.10**, entry 19).

Finally, the use of the catalytic systems previously selected for the Henry approach, confirm their tendency to promote preferentially the formation of the corresponding nitroalcohol (**Table 2.10**, entries 25 and 26), also in the absence of the additional base (**Table 2.10**, entry 26).



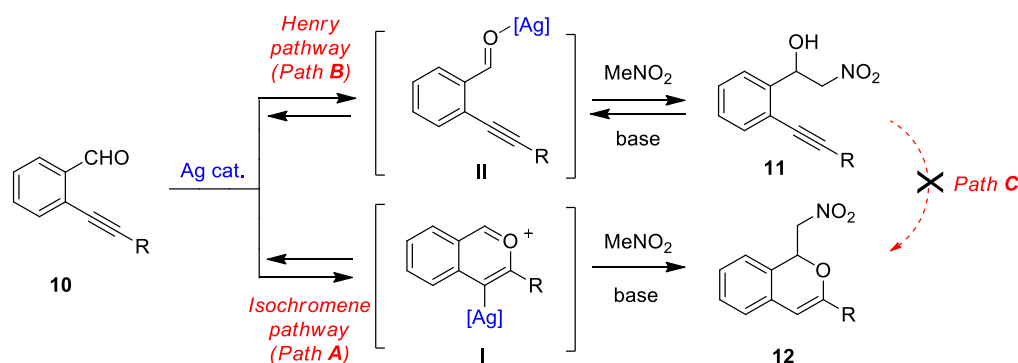
Entry	Catalyst	Base (equiv.)	MeNO ₂ (equiv.)	Solvent	t (h)	T (°C)	Yield 25a ^b (%)	Yield 26a ^b (%)	Rec. 24a (%)
1	6f-CuOTf	TEA (1)	50	CH ₂ Cl ₂	20	rt	(56)	-	(35)
2	6f-AgOTf	TEA (1)	50	CH ₂ Cl ₂	20	rt	(17)	(17)	(12)
3	6f-AgOTf	TEA (1)	50	CH ₂ Cl ₂	30	40	12	6	7
4	6f-AgOTf	TEA (1)	50	CH ₂ Cl ₂	30	60	11	4	4
5	6f-AgOTf	TEA (5)	50	CH ₂ Cl ₂	22	rt	45 (39)	-	11 (10)
6 ^c	6f-AgOTf	TEA ^c	^c	CH ₂ Cl ₂	22	rt	77	-	10
7	6f-AgOTf	TEA (1)	50	Tol	20	30	30	8	11
8	6f-AgOTf	TEA (1)	50	DMF	24	30	53	-	6
9	6f-AgOTf	TEA (1)	50	THF	22	rt	46	2	21
10	6f-AgOTf	TEA (1)	11	CH ₂ Cl ₂	22	rt	3	-	5
11	6f-AgOTf	TEA (1)	-	CH ₃ NO ₂	20	rt	39	29	-
12	AgOTf	TEA (1)	-	CH ₃ NO ₂	20	rt	-	15	15
13 ^d	6f-AgOTf	TEA (1)	500	CH ₂ Cl ₂	22	rt	18	24	-
14 ^d	6f-AgOTf	TEA (1)	500	CH ₂ Cl ₂	22	rt	25	33	-
15 ^d	6f-AgNTf₂	TEA (1)	500	CH ₂ Cl ₂	22	rt	16	29	5
16 ^d	6f-AgBF₄	TEA (1)	500	CH ₂ Cl ₂	22	rt	21 (18)	33 (30)	10 (9)
17 ^{d,e}	6f-AgBF₄	TEA (1)	500	CH ₂ Cl ₂	22	rt	60 (57)	19 (17)	-
18 ^{d,e}	6f-AgBF₄	TEA (1)	500	CH ₃ CN	22	rt	96	-	-
19 ^d	6f-AgBF₄	DIPEA (1)	500	CH ₂ Cl ₂	22	rt	36	27	-
20 ^d	6f-AgBF₄	DMAP (1)	500	CH ₂ Cl ₂	22	rt	50	-	4
21 ^d	6f-AgOTf	DBU (1)	500	CH ₂ Cl ₂	22	rt	11	4	16
22 ^d	6f-AgBF₄	NaHCO ₃ (1)	500	CH ₂ Cl ₂	22	rt	5	1	65
23 ^d	6f-AgOTf	Cs ₂ CO ₃ (1)	500	CH ₂ Cl ₂	22	rt	72	-	2
24 ^d	6f-AgNTf₂	K ₂ CO ₃ (1)	500	CH ₂ Cl ₂	22	rt	78	-	2
25 ^e	6s-AgBF₄	TEA (1)	500	CH ₂ Cl ₂	22	rt	57	15	8
26 ^e	8c-AgBF₄	-	500	CH ₂ Cl ₂	22	rt	60	15	13

^a Reactions were performed with [Ag(I)] (2.5 × 10⁻² mmol) in the solvent (1.25 mL) at a catalyst/aldehyde ratio of 1:10.

^b Yields based on initial **24a** calculated via ¹H NMR using 2,4-dinitrotoluene (DNT) as internal standard; isolated yields in brackets. Under these conditions, unreacted starting aldehyde did not always account for the rest of the reaction mass balance. In some cases, unidentified by-products derived from competitive side reactions were detected. ^c TEA (2.5 × 10⁻² mmol)/aldehyde/nitromethane ratio of 1:1:5. ^d Reaction performed with freshly distilled nitromethane. ^e In the presence of molecular sieves (4 Å).

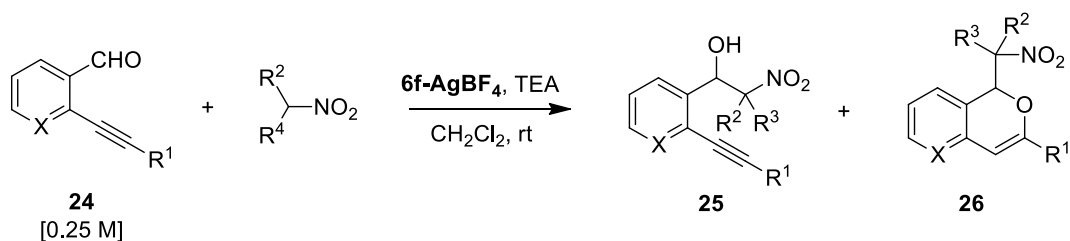
Table 2.10 – Study on the silver catalysed Henry reaction *versus* cycloisomerisation reaction.^a

With the aim to explain the behaviour observed, we made an additional experiment. Isolated **25a** was reacted in toluene at rt in the presence of 10 mol% of the silver(I) complex **6f-AgOTf**. After 24 h no reaction occurred and the TLC analysis showed the presence of unreacted **25a**. Upon addition of 10 mol% of TEA the mixture was reacted for additional 24 h at rt, then the crude was analysed by ^1H NMR which reveals the presence of unreacted **25a** (44%) along with traces of 2-[(4-methoxyphenyl)ethynyl]benzaldehyde **24a** ($\approx 5\%$), isochromene **25a** ($\approx 5\%$) and some unidentified by-products. This result suggests that the formation of the nitroalcohol **25a** (Path **B** in **scheme 2.39**) and the cascade synthesis of isochromene **26a** (Path **A** in **scheme 2.39**) are probably alternative and competitive pathways. According to reported metal catalysed domino synthesis of isochromenes in the presence of nucleophiles,^{78, 102 78, 102 78, 102} **26a** is most likely formed by nucleophilic attack of the nitronate anion on a preformed isochromenilium ion intermediate **I** (Path **A** in **scheme 2.39**), while a subsequent silver catalysed cycloisomerisation of the nitroalcohol **25a** (Path **C**) seems to be most unlikely. Endorsing this hypothesis, under our reaction conditions we never isolated or detected in the reactions crude the alternative isobenzofuran isomers obtained by Gong and co-workers (see **scheme 2.40**).



Scheme 2.40 – Alternative/competitive pathways in the reaction of 2-alkynylarylaldehydes and nitroalkanes.

Up to now, any attempt to obtain in an exclusive fashion the desired isochromene **26a** meet with failure, thus we decided to briefly investigate the substrate effect under the best reaction condition achieved for the synthesis of isochromenes (**Table 2.10**, entry 16). The results are reported in **Table 2.11**.



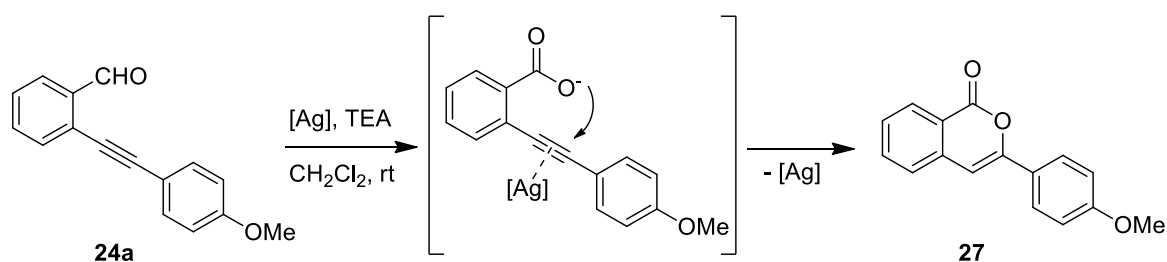
Entry	SM	R ¹	X	R ²	R ³	t (h)	Yield 25 ^b (%)	Yield 26 ^b (%)	Rec. SM (%)
1				H	H	22	25a 18	26a 30	9
2	24a	<i>p</i> -MeO-Ph	CH	Me	H	22	25b + 25b' 70 ^c	26b + 26b' 7 ^d	21
3				Me	Me	22	-	-	42 ^e
4	24b	<i>p</i> -Me-Ph	CH	H	H	22	25c 32	26c 31	5
5 ^f				H	H	22	25c 60	26c 5	9
6	24c	<i>p</i> -CF ₃ -Ph	CH	H	H	22	25d 45	26d traces	14
7	24d	Me ₃ Si	CH	H	H	22	25e 48	-	45
8 ^f				H	H	22	25e 83	-	15
9	24	<i>n</i> -Pr	CH	H	H	22	25f 15	26f 54	-
10	24f	<i>n</i> -Pr	N	H	H	1	25g 52	-	-
11	24g	<i>p</i> -MeO-Ph	N	H	H	22	25h 68	-	15
12 ^f				H	H	22	25h 78	-	-

^a Reactions were performed with [Ag(I)] (2.5 × 10⁻² mmol) in CH₂Cl₂ (1.25 mL) at a catalyst/TEA/aldehyde/nitromethane ratio of 1:1:10:500. ^b Isolated yields based on initial alkynylbenzaldehyde **10**. Under these conditions, unreacted starting aldehyde did not always account for the rest of the reaction mass balance. In some cases, unidentified by-products derived from competitive side reactions were detected. ^c Mixture of two diastereoisomers in 70:30 ratio. ^d Mixture of two diastereoisomers in 75:25 ratio calculated on the ¹H NMR. ^e In this case, the isocoumarin (29%) was recovered as major by-product. ^f In the presence of molecular sieves (4 Å).

Table 2.11 – Substrate effect in the divergent silver catalysed Henry *versus* cycloisomerisation reaction.^a

All tested *o*-alkynylarylaldehydes **24** were readily obtained in moderate to excellent yields by PdCl₂(PPh₃)₂ catalysed Sonogashira coupling reactions starting from commercially available 2-bromo(hetero)arylaldehydes and terminal acetylenes (see experimental section for details).

Compared to the model reaction (**Table 2.11**, entry 1) when nitroethane was used under standard conditions we observed the formation of only a small amount of distereoisomeric isochromenes **26b** and **26'b** (not separated), while the Henry products **25b** and **25'b** were recovered in 70:30 diastereoisomeric ratio in 70% overall yield (Table 5, entry 2). On the other hand, the reaction with bulkier 2-nitropropane gave the 3-(4-methoxyphenyl)isocumarine (**27**) (29%) as main reaction by-product, beside a huge amount of unreacted starting material (42%) (**Table 2.11**, entry 3). The formation of isocumarine **27** probably derived from the oxidation of the aldehyde **24a** to a carboxylic acid, which was transformed by the alkaline reaction condition in a carboxylate nucleophile able to make an intramolecular attack to the silver(I) activated triple bond¹⁰³¹⁰³¹⁰³ (**Scheme 2.41**).



Scheme 2.41 – Plausible path for the formation of isocumarine **27**.

The presence of a neutral aryl substituent on the alkynylbenzaldehyde **24b** gave an almost equal amount of nitroalcohol **25c**, and isochromene **26c**, (**Table 2.11**, entry 4). As already observed (**Table 2.10** entries 16 and 17), the presence of traces of water seems to be important to promote the formation of the isochromene products **26**. When the reaction of **24b** was performed under strictly anhydrous conditions in the presence of 4 Å molecular sieves, the yield of **26c** fall down while the yield of **25c** doubled (**Table 2.11**, compare entries 4 and 5). The presence of EWG on the aryl moiety was not suitable for the formation of the isochromene **26d**, and the corresponding nitroalcohol **25d** was the main product obtained (**Table 2.11**, entry 6). In addition, trimethylsilyl substituted alkynylbenzaldehyde **24d**, gave exclusively the nitroaldol product **25e** (**Table 2.11**, entry 7), and when the reaction was conducted in the presence of a water scavenger, the yield of **25e** skyrocket to 83 % (**Table 2.11**, entry 8). Alkyl substitution on the triple bond was the only substitution that lead a good selectivity in favour of the cyclic product (**Table 2.11**, entry 9). More basic and coordinating nicotinaldehyde derivatives **24g,h** yielded exclusively to the Henry products **25h** and **25i** (**Table 2.11**, entries 10 and 11). In the latter cases, the selectivity in favour of the Henry product could be explained by a speeding up of the nucleophilic attack of the nitronate anion to the aldehyde, promoted by the presence of an additional basic nitrogen on the pyridine moiety and by the EW

activating effect of the electron-poor pyridine on the proximate aldehyde group. Also in this case, the presence of molecular sieves resulted in higher yields of nitroalcohol **25i** (Table 2.11, entry 12).

2.7 Iron complexes

2.7.1 Synthesis

As already illustrated in the introduction, macrocyclic pyridine-containing ligands have been frequently devoted to the study of catalytic oxidation reactions. The first studies were inspired by nature and the understanding of metalloenzymes, which use molecular oxygen from air as the primary oxidant.¹⁰⁴

A common approach to the synthesis of pyridine-containing macrocyclic ligands consists of the modified Richman–Atkins procedure,⁸⁹ by treatment of an *N*-tosyl-protected polyamine with 2,6-*bis*(bromomethyl)pyridine, in the presence of K₂CO₃ as a base under heterogeneous conditions.

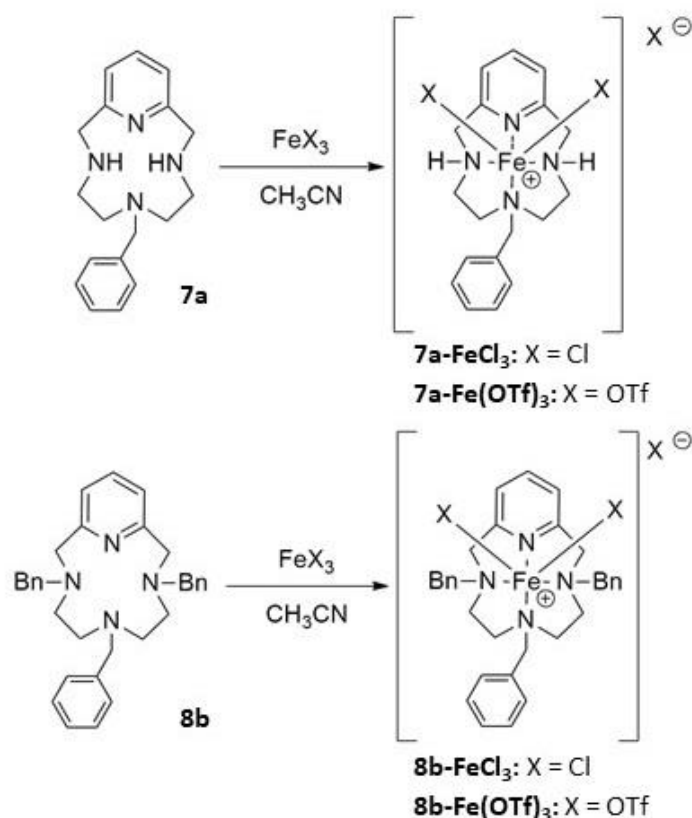
Costas and coworkers proposed this synthetic approach for their ligands, in which, after the hydrolysis, promoted by HBr, of the Ts protecting groups, the free-base ligand could be further functionalized. The iron(II) complex obtained by treating the corresponding ligand with [Fe^{II}(CF₃SO₃)₂(CH₃CN)₂], upon treatment with peracetic acid gave rise to the fastest non-*heme* oxo-iron complex for cyclohexane oxidation ever reported.¹⁰⁵ It also proved to be a good catalyst in alkene epoxidation with peracetic acid.

Triggered by these works and having synthesized a large number of pyridine-containing macrocycles, we decided to investigate the coordination properties of our ligands with transition metals other than copper(I) and silver(I). To do so, we needed to deprotect the sulfonyl protected nitrogens of the backbone of our macrocycles in order to increase the basicity of those nitrogens. In fact, nosyl and tosyl are extremely EW groups, resulting in a lower coordination ability of the nitrogens in position 3 and 9. Contrarily, a deprotection provides NH functions which donate easily the doublet to an incoming host like a transition metal. Moreover, the two -NH moieties could be further functionalized.

We choose Fe(III) as preferred metal for the oxidation of alkenes due to its well known great activity towards the generation of metal-oxo complexes and relative oxygen transfer reactions. The ideal ligand for preliminary coordination studies was the simplest one, i.e. **7a**, bearing only a benzyl group as pendant and without overcrowding substituents on the skeleton. The iron(III) sources chosen for this work were FeCl₃ and Fe(OTf)₃. The first one is one of the cheapest iron(III) commercially

available sources, the second one carries triflates as counteranions known for being “low-coordinating” ones and, for our purpose, a possible ideal candidate in order to leave more accessible space to the incoming substrate during the oxygen transfer step.

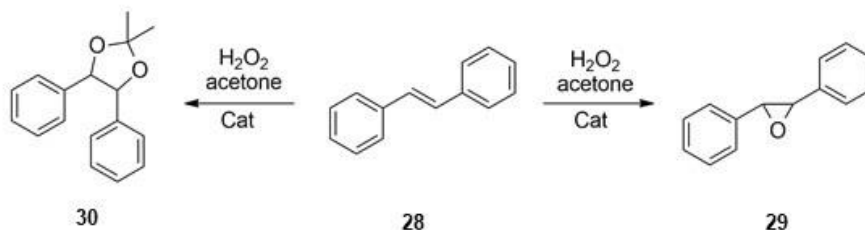
The complexes were obtained by treating an acetonitrile solution of the selected ligand with an acetonitrile solution of the metal source at room temperature. After one hour of stirring the acetonitrile was evaporated and *n*-hexane was added. The suspension was filtered in open-air atmosphere after 30 minutes of stirring leading to the desired complex without need of any further purification. All complexes were characterized by elemental analysis to have an idea of the purity and by mass analysis as detailed in the experimental chapter. Good results have been obtained by using the FAB (fast atomic bombardment) ionization technique and with NBA as matrix. Based on the ionization observed and the structure determination of parent metal complexes of other metals (see next subchapter), together with literature data, we propose for the metal complexes the structure depicted in **Scheme 2.42**, with the iron placed in an octahedral environment and only two X groups directly bounded to the metal.



Scheme 2.42 – Fe(III) PCL complexes obtained with the previously described procedure.

2.7.2 Fe(III) catalysis: highly selective alkene oxidation

The new Fe(III)-PcL complex **7a-FeCl₃** was fully characterized and used for the preliminary study of the catalytic activity and for determining the best conditions of the reaction between *trans*-stilbene and hydrogen peroxide (**Table 2.12**).



Entry	Catalyst	Solvent	Temp	Time	Epoxide (29) % Select (conv)	Acetal (30) % Select (conv)
1		acetone	RT	72h	90 (95)	-
2		acetone	60 °C	36h	77 (95)	-
3		acetone	30 °C	48h	95 (97)	-
4		CH ₃ CN	30 °C	48h	75 (99)	-
5	7a-FeCl₃	TFE	30 °C	48h	<i>no reaction</i>	-
6		H ₂ O	30 °C	48h	<i>no reaction</i>	-
7		H ₂ O/DCM	30 °C	48h	<i>no reaction</i>	-
8		<i>t</i> -BuOH	60 °C	48h	96 (45)	-
9		<i>t</i> -amyLOH	30 °C	48h	88 (32)	-
10		PhCl	30 °C	48h	<i>no reaction</i>	-
11		acetone	30 °C	48h	97 (95)	-
12	8b-FeCl₃	acetone ^a	60 °C	24h	95 (99)	-
13		acetone ^b	60 °C	24h	85 (58)	-
14	7a-Fe(OTf)₃	acetone ^a	60 °C	48h	-	65 (99)
15	8b-Fe(OTf)₃	acetone ^a	60 °C	24h	-	87 (99)
16	Fe(OTf)₃	acetone	60 °C	5 days	-	<i>traces</i>

General reaction conditions: Cat/substrate/H₂O₂ = 1/20/180, solvent = 10 mL, H₂O₂ 30% added 3eq every 12h.

^a Cat/substrate/H₂O₂ = 1/20/120. ^b Cat/substrate/H₂O₂ = 1/100/600.

Table 2.12 – Optimization of Fe(III) PcL catalyzed alkene oxidation.

First, we studied the reaction in different solvents and temperatures in order to find the best conditions. The reaction proceeded well using acetone, in presence of 5 mol% of **7a-FeCl₃**, leading

to the formation of the epoxide with very good selectivities at RT in 72 h (90%, entry 1, **Table 2.12**). Higher temperatures (60 °C) resulted in a faster reaction but in a loss of selectivity (77%, entry 3, **Table 2.12**), while the best combination was in acetone at 30 °C leading to the desired epoxide with almost full conversion and 95% of selectivity in 48 h (entry 2, **Table 2.12**). Other solvents like acetonitrile, *t*-BuOH and *tert*-amyl alcohol promoted also the reaction but with some limitations. In fact, with acetonitrile we obtained the total conversion of the starting material but with a lower selectivity compared to acetone (entry 4, **Table 2.12**). On the other hand, branched alcohols, known for being solvents compatible and often used in oxidations, showed good selectivities but with poor conversions (entries 8-9, **Table 2.12**). In all the other reaction media used, the reaction did not take place (*i.e.* water, chlorobenzene, TFE).

In the meantime, the corresponding **8b-FeCl₃** complex was synthesized with the procedure previously described and we were pleased to obtain a faster and more stable catalyst. In fact, using 5 mol% of this complex in acetone and at 60 °C, only the epoxide was selectively formed in 24 h (95% selectivity, 99% conversion, entry 12, **Table 2.12**). Moreover, a lower quantity of hydrogen peroxide was needed using this complex as the catalyst (6 eq instead of 9 eq). A lower catalyst loading of 1 mol% resulted in lower conversions and selectivities (entry 13, **Table 2.12**).

By exchanging the counteranion from chloride to triflate we were surprised to obtain a completely reverted chemoselectivity. In fact, by using complex **7a-Fe(OTf)₃**, the dimethyl acetal of the corresponding diol of *trans*-stilbene was obtained in a complete conversion and 65% of selectivity (no epoxide traces detected, the remaining yield attributed to benzaldehyde, entry 14, **Table 2.12**). Even in this case, by using **8b-Fe(OTf)₃**, the selectivity was improved to a respectable 87% (entry 15, **Table 2.12**).

In order to check if iron(III) triflate alone could have been responsible for this reverted selectivity we run also a blank reaction using the metal salt as given without the addition of any ligand nor additive. After 5 days, only few traces of diol/acetal were detected, confirming the actual activity and selectivity of our catalytic system (entry 16, **Table 2.12**).

In order to explain this change of behaviour dependant on the anion, we hypothesized an acidic environment leading to a protonated epoxide, resulting in the formation of a *sp*² carbocation subsequently undergoing to ring opening and transformation to the corresponding diol. Having in our hands the mass analysis of our iron(III) complexes and knowing their octahedral structure, we hypothesized that the third triflate anion, present in the second coordination sphere, transforms in

catalytic quantities of triflic acid in the protic environment of the reaction. This triflic acid would be the responsible of the protonation of the just formed epoxide leading to the formation of the diol/acetal product.

In order to confirm our hypothesis, we decided to perform some control experiments. First of all, the isolated *trans*-stilbene epoxide was reacted with catalytic triflic acid in acetone and actually formed the corresponding acetal in 8 hours, confirming the results reported in literature. Then, the isolated *trans*-stilbene epoxide was reacted also with our **8b-Fe(OTf)₃** complex in acetone leading to the same results obtained with the catalytic triflic acid and confirming our supposition.

We next moved to test the robustness of our catalytic system by performing several cycles in the same batch, seeing that the recovery of the catalyst was not possible after a single batch due to the celite filtration to which undergoes the reaction mixture in order to remove metal sources before the GC and GC-MS analyses. We were pleased to discover that both **8b-FeCl₃** and **8b-Fe(OTf)₃** were active for more cycles (respectively 3 and 5 cycles) before undergoing to inhibition from the formed product. Then we wondered if our catalytic system could find industrial application and to do so we started a cost evaluation of the process in collaboration with Prof. Ilenia Rossetti of our University (Department of Chemistry).

During the screening of several process alternatives, a common approach in the beginning stage in estimation of the feasibility of new chemical processes is the evaluation of the economic potential of level 2 (EP₂), based on material balances with current raw materials and product prices:

$$EP_2 = \text{Sales revenue} - \text{Raw material costs}$$

Where “sales revenue” represents the sum of product and byproduct selling prices times the relative amount necessary. If the EP₂ value is less than zero the process is not economic sustainable. Usually EP₂ is expressed as \$/time for continuous processes, however this study deals with a batch process. For our investigation all mass and volume values of reagents were related to 1 g of catalyst usage, which is the mass produced after one whole batch synthesis.

In particular, this formula was adopted:

$$EP_2 = \sum_k W_k P_k - \sum_i W_i P_i$$

Where W_k (g) and W_i (g) are the mass of the product and reagents respectively after the use of 1 g of catalyst, whereas P_k and P_i are the product selling price and the raw material costs respectively (including solvents). Raw materials costs and prices were obtained from Sigma Aldrich website.

In the beginning the cost of the catalyst per gram produced was evaluated. To this purpose the costs of all the synthetic steps of the catalyst were taken in count (**Figure 2.8**) Data and results for the catalyst cost calculation are reported in **Table 2.13**.

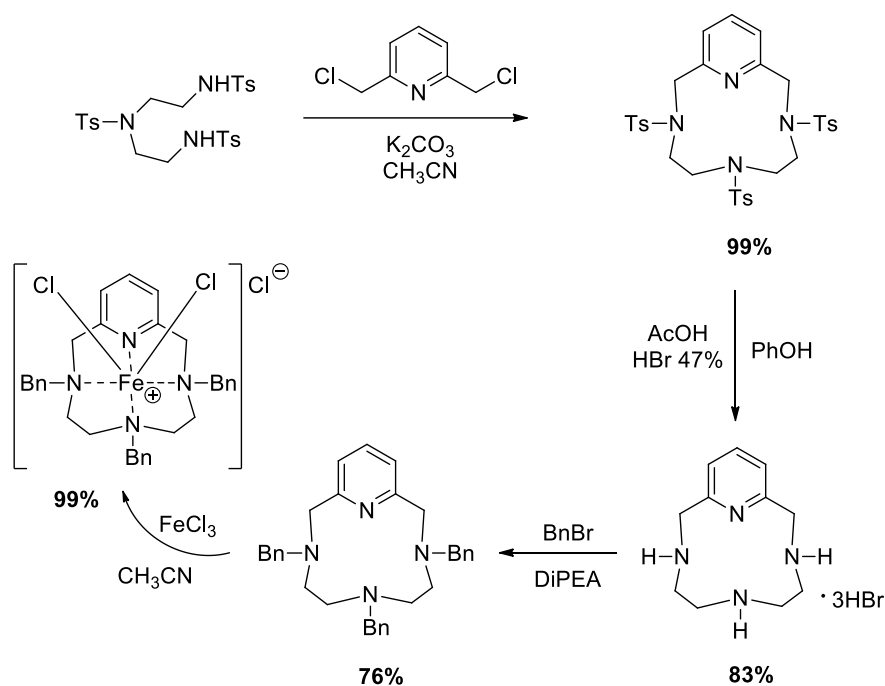


Figure 2.10 – Synthetic steps for the catalyst synthesis.

Reagent	Unit cost	Quantity for 1g of cat.	cost (€/g _{cat})
tritosyldiethylenetriamine	4,28 €/g	1 g	4,28
Py(CH ₂ Cl) ₂	50,80 €/g	0.3 g	15,24
potassium carbonate	0,08 €/g	0.8 g	0,064
HBr 47%	0,05 €/mL	17 mL	0,765
Acetic acid	0,04 €/mL	4 mL	0,152
Phenol	0,72 €/g	1.4 g	1,008
Benzyl Bromide	0,56 €/mL	0.4 mL	0,224
DiPEA	0,42 €/mL	2 mL	0,8
acetonitrile	0,02 €/mL	100 mL	1,5
Iron(III) trichloride hydrate	0,13 €/g	0.5 g	0.065
Total			24

Table 2.13 – Synthetic steps for the catalyst synthesis.

Then the EP₂ value was calculated considering the use of 1 gram of catalyst, which is the exact amount for having 200 cycles in catalytic tests. Table 2.14 report the data of the reagents involved in the reaction using the catalyst, whilst table 2.15 the calculation of EP₂.

Reagent per reaction	Unit cost	Quantity for 1g of cat.	cost (€/g _{cat})
<i>trans</i> -stilbene	1,40 €/g	0.090 g	0,13
H ₂ O ₂ 30%	0,04 €/mL	0.34 mL	0,0136
acetone	0,00025 €/mL	10mL	0,0025

Table 2.14 - Cost evaluation of reagents per catalytic cycle.

Catalytic data

Catalyst mass per reaction	15 mg
recycle of catalyst	3 cycles
number of cycles with 1 g	200
mass of transtilbene per cycle	0,09 g
mass of product per cycle	0,089 g
yield per cycle	93 %
Reagent costs per cycle	0,14 €
Reagent costs for 200 cycles	28 €/g _{cat}
Reagent + Cat	54 €/g _{cat}
Sales Revenue	219 €/g _{cat}
EP 2	167 €/g _{cat}

Table 2.15 – Economic potential (EP₂) of our catalytic system.

The process was compared to the traditional epoxidation strategies, which involve the use of stoichiometric oxidants, in particular the epoxidation with percarboxylic acids (the first one is the *m*-CPBA, while the second one is the TFPA). Both the processes were considered using acetone as solvent, which is the most commonly used option in these kind of oxidation reactions. Yields and reagents of industrial processes were obtained by Ullmann's Encyclopedia of Industrial Chemistry: Epoxides (DOI: 10.1002/14356007.a09_531). The calculation was carried out considering the same amount of transtilbene in the beginning of the process considered for the catalytic process previously described.

Reagent per reaction	Unit cost	Quantity	cost (€)
<i>m</i> -CPBA	1,40 €/g	0.086 g	0,12
<i>trans</i> stilbene	1,40 €/g	0.090 g	0,13
acetone	0,00025 €/mL	10mL	0,0025

Table 2.16 – Cost evaluation of epoxidation using *m*CPBA as oxidant.

In the case of TFPA the formation in situ was considered using H₂O₂ 70% and trifluoroacetic anhydride.

Reagent per reaction	Unit cost	Quantity	cost (€)
trifluoroacetic anhydride	1,28 €/g	0.105 g	0,13
H ₂ O ₂ 70%	1E-06 €/g	0.017 g	1,7E-05
trans stilbene	1,40 €/g	0.090 g	0,13
acetone	0,00025 €/mL	10 mL	0,0025

Table 2.17 – Cost evaluation of epoxidation using trifluorooperacetic acid generated *in situ* as oxidant.

Process	Cat-H ₂ O ₂	<i>m</i> -CPBA	TFPA
Catalyst mass per reaction	15 mg		
recycle of catalyst	3 cycles		
number of cycles with 1 g	200		
mass of transtilbene per cycle	0,09 g	0,09 g	0,09 g
mass of product per cycle	0,089 g	0,072 g	0,067 g
yield per cycle	93 %	75 %	70 %
Reagent costs per cycle	0,14 €	0,25 €	0,26 €
Reagent costs for 200 cycles	28 €	50 €	53 €
Reagent + Cat	54 €	-	-
Sales Revenue	219 €	177 €	165 €
EP 2	167 €	128 €	113 €

Table 2.18 – Comparison between economic potentials (EP2).



Figure 2.11 – Comparison between economic potentials (EP2).

The EP2 was positive and higher than traditional industrial processes. In addition, the problem for the conventional pathways without catalysts are the significant amount of waste generated, especially containing the acid analogue of the peracid used, which are often not easy to separate. With these preliminary studies in our hands we decided to study the scope of the reaction by using the catalysts **8b-FeCl₃** and **8b-Fe(OTf)₃**.

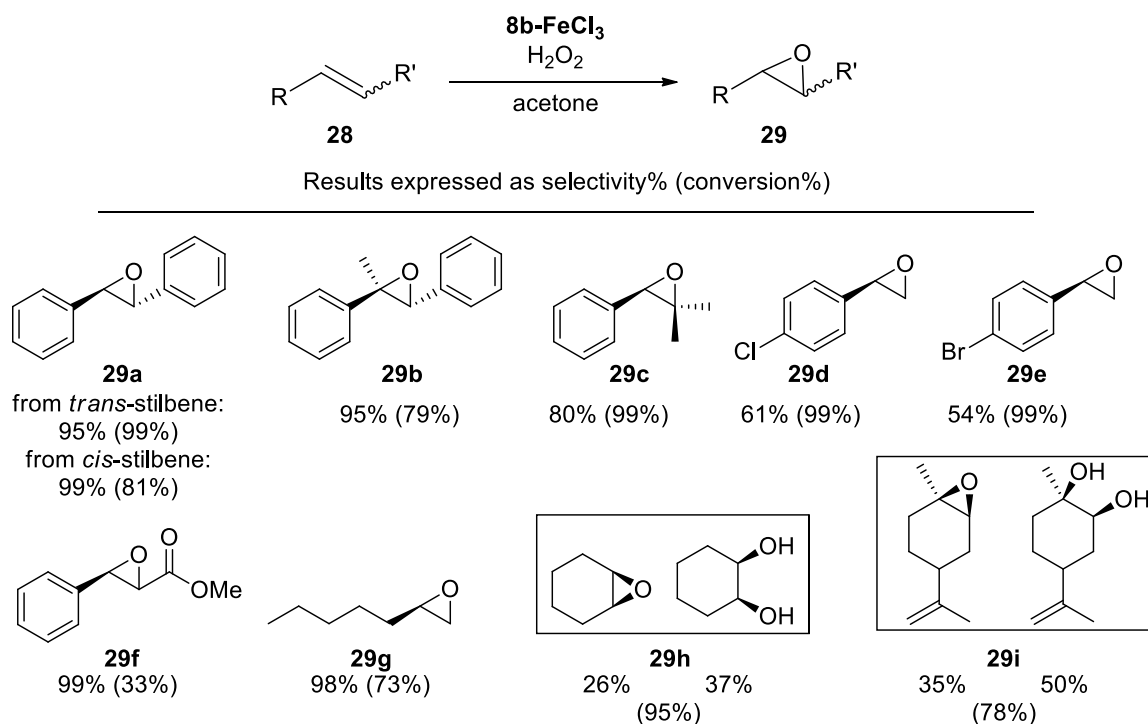
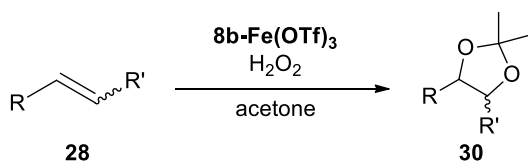


Table 2.19 – Scope of alkenes epoxidation catalyzed by **8b-FeCl₃**.

The catalytic system was found to tolerate a wide range of substrates. The reaction proceeds with excellent yields and selectivities for internal tri- and disubstituted alkenes (**Table 2.19**, products **29a,b,c**). The reaction shows a preference towards the formation of *trans* products, even starting from *cis* substrates (**Table 2.19**, products **29a**), possible evidence of a radicalic mechanism. In order to verify this hypothesis the model reaction was performed in presence of a radical trap such as BHT as found in the literature. The reaction proceeded to the formation of **29a**, excluding radical mechanism and driving our thoughts to a non-concerted mechanism. Electron-poor styrenes showed complete conversions but only moderate selectivities (**Table 2.19**, products **29d,e**) while electron-rich styrenes reacted giving only the corresponding aldehydes and acids demonstrating the too high oxidative activity of our catalytic system. More challenging substrates such as cinnamates, despite the modest conversion, gave excellent results in terms of selectivity (**Table 2.19**, products

29f). Aliphatic alkenes resulted in higher conversions and selectivities compared to those reported in the literature. 1-octene reacted to provide the corresponding epoxide in almost quantitative selectivity and very good yield (**Table 2.19**, product **29g**). On the other hand, cyclohexene produced the corresponding epoxide in only 26% of selectivity while the diol was found to be the main product of the reaction with a modest selectivity of 37% (**Table 2.19**, product **29h**). The rest of the yield was attributed to the plethora of oxidation products of cyclohexene. This result is the evidence of a preference to diol formation starting from endocyclic substrates and was confirmed even performing the reaction on limonene, where the corresponding diol was formed as main product with 50% of selectivity and complete regioselectivity towards the epoxidation of the internal double bond over the terminal one (**Table 2.19**, product **29i**).



Results expressed as selectivity% (conversion%)

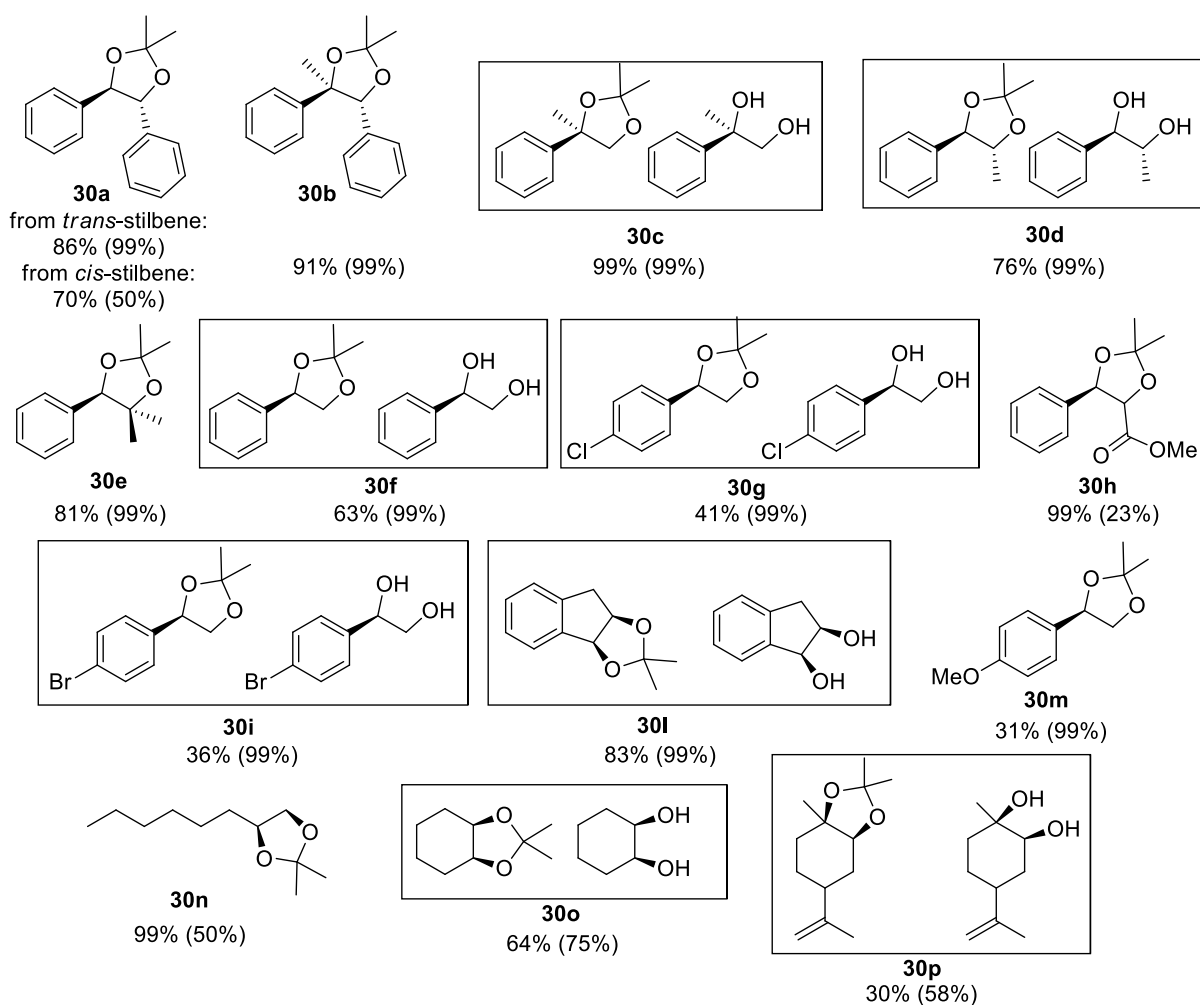


Table 2.20 – Scope of diol formation catalyzed by **8b-Fe(OTf)₃**.

By exchanging the counter anion from chloride to triflate, using **8b-Fe(OTf)₃**, the chemoselectivity of the reaction was completely changed providing the dimethyl acetal, coming from the corresponding diol selfprotecting in acetone solution. Generally, the dimethyl acetal was obtained as single product. In few cases traces of the corresponding non-protected diols were also detected by GC-MS. Given that the two products actually are the same species the results expressed in selectivity and conversion were given as sum of the two.

The reaction proceeds with excellent yields and selectivities for internal tri- and disubstituted alkenes (**Table 2.20**, products **30a,b,c,d,e**) and shows a preference towards the formation of *trans*

products, even starting from *cis* substrates, exactly like in the epoxidations previously reported. Styrenes were tolerated but showed lower selectivities (Table 2.20, products 30f,g,i,m) while challenging alkenes, such as indane and cinnamate, gave good results but with low conversions in the case of the last one (Table 2.20, products 30h,i). Even with aliphatic substrates the reaction proceeded well, giving excellent selectivity in the case of 1-octene (Table 2.20, product 30n) and reasonable results for cyclohexene and limonene (Table 2.20, products 30o,p) and in this last case with total regioselectivity for the internal double bond over the terminal one.

Other iron complexes were synthesized but these have not been used in catalysis yet. The ligands chosen for further structural studies on coordinated iron PCL were 7b, 7f and 7i. The first one was chosen because of its similarity with 7a, while also carrying a well-defined stereocenter. 7f was chosen as benchmark macrocycle for the aminoacid-derived PCLs. Finally, 7i was chosen as benchmark for the aminoacid-derived fully deprotected ligands (Figure 2.12).

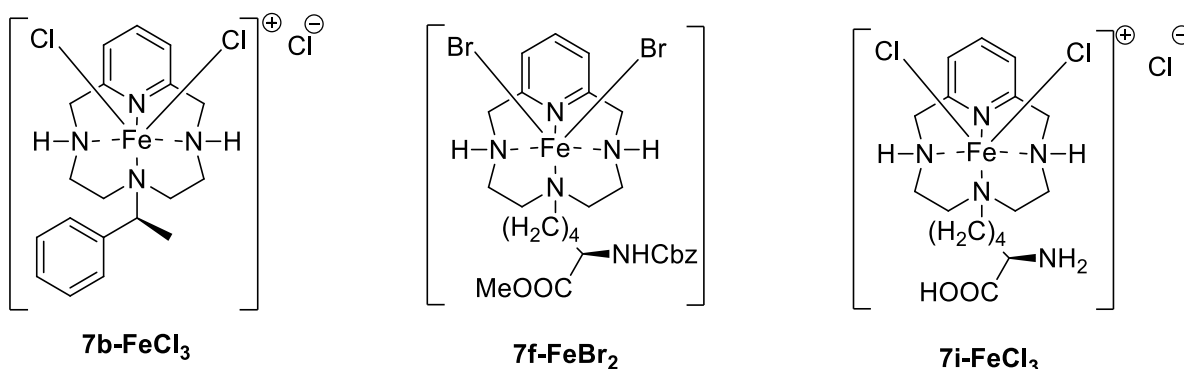


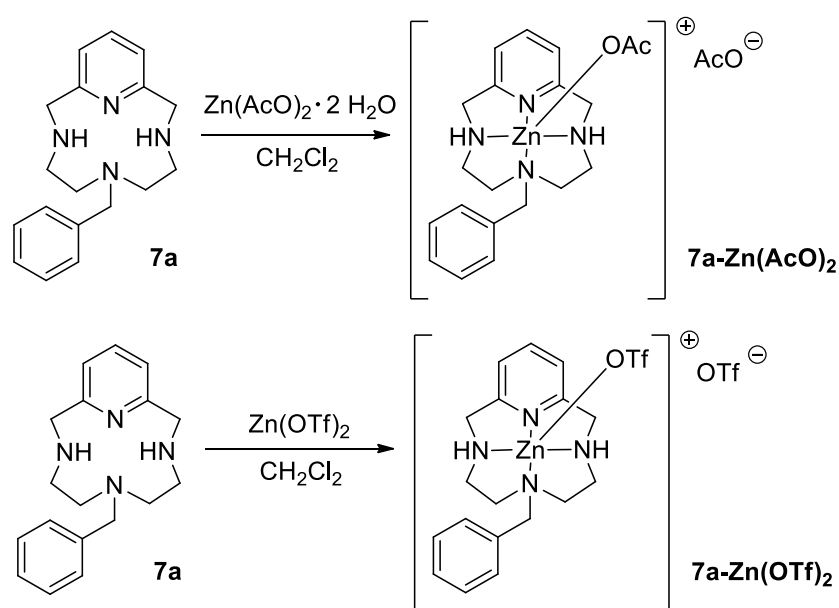
Figure 2.12 – Other iron PCL complexes.

2.8 Other metals

In the previous chapters, we have described the synthesis and application in catalysis of some metal complexes of our pyridine macrocycles. During the course of the thesis, we have synthesized also a plethora of other metal complexes with the objective either to prepare other possible catalysts to be used in the next future or to better understand the coordination modes of our ligands. In particular Zn(II), Cd(II), Co(II), Ru(II), Pd(II) and Ni(II) metal complexes were prepared.

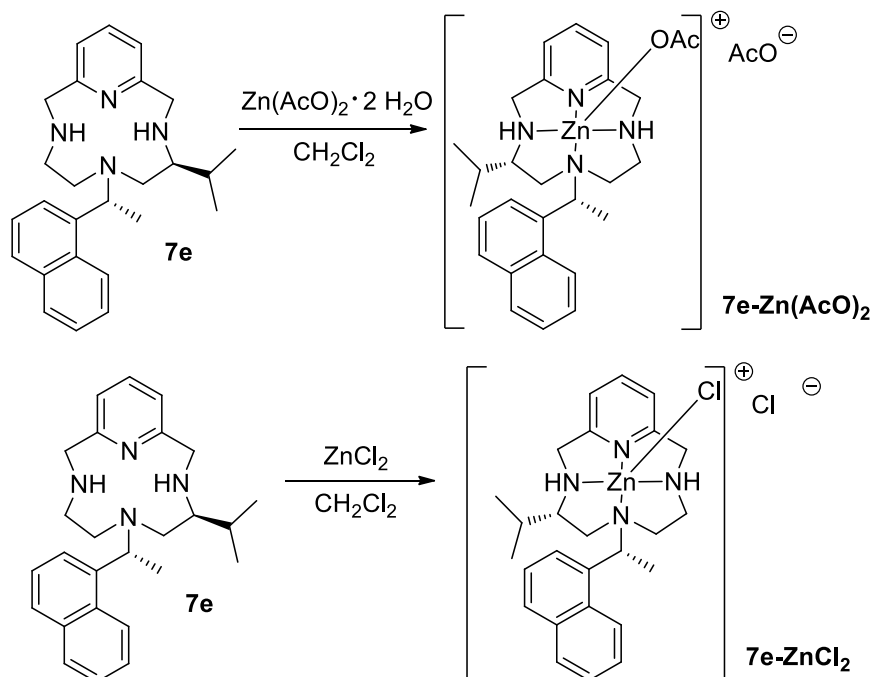
2.8.1 Zinc complexes

A logical extension of the coordination studies with copper and silver was the use of zinc. For this purpose, however, it was necessary as for iron, to remove the tosyl protecting groups of the starting macrocycle. **7a** and **7e** were chosen as model ligands for the coordination of Zn(II) salts. For the synthesis of zinc complexes, a solution of the selected ligand in acetonitrile was treated with a solution of the zinc salt in the same solvent. After one hour under stirring at rt, the solvent was evaporated and Et₂O was added. The resulting suspension was stirred for 15 minutes and filtered leading to the desired compound. At first, we started coordinating zinc(II) acetate to our simplest ligand, **7a** (Scheme 2.43). Then, in order to verify the effect of the anion, we switched to Zn(OTf)₂ (Scheme 2.43).



Scheme 2.43 – **7a** Zn complexes.

Then, we decided to coordinate also non-symmetrical monosubstituted ligands, such as **7e** (Scheme 2.44). To this purpose ZnCl_2 and $\text{Zn}(\text{AcO})_2$ were used as sources.

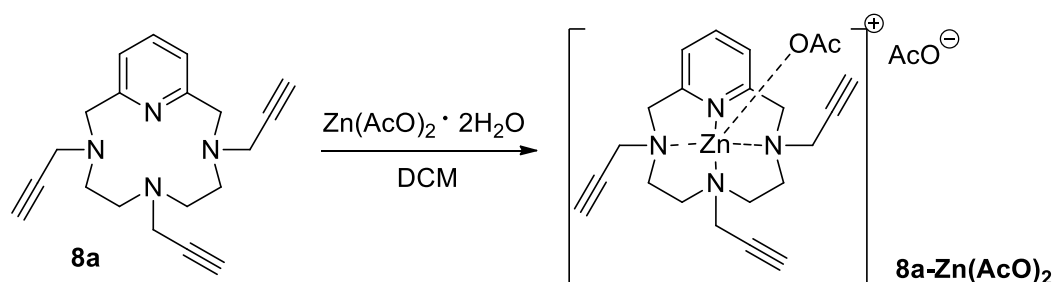


Scheme 2.44 – **7e** Zn complexes.

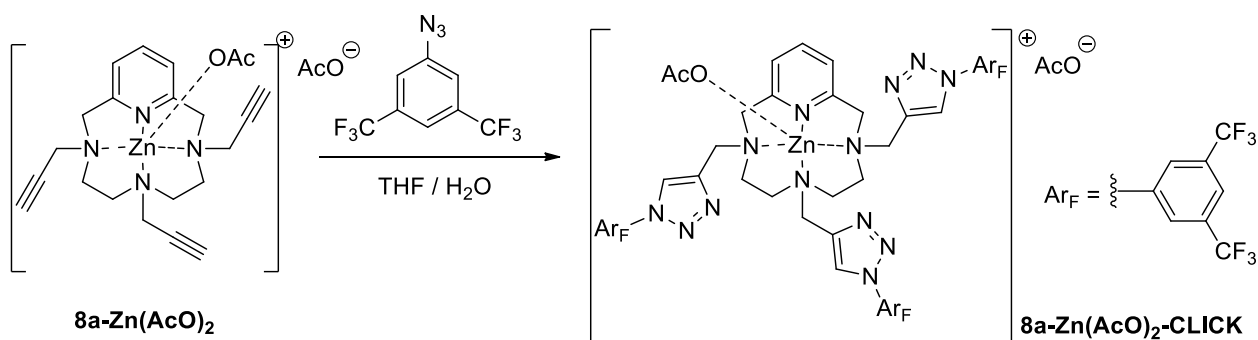
Elemental analyses confirmed the identity of the proposed metal complexes. An additional advantage of these complexes is the fact that, being diamagnetic, it is possible to follow the coordination by NMR studies. Thus, although up to now we were not able to grow crystals suitable for X-Ray analysis of good quality to have a structural characterization, NMR studies enabled us to propose the structures proposed in **scheme 2.43** and **2.44**. In fact, by careful integration of the signals in the ^1H NMR spectra, we were able to identify two protons bounded to nitrogen atoms, thus confirming that the ligand was neutral. Mass analyses instead suggested us that actually, of the two X^- anions only one is directly bound to the metal in the first coordination sphere (see Experimental Part). This hypothesis was supported also by a preliminary X-Ray analysis of 7e-ZnCl_2 that showed the zinc atom pentacoordinated in a strongly distorted square pyramidal geometry with a chlorine atom as apical ligand. Unfortunately, collected data are of very low quality and not suitable to be reported here.

Next, we moved towards the coordination of the new generation of PcL, the ones with three identical substituents on the three sp^3 nitrogen atoms. We studied macrocycle **8a** bearing three propargyl moieties and we synthesized the corresponding zinc(II) acetate complex (Scheme 2.45).

In this case, the zinc coordination has been used also as a protecting strategy for the macrocycle since the resulting complex was then further functionalized via triple Huisgen's condensation, also known as click chemistry (**Scheme 2.46**). The reaction, in fact, involves the use of a copper(I) salt, usually formed *in situ* by reduction of copper(II) with sodium ascorbate. In order to avoid the coordination of copper by the ligand, it was thus necessary to protect it by forming a zinc complex.



Scheme 2.45 – **8a-Zn(AcO)₂** complex.



Scheme 2.46 – **8a-Zn(AcO)₂** click complex.

In this last functionalization we choose 3,5-bis(trifluoromethyl)phenyl azide due to the presence of -CF₃ groups, helping us during ¹⁹F NMR analysis. The successful triple condensation is evident from ¹H, ¹³C and ¹⁹F NMR experiments (**Figure 2.12**).

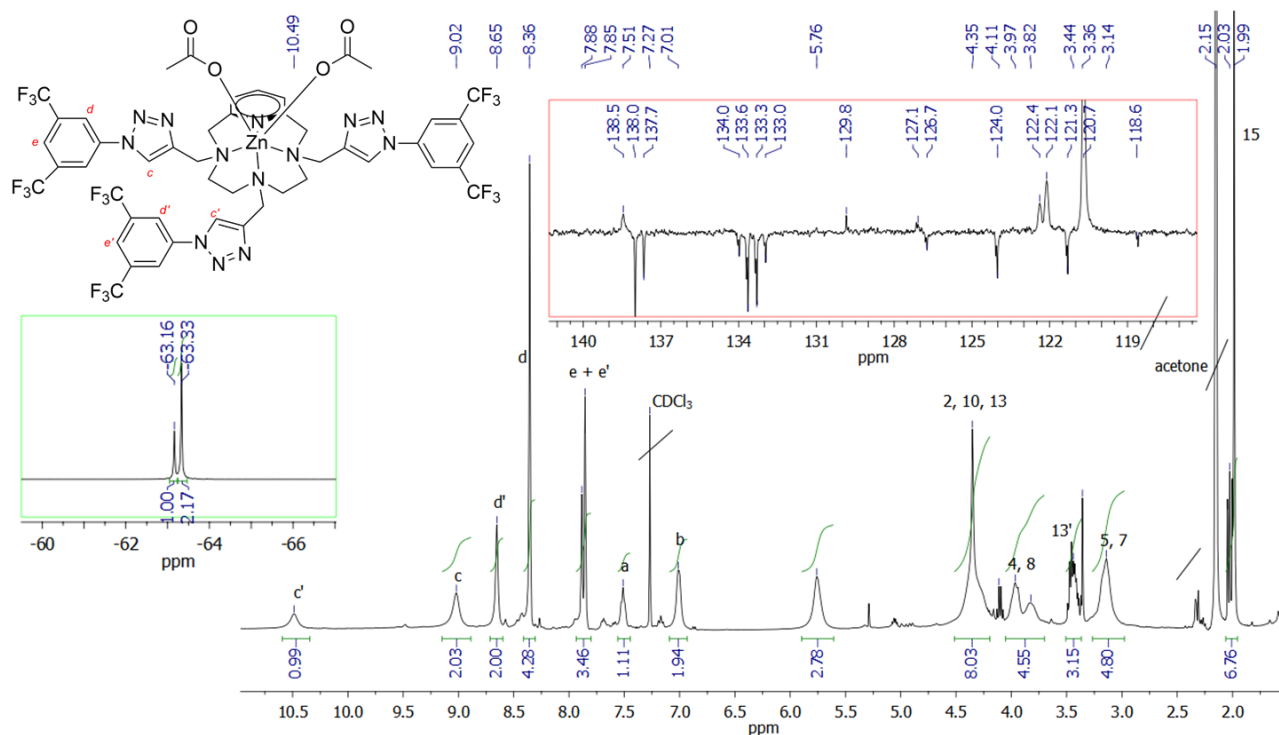
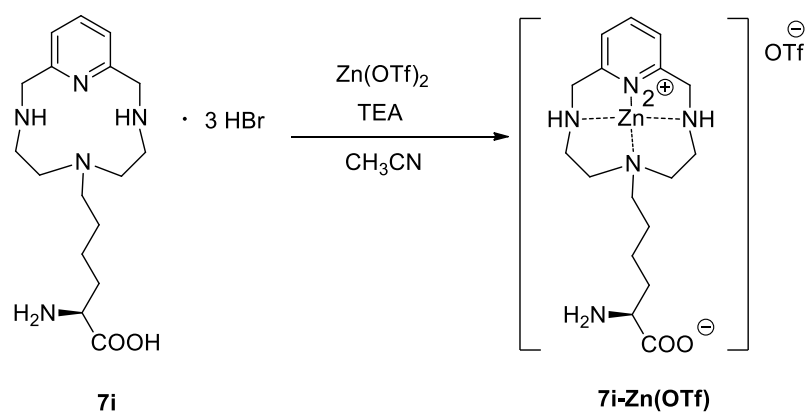


Figure 2.12 – ^1H and ^{19}F NMR experiments of complex **8a-Zn(AcO)₂-CLICK** in CDCl_3 .

In ^1H NMR, protons *c* and *c'* of the triazole moiety show integration 2:1 confirming the different nature of the two lateral substituents from the bottom one. The same can be noticed also for protons *d* and *d'*. In ^{13}C NMR experiment the expected quartets of CF_3 substituents are split in two almost overlapping quartets, with one of the two having half of the height compared to the other. Moreover, in ^{19}F NMR experiment two singlets of fluorine atoms are present with area ratio 1:2. In this case, data in our hands are not sufficient to discriminate between a penta- and a hexacoordinated central metal atom.

Finally, we decided to coordinate with $\text{Zn}(\text{OTf})_2$ also the fully deprotected lysine-derived ligand **7i**. For this synthesis we followed the already described procedure but in presence of 4 equivalents of TEA in order to remove the three HBr molecules. The precipitated product was directly filtered and washed with Et_2O in open air atmosphere (**Scheme 2.47**).



Scheme 2.47 – 7i-Zn complex.

In this case, by slow diffusion of acetone in water, we were able to grow crystals of sufficient quality for an X-Ray structural determination. As we expected, the acidic pendant is not innocent and coordinate to the zinc atom as acetate. However, instead of forming a monomer, despite the quite long alkyl chain, it prefers to crystallize as a trimer (**Figure 2.13**). The structure is highly symmetric and all the zinc atoms are hexacoordinated. Such an arrangement imposes to the whole crystal packing the presence of large voids (more than 38%), thus suggesting a potential application of this serendipitous MOF (metal-organic framework) for gas storage or catalytic purposes.

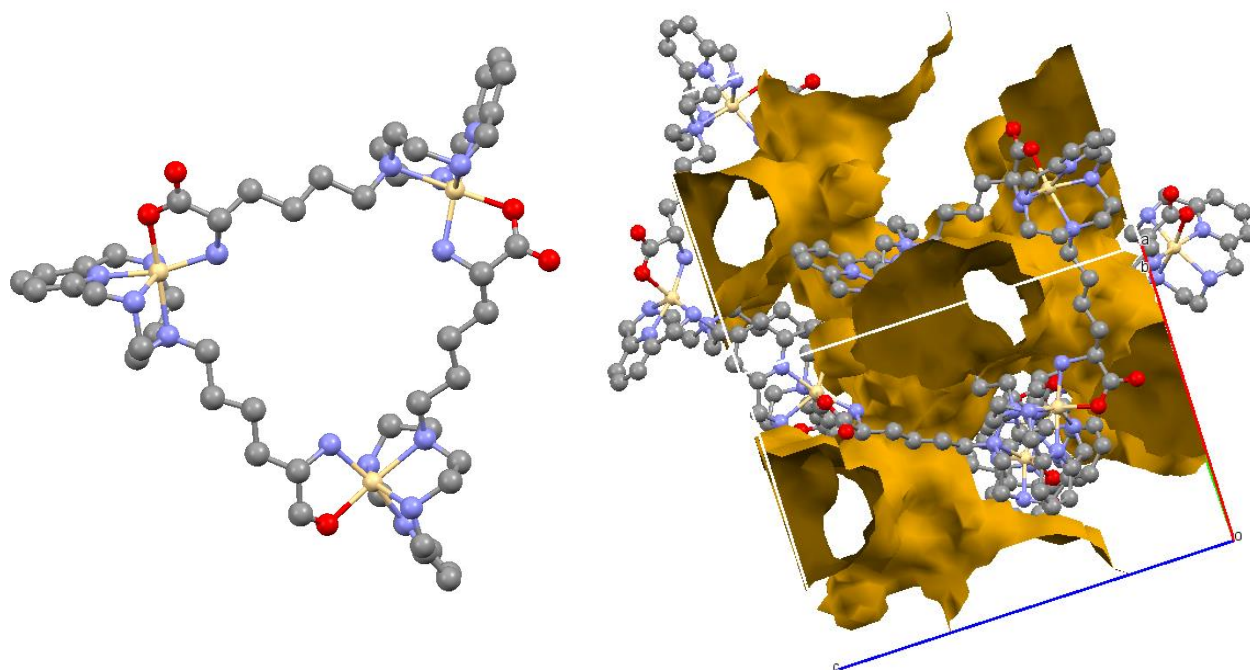
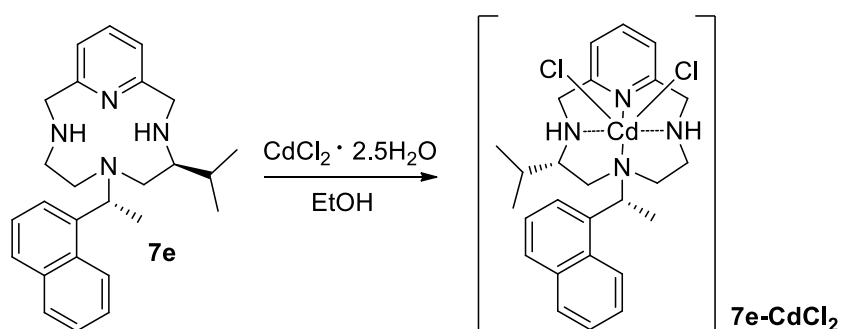


Figure 2.13 – Structure of compound **7i-Zn(OTf)** showing the trimeric arrangement of the zinc atoms (A) and crystal packing with voids evidenced (B).

2.8.2 Cadmium complexes

Knowing that very often cadmium complexes are isostructural with zinc ones, we decided to move on in the same group by coordinating cadmium(II) chloride. The complex was obtained by treating a solution of the ligand **7e** in EtOH with a solution of the metal salt in EtOH. The resulting mixture was refluxed and after cooling, the final precipitated complex was recovered by filtration (**Scheme 2.48**). In this case we were able to grow crystals of good quality. The structure is shown in **Figure 2.14** and confirmed our hypothesis that the ligand is not easily deprotonated. Actually, cadmium is hexacoordinated with two chloride atoms in *cis* position. Again, the presence of an heavy atom, allowed us to confirm the correct absolute configuration of all the stereocenters.



Scheme 2.48 – Synthesis of **7e-CdCl₂**.

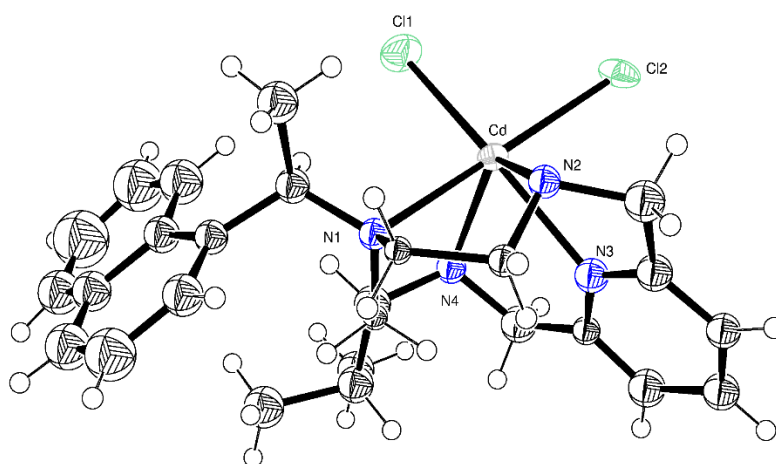


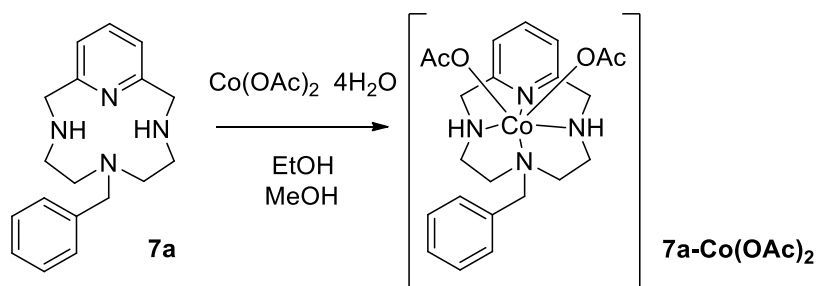
Figure 2.14 – Structure of compound **7e-CdCl₂** (thermal ellipsoids are shown at 50% probability level) Selected bond distances (Å) and angle (°): Cd-N1 2.45(3), Cd-N2 2.33(3), Cd-N3 2.39(3), Cd-N4 2.44(3), Cd-Cl1 2.504(1), Cd-Cl2 2.545(1), Cl1-Cd-Cl2 90.3(4).

2.8.3 Cobalt complexes

Being part of the first-row transition metals, cobalt(II) complexes are particularly relevant in catalysis thanks to their good activity and low cost. It was then a logical extension to our studies on iron coordination.

Co(II) PCL complexes were obtained by treating a solution of the selected ligand in EtOH with a solution of the Co(II) salt in MeOH. The resulting mixture was refluxed for one hour. The solvent was removed and replaced by Et₂O. The resulting suspension was stirred for 15 minutes, then the solid was recovered by filtration.

We started by coordinating the simplest PCL in our hands, ligand **7a**, with cobalt(II) acetate (**Scheme 2.49**). Of this Co (II) PCL complex single crystals were obtained by layering an alcoholic solution of the complex with *n*-hexane and an X-Ray diffraction study was performed (**Figure 2.15**).



Scheme 2.49 – Synthesis of **7a-Co(OAc)₂**.

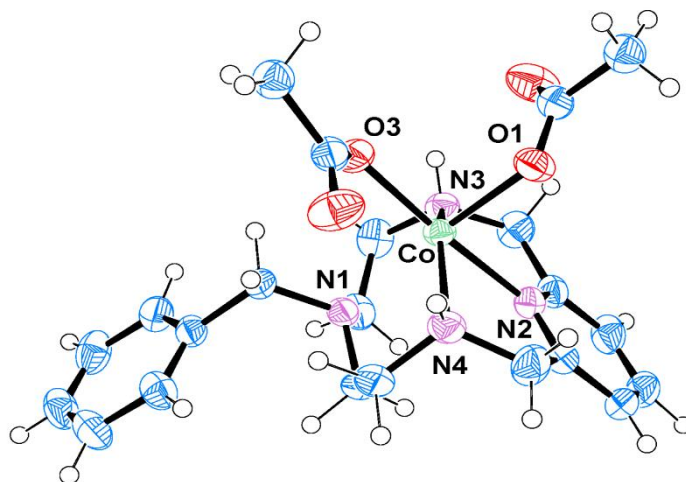
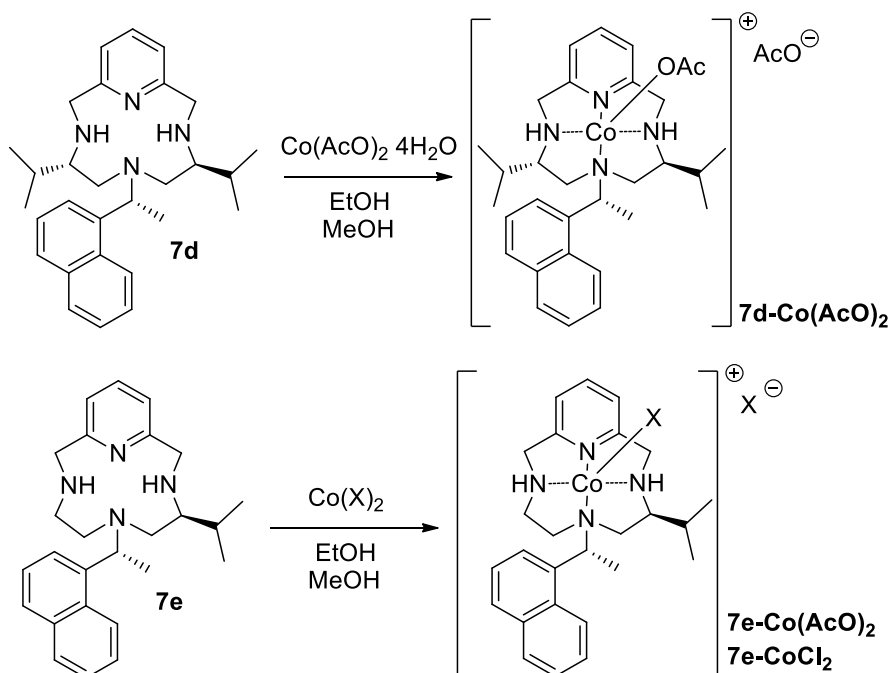


Figure 2.15 – Structure of compound **7a-Co(AcO)₂** (thermal ellipsoids are shown at 50% probability level) Selected bond distances (Å) and angle (°): Co-N1 2.305(2), Co-N2 2.099(2), Co-N3 2.201(3), Co-N4 2.207(3), Co-O1 2.080(2), Co-O3 2.033(2), O1-Co-O3 88.77(4).

Again, the macrocycle behaves as a neutral tetradentate ligand and two acetate molecules are completing the distorted octahedral geometry around the metal ion. The most interesting feature of this complex is the presence of two hydrogen bonds between the hydrogen atoms of the secondary amines of the macrocycle and the acetate residues. However, the complex does not show any tendency to lose acetic acid neither in the solid state nor in solution.

Mass spectra and elemental analyses confirmed us that a very similar coordination mode is found also for the cobalt(II) complexes of the chiral ligand **7d** and the monosubstituted non-symmetrical ligand **7e** (Scheme 2.50). In this last case two different cobalt(II) sources were used.



Scheme 2.50 – **7d** and **7e** Co complexes.

Just before completing the writing of this thesis, we obtained single crystals of sufficient quality for an X-Ray structural determination of a Co(II) complex obtained by treatment of ligand **8b** with $\text{Co}(\text{AcO})_2$. These crystals were obtained by dissolving the complex in DCM, not distilled, and by layering *n*-hexane. Much to our surprise, one of the two acetate ligands in the complex was selectively replaced by a chloride anion, located outside the coordination sphere of the metal. The distorted octahedral geometry at the metal is thus provided by the four nitrogen of the macrocycle, one acetate ion and an adventitious water molecule, as shown in **figure 2.16**. The water molecule is hydrogen bonded to the acetate.

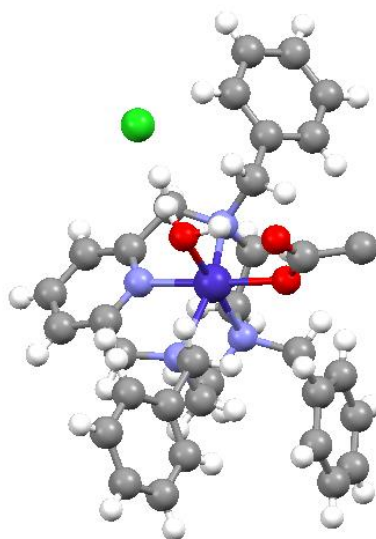
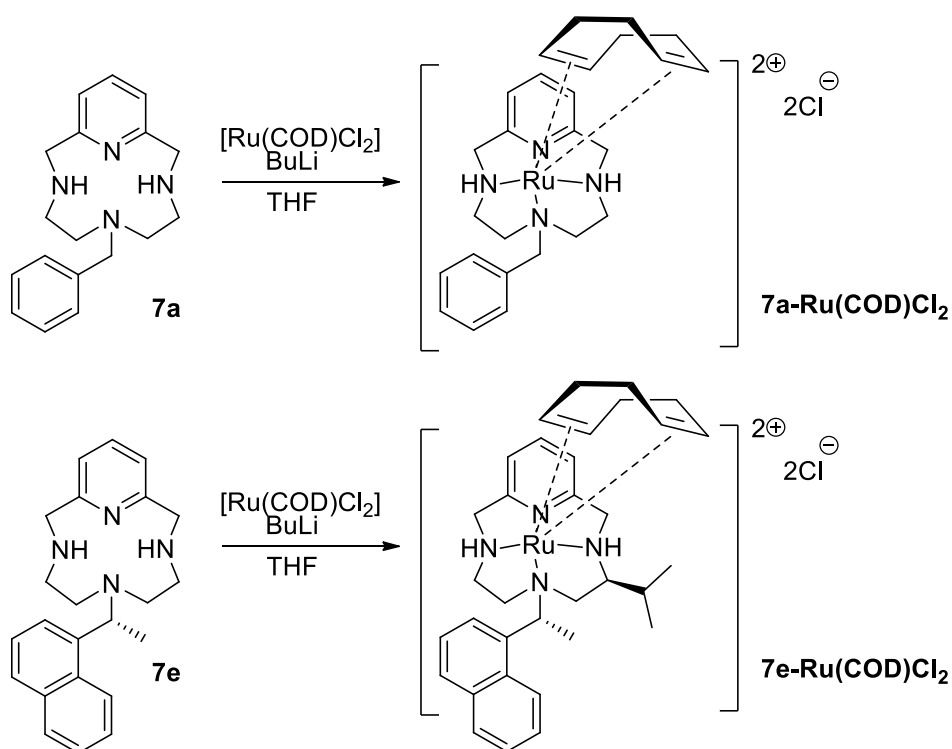


Figure 2.16 – Structure of compound **8b-Co(AcO)(Cl)**.

This again suggests that in these complexes X anionic ligands can be easily displaced and thus potential catalytic applications can be sought of.

2.8.4 Ruthenium complexes

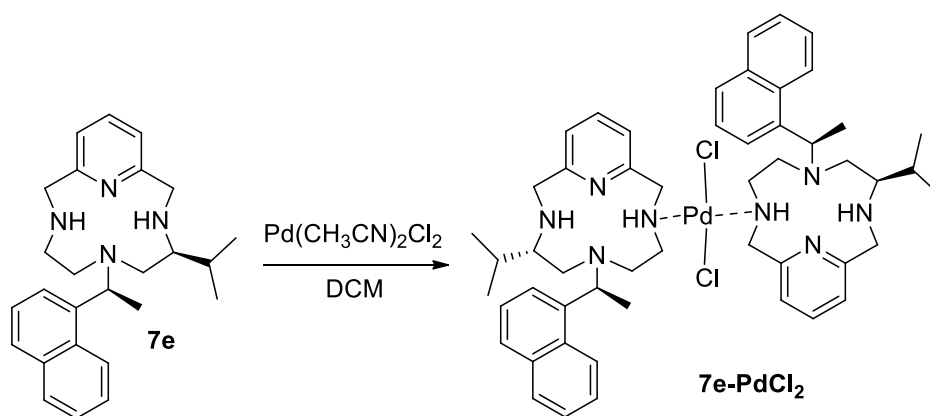
Having in our hands the good results obtained in the coordination of iron(III), we decided to move on in the same group by coordinating ligands **7a** and **7e** with Ru(COD)Cl₂ (**Scheme 2.51**). The complexes were obtained by treating a solution of the ligand in dry THF with a solution of BuLi in *n*-hexane. Ru(II) salt was added and the mixture was refluxed for 30 minutes. The precipitated solid was recovered by filtration and extracted in soxhlet until obtaining a brownish powder. Proposed structures are supported by the NMR data. Again, two N-H signals could be located, thus confirming the neutral behaviour of the ligand and the presence of a coordinated COD molecule was clearly seen. The formulation as an ion-separated complex was also supported by the low solubility in non-polar solvents. Good solubility was observed in water and DMSO. In this last solvent a conductance typical of an ionic compound was observed. Further evidences of the proposed structures were provided by both the MS spectra (FAB) and the elemental analyses. To confirm the presence of the two chloride atoms, an ion exchange reaction was performed, by using AgBF₄ in a DMSO solution. The precipitation of AgCl confirmed our assumption. Although in this case the products were obtained in very low yield, the weak acidity of the N-H groups in the free base macrocycle is confirmed by their lack of reactivity even with a strong base such as BuLi.



Scheme 2.51 – 7a and 7e Ru complexes.

2.8.5 Group 10 complexes

Ligand **7e** was also used for other coordinations with $PdCl_2$ and $NiCl_2$. In the first case a solution of the ligand in DCM was treated with a solution of $PdCl_2$ in DCM. After one hour of reflux the mixture was cooled down and the product was recovered by filtration (**Scheme 2.52**). Single crystals of this complex were obtained and X-ray diffraction was performed (**Figure 2.17**). Surprisingly we noticed that an interesting palladium-bridged dimer was obtained. Again, the identity of the stereocenters was confirmed.



Scheme 2.52 – 7e- $PdCl_2$ dimeric complex.

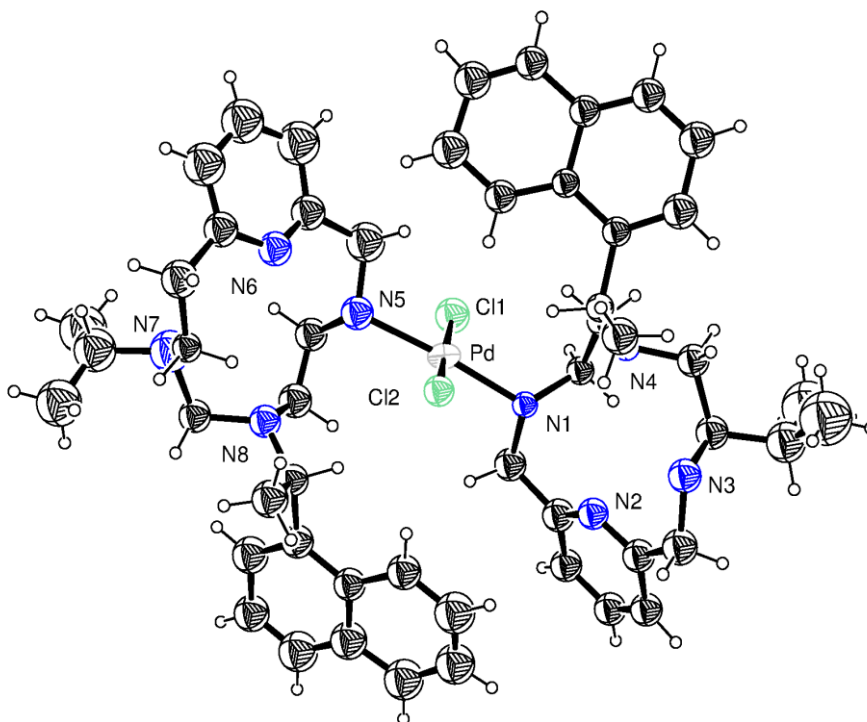
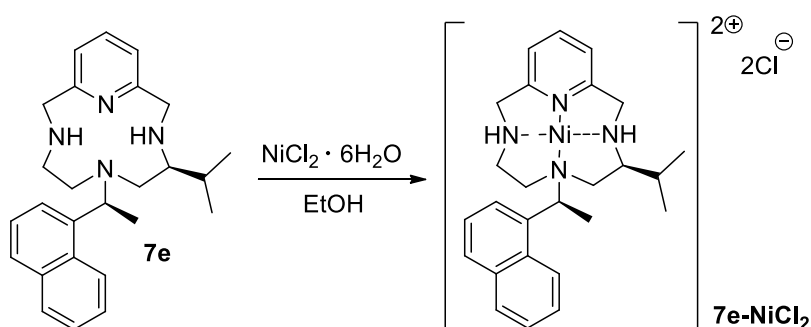


Figure 2.17 – Structure of compound **7e-PdCl₂** (thermal ellipsoids are shown at 50% probability level) Selected bond distances (Å) and angles (°): Pd-N1 2.014(1), Pd-N5 2.071(2), Pd-Cl1 2.283(7), Pd-Cl2 2.298(6), N1-Pd-N5 174.7(2), Cl1-Pd-Cl2 174.9(2).

In the case of NiCl₂ coordination, the procedure adopted was the same but replacing DCM with EtOH (**Scheme 2.53**). The identity of the complex was confirmed by mass spectrum and elemental analysis. Unfortunately, the low solubility in common solvents of the complex hampered any NMR study (the molecule is however diamagnetic) and probably imposes a serious limit to any possible application in catalysis. For this reason, we did not proceed to further studies.



Scheme 2.53 – **7e-NiCl₂** complex.

3. CONCLUSIONS

During these three years of PhD studies the reactivity and coordination behaviour of our class of Pyridine-containing Ligands (PcL) was studied deeply resulting in a better understanding of their structural features and of the final geometry of the corresponding transition metal complexes.

New ways of functionalizations were attempted and successfully realized and optimized, such as the synthesis of macrocycles bearing aminoacid-derived pendant arms or naturally functionalized ligands, such as with biotine or synthetic dipeptides, that in future could allow biological applications or catalysis in water media.

The new class of iron(III) PcL complexes demonstrated to be highly active in oxidation, as expected from studies reported in literature of iron complexes of similar ligands. The cost evaluation demonstrated that our iron(III) catalytic system is suitable for industrial application and competitive with the common synthetic industrial pathways.

Anyway, the complexes of our macrocycles demonstrated very good catalytic activity even in unpredictable fields leading us to the first example of silver(I) catalyzed Henry reaction with results comparable to the already reported Cu(I) and Zn(II) catalytic systems. The same complexes were also able to promote, even with modest results, two-step one-pot challenging isochromene cyclization versus nitroaldol reaction.⁸⁰

Moreover, the already studied Cu(I) PcL catalyzed carbene transfer, recently published by our group, was investigated also in new and different forms. Cyclopropanation of highly challenging substrates, such as vinylindoles, gave us excellent results in terms of yields and diastereoselectivities compared to other examples reported in literature. In future will be possible to develop also an enantioselective version of this transformation.

Last but not least, our Cu(I) catalytic system showed a wide range of applicability involving also Si-H, N-H, O-H bond insertion of carbenes, even deriving from different sources (diazo-compounds, enynones). The TON of 30.000 demonstrates the high activity of the catalytic system and will prompt our research group to the development of an industrially suitable methodology for the synthesis of such important compounds.¹⁰⁶

In future new catalytic applications for our transition metals PcL complexes will be studied and new functionalizations will be investigated. Moreover, the grafting of our catalysts on a proper stationary phase (already proposed in recent years for cyclopropanation)⁶³ will allow also for heterogeneous catalytic applications.

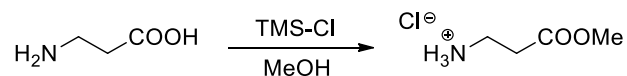
4. EXPERIMENTAL PART

General remarks

All the reactions that involved the use of reagents sensitive to oxygen or hydrolysis were carried out under an inert atmosphere. The glassware was previously dried in an oven at 110 °C and was set with cycles of vacuum and nitrogen. All chemicals and solvents were commercially available and were used as given except where specified. The chromatographic column separations were performed by a flash technique, using silica gel (pore size 60 Å, particle size 230–400 mesh, Merck grade 9385) or by gravimetric technique using basic Al₂O₃. For TLC, silica was used on TLC Alu foils with fluorescent indicator (254 nm) and the detection was performed by irradiation with UV light (λ = 254 nm or 366 nm). ¹H NMR analyses were performed with 200, 300, 400 or 600 MHz spectrometers at room temperature. The coupling constants (*J*) are expressed in hertz (Hz), and the chemical shifts (δ) in ppm. ¹³C NMR analyses were performed with the same instruments at 75.5, 100 or 150 MHz, and attached proton test (APT) sequence was used to distinguish the methine and methyl carbon signals from those arising from methylene and quaternary carbon atoms. All ¹³C NMR spectra were recorded with complete proton decoupling. The ¹H NMR signals of the ligands described in the following have been attributed by correlation spectroscopy (COSY) and nuclear Overhauser effect spectroscopy (NOESY) techniques. Assignments of the resonance in ¹³C NMR were made using the APT pulse sequence and heteronuclear single quantum correlation (HSQC) and heteronuclear multiple bond correlation (HMBC) techniques. Low resolution MS spectra were recorded with instruments equipped with electron ionization (EI), ESI/ion trap (using a syringe pump device to directly inject sample solutions), or fast atom bombardment (FAB) (for Pc-L and metal complexes) sources. The values are expressed as mass–charge ratio and the relative intensities of the most significant peaks are shown in brackets. Gaschromatographic analyses were performed with GC-FAST technique using a Shimadzu GC-2010 equipped with a Supelco SLB™-5ms capillary column. GC-MS analyses were performed using a ISQ™ QD Single Quadrupole GC-MS (Thermo Fisher) equipped with a VF-5ms (30 m x 0.25 mm i.d. x 0.25 μ m; Agilent Technology). Elemental analyses were recorded in the analytical laboratories of Università degli Studi di Milano. 2,6 pyridinedimethanol 2,6-dimesylate was synthesized as previously reported.

4.A Synthesis

Synthesis of β -alanine methyl ester hydrochloride

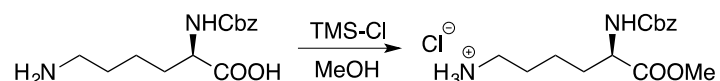


TMS-Cl (7.85 mmol) was added dropwise under stirring directly on β -alanine (3.55 mmol). Then MeOH (10.0 mL) was added dropwise carefully. The mixture was left to react 24h at RT, then the solvent was removed in vacuum leading to the product as a colourless oil.

Yield: 97%

^1H NMR (300MHz, D_2O) δ , ppm 3.81 (3H, s, OCH_3), 3.36 (2H, t, $J = 6.4$ Hz, CH_2), 2.89 (2H, t, $J = 6.5$ Hz, CH_2).

Synthesis of $\text{N}(\alpha)$ -Cbz-lysine methyl ester hydrochloride

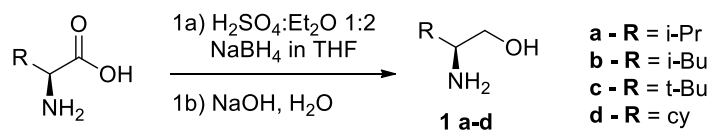


TMS-Cl (7.88 mmol) was added dropwise under stirring directly on $\text{N}(\alpha)$ -Cbz-lysine (3.57 mmol). Then MeOH (10.0 mL) was added dropwise carefully. The mixture was left to react 24h at RT, then the solvent was removed in vacuum leading to the product as a colourless oil.

Yield: 99%

^1H NMR (300 MHz, CDCl_3) δ 7.95 (s, 2H, H_{ar} Cbz), 7.31 (s, 4H, H_{ar} Cbz + NH), 5.07 (s, 2H, CH_2 Cbz), 4.92 (s, 2H, NH_2), 4.28 (s, 1H, CH), 3.69 (s, 2H, CH_2), 3.46 (s, 3H, OCH_3), 2.98 (s, 2H, CH_2), 1.75 (s, 4H, CH_2), 1.45 (s, 2H, CH_2).

4.1 Aminoalcohols

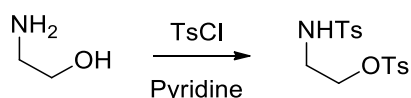


Aminoacid (100mmol) was added to a suspension of NaBH_4 (220mmol) in THF (100ml), at a temperature between 10 and 15°C. A chilled solution of H_2SO_4 conc. (6.6ml, 125mmol) and Et_2O (13.3ml) was carefully added monitoring the temperature. The solution was allowed to react overnight at room temperature, then MeOH (20ml) was carefully added drop by drop to destroy the unreacted NaBH_4 and the solution was concentrated to half the volume. The solution was diluted in 100mL of a 5N solution of NaOH in water and the volatile solvents were distilled away. Finally, the solution was allowed to reflux for three hours. The water layer was separated and the aminoalcohol was recovered as uncolored oil, concentrated in vacuum, and used without further purifications. The products were characterized by ^1H NMR spectroscopy and the results are according with the tabulated data.

Yields	L-valinol	94%
	L-leucinol	97%
	L-t-leucinol	98%
	L-cycloexylglicinol	95%

4.2 Tosyl protected aziridines

4.2.1 2-tosyl ammine ethyl toluene sulfonate

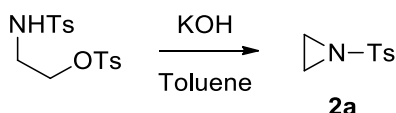


A solution of ethanolamine (12.1 mL, 200.0 mmol) in pyridine (20.0 mL) was added dropwise to a suspension of tosyl chloride (80.26 g, 421.0 mmol) in pyridine (50.0 mL) at -40 °C. The suspension was vigorously stirred for 2 hours at -10 °C then transferred in an ice bath. Ice was added to the suspension, the solid was filtered and washed with water, then it was dissolved in chloroform and washed again with water. The product obtained was recrystallized from ethanol as a yellow solid.

Yield: 55%

¹H NMR (400 MHz; CDCl₃; T = 300K) δ 7.76 (d, *J* = 8.2 Hz, 2H, ArH), 7.72 (d, *J* = 8.2 Hz, 2H, ArH), 7.37 (d, *J* = 8.0 Hz, 2H, ArH), 7.32 (d, *J* = 8.0 Hz, 2H, ArH), 4.83 (t, *J* = 6.1 Hz, 1H, NH), 4.07 (t, *J* = 5.1 Hz, 2H, CH₂O), 3.25 (pq *J* = 5.5 Hz, 2H, CH₂NH), 2.48 (s, 3H, CH₃), 2.45 (s, 3H, CH₃).

4.2.2 N-tosyl ariziridine

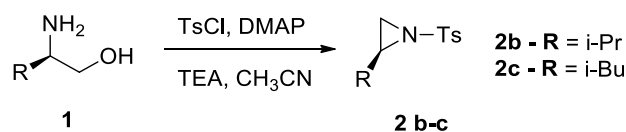


The reaction was carried out in air. A solution of KOH (5.516 g, 98.3 mmol) in water (30.0 mL) was added dropwise to a suspension of 2-tosyl ammine ethyl toluene sulfonate (10.651 g, 28.8 mmol) in toluene (80.0 mL). The resulting solution was stirred for 2 hours at room temperature, then diluted with water and toluene. The organic phase was washed with water obtaining a white solid **2a**. (MW 197.25 g/mol).

Yield: 88%

¹H NMR (400 MHz; CDCl₃; T = 300K) δ 7.85 (d, *J* = 8.2 Hz, 2H, ArH), 7.37 (d, *J* = 8.2 Hz, 2H, ArH), 2.47 (s, 4H, CH₂), 2.39 (s, 3H, CH₃).

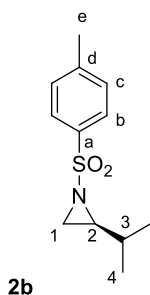
4.2.3 2-substituted N-tosyl ariziridine 2b-c



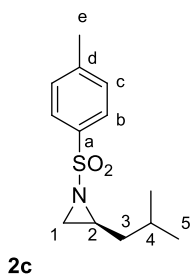
Aminoalcohol (30 mmol) was dissolved in CH₃CN dist. (125.0 ml) and TEA (120 mmol, 16.5 ml) was added. The solution was cooled to 0°C and tosylchloride (66 mmol) was added in four parts over one hour, followed by DMAP (3 mmol). The solution was allowed to react 20 hours at room temperature, then was concentrated, diluted with AcOEt and washed with brine (6x). The organic layer was anhydried with Na₂SO₄, filtered, concentrated in vacuum to give the pure products as white powder. The products were characterized by ¹H NMR spectroscopy and the results are according with the tabulated data.

Yields: **2b** 97%

2c 92%

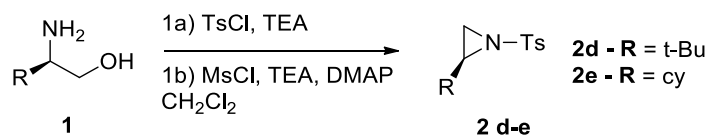


¹H NMR (300 MHz, CDCl₃, T = 300 K) δ = 7.83 (d, J = 8.6 Hz, 2H, H_b), 7.33 (d, J = 8.6 Hz, 2H, H_c), 2.61 (d, J = 7.0 Hz, 1H, H₁), 2.55-2.49 (m, 1H, H₂), 2.45 (s, 3H, H_e), 2.10 (d, J = 4.8 Hz, 1H, H₁), 1.42 (m, J = 7.0 Hz, 1H, H₃), 0.90 (d, J = 6.8 Hz, 3H, H₄), 0.80 (d, J = 7.0 Hz, 3H, H₄).



¹H NMR (300 MHz, CDCl₃, T = 300 K) δ = 7.83 (d, J = 8.6 Hz, 2H, H_b), 7.33 (d, J = 8.6 Hz, 2H, H_c), 2.82-2.80 (m, 1H, H₂), 2.65 (d, J = 7.0 Hz, 1H, H₁), 2.46 (s, 3H, H_e), 2.05 (d, J = 4.6 Hz, 1H, H₁), 1.42 (hep, J = 6.6 Hz, 1H, H₄), 1.42-1.30 (m, 2H, H₃), 0.91 (d, J = 6.6 Hz, 3H, H₅), 0.90 (d, J = 6.6 Hz, 3H, H₅).

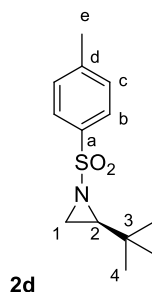
4.2.4 Aziridines 2d-e



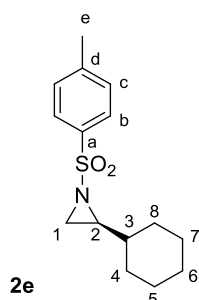
Aminoalcohol (26 mmol) and TEA (103 mmol) were dissolved in CH_2Cl_2 (75.0 ml) and the solution was cooled to 0°C then tosylchloride (28 mmol) was added. The solution was allowed to react at 0°C for 20 minutes, then for one hour at room temperature. The solvent was evaporated and AcOEt (100.0 ml) was added. The solid residuals were filtered and solvent was evaporated. CH_2Cl_2 (75.0 ml), TEA (103 mmol) and DMAP (26 mmol) were added and mesylchloride (52 mmol) was added dropwise. The solution became ever darker. After 2h30', the solvent was evaporated and AcOEt (150 ml) was added. The insoluble residuals were filtered and the product was obtained by concentrating the solution in vacuum. The products were characterized by ^1H NMR spectroscopy.

Yields: 2d 88%

2e 87%



^1H NMR (400 MHz; CDCl_3 ; T = 300K) δ 7.82 (d, J = 8.2 Hz, 2H, H_b), 7.32 (d, J = 8.2, 2H, H_c), 2.55 (dd, J = 7.6 Hz, 4.4 Hz, 1H, H₂), 2.51 (d, J = 7.6 Hz, 1H, H₁), 2.44 (s, 3H, H_e), 2.16 (d, J = 4.4 Hz, 1H, H₁), 1.36 (1 H, s), 0.78 (s, 9H, H₄).

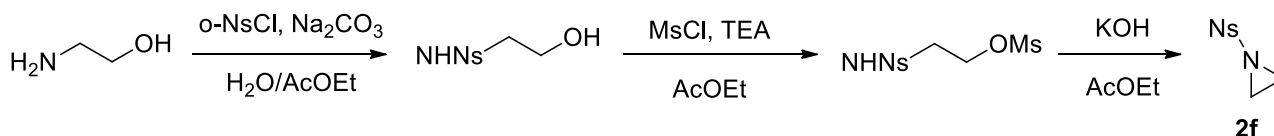


^1H NMR (400 MHz; CDCl_3 ; T = 300K) δ 7.85 (d, J = 8.1 Hz, 2H, H_b), 7.36 (d, J = 8.1 Hz, 2H, H_c), 2.62 (d, J = 7.0 Hz, 1H, H₁), 2.56 (ddd, J = 11.8, 6.0 Hz, 1H, H₂), 2.47 (s, 3H, H_e), 2.12 (d, J = 4.5 Hz, 1H, H_{1'}), 1.75-1.50 (b, 5H, H_{cy}), 1.25-0.90 (b, 6H, H_{cy})

^{13}C NMR (75 MHz; CDCl_3) δ 144.78 (C_b), 135.52 (C_d), 129.97 (C_a), 128.46 (C_c), 45.52 (C₂), 37.74 (C₃), 33.01 (C₁), 30.55 (C_{cy}), 30.00 (C_{cy}), 26.40 (C_{cy}), 25.94 (C_{cy}), 25.75 (C_{cy}), 22.01 (C_e)

4.3 Nosyl protected aziridines

4.3.1 *o*-Nosyl Aziridine 2f



Step 1

Ethanolamine (3.0 mL, 49.7 mmol) was added to a mixture of ethyl acetate (80.0 mL) and a solution of Na_2CO_3 (149.1 mmol) in water (200.0 mL). A solution of nosyl chloride (49.7 mmol) in ethyl acetate (40.0 mL) was added dropwise at 0°C . The reaction was left at room temperature for 4 hours and the product formation was evaluated with TLC chromatography (*n*-hexane/ethyl acetate = 4:6). The two layers were then separated, the organic phase was washed with brine, dried and evaporated. A slightly yellowish solid was obtained.

Yield: 92%

^1H NMR (300 MHz, CDCl_3 , $T = 300\text{K}$) δ 8.17 (m, 1H), 7.80 (m, 1H), 7.89 (m, 2H), 5.80 (s, 1H), 3.78 (m, 2H), 3.28 (dd, $J = 10.4, 5.8$ Hz, 2H), 1.90 (s, 1H).

Step 2

Triethylamine (69.0 mmol) was added to a solution of 2-nosyl amino ethanol (34.6 mmol) in ethyl acetate (94.0 mL) and the reaction mixture was cooled to 15°C . Keeping the temperature between 15 and 18°C , a solution of mesyl chloride (34.6 mmol) in ethyl acetate (2.7 mL) was added dropwise, leading to the formation of abundant white precipitate. After the addition the flask was left at room temperature for 4 hours and the product formation was evaluated with TLC chromatography (*n*-hexane/ethylacetate = 6:4). The precipitate was then filtered away and the solvent was washed with brine, dried and evaporated. A white solid was obtained.

Yield: 95%

^1H NMR (400 MHz, CDCl_3 , $T = 300\text{K}$) δ 8.17 (dd, $J = 5.8, 3.4$ Hz, 1H), 7.96-7.86 (m, 1H), 7.86-7.72 (m, 2H), 5.89 (t, $J = 5.7$ Hz, 1H), 4.32 (t, $J = 5.2$ Hz, 2H), 3.52 (m, 2H), 3.04 (s, 3H).

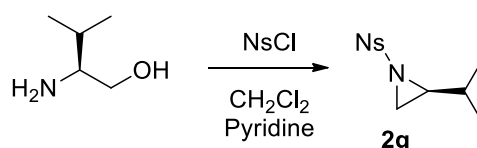
Step 3

KOH (28.5 mmol) in water (90.0 mL) was added to a solution of methanesulfonic acid 2-(2-nitrobenzenesulfonylamino) ethyl ester (28.5 mmol) in toluene (180.0 mL). The mixture was stirred for one hour, concentrated, diluted with ethyl acetate and the organic phase was washed with water and brine and dried over Na₂SO₄. The organic layer was concentrated and the crude was isolated as white solid.

Yield: 80%

¹H NMR (400 MHz, CDCl₃, T = 300K) δ 8.20-8.19 (m, 1H), 8.18-8.17 (m, 3H), 7.83-7.81 (m, 1H), 2.61 (s, 4H).

4.3.2 Nosyl protected (S)-isopropyl aziridine 2g

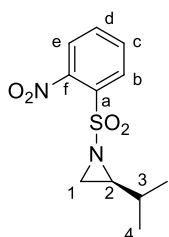


L-Valinol (576.1 mg, 5.6 mmol) was added to a solution of dichloromethane (35.0 mL) and pyridine (14.0 mL) at 0°C. A solution of ortho-nosyl chloride (727.0 mg, 12.3 mmol) in dichloromethane (35.0 mL) was dropwise and the solution is allowed to react at 0°C for 4 hours.

The mixture is diluted with 70 mL of dichloromethane and then washed three times 2M HCl (3 x 25.0 mL). The aqueous layers were washed again with dichloromethane (3 x 25.0 mL) and the collected organic phases were washed with aqueous KOH (3 x 50.0 mL), treated with Na₂SO₄ and concentrated in vacuum.

The crude was dissolved in dichloromethane (3.0 mL) and the pure product was obtained by precipitation, layering n-n-hexane on the solution.

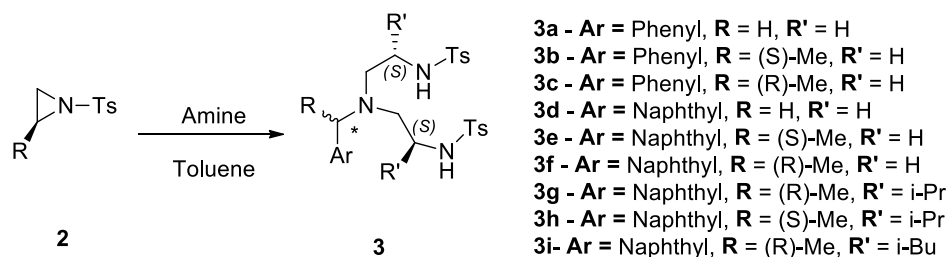
Yield: 84%



¹H NMR (400 MHz, CDCl₃, T = 300K) δ 8.22 (d, J = 5.3 Hz, 1H, H_{Ar}), 7.79 – 7.74 (m, 3H, H_{Ar}), 2.85-2.84 (m, 2H, H₁), 2.35-2.34 (m, 1H, H₂), 1.61-1.59 (m, 1H, H₃), 0.99 (d, J = 6.7, 3H, H₄), 0.93 (d, J = 6.7, 3H, H₄)

4.4 Bis-sulfonamides

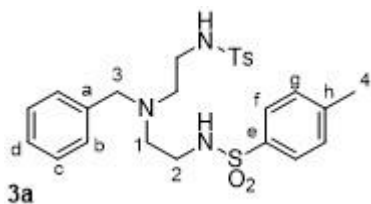
4.4.1 Bis-sulfonamides 3a-i



A solution of **2** (7.3 mmol) and amine (3.3 mmol – see **table 3.1**) in toluene (12.0 mL) and CH₃CN (8.0 mL) was stirred and refluxed for (see **table 3.1**). The mixture was dried and purified by column chromatography on silica using AcOEt/*n*-hexane = (see **table 3.1**) as eluent. Yields are reported in the **table 3.1**.

Table 3.1 – Reaction conditions for compounds 3a-i

Product	Amine	Reaction time	AcOEt/ <i>n</i> -hexane	Yield
3a	Benzylamine	4 hours	1:1	97%
3b	S-Benzylamine	4 hours	1:1	74%
3c	R-Benzylamine	4 hours	1:1	75%
3d	1- Naphthylmethylamine	5 hours	2:3	78%
3e	1-(S)-Naphthylethylamine	10 hours	2:3	97%
3f	1-(R)-Naphthylethylamine	10 hours	2:3	96%
3g	1-(R)-Naphthylethylamine	72 hours	3:7	40%
3h	1-(S)-Naphthylethylamine	72 hours	3:7	41%
3i	1-(R)-Naphthylethylamine	72 hours	3:7	43%

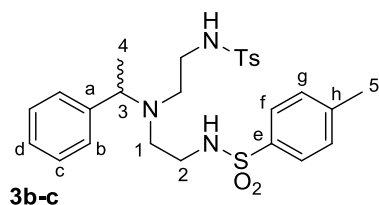


$^1\text{H NMR}$ (400 MHz; CDCl_3 ; T = 300K) δ 7.73 (d, J = 8.0 Hz, 4H, H_f), 7.29 (d, J = 8.0 Hz, 4H, H_g), 7.27-7.25 (m, 3H, H_{Ar}), 7.13 (m, 2H, H_{Ar}), 5.17 (br s, 2H, NH), 3.44 (s, 2H, H_3), 2.95 (m, 4H, H_1), 2.57 (m, 4H, H_2), 2.42 (s, 6H, H_4)

$^{13}\text{C NMR}$ (100 MHz; CDCl_3 ; T = 300K) δ 143.8 (C_h), 138.2 (C_e), 137.1 (C_a), 130.2 (C_f), 129.3 (C_b), 128.9 (C_c), 127.8 (C_d), 127.5 (C_g), 58.8 (C_3), 53.6 (C_1), 41.0 (C_2), 21.9 (C_4)

Elem. an. found: C, 60.0; H, 6.2; N, 8.6%
calculated: C, 59.9; H, 6.2; N, 8.4%

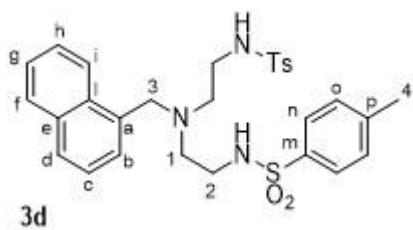
MS (EI) m/z 501 (M^+ 100%)



$^1\text{H NMR}$ (400 MHz; CDCl_3 ; T = 300K): δ 7.72 (d, J = 8.4 Hz, 4H, H_f), 7.34-7.28 (m, 7H, H_g , H_b , H_c), 7.18-7.16 (m, 2H, H_b' , H_c'), 4.85 (brs, 2H, NH), 3.73 (q, J = 6.9 Hz, 1H, H_3), 2.88 (m, 4H, H_2), 2.61 (m, 2H, H_1'), 2.43 (m, 6H, H_5), 2.42 (m, 2H, H_1), 1.30 (d, J = 6.9 Hz, 3H, H_4).

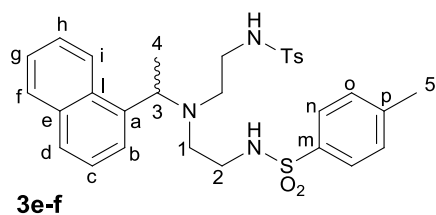
$^{13}\text{C NMR}$ (100 MHz; CDCl_3 ; T = 300K): δ 143.9 (C), 137.2 (C), 136.7 (C), 130.3 (C_g), 128.8 (C_b), 128.4 (C_c), 127.8 (C_d), 127.55 (C_f), 58.8 (C_3), 50.5 (C_1), 41.6 (C_2), 21.9 (C_5), 21.5 (C_4).

MS m/z 516.4 (M^+), 538.4 (90 + Na), 1053.1 (100 2M + Na).



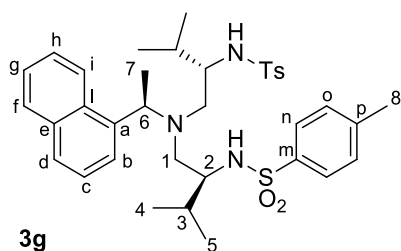
¹H NMR (300 MHz; CDCl₃; T = 300K) δ 8.14 (d, J = 8.3 Hz, 1H, H_i), 7.86 (d, J = 8.3 Hz, 1H, H_{Ar}), 7.78 (m, 1H, H_{Ar}), 7.54 (d, J = 8.0 Hz, 4H, H_n) overlapping with 7.61-7.49 (m, 2H, H_{Ar}), 7.42-7.32 (m, 2H, H_{Ar}), 7.19 (d, J = 8.0 Hz, 4H, H_o), 4.83 (bs, 2H, NH), 4.00 (br, 2H, H₃), 2.90 (m, 4H, H₁), 2.66 (m, 4H, H₂), 2.38 (s, 6H, H₄).

¹³C NMR (75 MHz; CDCl₃; T = 300K) δ 143.5 (C), 136.7 (C), 134.0 (C), 132.0 (C), 129.8 (CH), 129.0 (C_o), 127.1 (C_n), 126.3 (CH), 125.4 (CH), 123.7 (C_i), 54.2(CH₂), 40.8 (C₃), 21.6 (C₄). Signals relative to a quaternary carbon, three aromatic CH and a couple of CH₂ were not detected.



¹H NMR (400 MHz; CDCl₃; T = 300K): δ 8.36 (d, J = 8.6 Hz, 1H, H_{Ar}), 7.86 (d, J = 7.5 Hz, 1H, H_n), 7.76 (m, 1H, H_c), 7.67 (m, 1H, H_{Ar}), 7.54 (m, 1H, H_{Ar}), 7.50 (d, J = 8.0 Hz, 4H, H_o), 7.41-7.40 (m, 2H, H_b), 7.24 (d, J = 8.0, 4H, H_{Ar}), 4.69 (q, J = 6.7, 1H, H₃), 4.63 (brs, 2H, NH), 2.82-2.71 (m, 2H, H_{1'}), 2.69 (m, 4H, H₂), 2.56 (m, 2H, H₁), 2.42 (s, 6H, H₅), 1.46 (d, J = 6.7 Hz, 3H, H₄).

¹³C NMR (100 MHz; CDCl₃; T = 300K) δ 143.2 (CH), 138.3 (C_n), 136.7 (C_a), 134.9 (CH), 133.9 (C_i), 131.6 (C_p), 129.7 (CH), 128.3 (C_c), 126.6 (C_o), 124.2 (CH), 57.1 (CH), 51.1 (C₃), 41.8 (C_i), 21.5 (C₅), 12.7 (C₄).



¹H NMR (400 MHz; CDCl₃; T = 300K) δ 7.94 (m, 1H, H_i) 7.79(d, J = 8.0 Hz, 4H, H_n) overlapping with 7.79 (m, 1H, H_{Ar}), 7.73 (dd, J = 5.8 Hz, J = 3.4 Hz, 1H, H_{Ar}), 7.45-7.42 (m, 2H, H_{Ar}), 7.40-7.39 (m, 2H, H_{Ar}), 7.29 (d, J = 8.0 Hz, 4H, H_o), 4.66 (d, J = 7.9 Hz, 2H, NH), 4.59 (q, J = 6.6 Hz, 1H, H₆), 3.26 (m, 1H, H₂), 2.46 (dd, J = 13.4 Hz, J = 5.1 Hz, 2H, H₁), 2.41 (s, 6H, H₈), 1.55 (m, 2H, H₃), 1.20 (d, J = 6.6 Hz, 3H, H₇) 0.56 (d, J = 6.9 Hz, 6H, H₄), 0.19 (d, J = 6.8 Hz, 6H, H₅).

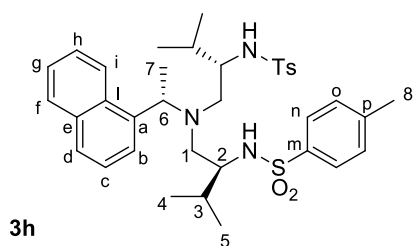
¹³C NMR (75 MHz; CDCl₃; T = 300K) δ 143.4 (C), 138.2 (C), 138.0 (C), 134.1 (C), 132.1 (C), 129.7 (C_n), 128.8 (CH), 128.2 (CH), 127.3 (C_o), 125.6 (CH), 125.5 (CH), 125.1 (CH), 125.0 (CH), 123.9 (CH), 56.6 (C₂), 53.6 (C₆), 52.3 (C₁), 27.6 (C₃), 21.6 (C₈), 19.3 (C₄), 14.8 (C₅), 12.4 (C₇).

¹⁵N NMR (40 MHz; CDCl₃; T = 300K) δ 94.0 (NHTs), 38.3 (NHC₆).

Elem. An. Found: C, 66.6; H, 7.6; N, 6.5%

Calculated: C, 66.5; H, 7.3; N, 6.5%

[α]_D²⁰ - 47.22 (c 1.37 in CHCl₃)



¹H NMR (300 MHz; CDCl₃; T = 300K) δ 8.73 (d, J = 8.2 Hz, 1H, H_i), 7.73 (d, J = 7.8 Hz, 2H, H_{Ar}), 7.70 (d, J = 8.3 Hz, 4H, H_n), 7.56 (pt, J = 8.2 Hz, 1H, H_{Ar}), 7.43-7.37 (m, 2H, H_{Ar}), 7.29 (m, 1H, H_{Ar}), 7.24 (d, J = 8.3 Hz, 4H, H_o), 5.36 (d, J = 5.4 Hz, 2H, NH), 5.13 (q, J = 6.5 Hz, 1H, H₆), 3.68 (m, 2H, H₂), 2.48-2.42 (m, 4H, H₁), overlapping with 2.42 (s, 6H, H₈), 1.76

(m, 2H, H₃), 1.48 (d, *J* = 6.5 Hz, 3H, H₇), 0.68 (d, *J* = 7.0 Hz, 6H, H₄), 0.35 (d, *J* = 7.0 Hz, 6H, H₅)

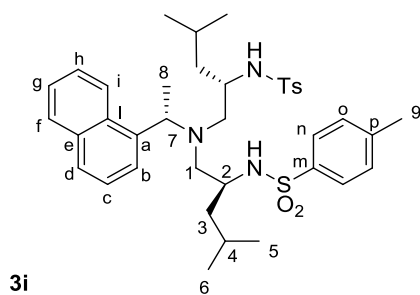
¹³C NMR (75 MHz; CDCl₃; T = 300K) δ 143.0 (C_p), 139.3 (C), 137.9 (C), 134.1 (C), 131.7 (C), 129.5 (C_n), 128.4 (CH), 127.4 (CH), 127.1 (C_o), 125.9 (CH), 125.2 (CH), 124.9 (CH), 124.6 (CH), 54.7 (C₂), 53.3 (C₆), 48.1 (C₁), 29.6 (C₃), 21.7 (C₈), 18.0 (C₄), 15.9 (C₅), 11.1 (C₇). A signal relative to an aromatic carbon was not detected.

Elem. An. Found: C, 66.4; H, 7.3; N, 6.7%

Calculated: C, 66.5; H, 7.3; N, 6.5%.

MS (EI) *m/z* 650 (M⁺+1).

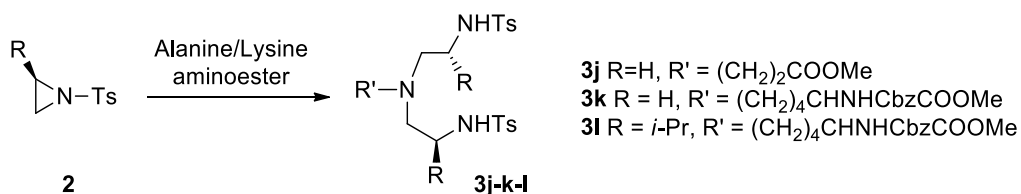
[α]_D²⁰ - 33.65 (c 0.28 in CHCl₃).



¹H NMR (300 MHz; CDCl₃) 8.02 (dd, *J* = 6.1, 3.4 Hz, 1H, H_h), 7.84-7.82 (m, 1H, H_{Ar}), 7.81 (d, *J* = 8.1 Hz, 4H, H_m), 7.77-7.74 (m, 1H, H_{Ar}), 7.46 (dd, *J* = 6.3, 3.2 Hz, 2H, H_{Ar}), 7.44 - 7.41 (m, 2H, H_{Ar}), 7.32 (d, *J* = 8.1 Hz, 4H, H_o), 4.70 (q, *J* = 6.6 Hz, 1H, H₇) 4.65-4.61 (m, 2H, NH), 3.29 (b, 2H, H₂), 2.70 (dd, *J* = 13.4, 5.3 Hz, 2H, H₁), 2.44 (s, 6H, H₉), 2.36 (dd, *J* = 13.4, 8.0 Hz, 2H, H_{1'}), 1.33 (d, *J* = 6.6 Hz, 3H, H₈), 1.28 (m, 2H, H₄), 0.93 (ddd, *J* = 13.8, 9.2, 4.6 Hz, 2H, H₃), 0.70 (ddd, *J* = 14.1, 9.1, 4.8 Hz, 2H, H_{3'}), 0.51 (d, *J* = 6.3 Hz, 6H, H_{5,6}), 0.50 (d, *J* = 6.4 Hz, 6H, H_{5',6'}).

¹³C NMR (75 MHz; CDCl₃) δ 143.66 (C_p), 138.67 (C_m), 138.58 (C_a), 134.30 (C_i), 132.60 (C_e), 129.99 (C_o), 129.19 (CH), 128.32 (CH), 127.56 (C_n), 126.26 (CH), 125.80 (C_h), 125.31 (CH), 125.24 (CH), 124.08 (CH), 57.52 (C₁), 54.25 (C₇), 51.05 (C₂), 43.28 (C₃), 24.57 (C₄), 23.31 (C_{5,6}), 21.96 (C_{5',6'}), 21.89 (C₉), 14.46 (C₈).

4.4.2 Synthesis of bis-sulfonamides 3j-k-l

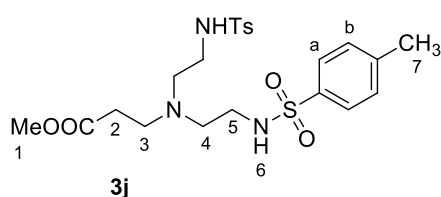


A solution of **2** (7.5 mmol in 8.0 mL of toluene) was added dropwise at 60°C over a period of 90 minutes to a suspension of aminoester hydrochloride (2.5 mmol) in toluene (4.0 mL) and CH₃CN (8.0 mL) and TEA (2.6 mmol). The resulting mixture was stirred and refluxed for 6h. The mixture was dried and purified by column chromatography on silica using AcOEt/*n*-hexane = 7:3 as eluent.

Yields: **3j** 48%

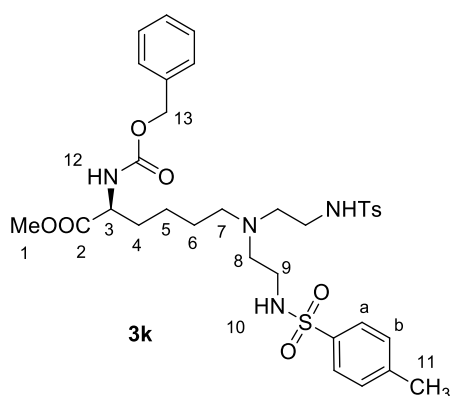
3k 69%

3l 35%



¹H NMR (300 MHz, CDCl₃) δ, ppm 7.77 (4H, d, *J* = 8.2 Hz, H_b), 7.30 (4H, d, *J* = 7.9 Hz, H_a), 5.50 (2H, m, H₆), 3.74 (3H, s, H₁), 2.88 (4H, m, CH₂), 2.50-2.33 (10H, m, H₇ + CH₂).

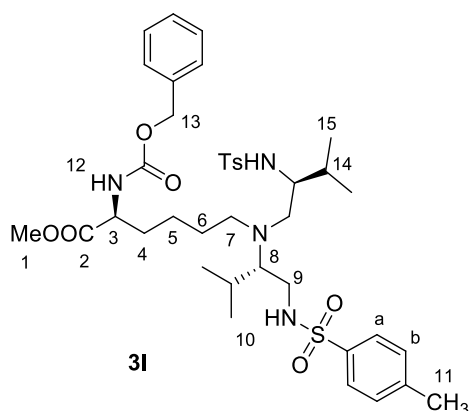
¹³C NMR (75 MHz, CDCl₃) δ, ppm 174.54 (C₂), 130.16 (C_b), 127.69 (C_a), 53.71 (C), 52.70 (C₁), 48.63 (C), 40.93 (C), 32.31 (C), 21.89 (C₇).



¹H NMR (400 MHz, CDCl₃) δ, ppm 7.75 (4H, d, *J* = 8.2 Hz, H_atosile), 7.35-7.28 (9H, m, H_b + H_{cbz}), 5.49 (1H, d, *J* = 8.1 Hz, H₁₂), 5.12 (2H, s, H₁₃), 4.35 (1H, m, H₃), 3.73 (3H, s, H₁), 3.01 (3H, br, CH₂), 2.63 (3H, br, CH₂), 2.44 (8H, m, H₁₁ + CH₂), 1.78 (2H, m, H₄), 1.64 (2H, m, H₅), 1.41 (2H, m, CH₂), 1.32-1.23 (2H, m, CH₂).

¹³C NMR (100 MHz, CDCl₃) δ, ppm 172.96 (C₂), 158.45 (C₁₃), 143.71 (C_{quaternary}tosyl), 137.01(C_{quaternary}Cbz), 129.93 (C_b), 128.68 (C_{Cbz}), 127.27 (C_a), 67.25 (C₁₃), 60.37 (C₃), 53.70 (CH₂), 52.71 (C₁), 40.47 (CH₂), 32.55 (C₄), 32.29 (C₅), 22.85 (CH₂), 21.66 (C₁₁), 21.19 (CH₂), 14.35 (CH₂).

[α]_D²⁰ 5.60° (c 0.75 in CH₂Cl₂)

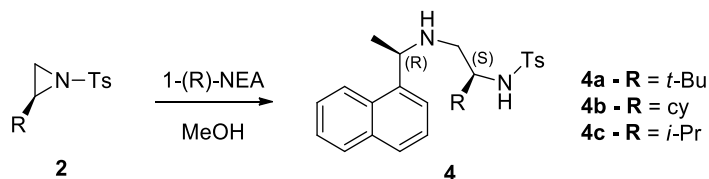


¹H NMR (400 MHz, CDCl₃) δ 7.79 (d, *J* = 8.2 Hz, 4H, H_a), 7.33 (m, 5H, H_{Ar}), 7.26 (m, 6H, H_{Ar}), 5.41 (m, 3H, NH_{12,10}), 5.11 (s, 2H, H₁₃), 4.38 (dd, *J* = 14.8, 6.2 Hz, 1H, H₃), 3.74 (s, 3H, H₁), 3.48 – 3.32 (m, 2H, CH₂), 2.40 (s, 8H, H₁₁ overlapping with CH₂), 2.29 (dd, *J* = 13.1, 5.0 Hz, 2H, CH₂), 2.20 (m, 1H, CH₂), 1.95 – 1.75 (m, 3H, H₈ + CH₂), 1.72 – 1.59 (m, 1H, CH₂), 1.41 – 1.16 (m, 6H, CH₂), 0.76 (dd, *J* = 10.8, 6.9 Hz, 12H, H₁₅)

¹³C NMR (100 MHz, CDCl₃) δ 143.0 (C_{quaternary}tosyl), 139.1 (C_{quaternary}Cbz), 129.6 (C_b), 128.7 (CH_{Cbz}), 128.3 (CH_{Cbz}), 127.1 (C_a), 67.1 (C₁₃), 56.2 (CH), 54.0 (CH₂), 53.9 (C₃), 53.4 (CH₂), 52.5 (C₁₃), 32.7 (C₄), 30.2 (C₁₄), 25.3 (CH₂), 23.1 (CH₂), 21.7 (C₁₁), 17.9 (C₁₅)

4.5 Mono-sulfonamides

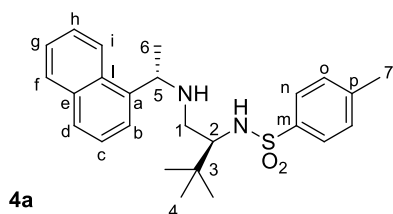
4.5.1 Synthesis of monosulfonamides 4a-c



Aziridine **2** (12.9 mmol) was dissolved in MeOH (4.2 ml) and 1-(*R*)-naphthylethylamine (13.2 mmol) is added. The solution was allowed to react to reflux for 8 hours.

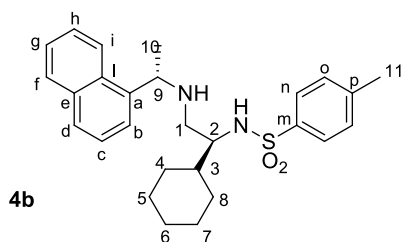
The crude was obtained by concentrating the solution in vacuum and was purified, if needed, by chromatographic column (*n*-*n*-hexane/AcOEt = 7:3).

Yields **4a:** 95%
 4b: 93%
 4c: 71%



¹H NMR (400 MHz; CDCl₃, 300 K) δ 8.02 (d, *J* = 7.9 Hz, 1H, H_h), 7.89-7.87 (m, 1H, H_{Ar}), 7.84 (d, *J* = 8.2 Hz, 2H, H_n), 7.76 (d, *J* = 8.1 Hz, 1H, H_{Ar}), 7.55-7.46 (m, 2H, H_{Ar}), 7.41 (d, *J* = 6.9 Hz, 1H, H_{Ar}), 7.29 (d, *J* = 8.1 Hz, 2H, H_o), 5.05 (b, 1H, NH), 4.37 (b, 1H, H₅), 3.16 (dd, *J* = 4.8 Hz, 5.7 Hz, 1H, H₂), 2.52-2.43 (m, 2H, H₁), 2.41 (s, 3H, H₇), 1.37 (d, *J* = 6.3 Hz, 3H, H₆), 0.79 (s, 9H, H₄). One NH signal is too broad to be detected.

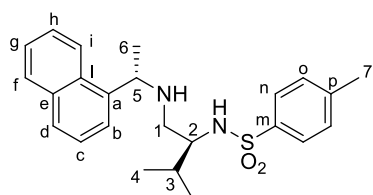
¹³C NMR (100 MHz; CDCl₃, 300 K) δ 143.27 (C_p), 138.43 (C_m), 133.95 (C_{Ar}), 131.12 (C_{Ar}), 129.62 (C_n), 129.04 (C_{Ar}), 127.44 (C_{Ar}), 127.19 (C_o), 125.95 (C_{Ar}), 125.66 (C_{Ar}), 125.50 (C_{naphthyl}), 122.58 (C_h), 122.44 (C_{Ar}), 61.78 (C₂), 53.72 (C₅), 47.59 (C₁), 34.61 (C₃), 26.98 (C₄), 23.52 (C₆), 21.49 (C₇).



4b

¹H NMR (400 MHz; CDCl₃; T = 300K) δ 8.03-8.00 (m, 1H, H_h), 7.89 (m, 1H, H_{Ar}), 7.78-7.75 (m, 3H, H_n and H_{Ar}), 7.52 (m, 4H, H_{Ar}), 7.27 (2H, d, J = 8.2 Hz, H_o), 5.09 (b, 1H, NH), 4.38 (pd, 1H, J = 6.4 Hz, H₉), 3.07 (pd, J = 4.5 Hz, 1H, NH), 2.51-2.37 (m, 3H, H₁ and H₂), 2.42 (3H, s, H₁₁), 1.68-1.58 (5H, m), 1.51-1.47 (m, 1H), 1.38 (3H, d, J = 6.5 Hz, H₁₀), 1.14-1.01 (m, 3H), 0.85-0.76 (m, 2H)

¹³C NMR (100 MHz; CDCl₃) δ 143.18 (C_p), 140.18 (C_a), 137.98 (C_m), 133.97 (C_i), 131.13 (C_e), 129.56 (C_n), 129.03 (C_{Ar}), 127.49 (C_{Ar}), 127.16 (C_o), 125.93 (C_{Ar}), 125.59 (C_{Ar}), 125.52 (C_{Ar}), 122.66 (C_h), 122.55 (C_{Ar}), 58.17 (C₂), 53.35 (C₉), 47.31 (C₁), 40.14 (C₃), 29.24 (C_{Cy}), 28.85 (C_{Cy}), 26.19 (C_{Cy}), 26.09 (C_{Cy}), 26.03 (C_{Cy}), 23.24 (C₁₀), 21.49 (C₁₁)

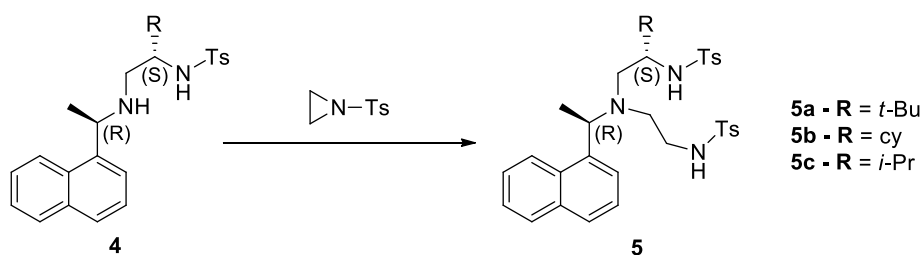


4c

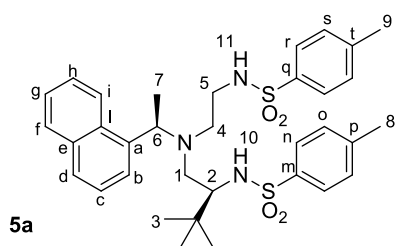
¹H NMR (300 MHz; CDCl₃; T = 300K) δ 8.03 (m, 1H, H_i), 7.89 (m, 1H, H_{Ar}), 7.78 (d, J = 8.4 Hz, 2H, H_n) overlapping with 7.79-7.75 (m, 1H, H_{Ar}), 7.52-7.45 (m, 4H, H_{Ar}), 7.25 (d, J = 8.4 Hz, 2H, H_o), 5.22 (br, 1H, NH), 4.35 (q, J = 6.6 Hz, 1H, H₅), 3.08 (m, 1H, H₂), 2.46-2.42 (m, 2H, H₁), 2.40 (s, 3H, H₇), 1.85 (dh, J = 13.4 Hz, J = 6.8 Hz, 1H, H₃), 1.36 (d, J = 6.6 Hz, 3H, H₆), 0.81 (d, J = 6.8 Hz, 3H, H₄), 0.78 (d, J = 6.8 Hz, 3H, H₄) One NH signal is too broad to be detected.

¹³C NMR (75 MHz; CDCl₃; T = 300K) δ 143.2 (C_{Ar}), 140.8 (C_{Ar}), 138.2 (C_{Ar}), 134.1 (C_{Ar}), 131.3 (C_{Ar}), 129.6 (C_o), 129.1 (C_{Ar}), 127.4 (C_{Ar}), 127.2 (C_{Ar}), 125.9 (C_{Ar}), 125.7 (C_{Ar}), 125.5 (C_{Ar}), 122.8 (C_i), 122.6 (C_{Ar}), 59.0 (C₂), 53.3 (C₆), 47.4 (C₁), 30.4 (C₃), 23.5 (C₇), 21.5 (C₈), 18.8 (C₄), 18.4 (C₅).

4.5.2 Monosubstituted bis-sulfonamides



Monoamine **4** (0.33mmol) was dissolved in MeOH (1ml) and N-Ts aziridine (0.33mmol) was added. The solution was allowed to react to reflux for 16 hours. The crude was obtained by concentrating the solution in vacuum and purified by chromatographic column (*n*-hexane/AcOEt = 7:3).



¹H NMR (300 MHz; CDCl₃) δ 8.18 (d, *J* = 8.4 Hz, 1H, H_h), 7.87-7.82 (m, 5 H, H_n, H_r, H_{Ar}), 7.76 (d, *J* = 8.0 Hz, 1H, H_{Ar}), 7.56-7.51 (m, 2H, H_{Ar}), 7.51-7.45 (m, 2H, H_{Ar}), 7.33-7.27 (m, 4H, H_o, H_s), 6.31 (b, 1H, NH₁₁), 4.84 (q, *J* = 6.8 Hz, 1H, H₆), 4.45 (d, *J* = 8.1 Hz, 1H, NH₁₀), 3.42-3.38 (m, 1H, H₂), 3.07-3.02 (m, 1H, H₅), 2.99-2.91 (m, 2H, H₅, H₄), 2.75-2.68 (m, 2H, H₄, H₁), 2.44 (s, 6H, H₈, H₉), 2.42-2.39 (m, 1H, H₁), 1.52 (d, *J* = 6.8 Hz, 3H, H₇), 0.54 (s, 9H, H₃).

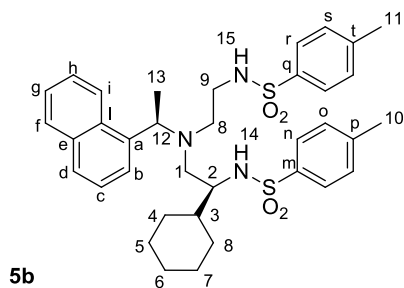
¹³C NMR (75 MHz; C₆D₆) δ 143.32 (C_p, C_t), 139.55 (C_m), 139.46 (C_a), 137.84 (C_q), 134.24 (C_i), 132.33 (C_e), 129.92 (C_o), 129.83 (C_s), 129.21 (CH), 127.93 (CH), 127.59 (C_n), 127.43 (C_r), 126.56 (CH), 125.90 (CH), 125.64 (CH), 124.93 (CH), 123.82 (C_h), 62.41 (C₂), 55.17 (C₆), 54.20 (C₁), 51.27 (C₄), 42.11 (C₅), 34.90 (C), 27.81 (C₃), 27.33 (C₃), 27.01 (C₃), 21.90 (C₈, C₉), 20.00 (C₇)

Elem. An. Found: C, 65.41; H, 7.10; N, 6.71

Calculated: C, 65.67; H, 6.97; N, 6.76

[α]_D²⁰ -15.41 (in CHCl₃)

MS (ESI) *m/z* 725.4 (M⁺), 747.5 (M⁺Na)



¹H NMR (400 MHz; CDCl₃) δ 8.13 (d, *J* = 8.3 Hz, 1H, H_h), 7.86 (d, *J* = 7.3 Hz, 1H, H_{Ar}), 7.77 (dd, *J* = 5.5 Hz, 3.9 Hz, 1H, H_{Ar}), 7.73 (d, *J* = 8.2 Hz, 2H, H_n), 7.64 (d, *J* = 8.2 Hz, 2H, H_r), 7.57-7.52 (m, 1H, H_{Ar}), 7.53-7.48 (m, 1H, H_{Ar}), 7.42-7.40 (m, 1H, H_{Ar}), 7.41 (s, 1H, H_{Ar}), 7.28 (m, 4H, H_o, H_s), 4.93 (t, *J* = 5.5 Hz, 1H, H₁₅), 4.63 (q, *J* = 6.6 Hz, 1H, H₁₂), 4.46 (d, *J* = 7.9 Hz, 1H, H₁₄), 3.07 (m, 1H, H₂), 3.03-2.98 (m, 1H, H₉), 2.91-2.83 (m, 1H, H₉), 2.83-2.76 (m, 1H, H₈), 2.70-2.64 (m, 1H, H₈), 2.53 (dd, *J* = 13.3, 8.4 Hz, 1H, H₁), 2.43 (s, 6H, H₁₀, H₁₁), 2.38 (dd, *J* = 13.3, 5.8 Hz, 1H, H₁), 1.39 (d, *J* = 6.6 Hz, 3H, H₁₃), 1.44 (m, 1H, H₇), 1.36 (m, 1H, H₆), 1.23 (m, 1H, H₅), 1.05 (m, 1H, H₈), 0.99 (m, 1H, H₃), 0.77-0.73 (m, 2H, H₇, H₆), 0.63 (m, 1H, H₈), 0.56 (m, 1H, H₄), 0.39 (ddd, *J* = 3.1, 12.1 Hz, 1H, H₄), 0.19 (m, 1H, H₅)

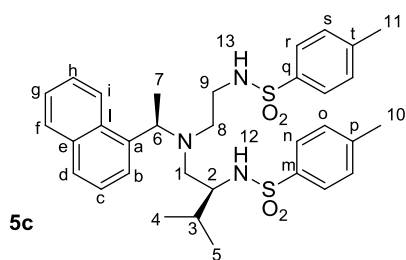
¹³C NMR (100 MHz; CDCl₃) δ 143.28 (C_p), 143.14 (C_t), 138.01 (C_a), 137.86 (C_m), 137.15 (C_q), 134.07 (C_i), 131.84 (C_e), 129.60 (C_o), 129.57 (C_s), 128.97 (CH), 128.20 (CH), 127.18 (C_m), 127.03 (C_r), 126.23 (CH), 125.71 (CH), 124.94 (CH), 124.75 (CH), 123.60 (C_h), 57.23 (C₂), 55.51 (C₁₂), 52.58 (C₁), 51.55 (C₈), 41.45 (C₉), 38.09 (C₃), 29.41 (C_{cy}), 26.17 (C_{cy}), 28.08 (C_{cy}), 25.97 (C_{cy}), 25.66 (C_{cy}), 21.50 (C₁₀, C₁₁), 12.92 (C₁₃)

Elem. An. Found: C, 66.91; H, 6.88; N, 6.37%

Calculated: C, 66.74; H, 7.00; N, 6.49%

[α]_D²⁰ -13.18 (in CHCl₃)

MS (ESI) m/z 670.6 (M⁺Na)



$^1\text{H NMR}$ (300 MHz; CDCl_3) δ 8.08 (d, $J = 8.2$ Hz, 1H, H_i), 7.85 (m, 1H, H_f), 7.77 (m, 1H, H_c), 7.71 (d, $J = 8.2$ Hz, 2H, H_n), 7.59 (d, $J = 8.2$ Hz, 2H, H_r), 7.52 (m, 2H, H_g , H_h), 7.42 (m, 2H, H_b , H_d), 7.28-7.24 (m, 4H, H_o , H_s), 4.82 (m, 1H, NH_{13}), 4.63 (q, $J = 6.6$ Hz, 1H, H_6), 4.30 (d, $J = 7.5$ Hz, 1H, NH_{12}), 3.14 (m, 1H, H_2), 2.83 (m, 2H, H_9 , $\text{H}_{9'}$), 2.70 (m, 2H, H_8 , $\text{H}_{8'}$), 2.46 (m, 2H, H_1 , $\text{H}_{1'}$), 2.42 (br, 6H, H_{10} , H_{11}), 1.40 (d, $J = 6.6$ Hz, 3H, H_7) overlapping with 1.41-1.39 (m, 1H, H_3), 0.44 (d, $J = 6.9$ Hz, 6H, H_4), 0.17 (d, $J = 6.8$ Hz, 6H, H_5).

$^{13}\text{C NMR}$ (75 MHz; CDCl_3) δ 143.5 (C_n), 143.2 (C_q), 138.3 (C_p), 137.9 (C_a), 137.2 (C_t), 134.2 (C), 131.9 (C_i), 129.8 (C_s), 129.7 (C_o), 129.1 (C_f), 128.4 (CH), 127.3 (C_r), 127.2 (C_n), 126.4 (CH), 125.9 (CH), 125.2 (CH), 124.9 (CH), 123.7 (C_i), 57.4 (C_2), 55.7 (C_6), 53.5 (C_1), 51.4 (C_8), 41.6 (C_9), 28.4 (C_3), 21.7 ($\text{C}_{11,10}$), 18.6 (C_4), 15.6 (C_5), 14.0 (C_7).

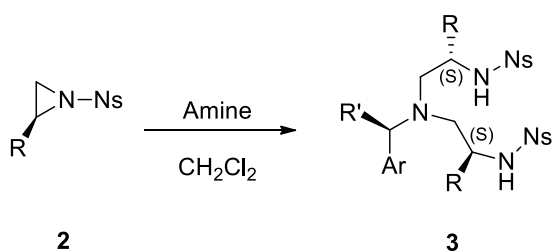
Elem. An. Found: C, 65.61; H, 7.02; N, 6.58%

Calculated: C, 65.21; H, 6.80; N, 6.91%

$[\alpha]_D^{20}$ -32.88 (c 0.420 in CHCl_3)

MS (ESI) m/z 608 (M+1)

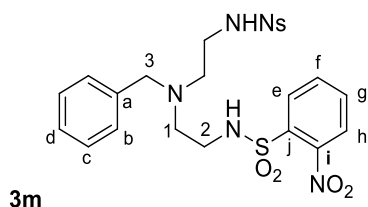
4.5.3 Synthesis of Ns-protected bis-sulfonamides



3m - R = H, R' = H, PG = Ns, Ar = Phenyl
3n - R = i-Pr, R' = (R)-Me, PG = Ns, Ar = Naphthyl
3o - R = H, R' = (R)-Me, PG = Ns, Ar = Naphthyl
3p - R = H, R' = (R)-Me, PG = Ns, Ar = Phenyl

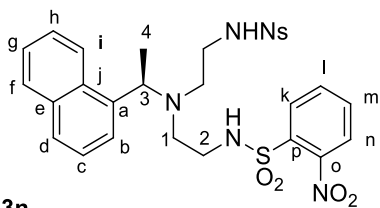
Amine (4.0 mmol – see **table 3.2**) was added to a solution of aziridine **2** (8.0 mmol) in distilled toluene (20 mL). The solution was allowed to reflux for (see **table 3.2**) and was monitored by TLC. The crude was recovered by concentrating the solution and was purified by chromatographic column (see **table 3.2**).

Product	Amine	Reaction time	AcOEt/ <i>n</i> -hexane	Yield
3m	Benzylamine	6 hours	7:3	70%
3n	1-(R)-Naphthylethylamine	40 hours	6:4	58%
3o	1-(R)-Naphthylethylamine	6 hours	8:2	60%
3p	1-(R)-Methyl Benzylamine	6 hours	7:3	75%



¹H NMR (300 MHz; CDCl₃) δ 8.04 (m, 2H, H₅), 7.83 (m, 2H, H₆), 7.79-7.66 (m, 4H, H_{Ar}), 7.37-7.04 (m, 5H, H_{Ar}), 5.63 (s, 2H, NH), 3.07 (t, J = 6.0 Hz, H₂), 2.63 (t, J = 6.0 Hz, H₁)

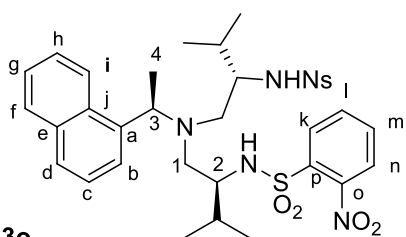
¹³C NMR (75 MHz; CDCl₃) δ 148.46 (C_i), 138.15 (C_a), 134.14 (C_g), 133.50 (C_j), 133.25 (C_f), 131.26 (C_h), 129.29 (CH), 129.02 (CH), 127.95 (CH), 125.91 (C_e), 59.4 (C₃), 54.02 (C₁), 41.79 (C₂)



3n

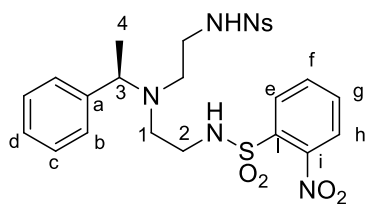
¹H NMR (300 MHz; CDCl₃) δ 8.06 (dd, *J* = 5.8, 3.4 Hz, 2H, H_h), 7.84 (dd, *J* = 5.8, 3.4 Hz, H_e), 7.72 (dd, *J* = 5.8, 3.4 Hz, 4H, H_{f,g}), 7.37-7.08 (m, 5H, H_{Ar}), 5.64 (s, 2H, NH), 3.58 (s, 1H, H₃), 3.09 (br, *J* = 6.0 Hz, H₂), 2.68 (br, *J* = 6.0 Hz, H₁)

¹³C NMR (100 MHz; CDCl₃) δ 148.2 (C), 133.9 (CH), 133.8 (CH), 133.3 (C), 133.0 (CH), 131.1 (CH), 129.1 (CH), 125.6 (CH), 59.4 (CH₂), 54.2 (CH₂), 42.1 (CH₂)



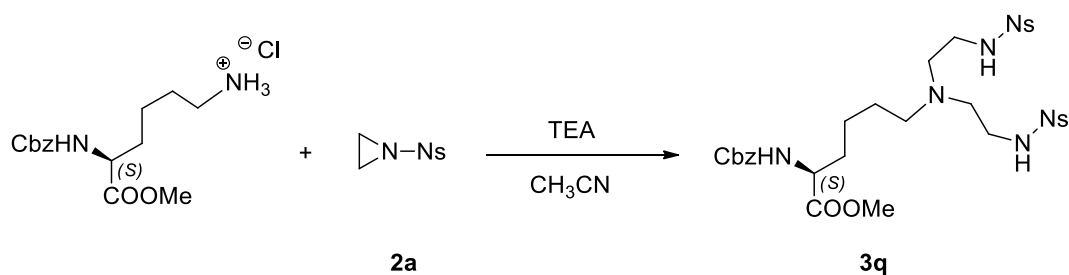
3o

¹H NMR (400 MHz, CDCl₃) δ 8.18 – 8.10 (m, 2H), 8.02 (d, *J* = 9.4 Hz, 1H), 7.87 (dd, *J* = 5.6, 3.6 Hz, 2H), 7.85 – 7.79 (m, 1H), 7.75 (ddd, *J* = 13.9, 6.2, 2.9 Hz, 4H), 7.46 (td, *J* = 6.5, 3.6 Hz, 4H), 5.16 (d, *J* = 7.7 Hz, 2H), 4.68 (q, *J* = 6.6 Hz, 1H), 3.45 (br, 1H), 2.57 (ddd, *J* = 18.0, 13.5, 7.4 Hz, 4H), 1.65 – 1.59 (m, 2H), 1.27 (d, *J* = 6.7 Hz, 3H), 0.53 (d, *J* = 6.9 Hz, 6H), 0.22 (d, *J* = 6.8 Hz, 6H).



3p

¹H NMR (300 MHz, CDCl₃) δ 8.07 (dd, *J* = 5.8, 3.3 Hz, 2H), 7.86 (q, *J* = 4.6, 3.6 Hz, 2H), 7.80 – 7.68 (m, 4H), 7.30 (m, 5H), 5.55 (s, 2H), 3.83 (q, *J* = 6.7 Hz, 1H), 3.01 (s, 4H), 2.71 (dt, *J* = 12.2, 5.9 Hz, 2H), 2.60 (dt, *J* = 13.2, 6.1 Hz, 2H), 1.37 (d, *J* = 6.8 Hz, 3H).

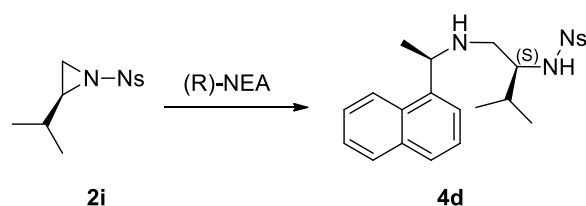


A solution of aziridine **2a** (12.0 mmol) in toluene (10.0 mL) was added dropwise at RT over a period of 90 minutes to a solution of TEA (4.1 mmol) and *N*(α)-Cbz lysine aminoester hydrochloride (4.0 mmol) in toluene (10.0 mL) and CH₃CN (5.0 mL). The solution was allowed to reflux for 10h and was monitored by TLC. The crude was recovered by concentrating the solution and **3q** was purified by chromatographic column using AcOEt/*n*-hexane 8:2 as eluent.

Yield: 25%

¹H NMR (300 MHz, CDCl₃) δ 8.20 – 8.12 (m, 2H), 7.93 – 7.85 (m, 2H), 7.80 – 7.74 (m, 4H), 5.78 (s, 2H), 3.77 (t, *J* = 5.0 Hz, 5H), 3.28 (q, *J* = 5.5 Hz, 5H), 1.76 (br, 5H).

4.5.4 Synthesis of Ns-protected mono-sulfonamide 4d

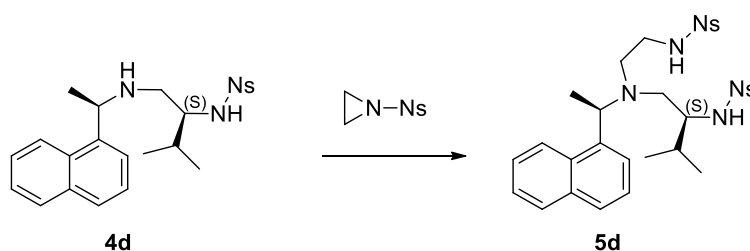


A solution of **2i** (2.5 mmol in 5.0 mL of toluene) was added to a solution of (R)-naphthyl ethylamine (2.5 mmol) in toluene (5.0 mL) and CH₃CN (5.0 mL). The resulting mixture was stirred and refluxed for 16h. The mixture was dried and purified by column chromatography on silica using AcOEt/*n*-hexane = 3:7 as eluent.

Yield: 65%

¹H NMR (400 MHz, CDCl₃) δ 8.22 – 8.16 (m, 2H), 8.13 (dd, *J* = 5.8, 3.4 Hz, 1H), 7.90 (dd, *J* = 5.8, 2.7 Hz, 1H), 7.79 – 7.66 (m, 9H), 5.57 (d, *J* = 8.0 Hz, 1H), 3.98 (dd, *J* = 5.8, 2.4 Hz, 1H), 3.60 (dd, *J* = 8.8, 4.5 Hz, 1H), 3.51 (qd, *J* = 9.4, 4.6 Hz, 2H), 2.82 (m, 4H), 2.32 (d, *J* = 3.7 Hz, 3H), 2.03 (dd, *J* = 13.5, 6.7 Hz, 1H), 1.68 – 1.64 (m, 1H), 1.63 – 1.52 (m, 6H).

4.5.5 Synthesis of Ns-protected mono-substituted bisulfonamide 5d



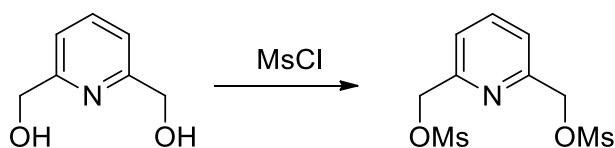
A solution of N-Ts aziridine (2.1 mmol in 5.0 mL of toluene) was added to a solution of **4e** (2.1 mmol) in toluene (5.0 mL). The resulting mixture was stirred and refluxed for 8h. The mixture was dried and **5e** was purified by column chromatography on silica using AcOEt/*n*-hexane = 3:7 as eluent.

Yield: 82%

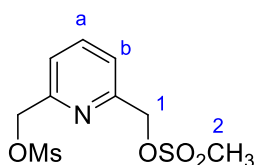
¹H NMR (300 MHz, CD₂Cl₂) δ 8.18 (d, *J* = 8.3 Hz, 1H), 8.10 (d, *J* = 7.5 Hz, 1H), 8.07 – 7.99 (m, 1H), 7.85 – 7.63 (m, 9H), 7.58 – 7.36 (m, 4H), 5.58 (br, 1H), 5.17 (d, *J* = 7.2 Hz, 1H), 4.70 (q, *J* = 6.3 Hz, 1H), 3.29 (br, *J* = 7.0 Hz, 1H), 3.11 (s, 2H), 2.92 (dd, *J* = 11.2, 5.6 Hz, 2H), 2.68 (dd, *J* = 13.4, 8.4 Hz, 1H), 2.51 (dd, *J* = 13.5, 5.8 Hz, 1H), 1.46 (d, *J* = 6.5 Hz, 3H), 0.34 (d, *J* = 6.9 Hz, 3H), 0.11 (d, *J* = 6.8 Hz, 3H).

4.6 Synthesis of macrocycles

4.6.1 Synthesis of 2,6-bis (OMs-methyl)-pyridine

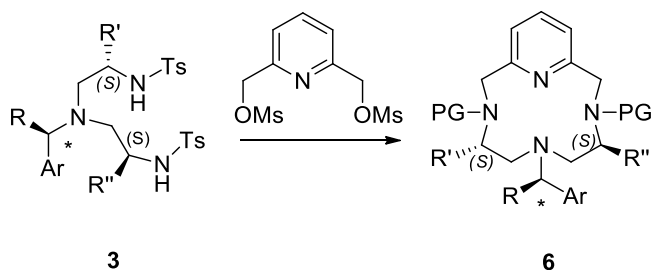


2,6-bismethanolpyridine (15.6 mmol) was suspended in AcOEt (45.0 mL) and TEA (10.9 mL, 78.0 mmol) was added. The temperature was set to 0°C and MsCl (3.6 mL, 46.7 mmol) was added dropwise. After 15', the reaction was quenched with a saturated NaHCO₃ (50 mL) solution in water and the product was extracted with AcOEt (3 x 40.0 mL). The organic layers were treated with Na₂SO₄ and concentrated in vacuum giving the final product as white powder (13.2 mmol, 85%).



¹H NMR (400 MHz; CDCl₃; T = 300 K) δ 7.88 (t, J = 7.8 Hz, 1H, H_a), 7.52 (d, J = 7.8 Hz, 2H, H_b), 5.36 (s, 4H, H₁), 3.13 (s, 6H, H₂).

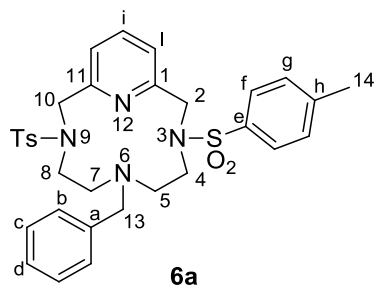
4.6.2 Synthesis of macrocycles 6a-q



- 6a** - Ar = Phenyl, R = R' = R'' = H, PG = Ts
6b - Ar = Phenyl, R = (S)-Me, R' = R'' = H, PG = Ts
6c - Ar = Phenyl, R = (R)-Me, R' = R'' = H, PG = Ts
6d - Ar = Naphthyl, R = R' = R'' = H, PG = Ts
6e - Ar = Naphthyl, R = (S)-Me, R' = R'' = H, PG = Ts
6f - Ar = Naphthyl, R = (R)-Me, R' = R'' = H, PG = Ts
6g - Ar = Naphthyl, R = (R)-Me, R' = R'' = i-Pr, PG = Ts
6h - Ar = Naphthyl, R = (S)-Me, R' = R'' = i-Pr, PG = Ts
6i - Ar = Naphthyl, R = (R)-Me, R' = R'' = i-Bu, PG = Ts
6j - Ar = Naphthyl, R = (R)-Me, R' = t.Bu, R'' = H, PG = Ts
6k - Ar = Naphthyl, R = (R)-Me, R' = Cy, R'' = H, PG = Ts
6l - Ar = Naphthyl, R = (R)-Me, R' = i-Pr, R'' = H, PG = Ts
6m - Ar = Phenyl, R = R' = R'' = H, PG = Ns
6n - Ar = Naphthyl, R = (R)-Me, R' = R'' = H, PG = Ns
6o - Ar = Naphthyl, R = (R)-Me, R' = R'' = i-Pr, PG = Ns
6p - Ar = Phenyl, R = (S)-Me, R' = R'' = H, PG = Ns
6q - Ar = Naphthyl, R = (R)-Me, R' = H, R'' = i-Pr, PG = Ns

2,6-(bis-mesyloxy)pyridine (1.5 mmol) in distilled CH₃CN (9 mL) was added dropwise to a suspension of K₂CO₃ (4.5 mmol) and bisulfonamide **3** (1.5 mmol) in distilled CH₃CN (25 mL). The reaction was allowed to react to reflux for (see table for reaction time). The reaction mixture was then quenched with water (25 mL) and washed with AcOEt (3 x 25 mL). The organic phases were concentrated in vacuum and the crude was purified by (see table).

Product	Reaction time	Purification	Yield	Product	Reaction time	Purification	Yield
6a	11 hours	Cristallized by layering <i>n</i> -hexane on warm AcOEt	88%	6j	35 hours	Column (<i>n</i> -hexane/AcOEt = 7:3)	47%
6b	11 hours	As for 6a	72%	6k	70 hours	As for 6j	48%
6c	11 hours	As for 6a	73%	6l	22 hours	As for 6k	55%
6d	45 hours	Column (Toluene/CH ₂ Cl ₂ /iPrOH = 90:10:5)	51%	6m	5 hours	Column (CH ₂ Cl ₂ /MeOH 10:0.3)	80%
6e	10 hours	As for 6a	80%	6n	5 hours	As for 6m	58%
6f	10 hours	As for 6a	78%	6o	32 hours	-	50%
6g	40 hours	Column (<i>n</i> -hexane/AcOEt = 6:4)	47%	6p	8 hours	-	85%
6h	53 hours	Column (<i>n</i> -hexane/CH ₂ Cl ₂ /iPrOH = 80:17.5:2.5)	50%	6q	15 hours	-	68%
6i	24 hours	As for 6h	67%				



¹H NMR (400 MHz; CDCl₃; T = 300 K): δ 7.78 (t, J = 7.7 Hz, 1H, H_i), 7.61 (d, J = 8.0 Hz, 4H, H_f), 7.38 (d, J = 7.7 Hz, 2H, H_i), 7.34–7.32 (m, 3H, H_{Ph}), 7.27 (d, J = 8.0 Hz, 4H, H_g), 7.20 (m, 2H, H_{Ph}), 4.37 (m, 4H, H₁₀ and H₂), 3.52 (s, 2H, H₁₃), 3.13 (m, 4H, H₄ and H₈), 2.45 (s, 6H, H₁₄), 2.32 (m, 4H, H₅ and H₇).

¹³C NMR (100 MHz; CDCl₃; T = 300 K): δ 154.9 (C₁), 143.3 (C_h), 139.2 (C_e), 138.8 (C_i), 136.0 (C_a), 129.7 (C_g), 128.6 (C_{Ph}), 128.3 (C_{Ph}), 128.2 (C_{Ph}), 127.1 (C_f), 124.0 (C_l), 59.4 (C₁₃), 54.3 (C₅), 50.0 (C₂), 44.2 (C₄), 21.5 (C₁₄).

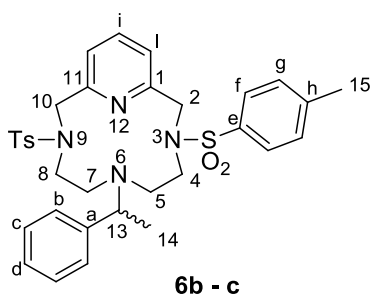
¹⁵N NMR (40 MHz; CDCl₃; T = 300 K): δ 312 (N₁₂), 94 (N-Ts), 32 (N₆).

Elem. an. Found: C, 63.6; H, 6.2; N, 9.2%

Calculated: C, 63.6; H, 6.0; N, 9.3%

MS (FAB) m/z (%) 605 (80) [MH]⁺, 449 (100) [M – Ts]⁺

UV-vis λ_{max} [nm], (log ε) = 241 (4.19); 263 (3.93) nm. (c 5.2 10⁻⁵ mol/L in CHCl₃ in 1 cm cuvettes)



¹H NMR (400 MHz; CDCl₃; T = 300 K): δ 7.78 (t, J = 7.7 Hz, 1H, H_n), 7.57 (d, J = 8.1 Hz, 4H, H_h), 7.40 (d, J = 7.7 Hz, 2H, H_o), 7.34–7.32 (m, 3H, H_{Ar}), 7.26 (d, J = 8.1 Hz, 4H, H_{Ar}), 7.20 (m, 2H, H_{Ar}), 4.32 (m, 4H, H₂ and H₁₀), 3.58 (q, J = 6.6 Hz, 1H, H₁₃), 3.13 (m, 2H, H₅), 3.00–2.92 (m, 2H, H₇), 2.44 (s, 6H, H₁₅), 2.23–2.19 (m, 4H, H₄ and H₈), 1.24 (d, J = 6.6 Hz, 3H, H₁₄).

¹³C NMR (75 MHz, CDCl₃; T = 300 K) δ 155.3 (C), 145.4 (C), 139.2 (C_n), 136.2 (CH), 130.1 (CH), 128.7 (CH), 127.6 (C_i), 127.5 (C_f), 127.3 (C_h), 124.6 (C_o), 61.7 (CH), 54.8 (C₂), 50.1 (C₄), 45.7 (C₅), 21.9 (C₁₅), 20.5 (C₁₄). One signal relative to an aromatic quaternary carbon was not detected.

¹⁵N NMR (40 MHz; CDCl₃; T = 300 K): δ 312 (N₁₂), 95 (N-Ts), 41 (N₆).

Elem. An. Found: C, 64.0; H, 6.2; N, 9.1%

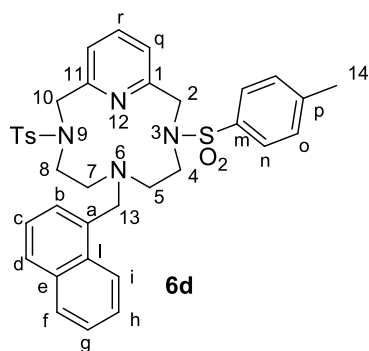
Calculated: C, 64.05; H, 6.2; N, 9.05%.

MS m/z 619 (M⁺100%), 516 (45).

IR ν (cm⁻¹) 1743.6 (w), 1594.1 (w), 1492.0 (w), 1460.1 (w), 1344.6 (m), 1160.6 (s).

[α]_D²⁰ -50 (c 1 in CHCl₃) (ligand **6b**).

50 (c 1 in CHCl₃) (ligand **6c**).

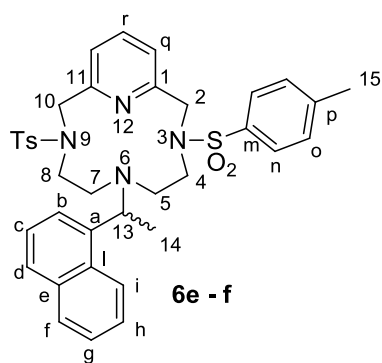


¹H NMR (300 MHz; CDCl₃; T = 300 K) δ 8.11 (d, J = 8.1 Hz, 1H, H_i), 7.90-7.83 (m, 2H, H_{Ar}), 7.76 (pst, J = 7.8 Hz, 1H, H_r), 7.50 (d, J = 8.2 Hz, 4H, H_n), overlapping with 7.52-7.23 (m, 6H, H_{Ar}), 7.19 (d, J = 8.2 Hz, 4H, H_o), 4.31 (br, 4H, H₂), 3.93 (br, 2H, H₁₃), 3.07 (m, 4H, H₄), 2.39 (s, 6H, H₁₄) overlapping with 2.36 (m, 4H, H₅).

¹³C NMR (75 MHz, CDCl₃; T = 400 K) δ 155.0 (C), 143.3 (C), 138.8 (C_r), 135.9 (C), 134.5 (C), 133.9 (C), 129.7 (C_o), 128.4 (C), 128.1 (C), 127.0 (C_n), 125.6 (C), 125.6 (C), 125.3 (C), 124.7 (C_i), 124.0 (C), 58.1 (C₁₃), 54.3 (C₂), 50.4 (C₅), 44.3 (C₄), 21.5 (C₁₄). A signal relative to an aromatic quaternary carbon and an aliphatic carbon were not detected.

Elem. An. Found: C, 66.2; H, 5.8; N, 8.4%

Calculated: C, 66.0; H, 5.8; N, 8.6%.



$^1\text{H NMR}$ (300 MHz; CDCl_3 ; T = 300 K): δ 8.16 (d, J = 8.4 Hz, 1H, H_i), 7.94 (d, J = 7.5 Hz, 1H, H_{Ar}), 7.87-7.77 (m, 2H, H_{Ar}), 7.56–7.54 (m, 4H, H_{Ar}), 7.43 (d, J = 7.5 Hz, 2H, H_{Ar}), 7.41 (d, J = 8.1 Hz, 4H, H_n), 7.13 (d, J = 8.1, 4H, H_o), 4.37 (q, J = 6.5 Hz, 1H, H_{13}), 4.27 (m, 4H, H_2 and CH_{10}), 3.09 (m, 2H, H_7), 2.82-2.85 (m, 2H, H_5), 2.37 (s, 6H, H_{15}), 2.28-2.32 (m, 4H, H_4 and H_8), 1.34 (d, J = 6.5 Hz, 3H, H_{14}).

$^{13}\text{C NMR}$ (75 MHz; CDCl_3 ; T = 300 K) δ 155.3 (C), 143.6 (C), 140.5 (C), 139.2 (C), 136.0 (C), 134.4 (C), 132.0 (C), 130.0 (C_n), 129.1 (CH), 127.9 (CH), 127.4 (C_o), 126.1 (CH), 125.8 (CH), 125.7 (CH), 124.8 (CH), 124.6 (CH), 124.5 (CH), 58.2 (C_{13}), 54.8 (C_2), 50.2 (C_4), 45.6 (C_5), 21.8 (C_{15}), 14.5 (C_{14}).

$^{15}\text{N NMR}$ (40 MHz; CDCl_3 ; T = 300 K): δ 313 (N_{12}), 39 (N_6). The signals relative to N(Ts) were not detected.

Elem. An. Found: C, 66.2; H, 6.2; N, 8.3%

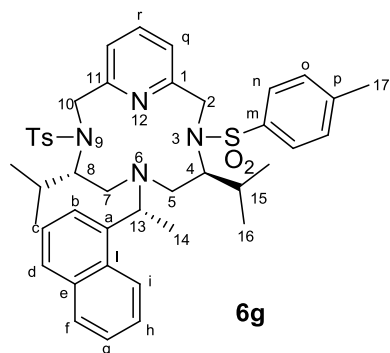
Calculated: C, 66.4; H, 6.0; N, 8.4%.

MS m/z 669 (M^+ 100%).

IR ν (cm^{-1}) 1595.1 (w), 1457.7 (w), 1357.0 (w), 1339.8 (s), 1253.4 (w), 1158.0 (s).

$[\alpha]_{\text{D}}^{20}$ -43 (c 1 in CHCl_3) (ligand **6e**)

+43 (c 1 in CHCl_3) (ligand **6f**)



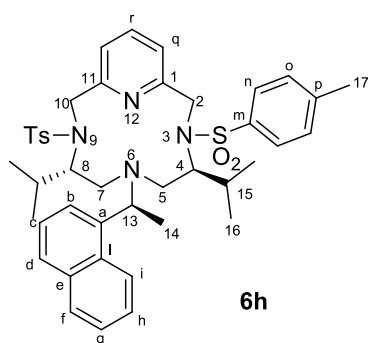
¹H NMR (300 MHz; CDCl₃; T = 300 K) δ 8.58 (d, J = 8.1 Hz, 1H, H_i), 7.89 (m, 1H, H_{Ar}), 7.83 (d, J = 8.1 Hz, 1H, H_{Ar}), 7.69 (d, J = 8.1 Hz, 1H, H_{Ar}), 7.64-7.42 (m, 8H, H_{Ar}), 7.12 (d, J = 7.8 Hz, 4H, H_o), 7.05 (m, 2H, H_{Ar}), 5.18 (m, 1H, H₁₃), 4.72 (m, 2H, H₂), 3.94-3.82 (m, 6H, H), 2.63-2.60 (m, 2H, H), 2.40 (m, 2H, H) overlapping with 2.33 (s, 6H, CH₁₇), 1.57 (d, J = 6.5 Hz, 3H, H₁₄), 0.44 (m, 12H, H₁₆).

¹³C NMR (75 MHz; CDCl₃; T = 300 K) δ 156.5 (C), 142.5 (C), 142.2 (C), 138.9 (C), 137.0 (CH), 134.2 (C), 131.7 (C), 129.2 (C_o), 128.9 (CH), 127.8 (C_n), 127.0 (CH), 126.0 (CH), 125.9 (CH), 125.8 (C_h), 125.2 (CH), 124.0 (C_i), 120.7 (CH), 66.5 (CH), 50.8 (CH₂), 49.5 (CH₂), 30.0 (CH), 23.8 (C₁₄), 21.5 (C₁₈), 21.1 (C₁₆). A signal relative to a CH was not detected.

¹⁵N NMR (40 MHz; CDCl₃; T = 300 K) δ 33.2 (N₆). The signals relative to N-Ts and N₁₂ were not detected.

Elem. An. Found: C, 68.4; H, 7.4; N, 7.1%
 Calculated: C, 68.6; H, 7.0; N, 7.4%.

MS (FAB) m/z 753 (M+1).



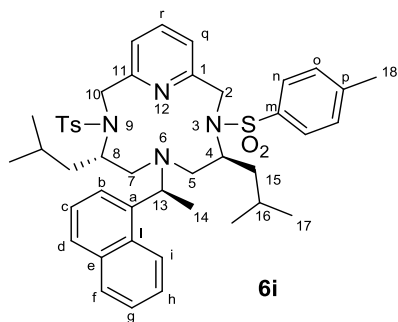
¹H NMR (300 MHz; CDCl₃; T = 300 K) δ 8.54 (m, 1H, H_i), 7.89 (m, 1H, H_{Ar}), 7.85 (d, J = 8.1 Hz, 1H, H_{Ar}), 7.77 (d, J = 8.1 Hz, 1H, H_{Ar}), 7.64-7.41 (m, 8H, H_{Ar}), 7.09-6.99 (m, 6H, H_{Ar}), 5.01 (m, 1H, H₁₃), 4.76 (m, 2H, H₂), 3.86 (m, 2H, H_{2'}), 3.77 (m, 2H, H₄), 3.55 (m, 2H, H₅), 2.36 (m, 2H, H_{5'}), 2.29 (s, 6H, CH₁₇), 1.48 (d, J = 6.6 Hz, 3H, CH₁₄), 1.34-1.23 (m, 2H, H₁₅), 0.60 (m, 6H, CH₁₆), 0.38 (m, 6H, CH₁₆).

¹³C NMR (75 MHz; CDCl₃; T = 300 K) δ 156.3 (C), 142.3 (C), 141.4 (C), 139.2 (C), 137.3 (CH), 134.1 (C), 132.5 (C), 128.9 (C_n), 128.8 (CH), 127.7 (C_o), 127.6 (CH), 126.7 (CH), 126.2 (CH), 125.4 (CH), 124.1 (CH), 120.7 (CH), 66.0 (C₄), 56.0 (C₁₃), 51.0 (C₅), 49.3 (C₂), 30.2 (C₁₅), 21.4 (C₁₇), 20.8 (C₁₄), 20.1 (C₁₆) overlapping with 20.1 (C₁₆).

Elem. An. Found: C, 68.6; H, 7.2; N, 7.4

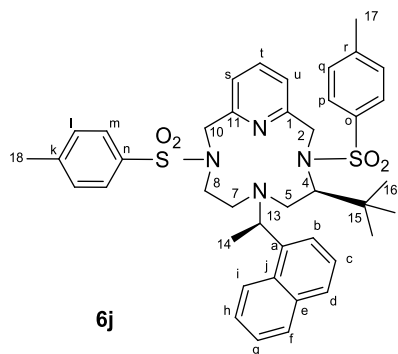
Calculated: C, 68.6; H, 7.0; N, 7.4

MS (FAB) m/z 753 (M+1).



¹H NMR (300 MHz; CDCl₃; T = 300 K) δ 8.29 (m, 1H, H_{Ar}), 7.85-7.84 (m, 1H, H_{Ar}), 7.79-7.69 (m, 3H, H_{Ar}), 7.58-7.43 (m, 6H, H_{Ar}), 7.38 (m, 1H, H_{Ar}), 7.30-7.25 (m, 4H, H_{Ar}), 4.90-4.88 (m, 1H, H₁₃), 4.79-4.74 (m, 1H, H₂), 4.45 (br, 1H, H₁₀), 3.99-3.94 (m, 1H, H₂), 3.86-3.81 (m, 1H, H₅), 3.65 (br, 1H, H₁₀), 3.50 (m, 1H, H₇), 3.05 (m, 1H, H₇), 2.94 (m, 1H, H₅), 2.43 (s, 6H, H₁₈), 1.43 (d, J = 6.2 Hz, 3H, H₁₄), 1.37-1.25 (m, 6H, H₁₅ and H₁₆), 0.76-0.21 (widespread, 12H, H₁₇)

¹³C NMR (75 MHz, CDCl₃) δ 143.07 (C), 140.68 (C), 138.56 (CH), 134.65 (C), 132.16 (C), 129.72 (CH), 129.05 (CH), 127.68 (CH), 127.63 (CH), 126.03 (CH), 125.74 (CH), 125.52 (CH), 124.89 (CH) 58.30 (C₁₃), 31.88 (C₂), 23.81 (C₁₈), 24.80 (C₄), 24.72 (C₁₆), 22.93 (C₅), 21.68 (C₁₇), 14.31 (C₁₄).



Two major conformers (1:1). Signals of the second conformer are reported as marked by *.

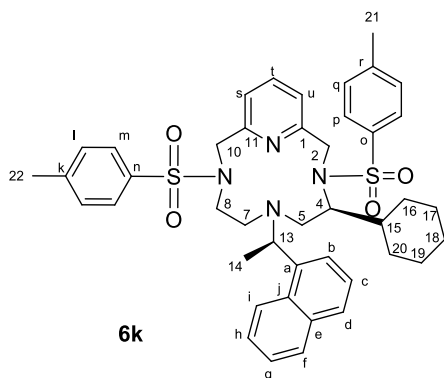
¹H NMR (300 MHz; CDCl₃, 300 K) δ 8.29-8.25 (m, 1H, H_h), 8.27-8.19 (m, 1H, H_h*), 7.91-7.86 (m, 2H, H_{Ar}), 7.79-7.76 (m, 4H, H_{Ar}), 7.64-7.59 (m, 1H, H_{Ar}), 7.55-7.36 (m, 13H, H_{Ar}), 7.31-7.20 (m, 10H, H_{Ar}), 7.08 (d, J = 7.6 Hz, 1H, H_{Ar}), 6.99 (d, J = 8.1, 2H, H_{Ar}), 6.73 (d, J = 7.6 Hz, 1H, H_{Ar}), 4.85 (d, J = 14.5, 2H, H₂₋₂*), 4.78 (q, J = 6.5 Hz, 1H, H₁₃), 4.62 (d, J = 15.2 Hz, 1H, H₁₀), 4.57 (q, J = 6.7 Hz, 1H, H₁₃*), 4.48 (d, J = 12.1 Hz, 1H, H₁₀*), 4.44 (d, J =

14.5 Hz, 1H, H₂), 4.43-4.35 (m, 1H, H₂*), 4.19 (d, *J* = 15.2 Hz, 1H, H₁₀), 4.03 (d, *J* = 9.1 Hz, 1H, H₄), 3.99 (d, *J* = 12.1 Hz, 1H, H₁₀*), 4.03 (d, *J* = 8.9 Hz, 1H, H₄*), 3.63 (dd, *J* = 13.4, 9.1 Hz, 2H, H₅, ₅*), 3.39-3.27 (m, 1H, H₈), 3.24-3.11 (m, 1H, H₈*), 3.08-2.95 (m, 2H, H₅, ₇), 2.93 – 2.82 (m, 2H, H₈, ₈*), 2.77 (d, *J* = 13.4 Hz, 1H, H₅*), 2.69-2.41 (m, 2H, H₇*), 2.46-2.30 (m, 12H, H₁₇₋₁₈ and H_{17*-18*}), 1.77-1.65 (m, 1H, H₇), 1.53 (d, *J* = 6.5 Hz, 3H, H₁₄), 1.52 (d, *J* = 6.7 Hz, 3H, H₁₄*), 0.94 (s, 9H, H₁₆), 0.91 (s, 9H, H₁₆)

¹³C NMR (75 MHz; CDCl₃, 300 K) δ 156.48 (C_{2,2*}), 155.96 (C₁₀), 155.58 (C_{10*}), 143.22 (C_k), 143.21 (C_{k*}), 143.05 (C_r), 142.96 (C_{r*}), 140.74 (C_a), 139.69 (C_{a*}), 139.58 (C_n), 139.57 (C_{n*}), 138.19 (C_t), 137.38 (C_{t*}), 137.17 (C_o), 136.94 (C_{o*}), 134.50 (C_j), 134.49 (C_{j*}), 132.19 (C_e), 131.99 (C_{e*}), 129.83 (2C_{ts}), 129.70 (2C_{ts}), 129.51 (2C_{ts}), 129.18 (2C_{ts}), 129.06 (2C_{ts}), 128.36 (2C_{ts}), 127.82 (C_{Ar}), 127.60 (2C_{Ar}), 127.45 (C_{Ar}), 127.14 (2C_{ts}), 127.12 (2C_{ts}), 125.97 (C_{Ar}), 125.64 (C_{Ar}), 125.48 (C_{Ar}), 125.46 (C_{Ar}), 125.42 (C_{Ar}), 125.33 (C_{Ar}), 125.29 (C_{Ar}), 124.46 (C_{Ar}), 124.18 (C_{Ar}), 123.91 (C_{Ar}), 123.75 (C_{Ar}), 123.49 (C_{Ar}), 123.17 (C_{Ar}), 121.53 (C_{Ar}), 69.03 (C₄), 68.02 (C_{4*}), 59.34 (C₁₃), 55.98 (C₁₀), 55.18 (C_{10*}), 54.92 (C₈), 52.81 (C₇), 50.65 (C_{2,2*}), 49.51 (C_{7*}), 47.62 (C_{8*}), 38.42 (C₁₅), 36.45 (C_{15*}), 29.26 (C₁₆), 29.05 (C_{16*}), 22.31 (C₁₄), 21.59 (C₁₈), 21.54 (C_{18*}), 21.51 (C₁₇), 21.47 (C_{17*}), 17.97 (C₁₄).

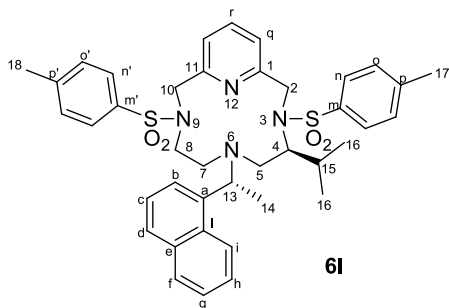
MS (FAB) m/z 751.5 (M⁺), 773.5 (M⁺Na).

[α]_D²⁰ - 64.3 (in CHCl₃).



¹H NMR (300 MHz; CDCl₃, 300 K) δ 8.57 (d, *J* = 8.6 Hz, 1H - H_h), 7.83-7.71 (m, 6H - H_{Ar}), 7.58-7.53 (m, 2H - H_{Ar}), 7.45-7.37 (m, 2H - H_{Ar}), 7.16-7.12 (m, 2H - H_{Ar}), 6.94 – 6.89 (m, 4H - H_{Ar}), 5.00-2.50 (m, 10H), 2.04 (s, 6H, H₂₁ and H₂₂), 1.70-0.65 (m, 16H).

¹³C NMR (75 MHz; CDCl₃, 300 K) δ 142.86 (C_{k-r}), 140.56 (C₁₁), 137.82 (C_{Ar}), 134.89 (C_{Ar}), 132.88 (C_{Ar}), 129.95 (4C_{Ts}), 129.55 (C_{Py}), 129.34 (C_{Ar}), 127.50 (C_{Ar}), 125.84 (C_{Ar}), 125.54 (C_{Ar}), 124.79 (C_h), 124.04 (C_{Ar}), 65.75, 31.51, 26.75, 26.63, 21.29 (C₂₁₋₂₂)



¹H NMR (300 MHz; CDCl₃; T = 300 K) δ 8.25 (m, 1H, H_i), 7.87 (m, 1H, H_{Ar}), 7.77 (d, J = 7.6 Hz, 1H, H_{Ar}), 7.65-7.62 (m, 2H, H_{Ar}), 7.50-7.40 (m, 7H, H_{Ar}), 7.26 (4H, covered by solvent residual peak), 7.17 (m, 2H, H_{Ar}), 4.80-4.20 (m, 4H, CH₂), 3.80-2.60 (m, 4H, CH₂), 2.43 (s, 3H, H₁₈), 2.37 (s, 3H, H₁₇), 2.00-1.76 (m, 1H, CH₂), 1.46 (d, J = 6.2 Hz, 3H, CH₁₄), 0.77 (m, 3H, CH₁₆), 0.59 (m, 3H, H₁₆). Some signals were too broad to be detected.

¹H NMR (400 MHz; C₆D₅CD₃; T = 373 K) δ 8.36 (d, J = 8.6 Hz, 1H, H_i), 7.68 (d, J = 8.0 Hz, 1H, H_{Ar}), 7.60-7.54 (m, 3H, H_{Ar}), 7.48-7.44 (m, 3H, H_{Ar}), 7.38 (pst, J = 7.5 Hz, 1H, H_{Ar}), 7.31 (d, J = 7.0 Hz, 1H, H_{Ar}), 7.27 (d, J = 7.0 Hz, 1H, H_{Ar}), 7.10-6.80 (m, 7H, H_{Ar} overlapped with toluene), 4.59 (q, J = 6.1 Hz, 1H, H₁₃), 4.29-4.14 (m, 4H, H₂ and H₁₀), 3.77 (m, 1H, H₈), 3.28-3.08 (m, 4H, H₄ and H₇), 2.93 (m, 1H, H₅), 2.08 (s, 3H, H₁₈), 2.05 (s, 3H, H₁₇), 2.01 (m, 1H, H₅), 1.88 (m, 1H, H₁₅), 1.46 (d, J = 6.6 Hz, 3H, H₁₄), 0.90 (d, J = 6.7 Hz, 3H, H₁₆), 0.69 (d, J = 6.7 Hz, 3H, H₁₆).

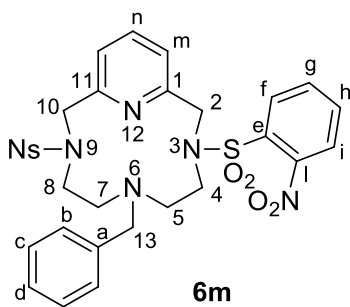
¹³C NMR (75 MHz; C₆D₅CD₃; T = 300 K) δ 156.3 (C), 156.2 (C), 141.9 (C), 134.5 (C), 132.1 (C), 129.2 (CH), 128.9 (CH), 128.8 (CH), 128.7 (CH), 127.8 (C), 127.8 (CH), 127.4 (CH), 126.9 (CH), 125.3 (CH), 125.2 (CH), 125.0 (CH), 124.0 (C_i), 123.2 (CH), 20.8 (CH), 20.7 (CH), 20.6 (CH). Signals relative to aromatic and aliphatic carbons were not detected.

Elem. An. Found: C, 67.1; H, 6.9; N, 7.6%

Calculated: C, 67.6; H, 6.5; N, 7.9%.

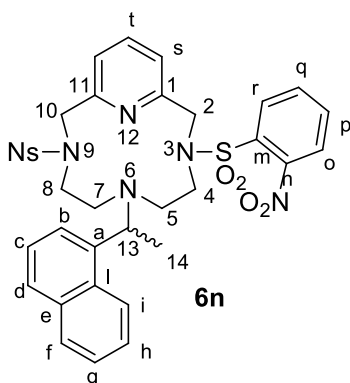
MS (EI) m/z 555 (M-NaphCH₃CH), 155 (NaphCH₃CH).

[α]_D²⁰ - 60.7 (c 1.01 in CHCl₃).

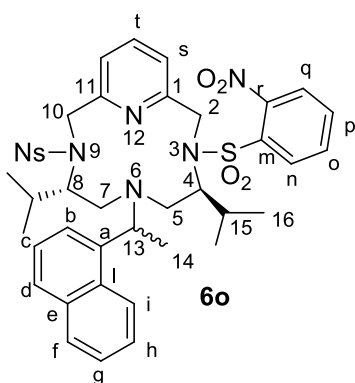


¹H NMR (400 MHz; CDCl₃; T = 300 K) δ 7.80 (m, 3H, H_{Ar}), 7.72-7.57 (m, 6H, H_{Ar}), 7.46 (d, J = 7.7 Hz, 2H, H_{Ar}), 7.34-7.23 (m, 4H, H_{Ar}), 7.19 (d, J = 6.3 Hz, 1H, H_{Ar}), 4.58 (s, 4H, H₂ and H₁₀), 3.53 (s, 2H, H₁₃), 3.38-3.15 (m, 4H, H₄ and H₈), 2.55-2.41 (m, 4H, H₅ and H₇)

¹³C NMR (75 MHz; CDCl₃, T = 300 K) δ 153.7 (CH), 139.3 (CH), 133.6 (CH), 131.8 (CH), 131.1 (CH), 129.0 (CH), 128.8 (CH), 128.4 (CH), 124.3 (CH), 59.4 (CH₂), 54.3 (CH₂), 49.8 (CH₂), 44.4 (CH₂)

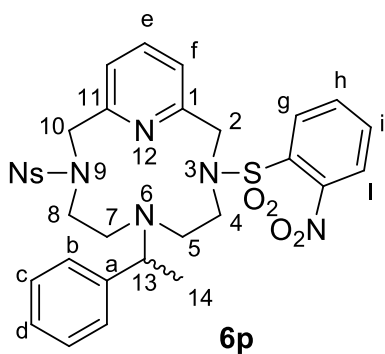


¹H NMR (400 MHz; CDCl₃; T = 300 K) δ 8.21-8.19 (s, 1H, H_{Ar}), 7.88-7.41 (m, 17H, H_{Ar}), 4.52 (s, 4H, H₂ and H₁₀), 4.41 (q, 1H, H₁₃), 3.22 (ddd, 2H, H₄), 2.98 (ddd, 2H, H₈), 2.51 (ddd, 2H, H₅), 2.38 (ddd, 2H, H₇), 1.38 (d, 3H, H₁₄)



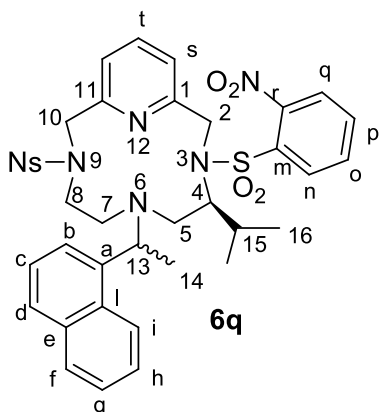
¹H NMR (300 MHz, Tol-d₈) δ 8.94 (m, 1H), 8.62 (m, 1H), 8.37 (m, 1H), 8.11 (m, 1H), 7.93 (m, 1H), 7.80 (s, 3H), 7.69 (d, *J* = 8.1 Hz, 2H), 7.55 (m, 6H), 7.41 – 7.23 (m, 4H), 6.91 (m, 4H), 6.79 (m, 3H), 6.68 (br, 8H), 5.69 (br, 1H), 5.50 (br, 1H), 5.01 (d, *J* = 16.2 Hz, 2H), 4.69 (m, 2H), 4.49 (m, 3H), 4.21 (m, 2H), 3.92 (m, 8H), 3.74 – 3.54 (m, 2H), 3.15 (d, *J* = 16.2 Hz, 2H), 1.81 (br, 4H), 1.74 (s, 2H), 1.46 (br, 6H), 1.35 (br, 5H), 1.18 (s, 4H), 0.52 (br, 3H), 0.39 (br, 6H), 0.27 (br, 6H).

¹³C NMR (75 MHz, Tol-d₈) δ 137.1 (CH), 134.8 (C), 132.5 (CH), 131.3 (CH), 130.4 (CH), 127.4 (CH), 126.1 (CH), 125.4 (C), 123.5 (CH), 121.7 (CH), 121.2 (CH), 118.6 (CH), 70.8 (CH₂), 67.1 (CH), 64.5 (CH₂), 60.0 (CH₂), 51.7 (CH₂), 50.2 (CH₂), 37.0 (CH), 30.3 (CH₂), 30.0 (CH₃), 23.9 (CH₃), 20.6 (CH₃).



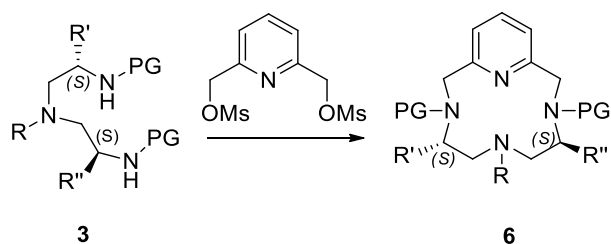
¹H NMR (400 MHz, CDCl₃) δ 7.91 – 7.78 (m, 1H, H_e), 7.78 – 7.69 (m, 5H), 7.64 (dd, *J* = 14.6, 7.0 Hz, 4H), 7.50 (d, *J* = 7.7 Hz, 2H), 7.30 (m, 3H), 7.22 (d, *J* = 7.4 Hz, 2H), 4.58 (q, *J* = 13.0 Hz, 4H, H_{2,10}), 3.62 (q, *J* = 6.5 Hz, 1H, H₁₃), 3.26 (dt, *J* = 15.9, 8.2 Hz, 2H), 3.12 (dt, *J* = 14.8, 7.6 Hz, 2H), 2.43 (br, 4H, 1.32 – 1.20 (m, 3H).

MS (EI) 681.3 m/z [M⁺]



¹H NMR (300 MHz, Tol-*d*₈, T = 353 K) δ 8.37 (d, *J* = 8.4 Hz, 1H), 7.73 – 7.22 (m, 13H), 7.21 – 6.77 (m, 20H), 4.70 (d, *J* = 6.5 Hz, 1H), 4.42 (ddd, *J* = 40.6, 17.5, 11.1 Hz, 6H), 3.91 – 3.75 (m, 1H), 3.47 – 3.04 (m, 6H), 2.82 (d, *J* = 27.4 Hz, 2H), 2.50 (d, *J* = 6.3 Hz, 2H), 1.73 (br, 2H), 1.45 (d, *J* = 6.5 Hz, 3H), 1.26 (dd, *J* = 18.5, 9.2 Hz, 5H), 0.72 (d, *J* = 6.6 Hz, 3H), 0.64 (d, *J* = 6.3 Hz, 3H), 0.55 – 0.29 (m, 2H).

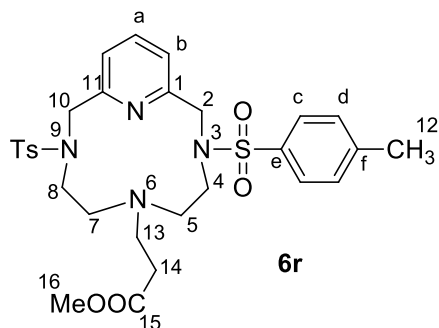
4.6.3 Synthesis of macrocycles 6r-u



6r - R = (CH₂)₂COOMe, R' = R'' = H, PG = Ts
6s - R = (CH₂)₄CHNHCBzCOOMe, R' = R'' = H, PG = Ts
6t - R = (CH₂)₄CHNHCBzCOOMe, R' = R'' = *i*Pr, PG = Ts
6u - R = (CH₂)₄CHNHCBzCOOMe, R' = R'' = H, PG = Ns

2,6-(bis-mesyloxy)pyridine (1.5 mmol) in distilled CH₃CN (9.0 mL) was added dropwise to a suspension of K₂CO₃ (4.5 mmol) and amine **3** (1.5 mmol) in distilled CH₃CN (25.0 mL). The reaction was allowed to react to reflux for (see table for reaction time). The reaction mixture was then quenched with water (25.0 mL) and washed with AcOEt (3 x 25.0 mL). The organic phases were concentrated in vacuum leading to the desired product with no further purification.

Product	Reaction time	Yield
6r	6h	97%
6s	6h	98%
6t	10h	95%
6u	10h	94%



¹H NMR (400 MHz, CDCl₃) δ 7.77–7.69 (m, 5H, H_{Ar}), 7.37–7.29 (m, 6H, H_{Ar}), 4.32 (s, 4H, CH₂), 3.64 (s, 3H, OCH₃), 3.10 (m, 4H, CH₂), 2.65 (m, 2H, CH₂), 2.44 (s, 6H, CH₃), 2.35–2.24 (m, 6H, CH₂)

¹³C NMR (100 MHz, CDCl₃) δ 172.8 (CO), 155.2 (C_{Ar}), 143.7 (C_{Ar}), 138.9 (CH_{Ar}), 130.0 (CH_{Ar}), 127.3 (CH_{Ar}), 124.2 (CH_{Ar}), 54.7 (CH₂), 51.7 (CH₂), 51.3 (OCH₃), 51.1 (CH₂), 45.2 (CH₂), 34.0 (CH₂), 22.9 (CH₂), 21.7 (CH₃)

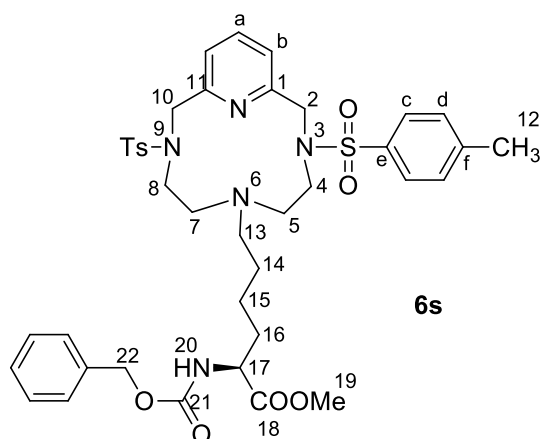
MS (ESI): m/z = 601.3 [MH]⁺

Elem. An. **Calculated:** C, 57.98; H, 6.04; N, 9.33

Found: C, 57.62; H, 5.92; N, 9.12

UV/vis λ_{\max} [nm] = 234 nm

IR (ATR) ν (cm⁻¹) 2949 (w), 1733 (CO), 1157



¹H NMR (300 MHz, CDCl₃) δ 7.73–7.69 (m, 5H, H_{ar}), 7.38–7.27 (m, 11H, H_{ar}), 5.29 (m, 1H, NH_{Cbz}), 5.11 (s, 2H, H₂₂), 4.39–4.28 (m, 5H, CH and CH₂), 3.74 (s, 3H, H₁₉), 3.10 (m, 4H, CH₂), 2.44 (s, 6H, H₁₂), 2.32–2.20 (m, 6H, CH₂), 1.79 (m, 1H, CH₂), 1.63 (m, 1H, CH₂), 1.36–1.16 (m, 4H, CH₂)

¹³C NMR (75 MHz, CDCl₃) δ 173.1 (CO), 155.1 (C), 143.7 (C_{Ar}), 138.9 (CH_{Ar}), 136.2 (C_{Ar}), 130.0 (CH_{Ar}), 128.7 (CH_{Ar}), 128.3 (CH_{Ar}), 127.3 (CH_{Ar}), 124.2 (CH_{Ar}), 67.1 (CH₂), 55.2 (CH₂), 54.6 (CH₂), 54.0 (CH₂), 52.5 (OCH₃), 51.8 (CH₂), 44.8 (CH₂), 32.6 (CH₂), 27.78 (CH₂), 22.8 (CH₂), 21.7 (CH₃)

MS (ESI) m/z = 792.4 [MH]⁺

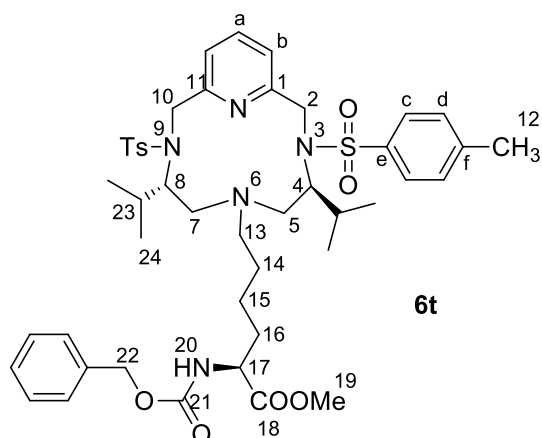
Elem. An. **Calculated:** C, 60.66; H, 6.24; N, 8.84

Found: C, 60.28; H, 5.96; N, 8.60

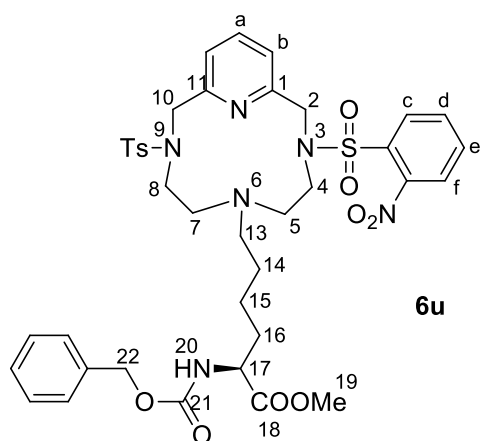
[α]_D (*c* 1.0 in CHCl₃) 3.82

UV/vis λ_{\max} [nm] = 234 nm

IR (ATR) ν (cm⁻¹) 3337 (NH), 2932 (w), 1750 (CO), 1152

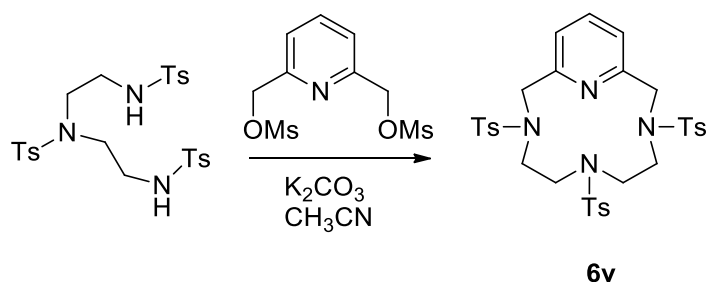


¹H NMR (300 MHz, CDCl₃) δ 7.85–7.45 (m, 3H, H_{Ar}), 7.39–7.13 (m, 9H, H_{Ar}), 7.12–6.83 (m, 3H, H_{Ar}) 5.40 (m, 1H, NH_{Cbz}), 5.11 (s, 2H, H₂₂), 4.73 (m, 1H), 4.39 (m, 1H, H₁₇), 3.74 (s, 3H, H₁₉), 3.58–3.35 (m, 1H), 3.26 (m, 1H), 2.40 (s, 3H, CH₁₂), 2.29 (s, 3H, H₁₂), 1.96–1.56 (m, 3H, CH₂), 1.47–1.20 (m, 3H, CH₂ + H₂₃), 1.05–0.69 (m, 12H, H₂₄)



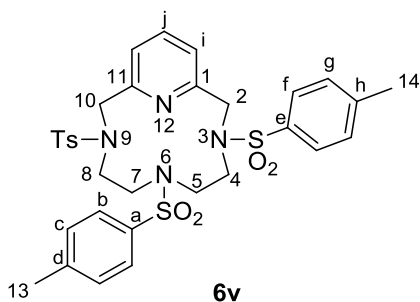
¹H NMR (300 MHz, CDCl₃) δ 8.03 (m, 2H, H_{Ar}), 7.75–7.50 (m, 6H, H_{Ar}), 7.45–7.30 (m, 8H, H_{Ar}), 5.40 (m, 1H, NH_{Cbz}), 5.10 (s, 2H, H₂₂), 4.60–4.30 (m, 4H), 3.74 (m, 4H, H₁₉ + H₁₇), 3.25–2.99 (m, 4H, CH₂), 2.92 (m, 2H, CH₂), 2.44–2.32 (m, 2H, CH₂), 1.85–1.19 (m, 8H, CH₂)

4.6.4 Synthesis of macrocycle 6v



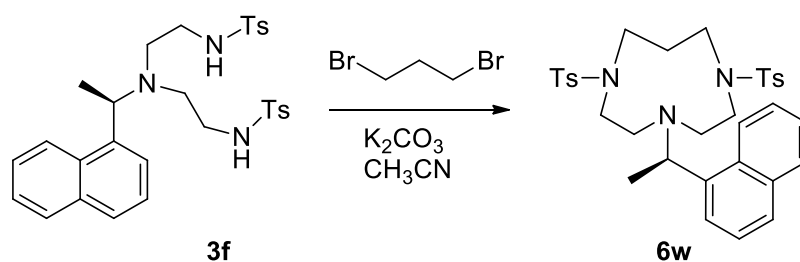
2,6 pyridinedimethanol 2,6-dimesylate (1.5 mmol) in distilled CH₃CN (9.0 mL) was added dropwise to a suspension of K₂CO₃ (4.5 mmol) and N,N',N''-tritosyldiethylenetriamine (1.5 mmol) in distilled CH₃CN (25.0 mL). The reaction was allowed to react to reflux for 3 hours. The reaction mixture was then quenched with water (25.0 mL) and washed with AcOEt (3 x 25.0 mL). The organic phases were concentrated in vacuum leading to the pure product as a white powder.

Yield: 99%



¹H NMR (300 MHz; CDCl₃; T = 300 K) δ 7.80 – 7.69 (m, 7H, H_{Ar}), 7.66 (d, *J* = 8.2 Hz, 2H, H_b), 7.44 (d, *J* = 7.7 Hz, 2H, H_c), 7.36 (d, *J* = 8.1 Hz, 4H, H_g), 7.29 (d, *J* = 7.9 Hz, 2H, H_i), 4.30 (s, 4H, H_{2,10}), 3.33 (t, *J* = 7.5 Hz, 4H, CH₂), 3.22 – 3.07 (m, 2H, CH₂), 2.77 (s, 2H, CH₂), 2.46 (s, 6H, H₁₄), 2.42 (s, 3H, H₁₃)

4.6.5 Synthesis of macrocycle 6w

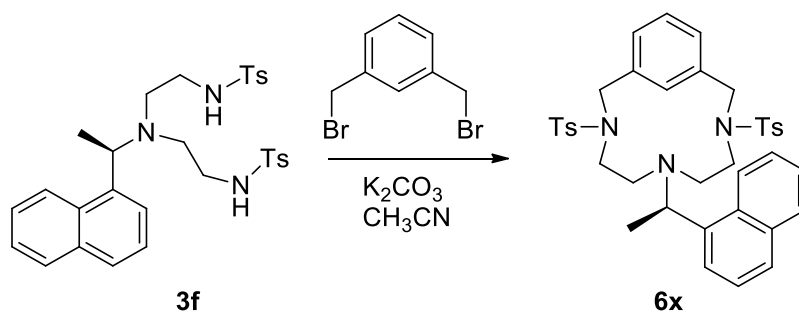


1,3 dibromopropane (1.5 mmol) in distilled CH₃CN (9.0 mL) was added dropwise to a suspension of K₂CO₃ (4.5 mmol) and bisulfonamide **3f** (1.5 mmol) in distilled CH₃CN (25.0 mL). The reaction was allowed to react to reflux for 6 hours. The reaction mixture was then quenched with water (25.0 mL) and washed with AcOEt (3 x 25.0 mL). The organic phases were concentrated in vacuum leading to the pure product as a white powder.

Yield: 99%

¹H NMR (300 MHz, CDCl₃) δ 8.64 (d, *J* = 8.8 Hz, 1H), 7.79 (d, *J* = 8.1 Hz, 1H), 7.75 – 7.55 (m, 6H), 7.45 (dt, *J* = 6.9, 5.0 Hz, 4H), 7.31 (s, 2H), 5.11 – 4.89 (m, 2H), 3.33 – 3.19 (m, 2H), 3.17 – 2.93 (m, 7H), 2.96 – 2.82 (m, 3H), 2.43 (s, 6H), 2.16 – 2.09 (m, 2H), 1.53 (d, *J* = 6.7 Hz, 3H).

4.6.6 Synthesis of macrocycle 6x



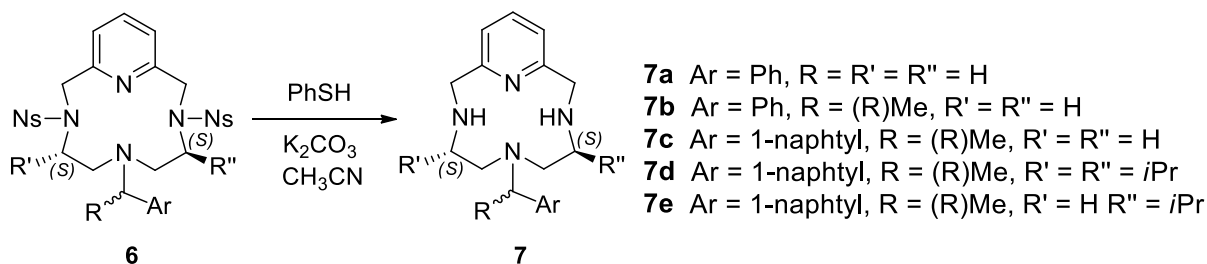
α,α' -Dibromo-m-xylene (1.2 mmol) in distilled CH_3CN (7.0 mL) was added dropwise to a suspension of K_2CO_3 (4.5 mmol) and bisulfonamide **3f** (1.2 mmol) in distilled CH_3CN (22.0 mL). The reaction was allowed to react to reflux for 6 hours. The reaction mixture was then quenched with water (20.0 mL) and washed with AcOEt (3 x 20.0 mL). The organic phases were concentrated in vacuum leading to the pure product as a white powder.

Yield: 99%

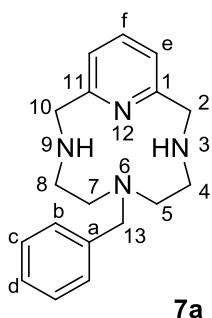
1H NMR (300 MHz, $CDCl_3$) δ 8.17 (d, $J = 8.4$ Hz, 1H), 7.92 (d, $J = 6.5$ Hz, 1H), 7.84 (d, $J = 7.2$ Hz, 1H), 7.55 – 7.39 (m, 9H), 7.37 – 7.20 (m, 9H), 4.46 – 4.33 (m, 1H), 4.18 (s, 4H), 2.90 – 2.76 (m, 2H), 2.70 – 2.51 (m, 2H), 2.44 (s, 7H), 2.29 (s, 3H), 1.38 (d, $J = 6.5$ Hz, 3H).

4.7 Deprotection of macrocycles

4.7.1 Deprotection of Nosyls



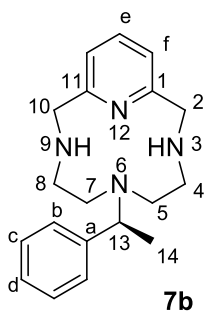
A solution of **6** (0.68 mmol), micronized potassium carbonate (2.72 mmol) and thiophenol (2.04 mmol) in distilled CH₃CN (17 mL) was allowed to react at 50 °C for 5 hours. Then CH₂Cl₂ (10 mL) is added. The mixture was extracted with a 1M solution of HCl (3 x 10 mL) and the aqueous phases were basified with NaOH. The suspension was extracted with CH₂Cl₂ (3 x 10 mL) and the organic phases were then treated with Na₂SO₄ and concentrated in vacuum. A yellowish powder was obtained.



Yield: 84%

¹H NMR (300 MHz; CDCl₃; T = 300K) δ 7.53 (t, J = 7.6 Hz, 1H, H_f), 7.40-7.19 (m, 5H, H_{a,b,c,d}), 6.99 (d, J = 7.6 Hz, 2H, H_e), 3.92 (s, 4H, H_{2,10}), 3.64 (s, 2H, H₁₃), 2.69-2.51 (m, 4H, H₄₋₈ overlapping with br NH), 2.42-2.25 (m, 4H, H_{5,7})

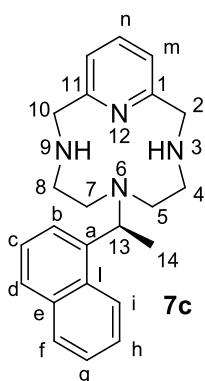
¹³C NMR (75 MHz; CDCl₃; T = 300K) δ 156.8 (C₁), 155.3 (CH), 138.0 (C), 137.6 (CH), 129.6 (CH), 128.7 (CH), 127.6 (CH), 120.8 (CH), 60.0 (CH₂), 54.0 (CH₂), 53.0 (CH₂), 46.8 (CH₂)



Yield 65%

¹H NMR (400 MHz, CDCl₃) δ 7.55 (t, *J* = 7.6 Hz, 1H), 7.43 – 7.33 (m, 5H), 6.99 (d, *J* = 7.6 Hz, 2H), 4.16 (q, *J* = 6.9 Hz, 1H), 3.93 (s, 4H), 2.76 – 2.56 (m, 4H), 2.49 (s, 6H), 1.48 (d, *J* = 6.9 Hz, 3H).

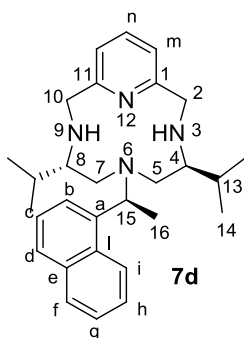
MS (EI) *m/z* 311.3 [M⁺]



Yield 78%

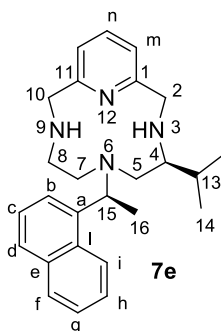
¹H NMR (400 MHz; CDCl₃; T = 300K) δ 8.59-8.56 (d, *J* = 8.61 Hz, 1H, H_n), 7.86 (d, *J* = 8.1 Hz, 1H, H_{Ar}), 7.82 (m, 1H, H_{Ar}), 7.56-7.41 (m, 5H, H_{Ar}), 6.91 (d, *J* = 7.6, 2H, H_{Ar}), 4.95 (q, *J* = 6.8, 1H, H₁₃), 3.88 (d, *J* = 16.8, 2H, H₂₋₁₀), 2.88-2.84 (m, 6H, H₄₋₈ and NH), 2.53-2.43 (m, 2H, H₅), 2.38-2.30 (m, 2H, H₇), 1.57 (d, *J* = 6.8, 3H, H₁₄)

¹³C NMR (100 MHz; CDCl₃; T = 300K) δ 158.04 (C_{Ar}), 139.31 (C_{Ar}), 136.24 (CH_{Ar}), 134.07 (C_{Ar}), 132.14 (C_{Ar}), 128.73 (CH_{Ar}), 128.01 (CH_{Ar}), 125.73 (CH_{Ar}), 125.32 (CH_{Ar}), 124.65 (CH_{Ar}), 119.76 (CH_{Ar}), 77.34 (C₂), 77.02 (C₁₀), 76.70 (C₄), 59.34 (C₁₃), 54.62 (C₈), 52.51 (C₅), 48.05 (C₇), 12.48 (C₁₄)



Yield 74%

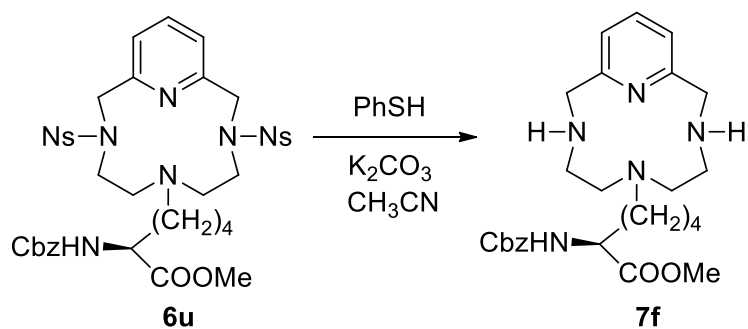
¹H NMR (300 MHz; CDCl₃; T = 300K) δ 8.21 (d, J = 8.7 Hz, 1H, H_n), 7.80 (d, J = 8.2 Hz, 1H, H_{Ar}), 7.77-7.68 (m, 1H, H_{Ar}), 7.54 (t, J = 7.6 Hz, 1H, H_a), 7.41-7.39 (m, 2H, H_{Ar}), 7.39-7.29 (m, 1H, H_{Ar}), 7.11-7.03 (m, 1H, H_{Ar}), 6.94 (d, J = 7.6 Hz, 2H, H_b), 4.85 (q, J = 6.6 Hz, 1H, H₁₅), 3.94 (d, J = 15.6 Hz, 2H, H₂₋₁₀), 3.49 (d, J = 15.6, 2H, H₂₋₁₀), 2.65-2.61 (m, 4H, H₄₋₈), 2.44-2.41 (m, 4H, H₅₋₇), 1.59 (d, J = 6.6, 3H, H₁₆) overlapped with (br, 2H, NH), 1.31-1.19 (m, 1H, H₁₃), 0.84 (d, J = 6.8 Hz, H₁₄), 0.76 (d, J = 6.8 Hz, H₁₄)



Yield 84%

¹H NMR (400 MHz, CDCl₃) δ 8.19 (d, J = 8.6 Hz, 1H), 7.79 (d, J = 8.0 Hz, 1H), 7.73 (d, J = 5.2 Hz, 1H), 7.51 (t, J = 7.7 Hz, 2H), 7.41 – 7.37 (m, 2H), 7.31 (dd, J = 14.4, 6.7 Hz, 1H), 7.07 (s, 1H), 6.91 (d, J = 7.6 Hz, 2H), 4.83 (d, J = 6.9 Hz, 1H), 3.91 (d, J = 15.9 Hz, 2H), 3.62 – 3.42 (m, 2H), 2.71 – 2.55 (m, 3H), 2.41 (m, 4H), 1.68 – 1.50 (m, 6H), 0.87 – 0.78 (d, J = 6.8 Hz, 6H), 0.76 (d, J = 6.8 Hz, 6H).

¹³C NMR (101 MHz, CDCl₃) δ 159.3 (C), 140.2 (C), 136.6 (CH), 133.9 (C), 132.1 (C), 128.8 (CH), 128.6, (CH) 127.9 (CH), 127.6 (CH), 125.8 (CH), 125.6 (CH), 125.3 (CH), 125.3 (CH), 125.1 (CH), 124.5 (CH), 124.5 (CH), 124.3 (CH), 124.2 (CH), 119.2 (CH), 62.0 (CH), 57.7 (CH), 57.5 (CH₂), 56.7 (CH₂), 54.9 (CH), 51.8 (CH₂), 32.0 (CH₃), 30.3 (CH₃), 19.3 (CH₃), 18.5 (CH₃), 17.8 (CH₃).

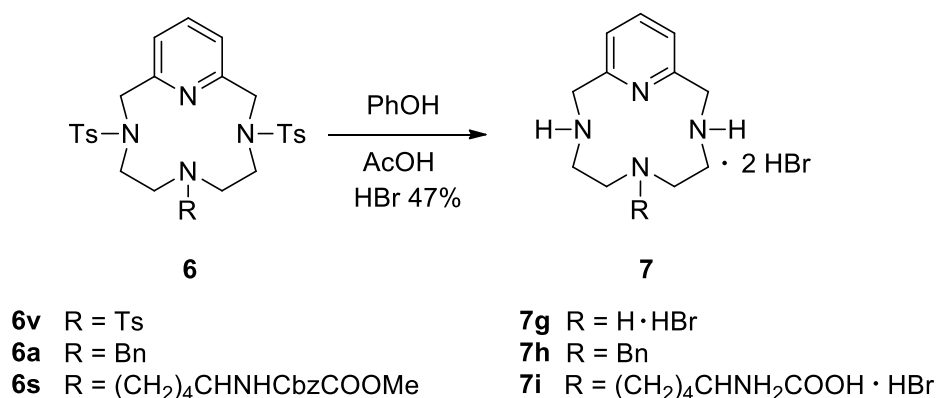


The general procedure for the deprotection of nosyls described above was performed also with **6u** leading to the formation of product **7f** with no need of further purification.

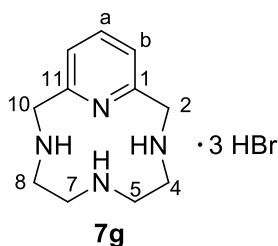
Yield 72%

¹H NMR (300 MHz, DMSO-*d*₆, T = 363 K) δ 7.73 – 7.53 (m, 1H), 7.40 – 7.05 (m, 7H), 5.03 (m, 2H), 4.54 (s, 1H), 4.27 (m, 1H), 3.77 (m, 2H), 3.63 (m, 2H), 2.67 – 2.57 (m, 2H), 2.57 – 2.45 (m, 3H), 2.40 (m, 2H), 1.68 (m, 2H), 1.43 – 1.21 (m, 2H).

4.7.2 Deprotection of Tosyls

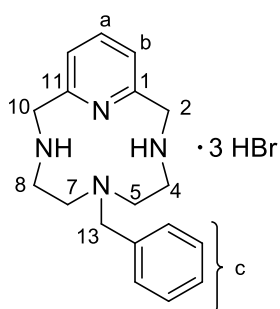


HBr 47% (80.0 mmol) was carefully added to a solution of phenol (8.0 mmol) and macrocycle **6** (1.0 mmol) in acetic acid (40.0 mmol). The reaction was refluxed for 10 hours and then concentrated in vacuum. The crude dark slime was washed with Et₂O (5 x 15.0 mL) and then dissolved in the minimum necessary amount of cold water. Cold acetone was added leading to the formation of the product **7** as a white heavy precipitate recovered by filtration.



Yield: 88%

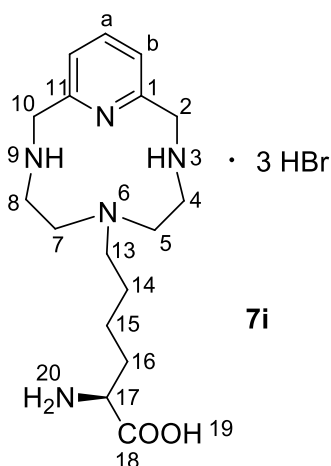
¹H NMR (300 MHz; D₂O; T = 300 K) δ 8.06 (t, *J* = 7.8 Hz, 1H, H_a), 7.58 (d, *J* = 7.8 Hz, 2H, H_b), 4.70 (s, 4H, H_{2,10}), 3.40 (br, 4H, H_{4,8}), 3.24 (br, 4H, H_{5,7})



7h

Yield: 71%

¹H NMR (300 MHz; D₂O; T = 300 K) δ 7,90-7,87 (1H, t, H_a), 7,41-7,37 (7H, m, H_{b+c}), 4,58 (4H, m, H_{2,10}), 3,81 (2H, s, H₁₃), 3,22-3,20 (4H, m, CH₂), 2,79-2,77 (4H, m, CH₂)



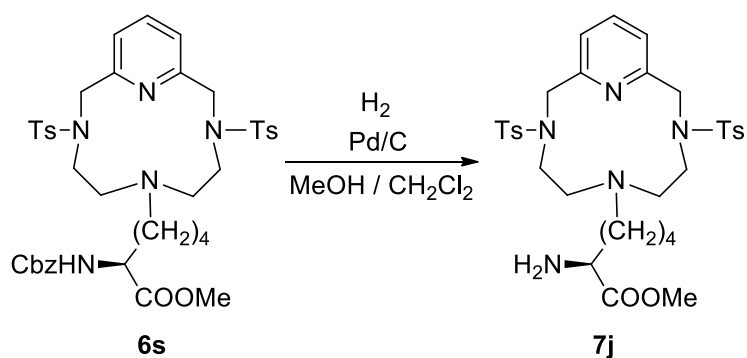
7i

Yield: 61%

¹H NMR (400 MHz, D₂O): δ 7.90 (t, J = 7.8 Hz, 1H, H_a), 7.40 (d, J = 7.8 Hz, 4H, H_b), 4.56 (m, 4H, H₂₊₁₀), 3.96 (pst, 1H, H₁₇), 3.74-3.39 (m, 2H, NH), 3.17 (s, 4H, H₅₊₇), 2.81 (s, 4H, H₄₊₈), 2.68 (pst, 1H), 1.91 (m, 2H, H₁₆), 1.55 (m, 2H, H₁₄), 1.34 (m, 2H, H₁₅).

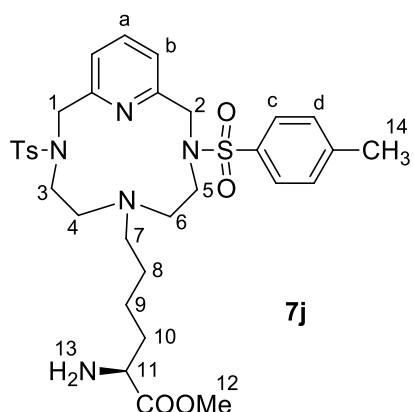
¹³C NMR (101 MHz, D₂O) δ 149.00 (C₁), 139.77 (C_a), 122.28 (C_b), 54.94 (C₁₃), 53.25 (C₁₇), 50.47 (C₄), 49.50 (C₂), 46.00 (C₅), 29.75 (C₁₆), 23.68 (C₁₄), 22.12 (C₁₅).

4.7.3 Other deprotections

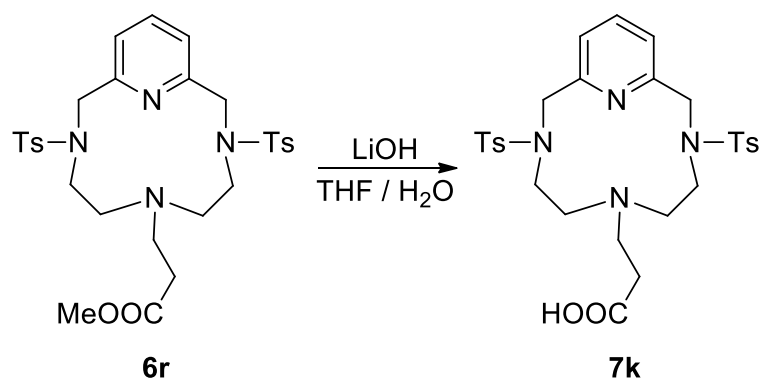


Macrocycle **6s** (0.787 g, 0.99 mmol) was dissolved in 38.0 mL of MeOH and 6.0 mL DCM. Pd/C was added and the resulting suspension was put under hydrogen atmosphere for 20h. The Pd/C was filtered on a celite pad and the solvent was dried in vacuum.

Yield 88%

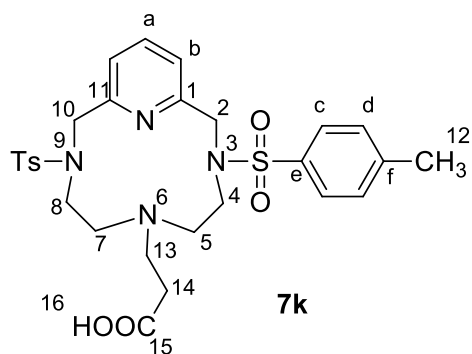


¹H NMR (300 MHz, CD₃OD) δ 7.87 (d, J = 8.3 Hz, 4H, H_c), 7.79 (q, J = 7.7 Hz, 1H, H_a), 7.52 (d, J = 8.1 Hz, 4H, H_d), 7.30 (d, J = 7.8 Hz, 2H, H_b), 4.66 (d, J = 15.7 Hz, 4H, H₂ + H₁₀), 4.20 (t, J = 6.5 Hz, 1H, H₁₇), 3.92 (s, 3H, H₁₉), 3.88 – 3.66 (m, 4H, CH₂), 3.54 (d, J = 25.0 Hz, 2H, CH₂), 3.19 (d, J = 17.4 Hz, 2H, CH₂), 2.47 (d, J = 15.2 Hz, 8H, H₁₂ + CH₂), 2.26 – 2.09 (m, 2H, CH₂), 2.08 – 1.93 (m, 2H, CH₂), 1.73 (d, J = 25.5 Hz, 2H, CH₂).



Macrocycle **6s** (0.285 g, 0.47 mmol) was dissolved in 15.0 mL of THF and 8.0 mL of H₂O. LiOH (0.081 g, 1.92 mmol) was added and the mixture was left to react at 0°C for 4h. Then, after 3h stirring at RT, LiOH was quenched with HCl. The solvent was concentrated and the precipitate was recovered by filtration.

Yield 89%



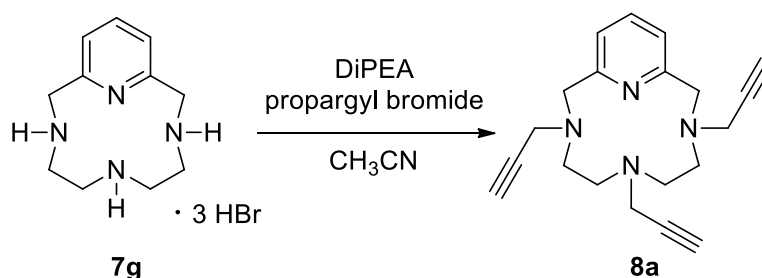
¹H NMR (300 MHz, CDCl₃) δ 7.80 – 7.68 (m, 5H, H_a + H_c), 7.34 (dd, *J* = 12.6, 7.9 Hz, 6H, H_b + H_d), 4.36 (s, 4H, H₂ + H₁₀), 3.34 – 3.21 (m, 4H, H₄ + H₈), 2.70 (dt, *J* = 21.3, 6.4 Hz, 6H, H₅ + H₇ + H₁₃), 2.46 (s, 6H, H₁₂), 2.42 (d, *J* = 5.9 Hz, 2H, H₁₄).

¹H NMR (400 MHz, CD₃OD) δ 7.87 (d, *J* = 8.2 Hz, 4H, H_c), 7.77 (t, *J* = 7.7 Hz, 1H, H_a), 7.49 (d, *J* = 8.1 Hz, 4H, H_d), 7.29 (d, *J* = 7.7 Hz, 2H, H_b), 4.61 (s, 8H, H₂ + H₁₀ + H₄ + H₈), 4.03 (t, *J* = 6.4 Hz, 2H, CH₂), 3.51 (s, 4H, H₅ + H₇), 2.63 (t, *J* = 6.5 Hz, 2H, CH₂), 2.47 (s, 6H, H₁₂).

Elem. An. Calculated for C₂₈H₃₄N₄O₆S₂: C 57.32; H 5.84; N 9.55. Found: C 54.69; H 5.50; N 8.69.

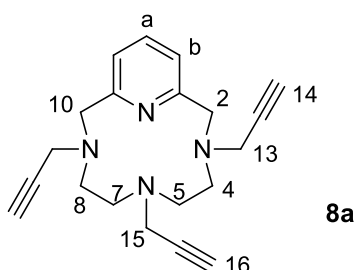
4.8 Functionalized ligands

4.8.1 Synthesis of ligand **8a**



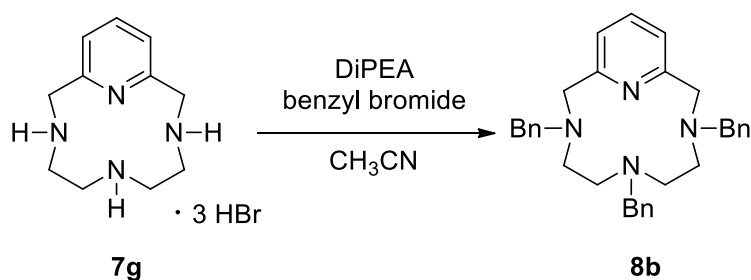
A solution of propargyl bromide (3.5 mmol) in acetonitrile (3.0 mL) was dropwise over a period of 15 minutes to a solution of ligand **7g** (1.0 mmol) and DIPEA (8.0 mmol) in acetonitrile (5.0 mL). The mixture was allowed to react over night, then was dried in vacuum and the crude was dissolved in DCM (7.0 mL). The organic solution was washed with H₂O (5 x 5.0 mL) and brine (3 x 5.0 mL) in order to remove the unreacted materials and the ammonium salt. The organic phase was then treated with Na₂SO₄ and dried in vacuum leading to product **8a** as an orange oil with no further purification.

Yield: 67%



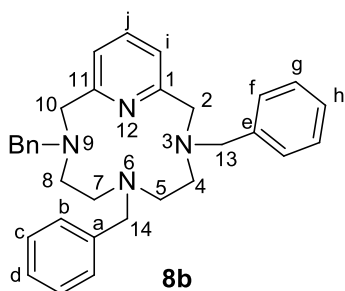
¹H NMR (300 MHz, CDCl₃) δ 7.60 (t, *J* = 7.1 Hz, 1H), 7.11 (d, *J* = 7.6 Hz, 2H), 3.94 (m, 4H), 3.56 (m, 4H), 3.32 (m, 2H), 2.66 (m, 8H), 2.27 (s, 2H), 2.16 (s, 1H).

4.8.2 Synthesis of ligand 8b



A solution of benzyl bromide (3.5 mmol) in acetonitrile (3.0 mL) was dropwise over a period of 15 minutes to a solution of ligand **7g** (1.0 mmol) and DiPEA (8.0 mmol) in acetonitrile (5.0 mL). The mixture was allowed to react over night, then was dried in vacuum and the crude was dissolved in DCM (7.0 mL). The organic solution was washed with H₂O (5 x 5.0 mL) and brine (3 x 5.0 mL) in order to remove the unreacted materials and the ammonium salt. The organic phase was then treated with Na₂SO₄ and dried in vacuum leading to product **8b** as a brown oil with no further purification.

Yield: 72%

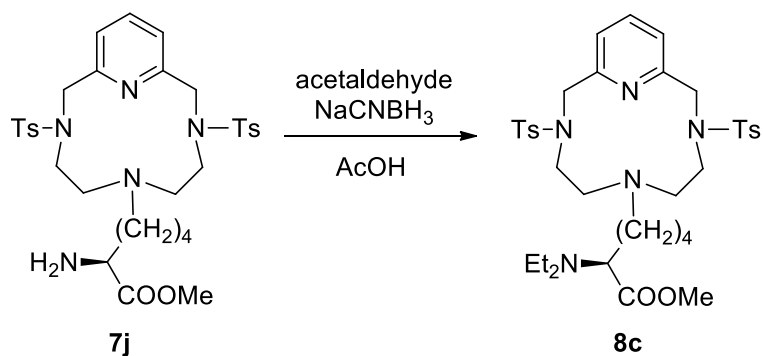


¹H NMR (300 MHz; CDCl₃; T = 300 K) δ 7.48 (t, *J* = 7.6 Hz, 1H, H_j), 7.42-7.15 (m, 15H), 6.84 (d, *J* = 7.7 Hz, 2H, H_i), 4.20 (s, 2H, H₁₄), 3.86 (s, 4H_{2,10}), 3.75-3.60 (m, 8H, H_{4,8,13}), 3.07 (br, 4H, H_{5,7})

¹³C NMR (101 MHz, D₂O) δ 159.1 (C₁), 138.0 (CH), 137.4 (C), 130.9 (CH), 129.9 (CH), 129.5 (CH), 129.4 (CH), 128.7 (CH), 128.0 (CH), 120.7 (CH), 61.8 (CH₂), 58.8 (CH₂), 52.7 (CH₂), 52.2 (CH₂), 50.1 (CH₂)

MS (EI) m/z 476.7 [M⁺].

4.8.3 Synthesis of ligand 8c



Ligand **7j** (0.88 mmol) was dissolved in AcOH (1.5 mL). NaCNBH₃ (2.65 mmol) was added and the mixture was let to stir 10 min at rt. Acetaldehyde (19.36 mmol) was added ver 72 h in small amounts (4 eq. every 12 h). The solvent was evaporated to dryness, then brine (10.0 mL) was added and the solution was extracted with DCM (5 x 10.0 mL). The organic phase was treated with Na₂SO₄ and the solvent was evaporated to dryness yielding to **8c** as a light yellow foam.

Yield: 61%

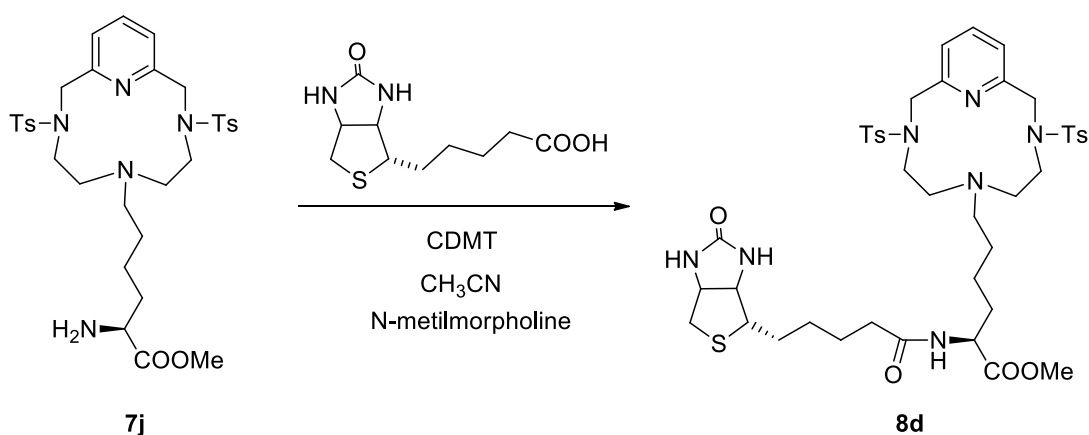
¹H NMR (400 MHz, CDCl₃) 7.72 (d, *J* = 8.2 Hz, 5H, H_{Ar}), 7.32 (t, *J* = 8.5 Hz, 6H, H_{Ar}), 4.34 (s, 4H, CH₂), 3.67 (s, 3H, OCH₃), 3.31 (t, *J* = 7.4 Hz, 1H, CH), 3.15–3.03 (m, 4H, CH₂), 2.70 (dq, *J* = 14.5, 7.2 Hz, 2H, CH₂), 2.51–2.40 (m, 8H, CH₂ + CH₃), 2.27 (dd, *J* = 16.6, 9.9 Hz, 6H, CH₂), 1.60 (ddd, *J* = 15.6, 14.6, 9.2 Hz, 2H, CH₂), 1.31 (m, 2H, CH₂), 1.02 (t, *J* = 7.1 Hz, 6H, CH₃)

¹³C NMR (100 MHz, CDCl₃) 174.2 (CO), 155.1 (C_{Ar}), 143.6 (C_{Ar}), 138.9 (CH_{Ar}), 136.2 (C_{Ar}), 130.0 (CH_{Ar}), 127.3 (CH_{Ar}), 124.2 (CH_{Ar}), 110.7 (CH), 63.2 (CH), 55.5 (CH₂), 54.8 (CH₂), 51.7 (CH₂), 51.1 (CH), 44.7 (CH₂), 29.9 (CH₂), 28.3 (CH₂), 24.1 (CH₂), 21.7 (CH₃), 14.1 (CH₃)

MS (ESI): *m/z* (%) = 712.3 (100) [MH]⁺

Elem. An. calcd for C₃₆H₅₁N₅O₆S₂: C, 60.56; H, 7.20; N, 9.81. Found: C, 60.22; H, 7.12; N, 10.02

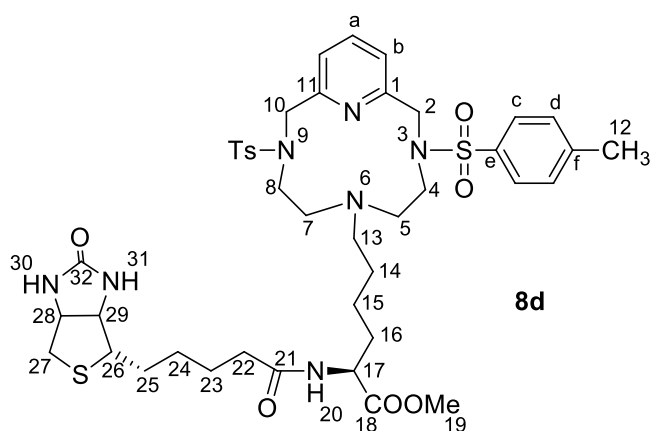
4.8.4 Synthesis of ligand 8d



Ligand **7j** (0.094 g, 0.143 mmol) was dissolved in 6.0 mL of acetonitrile. The other reagents were added in this order: biotin (0.035 g, 0.146 mmol), CDMT (0.027 g, 0.152 mmol) and 24.0 μL of *N*-methylmorpholine. The mixture was left to react at RT for 24h, then refluxed for 3h.

The solvent was concentrated, water was added and the water phase was washed with 3 x 15.0 mL of DCM. The organic phases were collected and dried leading to **8d**.

Yield 54%



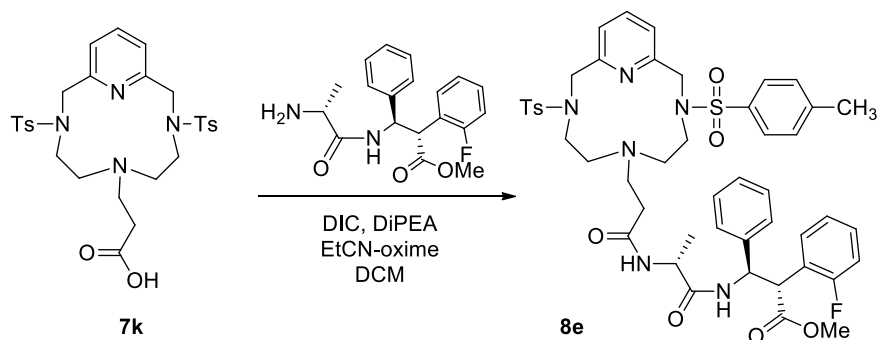
$^1\text{H NMR}$ (400 MHz, DMSO-d_6) δ 7.83 (t, $J = 7.6$ Hz, 1H, H_a), 7.77 (d, $J = 7.7$ Hz, 4H, H_c), 7.45 (d, $J = 7.8$ Hz, 4H, H_d), 7.28 (d, $J = 7.4$ Hz, 2H, H_b), 6.38 (d, $J = 18.8$ Hz, 2H, H_{30} s a 6.40 ppm + H_{31} s a 6.35 ppm), 4.29 (d, $J = 10.6$ Hz, 4H, $\text{H}_2 + \text{H}_{10} + \text{H}_{28}$), 4.11 (s, 1H, H_{29}), 3.77 (d, $J = 4.0$ Hz, 1H, H_{17}), 3.65 – 3.58 (m, 3H, H_{19}), 3.04 (s, 5H, $\text{H}_4 + \text{H}_8 + \text{H}_{26}$), 2.80 (dd, $J = 12.4, 4.9$ Hz, 1H, H_{27}), 2.57 (d, $J = 12.4$ Hz, 1H, H_{27}'), 2.41 (s, 6H, H_{12}), 2.31 (d, $J = 39.1$ Hz, 4H, $\text{H}_5 + \text{H}_7$), 2.26 (s, 4H, CH_2), 2.17 – 2.08 (m, 2H, H_{22}), 1.75 – 1.04 (m, 10H, CH_2).

¹³C NMR (101 MHz, DMSO-d₆) δ 172.61 (s, C₁₈), 172.12 (s, C₂₁), 162.44 (s, C₃₂), 154.82 (s, C₁ + C₁₁), 143.16 (s, C_e), 138.50 (s, C_a), 135.22 (s, C_f), 129.73 (s, C_d), 126.79 (s, C_a), 123.04 (s, C_b), 60.80 (s, C₂₉), 58.96 (s, C₂₈), 54.80 (s, C₂₅), 54.13 (s, C₂ + C₁₀ + CH₂), 53.92 (s, C₁₇), 51.50 (d, J = 8.9 Hz, C₁₉), 50.50 (s, C₅ + C₇), 44.89 (s, C₄ + C₈), 40.68 – 37.75 (m, DMSO-d₆ + CH₂), 34.46 (s, C₂₂), 30.56 (s, CH₂), 27.80 (d, J = 4.8 Hz, CH₂), 24.97 (s, CH₂), 22.67 (s, CH₂), 20.75 (s, C₁₂).

¹⁴N NMR (41 MHz, DMSO-d₆) δ 310.92 (s, 1N, N pyridine), 91.07 (s, 1N, N₂₀), 84.93 (s, 1N, N₃₀), 75.64 (s, 1N, N₃₁), 30.11 (s, 1N, N₆).

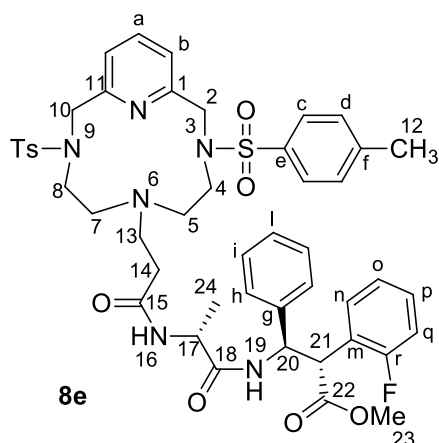
MS (ESI) m/z 885.

4.8.5 Synthesis of ligand 8e



A solution of compound **7k** (0.4 mmoles) and the selected dipeptide (0.4 mmoles) in DCM (0.1 M) was treated with DIC (1.1 equivalents), ethylencianooxime (1.1 equivalents) and DiPEA (1.1 equivalents). The resulting mixture was stirred at RT for 12 hours. The solvent was dried and the crude was purified with SiO₂ flash column chromatography using DCM/MeOH 20 : 1 as the eluent.

Yield: 60%



$^1\text{H NMR}$ (400 MHz, CDCl_3) δ 7.71 (dd, $J = 16.9, 9.7$ Hz, 6H, H_{ar}), 7.54 (s, 2H, H_{ar}), 7.38 – 7.10 (m, 11H, H_{ar}), 7.04 (t, $J = 9.0$ Hz, 1H, H_{q}), 5.68 (t, $J = 8.5$ Hz, 1H, H_{20}), 4.46 (d, $J = 10.1$ Hz, 1H, H_{21}), 4.40 – 4.28 (m, 4H, $\text{H}_2 + \text{H}_{10}$), 4.23 – 4.13 (m, 1H, H_{17}), 3.47 (s, 3H, H_{23}), 3.12 (s, 4H, $\text{H}_4 + \text{H}_8$), 2.43 (d, $J = 14.2$ Hz, 12H, H_{12} s a 2.44 ppm + $\text{H}_5 + \text{H}_7 + \text{CH}_2$), 2.11 (d, $J = 19.0$ Hz, 2H, CH_2), 1.60 (s, 2H, NH), 1.05 (d, $J = 5.9$ Hz, 3H, H_{24}).

$^{13}\text{C NMR}$ (101 MHz, CDCl_3) δ 170.97 ($\text{C}_{18} + \text{C}_{22}$), 154.99 (C_{ar}), 143.78 (C_{ar}), 138.84 (C_{ar}), 135.71 (C_{ar}), 129.99 (C_{ar}), 129.76 (C_{ar}), 127.89 (C_{ar}), 127.24 (C_{ar}), 124.54 (C_{ar}), 123.91 (C_{ar}), 115.24 (d, $J = 23.0$ Hz, C_{q}), 54.49 (C_{20}), 52.17 (C_{23}), 50.75 ($\text{C}_5 + \text{C}_7 + \text{CH}_2$), 48.94 (C_{21}), 48.40 (C_{17}), 44.29 ($\text{C}_4 + \text{C}_8$), 32.99 (CH_2), 21.55 (C_{12}), 16.42 (C_{24}).

$^{19}\text{F NMR}$ (282 MHz, CDCl_3) δ -117.93 (1F, F_{r})

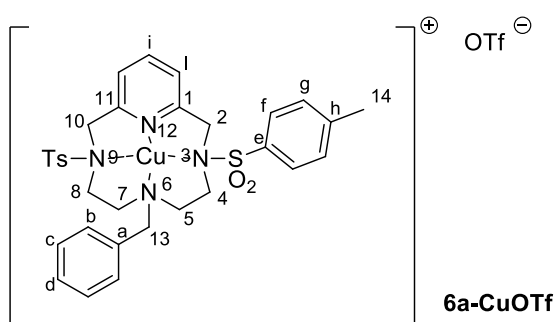
MS (ESI) m/z 914

4.9 Copper complexes

4.9.1 Method 1:

Copper(I) triflate benzene complex (40 mg, 0.08 mmol) was added to a solution of **6** (0.16 mmol) in dichloroethane (5 mL). The solution was stirred at room temperature for 1 hour, toluene (10 mL) was layered. After standing at room temperature for 16 hours, the white precipitated was filtered and dried in vacuum under nitrogen atmosphere.

Yields	6a-CuOTf:	95%
	6d-CuOTf:	98%
	6e-CuOTf:	97%



¹H NMR (400 MHz; CDCl₃): δ 7.79 (m, 4H, H_{Ts}), 7.74 (m, 1H, H_{Ar}), 7.64 (m, 1H, H_{Ar}), 7.58–7.53 (m, 2H, H_{Ar}), 7.46 (m, 2H, H_{Ar}), 7.42–7.40 (m, 4H, H_{Ts}), 7.34 (m, 1H, H_{Ar}), 7.09 (m, 1H, H_{Ar}), 5.14 (m, 1H, CH₂), 4.94 (m, 2H, H₁₃), 4.50 (d, J = 17.2 Hz, 1H, CH₂), 4.39 (m, 1H, CH₂), 4.23 (d, J = 17.2 Hz, 1H, CH₂), 4.07 (m, 1H, CH₂), 3.82 (m, 2H, CH₂), 3.40 (m, 1H, CH₂), 3.26–3.10 (m, 3H, CH₂), 2.51 (s, 3H, H₁₄), 2.48 (s, 3H, H₁₄), 2.28 (m, 1H, CH₂)

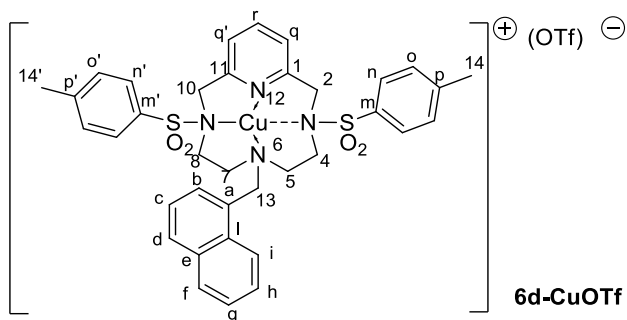
¹³C NMR (100 MHz; CDCl₃) δ 157.1 (C), 139.4 (C), 139.0 (C), 131.3 (CH), 130.6 (CH), 130.4 (CH), 130.3 (C), 130.0 (CH), 128.7 (CH), 127.8 (CH), 125.9 (CH), 124.1 (CH), 121.5 (CH), 58.7 (CH₂), 56.1 (CH₂), 53.9 (CH₂), 52.8 (CH₂), 50.1 (CH₂), 48.4 (C₁₃), 45.6 (CH₂), 21.6 (C₁₄)

¹⁵N NMR (40 MHz; CDCl₃; T = 300 K): δ 278 (N₁₂), 92 (N_{Ts}), 46 (N₆)

¹⁹F NMR (376 MHz; CDCl₃; T = 300 K): δ -78.3

Elem. an. Found: C, 48.6; H, 4.6; N, 6.7%

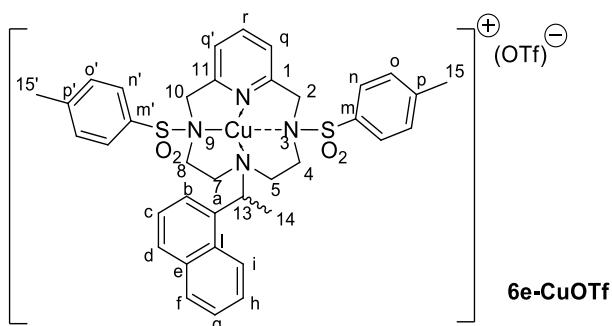
Calculated: C, 48.5; H, 4.4; N, 6.9%



¹H NMR (300 MHz; CDCl₃; T = 300 K) δ 8.97 (d, J = 7.8 Hz, 1H, H_i), 8.08-8.05 (m, 2H, H_{Ar}), 7.92 (m, 1H, H_{Ar}), 7.85-7.75 (m, 2H, H_r), 7.65-7.52 (m, 7H, H_{Ar}), 7.42-7.37 (m, 4H, H_{Ar}), 7.27-7.17 (m, 2H, H_{Ar}), 4.89 (d, J = 14.7 Hz, 2H, H₂ and H₁₀), 4.46 (m, 2H, H₁₃), 3.68 (d, J = 14.7 Hz, 2H, H₂ and H₁₀), 3.53 (m, 2H, H₄ and H₈), 2.93 (m, 2H, H₄ and H₈), 2.82 (m, 2H, H₅ and H₇), 2.50 (s, 6H, H₁₄), overlapping with 2.58-2.50 (m, 2H, H₅ and H₇)

Elem. An. Found: C, 51.4; H, 4.3; N, 6.1

Calculated: C, 51.2; H, 4.4; N, 6.6



¹H NMR (400 MHz; CDCl₃; T = 300 K) δ 8.93 (d, J = 8.1 Hz, 1H, H_i), 8.07 (d, J = 8.3 Hz, 1H, H_r), 7.92-7.88 (m, 3H, H_{Ar}), 7.82-7.74 (m, 2H, H_{Ar}), 7.69-7.62 (m, 2H, H_b and H_c), 7.53-7.48 (m, 3H, H_{Ar}), 7.39-7.36 (m, 3H, H_{Ar}), 7.29 (m, 2H, H_o), 7.05 (d, J = 7.5 Hz, 1H, H_q), 5.59 (q, J = 6.5 Hz, 1H, H₁₃), 5.31 (d, J = 16.4 Hz, 1H, H₁₀), 4.69 (m, 1H, H₇), 4.35 (m, 1H, H₂), 3.94 (d, J = 16.6 Hz, 1H, H_{10'}), 3.18 (m, 1H, H_{2'}), 3.04 (d, J = 14.2 Hz, 1H, H₈), 2.88-2.82 (m, 3H, CH₂), 2.56 (s, 3H, H₁₅), 2.42 (s, 3H, H₁₅), 2.34 (m, 2H, CH₂), 2.21 (d, J = 14.2 Hz, 1H, H₅), 1.69 (d, J = 6.5 Hz, 3H, H₁₄)

¹³C NMR (100 MHz; CDCl₃; T = 300 K) δ 156.2 (C₁₁), 152.9 (C₂), 146.2 (CH), 145.9 (CH), 140.0 (C_r), 137.2 (C_a), 134.1 (C_f), 131.9 (CH), 131.5 (CH), 130.6 (C_{o'}), 130.0 (C_o), 129.2 (C_n), 128.9 (CH), 128.3 (CH), 128.2 (CH), 126.7 (C_b), 126.0 (C_c), 125.2 (C_{q'}), 124.7 (C_g),

124.6 (CH), 124.1 (CH), 118.2 (C_h), 94.2 (C_i), 56.5 (C₂), 56.1 (C₁₀), 53.1 (C₁₃), 51.0 (C₅),
48.9 (C₇), 45.9 (C₄), 21.7 (C_{15'}), 21.5 (C₁₅), 12.9 (C₁₄)

¹⁵N NMR (40 MHz; CDCl₃; T = 300 K) δ 245 (N₁₂), 51 (N₆). The signals relative to N-Ts were not detected

¹⁹F NMR (376 MHz; CDCl₃; T = 300 K) δ - 78.6 (s)

IR ν (cm⁻¹) 1447.0 (w), 1343.5 (w), 1223.5 (w), 1260.9 (s), 1223.5 (m), 1165.4 (s), 1085.3 (w),
1029.5 (s), 802.6 (w), 759.7 (m), 720.4 (m), 710.0 (m), 660.5 (s), 637.6 (s)

Elem. An.: Found: C, 51.6; H, 4.9; N, 6.7

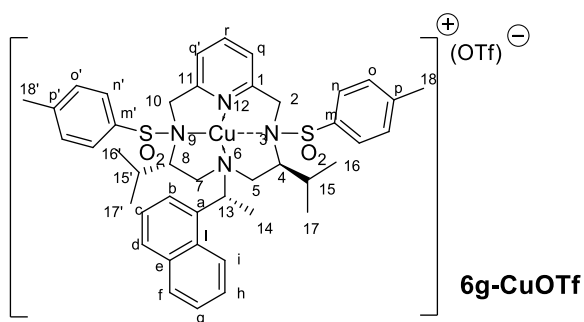
Calculated: C, 51.9; H, 4.6; N, 6.4

[α]_D²⁰ - 115 (c 0.5 in CHCl₃)

4.9.2 Method 2:

Copper(I) triflate benzene complex (30.0 mg, 0.06 mmol) was added to a solution of **6** or **7** or **8** (0.12 mmol) in dichloroethane (10.0 mL). The solution was stirred at room temperature for 1 hour, then was concentrated to half volume and *n*-hexane was layered until the product precipitates as white powder. The white precipitated was filtered and dried in vacuum under nitrogen atmosphere.

Yields	6g-CuOTf:	97%
	6j-CuOTf:	97%
	6k-CuOTf:	98%
	7j-CuOTf:	21% (<i>not soluble in the common NMR solvents</i>)
	8d-CuOTf:	38%



¹H NMR (300 MHz; CDCl₃) δ 8.68 (d, *J* = 8.7 Hz, 1H, H_i), 7.93 (d, *J* = 8.0 Hz, 1H, H_{Ar}), 7.87 (d, *J* = 8.1 Hz, 4H, H_n), 7.80-7.69 (m, 3H, H_{Ar}), 7.62-7.40 (m, 7H, H_{Ar}), 7.23-7.16 (m, 2H, H_{Ar}), 5.95 (q, *J* = 6.6 Hz, 1H, H₁₄), 5.25 (d, *J* = 20 Hz, 1H, H₂), 4.79 (d, *J* = 12.7 Hz, 1H, H₇), 4.71 (d, *J* = 14.6 Hz, 1H, H₁₀), 4.62 (d, *J* = 20 Hz, 1H, H_{2'}), overlapping with 4.61 (m, 1H, H₈), 4.01 (d, *J* = 14.6 Hz, 1H, H_{10'}), 2.78 (d, *J* = 12.7 Hz, 1H, H_{7'}), 2.57 (s, 3H, CH₁₈), overlapping with 2.57 (m, 1H, H₄), 2.52 (s, 3H, H_{18'}), 2.42-2.37 (m, 1H, H₅), 2.30-2.15 (m, 2H, H_{5'} and H_{15'}), 2.10 (d, *J* = 6.8 Hz, 3H, H₁₄), 1.59 (m, 1H, H₁₅), 0.90 (d, *J* = 6.7 Hz, 3H, CH_{16'}), 0.68 (d, *J* = 6.2 Hz, 3H, H₁₇), 0.29 (d, *J* = 6.5 Hz, 3H, H₁₇), -0.49 (d, *J* = 6.2 Hz, 3H, H₁₆)

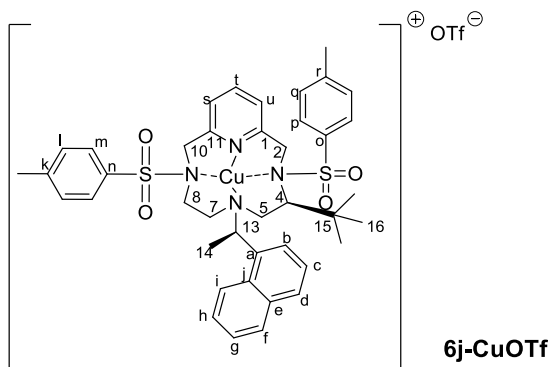
¹³C NMR (75 MHz; CDCl₃) δ 155.7 (C₁₁), 151.2 (C₁), 145.6 (C_{p'}), 145.3 (C_p), 140.4 (CH), 134.8 (C_a), 134.5 (C_i), 133.9 (C), 132.1 (C), 131.5 (CH), 130.4 (C_o), 129.8 (CH), 129.3 (CH), 128.9 (CH), 127.7 (CH_h), 127.3 (CH), 126.4 (CH), 125.2 (CH), 124.8 (CH), 124.5 (CH), 123.9 (CH), 122.8 (C_i), 64.7 (C₄), 62.0 (C₈), 57.4 (C₅), 57.1 (C₁₀), 56.4 (C₁₃), 55.5 (C₇), 46.8 (C₂),

29.9 (C_{15'}), 27.1 (C₁₅), 24.5 (C₁₄), 22.4 (C_{16'}), 21.9 (C_{18 and 18'}), 21.3 (C_{17'}), 20.3 (C₁₇), 18.5 (C₁₆)

¹⁹F NMR (282 MHz; CDCl₃; T = 300 K) δ - 78.58 (s)

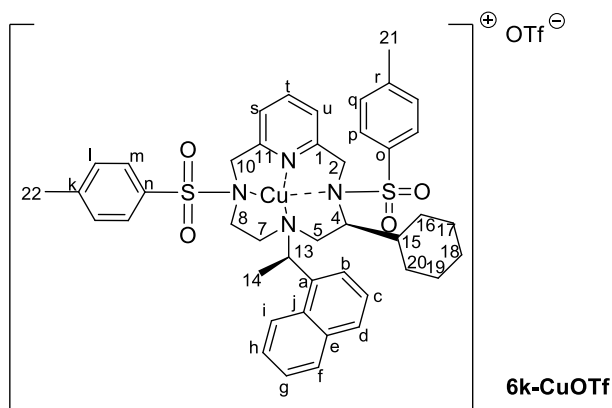
Elem. An. Found: C, 54.7; H, 5.2; N, 5.7

Calculated: C, 54.7; H, 5.4; N, 5.8



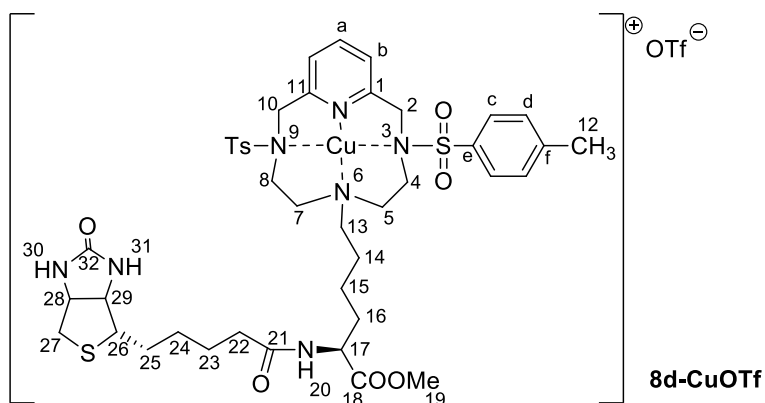
¹H NMR (300 MHz; CDCl₃) δ 8.59 (d, *J* = 7.3 Hz, 1H, H_h), 8.06-7.12 (m, 17H), 6.00 (m, 1H, H₁₄), 5.25 (d, *J* = 18.9 Hz, 1H, H₂), 4.81-4.64 (m, 3H, H_{2'}, H₈ and H₁₀), 4.60-4.55 (m, 1H, H₄), 3.63 (d, *J* = 15.4 Hz, 1H, H_{10'}), 3.14 (d, *J* = 13.2 Hz, 1H, H_{8'}), 2.96 (m, 1H, H_{7,7'}), 2.79-2.36 (m, 2H, H_{5,5'}), 2.57-2.55 (m, 6H, H₁₇ and H₁₈), 2.15 (m, 3H, H₁₄), 0.35 (s, 9H, H₁₆).

¹³C NMR (75 MHz; CDCl₃) δ 154.59 (C₂), 152.91 (C₁₀), 147.18 (C_r), 145.81 (C_k), 140.38 (C_t), 136.25 (C_a), 134.78 (C_{Ar}), 133.71 (C_{Ar}), 132.07 (C_{Ar}), 131.13 (C_{Ar}), 132.07 (C_{Ar}), 131.13 (C_{Ar}), 130.63 (C_{Ar}), 130.29 (C_{Ar}), 129.89 (C_{Ar}), 129.82 (C_{Ar}), 129.11 (C_{Ar}), 128.72 (C_{Ar}), 128.28 (C_{Ar}), 128.17 (C_{Ar}), 127.66 (C_{Ar}), 126.52 (C_{Ar}), 125.71 (C_{Ar}), 124.60 (C_{Ar}), 123.85 (C_{Ar}), 122.70 (C_{Ar}), 62.40 (C₄), 56.47 (C₁₃), 56.35 (C₁₀), 55.69 (C₅), 52.49 (C₈), 49.68 (C₇), 48.46 (C₂), 35.10 (C₁₅), 27.65 (C₁₆), 24.92 (C₁₄), 22.11 (C₁₇ and C₁₈)



¹H NMR (300 MHz; CDCl₃) δ 8.67 (d, *J* = 8.7 Hz, 1H, H_h), 7.95 (d, *J* = 8.0 Hz, 1H, H_{Ar}), 7.88-7.78 (m, 6H, H_{Ar}), 7.67-7.58 (m, 4H), 7.54-7.52 (m, 4H, H_l, H_q), 7.29 (d, *J* = 4.9 Hz, 1H - H_s), 7.16 (d, *J* = 7.4 Hz, 1H - H_u), 5.96 (d, *J* = 6.9 Hz, 1H - H₁₃), 5.17 (d, *J* = 19.5 Hz, 1H - H₂), 4.75-4.66 (m, 1H - H₇), 4.70 (d, *J* = 15.6 Hz, 1H - H₁₀), 4.58 (m, 1H - H₄), 4.44 (d, *J* = 19.5 Hz, 1H - H_{2'}), 3.56 (d, *J* = 15.6 Hz, 1H - H_{10'}), 3.00-2.76 (m, 3H, H_{7'}, H_{8-8'}), 2.55 (s, 3H, H₂₁), 2.54 (s, 3H, H₂₂), 2.54-2.47 (m, 1H, H₅), 2.34 (d, *J* = 6.5 Hz, 1H - H_{5'}), 1.66-1.54 (m, 2H, H₂₀ - H₁₇), 1.40-1.36 (m, 1H, H₁₈), 1.16-1.10 (m, 1H, H₁₅), 1.05-0.96 (m, 2H, H₁₉ - H₁₇), 0.77-0.70 (m, 2H, H_{20'} - H_{19'}), 0.68-0.56 (m, 1H, H_{18'}), 0.17 (d, *J* = 11.6 Hz, 1H - H₁₆), -1.22 (d, *J* = 11.6 Hz, 1H - H_{16'})

¹³C NMR (75 MHz; CDCl₃) δ 155.23 (C₁₁), 152.26 (C₁), 147.07 (C_r), 145.52 (C_k), 140.06 (C_t), 135.62 (C_a), 134.77 (C_j), 133.29 (C_n), 132.17 (C_e), 131.05 (C_{Ts}), 129.88 (C_{Ar}), 129.77 (C_{Ar}), 129.21 (C_m), 128.72 (C_{Ar}), 128.54 (C_o), 127.55 (C_{Ar}), 126.43 (C_{Ar}), 125.63 (C_{Ts}), 125.04 (C_{Ts}), 123.31 (C_u), 123.09 (C_s), 123.04 (C_h), 61.74 (C₄), 56.32 (C₅ - C₁₀), 56.00 (C₁₃), 51.81 (C₇), 49.20 (C₂), 46.80 (C₈), 36.48 (C₁₅), 30.30 (C₁₆), 29.35 (C₁₇), 29.06-25.96 (C₂₀ - C₁₈ - C₁₉), 24.27 (C₁₄), 22.13 (C₂₁), 22.08 (C₂₂)



¹H NMR (400 MHz, DMSO-*d*₆) δ 7.88 (dd, *J* = 14.2, 7.8 Hz, 5H, H_a piridina + H_c tostile), 7.52 (d, *J* = 7.9 Hz, 4H, H_d tostile), 7.46 (d, *J* = 7.7 Hz, 2H, H_b piridina), 6.39 (d, *J* = 29.1 Hz, 3H, H₃₀ s a 6.40 ppm + H₃₁ s a 6.35 ppm + H₂₀), 4.61 (d, *J* = 17.2 Hz, 2H, H₂ + H₁₀), 4.34 – 4.27 (m, 2H, H₂₈), 4.19 (d, *J* = 17.1 Hz, 2H, H_{2'} + H_{10'}), 4.16 – 4.10 (m, 2H, H₂₉), 4.07 (s, 2H, H₅ + H₇), 3.80 (d, *J* = 10.1 Hz, 4H, H₁₉ + H₁₆), 3.60 (s, 2H, H₄ + H₈), 3.51 (s, 2H, H₂₂), 3.34 (s, 2H, H₄ + H₈), 3.17 (s, 1H, H_{16'}), 3.10 (s, 3H, H₅ + H₇ + H₂₆), 2.82 (dd, *J* = 12.5, 4.9 Hz, 1H, H₂₇), 2.78 (s, 1H, H₁₇), 2.58 (d, *J* = 12.4 Hz, 1H, H_{27'}), 2.45 (s, 6H, H₁₂), 2.20 (s, 2H, H₁₃), 1.69 – 1.21 (m, 10H, CH₂)

¹³C NMR (101 MHz, DMSO-*d*₆) δ 174.12 (C₁₈), 162.43 (C₂₁ + C₃₂), 157.61 (C₁ + C₁₁), 144.21 (C_e), 138.93 (C_a), 133.02 (C_f), 129.90 (C_d), 127.34 (C_c), 121.13 (C_b), 60.78 (C₂₉), 58.91 (C₂₈), 55.09 (C₂₆), 52.68 (C₁₉), 52.32 (C₁₆), 51.38 (C₂ + C₁₀), 48.26 (C₄ + C₈), 45.22 (C₅ + C₇), 42.27 (C₁₇), 41.24 (C₂₂), 33.20 (C₁₃), 27.78 (CH₂), 24.25 (CH₂), 20.77 (C₁₂)

¹⁴N NMR (41 MHz, DMSO-*d*₆) δ 278.15 (s, 1N, N piridina), 85.17 (s, 1N, N₃₀), 75.81 (s, 1N, N₃₁)

Elem An. Calculated for C₄₃H₅₇CuF₃N₇O₁₁S₄: C 47.09; H 5.24; N 8.94

Found: C 47.71; H 5.42; N 8.88

MS (MALDI) *m/z* 946.8

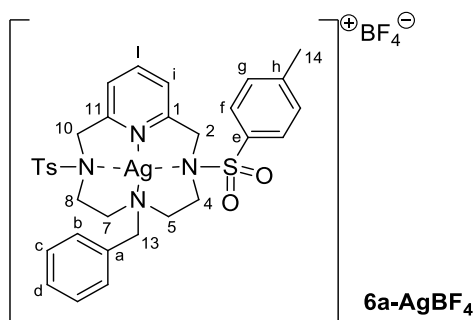
4.10 Silver complexes

4.10.1 Synthesis of silver BF₄ complexes

General Procedure

Silver tetrafluoroborate (165.0 mg, 0.85 mmol) was added to a solution of ligand **6** or **7** or **8** in dichloroethane (20.0 mL). The solution – kept in the dark until the final isolation of the product – was stirred at room temperature for one hour. The solvent was then concentrated to 3.0 mL and distilled *n*-hexane was added causing the precipitation of the product. The precipitate was recovered by filtration and dried in vacuum.

Yields	6a-AgBF₄:	91%
	6b-AgBF₄:	93%
	6d-AgBF₄:	90%
	6f-AgBF₄:	98%
	6r-AgBF₄:	99%
	6s-AgBF₄:	99%
	7j-AgBF₄:	75%
	7k-AgBF₄:	77%
	8c-AgBF₄:	97%
	8d-AgBF₄:	55%
	8e-AgBF₄:	37%



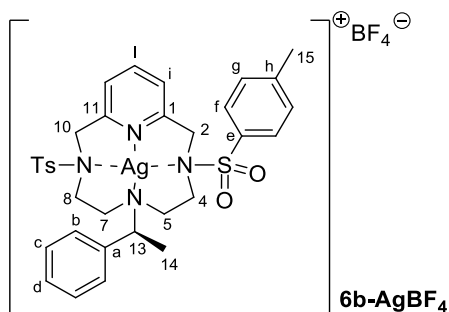
¹H NMR (300 MHz, CDCl₃, T = 300 K): δ = 7.77 (t, J = 7.7 Hz, 1H) overlapping with 7.74 (d, J = 8.0 Hz, 4H), 7.60 (d, J = 6.9 Hz, 2H), 7.45 (d, J = 8.0 Hz, 4H) overlapping with 7.42 (m, 3H), 7.28 (d, J = 7.7 Hz, 2H), 5.04 (d, J = 15.2 Hz, 2H), 3.97 (s, 2H), 3.70 (d, J = 15.2 Hz, 2H), 3.51 (m, 2H), 2.94 (m, 2H), 2.65 (m, 2H), 2.49 (s, 6H), 2.06 (m, 2H)

¹³C NMR (100 MHz, CDCl₃, T = 300 K) δ 153.4, 145.9, 140.5, 135.6, 130.9, 130.7, 130.6, 128.8, 128.6, 128.4, 125.0, 58.4, 56.3, 52.9, 47.5, 21.9

¹⁹F NMR (282 MHz, CDCl₃, T = 300 K): δ = -152.8

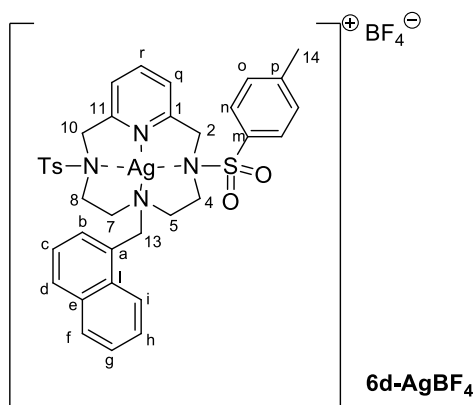
MS (FAB) m/z (%) = 711 m/z (100) [M⁺ - BF₄], 605 (94) [MH - AgBF₄]⁺

UV/vis (5.2x10⁻⁵ mol/L, CHCl₃ in 1cm cuvettes): λ_{max} [nm], (log ϵ) = 243 (4.26); 263 (3.89) nm



¹H NMR (300 MHz, CDCl₃, T = 300 K) δ = 7.82 (m, 5H, H_{Ar}), 7.51 (m, 4H, H_{Ar}), 7.46 (m, 4H, H_{Ar}), 7.39 (m, 2H, H_{Ar}), 7.26 (m, 1H, H_{Ar}), 5.10 (d, J = 16.1 Hz, 1H, H₂), 4.99 (d, J = 14.8 Hz, 1H, H₁₀), 4.82 (q, J = 6.7 Hz, 1H, H₁₃), 4.33 (br, 1H), 3.96 (br, 1H), 3.87 (d, J = 16.1 Hz, 1H, H₂), 3.65 (d, J = 14.8 Hz, 1H, H₁₀), 3.64 (br, 1H), 3.15 (br, 1H), 2.76 (m, 1H), 2.54 (s, 3H, H₁₅), 2.53 (s, 1H, H₁₅), 2.45 (br, 1H), 1.95 (br, 1H), 1.86 (br, 1H), 1.80 (d, J = 6.7 Hz, 3H, H₁₄).

¹⁹F NMR (225 MHz, CDCl₃, T = 300 K) δ = -152.85 (¹⁰BF₄), -152.90 (¹¹BF₄).



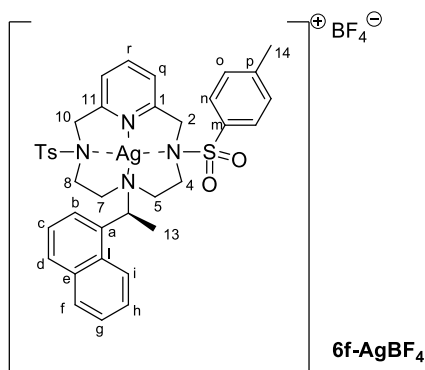
¹H NMR (300 MHz, CDCl₃, T = 300 K): δ 9.16 (d, J = 8.1 Hz, 1H, H_i), 8.12 (d, J = 8.1 Hz, 1H, H_f), 7.99 (d, J = 8.1 Hz, 1H, H_d), 7.90 (m, 1H, H_h), 7.81 (t, J = 7.9 Hz, 1H, H_r), 7.72 (m, 1H, H_b), 7.67-7.59 (m, 2H, H_c and H_g) overlapping with 7.59 (d, J = 7.8 Hz, 4H, H_n), 7.41 (d, J = 7.8 Hz, 4H, H_o), 7.24 (d, J = 7.9 Hz, 2H, H_q), 4.89 (d, J = 15.0 Hz, 2H, H² and H₁₀), 4.35 (br s, 2H, H₁₃), 3.50 (d, J = 15.0 Hz, 2H, H_{2'} and H_{10'}) overlapping with 3.51-3.48 (m, 2H, CH₂), 2.81 (m, 2H, CH₂), 2.59 (m, 2H, CH₂), 2.49 (s, 6H, H₁₄), 2.13 (m, 2H, CH₂)

¹³C NMR (75 MHz, CDCl₃, T = 300 K): δ 154.0 (C₁), 146.0 (C_p), 141.0 (C_r), 135.3 (C_m), 133.8 (C), 133.2 (C), 132.5 (C_f), 131.1 (C), 130.8 (C_o), 130.7 (C_b), 130.0 (C_d), 128.6 (C_n), 127.1 (C_h), 126.4 (CH), 125.8 (CH), 125.3 (C_q), 112.3 (C_i), 56.4 (C₁₃), 56.3 (C₂ and C₁₀), 54.7 (CH₂), 48.3 (CH₂), 22.1 (C₁₄)

¹⁹F NMR (282 MHz, CDCl₃, T = 300 K): δ -152.8

MS (FAB) m/z (%) = 761/763 (90/100) [M - BF₄]⁺, 655 (37) [MH - AgBF₄]⁺

Elem. An. Found: C, 50.75; H, 4.61; N, 6.43 Calculated: C, 50.90; H, 4.51; N, 6.60



¹H NMR (400 MHz, CDCl₃): δ 9.42 (pst, *J* = 7.1 Hz, 1H, H_i), 8.15 (d, *J* = 8.3 Hz, 1H, H_{Ar}), 8.00 (m, 1H, H_h), 7.94 (d, *J* = 7.5 Hz, 1H, H_{Ar}), 7.87 (d, *J* = 8.2 Hz, 2H, H_n), 7.83 (pst, *J* = 7.8 Hz, 1H, H_r), 7.68–7.62 (m, 3 H, H_{Ar}), 7.52 (d, *J* = 8.2 Hz, 2H, H_o), 7.38 (d, *J* = 8.2 Hz, 2H, H_n), 7.33 (d, *J* = 7.9 Hz, 1H, H_q), 7.29 (d, *J* = 8.2 Hz, 2H, H_o), 7.08 (d, *J* = 7.6 Hz, 1H, H_q), 5.66 (q, *J* = 6.7 Hz, 1H, H₁₃), 5.11 (d, *J* = 15.4 Hz, 1H, H₂), 4.70 (m, 1H, H₄), 4.40 (d, *J* = 13.9 Hz, 1H, H₁₀), 3.64 (d, *J* = 15.4 Hz, 1 H, H₂), 3.04 (d, *J* = 13.9 Hz, 1H, H₁₀), 2.99–2.95 (m, 2H, CH₂), 2.63 (m, 1H, CH₂), 2.54 (s, 3H, H₁₄), 2.49 (m, 1H, CH₂), 2.41 (s, 3H, H₁₄), 2.41–2.09 (m, 3H, CH₂)

¹³C NMR (100 MHz, CDCl₃): δ 154.3 (C₁), 152.6 (C₁₁), 145.9 (C_p), 145.7 (C_{p'}), 141.3 (CH_r), 137.4 (C), 135.2 (C), 133.8 (CH), 132.4 (C), 131.8 (C), 130.8 (CH_o), 130.3 (CH_{o'}), 129.7 (C), 129.6 (CH), 128.7 (CH_{r'}), 128.3 (CH_n), 127.7 (CH), 126.30 (CH), 126.26 (CH), 125.5 (CH), 125.3 (CH), 125.1 (CH_h), 104.7 (CH_i), 56.7 (C₂), 56.4 (C₁₀), 51.8 (C₁₃), 49.2 (CH₂), 48.9 (CH₂), 48.8 (CH₂), 45.5 (CH₂), 9.0 (C₁₄)

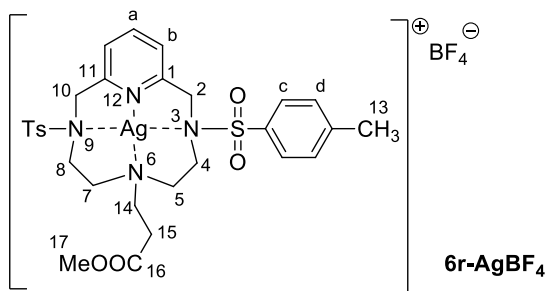
¹⁹F NMR (282 MHz, CDCl₃): δ -153.03 (¹⁰BF₄), -153.08 (¹¹BF₄)

¹¹B NMR (128 MHz, CDCl₃): δ -1.39 (p, *J*_{B-F} = 1.1 Hz)

¹⁵N NMR (40 MHz, CDCl₃): δ 265 (N₁₂), 101 and 97 (N₃ and N₉), 40 (N₆)

¹⁰⁹Ag NMR (19 MHz, CDCl₃): δ 536

Elem. An. C₃₇H₄₀AgBF₄N₄O₄S₂: calcd. C 51.46, H 4.67, N 6.49; found C 51.15, H 4.57, N 6.21



¹H NMR (400 MHz, CDCl₃): δ 7.91-7.70 (5H, m, H_c + H_a), 7.45 (4H, d, *J* = 7.8 Hz, H_d), 7.32-7.28 (2H, m, H_b), 5.04 (2H, d, *J* = 14.5 Hz, H₂ + H₁₀), 3.79 (3H, s, H₁₄), 3.72-3.60 (2H, m, H₂' + H₁₀'), 3.50-3.43 (2H, m, H₁₂), 3.05 (2H, br, CH₂), 2.92-2.76 (4H, br, H₇ + H₅), 2.72-2.58 (2H, br, CH₂), 2.49 (6H, s, H₁₅), 2.11 (2H, br, H₁₁)

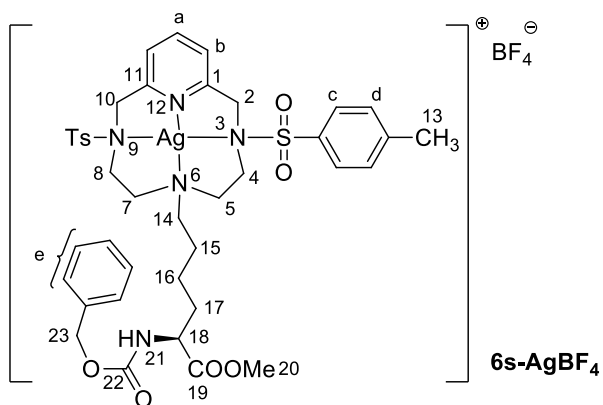
¹³C NMR (100 MHz, CDCl₃): δ 145.26 (C_{quaternary}tosyl), 140.2 (C_a), 130.2 (C_d), 127.8 (C_c), 125.0 (C_b), 56.0 (C₂ + C₁₀), 52.7 (C), 52.3 (C₁₄), 48.4 (C), 46.4 (C), 45.1 (C), 21.3 (C₁₇)

IR (ATR): 1727 cm⁻¹ (ν_{C=O}, ester), 1161 cm⁻¹ (sulfonamide)

UV-vis: (CH₂Cl₂): λ_{MAX} (log ε) 237 nm (4.44), 264 nm (3.96)

MS (FAB⁺) *m/z* 709 [M]⁺

Elem. An. C₂₉H₃₆N₄O₆S₂AgBF₄ Calculated: C, 43.79; H, 4.56; N, 7.04
Found: C, 41.89; H, 4.42; N, 6.52



¹H NMR (300 MHz, CDCl₃) δ 7.86-7.62 (5H, m, H_a + H_c), 7.49-7.27 (11H, m, H_b + H_d + H_e), 5.61 (1H, m, H₂₁), 5.23-4.92 (4H, m, H₂₃ + H₂ + H₁₀), 4.51 (1H, m, H₁₈), 3.76-3.61 (5H, s, H₂₀ + H_{2'} + H_{10'}), 3.46 (1H, br, CH₂), 3.29 (1H, br, CH₂), 2.97 (1H, br, CH₂), 2.80-2.54 (4H, m, CH₂), 2.53-2.25 (7H, m, H₁₃ + CH₂), 2.09 (1H, br, CH₂), 1.94 (1H, m, CH₂), 1.78 (3H, m, CH₂), 1.60 (2H, m, CH₂), 1.25 (2H, br, CH₂)

¹³C NMR (75 MHz, CDCl₃) δ 173.36 (C₁₉), 157.06 (C₂₂), 153.77 (C₁), 146.06 (C_{quaternarytosyl}), 140.36 (C_a), 130.90 (C), 130.37 (C_d), 128.58 (C_{quaternarytosyl}), 128.02 (C_{cbz}), 127.90 (C_c), 125.34 (C), 124.82 (C_b), 67.17 (C₂₃), 56.37 (C₂ + C₁₀), 53.43 (C), 53.41 (C), 53.37 (C₁₈), 52.39 (C₂₀), 46.69 (C), 29.60 (C), 22.63 (C), 21.47 (C₁₃)

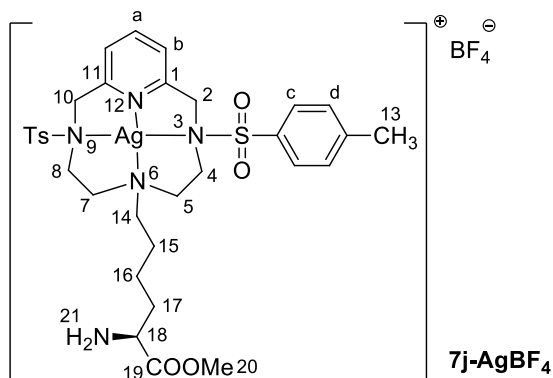
IR (ATR): 2351 cm⁻¹ (NC=O, amide), 1718 cm⁻¹ (ν_{C=O}, ester), 1160 cm⁻¹ (sulfonamide)

UV-vis (CH₂Cl₂): λ_{MAX} (log ε) 237 nm (4.37), 264 nm (3.86)

Elem. An. C₄₀H₄₉N₅O₈S₂AgBF₄ Calculated C, 48.96; H, 5.01; N, 7.10

Found: C, 51.54; H, 5.16; N, 7.16

MS (FAB⁺) *m/z* 900 [M]⁺

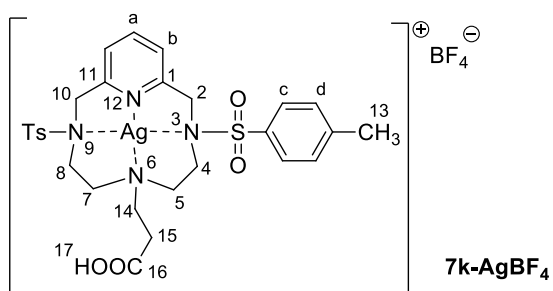


¹H NMR (300 MHz, CD₃OD) δ 7.93–7.67 (m, 5H, H_a + H_c), 7.53–7.20 (m, 6H, H_b + H_d), 4.61 (d, *J* = 17.4 Hz, 2H, NH₂), 4.44–4.14 (m, 2H, CH₂), 4.06 (d, *J* = 17.1 Hz, 2H, CH₂), 3.81–3.53 (m, 4H, H₂₀ + CH₂), 3.50–3.27 (m, 4H, CH₂), 3.20–2.91 (m, 3H, CH₂ + CH), 2.45 (s, 6H, H₁₃), 2.23–1.77 (m, 4H, CH₂), 1.74–1.51 (m, 2H, CH₂).

¹³C NMR (75 MHz, CD₃OD) δ 159.3 (CO), 146.5 (C_{Ar}), 140.3 (CH_{Ar}), 134.7 (C_{Ar}), 131.4 (CH_{Ar}), 131.0 (CH_{Ar}), 129.1 (CH_{Ar}), 128.2 (CH_{Ar}), 122.6 (CH_{Ar}), 67.8 (CH₂), 53.9 (CH), 53.7 (OCH₃), 53.4 (CH₂), 46.7 (CH₂), 43.6 (CH₂), 23.2 (CH₂), 21.5 (CH₃), 20.2 (CH₂)

MS (FAB⁺): *m/z* (%) = 766 (100); 764 (97%); 767 (40%); 765 (38%) [M - BF₄]⁺

Elem An. C₃₂H₄₃AgBF₄N₅O₆S₂ Calculated: C, 45.08; H, 5.08; N, 8.21
Found: C, 44.96; H, 5.42; N, 7.93

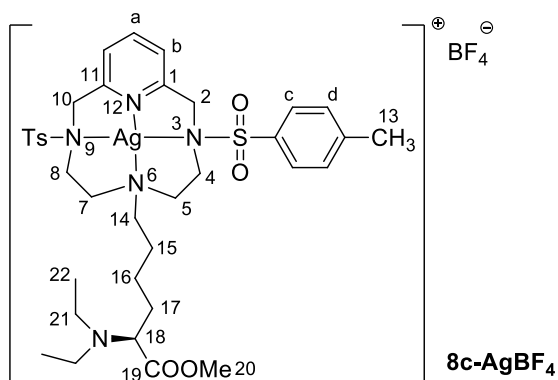


¹H NMR (300 MHz, DMSO-*d*₆) δ 8.03-7.61 (5H, m, H_{Ar}), 7.61-7.20 (6H, m, H_{Ar}), 4.88-3.64 (6H, br, CH₂), 3.12-2.68 (4H, br, CH₂), 2.47 (6H, s, H₁₃)

IR (ATR): 1741 cm⁻¹ (ν_{C=O}, COOH), 1158 cm⁻¹ (sulfonamide)

UV-vis (CH₂Cl₂): λ_{MAX} (log ε) 237 nm (4.37), 264 nm (3.85)

Elem. An. C₂₈H₃₄N₄O₆S₂AgBF₄ Calculated: C, 43.04; H, 4.89; N, 7.17
Found: C, 39.40; H, 4.21; N, 8.49

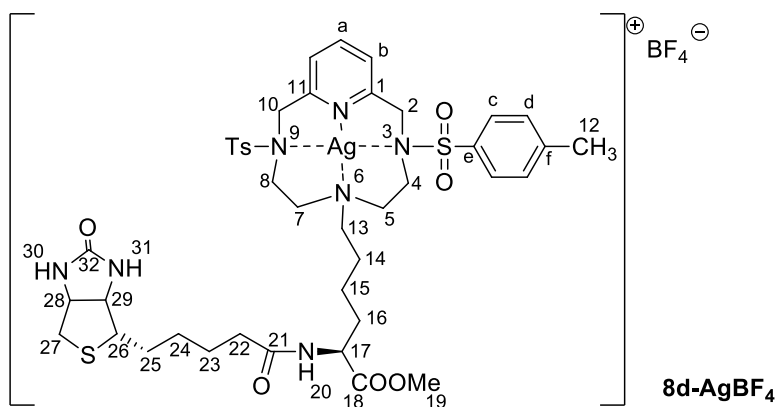


¹H NMR (600 MHz, CDCl₃) δ 7.78 (br, 5H, H_{a+c}), 7.46 (br, 4H, H_{Ar}), 7.32–7.26 (m, 2H, H_{Ar}) 5.09 (d, *J* = 13.8 Hz, 2H, CH₂), 3.82–3.58 (m, 6H, H₂₀ + CH₂), 3.20 (s, 1H, H₁₈), 3.09–2.79 (m, 4H, CH₂), 2.70–2.54 (m, 6H, CH₂), 2.48 (s, 6H, H₁₃), 2.23–2.05 (m, 2H, CH₂), 2.02–1.81 (m, 3H, CH₂), 1.75–1.45 (m, 2H, CH₂), 1.27 (br, 2H, CH₂), 1.15 (br, 6H, H₂₂)

¹³C NMR (151 MHz, CDCl₃) δ 153.7 (C_{Ar}), 145.8 (C_{Ar}), 140.6 (CH_{Ar}), 130.7 (CH_{Ar}), 128.7 (CH_{Ar}), 128.6 (CH_{Ar}), 125.0 (CH_{Ar}), 56.5 (CH₂), 21.8 (CH₃)

MS (FAB): *m/z* (%) 822 (100); 820 (97); 821 (40); 823 (38) [M-BF₄]⁺

Elem. An. C₃₆H₅₁AgBF₄N₅O₆S₂ Calculated: C, 47.59; H, 5.66; N, 7.71
Found: C, 47.62; H, 5.32; N, 7.75

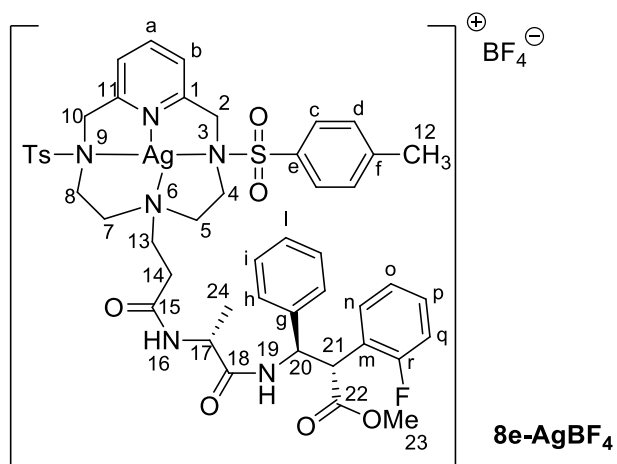


¹H NMR (400 MHz, DMSO-*d*₆) δ 7.88 (dd, *J* = 14.2, 7.8 Hz, 5H, H_a + H_c), 7.52 (d, *J* = 7.9 Hz, 4H, H_d), 7.46 (d, *J* = 7.7 Hz, 2H, H_b), 6.39 (d, *J* = 29.1 Hz, 3H, H₃₀ + H₃₁ + H₂₀), 4.61 (d, *J* = 17.2 Hz, 2H, H₂ + H₁₀), 4.34 – 4.27 (m, 2H, H₂₈), 4.19 (d, *J* = 17.1 Hz, 2H, H_{2'} + H_{10'}), 4.16 – 4.10 (m, 2H, H₂₉), 4.07 (s, 2H, H₅ + H₇), 3.80 (d, *J* = 10.1 Hz, 4H, H₁₉ + H₁₆), 3.60 (s, 2H, H₄ + H₈), 3.51 (s, 2H, H₂₂), 3.34 (s, 2H, H₄ + H₈), 3.17 (s, 1H, H_{16'}), 3.10 (s, 3H, H₅ + H₇ + H₂₆), 2.82 (dd, *J* = 12.5, 4.9 Hz, 1H, H₂₇), 2.78 (s, 1H, H₁₇), 2.58 (d, *J* = 12.4 Hz, 1H, H_{27'}), 2.45 (s, 6H, H₁₂), 2.20 (s, 2H, H₁₃), 1.69 – 1.21 (m, 10H, CH₂)

¹³C NMR (101 MHz, DMSO-*d*₆) δ 174.1 (C₁₈), 162.4 (C₂₁ + C₃₂), 157.6 (C₁ + C₁₁), 144.2 (C_e), 138.9 (C_a), 133.0 (C_f), 129.90 (C_d), 127.3 (C_c), 121.1 (C_b), 60.8 (C₂₉), 58.9 (C₂₈), 55.1 (C₂₆), 52.7 (C₁₉), 52.3 (C₁₆), 51.4 (C₂ + C₁₀), 48.3 (C₄ + C₈), 45.2 (C₅ + C₇), 42.3 (C₁₇), 41.2 (C₂₂), 33.2 (C₁₃), 27.8 (CH₂), 24.3 (CH₂), 20.8 (C₁₂)

Elem An. C₄₂H₅₇AgBF₄N₇O₈S₃ Calculated: C 46.76; H 5.33; N 9.09
 Found: C 47.31; H 5.47; N 8.89

MS (MALDI) *m/z* 992.25



¹H NMR (300 MHz, CDCl₃) δ 5.06 (d, *J* = 14.8 Hz, 2H, H₂ + H₁₀), 3.67 (d, *J* = 14.2 Hz, 2H, H₂' + H₁₀'), 3.51 (s, 3H, H₂₃), 2.51 (d, *J* = 5.3 Hz, 6H, H₁₂ + H₁₂)

¹⁹F NMR (282 MHz, CDCl₃) δ -116.25 (1F, F_r), -151.34 (4F, F_{anion})

Elem. An. C₄₇H₅₃AgBF₅N₆O₈S₂ Calculated: C 50.96; H 4.82; N 7.59 Found: C 52.20; H 5.03; N 7.08

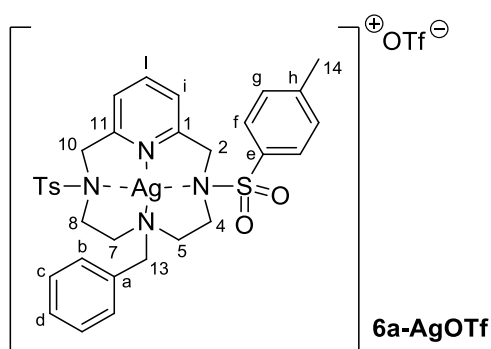
MS (FAB): m/z 1019

4.10.2 Synthesis of silver OTf complexes

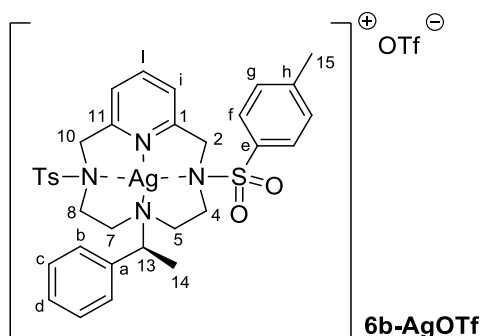
General Procedure:

Silver triflate (89.0 mg, 0.34 mmol) was added to a solution of **6** or **7** or **8** in dichloroethane (17.0 ml). The solution – kept in the dark until the final isolation of the product – was stirred at room temperature for one hour. The solvent was then concentrated to 3.0 mL and distilled *n*-hexane was added causing the precipitation of the product. The precipitate was recovered by filtration and dried in vacuum.

Yields	6a-AgOTf:	94%
	6b-AgOTf:	92%
	6d-AgOTf:	91%
	6r-AgOTf:	98%
	6s-AgOTf:	97%

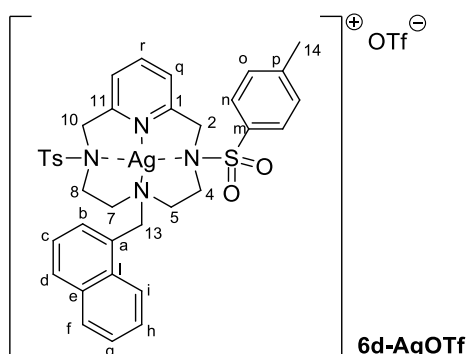


¹H NMR	(300 MHz, CDCl ₃): δ 7.83 (t, <i>J</i> = 7.7 Hz, 1H), 7.72 (d, <i>J</i> = 8.0 Hz, 4H), 7.65 (d, <i>J</i> = 7.1 Hz, 2H), 7.50 (m, 3H) overlapping with 7.45 (d, <i>J</i> = 8.0 Hz, 4H), 7.33 (d, <i>J</i> = 7.7 Hz, 2H), 5.01 (d, <i>J</i> = 14.9 Hz, 2H), 3.89 (s, 2H) overlapping with 3.85 (m, 2H), 3.53 (m, 2H), 3.04 (m, 2H), 2.87 (m, 2H), 2.51 (s, 6H), 2.22 (m, 2H)
¹³C NMR	(75 MHz, CDCl ₃): δ 153.7, 145.9, 140.5, 136.0, 130.9, 130.7, 130.6, 129.1, 128.7, 128.2, 125.0, 58.9, 56.4, 53.5, 47.7, 21.8
¹⁹F NMR	(282 MHz, CDCl ₃): δ -78.7 (anion)
MS (FAB)	<i>m/z</i> (%) = 711 <i>m/z</i> (100) [M ⁺ – CF ₃ SO ₃], 605 (90) [MH – AgCF ₃ SO ₃] ⁺
UV/vis	(5.1 10 ⁻⁵ mol/L, CHCl ₃ in 1cm cuvettes): λ _{max} [nm], (log ε) = 242 (4.32); 263 (3.94)



¹H NMR (300 MHz, CDCl₃) δ 7.80 (m, 5H, H_{Ar}), 7.43 (m, 10H, H_{Ar}), 7.29 (m, 1H, H_{Ar}), 5.07 (d, *J* = 15.2 Hz, 1H, H₂), 4.92 (d, *J* = 14.6 Hz, 1H, H₂), 4.69 (br, 1H, H₁₃), 3.98 (br, 2H), 3.69 (m, 2H), 3.11 (br, 1H), 2.83 (br, 1H), 2.62 (m, 1H), 2.51 (s, 6H, H₁₅), 2.44 (m, 1H), 1.97 (m, 1H), 1.84 (m, 1H), 1.77 (d, *J* = 6.8 Hz, 3H, H₁₄)

¹⁹F NMR (225 MHz, CDCl₃) δ -78.37 (anion)



¹H NMR (300 MHz, CDCl₃): δ 9.18 (d, *J* = 8.4 Hz, 1H, H_i), 8.12 (d, *J* = 8.4 Hz, 1H, H_f), 8.00 (d, *J* = 8.1 Hz, 1H, H_d), 7.92 (m, 1H, H_h), 7.84 (t, *J* = 7.7 Hz, 1H, H_r), 7.73 (m, 1H, H_b), 7.69-7.62 (m, 2H, H_c and H_g), 7.59 (d, *J* = 8.2 Hz, 4H, H_n), 7.41 (d, *J* = 8.2 Hz, 4H, H_o), 7.26 (d, *J* = 7.7 Hz, 2H, H_q), 4.88 (d, *J* = 15.0 Hz, 2H, H₂ and H₁₀), 4.36 (br s, 2H, H₁₃), 3.59 (d, *J* = 15.0 Hz, 2H, H_{2'} and H_{10'}) overlapping with 3.57-3.49 (m, 2H, CH₂), 2.84 (m, 2H, CH₂), 2.74 (m, 2H, CH₂), 2.50 (s, 6H, H₁₄), 2.26 (m, 2H, CH₂)

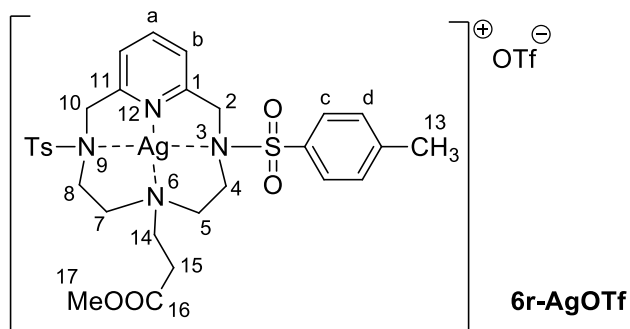
¹³C NMR (75 MHz, CDCl₃): δ 154.1 (C₁), 146.0 (C_p), 141.0 (C_r), 135.3 (C_m), 133.7 (C), 133.2 (C), 132.7 (C_f), 131.2 (C), 130.8 (C_o) overlapping with 130.8 (C_b), 130.1 (C_d), 128.6 (C_n), 127.1 (C_h), 126.5 (C_h), 125.9 (C_h), 125.4 (C_q), 112.4 (C_i, *J*¹H-¹³C = 156.8 Hz), 56.6 (C₁₃), 56.4 (C₂ and C₁₀), 54.8 (CH₂), 48.3 (CH₂), 22.1 (C₁₄)

¹⁹F NMR (282 MHz, CDCl₃): δ -78.5 (anion)

MS (FAB) m/z (%) = 761/763 (90/100) $[M - CF_3SO_3]^+$, 655 (35) $[MH - AgCF_3SO_3]^+$

Elem. An. Found: C, 48.41; H, 4.52; N, 6.02

Calculated: C, 48.74; H, 4.20; N, 6.14



¹H NMR (300 MHz, CDCl₃) δ 7.86 (1H, t, J = 7.7 Hz, H_a), 7.76 (4H, d, J = 8.2 Hz, H_c), 7.46 (4H, d, J = 8.2 Hz, H_d), 7.31 (2H, d, J = 7.7 Hz, H_b), 5.04 (2H, d, J = 14.6 Hz, H₁₀ + H₂), 3.72 (3H, s, H₁₇), 3.69 (2H, d, J = 14.8 Hz, H_{10'} + H_{2'}), 3.46 (2H, m, CH₂), 3.04 (2H, m, CH₂), 2.95-2.63 (6H, m, CH₂), 2.48 (8H, m, H₁₃ + CH₂)

¹³C NMR (75 MHz, CDCl₃) δ 153.04 (C), 145.43 (C_{quaternarytosyl}), 140.48 (C_a), 130.25 (C_d), 127.87 (C_c), 125.12 (C_b), 56.14 (C₂ + C₁₀), 52.98 (C), 52.51 (C₁₄), 48.46 (C), 46.57 (C), 31.49 (C), 21.41 (C₁₅)

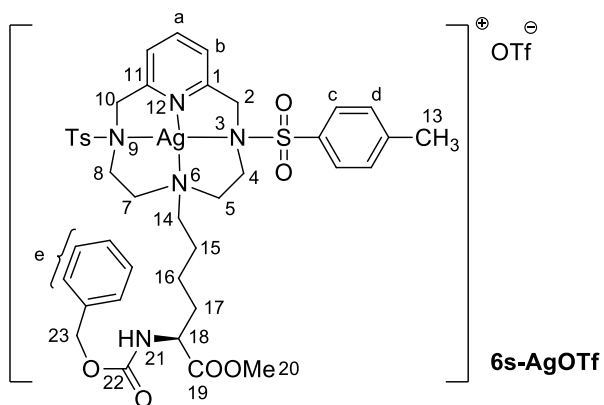
IR (ATR): 1728 cm⁻¹ (ν_{C=O}, ester), 1155 cm⁻¹ (sulfonamide)

UV-vis (CH₂Cl₂): λ_{MAX} (log ε) 237 nm (4.47), 264 nm (4.02)

MS (FAB) m/z 709 [M]⁺

Elem. An. C₃₀H₃₆N₄O₉S₃AgF₃ Calculated: C, 42.01; H, 4.23; N, 6.53

Found: C, 42.13; H, 4.16; N, 6.49



¹H NMR (300 MHz, CDCl₃) δ 7.85 (1H, t, *J* = 7.7 Hz, H_a), 7.80-7.68 (4H, m, H_c), 7.49-7.28 (11H, m, H_{Ar}Cbz + H_d + H_b), 5.56 (1H, m, H₂₁), 5.17 (2H, s, H₂₃), 5.14-5.05 (2H, m, H₂), 4.52 (1H, m, H₁₈), 3.76 (3H, s, H₂₀), 3.73-3.67 (2H, m, H₁₀), 3.48 (2H, m, CH₂), 2.30 (1H, m, CH₂), 3.03 (1H, m, CH₂), 2.88-2.55 (4H, m, CH₂), 2.51 (6H, s, H₁₃), 2.17 (2H, m, CH₂), 1.95 (1H, m, CH₂), 1.81 (2H, m, CH₂), 1.59 (2H, m, CH₂), 1.25 (2H, m, CH₂)

IR (ATR): 1717 cm⁻¹ (ν_{C=O}, ester), 1156 cm⁻¹ (sulfonamide)

UV-vis (CH₂Cl₂): λ_{MAX} (log ε) 237 nm (4.43), 264 nm (3.97)

MS (FAB) *m/z* 900 [M]⁺

Elem. An. C₄₁H₄₉N₅O₁₁S₃AgF₃ Calculated: C, 46.95; H, 4.71; N, 6.68

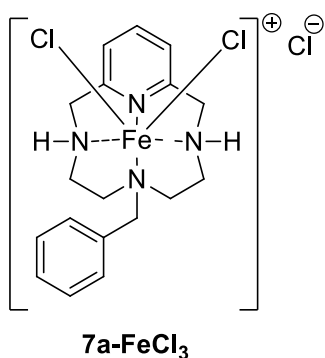
Found: C, 44.47; H, 4.35; N, 6.17

4.11 Iron complexes

General procedure

A solution of iron (II) or iron (III) salt (0.85 mmol) [see table below] in acetonitrile (3.0 mL) was added dropwise to a solution of ligand **7** or **8** in acetonitrile (5.0 mL). A change to dark-red/brown colour was observed. The mixture was left to react for 1 hour at RT, then the solvent was evaporated and the residual dense oil was treated with Et₂O (5.0 mL). The suspension was left to stir for 1 hour during which the dense oil turned to brown powder. The precipitate was then recovered by filtration and dried in vacuum.

Yields	7a-FeCl₃	94%	[iron source: FeCl ₃ · 6H ₂ O]
	7a-Fe(OTf)₃	95%	[iron source: Fe(OTf) ₃ anhydrous]
	7b-FeCl₃	91%	[iron source: FeCl ₃ · 6H ₂ O]
	7f-FeBr₂	88%	[iron source: FeBr ₂ anhydrous]
	7i-FeCl₃	45%	[iron source: FeCl ₃ · 6H ₂ O]
	8b-FeCl₃	97%	[iron source: FeCl ₃ · 6H ₂ O]
	8b-Fe(OTf)₃	93%	[iron source: Fe(OTf) ₃ anhydrous]



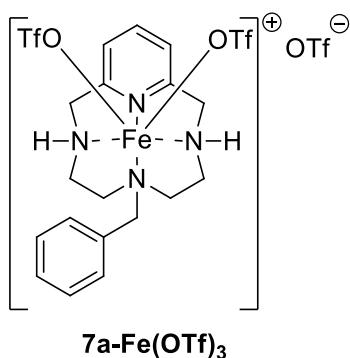
MS (FAB)

m/z (%) 422 (100), 424 (63) [M-Cl]

Elem. An.

C₁₈H₂₄Cl₃FeN₄ Calculated: C 47,14; H 5,27; N 12,22

Found: C 47,81; H 5,39; N 12,47



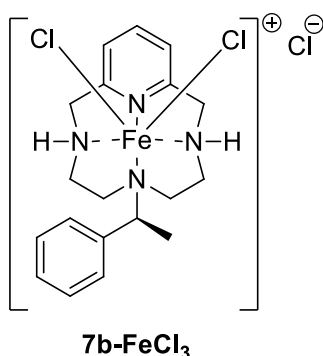
MS (FAB)

m/z (%) 501 (100), 503 (27) [M-2OTf]

Elem. An.

C₂₁H₂₄F₉FeN₄O₉S₃ Calculated: C 31,55; H 3,03; N 7,01

Found: C 32,01; H 3,84; N 7,89



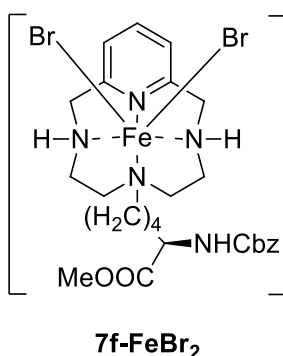
MS (FAB)

m/z (%) 401 (100), 403 (63) [M-2Cl]

Elem. An.

C₁₉H₂₆Cl₃FeN₄ Calculated: C 48,28; H 5,54; N 11,85

Found: C 48,45; H 5,85; N 11,47



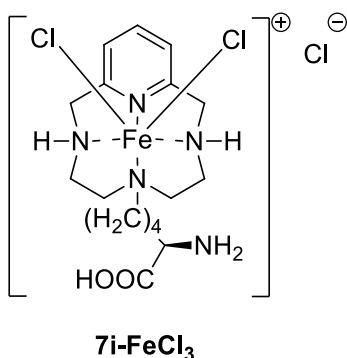
MS (FAB)

m/z (%) 699 (100), 697 (58), 701 (49) [M⁺]

Elem. An.

C₂₆H₃₇Br₂FeN₅O₄ Calculated: C 44,66; H 5,33; N 10,02

Found: C 58,12; H 6,67; N 11,02



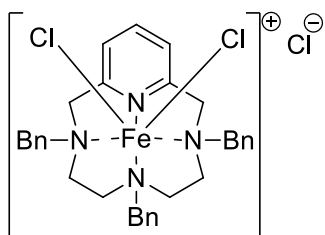
MS (FAB)

m/z (%) 461 (100), 463 (65) [M-Cl]

Elem. An.

C₁₇H₂₉Cl₃FeN₅O₂ Calculated: C 41,03; H 5,87; N 14,07

Found: C 40,70; H 6,07; N 14,54



8b-FeCl₃

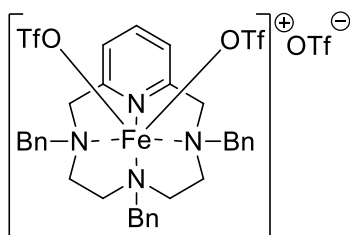
MS (FAB)

m/z (%) 567 (100), 569 (62) [M-2Cl]

Elem. An.

C₃₂H₃₆Cl₃FeN₄ Calculated: C 60,16; H 5,68; N 8,77

Found: C 58,99; H 6,09; N 9,13



8b-Fe(OTf)₃

MS (FAB)

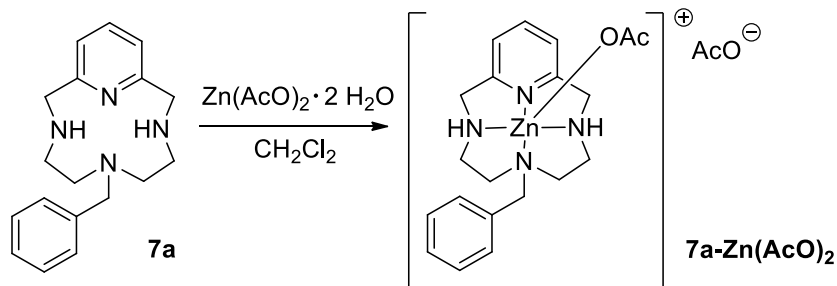
m/z (%) 830 (100), 831 (37) [M-OTf]

Elem. An.

C₃₅H₃₆F₉FeN₄O₉S₃ Calculated: C 42,91; H 3,70; N 5,72

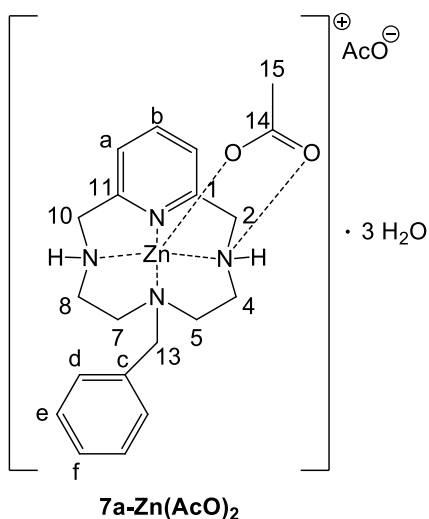
Found: C 42,24; H 4,04; N 6,18

4.12 Zinc complexes



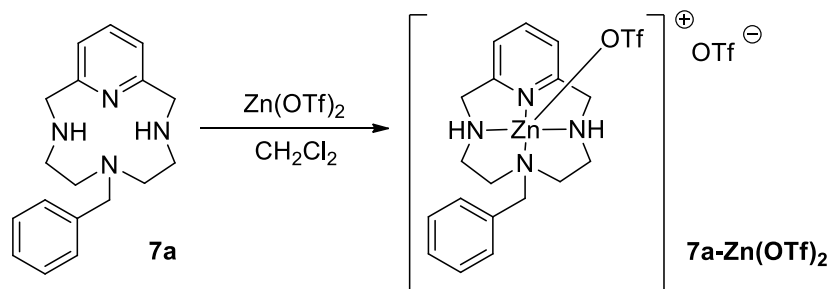
A solution of $\text{Zn(AcO)}_2 \cdot 2 \text{H}_2\text{O}$ (0.15 mmol) in dry DCM (7.0 mL) was added dropwise to a solution of ligand **7a** (0.15 mmol) in dry DCM (3.0 mL). The mixture was left to react for 2 hours, then the solvent was evaporated and *n*-hexane (8.0 mL) was added. The resulting suspension was stirred for 30 minutes, then the product was recovered by filtration as a pale yellow solid.

Yield: 83%



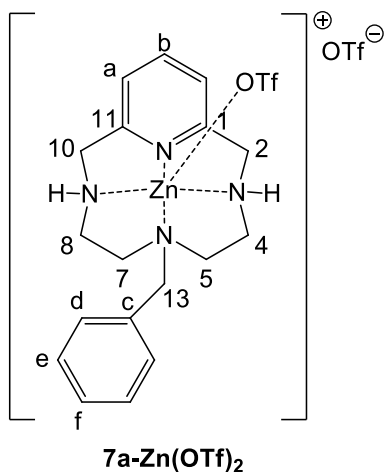
¹H NMR (400 MHz, CDCl₃) δ 7.82 (t, $J = 7.5$ Hz, 1H, H_b), 7.34 (m, 3H, H_e, H_f), 7.24 (d, $J = 7.5$ Hz, 2H, H_a), 7.11 (m, 2H, H_d), 4.78 (dd, $J = 16.6, 6.8$ Hz, 2H, H_{10'}, H_{2'}), 4.54 (s, 2H, H_{NH}), 4.05 (s, 2H, H₁₃), 3.75 (d, $J = 16.8$ Hz, 2H, H₁₀, H₂), 2.81 (d, $J = 13.2$ Hz, 2H, H_{5,7}), 2.60 (d, $J = 13.6$ Hz, 2H, H_{4,8}), 1.46 (t, $J = 13.6$ Hz, 2H)

MS (FAB) m/z 473.3 [$M + 3\text{H}_2\text{O} - \text{CH}_3\text{COO}^-$], 419.3 [$M - \text{CH}_3\text{COO}^-$]



A solution of Zn(OTf)_2 (0.15 mmol) in dry DCM (7.0 mL) was added dropwise to a solution of ligand **7a** (0.15 mmol) in dry DCM (3.0 mL). The mixture was left to react for 2 hours, then the solvent was evaporated and *n*-hexane (8.0 mL) was added. The resulting suspension was stirred for 30 minutes, then the product was recovered by filtration as a pale yellow solid.

Yield: 83%

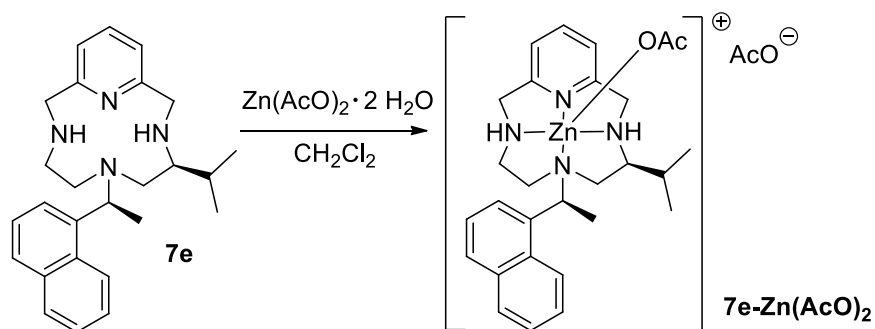


¹H NMR (300 MHz, CDCl_3) δ 8.07 (t, $J = 7.7$ Hz, 1H), 7.49 (d, $J = 7.7$ Hz, 2H), 7.37 (d, $J = 6.4$ Hz, 3H), 7.23 (d, $J = 7.2$ Hz, 2H), 4.98 (d, $J = 5.5$ Hz, 2H), 4.44 (dd, $J = 17.9, 7.5$ Hz, 2H), 3.92 (d, $J = 18.1$ Hz, 2H), 3.83 (s, 1H), 3.47 (dd, $J = 14.7, 13.6$ Hz, 2H), 2.64 (d, $J = 12.9$ Hz, 4H), 2.54 – 2.45 (m, 2H), 1.44 – 1.28 (m, 2H).

¹³C NMR (75 MHz, $\text{DMSO-}d_6$) δ 155.0 (C), 141.9 (CH), 133.0 (CH), 132.5 (C), 129.0 (CH), 122.1 (CH), 53.4 (CH_2), 50.8 (CH_2), 48.2 (CH_2).

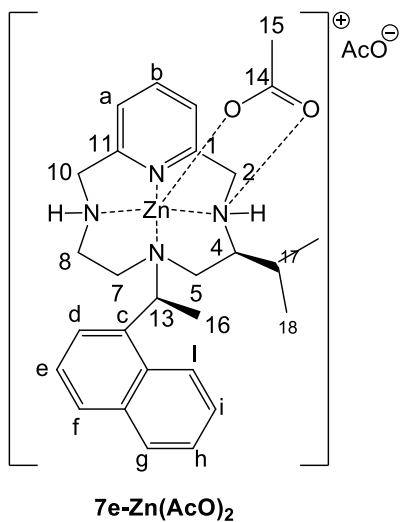
¹⁹F NMR (282 MHz, Methylene Chloride- d_2) δ -78.01.

MS (FAB) m/z 359 [M -H -2OTf]



A solution of $\text{Zn}(\text{AcO})_2 \cdot 2 \text{H}_2\text{O}$ (0.18 mmol) in dry DCM (8.0 mL) was added dropwise to a solution of ligand **7e** (0.18 mmol) in dry DCM (4.0 mL). The mixture was left to react for 2 hours, then the solvent was evaporated and *n*-hexane (8.0 mL) was added. The resulting suspension was stirred for 30 minutes, then the product was recovered by filtration as a pale yellow solid.

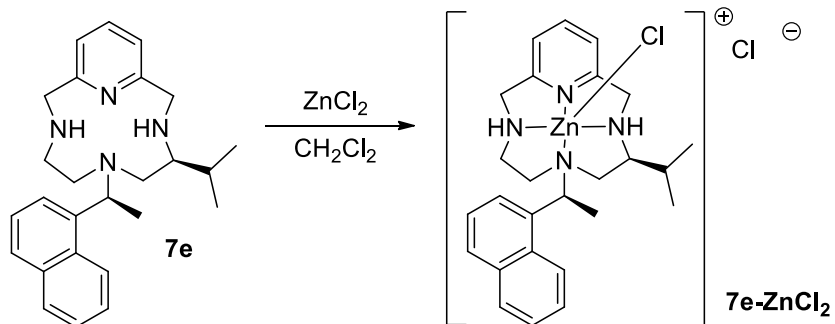
Yield: 68%



MS (FAB) m/z 525 $[\text{M} + 2\text{H}_2\text{O} - 2\text{CH}_3\text{COO}^-]$

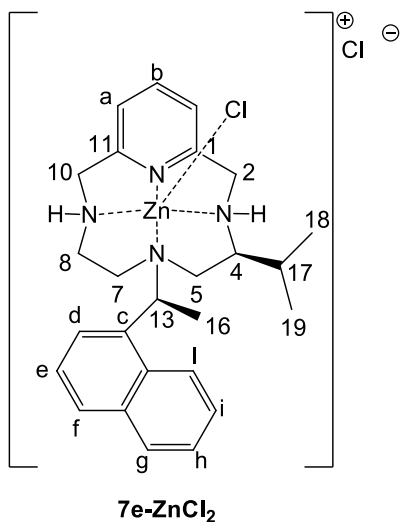
Elem. An. $\text{C}_{32}\text{H}_{44}\text{N}_4\text{O}_6\text{Zn}$ Calculated: C 59,49; H 6,86; N 8,67

Found: C 58,52; H 6,88; N 8,46



A solution of ZnCl_2 (0.2 mmol) in dry DCM (8.0 mL) was added dropwise to a solution of ligand **7e** (0.2 mmol) in dry DCM (4.0 mL). The mixture was left to react for 2 hours, then the solvent was evaporated and *n*-hexane (8.0 mL) was added. The resulting suspension was stirred for 30 minutes, then the product was recovered by filtration as a pale yellow solid.

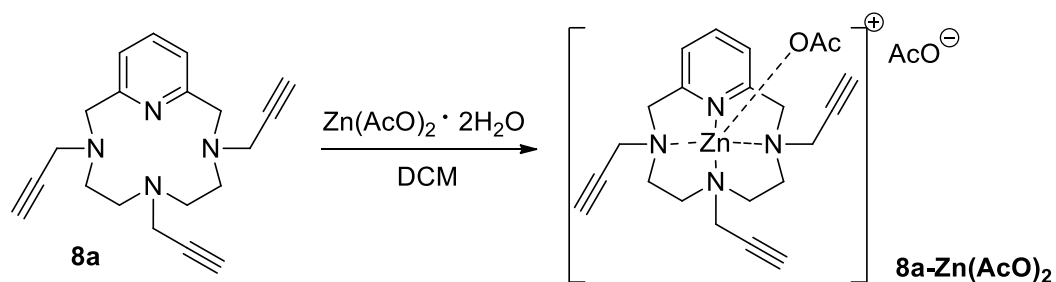
Yield: 88%



MS (FAB) m/z 501 [M - Cl⁻]

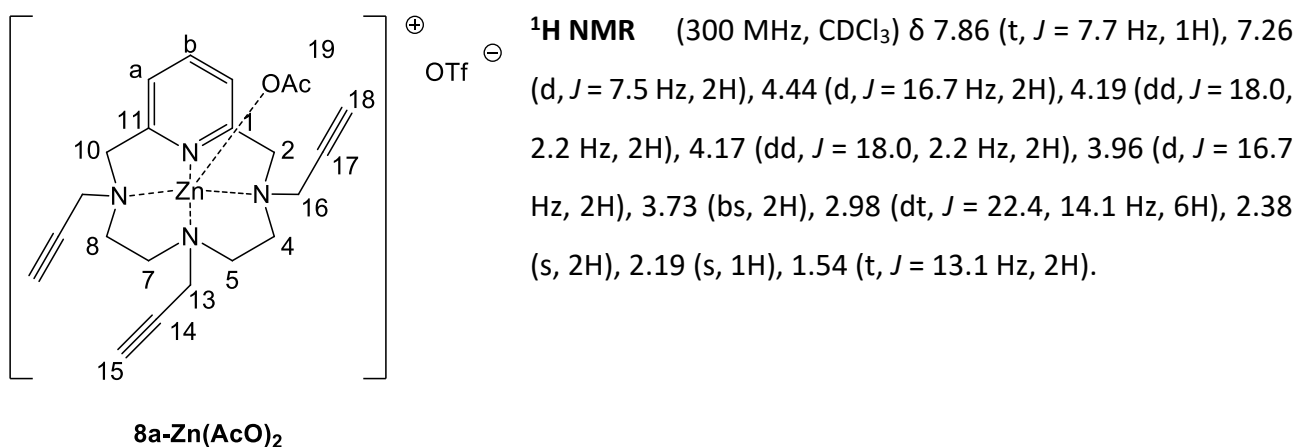
Elem. An. $\text{C}_{26}\text{H}_{34}\text{Cl}_2\text{N}_4\text{Zn}$ (+2 H_2O) Calculated: C 52,34; H 6,66; N 9,75

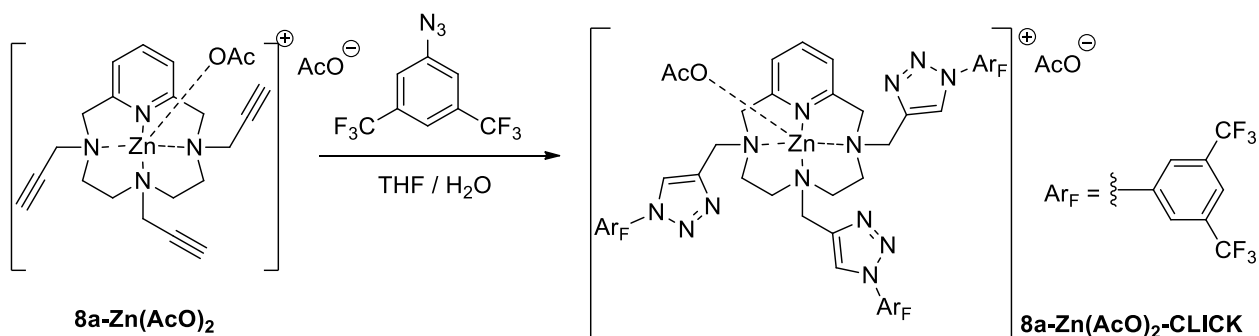
Found: C 53,01; H 6,42; N 9,86



A solution of $\text{Zn(AcO)}_2 \cdot 2 \text{H}_2\text{O}$ (0.42 mmol) in dry DCM (10.0 mL) was added dropwise to a solution of ligand **8a** (0.42 mmol) in dry DCM (5.0 mL). The mixture was left to react for 2 hours, then the solvent was evaporated and *n*-hexane (10.0 mL) was added. The resulting suspension was stirred for 30 minutes, then the product was recovered by filtration as a pale yellow solid.

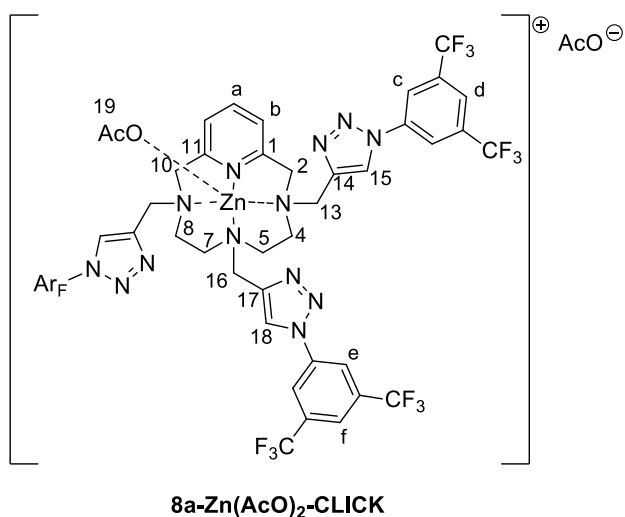
Yield: 97%





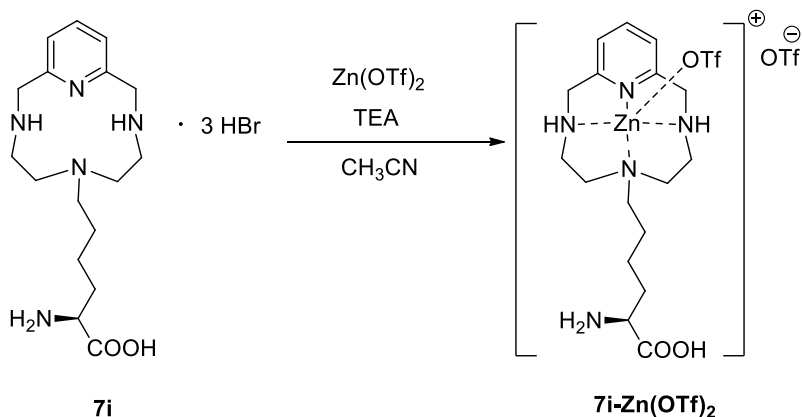
A solution of **8a-Zn(AcO)₂** (0.12 mmol) in dry THF (10.0 mL) was added dropwise to a solution of CuSO₄ (0.43 mmol) and Na-ascorbate (0.43 mmol) in H₂O (5.0 mL). 3,5 *bis*-CF₃ phenylazide (0.43 mmol) was added in one portion and the resulting mixture was left to react over night, then the solvent was evaporated and DCM (10.0 mL) was added. The organic layer was washed with brine (3 x 7.0mL), treated with Na₂SO₄ and dried in vacuum leading to the product as a pale yellow solid.

Yield: 97%



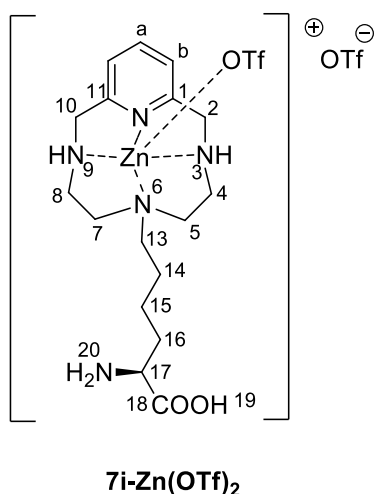
¹H NMR (400 MHz, CDCl₃) δ 10.49 (s, 1H), 9.02 (s, 2H), 8.65 (s, 2H), 8.36 (s, 4H), 7.88 (s, 1H), 7.85 (s, 2H), 7.51 (t, 1H), 7.01 (d, 2H), 5.76 (bs, 3H), 4.35 (m, 8H), 3.97 (m, 2H), 3.82 (m, 2H), 3.44 (m, 2H), 3.14 (m, 4H), 1.99 (s, 6H, AcO).

¹³C NMR (101 MHz, CDCl₃) δ 173.1 (C₁₆), 138.5 (C_a), 138.0 (C_g), 137.7 (C_{g'}), 132.5 (q, J_{CF} 30Hz, C_f), 132.5 (q, J_{CF} 30Hz, C_{f'}), 122.7 (q, J_{CF} 135Hz, C₁₇), 122.6 (q, J_{CF} 135Hz, C_{17'}), 122.4 (C_c), 122.1 (C_{d'}), 120.7 (C_d, C_b), 58.3 (C₁₃), 51.9 (C₂, C₁₀), 51.7 (C_{13'}), 46.2 (C₅, C₇).



A solution of $\text{Zn}(\text{AcO})_2 \cdot 2 \text{H}_2\text{O}$ (0.42 mmol) in dry acetonitrile (10.0 mL) was added dropwise to a solution of ligand **7i** (0.42 mmol) and TEA (1.3 mmol) in dry acetonitrile (5.0 mL). The mixture was left to react for 2 hours, then the solvent was evaporated and *n*-hexane (10.0 mL) was added. The resulting suspension was stirred for 30 minutes, then the product was recovered by filtration as a pale yellow solid.

Yield: 97%



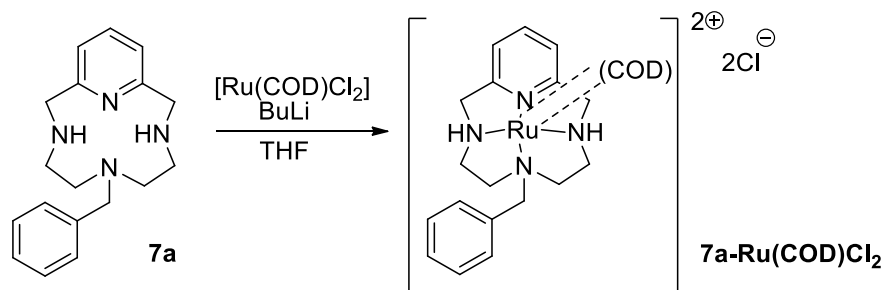
¹H NMR (400 MHz, D₂O): δ 8.03 (t, $J = 7.8$ Hz, 1H, H_a), 7.47 (d, $J = 7.8$ Hz, 2H, H_b), 4.56 – 4.41 (pst, 2H, H₂₊₁₀), 3.99 (m, 2H, H_{2'+10'}), 3.58 (m 1H, H₁₇), 3.40 (m, 2H, H₁₃), 3.08 – 2.57 (m, 8H, CH₂), 2.07 – 1.37 (m, 6H, CH₂).

¹³C NMR (101 MHz, D₂O): δ 154.30 (C₁), 141.17 (C_a), 121.66 (C_b), 54.38 (CH), 52.38 (C₂₊₁₂), 50.88 (CH₂), 46.69 (CH₂), 31.25(CH₂), 22.44 (CH₂), 20.34 (CH₂).

¹⁹F NMR (282 MHz, Deuterium Oxide): δ -79.11 (CF triflate).

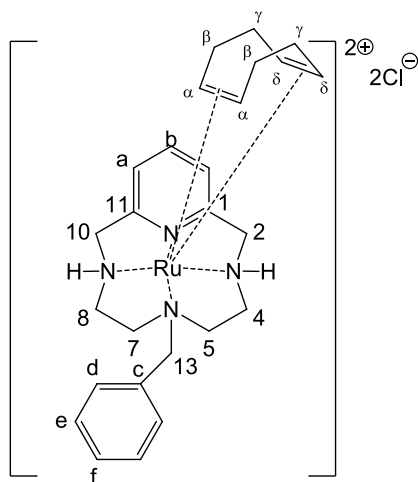
MS (FAB⁺) m/z 398 [M]²⁺

4.13 Other transition metal complexes



To a solution of **7a** (271.6 mg; 0.9 mmol) in distilled THF (14.0 mL), was added of BuLi (0.8 mL, 1.8 mmol) in *n*-hexane (5.0 mL) solution. During the addition the mixture changed its color from yellow to dark red and Ru(COD)Cl₂ (260.2 mg, 0.9 mmol) was added. The reaction was refluxed for 30 minutes and then filtered. The precipitate was then extracted in soxhlet for 15 hours using the filtrated solution. The solid was then recovered from the soxhlet giving the complex as brownish powder.

Yield: 45%

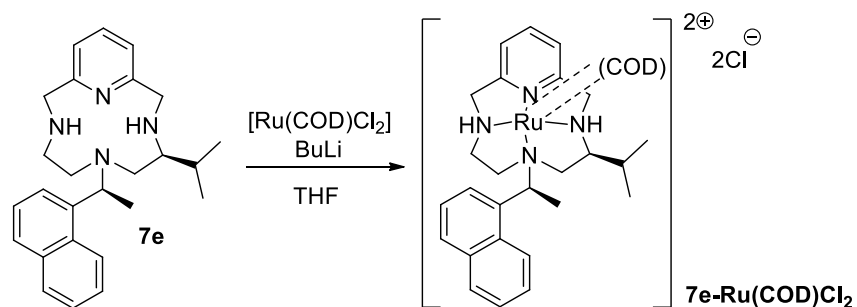


7a-Ru(COD)Cl₂

¹H NMR (400 MHz, DMSO) δ 7.93 (t, $J = 7.9$ Hz, 1H, H_b), 7.69 (s, 2H, NH), 7.57 (d, $J = 7.9$ Hz, 2H, H_a), 7.41 – 7.37 (m, 3H, H_{Ar}), 7.30 – 7.22 (m, 2H, H_{Ar}), 5.30 (dd, $J = 18.6, 6.4$ Hz, 2H, H_{2,10}), 4.60 (d, $J = 18.6$ Hz, 2H, H_{2,10}), 4.54 (s, 2H, H _{δ}), 4.23 (t, $J = 13.9$ Hz, 2H, H_{4,8}), 3.98 (s, 2H, H₁₃), 3.48 (s, 2H, H _{α}), 3.35 (s, 2H, H_{4,8}), 2.85 – 2.61 (m, 4H, H _{γ}), overlapped 2.72 (d, $J = 13.9$ Hz, 2H, H_{5,7}), 2.37 – 2.14 (m, 4H, H _{β}), 2.00 (t, $J = 13.9$ Hz, 2H, H_{5,7})

¹³C NMR (300 MHz, DMSO) δ 160.26(C_{1,11}), 138.61(C_a), 133.83(CH), 131.07(C), 128.79 (CH), 120.39 (CH_b), 86.67 (C _{α}), 85.09 (C _{δ}), 64.95 (C₂ and C₁₁), 59.17(C₄ and C₈), 52.41(C₅ and C₇), 51.77(C₁₃), 29.53(C _{β}), 28.97(C _{γ})

MS (FAB) m/z 505 (M⁺) [considering the ligand deprotonated on both N-H]

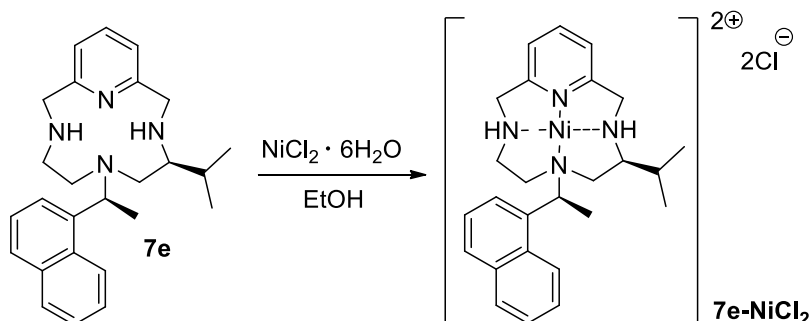


To a solution of **7e** (0.9 mmol) in distilled THF (15.0 mL), was added of BuLi (1.8 mmol) in *n*-hexane (5.0 mL) solution. During the addition the mixture changed its color from yellow to dark red and Ru(COD)Cl₂ (0.9 mmol) was added. The reaction was refluxed for 30 minutes and then filtered. The precipitate was then extracted in soxhlet for 15 hours using the filtrated solution. The solid was then recovered from the soxhlet giving the complex as brownish powder.

Yield: 62% [Not soluble in the common NMR solvents]

MS (FAB) m/z (%) 612 (100), 611 (58), 614 (54) [M-2Cl]

Elem. An. C₃₆H₄₆N₄Cl₂Ru Calculated: C 59,81; H 6,79; N 8,21
 Found: C 57,91; H 6,47; N 8,72

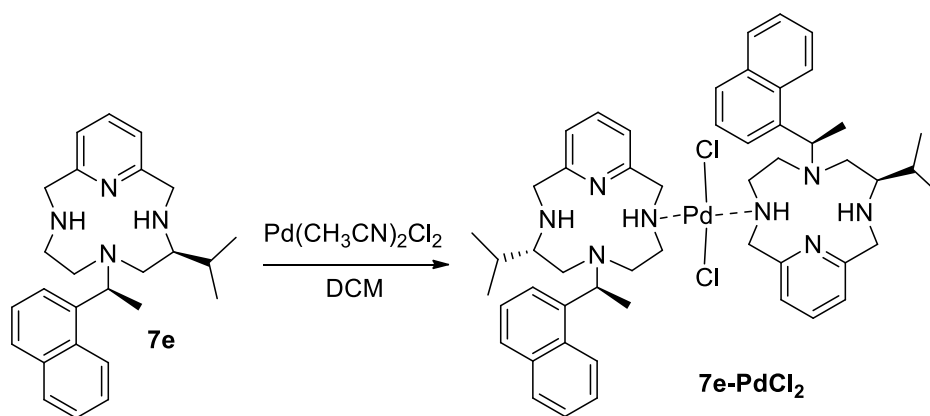


A solution of NiCl₂ · 6H₂O (0.29 mmol) in EtOH (2.0 mL) was added dropwise to a solution of **7e** (0.29 mmol) in EtOH (2.0 mL). The mixture changed colour from yellow to dark green and the product started to precipitate. The mixture was refluxed for 1 hour, then cooled and the complex was recovered by filtration as a light green powder.

Yield 51% [Not soluble in the common NMR solvents]

MS (FAB) m/z (%) 460 (100) [M-2Cl]

Elem. An. C₂₆H₃₄N₄Cl₂Ni Calculated: C 58,68; H 6,44; N 10,53
 Found: C 57,95; H 6,49; N 10,72

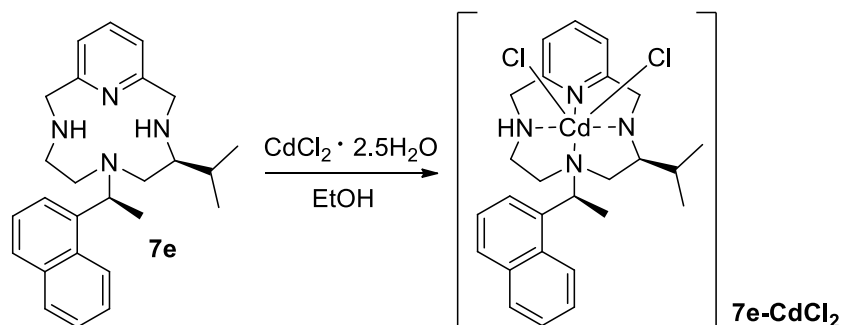


A solution of Pd(CH₃CN)₂Cl₂ (0.27 mmol) in DCM (8.0 mL) was added dropwise to a solution of **7e** (0.27 mmol) in DCM (2.0 mL). The mixture was refluxed for 1 hour, then cooled and the complex was recovered by filtration as a light grey powder.

Yield 87%

MS (FAB) m/z (%) 983 [M⁺]

Elem. An. C₅₂H₆₈N₈Cl₂Pd Calculated: C 63,57; H 6,98; N 11,41
 Found: C 63.52; H 6,77; N 10,78



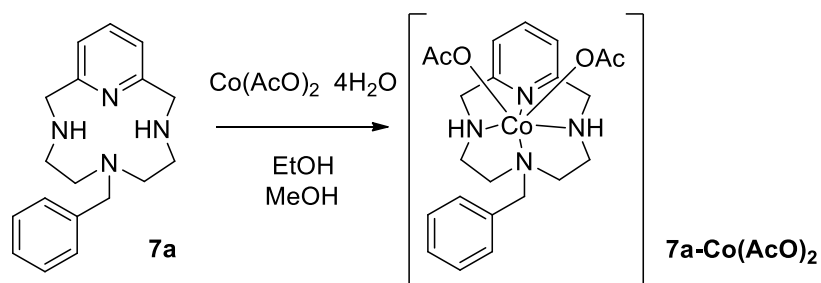
A solution of $\text{CdCl}_2 \cdot 2.5 \text{H}_2\text{O}$ (0.32 mmol) in EtOH (8.0 mL) was added dropwise to a solution of **7e** (0.32 mmol) in EtOH (4.0 mL). The mixture changed colour from yellow to white and the product started to precipitate. The mixture was refluxed for 1 hour, then cooled and the complex was recovered by filtration as a white powder.

Yield 72% [Not soluble in the common NMR solvents]

MS (FAB) m/z (%) 550 (100), 548 (75) [M^+]

Elem. An. $\text{C}_{26}\text{H}_{33}\text{N}_4\text{ClCd}$ Calculated: C 56,84; H 6,05; N 10,20

Found: C 56.01; H 5,55; N 10,09



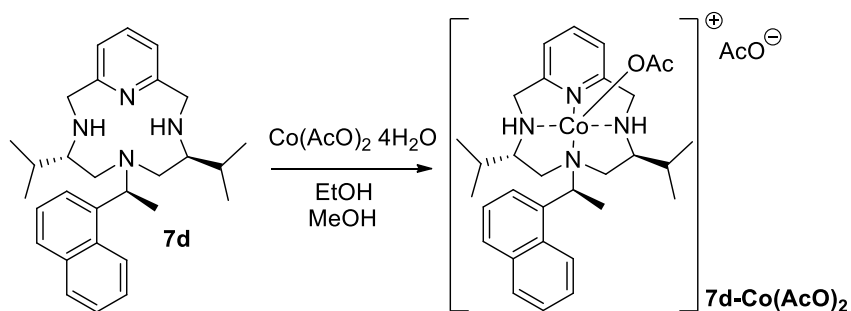
A solution of $\text{Co}(\text{AcO})_2 \cdot 4 \text{H}_2\text{O}$ (0.35 mmol) in MeOH (7.0 mL) was added dropwise to a solution of **7a** (0.35 mmol) in EtOH (5.0 mL). The mixture changed colour from yellow to purple and was refluxed for 1 hour, then cooled and the complex was recovered by filtration as a lilac powder.

Yield 75%

MS (FAB) m/z (%) 473 [M^+]

Elem. An. $\text{C}_{22}\text{H}_{30}\text{CoN}_4\text{O}_2$ Calculated: C 55,81; H 6,39; N 11,83

Found: C 55.05; H 5,96; N 11.02



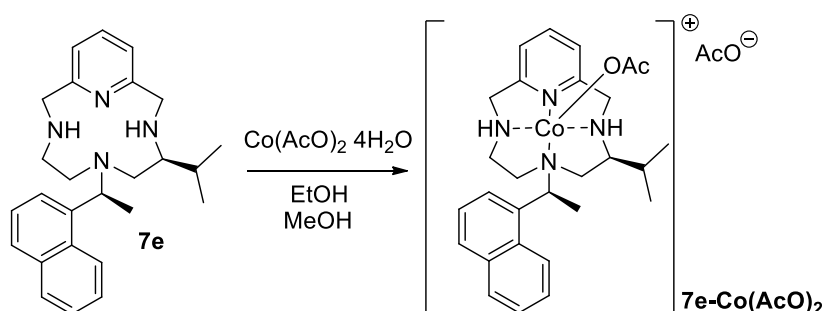
A solution of $\text{Co}(\text{AcO})_2 \cdot 4\text{H}_2\text{O}$ (0.30 mmol) in MeOH (7.0 mL) was added dropwise to a solution of **7d** (0.30 mmol) in EtOH (4.0 mL). The mixture changed colour from yellow to purple and was refluxed for 1 hour, then cooled and the complex was recovered by filtration as a lilac powder.

Yield 85%

MS (FAB) m/z (%) 566 [M - AcO]

Elem. An. $\text{C}_{33}\text{H}_{46}\text{CoN}_4\text{O}_4$ Calculated: C 63,76; H 7,46; N 9,01

Found: C 60,08; H 6,98; N 7,87



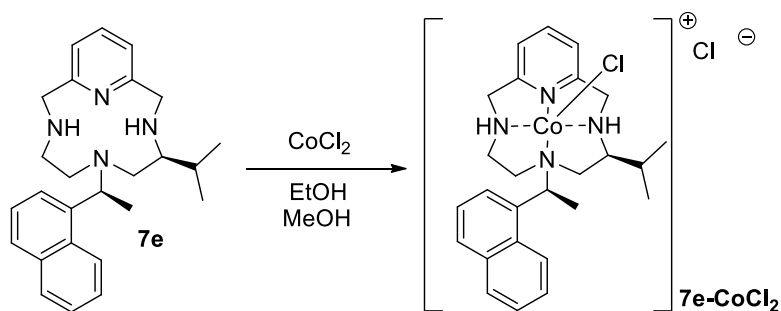
A solution of $\text{Co}(\text{AcO})_2 \cdot 4\text{H}_2\text{O}$ (0.31 mmol) in MeOH (7.0 mL) was added dropwise to a solution of **7e** (0.31 mmol) in EtOH (4.0 mL). The mixture changed colour from yellow to purple and was refluxed for 1 hour, then cooled and the complex was recovered by filtration as a lilac powder.

Yield 81%

MS (FAB) m/z (%) 520 [M - AcO]

Elem. An. $\text{C}_{30}\text{H}_{40}\text{CoN}_4\text{O}_4$ Calculated: C 62,17; H 6,96; N 9,67

Found: C 60,18; H 7,05; N 8,69



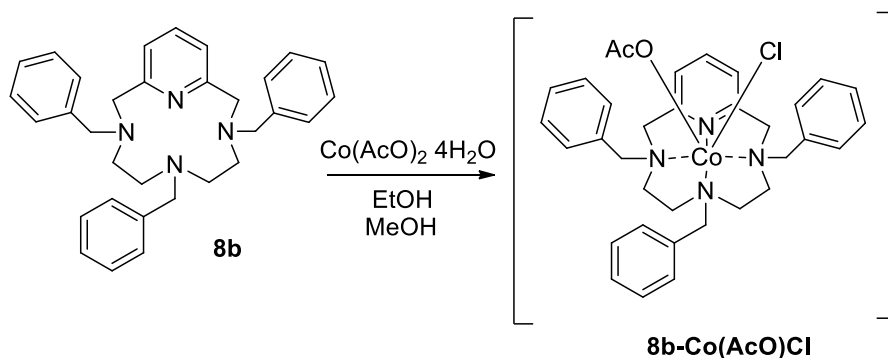
A solution of CoCl_2 (0.37 mmol) in MeOH (7.0 mL) was added dropwise to a solution of **7e** (0.37 mmol) in EtOH (4.0 mL). The mixture changed colour from yellow to purple and was refluxed for 1 hour, then cooled and the complex was recovered by filtration as a lilac powder.

Yield 65%

MS (FAB) m/z (%) 496 [M - Cl]

Elem. An. $\text{C}_{26}\text{H}_{33}\text{N}_4\text{CoCl}_2$ Calculated: C 58,65; H 6,44; N 10,42

Found: C 57,43; H 5,98; N 9,42



A solution of CoCl_2 (0.37 mmol) in MeOH (7.0 mL) was added dropwise to a solution of **7e** (0.37 mmol) in EtOH (4.0 mL). The mixture changed colour from yellow to purple and was refluxed for 1 hour, then cooled and the complex was recovered by filtration as a lilac powder.

Yield 65%

MS (FAB) m/z (%) 665 [M - Cl + 4 H₂O]

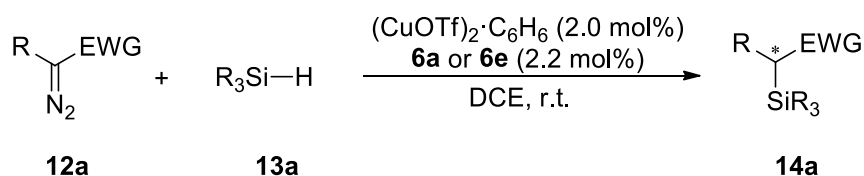
Elem. An. $\text{C}_{34}\text{H}_{39}\text{N}_4\text{ClCoO}_2$ Calculated: C 64,81; H 6,24; N 8,89

Found: C 63,77; H 6,02; N 9,12

4.B Catalysis

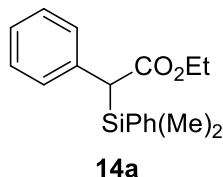
4.14 X-H carbene insertion¹⁰⁶

Copper-catalyzed Si-H bond carbene insertion using diazo compounds



Representative procedure for the synthesis of compounds 3:

Under Ar atmosphere, a solution of **6a** or **6e** (0.0044 mmol) and [(CuOTf)₂·C₆H₆] (0.002 mmol) in 1,2-dichloroethane (1.0 mL) was stirred for 1h at rt. The silane **13** (0.6 mmol) was added, followed by the slow addition during 1.5 h of a solution of the diazocompound **12** (0.2 mmol) in 1,2-dichloroethane (1.0 mL) using a syringe pump. The resulting mixture was stirred at this temperature until disappearance of the starting material (checked by TLC analysis). The solvent was removed under vacuum. The resulting residue was purified by flash column chromatography (SiO₂, hexanes : ethyl acetate) to afford **14**.



Ethyl 2-(dimethyl(phenyl)silyl)-2-phenylacetate (14a): The representative procedure was followed using dimethylphenylsilane (**13a**, 90 μ L, 0.6 mmol) and ethyl diazo(phenyl)acetate (**12a**, 38.0 mg, 0.2 mmol). After 18 h, purification by flash chromatography (SiO₂, hexane/EtOAc = 20:1) yielded **14a** (51.0 mg, 85% with **6a**; 55.0 mg, 92% with **6e**) as a colourless oil.

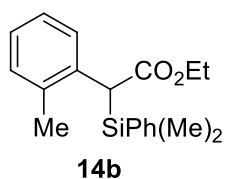
¹H NMR (300 MHz, CDCl₃): 0.35 (s, 3H), 0.40 (s, 3H), 1.14 (t, *J* = 7.1 Hz, 3H), 3.62 (s, 1H), 4.03 (qd, *J* = 7.1, 1.6 Hz, 2H), 7.10-7.51 (m, 10H).

¹³C NMR (75 MHz, CDCl₃): -4.5 (CH₃), -3.9 (CH₃), 14.3 (CH₃), 46.3 (CH), 60.3 (CH₂), 125.7 (CH), 127.8 (CH), 128.1 (CH), 128.5 (CH), 129.7 (CH), 134.2 (CH), 135.7 (C), 136.2 (C), 172.8 (C).

HR-MS (EI) calc. for C₁₈H₂₂NaO₂Si [M+Na⁺] 321.1281, found 321.1282.

HPLC: Chiralcel OD-H column (250 mm); detected at 230 nm; hexane/*i*-propanol = 97:3; flow = 0.7 mL/min; Retention time: 6.6 min, 12.5 min.

The spectroscopic data are in agreement with those previously reported.



Ethyl 2-(dimethyl(phenyl)silyl)-2-(*o*-tolyl)acetate (14b): The representative procedure was followed using **13a** (90 μ L, 0.6 mmol) and **12b** (41.0 mg, 0.2 mmol). After 18 h, purification by flash chromatography (SiO₂, hexane/EtOAc = 20:1) yielded **14b** (52.0 mg, 83% with **6a**; 54.0 mg, 87% with **6e**) as a colourless oil.

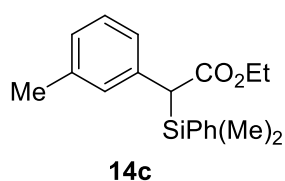
¹H NMR (300 MHz, CDCl₃): 0.34 (s, 3H), 0.43 (s, 3H), 1.16 (t, $J = 7.1$ Hz, 3H), 2.06 (s, 3H), 3.88 (s, 1H), 4.05 (qd, $J = 7.1, 1.7$ Hz, 2H), 7.01-7.11 (m, 2H), 7.12-7.21 (m, 1H), 7.26-7.43 (m, 5H), 7.61 (d, $J = 7.6$ Hz, 1H).

¹³C NMR (75 MHz, CDCl₃): -4.1 (CH₃), -3.5 (CH₃), 14.4 (CH₃), 20.5 (CH₃), 40.7 (CH), 60.4 (CH₂), 125.7 (CH), 125.8 (CH), 127.8 (CH), 129.1 (CH), 129.7 (CH), 130.2 (CH), 134.1 (CH), 134.6 (C), 135.0 (C), 136.1 (C), 172.9 (C).

HR-MS (ESI) calc. for C₁₉H₂₄NaO₂Si [M+Na⁺] 335.1438, found 335.1439.

HPLC: Chiralcel OD-H column (250 mm); detected at 235 nm; hexane/*i*-propanol = 97:3; flow = 0.7 mL/min; Retention time: 6.3 min, 8.0 min.

The spectroscopic data are in agreement with those previously reported.



Ethyl 2-(dimethyl(phenyl)silyl)-2-(*m*-tolyl)acetate (14c): The representative procedure was followed using **13a** (90 μ L, 0.6 mmol) and **12c** (41.0 mg, 0.2 mmol). After 24 h, purification by flash chromatography (SiO₂, hexane/EtOAc = 20:1) yielded **14c** (52.0 mg, 83% with **6a**; 59.0 mg, 94% with **6e**) as a colourless oil.

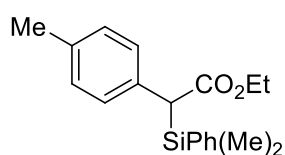
¹H NMR (300 MHz, CDCl₃): 0.33 (s, 3H), 0.37 (s, 3H), 1.11 (t, $J = 7.1$ Hz, 3H), 2.28 (s, 3H), 3.56 (s, 1H), 4.00 (qd, $J = 7.1, 1.2$ Hz, 2H), 6.92-7.17 (m, 4H), 7.29-7.46 (m, 5H).

¹³C NMR (75 MHz, CDCl₃): -4.5 (CH₃), -3.9 (CH₃), 14.3 (CH₃), 21.6 (CH₃), 46.1 (CH), 60.3 (CH₂), 125.6 (CH), 126.5 (CH), 127.7 (CH), 128.0 (CH), 129.3 (CH), 129.7 (CH), 134.2 (CH), 135.8 (C), 136.0 (C), 137.6 (C), 172.8 (C).

HR-MS (ESI) calc. for C₁₉H₂₄NaO₂Si [M+Na⁺] 335.1438, found 335.1438.

HPLC: Chiralcel OD-H column (250 mm); detected at 235 nm; hexane/*i*-propanol = 97:3; flow = 0.7 mL/min; Retention time: 6.2 min, 12.0 min.

The spectroscopic data are in agreement with those previously reported.



14d

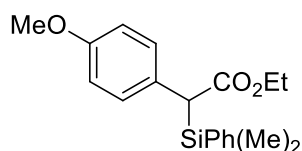
Ethyl 2-(dimethyl(phenyl)silyl)-2-(*p*-tolyl)acetate (14d): The representative procedure was followed using **13a** (90 μL, 0.6 mmol) and **12d** (41.0 mg, 0.2 mmol). After 18 h, purification by flash chromatography (SiO₂, hexane/EtOAc = 20:1) yielded **14d** (51.0 mg, 82% with **6a**; 52.0 mg, 83% with **6e**) as a colourless oil.

¹H NMR (300 MHz, CDCl₃): 0.32 (s, 3H), 0.36 (s, 3H), 1.10 (t, *J* = 7.1 Hz, 3H), 2.30 (s, 3H), 3.56 (s, 1H), 3.99 (qd, *J* = 7.1, 2.5 Hz, 2H), 7.04 (d, *J* = 8.0 Hz, 2H), 7.13 (d, *J* = 8.2 Hz, 2H), 7.28-7.46 (m, 5H).

¹³C NMR (75 MHz, CDCl₃): -4.5 (CH₃), -3.8 (CH₃), 14.3 (CH₃), 21.1 (CH₃), 45.8 (CH), 60.3 (CH₂), 127.8 (CH), 128.4 (CH), 128.9 (CH), 129.7 (CH), 133.0 (C), 134.2 (CH), 135.2 (C), 135.9 (C), 172.9 (C).

HR-MS (ESI) calc. for C₁₉H₂₄NaO₂Si [M+Na⁺] 335.1438, found 335.1439.

HPLC: Chiralcel OD-H column (250 mm); detected at 235 nm; hexane/*i*-propanol = 97:3; flow = 0.7 mL/min; Retention time: 6.2 min, 8.9 min.



14e

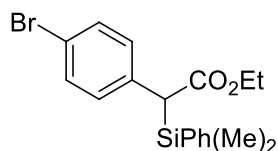
Ethyl 2-(dimethyl(phenyl)silyl)-2-(4-methoxyphenyl)acetate (14e): The representative procedure was followed using **13a** (90 μ L, 0.6 mmol) and **12e** (44.0 mg, 0.2 mmol). After 18 h, purification by flash chromatography (SiO₂, hexane/EtOAc = 20:1) yielded **14e** (47.0 mg, 72% with **6a**; 59.0 mg, 90% with **6e**) as a colourless oil.

¹H NMR (300 MHz, CDCl₃): 0.34 (s, 3H), 0.38 (s, 3H), 1.13 (t, $J = 7.1$ Hz, 3H), 3.56 (s, 1H), 3.80 (s, 3H), 4.02 (qd, $J = 7.1, 2.0$ Hz, 2H), 6.80 (d_{ap}, $J = 8.8$ Hz, 2H), 7.16 (d_{ap}, $J = 8.8$ Hz, 2H), 7.30-7.48 (m, 5H).

¹³C NMR (75 MHz, CDCl₃): -4.5 (CH₃), -4.0 (CH₃), 14.2 (CH₃), 45.0 (CH), 55.2 (CH₃), 60.2 (CH₂), 113.5 (CH), 127.6 (CH), 128.1 (C), 129.4 (CH), 129.5 (CH), 134.1 (CH), 135.8 (C), 157.6 (C), 172.9 (C).

HR-MS (ESI) calc. for C₁₉H₂₄NaO₃Si [M+Na⁺] 351.1387, found 351.1386.

HPLC: Chiralcel OD-H column (250 mm); detected at 240 nm; hexane/*i*-propanol = 97:3; flow = 0.7 mL/min; Retention time: 8.7 min, 19.9 min.



14f

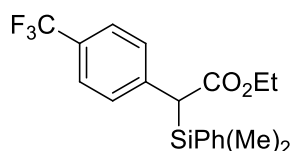
Ethyl 2-(4-bromophenyl)-2-(dimethyl(phenyl)silyl)acetate (314f): The representative procedure was followed using **13a** (90 μ L, 0.6 mmol) and **12f** (44.0 mg, 0.2 mmol). After 18 h, purification by flash chromatography (SiO₂, hexane/EtOAc = 20:1) yielded **14f** (61.0 mg, 81% with **6a**; 71.0 mg, 94% with **6e**) as a colourless oil.

¹H NMR (300 MHz, CDCl₃): 0.33 (s, 3H), 0.36 (s, 3H), 1.12 (t, $J = 7.1$ Hz, 3H), 3.56 (s, 1H), 4.02 (qd, $J = 7.1, 1.5$ Hz, 2H), 7.09 (d, $J = 8.5$ Hz, 2H), 7.29-7.43 (m, 7H).

¹³C NMR (75 MHz, CDCl₃): -4.4 (CH₃), -4.0 (CH₃), 14.3 (CH₃), 45.8 (CH), 60.5 (CH₂), 119.6 (C), 127.9 (CH), 129.9 (CH), 130.2 (CH), 131.1 (CH), 134.2 (CH), 135.2 (C), 135.3 (C), 172.4 (C).

HR-MS (ESI) calc. for C₁₈H₂₁BrO₂Si [M⁺] 376.0489, found 376.0495.

HPLC: Chiralcel OD-H column (250 mm); detected at 245 nm; hexane/*i*-propanol = 98:2; flow = 0.7 mL/min; Retention time: 8.8 min, 9.6 min.



14g

Ethyl 2-(dimethyl(phenyl)silyl)-2-(4-(trifluoromethyl)phenyl)acetate (14g): The representative procedure was followed using **13a** (90 μ L, 0.6 mmol) and **12g** (44.0 mg, 0.2 mmol). After 48 h, purification by flash chromatography (SiO₂, hexane/EtOAc = 20:1) yielded **14g** (46.0 mg, 63% with **6a**; 47.0 mg, 65% with **6e**) as a colourless oil.

¹H NMR (300 MHz, CDCl₃): 0.34 (s, 3H), 0.37 (s, 3H), 1.13 (t, $J = 7.1$ Hz, 3H), 3.67 (s, 1H), 4.03 (qd, $J = 7.1, 1.5$ Hz, 2H), 7.29-7.42 (m, 7H), 7.46 (d, $J = 8.2$ Hz, 2H).

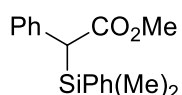
¹³C NMR (75 MHz, CDCl₃): -4.5 (CH₃), -4.1 (CH₃), 14.3 (CH₃), 46.5 (CH), 60.6 (CH₂), 125.0 (q, $J = 3.7$ Hz, CH), 127.9 (CH), 128.6 (CH), 130.0 (CH), 134.1 (CH), 134.9 (C), 140.5 (C), 172.2 (C) (two quaternary carbons could not be located).

¹⁹F NMR (282 MHz, CDCl₃): -62.30 (CF₃).

HR-MS (ESI) calc. for C₁₉H₂₁F₃NaO₂Si [M+Na⁺] 389.1161, found 389.1157.

The spectroscopic data are in agreement with those previously reported.

HPLC: Chiralcel OD-H column (250 mm); detected at 230 nm; hexane/*i*-propanol = 98:2; flow = 0.7 mL/min; Retention time: 16.4 min, 23.0 min.



14h

Methyl 2-(dimethyl(phenyl)silyl)-2-phenylacetate (14h): The representative procedure was followed using **13a** (90 μ L, 0.6 mmol) and **12h** (35.0 mg, 0.2 mmol). After 18 h, purification by flash chromatography (SiO₂, hexane/EtOAc = 20:1) yielded **14h** (48.0 mg, 84% with **6a**; 51.0 mg, 89% with **6e**) as a colourless oil.

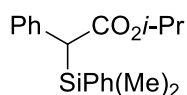
¹H NMR (300 MHz, CDCl₃): 0.33 (s, 3H), 0.36 (s, 3H), 3.56 (s, 3H), 3.61 (s, 1H), 7.11-7.25 (m, 5H), 7.29-7.43 (m, 5H).

¹³C NMR (75 MHz, CDCl₃): -4.4 (CH₃), -4.0 (CH₃), 46.2 (CH), 51.4 (CH₃), 125.8 (CH), 127.8 (CH), 128.2 (CH), 128.5 (CH), 129.8 (CH), 134.1 (CH), 135.6 (C), 136.1 (C), 173.2 (C).

HR-MS (ESI) calc. for C₁₇H₂₀NaO₂Si [M+Na⁺] 307.1125, found 307.1125.

HPLC: Chiralcel OD-H column (250 mm); detected at 235 nm; hexane/*i*-propanol = 97:3; flow = 0.7 mL/min; Retention time: 7.1 min, 16.9 min.

The spectroscopic data are in agreement with those previously reported.



14i

Isopropyl 2-(dimethyl(phenyl)silyl)-2-phenylacetate (14i): The representative procedure was followed using di **13a** (90 μ L, 0.6 mmol) and **12i** (41.0 mg, 0.2 mmol). After 48 h, purification by flash chromatography (SiO₂, hexane/EtOAc = 20:1) yielded **14i** (47.0 mg, 75% with **6a**; 49.0 mg, 78% with **6e**) as a colourless oil.

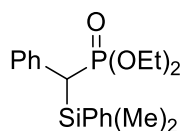
¹H NMR (300 MHz, CDCl₃): 0.31 (s, 3H), 0.38 (s, 3H), 1.05 (d, *J* = 6.3 Hz, 3H), 1.15 (d, *J* = 6.3 Hz, 3H), 3.57 (s, 1H), 4.90 (hept, *J* = 6.3 Hz, 1H), 7.09-7.25 (m, 5H), 7.29-7.45 (m, 5H).

¹³C NMR (75 MHz, CDCl₃): -4.4 (CH₃), -3.8 (CH₃), 21.9 (CH₃), 22.1 (CH₃), 46.3 (CH), 67.8 (CH), 125.7 (CH), 127.8 (CH), 128.1 (CH), 128.5 (CH), 129.7 (CH), 134.3 (CH), 135.8 (C), 136.4 (C), 172.3 (C).

HR-MS (ESI) calc. for C₁₉H₂₄NaO₂Si [M+Na⁺] 335.1838, found 335.1434.

HPLC: Chiralcel OD-H column (250 mm); detected at 230 nm; hexane/*i*-propanol = 97:3; flow = 0.7 mL/min; Retention time: 6.1 min, 7.0 min.

The spectroscopic data are in agreement with those previously reported.



14j

Diethyl ((dimethyl(phenyl)silyl)(phenyl)methyl)phosphonate (14j): The representative procedure was followed using dimethylphenylsilane **13a** (90 μ L, 0.6 mmol) and **12j** (51.0 mg, 0.2 mmol). After 8 h at 60°C, purification by flash chromatography (SiO₂, hexane/EtOAc = 20:1) yielded **14j** (40.0 mg, 55% with **6e**) as a colourless oil.

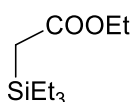
¹H NMR (300 MHz, CDCl₃): 0.35 (s, 3H), 0.52 (s, 3H), 1.02 (t, *J* = 7.1 Hz, 3H), 1.12 (t, *J* = 7.1 Hz, 3H), 2.87 (d, *J* = 24.4 Hz, 1H), 3.68-3.99 (m, 4H), 7.05-7.22 (m, 5H), 7.24-7.44 (m, 5H).

¹³C NMR (75 MHz, CDCl₃): -3.1 (d, *J* = 2.4 Hz, CH₃), -2.9 (CH₃), 16.2 (CH₃), 16.3 (CH₃), 37.2 (d, *J* = 126.4 Hz, CH), 61.1 (d, *J* = 6.6 Hz, CH₂), 62.4 (d, *J* = 6.8 Hz, CH₂), 125.7 (d, *J* = 2.7 Hz, CH), 127.6 (CH), 128.3 (CH), 129.4 (CH), 129.6 (d, *J* = 8.3 Hz, CH), 134.33 (CH), 134.69 (d, *J* = 7.0 Hz, C), 136.73 (d, *J* = 4.0 Hz, C).

HR-MS (ESI) calc. for C₁₉H₂₇O₃PSi [M+H⁺] 363.1540, found 363.1541.

HPLC: Chiralcel AD-H column (250 mm); detected at 220 nm; hexane/*i*-propanol = 95:5; flow = 0.7 mL/min; Retention time: 13.1 min, 14.4 min.

The spectroscopic data are in agreement with those previously reported.



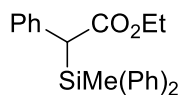
14k

Ethyl 2-(triethylsilyl)acetate (14k): The representative procedure was followed using **13c** (96 μL, 0.6 mmol) and **12m** (25 μL of a solution at 87% w/w, 0.2 mmol). After 18 h, purification by flash chromatography (SiO₂, hexane/EtOAc = 20:1) yielded **14k** (39.0 mg, 96%) as a colourless oil.

¹H NMR (300 MHz, CDCl₃): 0.62 (q, *J* = 7.9 Hz, 6H), 0.96 (t, *J* = 7.9 Hz, 9H), 1.23 (t, *J* = 7.1 Hz, 3H), 1.88 (s, 2H), 4.08 (q, *J* = 7.1 Hz, 2H).

¹³C NMR (75 MHz, CDCl₃): 3.9 (CH₃), 7.4 (CH₂), 14.8 (CH₃), 22.3 (CH₂), 60.2 (CH₂), 173.8 (C).

The spectroscopic data are in agreement with those previously reported.



14l

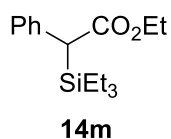
Ethyl 2-(methyldiphenylsilyl)-2-phenylacetate (14l): The representative procedure was followed using **13b** (120 μL, 0.6 mmol) and **12a** (38.0 mg, 0.2 mmol). After 18 h, purification by flash chromatography (SiO₂, hexane/EtOAc = 20:1) yielded **14l** (56.0 mg, 78% with **6a**; 60.0 mg, 83% with **6e**) as a colourless oil.

¹H NMR (300 MHz, CDCl₃): 0.62 (s, 3H), 1.01 (t, *J* = 7.2 Hz, 3H), 3.85-3.99 (m, 2H), 4.00 (s, 1H), 7.08-7.48 (m, 13H), 7.51-7.63 (m, 2H).

¹³C NMR (75 MHz, CDCl₃): -5.2 (CH₃), 14.1 (CH₃), 45.0 (CH), 60.5 (CH₂), 125.9 (CH), 127.8 (CH), 127.9 (CH), 128.1 (CH), 129.0 (CH), 129.8 (CH), 129.9 (CH), 133.8 (CH), 134.2 (C), 135.1 (C), 135.3 (CH), 135.7 (C), 172.7 (C).

HR-MS (EI) calc. for C₂₃H₂₄NaO₂Si [M+Na⁺] 383.1438, found 383.1437.

HPLC: Chiralcel OD-H column (250 mm); detected at 230 nm; hexane/*i*-propanol = 97:3; flow = 0.7 mL/min; Retention time: 6.7 min, 10.4 min.



Ethyl 2-phenyl-2-(triethylsilyl)acetate (14m): The representative procedure was followed using **13c** (96 μL, 0.6 mmol) and **12a** (38.0 mg, 0.2 mmol). After 24 h, purification by flash chromatography (SiO₂, hexane/EtOAc = 20:1) yielded **14m** (46.0 mg, 82% with **6a**; 51.0 mg, 91% with **6e**) as a colourless oil.

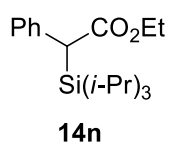
¹H NMR (300 MHz, CDCl₃): 0.59 (ddd, *J* = 10.6, 7.9, 1.7 Hz, 6H), 0.91 (t, *J* = 7.9 Hz, 9H), 1.28 (t, *J* = 7.1 Hz, 3H), 3.51 (s, 1H), 4.13 (qd, *J* = 7.1, 2.0 Hz, 2H), 7.04-7.43 (m, 5H).

¹³C NMR (75 MHz, CDCl₃): 2.9 (CH₂), 7.2 (CH₃), 14.5 (CH₃), 43.0 (CH), 60.3 (CH₂), 125.6 (CH), 128.2 (CH), 128.6 (CH), 136.5 (C), 173.3 (C).

HR-MS (EI) calc. for C₁₆H₂₆NaO₂Si [M+Na⁺] 301.1594, found 301.1594.

HPLC: Chiralcel OD-H column (250 mm); detected at 230 nm; hexane/*i*-propanol = 97:3; flow = 0.7 mL/min; Retention time: 5.7 min, 8.0 min.

The spectroscopic data are in agreement with those previously reported.



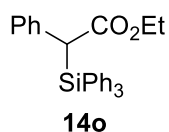
Ethyl 2-phenyl-2-(triisopropylsilyl)acetate (14n): The representative procedure was followed using **13d** (123 μ L, 0.6 mmol) and **12a** (38.0 mg, 0.2 mmol). After 24 h, purification by flash chromatography (SiO₂, hexane/EtOAc = 20:1) yielded **14n** (39.0 mg, 61% with **6a**; 44.0 mg, 68% with **6e**) as a colourless oil.

¹H NMR (300 MHz, CDCl₃): 0.99 (d, J = 7.2 Hz, 9H), 1.06 (d, J = 7.1 Hz, 9H), 1.13-1.32 (m, 6H), 3.68 (s, 1H), 4.11 (qd, J = 7.2, 2.2 Hz, 2H), 7.16 (t, J = 7.3 Hz, 1H), 7.27 (t, J = 7.4 Hz, 2H), 7.41 (d, J = 7.2 Hz, 2H).

¹³C NMR (75 MHz, CDCl₃): 11.7 (CH), 14.5 (CH₃), 18.7 (CH₃), 18.8 (CH₃), 41.7 (CH), 60.5 (CH₂), 125.8 (CH), 128.2 (CH), 129.6 (CH), 137.1 (C), 173.8 (C).

HR-MS (EI) calc. for C₁₉H₃₂NaO₂Si [M+Na⁺] 343.2064, found 343.2069.

HPLC: Chiralcel OD-H column (250 mm); detected at 220 nm; hexane/*i*-propanol = 97:3; flow = 0.7 mL/min; Retention time: 5.4 min, 6.3 min.



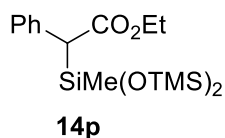
Ethyl 2-phenyl-2-(triphenylsilyl)acetate (14o): The representative procedure was followed using **13e** (156.0 mg, 0.6 mmol) and **12a** (38.0 mg, 0.2 mmol). After 24 h, purification by flash chromatography (SiO₂, hexane/EtOAc = 20:1) yielded **14o** (33 mg, 39% with **6a**; 57.0 mg, 67% with **6e**) as a white solid.

¹H NMR (300 MHz, CDCl₃): 0.94 (t, J = 7.1 Hz, 3H), 3.90 (qd, J = 7.1, 1.9 Hz, 2H), 4.25 (s, 1H), 7.12 (s, 5H), 7.28-7.46 (m, 15H).

¹³C NMR (75 MHz, CDCl₃): 13.9 (CH₃), 44.8 (CH), 60.7 (CH₂), 126.2 (C), 127.8 (CH), 128.1 (CH), 130.0 (CH), 130.1 (CH), 132.4 (CH), 135.4 (C), 136.7 (CH), 172.7 (C).

HR-MS (EI) calc. for C₂₈H₂₆NaO₂Si [M+Na⁺] 445.1594, found 445.1596.

HPLC: Chiralcel OD-H column (250 mm); detected at 230 nm; hexane/*i*-propanol = 97:3; flow = 0.7 mL/min; Retention time: 6.5 min, 8.5 min.



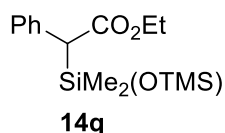
Ethyl 2-(1,1,1,3,5,5,5-heptamethyltrisiloxan-3-yl)-2-phenylacetate (14p): The representative procedure was followed using 0.005 mmoles of [(CuOTf)₂·C₆H₆], 0.011 mmoles of the Ligand (**6a** or **6e**), **13f** (163 μL, 0.6 mmol) and **12a** (38.0 mg, 0.2 mmol). After 24 h, purification by flash chromatography (SiO₂, hexane/EtOAc = 20:1) yielded **14p** (62.0 mg, 80% with **6a**; 63.0 mg, 82% with **6e**) as a colourless oil.

¹H NMR (300 MHz, CDCl₃): 0.01 (s, 18H), 0.10 (s, 3H), 1.27 (t, *J* = 7.1 Hz, 3H), 3.39 (s, 1H), 4.04-4.23 (m, 2H), 7.16 (tt, *J* = 7.2, 1.5 Hz, 1H), 7.26 (t, *J* = 7.4 Hz, 2H), 7.32-7.37 (m, 2H).

¹³C NMR (75 MHz, CDCl₃): 1.4 (CH₃), 1.7 (CH₃), 14.5 (CH₃), 47.8 (CH), 60.4 (CH₂), 125.8 (CH), 128.1 (CH), 129.1 (CH), 136.1 (C), 172.3 (C).

HR-MS (EI) calc. for C₁₇H₃₃O₄Si₃ [M+H⁺] 385.1681, found 385.1687.

HPLC: Chiralcel OD-H column (250 mm); detected at 220 nm; hexane/*i*-propanol = 97:3; flow = 0.7 mL/min; Retention time: 5.1 min, 6.1 min.



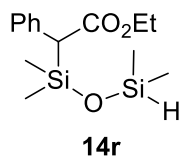
Ethyl 2-(1,1,3,3,3-pentamethyldisiloxanyl)-2-phenylacetate (14q): The representative procedure was followed using **13g** (117 μL, 0.6 mmol) and **12a** (38.0 mg, 0.2 mmol). After 18 h, purification by flash chromatography (SiO₂, hexane/EtOAc = 20:1) yielded **14q** (53.0 mg, 85% with **6e**) as a colourless oil.

¹H NMR (300 MHz, CDCl₃): 0.01 (s, 9H), 0.11 (d, *J* = 2.6 Hz, 6H), 1.28 (t, *J* = 7.1 Hz, 3H), 3.45 (s, 1H), 4.15 (q, *J* = 7.1 Hz, 2H), 7.17 (t, *J* = 7.2 Hz, 1H), 7.27 (t, *J* = 7.5 Hz, 2H), 7.35 (d, *J* = 7.1 Hz, 2H).

¹³C NMR (75 MHz, CDCl₃): -0.4 (CH₃), 1.8 (CH₃), 14.5 (CH₃), 48.2 (CH), 60.4 (CH₂), 125.7 (CH), 128.2 (CH), 128.8 (CH), 136.3 (C), 172.5 (C).

HR-MS (EI) calc. for C₁₅H₂₆NaO₃Si₂ [M+Na⁺] 333.1313, found 333.1313.

HPLC: Chiralcel OD-H column (250 mm); detected at 220 nm; hexane/*i*-propanol = 97:3; flow = 0.7 mL/min; Retention time: 5.4 min, 7.5 min.



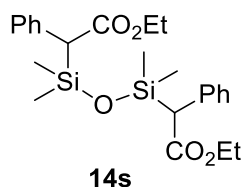
Ethyl 2-phenyl-2-(1,1,3,3-tetramethyldisiloxanyl)acetate (14r): The representative procedure was followed using **13h** (106 μ L, 0.6 mmol) and **12a** (38.0 mg, 0.2 mmol). After 24 h, purification by flash chromatography (SiO₂, hexane/EtOAc = 20:1) yielded **14r** (56.0 mg, 94% with **6a**; 56.0 mg, 95% with **6e**) as a colourless oil.

¹H NMR (300 MHz, CDCl₃): 0.10 (d, *J* = 2.8 Hz, 6H), 0.13 (s, 6H), 1.28 (t, *J* = 7.1 Hz, 3H), 3.47 (s, 1H), 4.15 (q, *J* = 7.1 Hz, 2H), 4.61 (dt, *J* = 5.5, 2.8 Hz, 1H), 7.13-7.22 (m, 1H), 7.24-7.31 (m, 2H), 7.32-7.39 (m, 2H).

¹³C NMR (75 MHz, CDCl₃): -0.7 (CH₃), 0.7 (CH₃), 14.5 (CH₃), 48.1 (CH), 60.5 (CH₂), 125.8 (CH), 128.3 (CH), 128.8 (CH), 136.1 (C), 172.5 (C).

HR-MS (EI) calc. for C₁₄H₂₄NaO₃Si₂ [M+Na⁺] 319.1156, found 319.1157.

HPLC: Chiralcel OD-H column (250 mm); detected at 225 nm; hexane/*i*-propanol = 97:3; flow = 0.7 mL/min; Retention time: 5.3 min, 7.3 min.



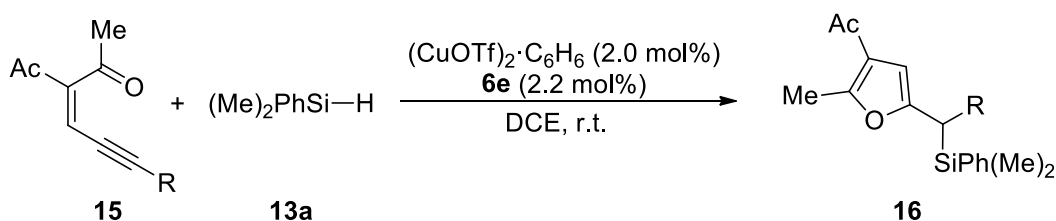
Diethyl 2,2'-(1,1,3,3-tetramethyldisiloxane-1,3-diyl)bis(2-phenylacetate) (14s): The representative procedure was followed using **13h** (36 μ L, 0.2 mmol) and **12a** (200.0 mg, 1 mmol, 5.0 equiv.). After 18 h, purification by flash chromatography (SiO₂, hexane/EtOAc = 20:1) yielded **14s** (72.0 mg, 79% with **6e**) as a colourless oil. (**14s** is a mixture of diastereoisomers).

¹H NMR (300 MHz, CDCl₃): -0.03 (d, *J* = 2.3 Hz, 6H), 0.03 (d, *J* = 1.3 Hz, 6H), 1.25 (td, *J* = 7.1, 1.9 Hz, 6H), 3.39 (s, 2H), 4.12 (q, *J* = 7.1 Hz, 4H), 7.04-7.38 (m, 10H).

¹³C NMR (75 MHz, CDCl₃): -0.9 (CH₃), -0.6 (CH₃), 14.5 (CH₃), 48.0 (CH), 60.5 (CH₂), 125.9 (CH), 128.3 (CH), 128.8 (CH), 136.0 (C), 172.3 (C).

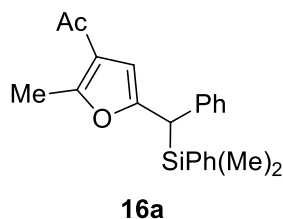
HR-MS (EI) calc. for C₂₄H₃₅O₅Si₂ [M+H⁺] 459.2018, found 459.2018.

Copper-catalyzed Si–H bond carbene insertion using enynones.



Representative procedure for the synthesis of compounds **16**:

Under Ar atmosphere, a solution of **6e** (0.0044 mmoles) and [(CuOTf)₂·C₆H₆] (0.002 mmoles) in 1,2-dichloroethane (1.0 mL) was stirred for 1h at rt. Silane **13a** (0.6 mmoles) was added, followed by the slow addition during 1.5 h of a solution of the enynone **15** (0.2 mmoles) in 1,2-dichloroethane (1.0 mL) using a syringe pump. The resulting mixture was stirred at this temperature until disappearance of the starting material (checked by TLC analysis). The solvent was removed under vacuum. The resulting residue was purified by flash column chromatography (SiO₂, hexanes:ethyl acetate) to afford **16**.



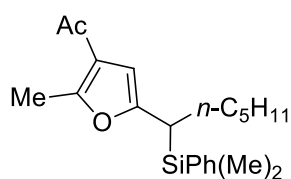
1-(5-((dimethyl(phenyl)silyl)(phenyl)methyl)-2-methylfuran-3-yl)ethanone (16a): The representative procedure was followed using **13a** (90 μ L, 0.6 mmol) and **15a** (42.0 mg, 0.2 mmol). After 18 h, purification by flash chromatography (SiO₂, hexane/EtOAc = 20:1) yielded **16a** (43.0 mg, 61% with **6e**) as a pale yellow oil.

¹H NMR (300 MHz, CDCl₃): 0.33 (s, 6H), 2.32 (s, 3H), 2.53 (s, 3H), 3.70 (s, 1H), 6.16 (s, 1H), 6.96-7.06 (m, 2H), 7.09-7.41 (m, 8H).

¹³C NMR (75 MHz, CDCl₃): -3.8 (CH₃), -3.6 (CH₃), 14.5 (CH₃), 29.3 (CH₃), 38.3 (CH), 106.5 (CH), 122.3 (C), 125.6 (CH), 127.7 (CH), 128.1 (CH), 128.4 (CH), 129.5 (CH), 134.3 (CH), 136.6 (C), 139.7 (C), 154.1 (C), 156.9 (C), 194.5 (C).

HR-MS (EI) calc. for C₂₂H₂₄NaO₂Si [M+Na⁺] 371.1443, found 371.1434.

HPLC: Chiralcel OD-H column (250 mm); detected at 235 nm; hexane/*i*-propanol = 98:2; flow = 0.7 mL/min; Retention time: 11.0 min, 11.9 min.



16b

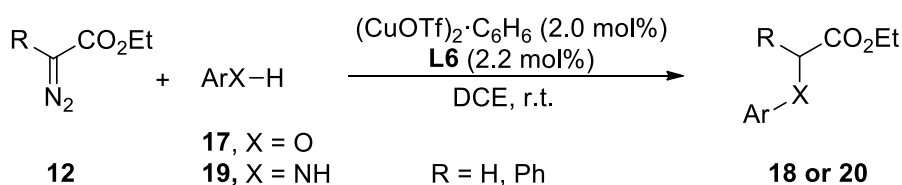
1-(5-(1-(dimethyl(phenyl)silyl)hexyl)-2-methylfuran-3-yl)ethanone (16b): The representative procedure was followed using **13a** (90 μ L, 0.6 mmol) and **15b** (41.0 mg, 0.2 mmol). After 18 h, purification by flash chromatography (SiO₂, hexane/EtOAc = 20:1) yielded **16b** (48.0 mg, 70% with **6e**) as a pale yellow oil.

¹H NMR (300 MHz, CDCl₃): 0.23 (s, 3H), 0.31 (s, 3H), 0.81 (t, *J* = 6.7 Hz, 3H), 1.06-1.37 (m, 6H), 1.45-1.69 (m, 2H), 2.24 (dd, *J* = 11.1, 4.2 Hz, 1H), 2.35 (s, 3H), 2.49 (s, 3H), 5.97 (s, 1H), 7.30-7.38 (m, 3H), 7.42 (dt, *J* = 6.1, 2.8 Hz, 2H).

¹³C NMR (75 MHz, CDCl₃): -4.8 (CH₃), -3.8 (CH₃), 14.2 (CH₃), 14.5 (CH₃), 22.6 (CH₂), 28.3 (CH₂), 29.1 (CH₂), 29.3 (CH₂), 29.4 (CH₃), 31.6 (CH), 104.4 (CH), 122.3 (C), 127.8 (CH), 129.3 (CH), 134.0 (CH), 137.4 (C), 155.8 (C), 156.2 (C), 194.7 (C).

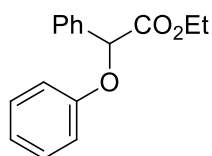
HR-MS (EI) calc. for C₂₁H₃₀NaO₂Si [M+Na⁺] 365.1913, found 365.1910.

Copper-catalyzed O–H/N–H bond carbene insertion using diazo compounds



Representative procedure for the synthesis of compounds **18** and **20**:

Under Ar atmosphere, a solution of **6e** (0.0044 mmoles) and [(CuOTf)₂·C₆H₆] (0.002 mmoles) in 1,2-dichloroethane (1.0 mL) was stirred for 1h at rt. The substrate **17** or **19** (0.6 mmoles) was added, followed by the slow addition during 1.5 h of a solution of the diazo compound **12** (0.2 mmoles) in 1,2-dichloroethane (1.0 mL) using a syringe pump. The resulting mixture was stirred at this temperature until disappearance of the starting material (checked by TLC analysis). The solvent was removed under vacuum. The resulting residue was purified by flash column chromatography (SiO₂, hexanes:ethyl acetate) to afford **18** or **20**.



18a

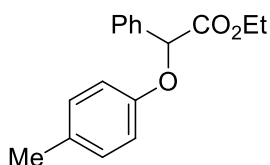
Ethyl 2-phenoxy-2-phenylacetate (18a): The representative procedure was followed using phenol (**17a**, 56.0 mg, 0.6 mmol) and **12a** (38.0 mg, 0.2 mmol). After 18 h, purification by flash chromatography (SiO₂, hexane/EtOAc = 20:1) yielded **18a** (42.0 mg, 83%) as a colourless oil.

¹H NMR (300 MHz, CDCl₃): 1.21 (t, *J* = 7.1 Hz, 3H), 4.13 - 4.29 (m, 2H), 5.63 (s, 1H), 6.96 (m, 3H), 7.27 (m, 2H), 7.35 - 7.45 (m, 3H), 7.59 (dd, *J* = 7.7, 1.6 Hz, 2H).

¹³C NMR (75 MHz, CDCl₃): 14.2 (CH₃), 61.7 (CH₂), 78.9 (CH), 115.7 (CH), 121.9 (CH), 127.2 (CH), 128.9 (CH), 129.0 (CH), 129.7 (CH), 135.7 (C), 157.5 (C), 170.1 (C).

MS (EI) calc. for C₁₆H₁₆O₃ [M⁺] 256.1, found 256.

The spectroscopic data are in agreement with those previously reported.



18b

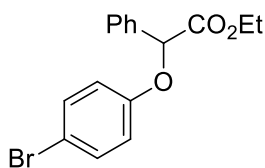
Ethyl 2-phenyl-2-(*p*-tolylloxy)acetate (18b): The representative procedure was followed using *p*-cresol (**17b**, 65.0 mg, 0.6 mmol) and **12a** (38.0 mg, 0.2 mmol). After 18 h, purification by flash chromatography (SiO₂, hexane/EtOAc = 20:1) yielded **18b** (39.5 mg, 73%) as a colourless oil.

¹H NMR (300 MHz, CDCl₃): 1.21 (t, *J* = 7.1 Hz, 3H), 2.27 (s, 3H), 4.07-4.31 (m, 2H), 5.59 (s, 1H), 6.85 (d, *J* = 8.6 Hz, 2H), 7.06 (d, *J* = 8.3 Hz, 2H), 7.32-7.46 (m, 3H), 7.58 (d, *J* = 6.1 Hz, 2H).

¹³C NMR (75 MHz, CDCl₃): 14.2 (CH₃), 20.6 (CH₃), 61.7 (CH₂), 79.0 (CH), 115.5 (CH), 127.2 (CH), 128.9 (CH), 129.0 (CH), 130.1 (CH), 131.2 (C), 135.8 (C), 155.4 (C), 170.2 (C).

HR-MS (ESI) calc. for C₁₇H₁₈NaO₃ [M+Na⁺] 293.1148, found 293.1150.

HPLC: Chiralcel OD-H column (250 mm); detected at 220 nm; hexane/*i*-propanol = 99:1; flow = 0.7 mL/min; Retention time: 16.4 min, 20.8 min.



18c

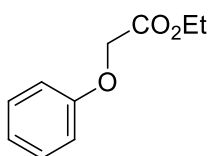
Ethyl 2-(4-bromophenoxy)-2-phenylacetate (18c): The representative procedure was followed using 4-bromophenol (**17c**, 104.0 mg, 0.6 mmol) and **12a** (38.0 mg, 0.2 mmol). After 18 h, purification by flash chromatography (SiO₂, hexane/EtOAc = 20:1) yielded **18c** (43.5 mg, 65%) as a colourless oil.

¹H NMR (300 MHz, CDCl₃): 1.21 (t, *J* = 7.1 Hz, 3H), 4.12 - 4.27 (m, 2H), 5.57 (s, 1H), 6.84 (d, *J* = 8.9 Hz, 2H), 7.31 - 7.45 (m, 5H), 7.50 - 7.61 (m, 2H).

¹³C NMR (75 MHz, CDCl₃): 14.2 (CH₃), 61.9 (CH₂), 79.1 (CH), 114.3 (C), 117.5 (CH), 127.2 (CH), 129.0 (CH), 129.2 (CH), 132.6 (CH), 135.2 (C), 156.6 (C), 169.7 (C).

(The product contains traces of the ester used for the synthesis of the diazo-compound)

MS (EI) calc. for C₁₆H₁₅BrO₃ [M⁺] 234.0, found 234.



18d

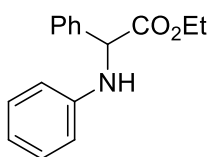
Ethyl 2-phenoxyacetate (18d): The representative procedure was followed using phenol (**17a**, 56.0 mg, 0.6 mmol) and **12m** (25 μ L of a solution at 87% w/w, 0.2 mmol). After 18 h, purification by flash chromatography (SiO₂, hexane/EtOAc = 20:1) yielded **18d** (32.0 mg, 90%) as a colourless oil.

¹H NMR (300 MHz, CDCl₃): 1.29 (t, J = 7.1 Hz, 3H), 4.27 (q, J = 7.1 Hz, 2H), 4.61 (s, 2H), 6.91 (d, J = 8.0 Hz, 2H), 6.99 (t, J = 7.4 Hz, 1H), 7.29 (t, J = 8.0 Hz, 2H).

¹³C NMR (75 MHz, CDCl₃): 14.3 (CH₃), 61.5 (CH₂), 65.6 (CH₂), 114.8 (CH), 121.9 (CH), 129.7 (CH), 158.0 (C), 169.1 (C).

MS (EI) calc. for C₁₀H₁₂O₃ [M^+] 180.1, found 180.

The spectroscopic data are in agreement with those previously reported.



20a

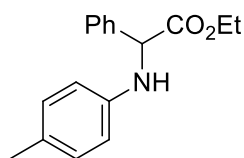
Ethyl 2-phenyl-2-(phenylamino)acetate (20a): The representative procedure was followed using aniline (**19a**, 54 μ L, 0.6 mmol) and **12a** (38.0 mg, 0.2 mmol). After 18 h, purification by flash chromatography (SiO₂, hexane/EtOAc = 20:1) yielded **20a** (41.0 mg, 81%) as a white solid.

¹H NMR (300 MHz, CDCl₃): 1.22 (t, J = 7.1 Hz, 3H), 4.07-4.33 (m, 2H), 4.97 (d, J = 5.2 Hz, 1H), 5.07 (d, J = 5.8 Hz, 1H), 6.57 (d, J = 7.7 Hz, 2H), 6.70 (t, J = 7.3 Hz, 1H), 7.13 (dd, J = 8.5, 7.4 Hz, 2H), 7.29-7.40 (m, 3H), 7.51 (d, J = 6.6 Hz, 2H).

¹³C NMR (75 MHz, CDCl₃): 14.2 (CH₃), 60.9 (CH), 62.0 (CH₂), 113.5 (CH), 118.2 (CH), 127.3 (CH), 128.3 (CH), 128.9 (CH), 129.4 (CH), 137.8 (C), 146.1 (C), 172.0 (C).

HR-MS (ESI) calc. for C₁₆H₁₈NO₂ [$M+H^+$] 256.1332, found 256.1333.

The spectroscopic data are in agreement with those previously reported.



20b

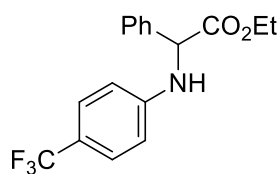
Ethyl 2-phenyl-2-(p-tolylamino)acetate (20b): The representative procedure was followed using 4-methylaniline (**19b**, 65.0 mg, 0.6 mmol) and **12a** (38.0 mg, 0.2 mmol). After 18 h, purification by flash chromatography (SiO₂, hexane/EtOAc = 20:1) yielded **20b** (47.0 mg, 88%) as a white solid.

¹H NMR (300 MHz, CDCl₃): 1.23 (t, *J* = 7.1 Hz, 3H), 2.22 (s, 3H), 3.99 - 4.32 (m, 2H), 5.07 (s, 1H), 6.52 (d, *J* = 8.4 Hz, 2H), 6.96 (d, *J* = 8.1 Hz, 2H), 7.26 - 7.43 (m, 3H), 7.52 (m, 2H).

¹³C NMR (75 MHz, CDCl₃): 14.1 (CH₃), 20.5 (CH₃), 61.3 (CH), 61.8 (CH₂), 113.8 (CH), , 127.3 (CH), 127.4 (C), 128.3 (CH), 128.9 (CH), 129.8 (CH), 137.9 (C), 143.8 (C), 172.0 (C).

MS (EI) calc. for C₁₇H₁₉NO₂ [M⁺] 269.1, found 269.

The spectroscopic data are in agreement with those previously reported.



20c

Ethyl 2-phenyl-2-((4-(trifluoromethyl)phenyl)amino)acetate (20c): The representative procedure was followed using 4-trifluoromethylaniline (**19c**, 97.0 mg, 0.6 mmol) and **12a** (38.0 mg, 0.2 mmol). After 18 h, purification by flash chromatography (SiO₂, hexane/EtOAc = 20:1) yielded **20c** (55.0 mg, 85%) as a white solid.

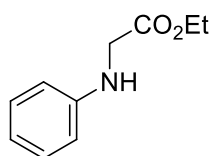
¹H NMR (300 MHz, CDCl₃): 1.23 (t, *J* = 7.1 Hz, 3H), 4.02 - 4.37 (m, 2H), 5.09 (s, 1H), 6.57 (d, *J* = 8.5 Hz, 2H), 7.29 - 7.42 (m, 5H), 7.49 (dd, *J* = 7.8, 1.4 Hz, 2H).

¹³C NMR (75 MHz, CDCl₃): 14.1 (CH₃), 60.4 (CH), 62.2 (CH₂), 112.8 (CH), 119.8 (q, *J*²_{C-F} = 32.6 Hz, C), 121.4 (q, *J*¹_{C-F} = 271.0 Hz, CF₃), 126.7 (q, *J*³_{C-F} = 4.1 Hz, CH), 127.2 (CH), 128.6 (CH), 129.1 (CH), 137.0 (C), 148.4 (C), 171.4 (C).

¹⁹F NMR (282 MHz, CDCl₃): -61.47 (CF₃).

MS (EI) calc. for C₁₇H₁₆F₃NO₂ [M⁺] 323.1, found 323.

The spectroscopic data are in agreement with those previously reported.



20d

Ethyl 2-(phenylamino)acetate (20d): The representative procedure was followed using 4-trifluoromethylaniline (**19a**, 97.0 mg, 0.6 mmol) and **12m** (25 μ L of a solution at 87% w/w, 0.2 mmol). After 18 h, purification by flash chromatography (SiO₂, hexane/EtOAc = 20:1) yielded **20d** (32.6 mg, 91%) as a white solid.

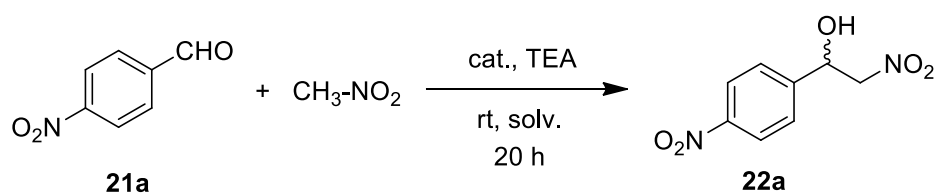
¹H NMR (300 MHz, CDCl₃): 1.31 (t, *J* = 7.1 Hz, 3H), 3.91 (s, 2H), 4.26 (q, *J* = 7.1 Hz, 2H), 6.63 (d, *J* = 7.8 Hz, 2H), 6.77 (t, *J* = 7.3 Hz, 1H), 7.21 (t, *J* = 7.9 Hz, 2H).

¹³C NMR (75 MHz, CDCl₃): 14.3 (CH₃), 46.0 (CH₂), 61.4 (CH₂), 113.2 (CH), 118.3 (CH), 129.4 (CH), 147.1 (C), 171.3 (C).

MS (EI) calc. for C₁₀H₁₃NO₂ [M⁺] 179.1, found 179.

The spectroscopic data are in agreement with those previously reported.

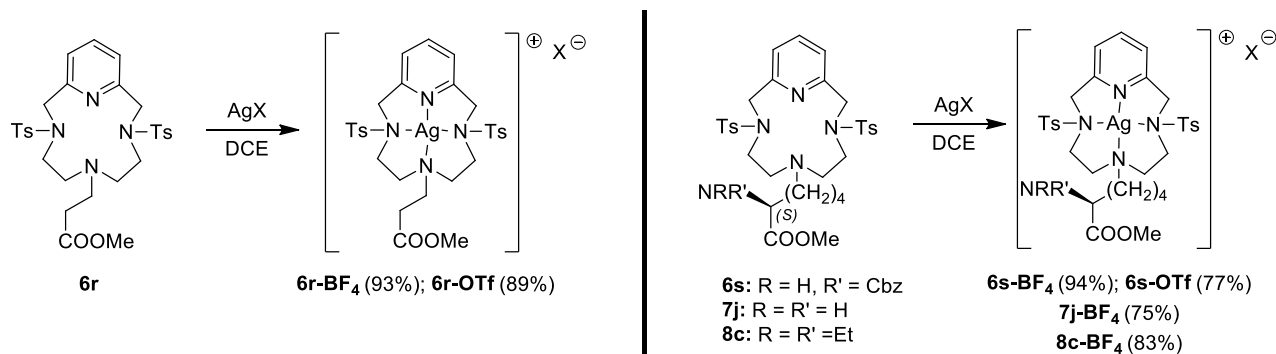
4.15 Silver catalysed Henry reaction⁸⁰



Entry	Cat.	X	Solv.	Base	Yield (%) ^b
1	Ag(OTf)		CH ₂ Cl ₂	TEA	21
2 ^c	Ag(BF ₄)		CH ₂ Cl ₂	Cs ₂ CO ₃	25
3 ^d	-		CH ₂ Cl ₂	TEA	35
4	6f-Ag	OTf	CH ₂ Cl ₂	TEA	84
5	6f-Ag	BF₄	CH ₂ Cl ₂	TEA	75
6 ^e	6f-Ag	BF₄	CH ₂ Cl ₂	TEA	85
7	6f-Ag	OTf	CH ₃ NO ₂	TEA	84
8	6f-Ag	OTf	Tol	TEA	60
9	6f-Cu	OTf	CH ₂ Cl ₂	TEA	85

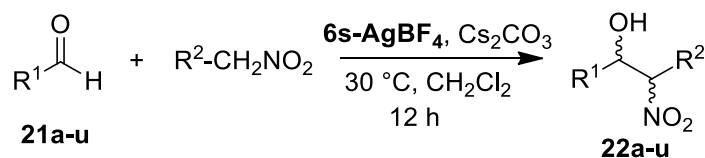
^a Reactions were performed with [Ag(I)] (3.2 × 10⁻² mmol) in the solvent (5 mL) at a cat./base/aldehyde/nitromethane ratio of 1:1:10:50 at rt for 20 h; lower catalyst loadings (1 mol%), resulted in very slow reactions. ^b Isolated yields based on initial 4-nitrobenzaldehyde; unreacted aldehyde accounted for the rest of the reaction mass balance.

^c T = 30 °C, t = 6 h. ^d Reaction conditions in the absence of metal catalyst: TEA/aldehyde/nitromethane ratio of 1:10:500 at rt for 20 h. Unreacted 4-nitrobenzaldehyde did not account for the rest of the reaction mass balance and some unidentified by-products derived from competitive side reactions were observed. ^e In the presence of molecular sieves (4 Å).



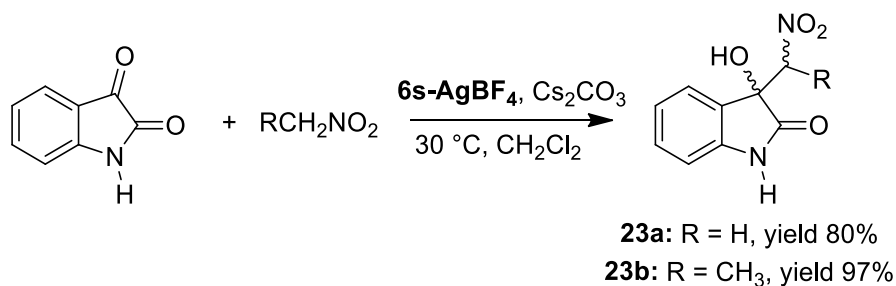
Entry	Cat.	X	Base	Solv.	t (h)	T (°C)	Yield 22a (%) ^b
1	6r-Ag	OTf	TEA	CH ₂ Cl ₂	20	rt	60
2	6r-Ag	OTf	TEA	Tol	40	rt	15
3	6r-Ag	OTf	DiPEA	CH ₂ Cl ₂	20	rt	53
4	6r-Ag	OTf	DMAP	CH ₂ Cl ₂	20	rt	53
5	6r-Ag	OTf	Morfoline	CH ₂ Cl ₂	20	rt	50
6	6r-Ag	OTf	K ₂ CO ₃	CH ₂ Cl ₂	20	rt	45
7	6r-Ag	OTf	Cs ₂ CO ₃	CH ₂ Cl ₂	20	rt	70
8	6r-Ag	BF₄	Cs ₂ CO ₃	CH ₂ Cl ₂	20	rt	70
9	6s-Ag	OTf	TEA	CH ₂ Cl ₂	20	rt	67
10	6s-Ag	BF₄	TEA	CH ₂ Cl ₂	20	rt	65
11	6s-Ag	BF₄	DiPEA	CH ₂ Cl ₂	20	rt	75
12	6s-Ag	BF₄	Cs ₂ CO ₃	CH ₂ Cl ₂	20	rt	90
13	6s-Ag	BF₄	Cs ₂ CO ₃	CH ₂ Cl ₂	20	30	95
14	6s-Ag	BF₄	Cs ₂ CO ₃	CH ₂ Cl ₂	12	30	92
15	6s-Ag	BF₄	Cs ₂ CO ₃	CH ₂ Cl ₂	6	30	75
16	6s-Ag	BF₄	Cs ₂ CO ₃	CH ₂ Cl ₂	3	30	45
17	6s-Ag	OTf	-	CH ₂ Cl ₂	20	rt	25
18	-	-	Cs ₂ CO ₃	CH ₂ Cl ₂	20	30	55
19 ^c	7j-Ag	BF₄	-	CH ₂ Cl ₂	20	rt	-
20 ^c	7j-Ag	BF₄	-	MeNO ₂	20	rt	-
21	7j-Ag	BF₄	-	MeOH	20	rt	- ^d
22	8c-Ag	BF₄	Cs ₂ CO ₃	CH ₂ Cl ₂	12	30	90
23	8c-Ag	BF₄	-	CH ₂ Cl ₂	12	30	64

^a Reactions were performed with [Ag(I)] (3.2 × 10⁻² mmol) in the solvent (5 mL) at a cat./base/aldehyde/nitromethane ratio of 1:1:10:50 in the presence of molecular sieves (4 Å). ^b Yields based on initial 4-nitrobenzaldehyde calculated via ¹H NMR using 2,4-dinitrotoluene (DNT) as internal standard; unreacted aldehyde accounted for the rest of the reaction mass balance. ^c The metal complex **7j-BF₄** is not soluble in the reaction medium: no reaction after 20 h as judged by TLC analysis. ^d Dimethyl acetal derived from the nucleophilic attack of MeO⁻ on the 4-nitrobenzaldehyde was recovered in 25% yield (see SI).



Entry	R ¹	R ²	Product	<i>syn/anti</i> ^b	Yield ^c (%)
1	4-NO ₂ C ₆ H ₄	H	22a	-	92 (90)
2	4-CNC ₆ H ₄	H	22b	-	83 (80)
3	4-CF ₃ C ₆ H ₄	H	22c	-	93 (92)
4	4-BrC ₆ H ₄	H	22d	-	85 (82)
5	4-ClC ₆ H ₄	H	22e	-	83 (80)
6	4-FC ₆ H ₄	H	22f	-	70 (64)
7	C ₆ H ₅	H	22g	-	60 (55)
8 ^d	4-MeC ₆ H ₄	H	22h	-	15
9	4-Bu ^t C ₆ H ₄	H	-	-	n.d.
10	4-MeOC ₆ H ₄	H	-	-	n.d.
11	4-Et ₂ NC ₆ H ₄	H	-	-	n.d.
12	C ₆ F ₅	H	22i	-	72 (68)
13	3,5-(CF ₃) ₂ C ₆ H ₄	H	22j	-	70 (66)
14	2-NO ₂ C ₆ H ₄	H	22k	-	97 (95)
15	2-BrC ₆ H ₄	H	22l	-	72 (65)
16	2,6-Cl ₂ C ₆ H ₄	H	22m	-	70 (68)
17	2-MeOC ₆ H ₄	H	22n	-	10
18	3-MeOC ₆ H ₄	H	-	-	n.d.
19	Cy	H	-	-	n.d.
20		H	-	-	n.d.
21		H	-	-	n.d.
22		H	22o	-	65 (62)
23		H	22p	-	10
24	4-NO ₂ C ₆ H ₄	CH ₃	22q	60:40	95 (90)
25 ^e	4-NO ₂ C ₆ H ₄	CH ₃	22q	60:40	90
26	2-NO ₂ C ₆ H ₄	CH ₃	22r	45:55	96 (93)
27	4-CF ₃ C ₆ H ₄	CH ₃	22s	51:49	93 (89)
28	4-ClC ₆ H ₄	CH ₃	22t	61:39	80 (75)
29	C ₆ H ₅	CH ₃	22u	55:45	75 (60)

^a Reactions were performed with [Ag(I)] (3.2×10^{-2} mmol) in CH₂Cl₂ (5 mL) at a cat./Cs₂CO₃/aldehyde/nitromethane ratio of 1:1:10:50 in the presence of molecular sieves (4 Å) at 30 °C for 12 h. ^b *Syn/anti* ratio determined by ¹H NMR. ^c Yields based on initial aldehyde calculated via ¹H NMR using 2,4-dinitrotoluene (DNT) as internal standard (isolated yields); unreacted aldehyde accounted for the rest of the reaction mass balance. ^d Reaction performed with complex **6r-BF₄** as catalyst. ^e Reaction performed with complex **8d-BF₄** as catalyst and in the absence of Cs₂CO₃.



2-nitro-1-(4-nitrophenyl)ethanol **22a**. Yield 90% (62 mg); ¹H NMR (400 MHz, CDCl₃, δ) 8.27 (d, J = 8.6 Hz, 2H, H_{Ar}), 7.63 (d, J = 8.5 Hz, 2H, H_{Ar}), 5.60 (dd, J = 7.7, 3.4 Hz, 1H, CH), 4.68 – 4.40 (m, 2H, CH₂), 3.12 (bs, 1H, OH). Spectral data are consistent with literature values.

4-(1-hydroxy-2-nitroethyl)benzotrile **22b**. Yield 80% (49 mg); ¹H NMR (300 MHz, CDCl₃, δ) 7.71 (d, J = 8.4 Hz, 2H, H_{Ar}), 7.56 (d, J = 8.1 Hz, 2H, H_{Ar}), 5.55 (dd, J = 7.9, 3.8 Hz, 1H, CH), 4.68 – 4.43 (m, 2H, CH₂), 3.11 (bs, 1H, OH). Spectral data are consistent with literature values.

2-nitro-1-(4-(trifluoromethyl)phenyl)ethanol **22c**. Yield 92% (69 mg); ¹H NMR (300 MHz, CDCl₃, δ) 7.68 (d, J = 8.3 Hz, 2H, H_{Ar}), 7.56 (d, J = 8.2 Hz, 2H, H_{Ar}), 5.56 (d, J = 6.6 Hz, 1H, CH), 4.70 – 4.45 (m, 2H, CH₂), 2.96 (bs, 1H, OH). Spectral data are consistent with literature values.

1-(4-bromophenyl)-2-nitroethanol **22d**. Yield 82% (65 mg); ¹H NMR (300 MHz, CDCl₃, δ) 7.54 (d, J = 8.4 Hz, 2H, H_{Ar}), 7.29 (d, J = 8.2 Hz, 2H, H_{Ar}), 5.44 (dd, J = 9.2, 3.3 Hz, 1H, CH), 4.61 – 4.46 (m, 2H, CH₂), 2.88 (bs, 1H, OH). Spectral data are consistent with literature values.

1-(4-chlorophenyl)-2-nitroethanol **22e**. Yield 80% (52 mg); ¹H NMR (600 MHz, CDCl₃, δ) 7.38 (d, J = 8.6 Hz, 2H, H_{Ar}), 7.34 (d, J = 8.5 Hz, 2H, H_{Ar}), 5.44 (d, J = 9.5 Hz, 1H, CH), 4.57 (dd, J = 13.3, 9.5 Hz, 1H, CH₂), 4.49 (dd, J = 13.3, 3.1 Hz, 1H, CH₂), 3.01 (d, J = 3.6 Hz, 1H, OH). Spectral data are consistent with literature values.

1-(4-fluorophenyl)-2-nitroethanol **22f**. Yield 64% (38 mg); ¹H NMR (300 MHz, CDCl₃, δ) 7.39 (dd, J = 8.4, 5.2 Hz, 2H, H_{Ar}), 7.10 (pst, J = 8.6 Hz, 2H, H_{Ar}), 5.46 (d, J = 9.1 Hz, 1H, CH), 4.63 – 4.47 (m, 2H, CH₂), 2.82 (bs, 1H, OH). Spectral data are consistent with literature values.

2-nitro-1-phenylethanol **22g**. Yield 55% (29 mg); ^1H NMR (300 MHz, CDCl_3 , δ) 7.42 – 7.29 (m, 5H, H_{Ar}), 5.48 (dd, $J = 9.3, 3.2$ Hz, 1H, CH), 4.66 – 4.50 (m, 2H, CH_2), 1.56 (bs, 1H, OH exchanging with water). Spectral data are consistent with literature values.

2-nitro-1-(perfluorophenyl)ethanol **22i**. Yield 68% (56 mg); ^1H NMR (300 MHz, CDCl_3 , δ) 5.87 (ddd, $J = 9.2, 5.8, 3.5$ Hz, 1H, CH), 5.02 (dd, $J = 13.9, 9.4$ Hz, 1H, CH_2), 4.61 (dd, $J = 14.0, 3.4$ Hz, 1H, CH_2), 3.08 (d, $J = 6.0$ Hz, 1H, OH). Spectral data are consistent with literature values.

2-nitro-1-(2-nitrophenyl)ethanol **22k**. Yield 95% (65 mg); ^1H NMR (300 MHz, CDCl_3 , δ) 8.07 (d, $J = 8.2$ Hz, 1H, H_{Ar}), 7.95 (d, $J = 7.9$ Hz, 1H, H_{Ar}), 7.75 (pst, $J = 7.6$ Hz, 1H, H_{Ar}), 7.56 (pst, $J = 7.8$ Hz, 1H, H_{Ar}), 6.05 (dd, $J = 9.0, 2.0$ Hz, 1H, CH), 4.87 (dd, $J = 13.8, 2.3$ Hz, 1H, CH_2), 4.55 (dd, $J = 13.8, 9.1$ Hz, 1H, CH_2), 3.23 (bs, 1H, OH). Spectral data are consistent with literature values.

1-(2-bromophenyl)-2-nitroethanol **22l**. Yield 65% (51 mg); ^1H NMR (300 MHz, CDCl_3 , δ) 7.67 (d, $J = 7.9$ Hz, 1H, H_{Ar}), 7.57 (d, $J = 8.0$ Hz, 1H, H_{Ar}), 7.41 (pst, $J = 7.1$ Hz, 1H, H_{Ar}), 7.22 (pst, $J = 7.7$ Hz, 1H, H_{Ar}), 5.96 – 5.70 (m, 1H, CH), 4.70 (dd, $J = 13.7, 2.3$ Hz, 1H, CH_2), 4.44 (dd, $J = 13.7, 9.6$ Hz, 1H, CH_2), 2.94 (d, $J = 4.0$ Hz, 1H, OH). Spectral data are consistent with literature values.

1-(2,6-dichlorophenyl)-2-nitroethanol **22m**. Yield 68% (51 mg); ^1H NMR (300 MHz, CDCl_3 , δ) 7.37 (m, 2H, H_{Ar}), 7.32 – 7.20 (m, 2H, H_{Ar}), 6.38 – 6.21 (m, 1H, CH), 5.17 (dd, $J = 13.1, 10.1$ Hz, 1H, CH_2), 4.56 (dd, $J = 13.1, 3.4$ Hz, 1H, CH_2), 3.24 (d, $J = 8.3$ Hz, 1H, OH). Spectral data are consistent with literature values.

1-(furan-2-yl)-2-nitroethanol **22o**. Yield 62% (31 mg); ^1H NMR (400 MHz, CDCl_3 , δ) 7.40 (s, 1H, H_{Ar}), 6.55 – 6.23 (m, 2H, H_{Ar}), 5.51 – 5.38 (m, 1H, CH), 4.76 (dd, $J = 13.4, 9.0$ Hz, 1H, CH_2), 4.65 (dd, $J = 13.4, 3.6$ Hz, 1H, CH_2), 3.18 (bs, 1H, OH). Spectral data are consistent with literature values.

2-nitro-1-(4-nitrophenyl)propan-1-ol **22q**. Yield 90% (65 mg); Diastereomeric ratio (*syn/anti* 60:40) determined by ^1H NMR. *Syn* isomer: ^1H NMR (400 MHz, CDCl_3 , δ) 8.25 – 8.21 (m, 2H, H_{Ar}), 7.60 – 7.56 (m, 2H, H_{Ar}), 5.18 (d, $J = 6.6$ Hz, 1H, CH), 4.79 – 4.72 (m, 1H, CH), 3.15 (bs, 1H, OH), 1.37 (d, $J = 6.6$ Hz, 3H, CH_3). *Anti* isomer: ^1H NMR (400 MHz, CDCl_3 , δ) 8.25 – 8.21 (m, 2H, H_{Ar}), 7.60 – 7.56 (m, 2H, H_{Ar}), 5.55 (m, 1H, CH), 4.79 – 4.72 (m, 1H, CH), 3.15 (bs, 1H, OH), 1.48 (d, $J = 6.6$ Hz, 3H, CH_3). Spectral data are consistent with literature values.

2-nitro-1-(2-nitrophenyl)propan-1-ol **22r**. Yield 93% (67 mg); Diastereomeric ratio (*syn/anti* 45:55) determined by ^1H NMR. *Syn* isomer: ^1H NMR (400 MHz, CDCl_3 , δ) 8.00 (dd, $J = 8.2, 0.9$ Hz, 1H, H_{Ar}),

7.73 – 7.69 (m, 2H, H_{Ar}), 7.56 – 7.53 (m, 1H, H_{Ar}), 5.71 (d, *J* = 6.6 Hz, 1H, CH), 5.01 – 4.95 (m, 1H, CH), 3.34 (bs, 1H, OH), 1.56 – 1.51 (m, 3H, CH₃). *Anti* isomer: ¹H NMR (400 MHz, CDCl₃, δ) 8.08 (dd, *J* = 8.2, 1.4 Hz, 1H, H_{Ar}), 7.93 (d, *J* = 7.9 Hz, 1H, H_{Ar}), 7.73 – 7.69 (m, 1H, H_{Ar}), 7.56 – 7.53 (m, 1H, H_{Ar}), 6.09 (d, *J* = 2.6 Hz, 1H, CH), 4.79 – 4.72 (m, 1H, CH), 3.15 (bs, 1H, OH), 1.56 – 1.51 (d, *J* = 6.0 Hz, 3H, CH₃). Spectral data are consistent with literature values.

2-nitro-1-(4-(trifluoromethyl)phenyl)propan-1-ol **22s**. Yield 71% (89 mg); Diastereomeric ratio (*syn/anti* 51:49) determined by ¹H NMR. *Syn* isomer: ¹H NMR (600 MHz, CDCl₃, δ) 7.69 – 7.66 (m, 2H, H_{Ar}), 7.54 – 7.51 (m, 2H, H_{Ar}), 5.13 (d, *J* = 8.6 Hz, 1H, CH), 4.76 (dq, *J* = 8.6, 6.9 Hz, 1H, CH), 1.37 (d, *J* = 6.9 Hz, 3H, CH₃). *Anti* isomer: ¹H NMR (600 MHz, CDCl₃, δ) 7.69 – 7.66 (m, 2H, H_{Ar}), 7.54 – 7.51 (m, 2H, H_{Ar}), 5.50 (d, *J* = 3.4 Hz, 1H, CH), 4.70 (qd, *J* = 6.8, 3.4 Hz, 1H, CH), 1.50 (d, *J* = 6.8 Hz, 3H, CH₃). OH signal appeared as a very broad signal around 3.5 – 1.8 ppm. Spectral data are consistent with literature values.

2-nitro-1-(4-chlorophenyl)propan-1-ol **22t**. Yield 75% (52 mg); Diastereomeric ratio (*syn/anti* 61:39) determined by ¹H NMR. *Syn* isomer: ¹H NMR (300 MHz, CDCl₃, δ) 7.39 – 7.35 (m, 2H, H_{Ar}), 7.33 – 7.26 (m, 2H, H_{Ar}), 5.02 (d, *J* = 8.9 Hz, 1H, CH), 4.76 – 4.70 (m, 1H, CH), 2.67 (br, 1H, OH), 1.33 (dd, *J* = 6.8, 1.6 Hz, 3H, CH₃). *Anti* isomer: ¹H NMR (300 MHz, CDCl₃, δ) 7.39 – 7.35 (m, 2H, H_{Ar}), 7.33 – 7.26 (m, 2H, H_{Ar}), 5.37 (br, 1H, CH), 4.68 – 4.62 (m, 1H, CH), 2.77 (br, 1H, OH), 1.49 (dd, *J* = 6.8, 1.5 Hz, 3H, CH₃). Spectral data are consistent with literature values.

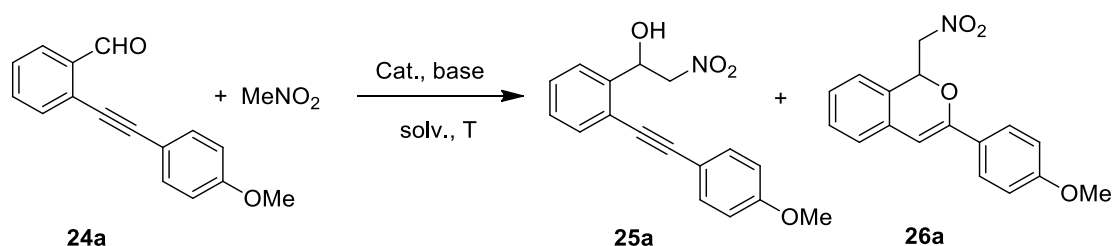
2-nitro-1-phenylpropan-1-ol **22u**. Yield 60% (35 mg); Diastereomeric ratio (*syn/anti* 55:45) determined by ¹H NMR. *Syn* isomer: ¹H NMR (400 MHz, CDCl₃, δ) 7.41 – 7.36 (m, 5H, H_{Ar}), 5.03 (dd, *J* = 9.0, 3.0 Hz, 1H, CH), 4.77 (dq, *J* = 9.0, 6.8 Hz, 1H, CH), 2.58 (d, *J* = 3.0 Hz, 1H, OH), 1.32 (d, *J* = 6.8 Hz, 3H, CH₃). *Anti* isomer: ¹H NMR (300 MHz, CDCl₃, δ) 7.41 – 7.36 (m, 5H, H_{Ar}), 5.40 (pst, *J* = 3.5 Hz, 1H, CH), 4.70 (qd, *J* = 6.8, 3.6 Hz, 1H, CH), 2.70 (d, *J* = 3.5 Hz, 1H, OH), 1.51 (d, *J* = 6.8 Hz, 3H, CH₃). Spectral data are consistent with literature values.

3-hydroxy-3-(nitromethyl)indolin-2-one **23a**. Yield 80% (53 mg); ¹H NMR (300 MHz, DMSO-d₆, δ) 10.54 (s, 1H, NH), 7.40 (dd, *J* = 7.3, 1.2 Hz, 1H, H_{Ar}), 7.27 (m, 1H, H_{Ar}), 7.10 – 6.82 (m, 2H, H_{Ar}), 6.74 (d, *J* = 1.0 Hz, 1H, OH), 5.15 – 4.82 (m, 2H, CH₂). Spectral data are consistent with literature values.

3-hydroxy-3-(nitroethyl)indolin-2-one **23b**. The product was not isolated; the yield and the diastereoisomeric ratio (6:4) were determined by ¹H NMR (internal standard 2,4-dinitrotoluene).

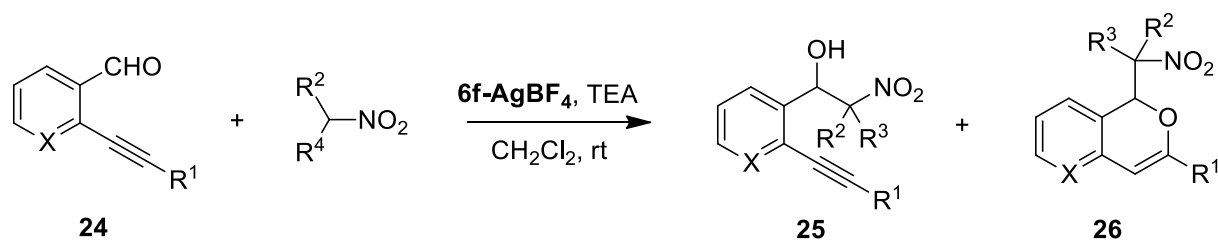
Major isomer: ^1H NMR (300 MHz, DMSO- d_6 , δ) 8.12 – 6.75 (m, 4H, H_{Ar}), 5.03 (m, 1H, CH), 1.34 (d, J = 6.8 Hz, 3H, CH_2). Minor isomer: ^1H NMR (300 MHz, DMSO- d_6 , δ) 8.12 – 6.75 (m, 4H, H_{Ar}), 5.04 (m, 1H, CH), 1.66 (d, J = 6.8 Hz, 3H, CH_2). Spectral data are consistent with literature values.

4.16 One-pot isochromene cycloisomerization vs Henry reaction⁸⁰



Entry	Catalyst	Base (equiv.)	MeNO_2 (equiv.)	Solvent	t (h)	T (°C)	Yield 25a ^b (%)	Yield 26a ^b (%)	Rec. 24a (%)
1	6f-CuOTf	TEA (1)	50	CH_2Cl_2	20	rt	(56)	-	(35)
2	6f-AgOTf	TEA (1)	50	CH_2Cl_2	20	rt	(17)	(17)	(12)
3	6f-AgOTf	TEA (1)	50	CH_2Cl_2	30	40	12	6	7
4	6f-AgOTf	TEA (1)	50	CH_2Cl_2	30	60	11	4	4
5	6f-AgOTf	TEA (5)	50	CH_2Cl_2	22	rt	45 (39)	-	11 (10)
6 ^c	6f-AgOTf	TEA ^c	^c	CH_2Cl_2	22	rt	77	-	10
7	6f-AgOTf	TEA (1)	50	Tol	20	30	30	8	11
8	6f-AgOTf	TEA (1)	50	DMF	24	30	53	-	6
9	6f-AgOTf	TEA (1)	50	THF	22	rt	46	2	21
10	6f-AgOTf	TEA (1)	11	CH_2Cl_2	22	rt	3	-	5
11	6f-AgOTf	TEA (1)	-	CH_3NO_2	20	rt	39	29	-
12	AgOTf	TEA (1)	-	CH_3NO_2	20	rt	-	15	15
13 ^d	6f-AgOTf	TEA (1)	500	CH_2Cl_2	22	rt	18	24	-
14 ^d	6f-AgOTf	TEA (1)	500	CH_2Cl_2	22	rt	25	33	-
15 ^d	6f-AgNTf₂	TEA (1)	500	CH_2Cl_2	22	rt	16	29	5
16 ^d	6f-AgBF₄	TEA (1)	500	CH_2Cl_2	22	rt	21 (18)	33 (30)	10 (9)
17 ^{d,e}	6f-AgBF₄	TEA (1)	500	CH_2Cl_2	22	rt	60 (57)	19 (17)	-
18 ^{d,e}	6f-AgBF₄	TEA (1)	500	CH_3CN	22	rt	96	-	-
19 ^d	6f-AgBF₄	DIPEA (1)	500	CH_2Cl_2	22	rt	36	27	-
20 ^d	6f-AgBF₄	DMAP (1)	500	CH_2Cl_2	22	rt	50	-	4
21 ^d	6f-AgOTf	DBU (1)	500	CH_2Cl_2	22	rt	11	4	16
22 ^d	6f-AgBF₄	NaHCO_3 (1)	500	CH_2Cl_2	22	rt	5	1	65
23 ^d	6f-AgOTf	Cs_2CO_3 (1)	500	CH_2Cl_2	22	rt	72	-	2
24 ^d	6f-AgNTf₂	K_2CO_3 (1)	500	CH_2Cl_2	22	rt	78	-	2
25 ^e	6s-AgBF₄	TEA (1)	500	CH_2Cl_2	22	rt	57	15	8
26 ^e	8c-AgBF₄	-	500	CH_2Cl_2	22	rt	60	15	13

^a Reactions were performed with $[\text{Ag(I)}]$ (2.5×10^{-2} mmol) in the solvent (1.25 mL) at a catalyst/aldehyde ratio of 1:10. ^b Yields based on initial **24a** calculated via ¹H NMR using 2,4-dinitrotoluene (DNT) as internal standard; isolated yields in brackets. Under these conditions, unreacted starting aldehyde did not always account for the rest of the reaction mass balance. In some cases, unidentified by-products derived from competitive side reactions were detected. ^c TEA (2.5×10^{-2} mmol)/aldehyde/nitromethane ratio of 1:1:5. ^d Reaction performed with freshly distilled nitromethane. ^e In the presence of molecular sieves (4 Å).



Entry	SM	R ¹	X	R ²	R ³	t (h)	Yield 25 ^b (%)	Yield 26 ^b (%)	Rec. SM (%)
1				H	H	22	25a 18	26a 30	9
2	24a	<i>p</i> -MeO-Ph	CH	Me	H	22	25b + 25b' 70 ^c	26b + 26b' 7 ^d	21
3				Me	Me	22	-	-	42 ^e
4	24b	<i>p</i> -Me-Ph	CH	H	H	22	25c 32	26c 31	5
5 ^f				H	H	22	25c 60	26c 5	9
6	24c	<i>p</i> -CF ₃ -Ph	CH	H	H	22	25d 45	26d traces	14
7	24d	Me ₃ Si	CH	H	H	22	25e 48	-	45
8 ^f				H	H	22	25e 83	-	15
9	24e	<i>n</i> -Pr	CH	H	H	22	25f 15	26f 54	-
10	24f	<i>n</i> -Pr	N	H	H	1	25g 52	-	-
11	24g	<i>p</i> -MeO-Ph	N	H	H	22	25h 68	-	15
12 ^f				H	H	22	25h 78	-	-

^a Reactions were performed with [Ag(I)] (2.5 × 10⁻² mmol) in CH₂Cl₂ (1.25 mL) at a catalyst/TEA/aldehyde/nitromethane ratio of 1:1:10:500. ^b Isolated yields based on initial alkynebenzaldehyde **24**. Under these conditions, unreacted starting aldehyde did not always account for the rest of the reaction mass balance. In some cases, unidentified by-products derived from competitive side reactions were detected. ^c Mixture of two diastereoisomers in 70:30 ratio. ^d Mixture of two diastereoisomers in 75:25 ratio calculated on the ¹H NMR. ^e In this case, the isocoumarin **26** (29%) was recovered as major by-product. ^f In the presence of molecular sieves (4 Å).

1-(2-((4-methoxyphenyl)ethynyl)phenyl)-2-nitroethanol 25a. Yield 18% (13 mg); ¹H NMR (300 MHz, CDCl₃, δ) 7.62 (d, *J* = 7.7 Hz, 1H, H_{Ar}), 7.55 – 7.44 (m, 3H, H_{Ar}), 7.37 (td, *J* = 7.6, 1.3 Hz, 1H, H_{Ar}), 7.31 (td, *J* = 7.5, 1.3 Hz, 1H, H_{Ar}), 6.88 (d, *J* = 8.9 Hz, 2H, H_{Ar}), 5.98 (dd, *J* = 9.8, 1.8 Hz, 1H, CH), 4.79 (dd, *J* = 13.0, 2.4 Hz, 1H, CH₂), 4.50 (dd, *J* = 13.0, 9.9 Hz, 1H, CH₂), 3.81 (s, 3H, CH₃). 2.94 (s, 1H, OH). Spectral data are consistent with literature values.

3-(4-methoxyphenyl)-1-(nitromethyl)-1H-isochromene 26a. Yield 30% (22 mg); ¹H NMR (300 MHz, CDCl₃, δ) 7.62 – 7.55 (m, 2H, H_{Ar}), 7.31 (td, *J* = 7.5, 1.1 Hz, 1H, H_{Ar}), 7.20 (td, *J* = 7.5, 1.1 Hz, 1H, H_{Ar}), 7.12 (dd, *J* = 11.4, 7.6 Hz, 2H, H_{Ar}), 6.93 – 6.86 (m, 2H, H_{Ar}), 6.37 (s, 1H, Csp²-H), 6.11 (dd, *J* = 10.3, 3.2 Hz, 1H, CH), 4.95 (dd, *J* = 12.3, 10.3 Hz, 1H, CH₂), 4.35 (dd, *J* = 12.3, 3.2 Hz, 1H, CH₂), 3.82 (s, 3H, CH₃). Spectral data are consistent with literature values.

2-nitro-1-(2-(p-tolyethynyl)phenyl)ethanol 25c. Yield 32% (23 mg) Table 5, entry 4; yield 60% (42 mg) Table 5, entry 5; ¹H NMR (300 MHz, CDCl₃, δ) 7.59 (d, *J* = 7.6 Hz, 1H, H_{Ar}), 7.49 (dd, *J* = 7.6, 1.1 Hz, 1H, H_{Ar}), 7.43 (d, *J* = 8.1 Hz, 2H, H_{Ar}), 7.35 (td, *J* = 7.6, 1.3 Hz, 1H, H_{Ar}), 7.28 (td, *J* = 7.5, 1.2 Hz, 1H, H_{Ar}), 7.14 (d, *J* = 7.9 Hz, 2H, H_{Ar}), 5.94 (dd, *J* = 9.8, 2.2 Hz, 1H, CH), 4.74 (dd, *J* = 13.1, 2.4 Hz, 1H, CH₂), 4.45 (dd, *J* = 13.1, 9.9 Hz, 1H, CH₂), 2.95 (s, 1H, OH), 2.34 (s, 3H, CH₃). Spectral data are consistent with literature values.

1-(nitromethyl)-3-(p-tolyl)-1H-isochromene 26c. Yield 31% (22 mg) Table 5, entry 4; yield 5% (4 mg) Table 5, entry 5; ¹H NMR (400 MHz, CDCl₃, δ) 7.55 (d, *J* = 7.9 Hz, 2H, H_{Ar}), 7.32 (t, *J* = 7.5 Hz, 1H, H_{Ar}), 7.27 – 7.04 (m, 5H, H_{Ar}), 6.45 (s, 1H, Csp²-H), 6.13 (dd, *J* = 10.2, 2.7 Hz, 1H, CH), 4.95 (dd, *J* = 12.3, 7.2 Hz, 1H, CH₂), 4.36 (dd, *J* = 12.3, 3.0 Hz, 1H, CH₂), 2.37 (s, 3H, CH₃). Spectral data are consistent with literature values.

4.17 Fe(III) catalysed alkene oxidation

General catalytic procedure

The catalyst (0.025 mmol), the substrate (0.5 mmol) and dodecane (60 μ L, used as GC internal standard) were dissolved in acetone (10.0 mL). H₂O₂ 30% (1.5 mmol) was added and the mixture was heated for 10 hours at 60 °C. Then H₂O₂ 30% (1.5 mmol) was added and the mixture was heated for further 12-14 hours. After this period the catalyst was removed by filtration on celite pad and a sample of the so-obtained crude ($c = 0.1$ mg/mL) was used for GC and GC-MS analyses.

General GC method

Gaschromatographic analyses were performed with GC-FAST technique using a Shimadzu GC-2010 equipped with a Supelco SLBTM-5ms capillary column. Dodecane was used as the internal standard. The samples were prepared with a concentration of 0.1 mg/mL in DCM.

PTV parameters:

Temperature = 120 °C

Injection mode: SPLIT

Pressure = 2.54 bar

Total flow = 11 mL/min

Column flow = 0.32 mL/min

Linear velocity = 32.6 cm/s

Purge flow = 1 mL/min

Split Ratio = 30

FID parameters:

Temperature = 280 °C

Make-up gas: N₂/air

H₂ flow = 40 mL/min

Make-up flow = 30 mL/min

Air flow = 400 mL/min

Column program:

RATE	Temperature	Holding Time
-	120 °C	0 min
25 °C/min	270 °C	3 min

General GC-MS methods

Instrument: ThermoFisher, GC-MS Single quadrupole TRACE1300 ISQQD

Column: VF-5ms (30 m x 0.25 mm i.d. x 0.25 µm; Agilent Technology).

Injector: SSL (split, splitless).

METHOD A:

Mode: Split.

T. injector = 290 °C

Split Flow = 30 mL/min

Split Ratio = 25

Carrier Flow = 1.2 mL/min

Purge Flow = 5 mL/min

Vacuum Compensation: on

Gas-saver Flow = 20 mL/min

Gas-saver Time = 2 min

Oven:

RATE	Temperature	Holding Time
-	120 °C	1 min
15 °C/min	220 °C	1 min
20 °C/min	250 °C	5 min

Mass:

Ion source T. = 270 °C

Transfer line T. = 270 °C

Ionization mode = EI

Delay time = 3 min

Range Mass = 50 – 500

Dwell Times = 0.2 sec

METHOD B:

Mode: Split.

T. injector = 280 °C

Split Flow = 30 mL/min

Split Ratio = 25

Carrier Flow = 1.2 mL/min

Purge Flow = 5 mL/min

Vacuum Compensation: on

Gas-saver Flow = 20 mL/min

Gas-saver Time = 2 min

Oven:

RATE	Temperature	Holding Time
-	50 °C	1 min
15 °C/min	180 °C	1 min
20 °C/min	240 °C	2 min

Mass:

Ion source T. = 270 °C

Transfer line T. = 270 °C

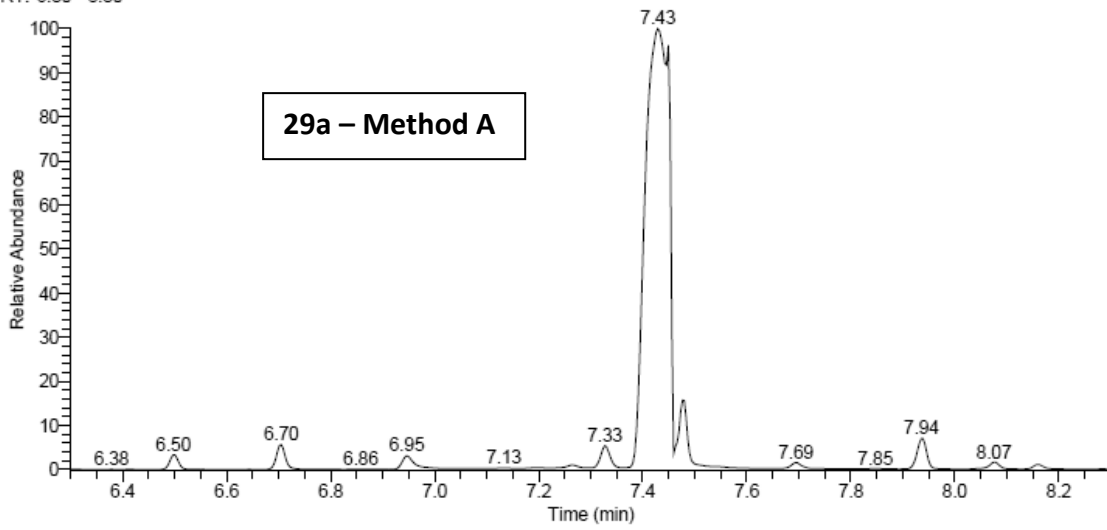
Ionization mode = EI

Delay time = 3 min

Range Mass = 50 – 500

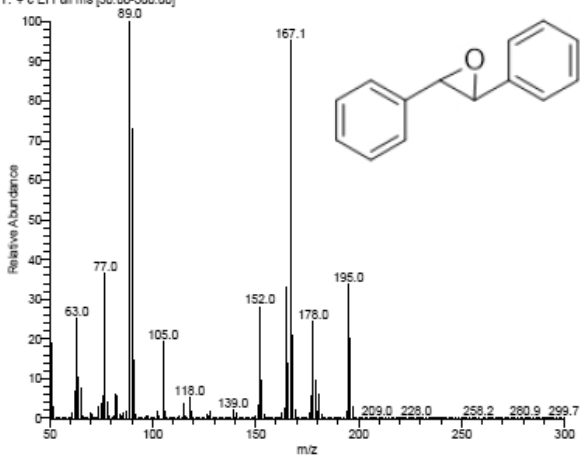
Dwell Times = 0.2 sec

RT: 6.30 - 8.30

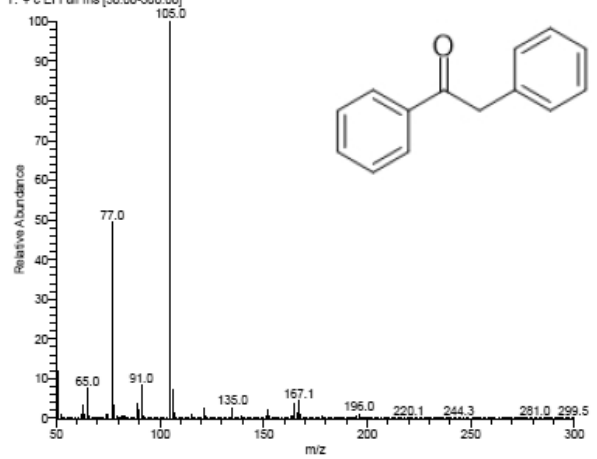


NL:
1.89E9
TIC MS
GT704

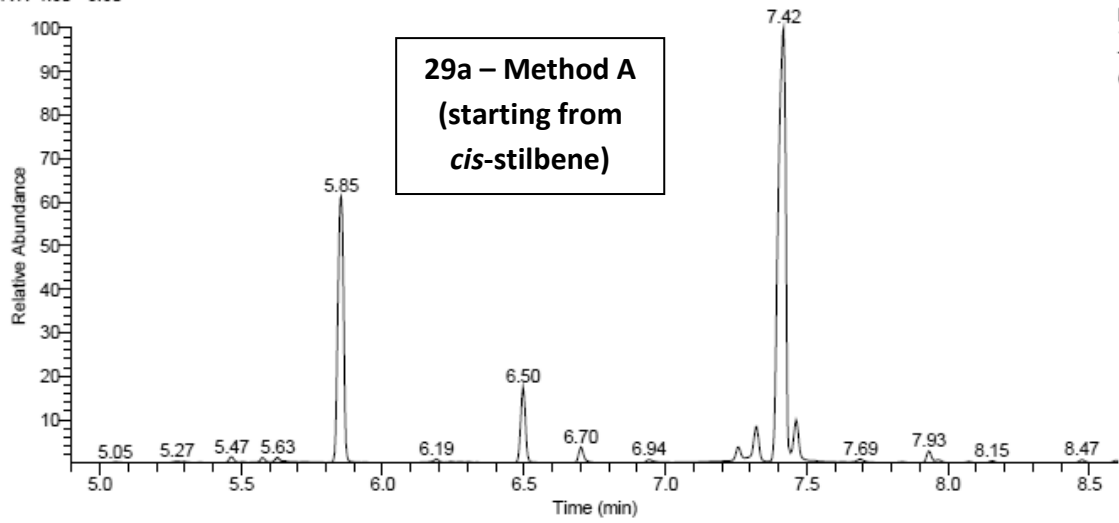
gt704 #1303 RT: 7.43 AV: 1 NL: 2.68E8
T: + c EI Full ms [50.00-500.00]



gt704 #1318 RT: 7.48 AV: 1 NL: 1.24E8
T: + c EI Full ms [50.00-500.00]

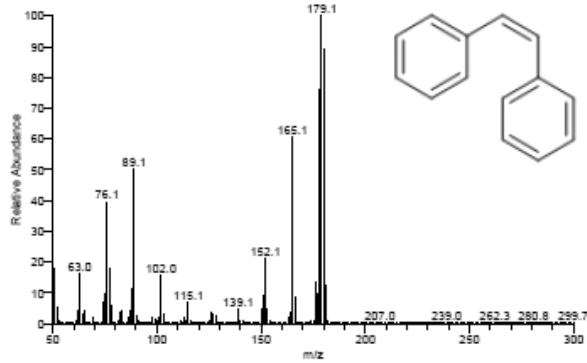


RT: 4.90 - 8.60

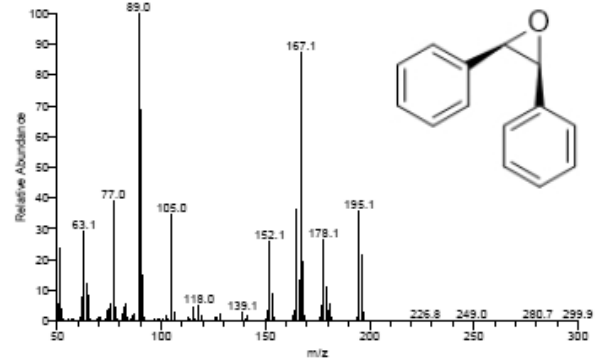


NL:
1.08E9
TIC MS
GT716bis

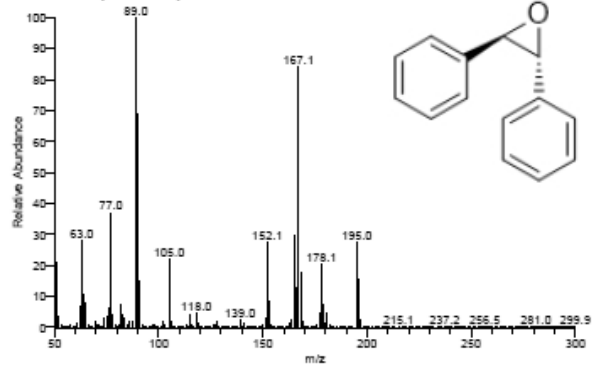
gt716bis #839 RT: 5.85 AV: 1 NL: 9.41E7
T: + c EI Full ms [50.00-500.00]



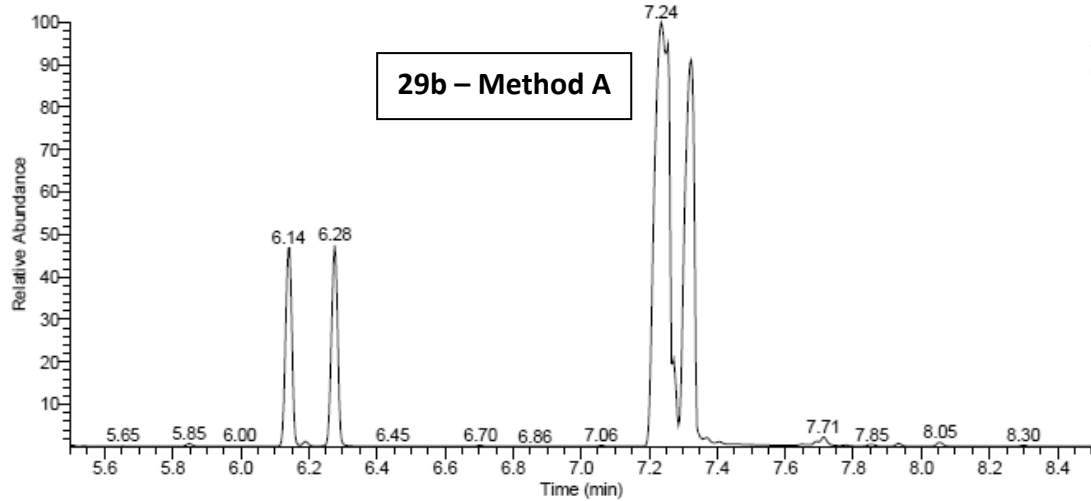
gt716bis #1030 RT: 6.50 AV: 1 NL: 2.36E7
T: + c EI Full ms [50.00-500.00]



gt716bis #1300 RT: 7.42 AV: 1 NL: 1.51E8
T: + c EI Full ms [50.00-500.00]

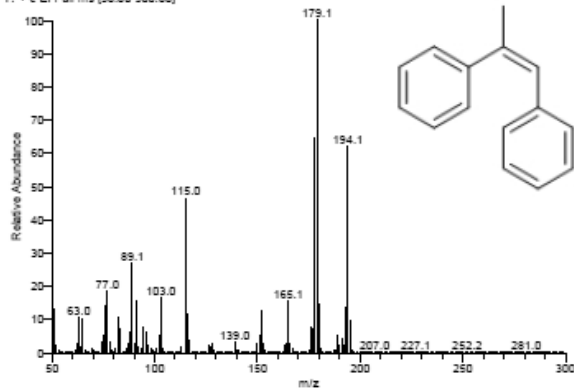


RT: 5.50 - 8.50

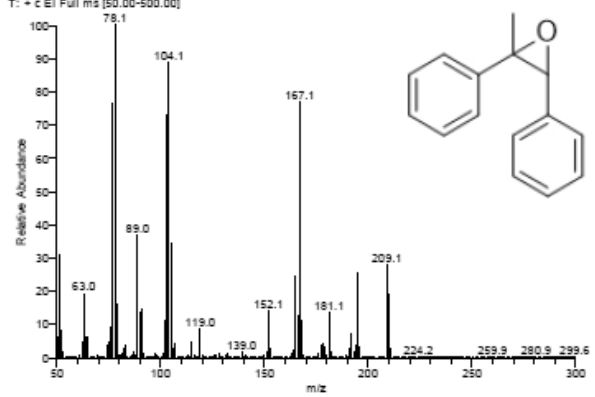


NL:
1.33E9
TIC MS
GT719bis

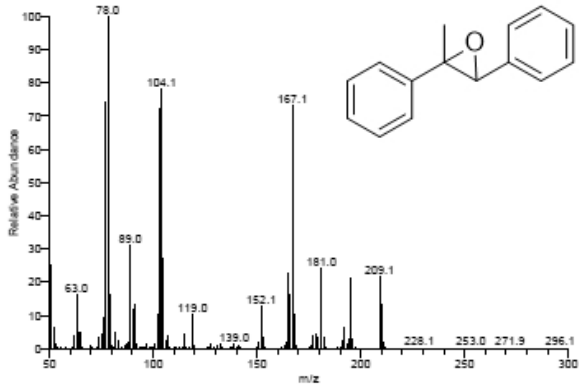
GT719bis #524 RT: 6.14 AV: 1 NL: 9.52E7
T: + c EI Full ms [50.00-500.00]



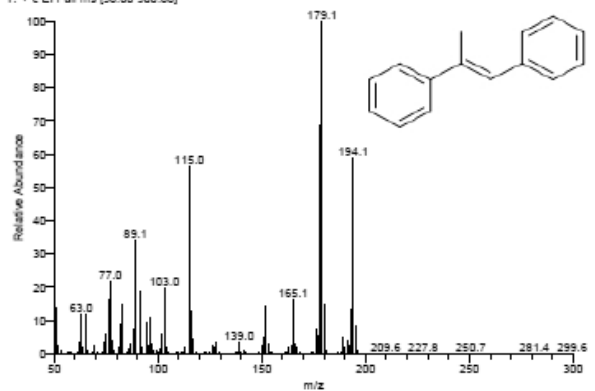
GT719bis #965 RT: 6.28 AV: 1 NL: 6.58E7
T: + c EI Full ms [50.00-500.00]



GT719bis #1247 RT: 7.24 AV: 1 NL: 1.59E8
T: + c EI Full ms [50.00-500.00]



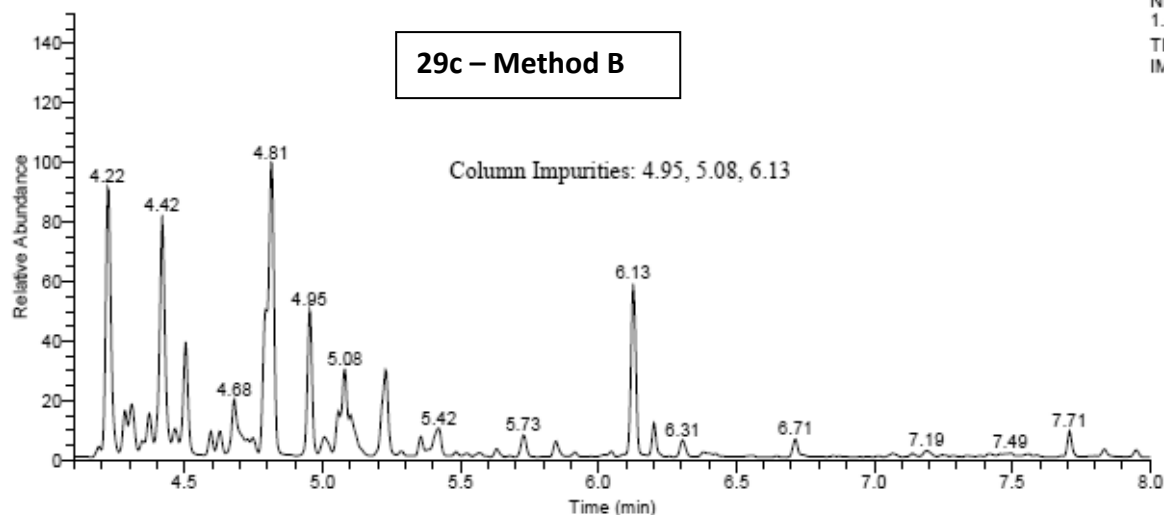
GT719bis #1274 RT: 7.33 AV: 1 NL: 1.50E8
T: + c EI Full ms [50.00-500.00]



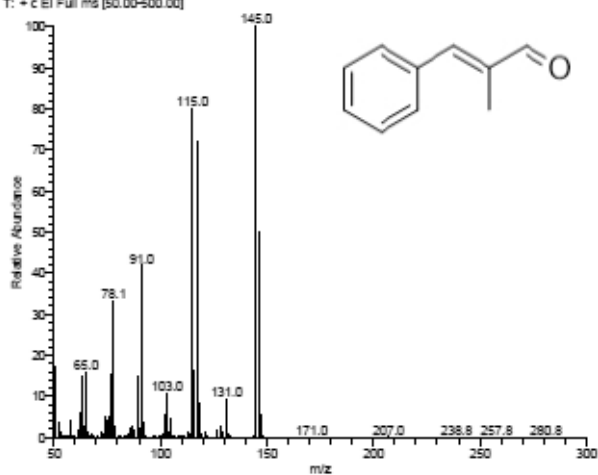
RT: 4.10 - 8.00

29c - Method B

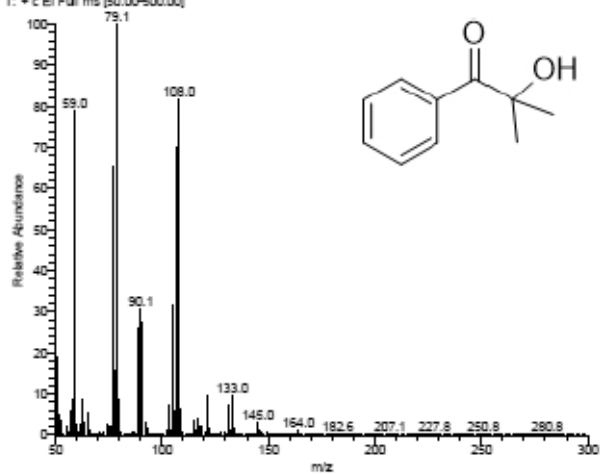
NL:
1.64E8
TIC MS
IM49



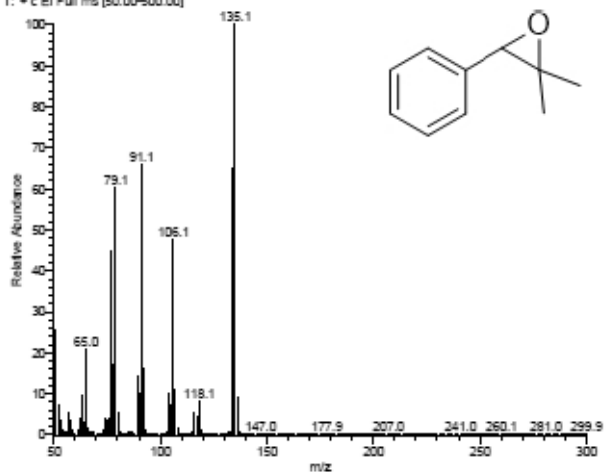
IM49 #350 RT: 4.22 AV: 1 NL: 2.53E7
T: + c EI Full ms [50.00-500.00]



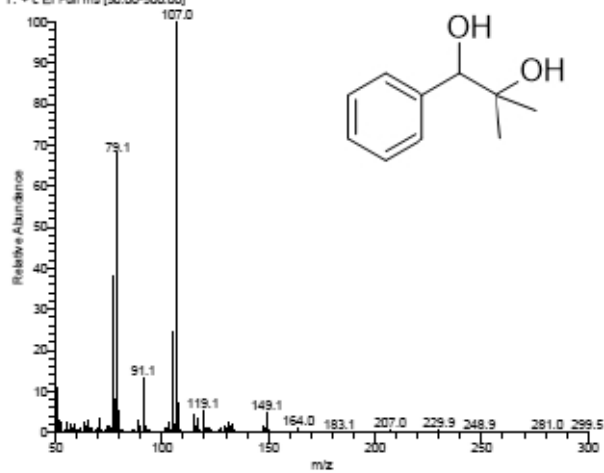
IM49 #418 RT: 4.42 AV: 1 NL: 1.94E7
T: + c EI Full ms [50.00-500.00]



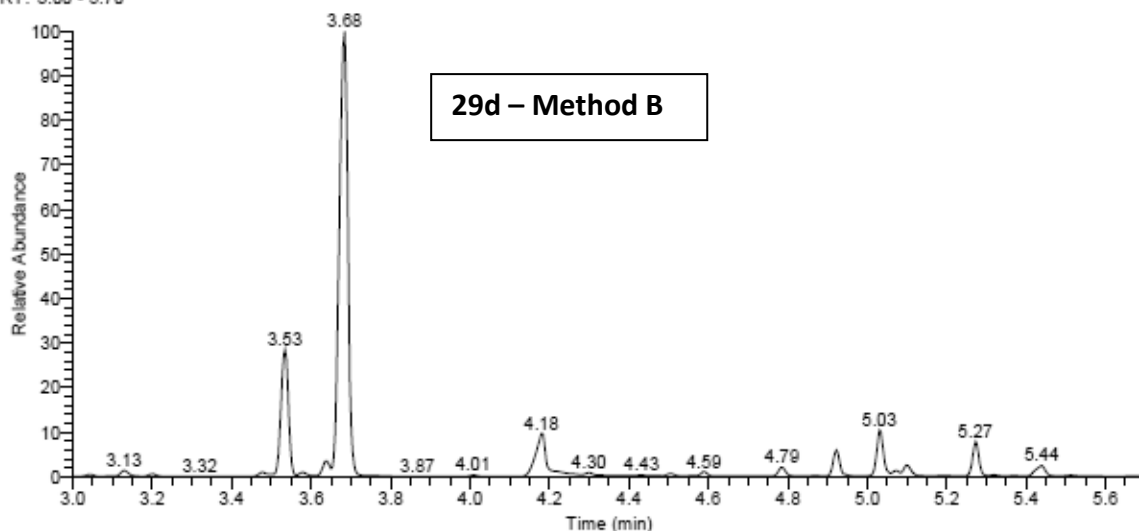
IM49 #527 RT: 4.79 AV: 1 NL: 1.20E7
T: + c EI Full ms [50.00-500.00]



IM49 #657 RT: 5.23 AV: 1 NL: 1.35E7
T: + c EI Full ms [50.00-500.00]

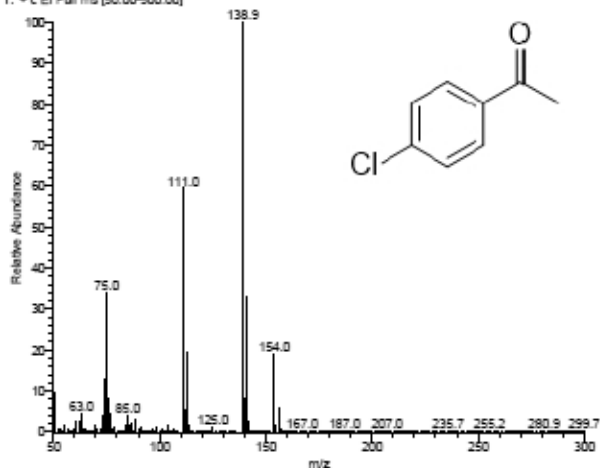


RT: 3.00 - 5.70

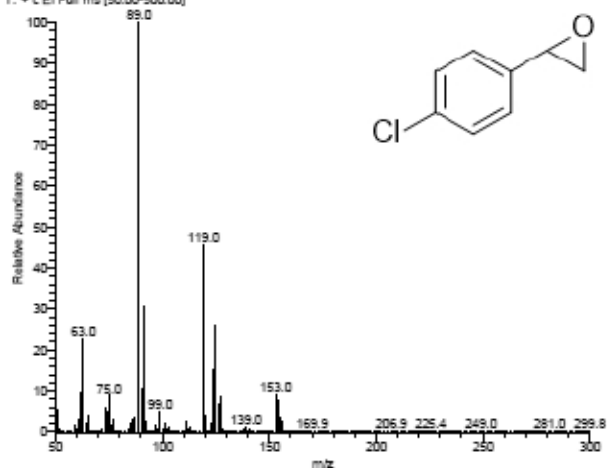


NL:
1.21E9
TIC MS
CF128

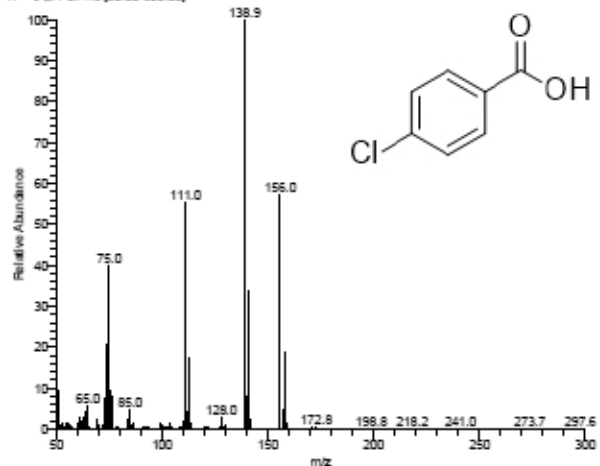
c128#157 RT: 3.53 AV: 1 NL: 8.78E7
T: + c EI Full ms [50.00-500.00]



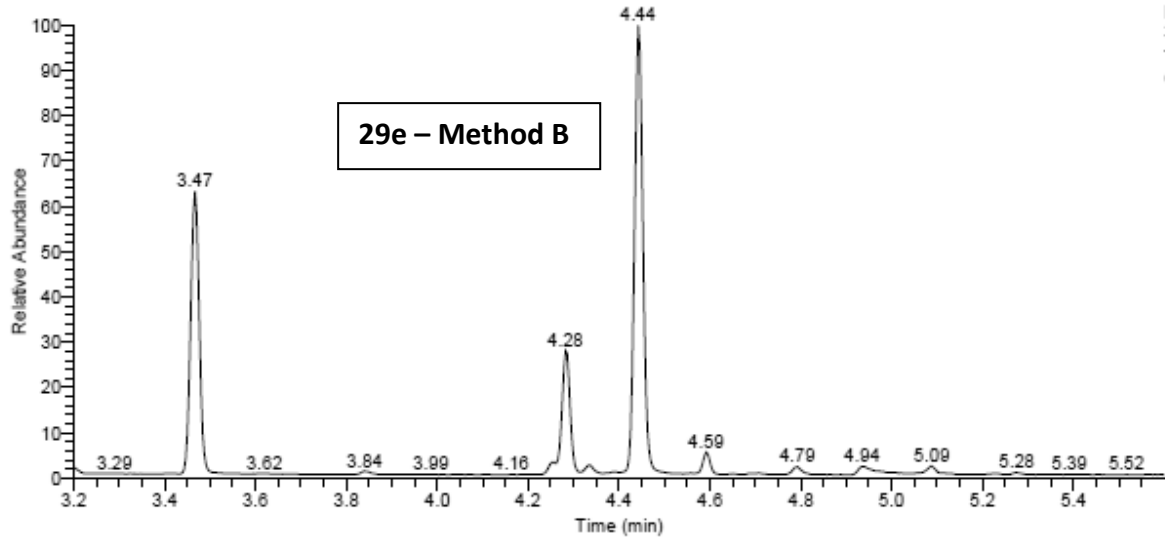
c128#201 RT: 3.68 AV: 1 NL: 3.04E9
T: + c EI Full ms [50.00-500.00]



c128#348 RT: 4.18 AV: 1 NL: 2.49E7
T: + c EI Full ms [50.00-500.00]

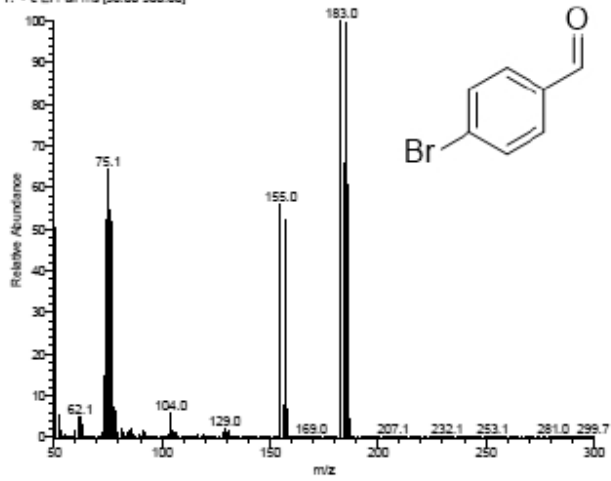


RT: 3.20 - 5.60

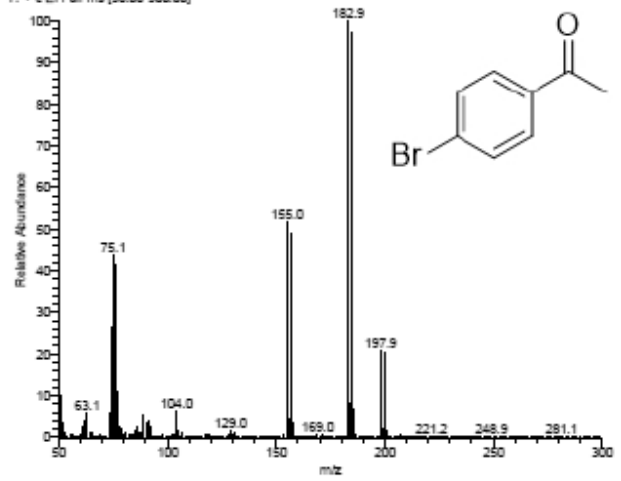


NL:
3.50E8
TIC MS
CF135

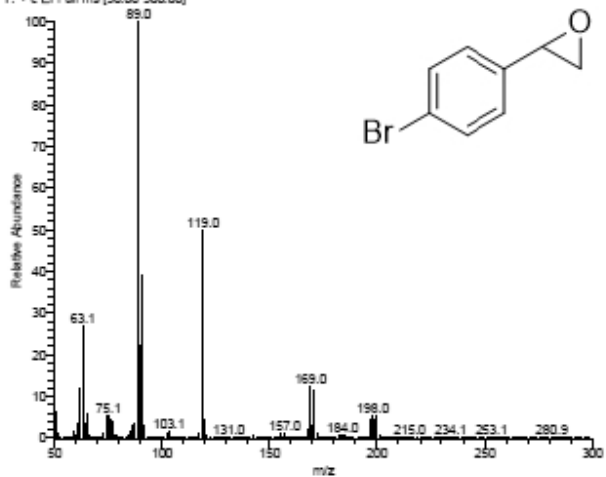
c135 #139 RT: 3.47 AV: 1 NL: 2.40E7
T: + c EI Full ms [50.00-500.00]



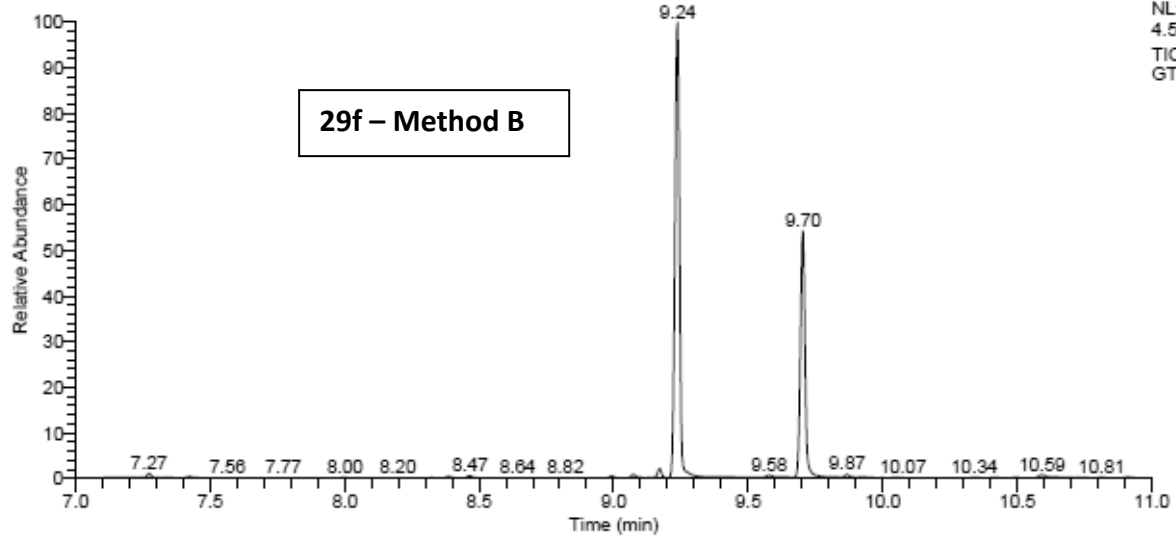
c135 #377 RT: 4.28 AV: 1 NL: 1.40E7
T: + c EI Full ms [50.00-500.00]



c135 #434 RT: 4.44 AV: 1 NL: 7.98E7
T: + c EI Full ms [50.00-500.00]

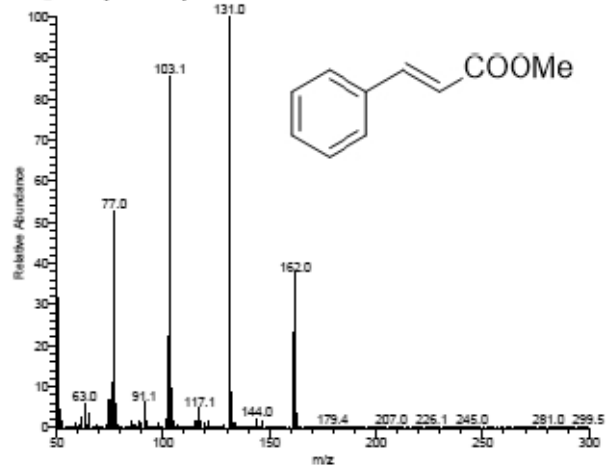


RT: 7.00 - 11.00

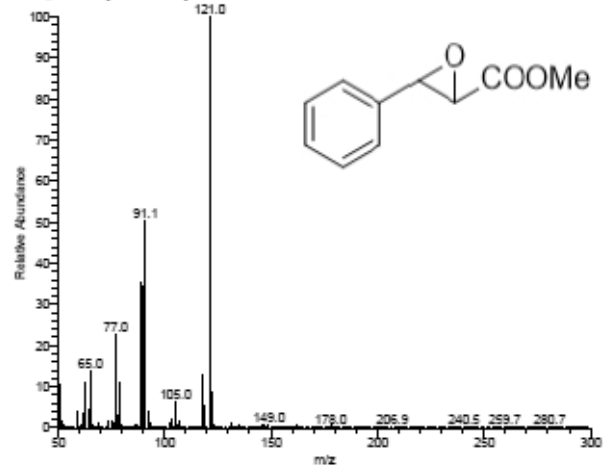


NL:
4.53E8
TIC MS
GT726

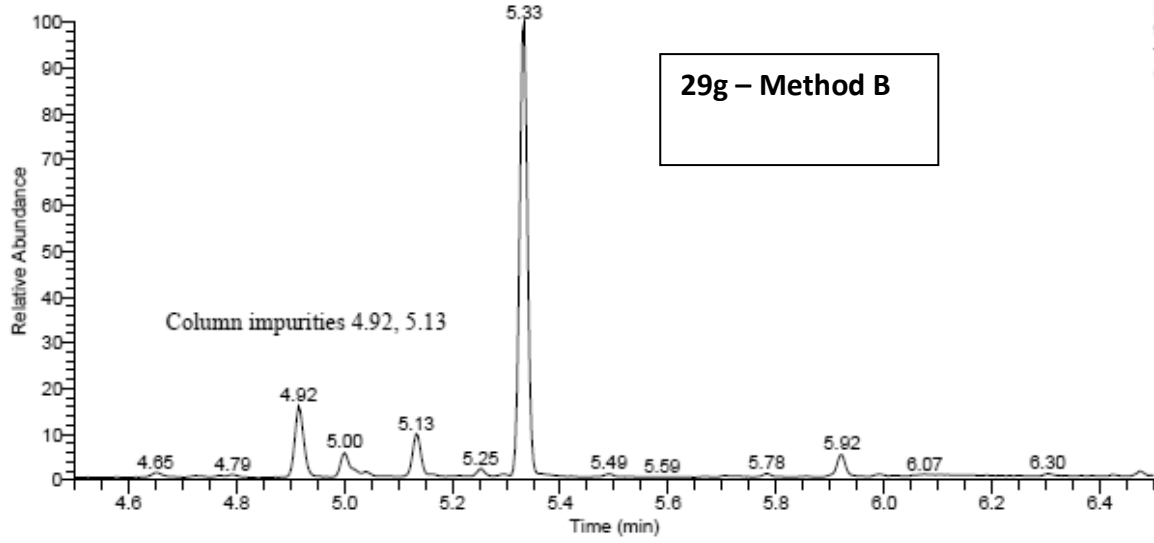
g726 #1836 RT: 9.24 AV: 1 NL: 8.10E7
T: + c EI Full ms [50.00-500.00]



g726 #1971 RT: 9.70 AV: 1 NL: 6.34E7
T: + c EI Full ms [50.00-500.00]

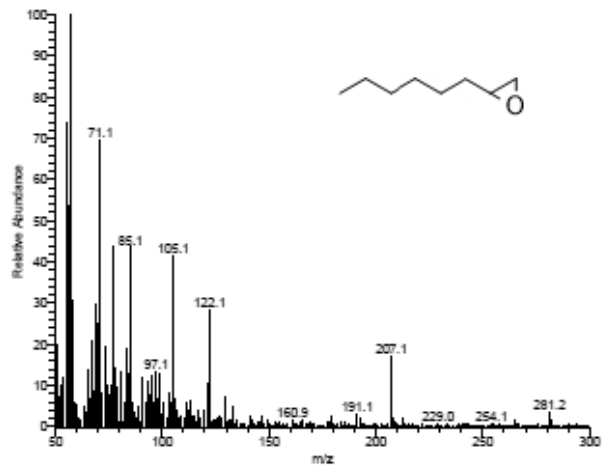


RT: 4.50 - 6.50

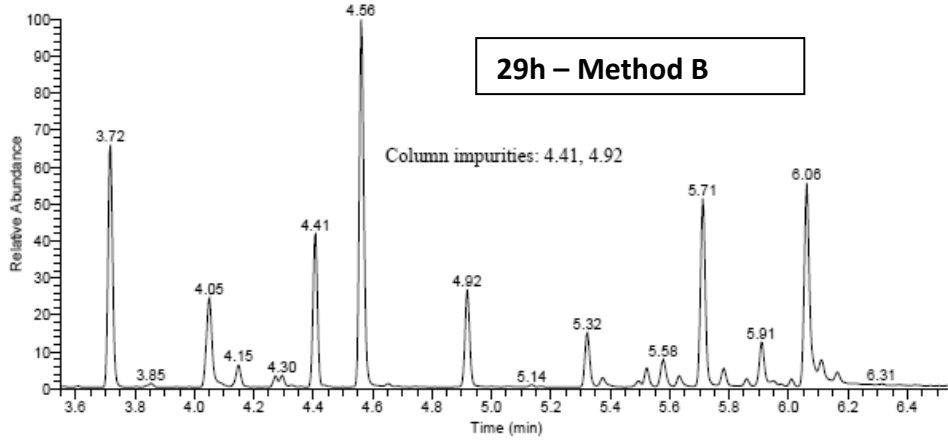


NL:
9.58E7
TIC MS
GT725_BIS

GT725_BIS #1283 RT: 7.36 AV: 1 NL: 1.15E5
T: + c EI Full ms [50.00-500.00]

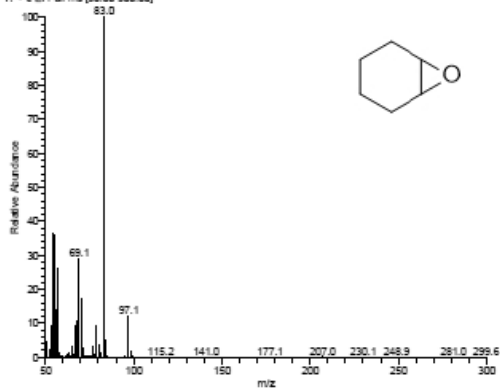


RT: 3.55 - 6.55

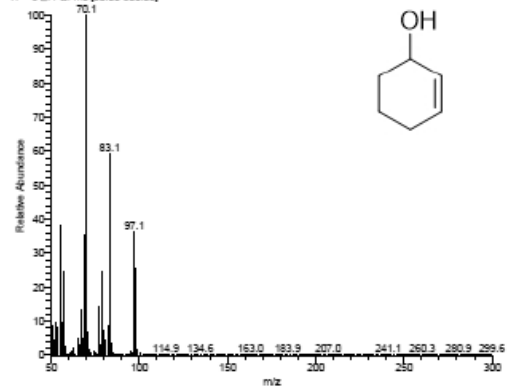


NL:
1.34E8
TIC MS
IM50_BIS

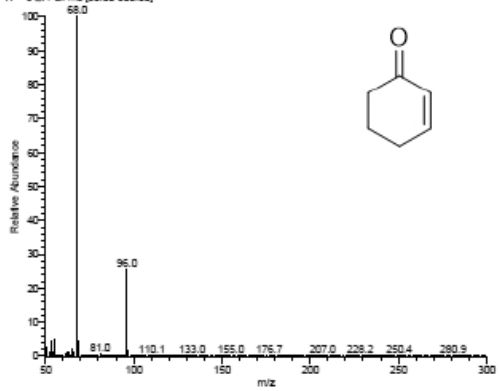
IM50_bis #213 RT: 3.72 AV: 1 NL: 2.13E7
T: + c EI Full ms [50.00-500.00]



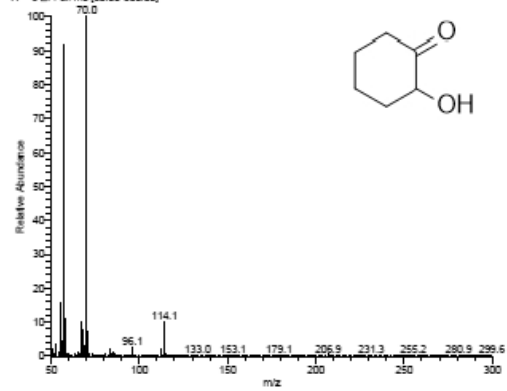
IM50_bis #310 RT: 4.05 AV: 1 NL: 6.89E6
T: + c EI Full ms [50.00-500.00]



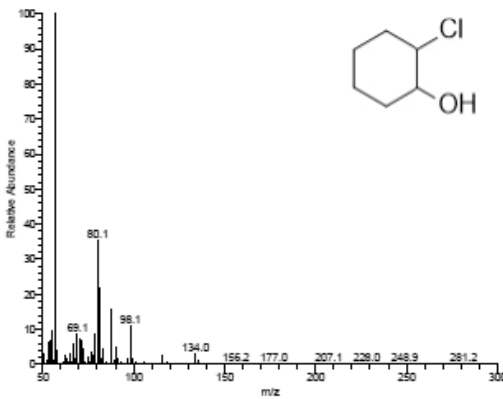
IM50_bis #439 RT: 4.95 AV: 1 NL: 7.04E7
T: + c EI Full ms [50.00-500.00]



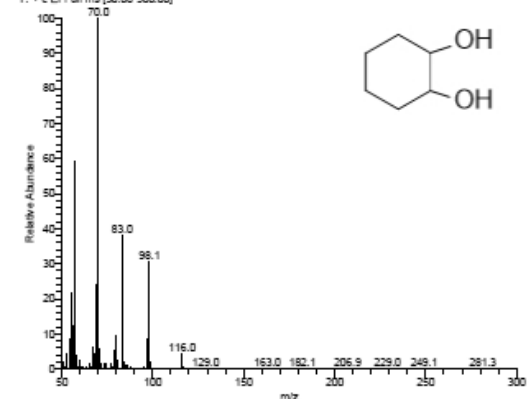
IM50_bis #683 RT: 5.32 AV: 1 NL: 6.80E6
T: + c EI Full ms [50.00-500.00]



IM50_bis #798 RT: 5.71 AV: 1 NL: 2.26E7
T: + c EI Full ms [50.00-500.00]



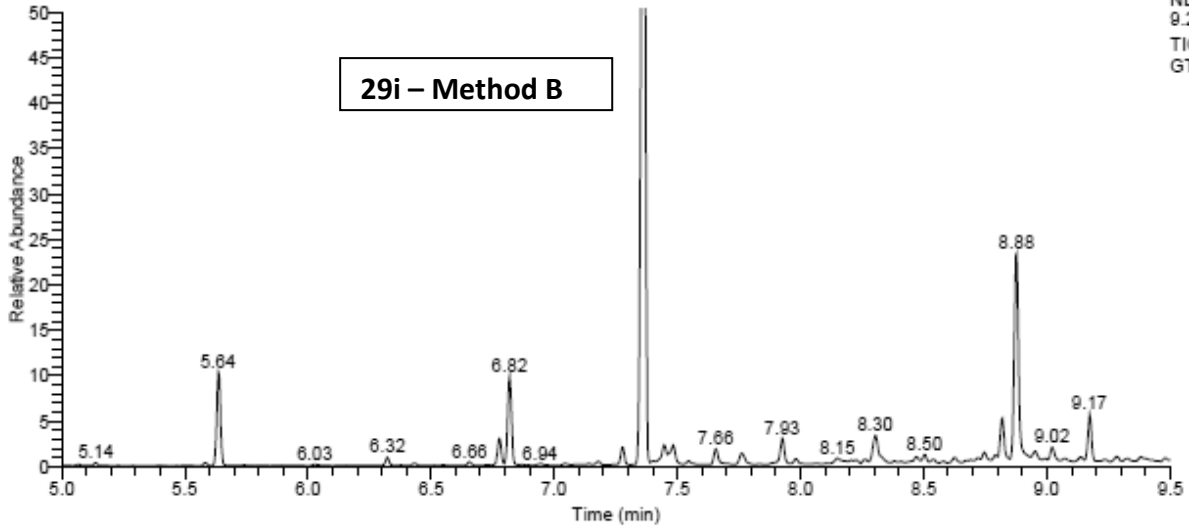
IM50_bis #801 RT: 6.06 AV: 1 NL: 2.02E7
T: + c EI Full ms [50.00-500.00]



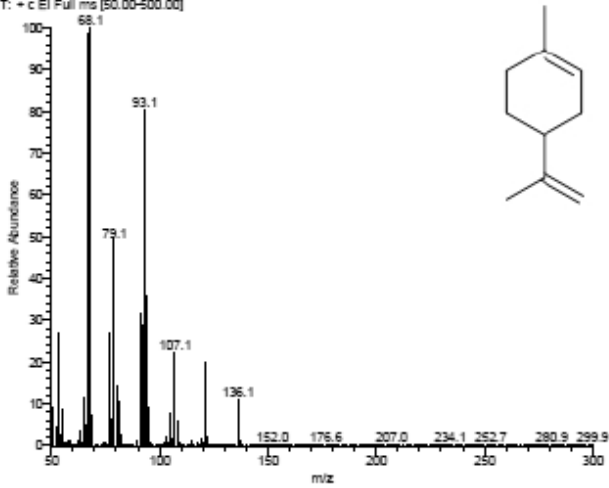
RT: 5.00 - 9.50

NL:
9.27E8
TIC MS
GT732

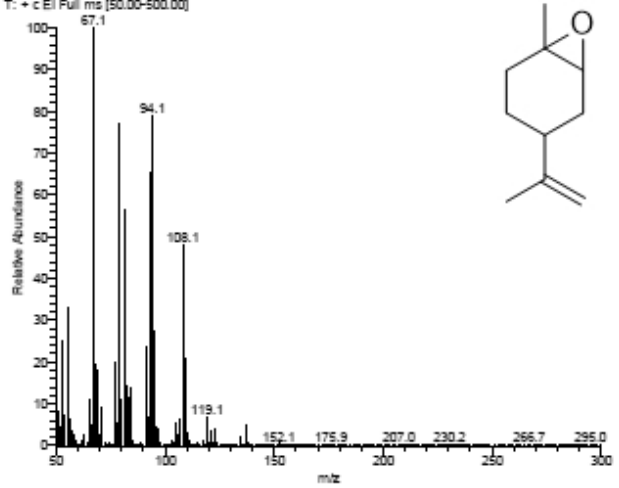
29i - Method B



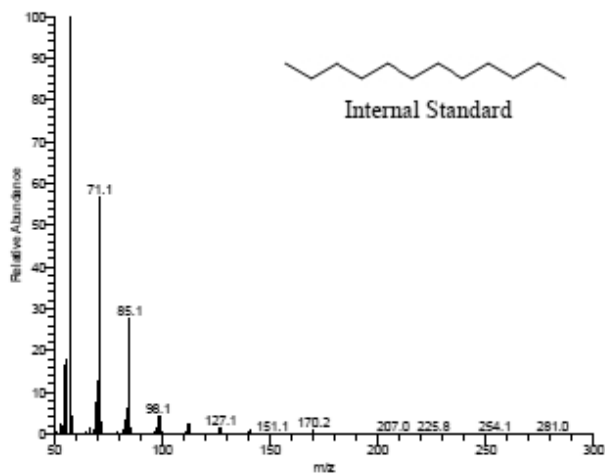
gt732 #777 RT: 5.64 AV: 1 NL: 1.41E7
T: + c EI Full ms [50.00-500.00]



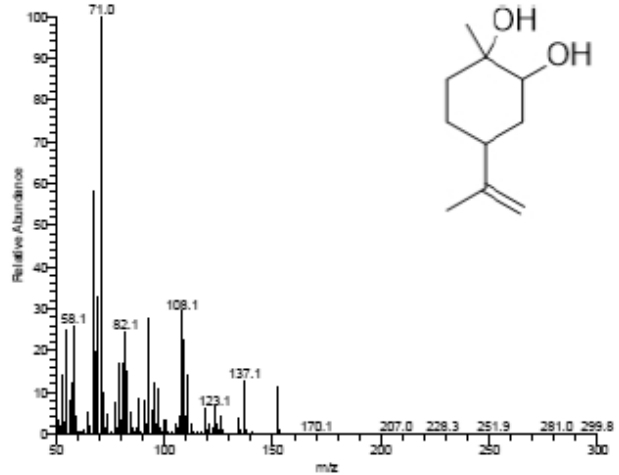
gt732 #1124 RT: 6.82 AV: 1 NL: 1.16E7
T: + c EI Full ms [50.00-500.00]



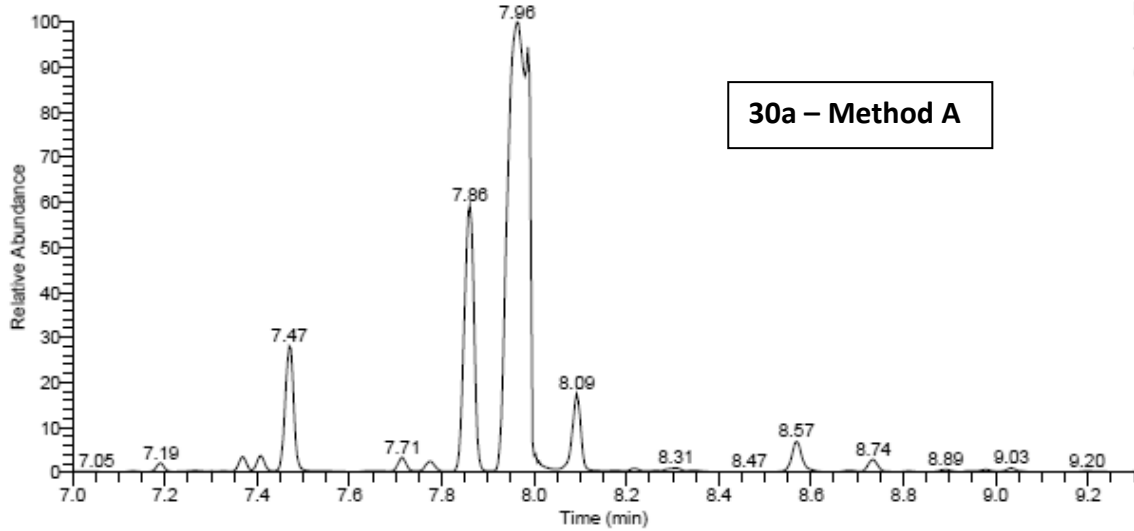
gt732 #1283 RT: 7.36 AV: 1 NL: 3.23E8
T: + c EI Full ms [50.00-500.00]



gt732 #1730 RT: 8.88 AV: 1 NL: 2.78E7
T: + c EI Full ms [50.00-500.00]

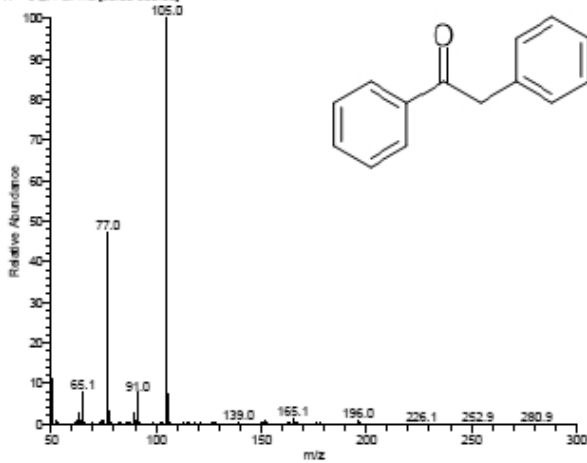


RT: 7.00 - 9.30

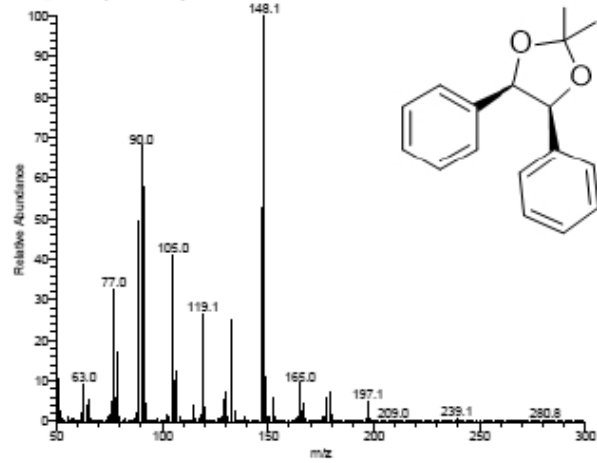


NL:
1.94E9
TIC MS
GT713

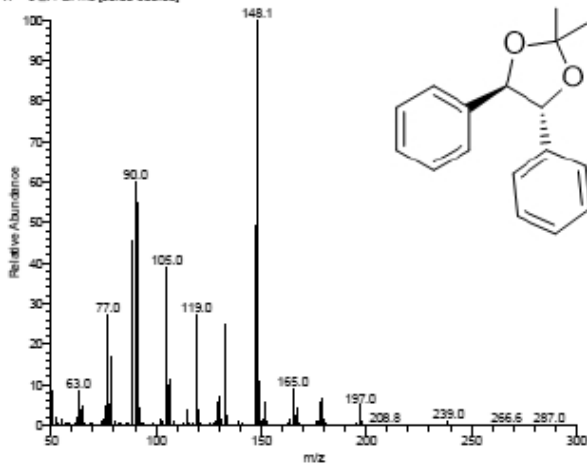
g713 #1315 RT: 7.47 AV: 1 NL: 2.61E8
T: + c EI Full ms [50.00-500.00]



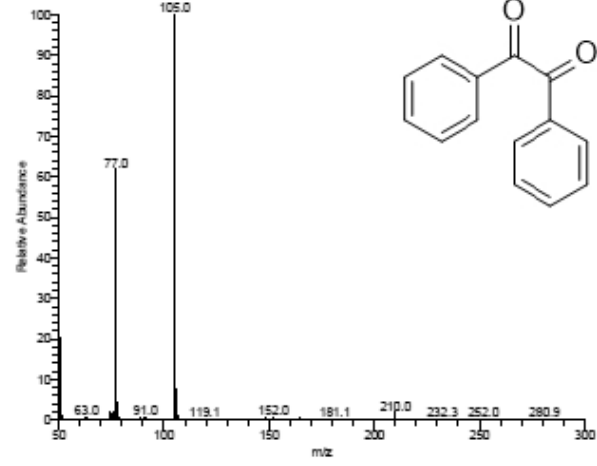
g713 #1430 RT: 7.96 AV: 1 NL: 1.76E8
T: + c EI Full ms [50.00-500.00]



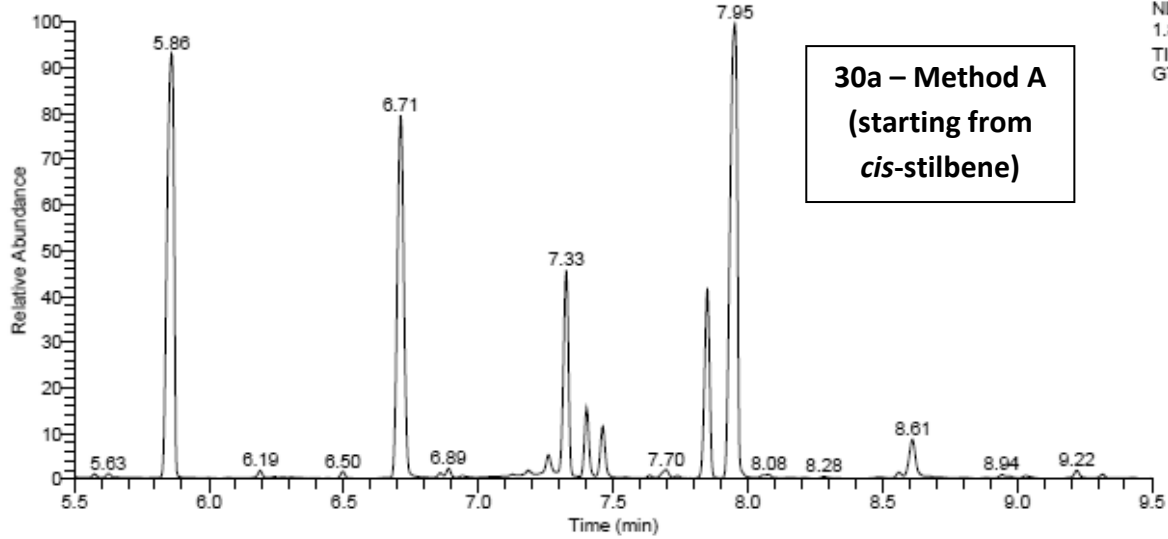
g713 #1459 RT: 7.96 AV: 1 NL: 3.12E8
T: + c EI Full ms [50.00-500.00]



g713 #1497 RT: 8.09 AV: 1 NL: 1.39E8
T: + c EI Full ms [50.00-500.00]

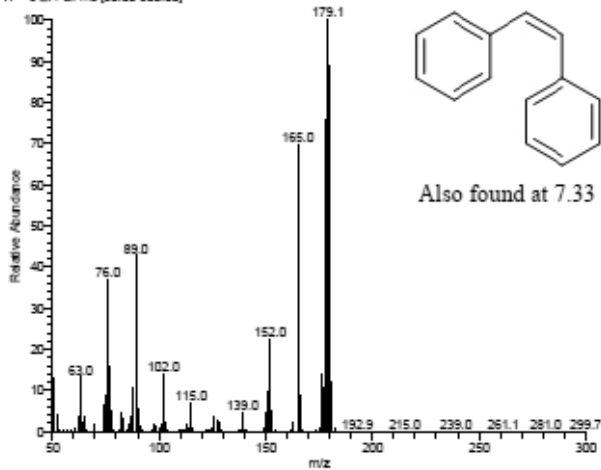


RT: 5.50 - 9.50

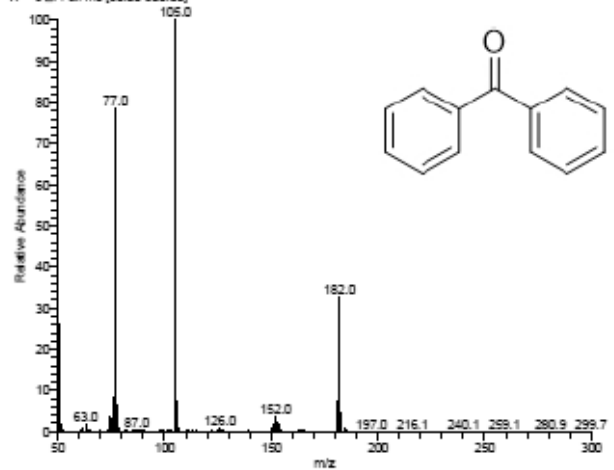


NL:
1.84E9
TIC MS
GT717

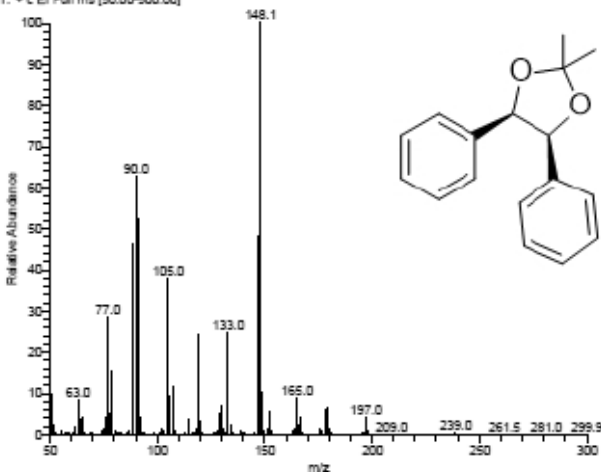
GT717#842 RT: 5.86 AV: 1 NL: 2.54E8
T: + c EI Full ms [50.00-500.00]



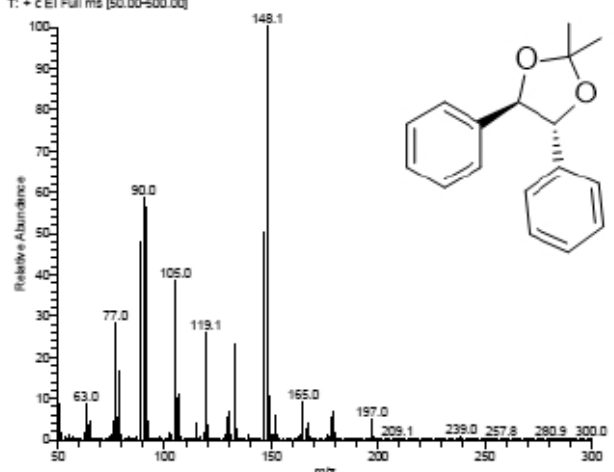
g717#1092 RT: 6.71 AV: 1 NL: 4.71E8
T: + c EI Full ms [50.00-500.00]



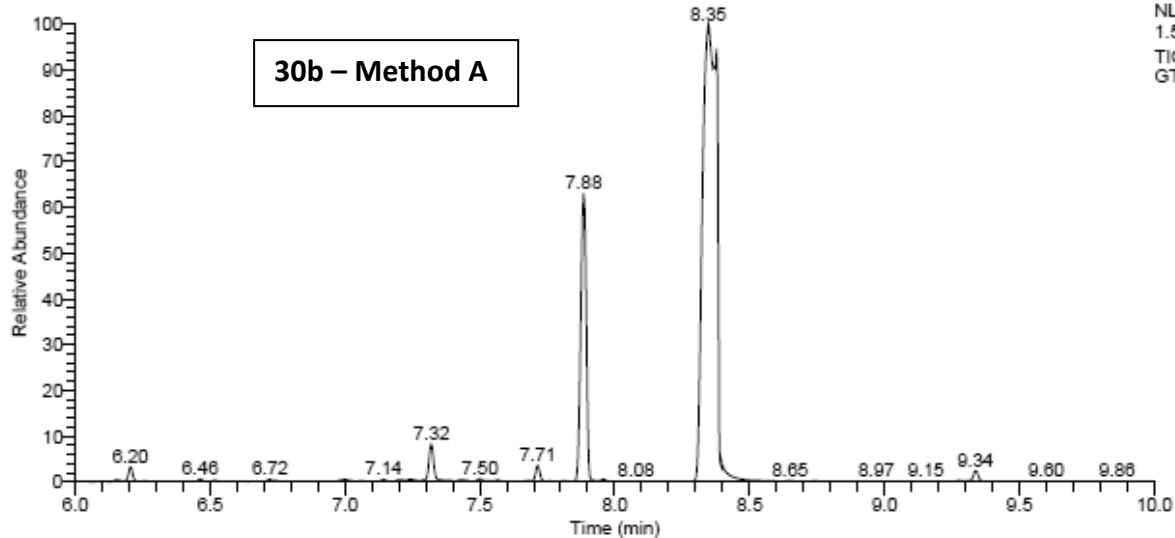
g717#1427 RT: 7.85 AV: 1 NL: 1.28E8
T: + c EI Full ms [50.00-500.00]



g717#1456 RT: 7.95 AV: 1 NL: 2.93E8
T: + c EI Full ms [50.00-500.00]

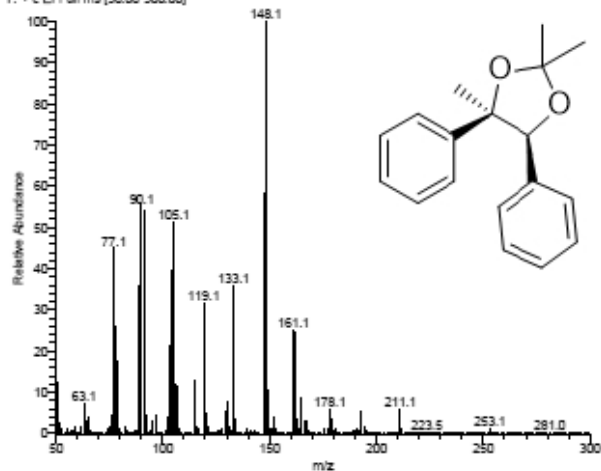


RT: 8.00 - 10.00

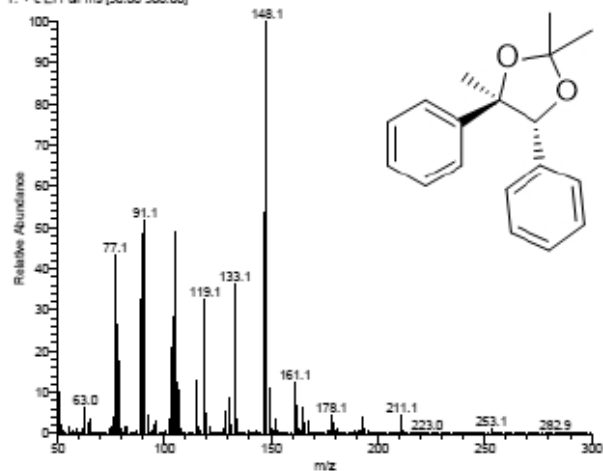


NL:
1.55E9
TIC MS
GT720

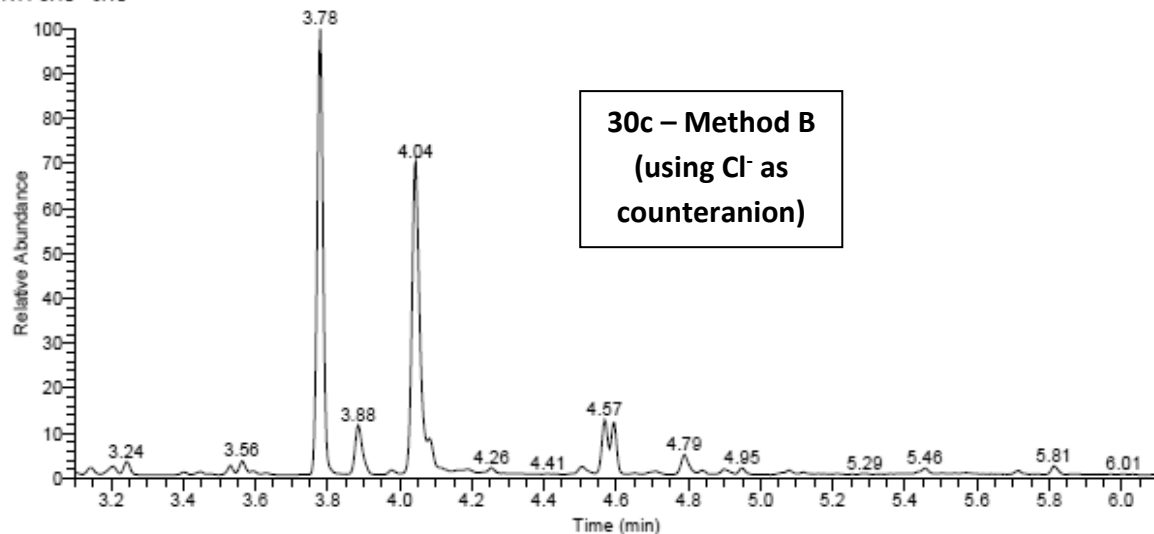
gt720#1436 RT: 7.88 AU: 1 NL: 1.08E8
T: + c EI Full ms [50.00-500.00]



gt720#1574 RT: 8.35 AU: 1 NL: 2.07E8
T: + c EI Full ms [50.00-500.00]

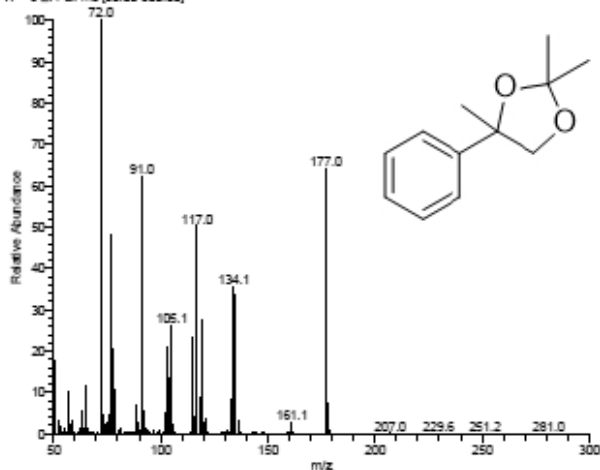


RT: 3.10 - 6.10

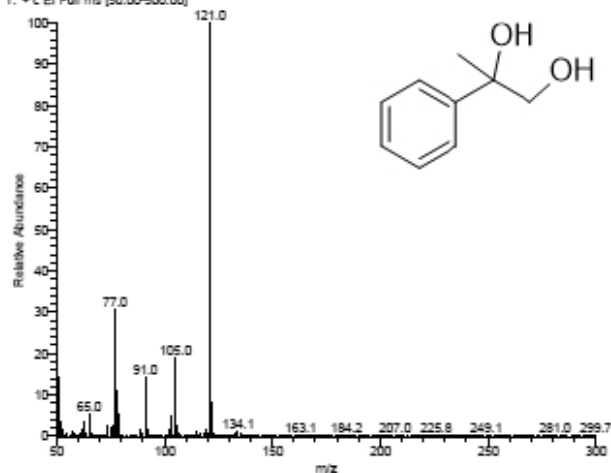


NL:
1.11E8
TIC MS
IM51(nome
file im50tris)

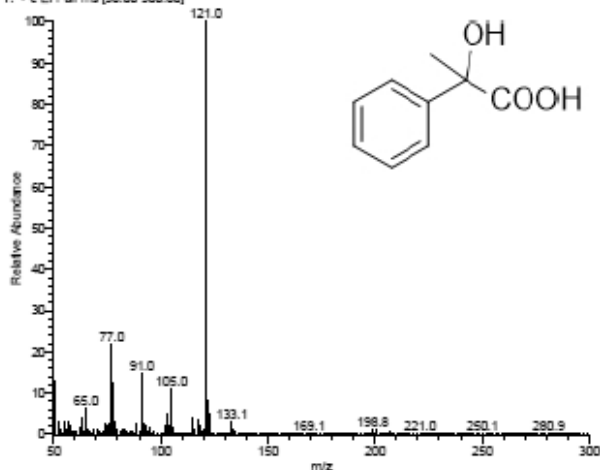
Im51(nome file im50tris) #230 RT: 3.78 AV: 1 NL: 1.59E7
T: + c EI Full ms [50.00-500.00]



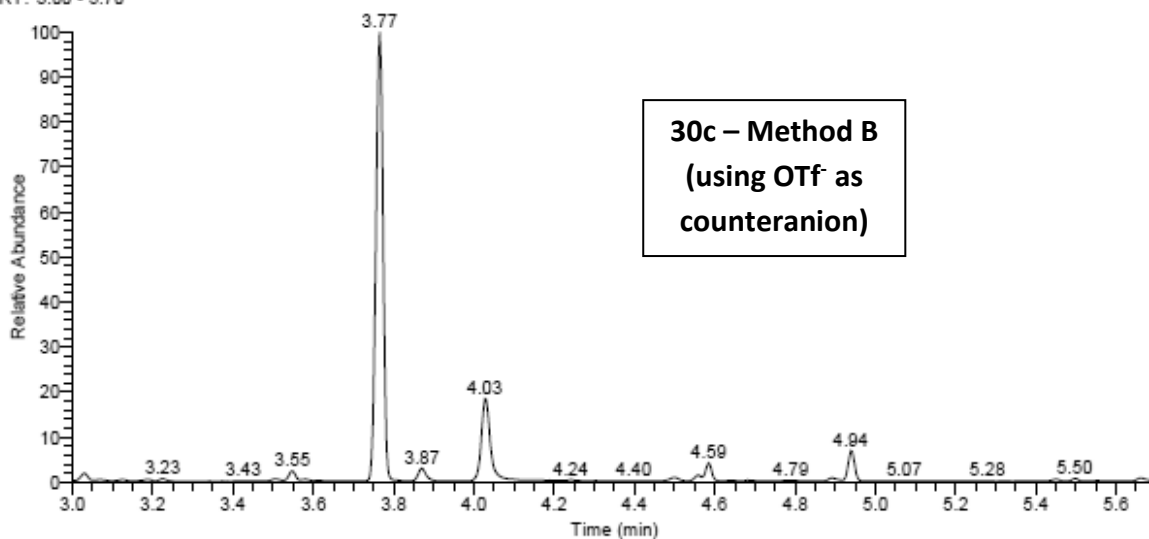
Im51(nome file im50tris) #307 RT: 4.04 AV: 1 NL: 2.95E7
T: + c EI Full ms [50.00-500.00]



Im51(nome file im50tris) #462 RT: 4.57 AV: 1 NL: 5.02E6
T: + c EI Full ms [50.00-500.00]

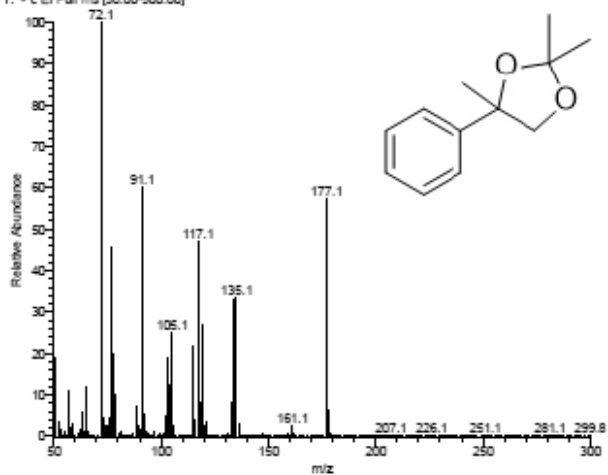


RT: 3.00 - 5.70

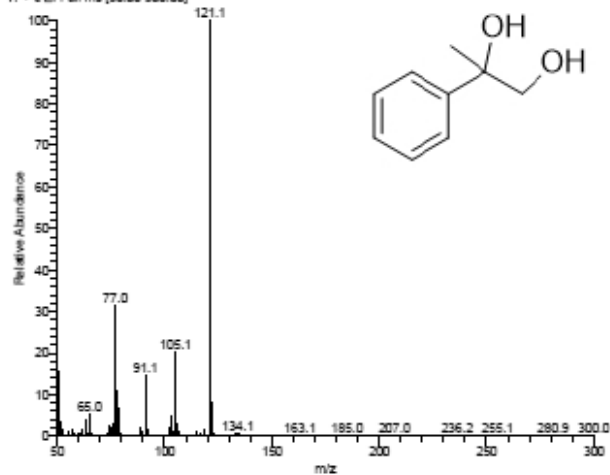


NL:
4.29E8
TIC MS
GT738

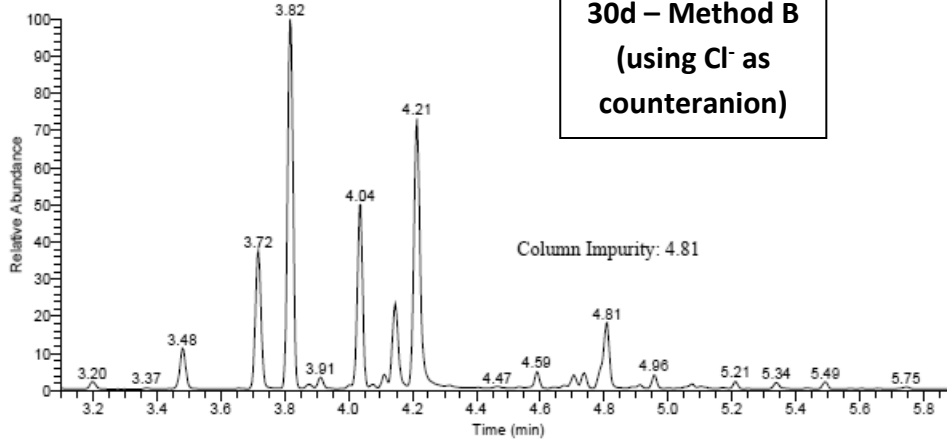
gt738 #227 RT: 3.77 AV: 1 NL: 5.81E7
T: + c EI Full ms (50.00-500.00)



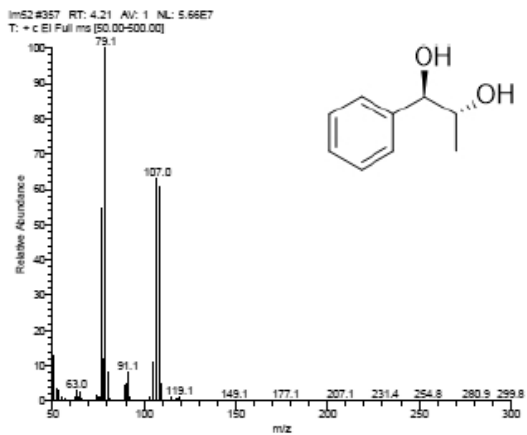
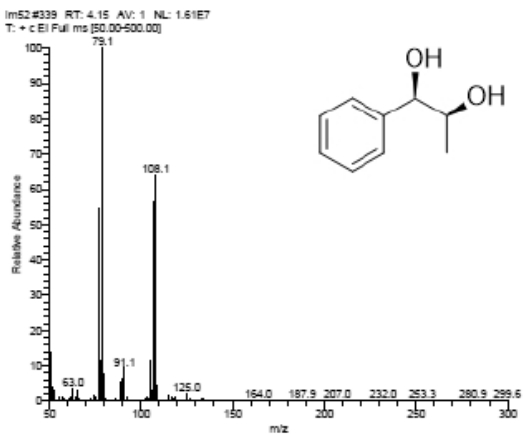
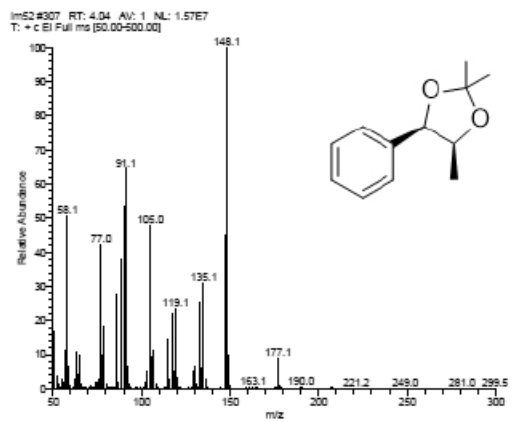
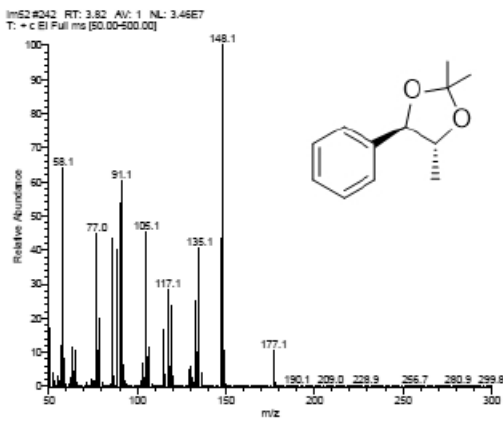
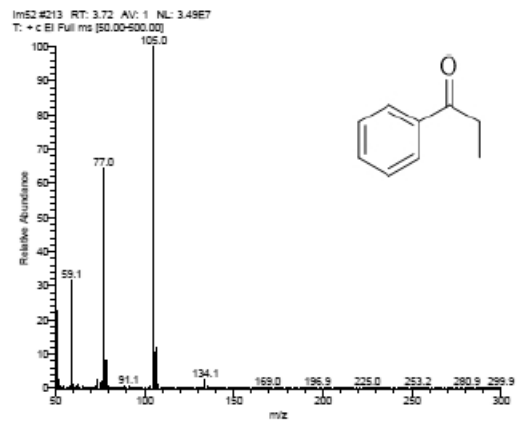
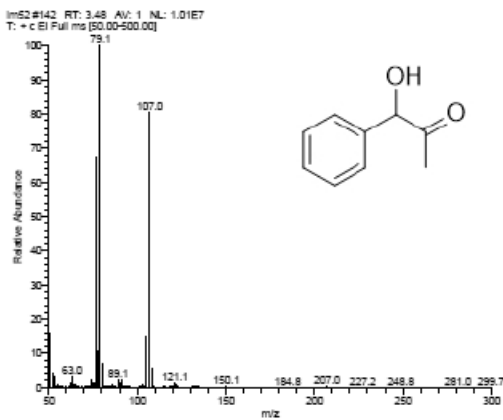
gt738 #304 RT: 4.03 AV: 1 NL: 2.92E7
T: + c EI Full ms (50.00-500.00)



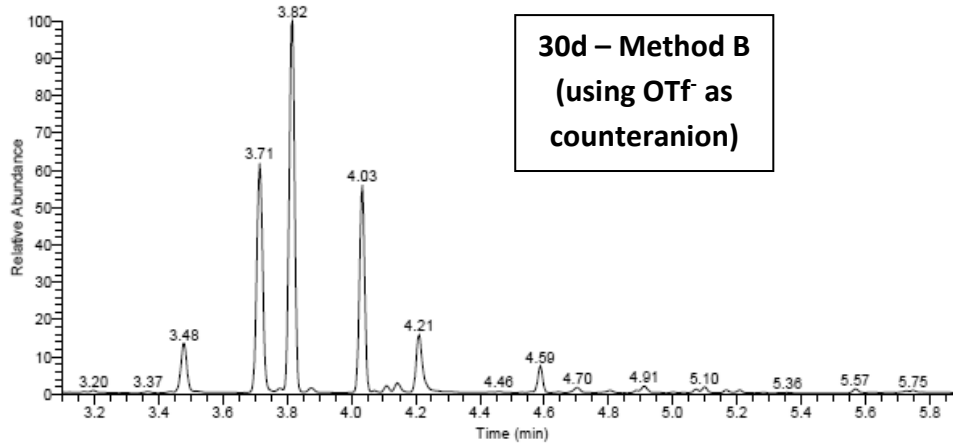
RT: 3.10 - 5.90



NL:
3.06E8
TIC MS
IM52



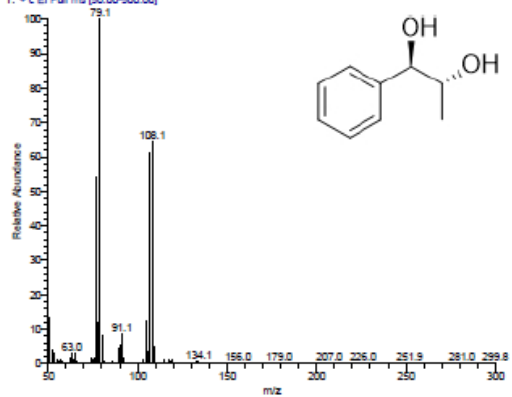
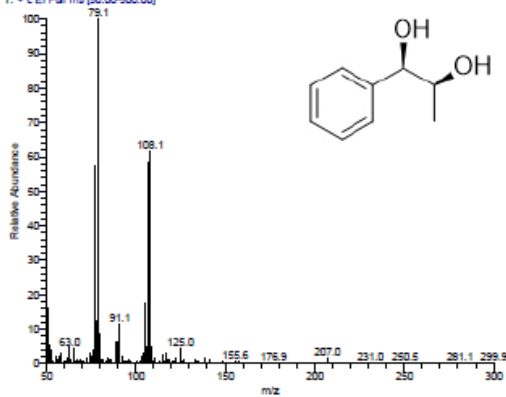
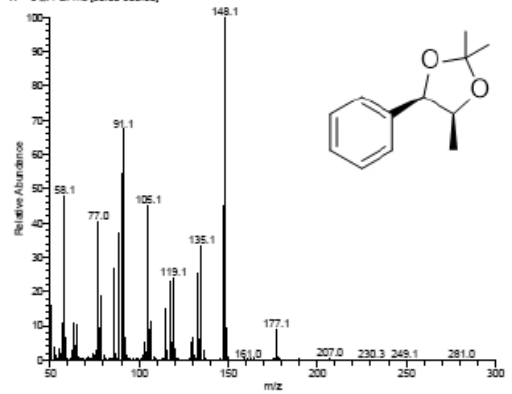
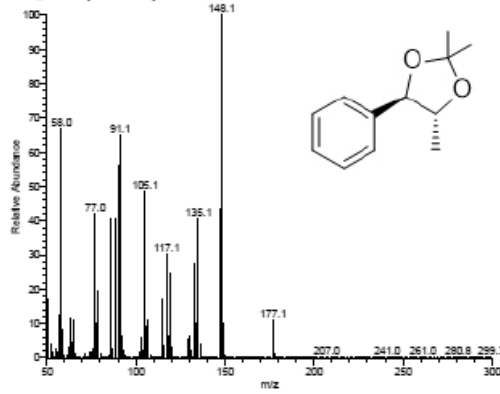
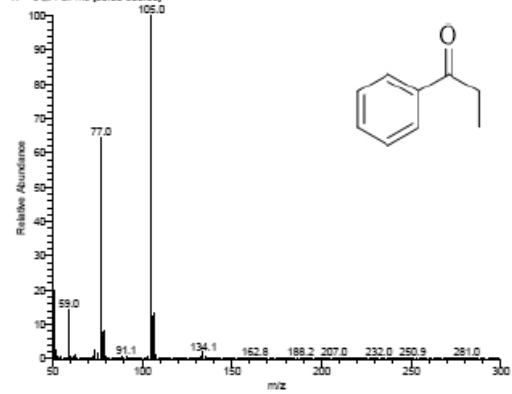
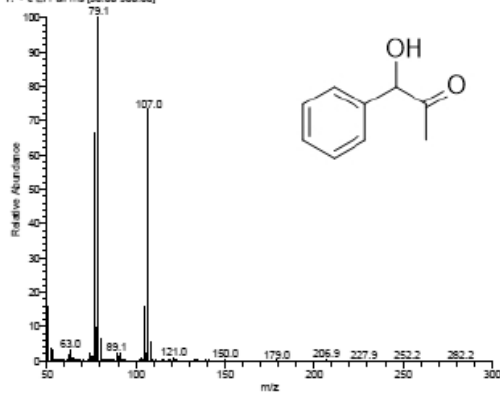
RT: 3.10 - 5.90



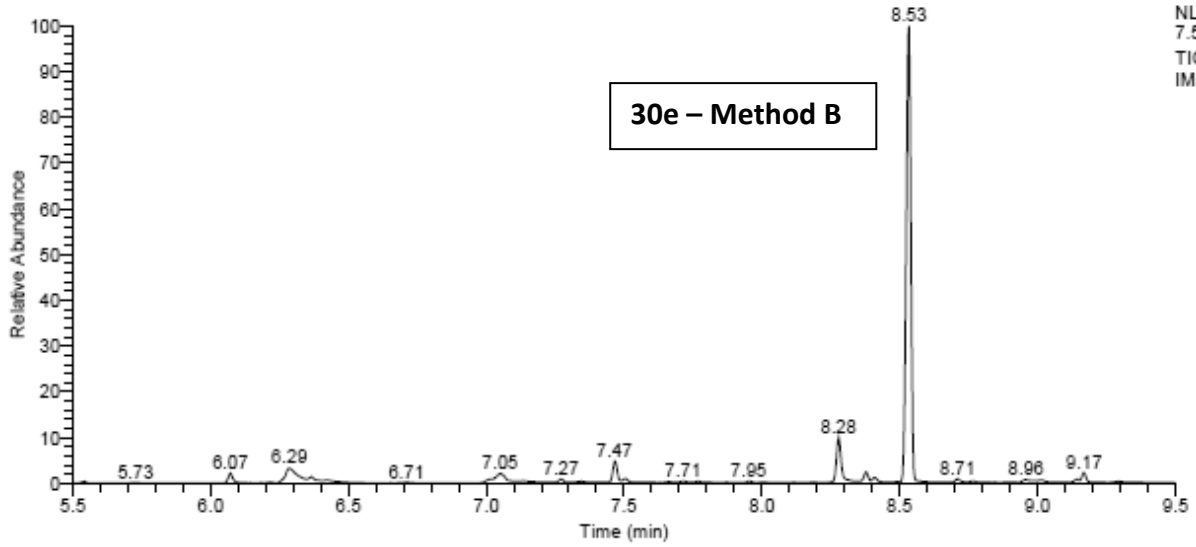
**30d – Method B
(using OTf as
counteranion)**

NL:
4.18E8
TIC MS
IM54

ImS4 #142 RT: 3.48 AV: 1 NL: 1.70E7
T: + c EI Full ms [50.00-500.00]

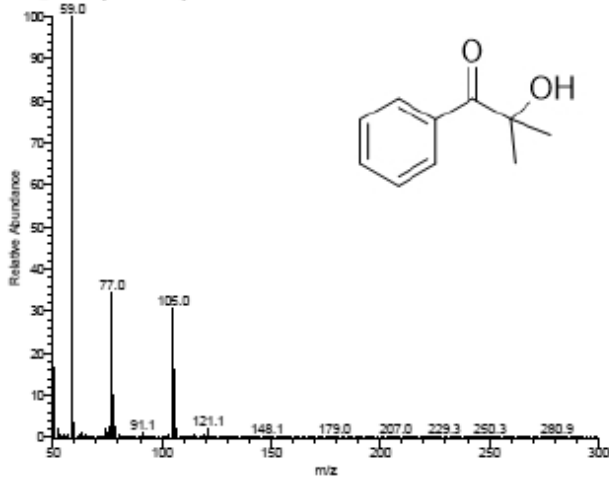


RT: 5.50 - 9.50

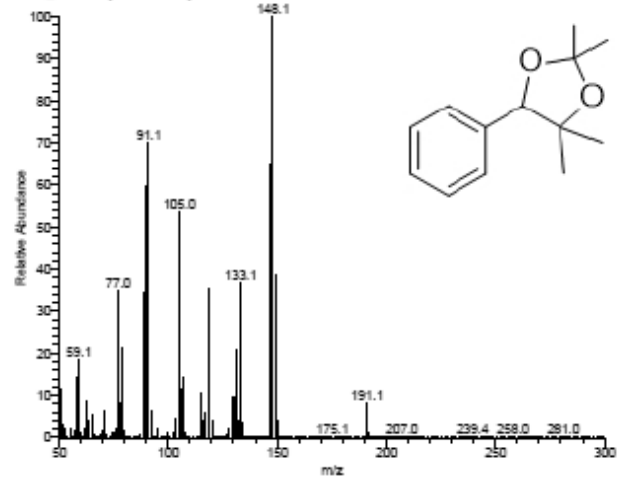


NL:
7.51E8
TIC MS
IM56

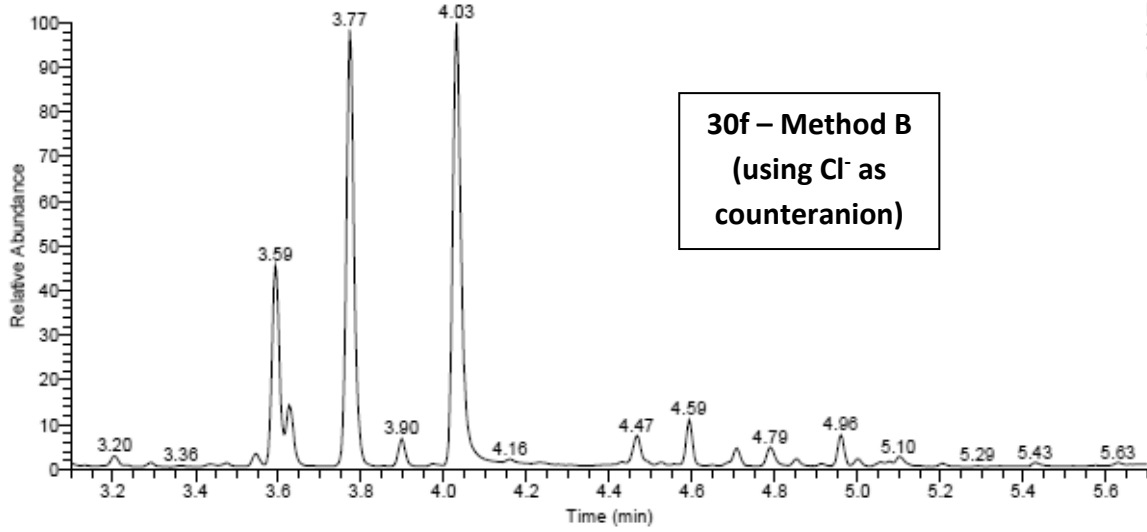
Im56 #1553 RT: 8.28 AV: 1 NL: 3.12E7
T: + c EI Full ms [50.00-500.00]



Im56 #1627 RT: 8.53 AV: 1 NL: 9.38E7
T: + c EI Full ms [50.00-500.00]

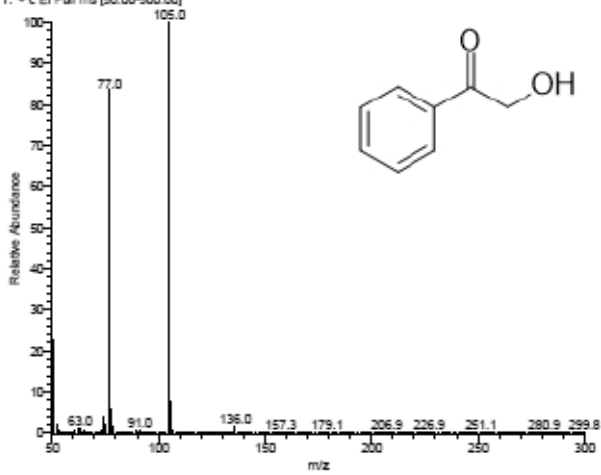


RT: 3.10 - 5.70

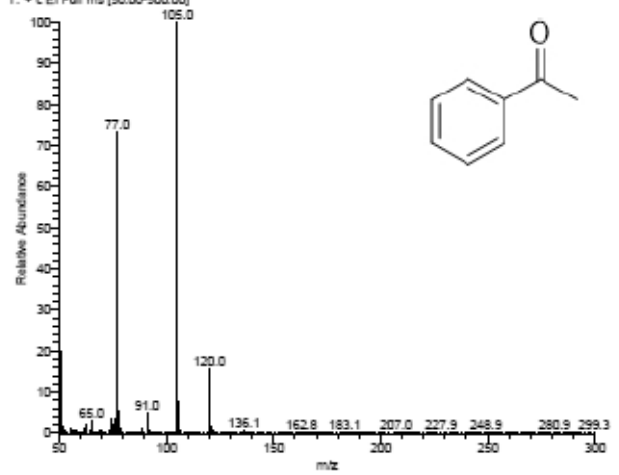


NL:
2.01E8
TIC MS
CF129

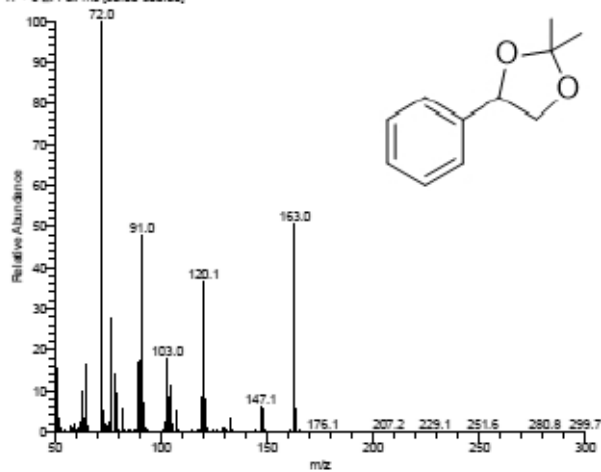
d129#174 RT: 3.59 AV: 1 NL: 3.29E7
T: + c EI Full ms [50.00-500.00]



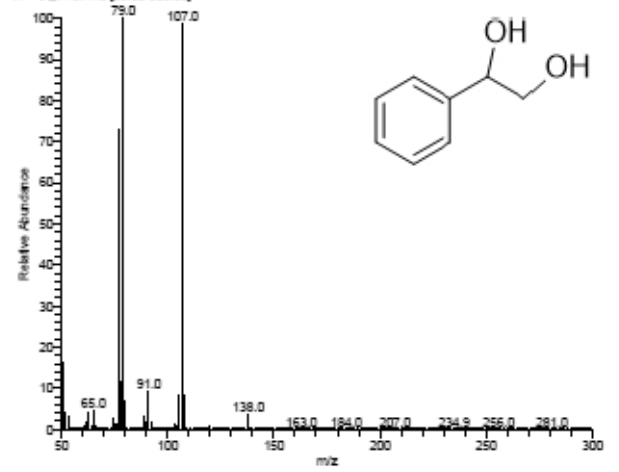
d129#183 RT: 3.62 AV: 1 NL: 7.64E6
T: + c EI Full ms [50.00-500.00]



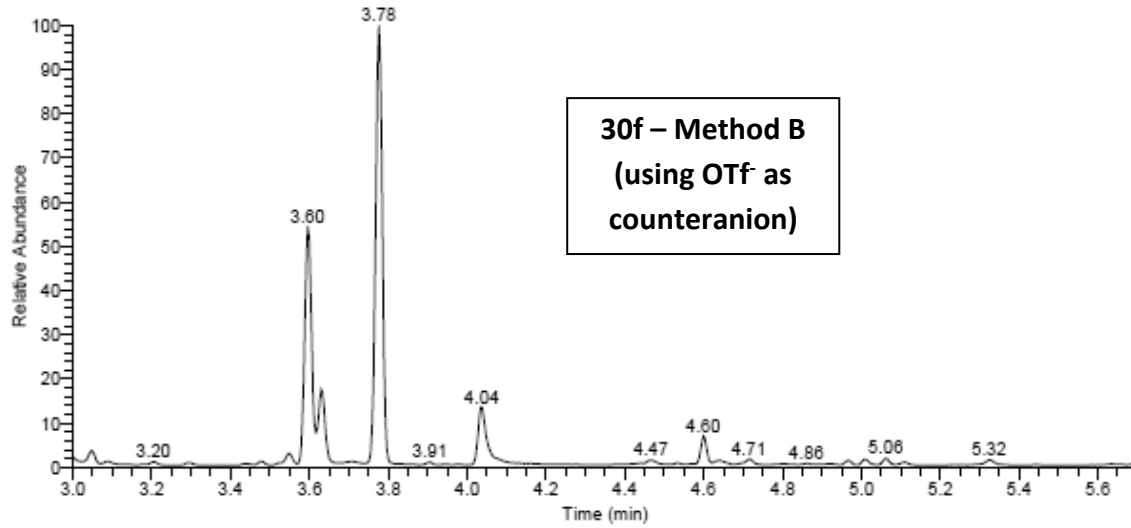
d129#227 RT: 3.77 AV: 1 NL: 3.47E7
T: + c EI Full ms [50.00-500.00]



d129#304 RT: 4.03 AV: 1 NL: 5.29E7
T: + c EI Full ms [50.00-500.00]

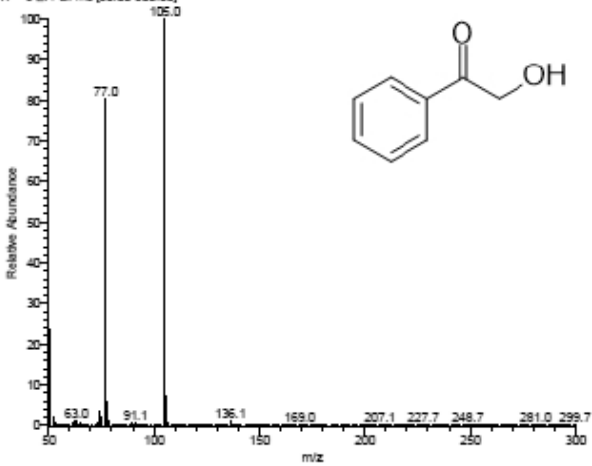


RT: 3.00 - 5.70

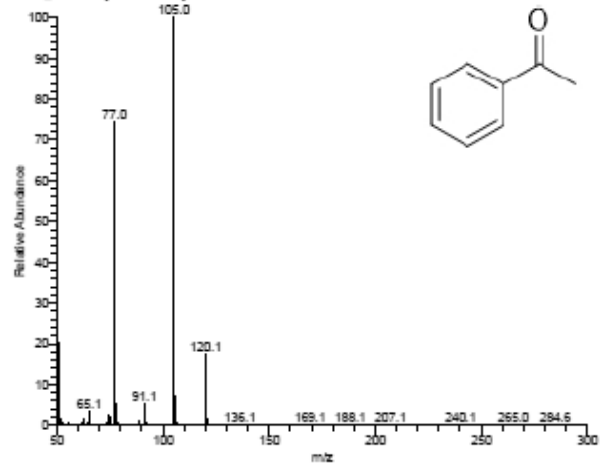


NL:
1.95E8
TIC MS
GT737

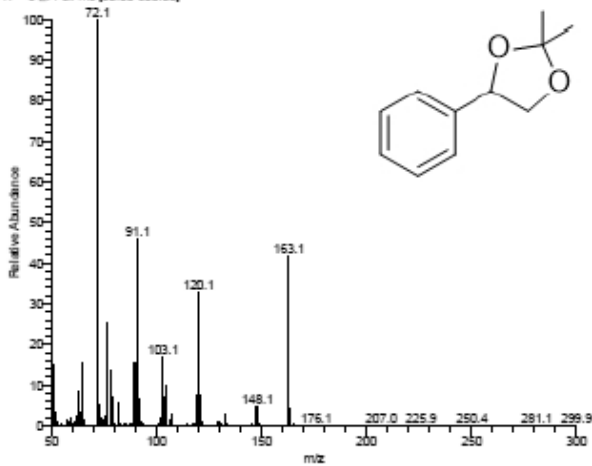
g737 #177 RT: 3.60 AV: 1 NL: 4.18E7
T: + c EI Full ms [50.00-500.00]



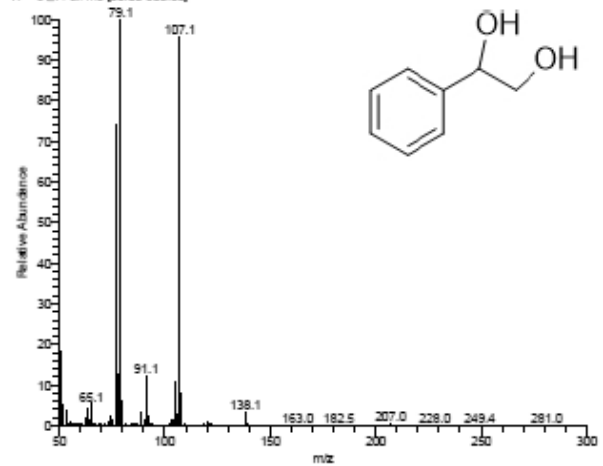
g737 #186 RT: 3.63 AV: 1 NL: 1.33E7
T: + c EI Full ms [50.00-500.00]



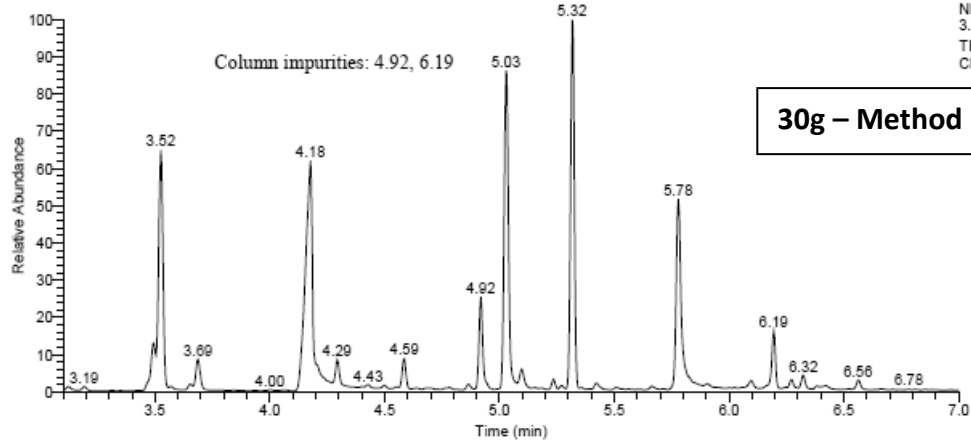
g737 #230 RT: 3.78 AV: 1 NL: 3.94E7
T: + c EI Full ms [50.00-500.00]



g737 #307 RT: 4.04 AV: 1 NL: 5.78E6
T: + c EI Full ms [50.00-500.00]

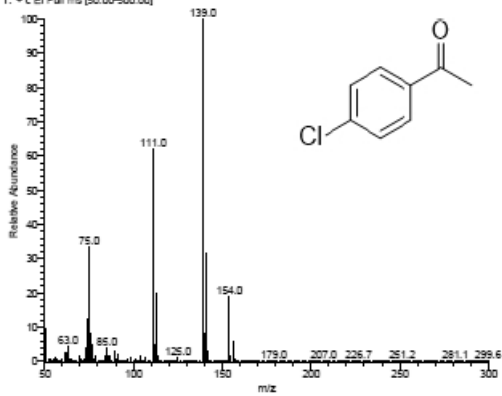


RT: 3.10 - 7.00

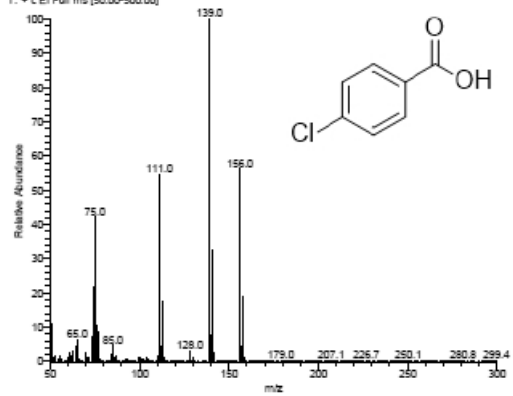


NL:
3.36E8
TIC MS
CF137

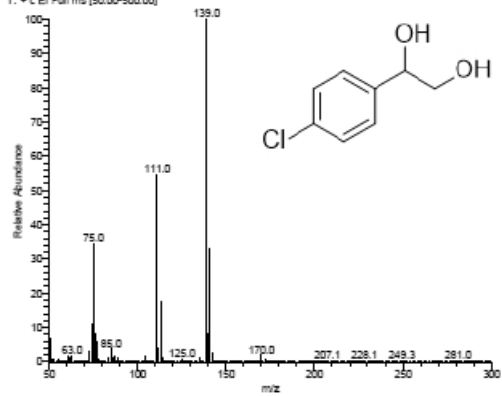
cf137#154 RT: 3.52 AV: 1 NL: 5.23E7
T: + c EI Full ms [50.00-500.00]



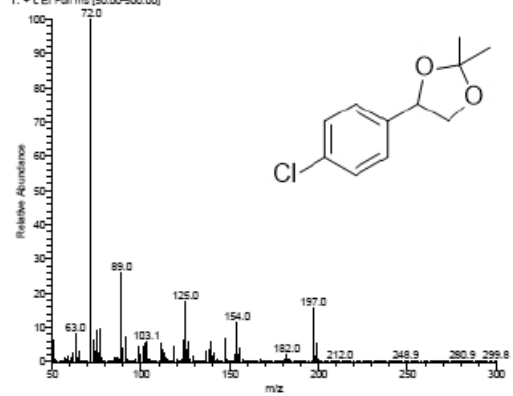
cf137#348 RT: 4.18 AV: 1 NL: 3.95E7
T: + c EI Full ms [50.00-500.00]



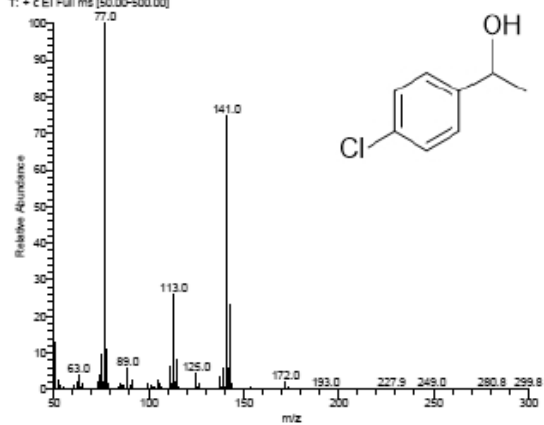
cf137#596 RT: 5.03 AV: 1 NL: 8.78E7
T: + c EI Full ms [50.00-500.00]



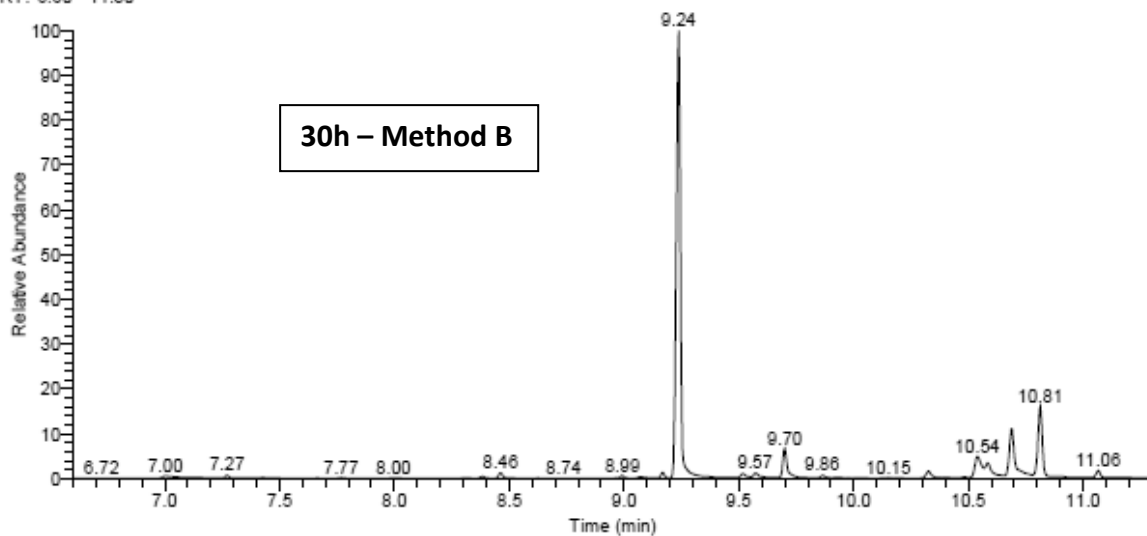
cf137#683 RT: 5.32 AV: 1 NL: 9.17E7
T: + c EI Full ms [50.00-500.00]



cf137#818 RT: 5.78 AV: 1 NL: 4.85E7
T: + c EI Full ms [50.00-500.00]

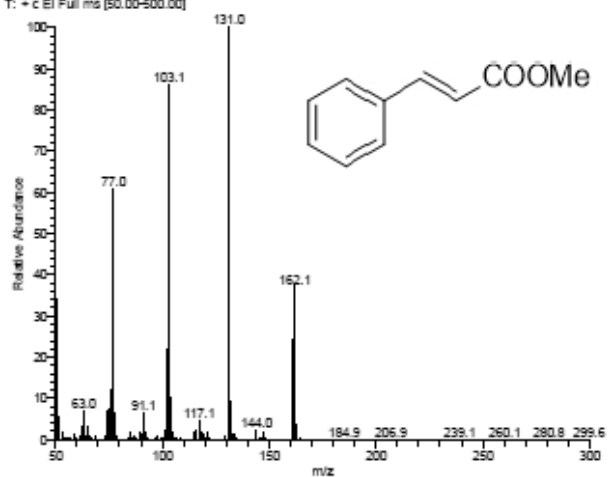


RT: 6.60 - 11.30

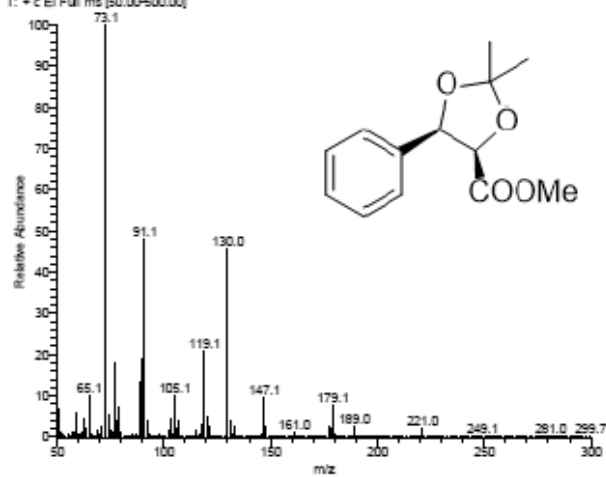


NL:
9.34E8
TIC MS
IM58

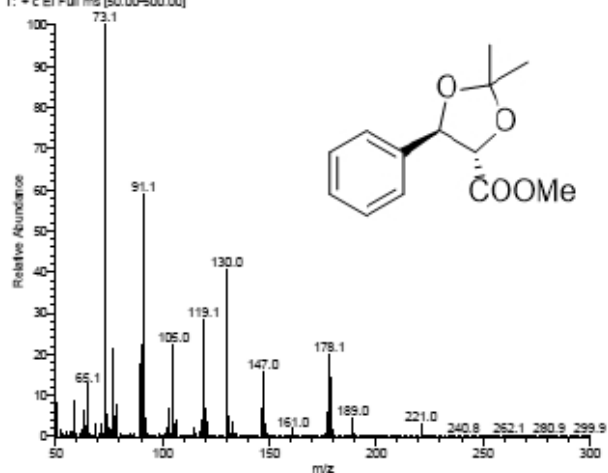
Im58 #1836 RT: 9.24 AV: 1 NL: 1.68E8
T: + c EI Full ms [50.00-500.00]



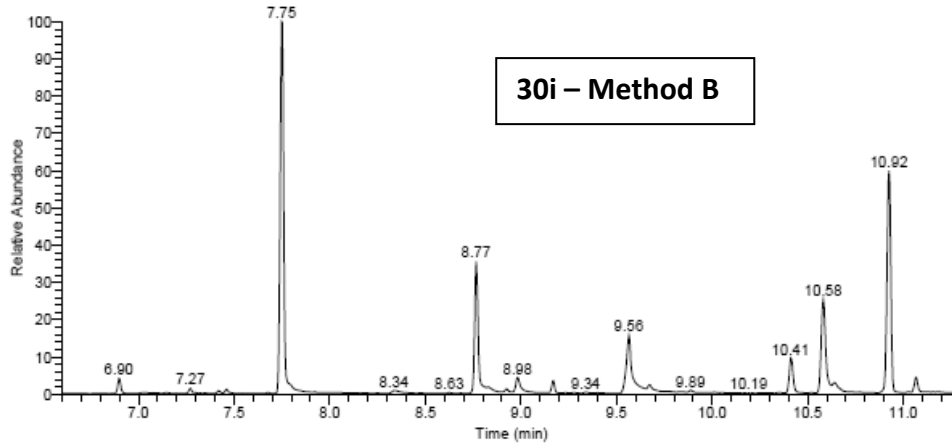
Im58 #2262 RT: 10.69 AV: 1 NL: 2.50E7
T: + c EI Full ms [50.00-500.00]



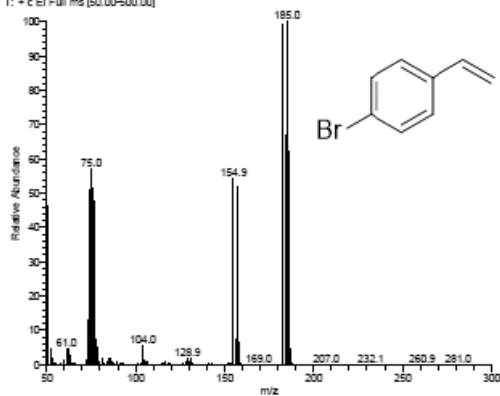
Im58 #2297 RT: 10.81 AV: 1 NL: 2.69E7
T: + c EI Full ms [50.00-500.00]



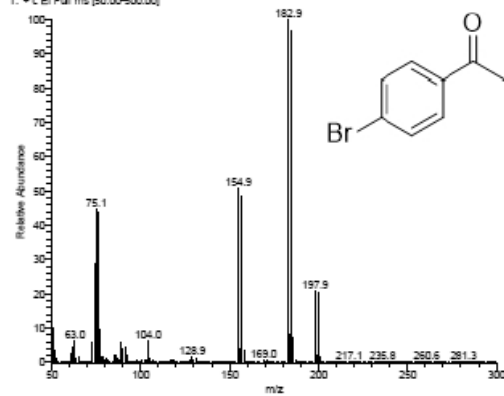
RT: 6.60 - 11.30



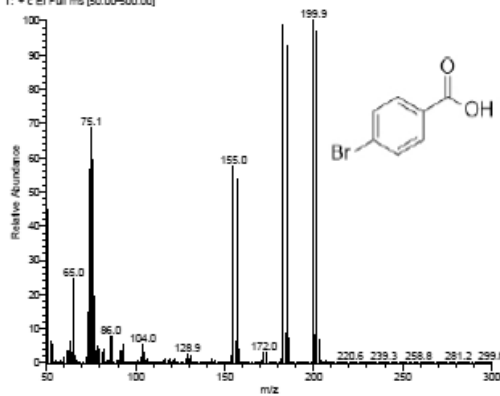
Im57 #1397 RT: 7.75 AV: 1 NL: 5.57E7
T: + c EI Full ms [50.00-500.00]



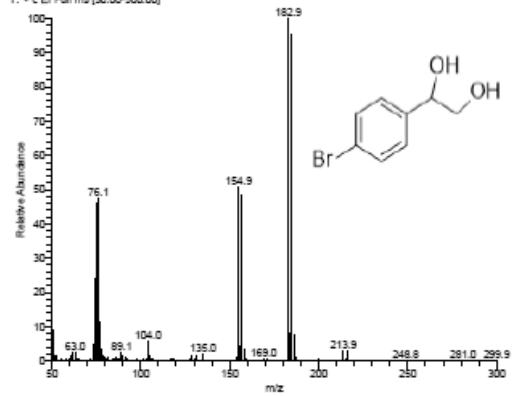
Im57 #1697 RT: 8.77 AV: 1 NL: 2.58E7
T: + c EI Full ms [50.00-500.00]



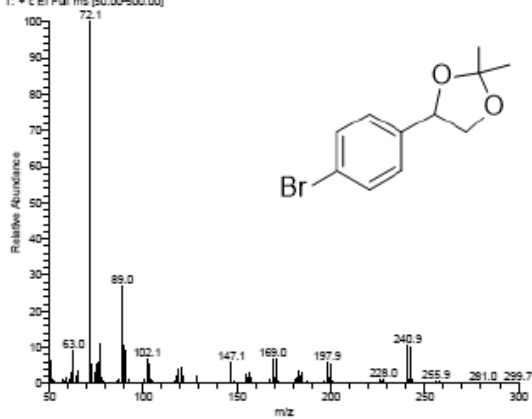
Im57 #1930 RT: 9.56 AV: 1 NL: 6.84E6
T: + c EI Full ms [50.00-500.00]



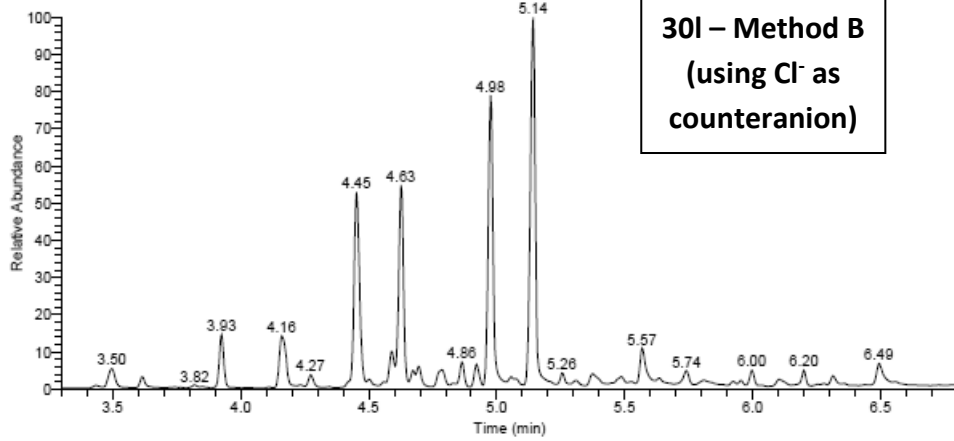
Im57 #2230 RT: 10.58 AV: 1 NL: 2.17E7
T: + c EI Full ms [50.00-500.00]



Im57 #2330 RT: 10.92 AV: 1 NL: 7.78E7
T: + c EI Full ms [50.00-500.00]

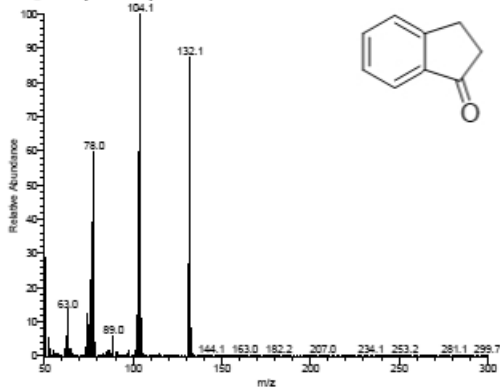


RT: 3.30 - 6.80

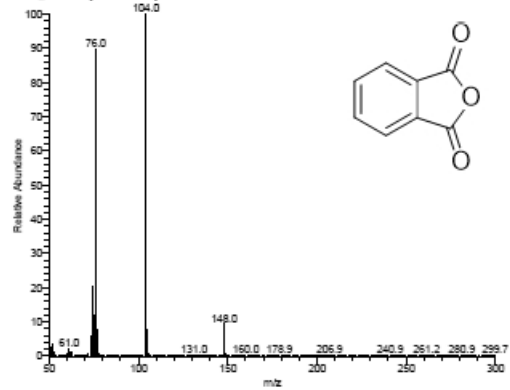


NL:
3.79E8
TIC MS
IM48_17070
6131125

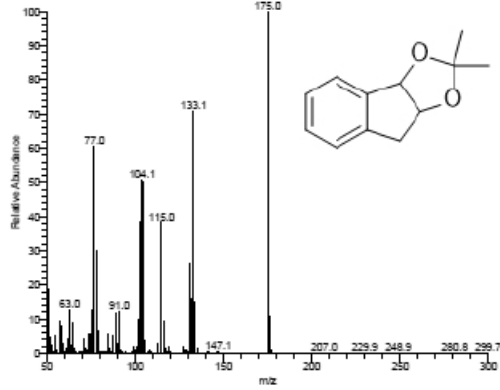
IM48_170706131125#274 RT: 3.93 AV: 1 NL: 8.81E5
T: + c EI Full ms [50.00-500.00]



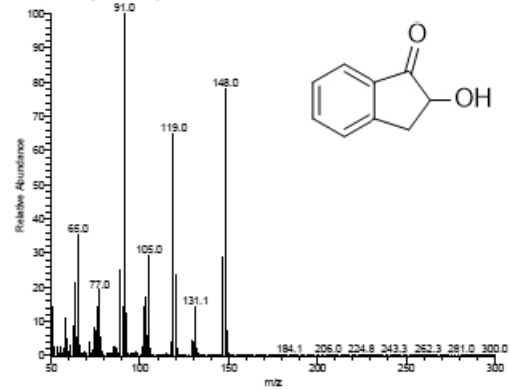
IM48_170706131125#342 RT: 4.16 AV: 1 NL: 1.85E7
T: + c EI Full ms [50.00-500.00]



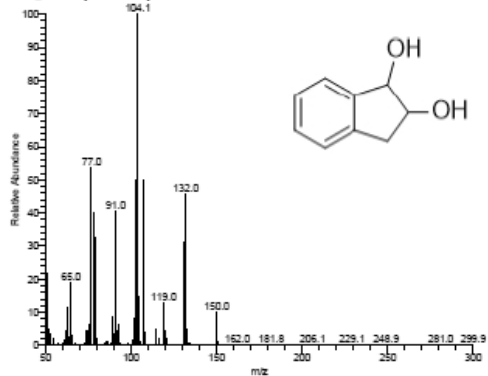
IM48_170706131125#427 RT: 4.45 AV: 1 NL: 2.62E7
T: + c EI Full ms [50.00-500.00]



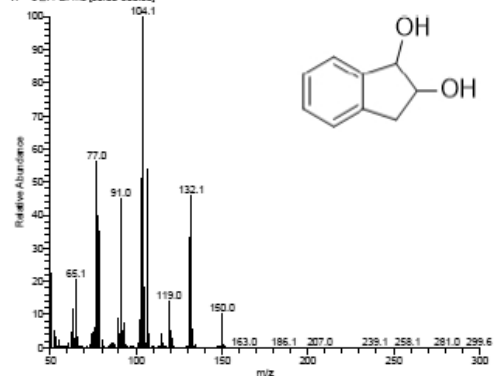
IM48_170706131125#480 RT: 4.63 AV: 1 NL: 3.00E7
T: + c EI Full ms [50.00-500.00]



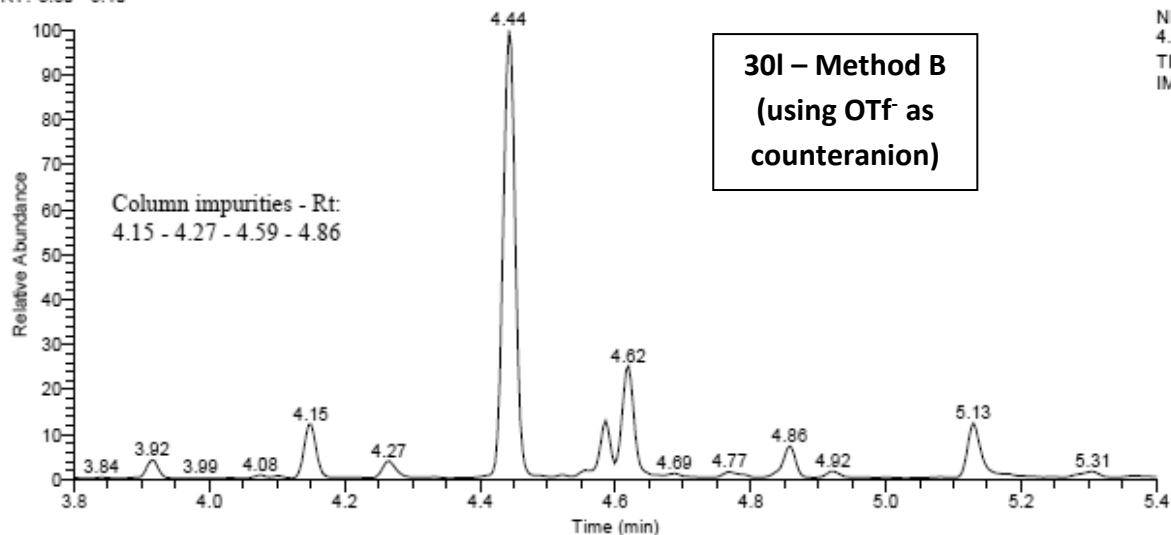
IM48_170706131125#583 RT: 4.98 AV: 1 NL: 4.40E7
T: + c EI Full ms [50.00-500.00]



IM48_170706131125#630 RT: 5.14 AV: 1 NL: 5.44E7
T: + c EI Full ms [50.00-500.00]

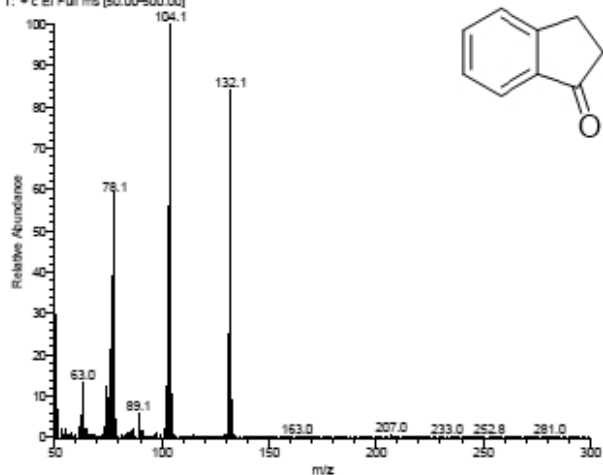


RT: 3.80 - 5.40

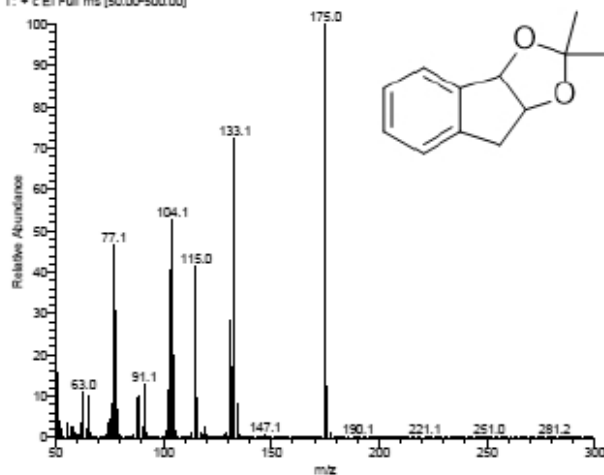


NL:
4.65E8
TIC MS
IM55

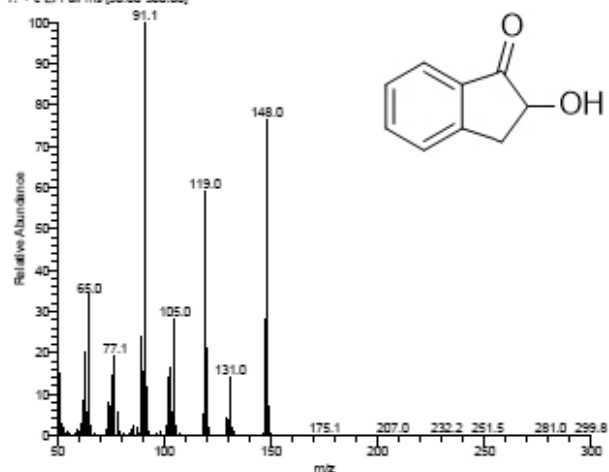
IM55 #271 RT: 3.92 AV: 1 NL: 3.40E6
T: + c EI Full ms [50.00-500.00]



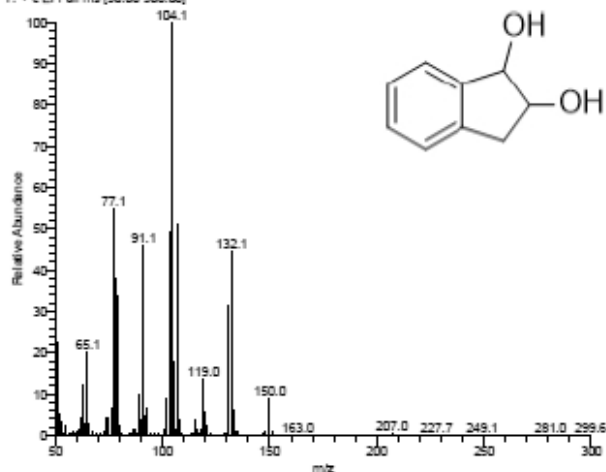
IM55 #424 RT: 4.44 AV: 1 NL: 6.59E7
T: + c EI Full ms [50.00-500.00]



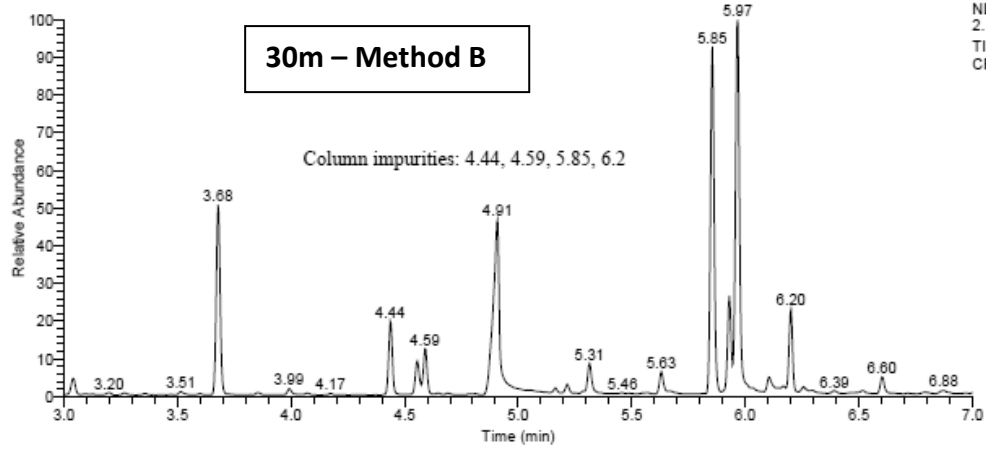
IM55 #477 RT: 4.62 AV: 1 NL: 1.90E7
T: + c EI Full ms [50.00-500.00]



IM55 #527 RT: 5.13 AV: 1 NL: 8.69E6
T: + c EI Full ms [50.00-500.00]

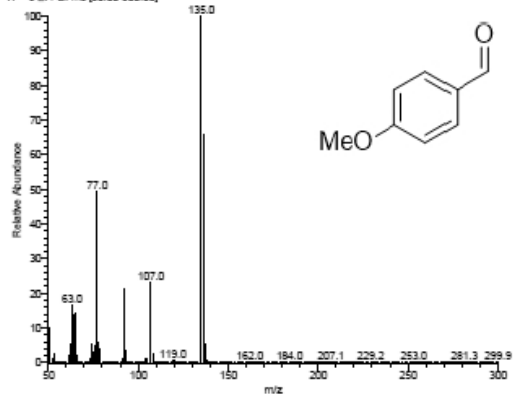


RT: 3.00 - 7.00

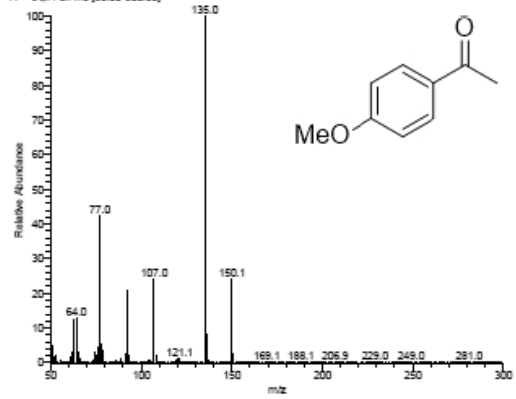


NL:
2.10E8
TIC MS
CF138

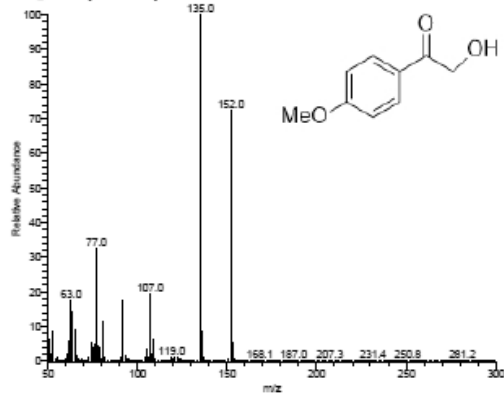
c136 #501 RT: 3.68 AV: 1 NL: 2.69E7
T: + c EI Full ms [50.00-500.00]



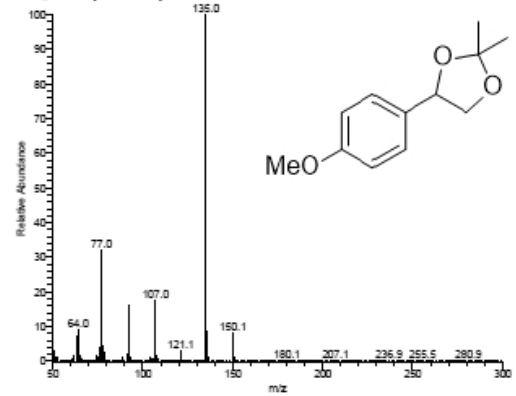
c136 #424 RT: 4.44 AV: 1 NL: 1.32E7
T: + c EI Full ms [50.00-500.00]



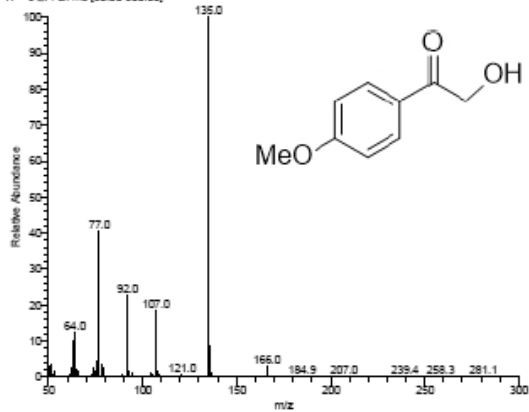
c136 #562 RT: 4.91 AV: 1 NL: 2.50E7
T: + c EI Full ms [50.00-500.00]



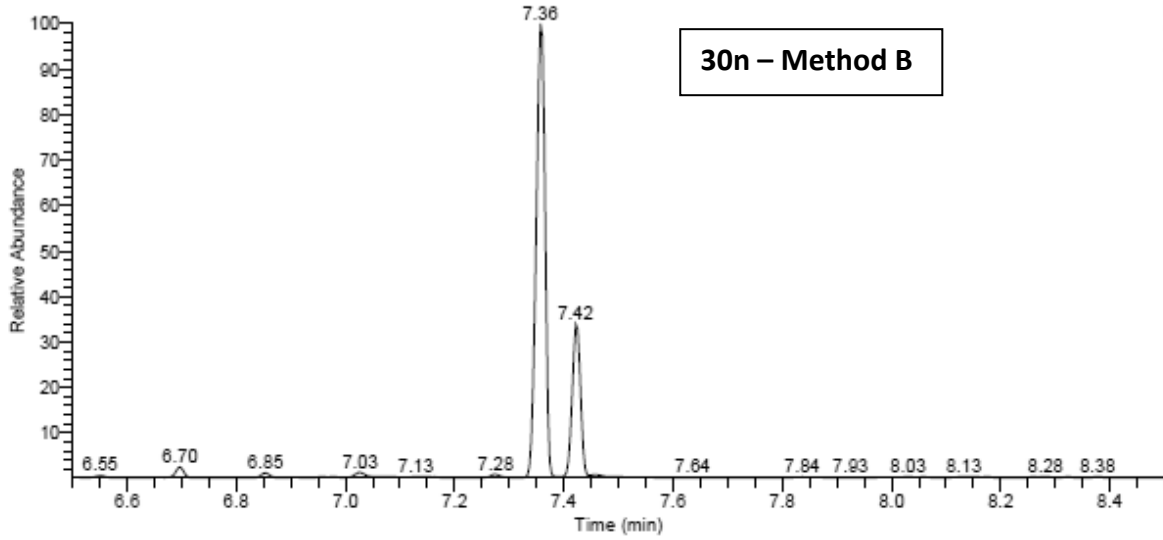
c136 #962 RT: 5.93 AV: 1 NL: 2.30E7
T: + c EI Full ms [50.00-500.00]



c136 #874 RT: 5.97 AV: 1 NL: 6.77E7
T: + c EI Full ms [50.00-500.00]

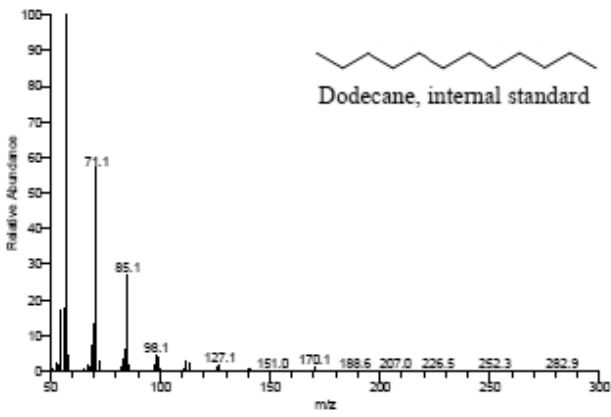


RT: 6.50 - 8.50

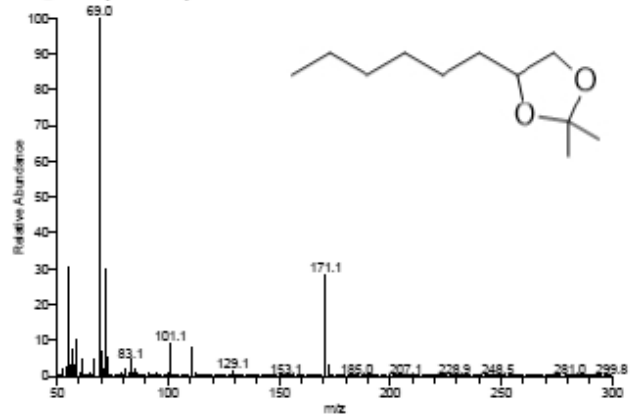


NL:
1.01E9
TIC MS
GT740BIS

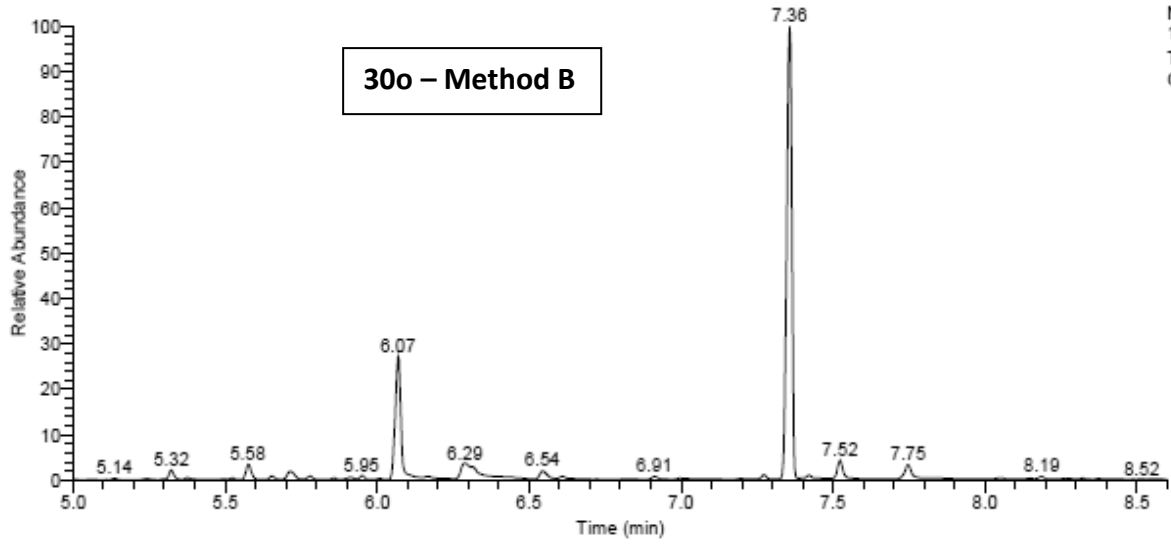
gt740bis#1283 RT: 7.36 AV: 1 NL: 3.41E8
T: + c EI Full ms [50.00-500.00]



gt740bis#1300 RT: 7.42 AV: 1 NL: 9.93E7
T: + c EI Full ms [50.00-500.00]

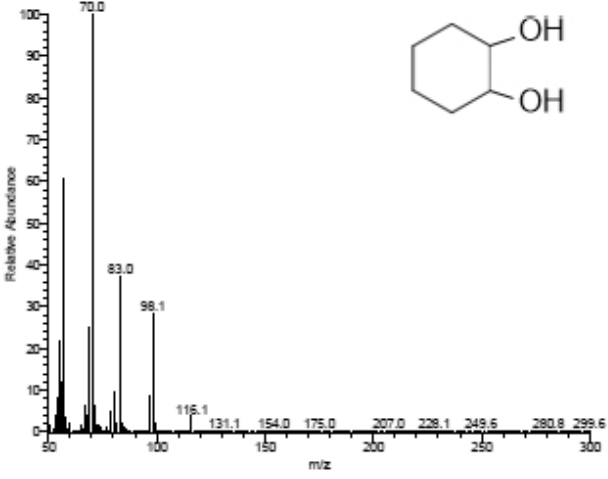


RT: 5.00 - 8.60

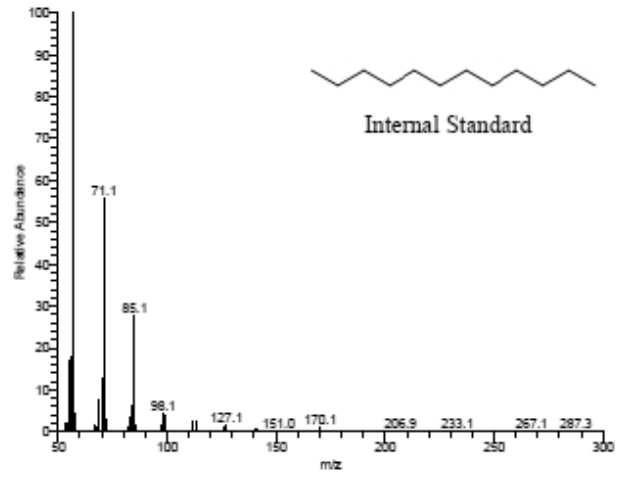


NL:
1.07E9
TIC MS
GT741BIS

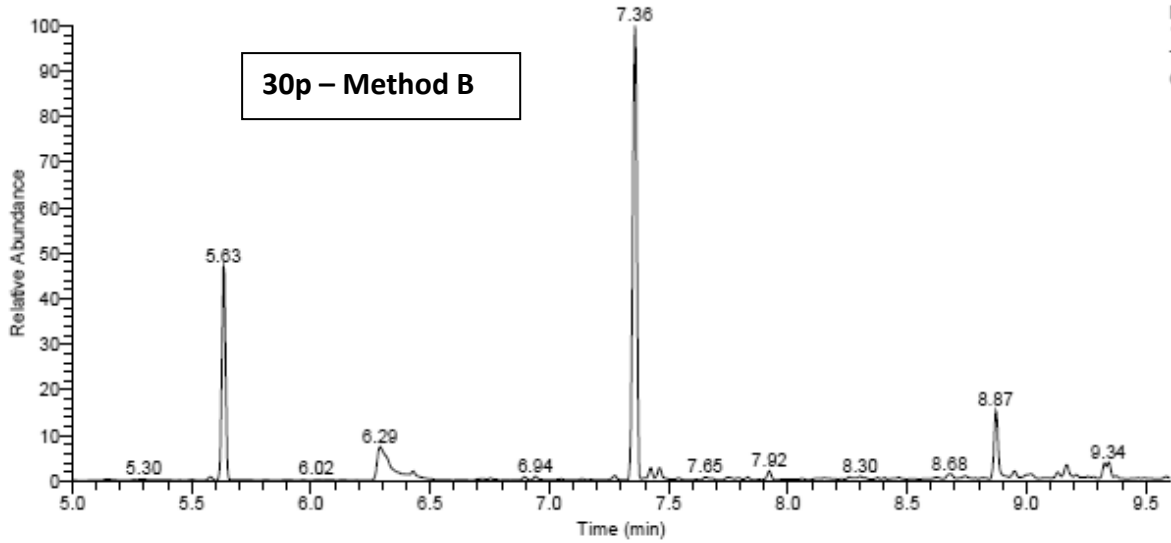
gt741bis #903 RT: 6.07 AV: 1 NL: 7.96E7
T: + c EI Full ms [50.00-500.00]



gt741bis #1283 RT: 7.36 AV: 1 NL: 3.98E8
T: + c EI Full ms [50.00-500.00]

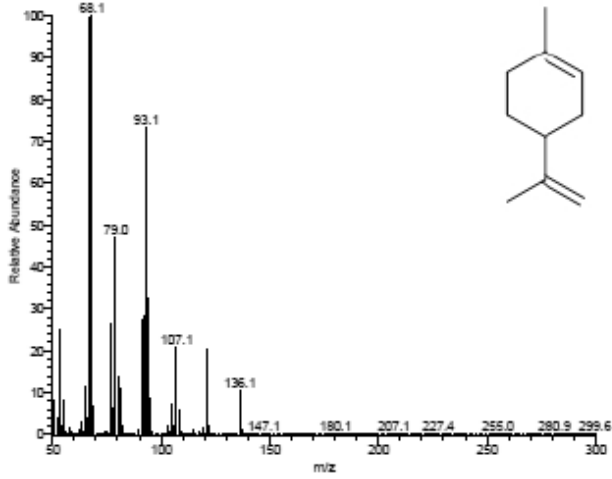


RT: 5.00 - 9.00

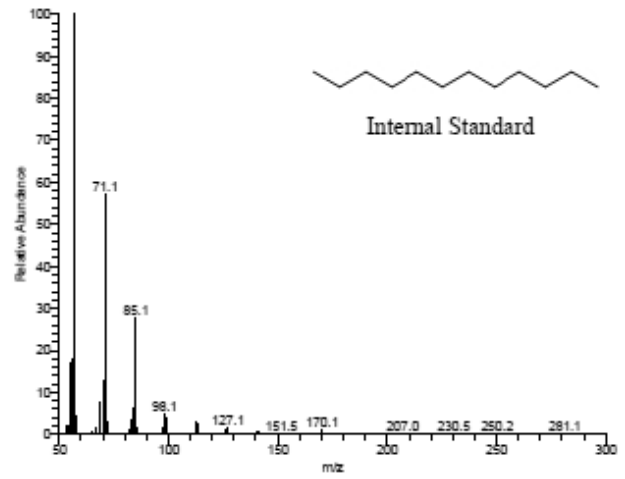


NL:
1.15E9
TIC MS
GT742BIS

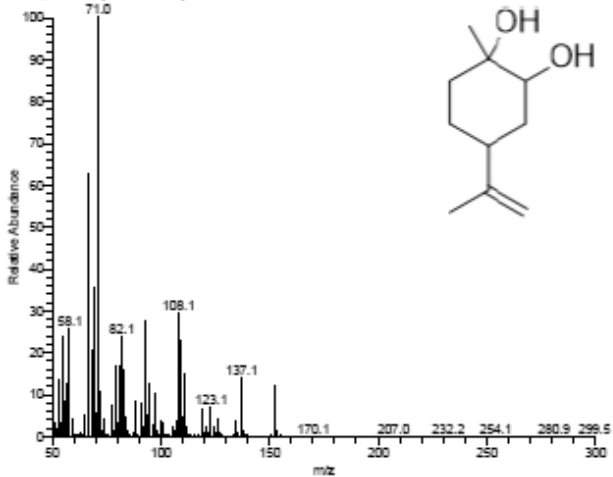
g742bis#774 RT: 5.63 AV: 1 NL: 7.09E7
T: + c EI Full ms [50.00-500.00]



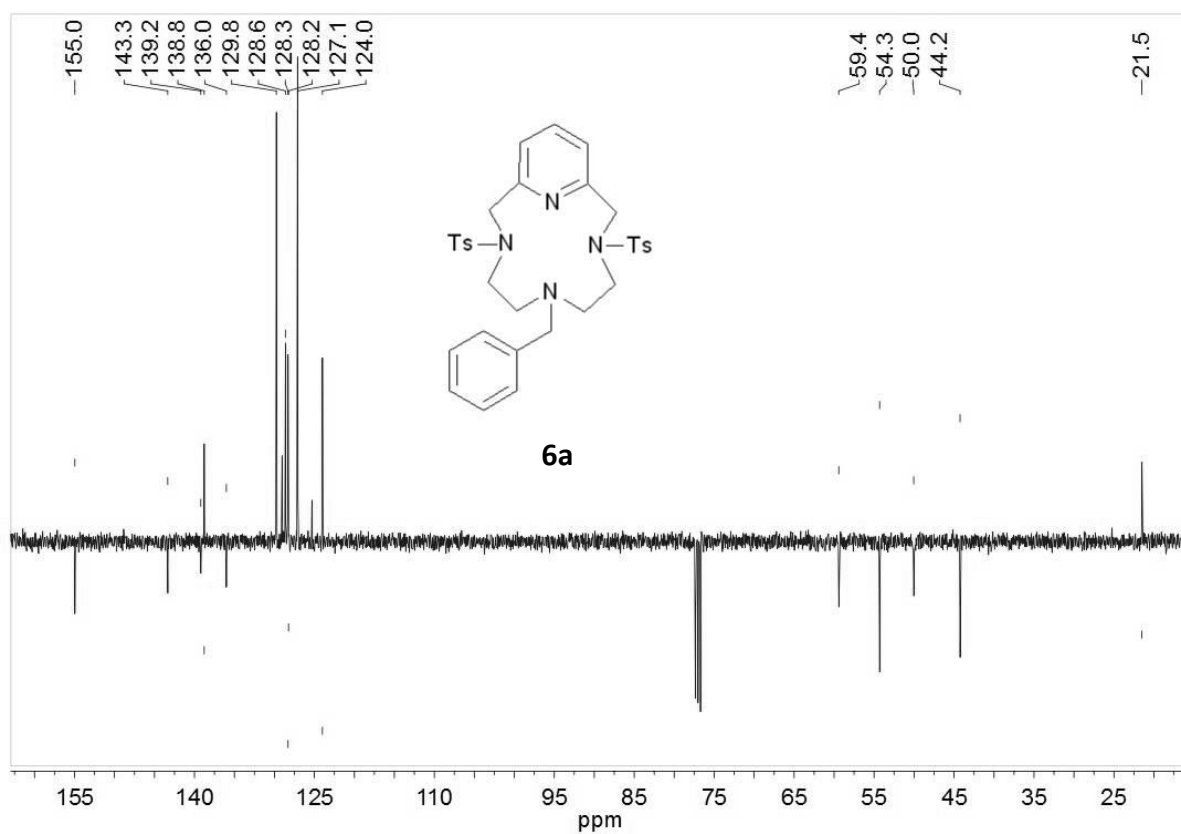
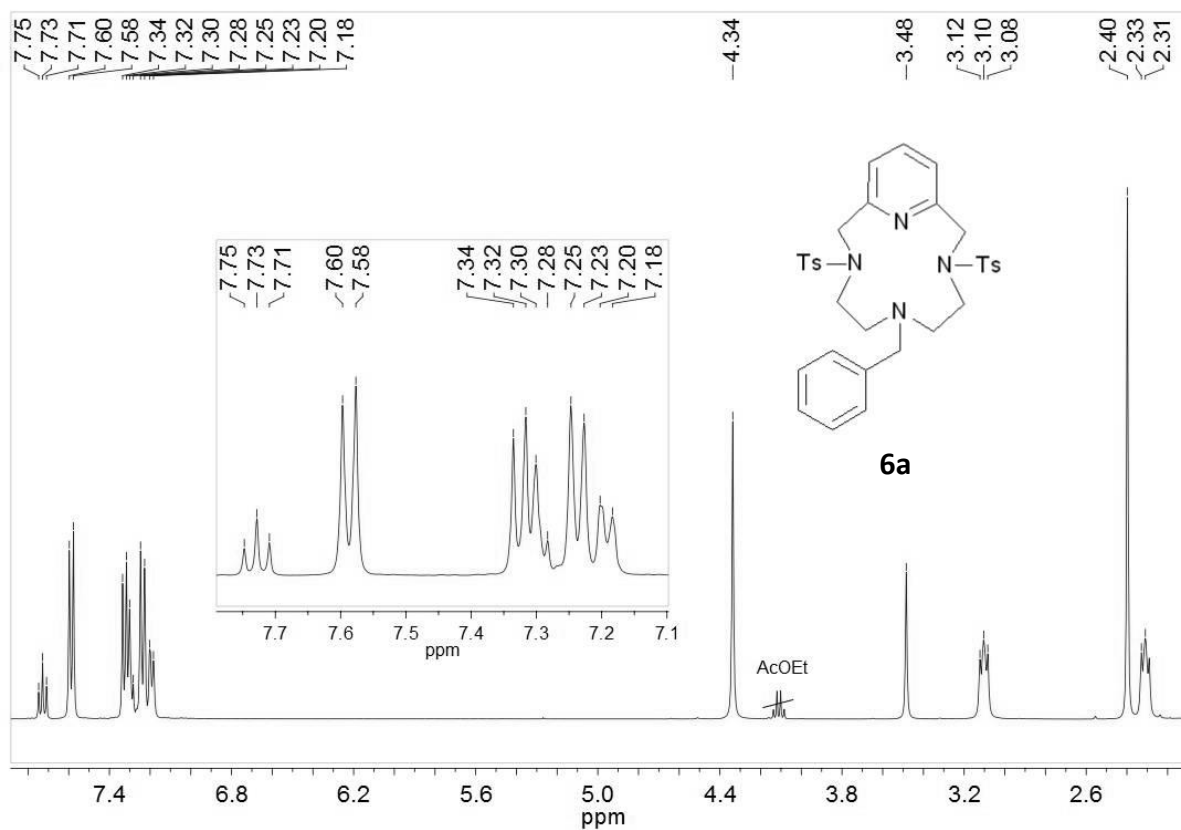
g742bis#1283 RT: 7.36 AV: 1 NL: 3.90E8
T: + c EI Full ms [50.00-500.00]

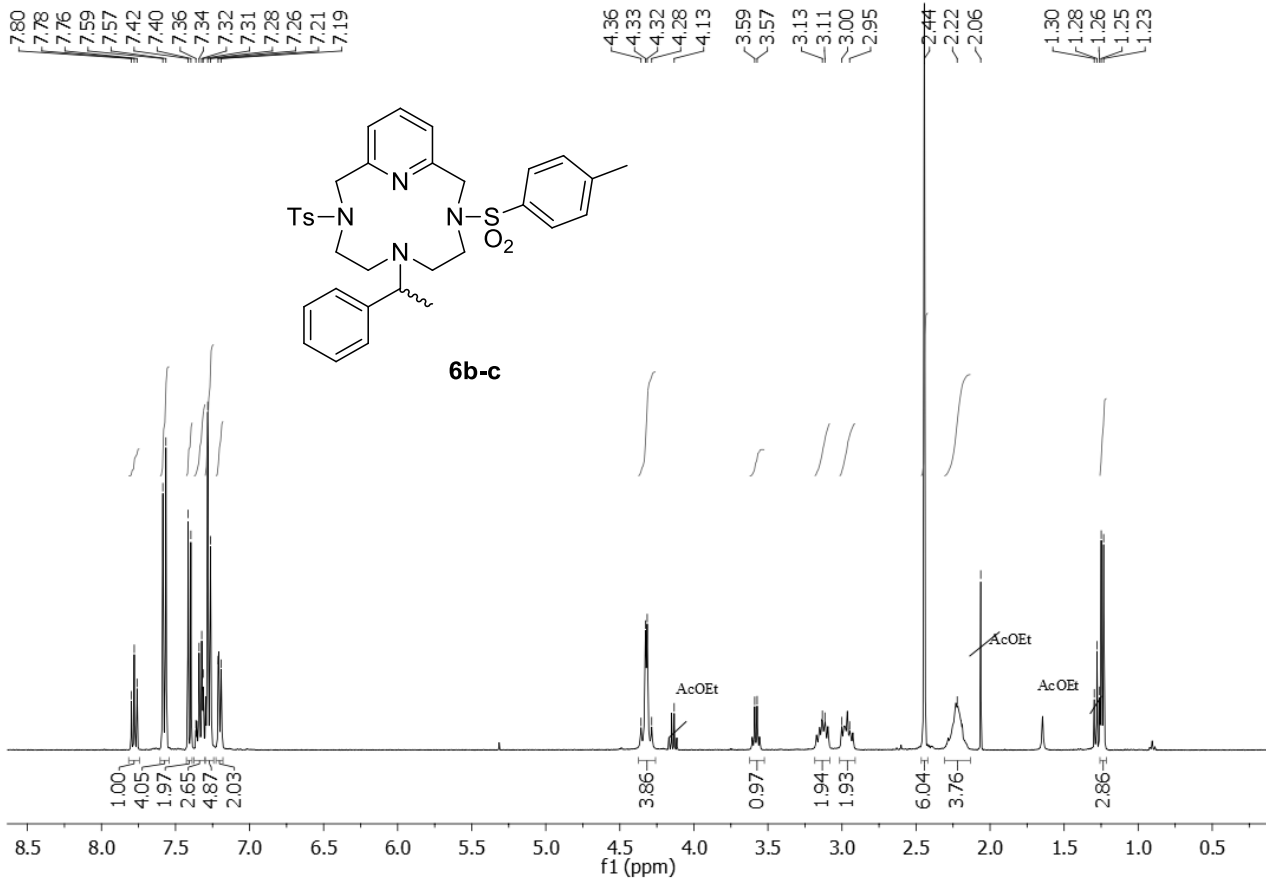


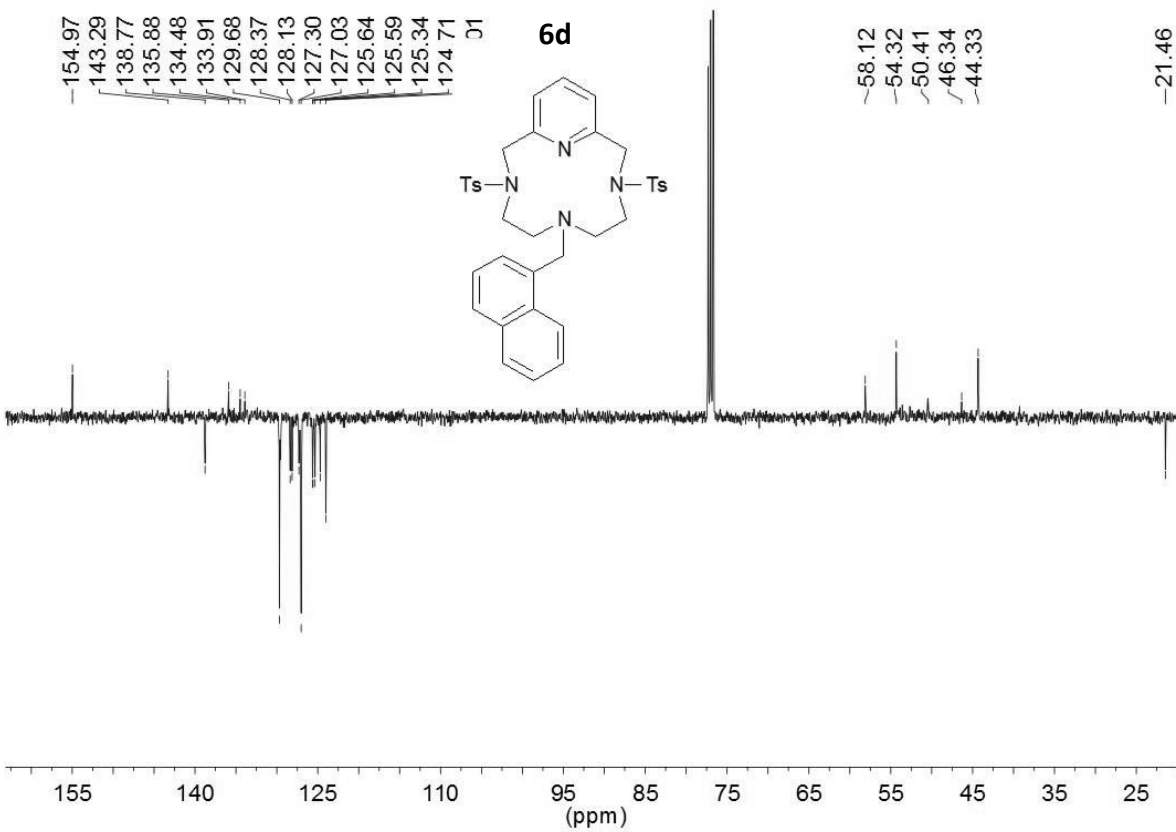
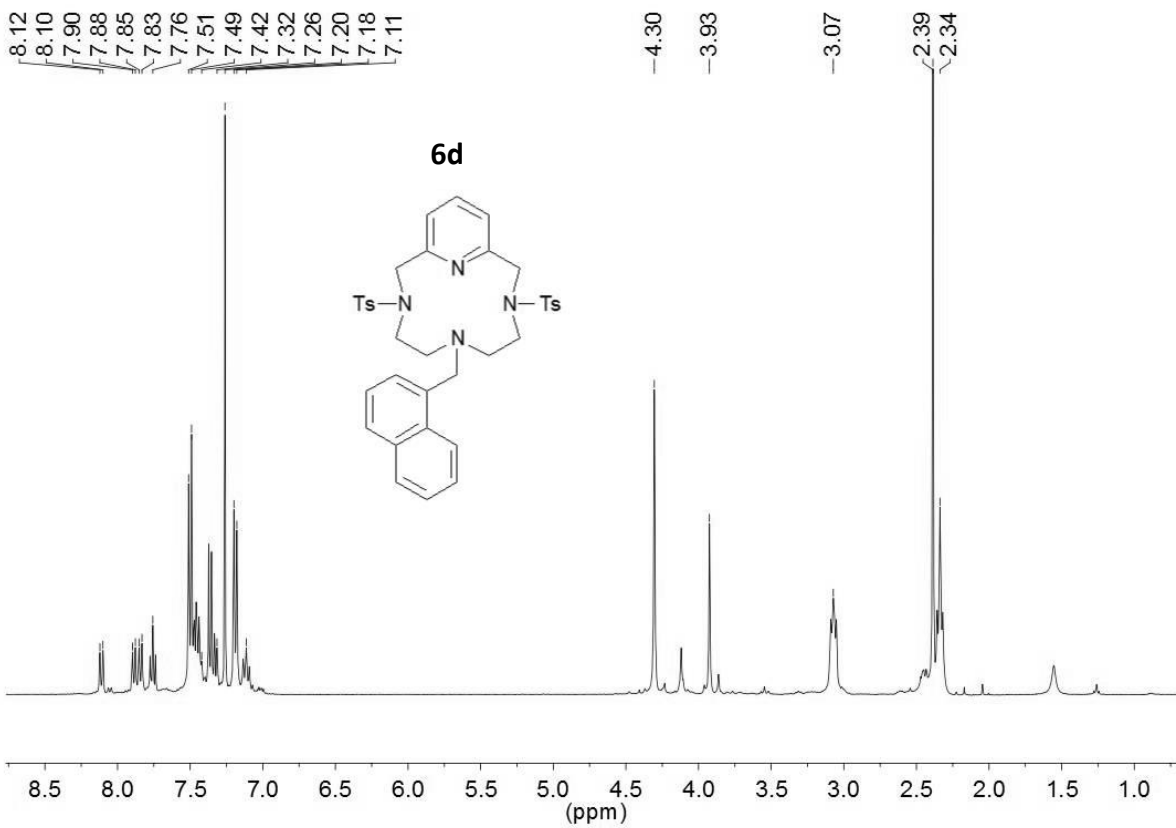
g742bis#1727 RT: 8.87 AV: 1 NL: 2.65E7
T: + c EI Full ms [50.00-500.00]

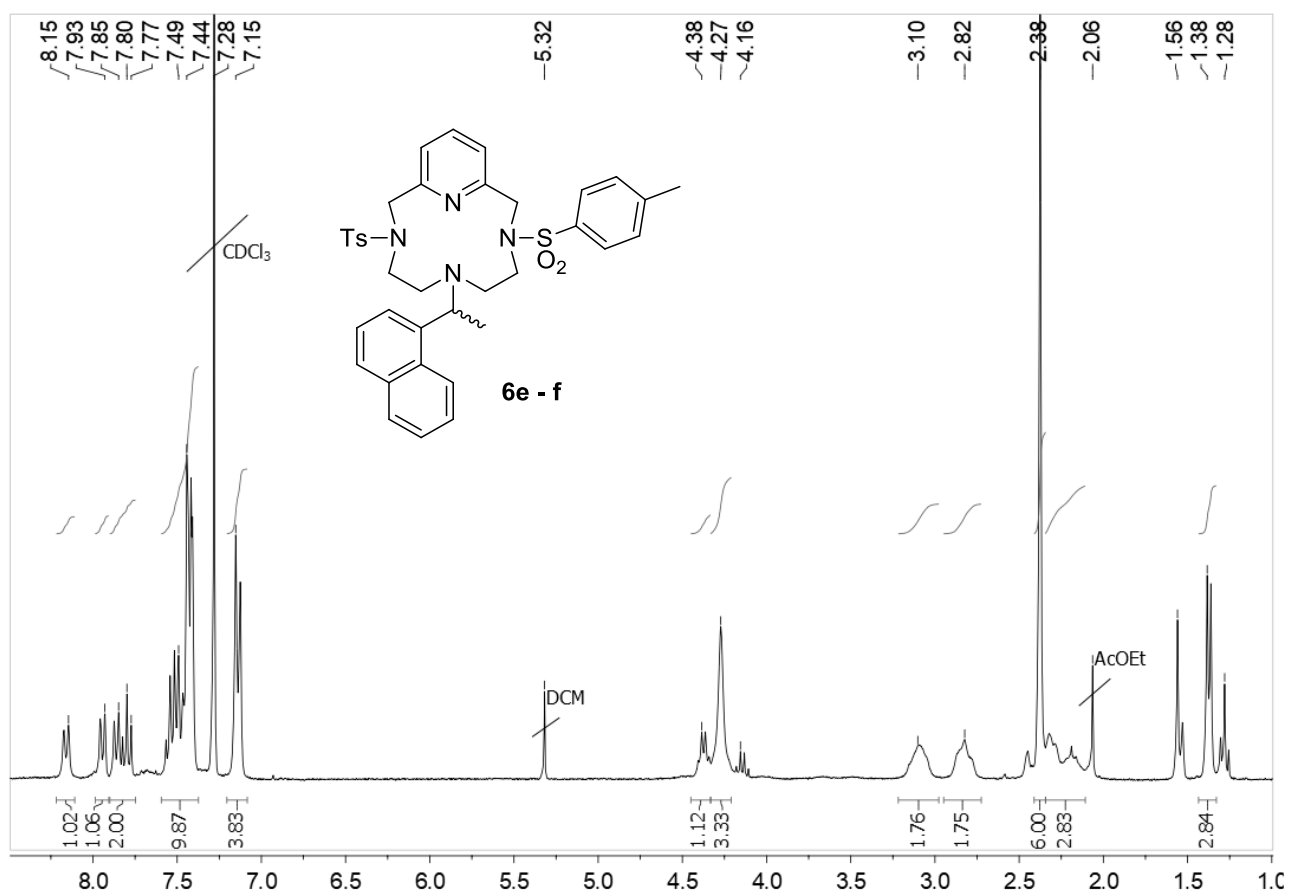


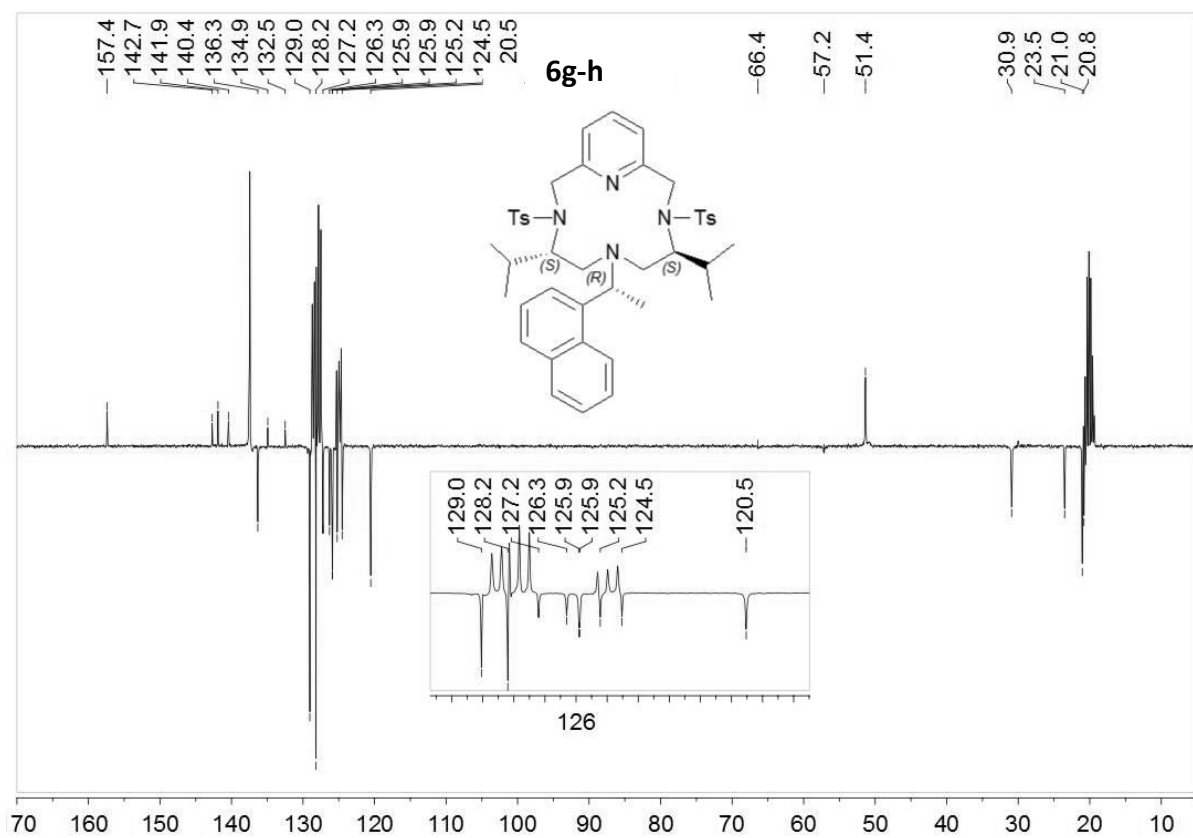
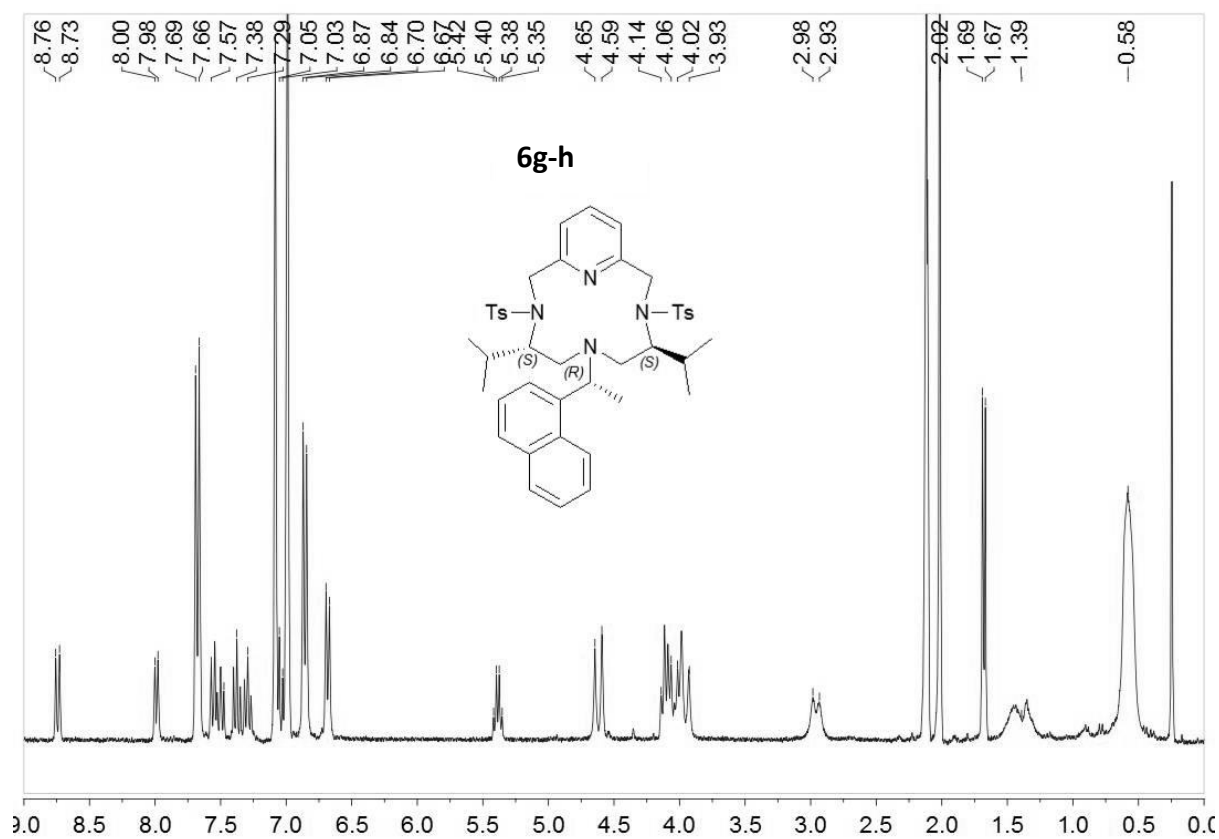
4.18 NMR-spectra of selected Ligands and Complexes

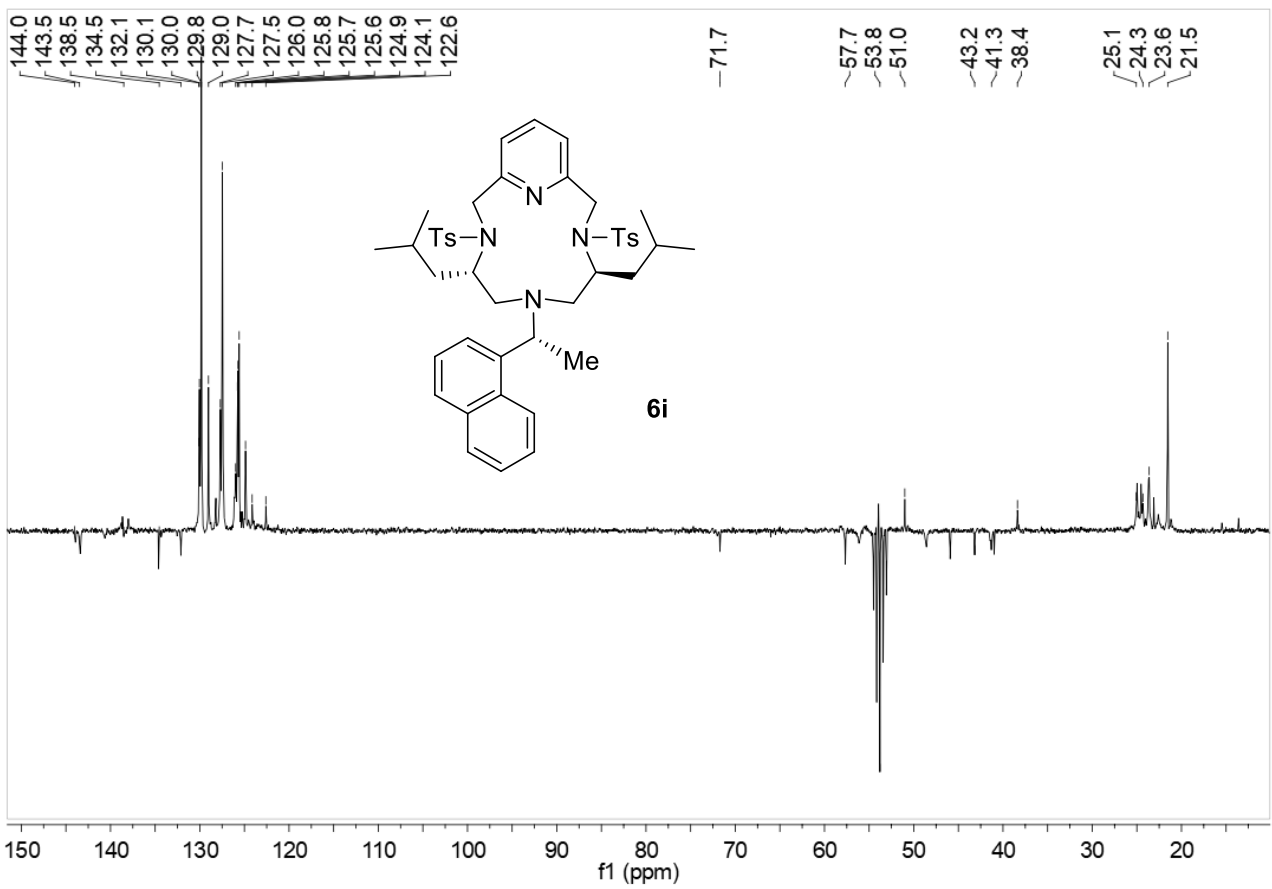
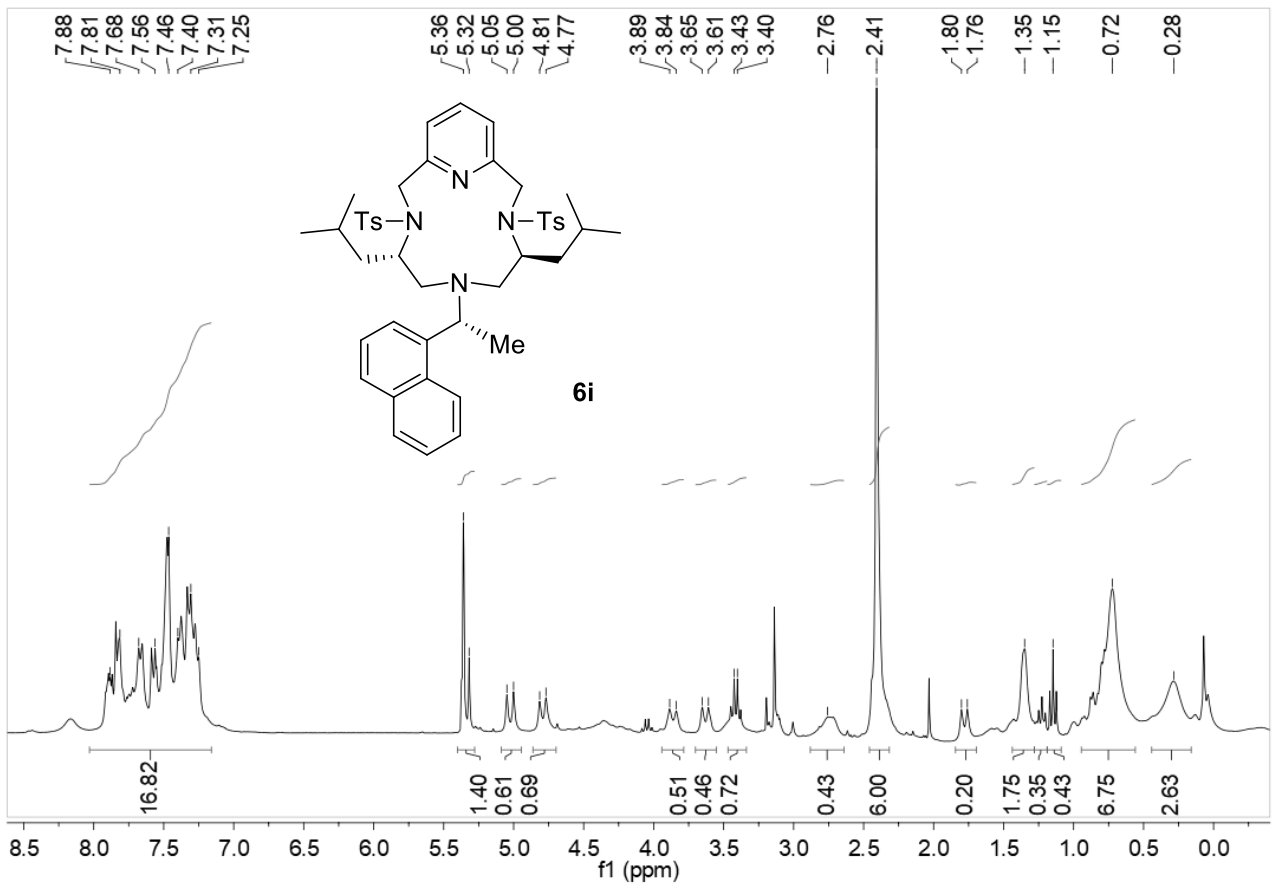


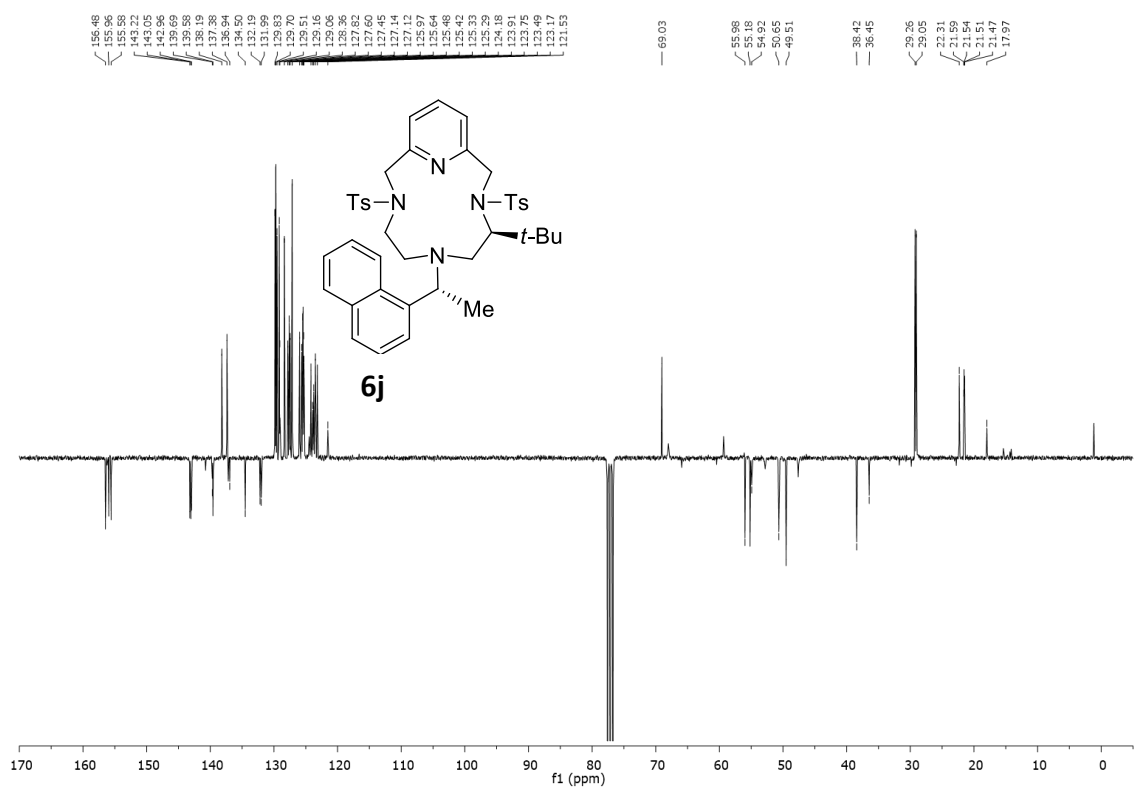
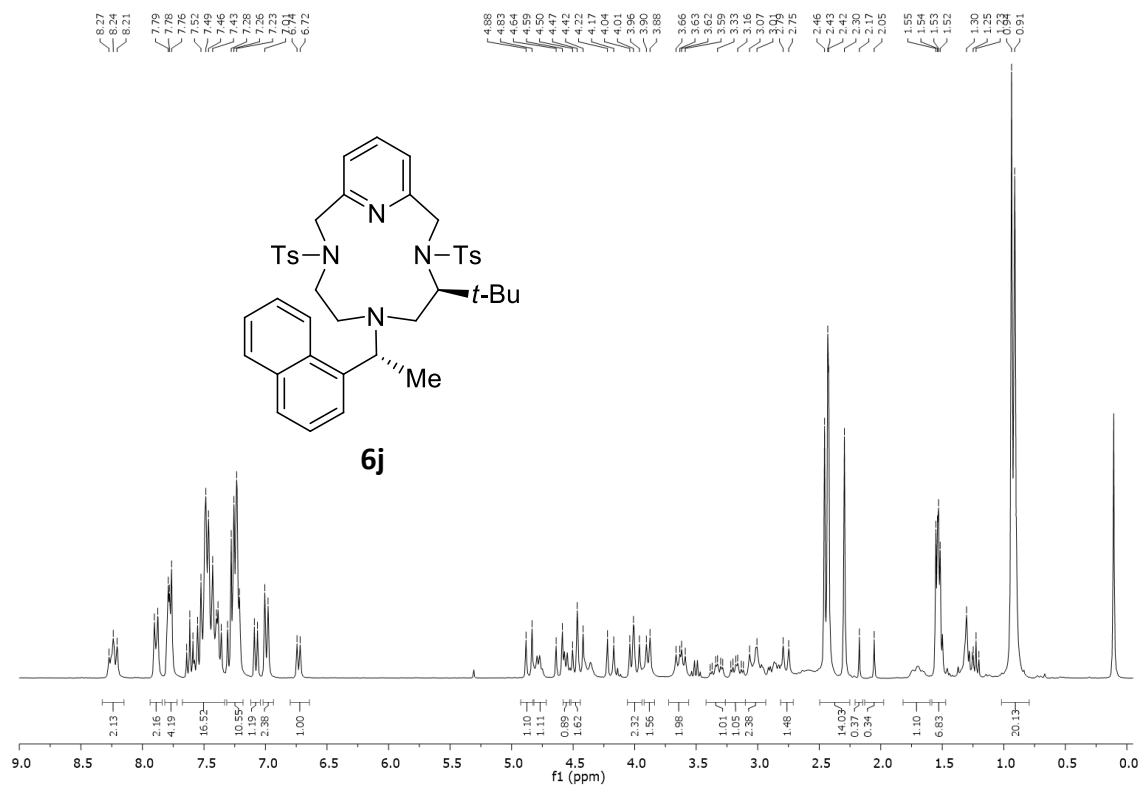


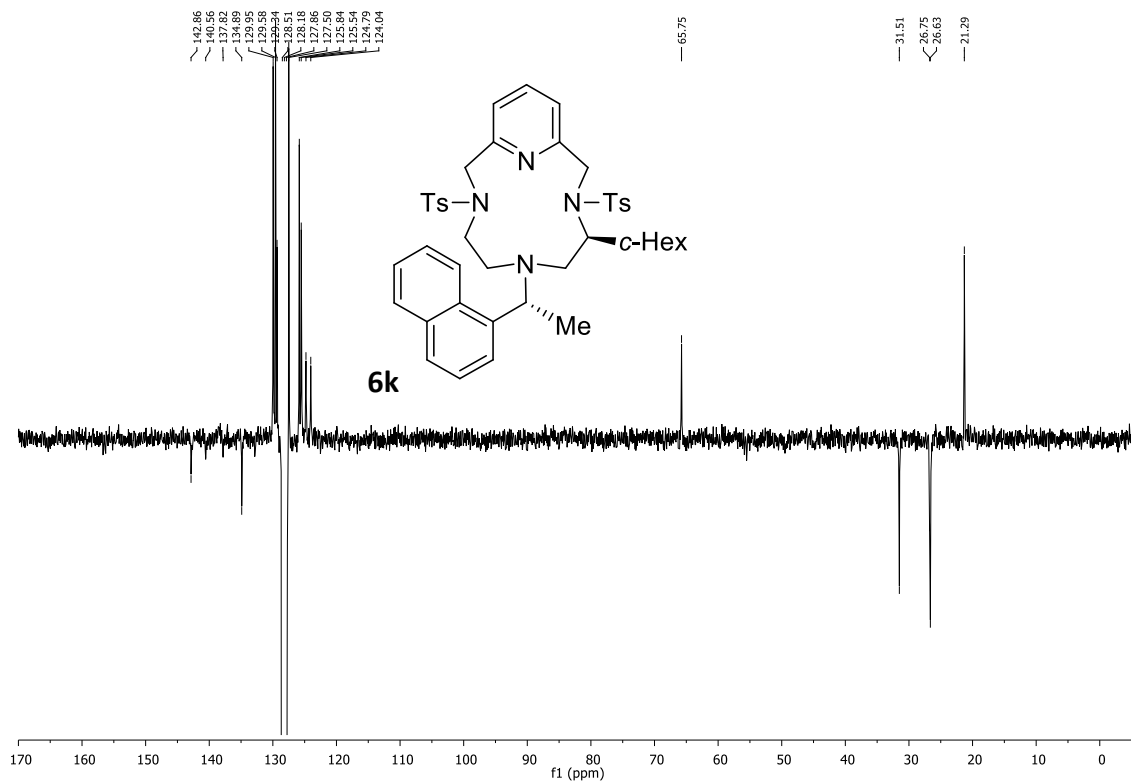
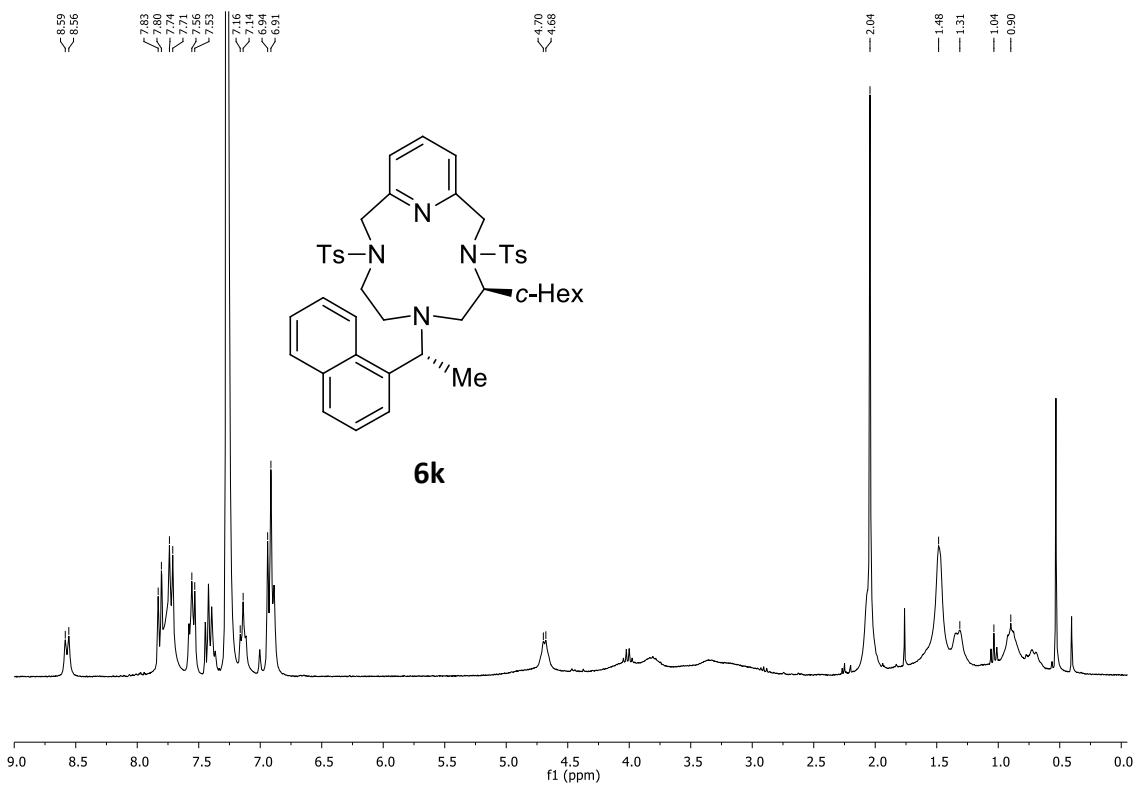


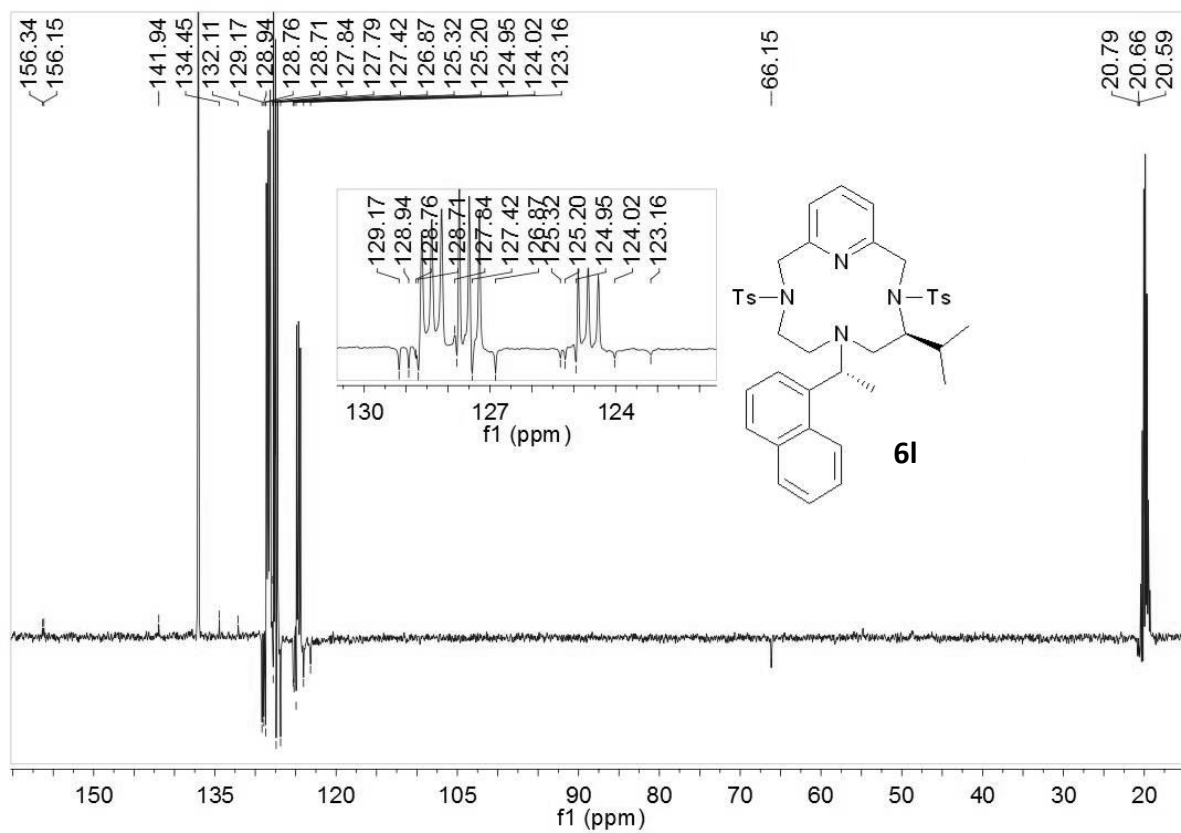
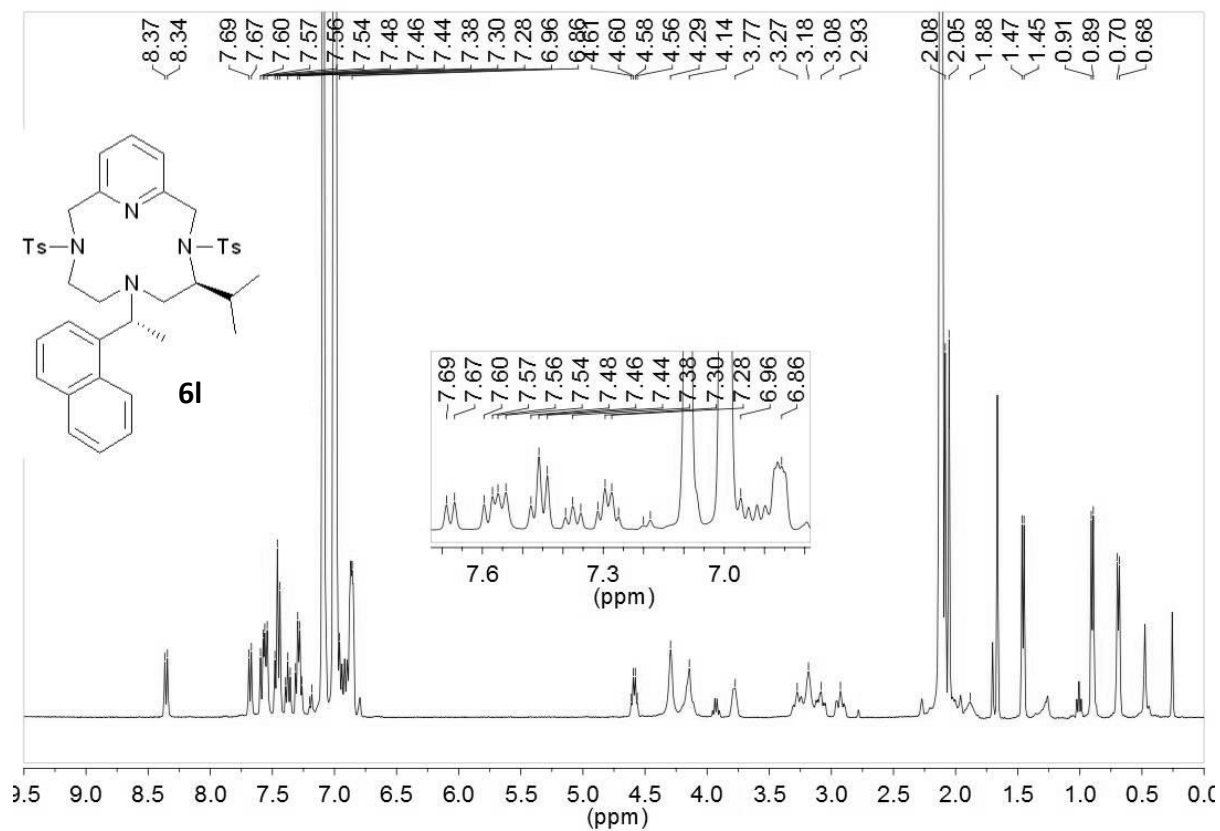


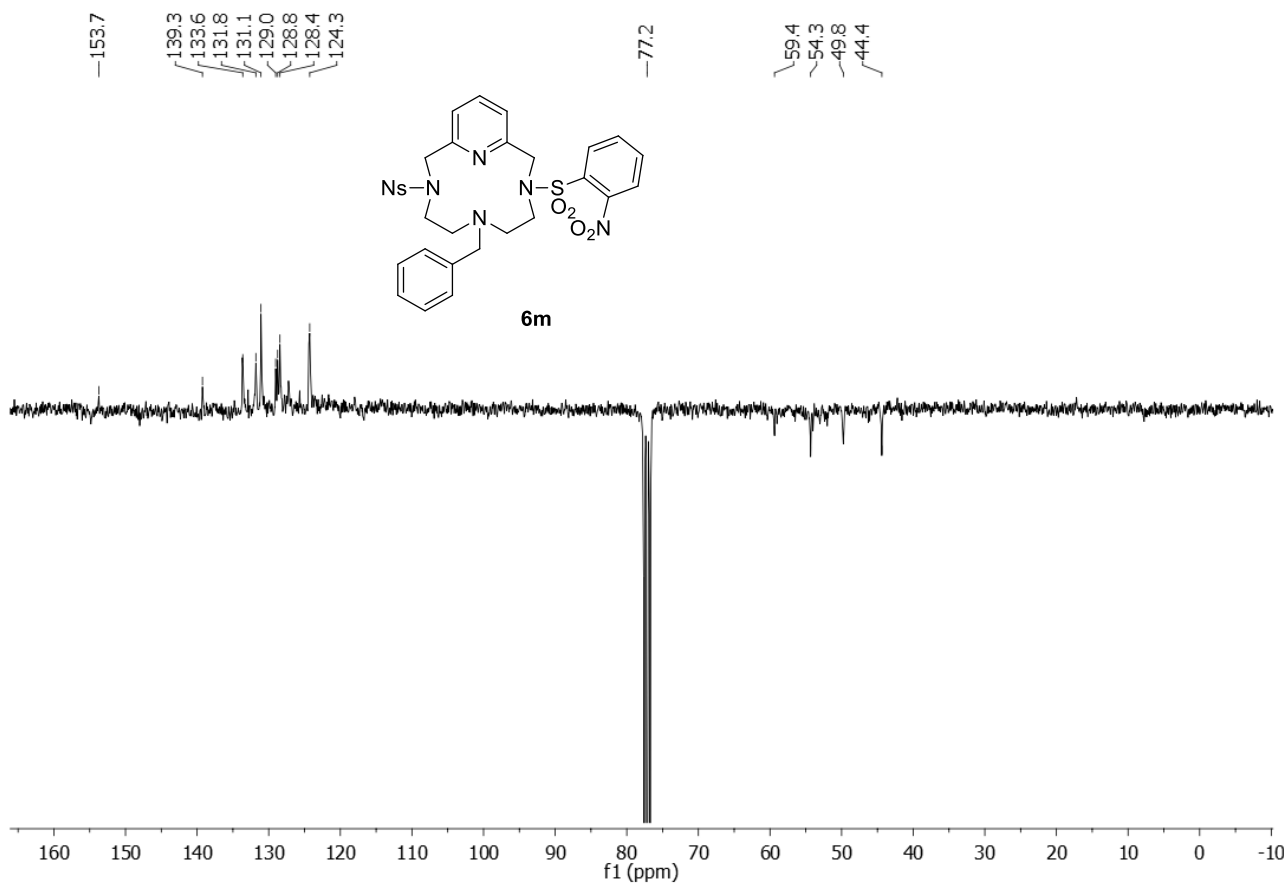
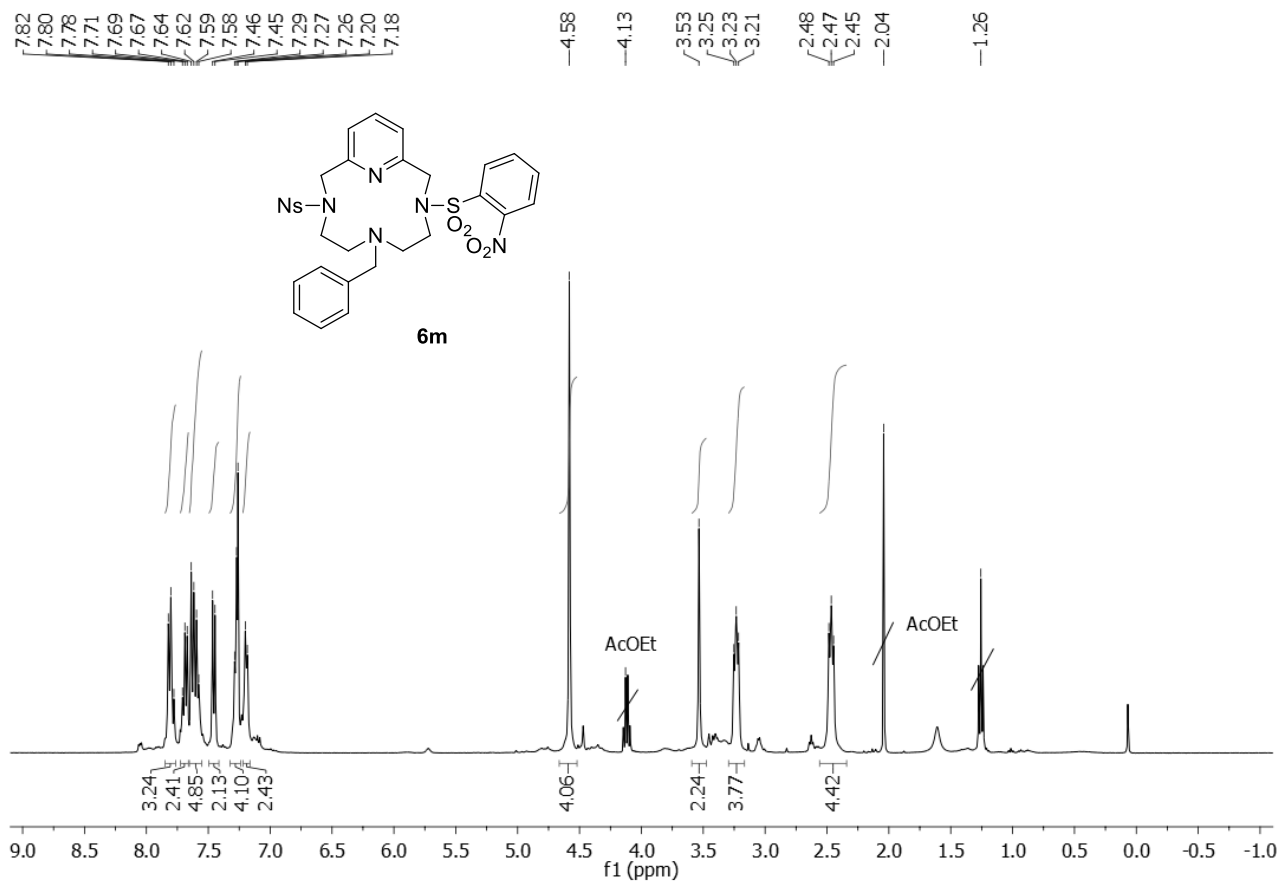


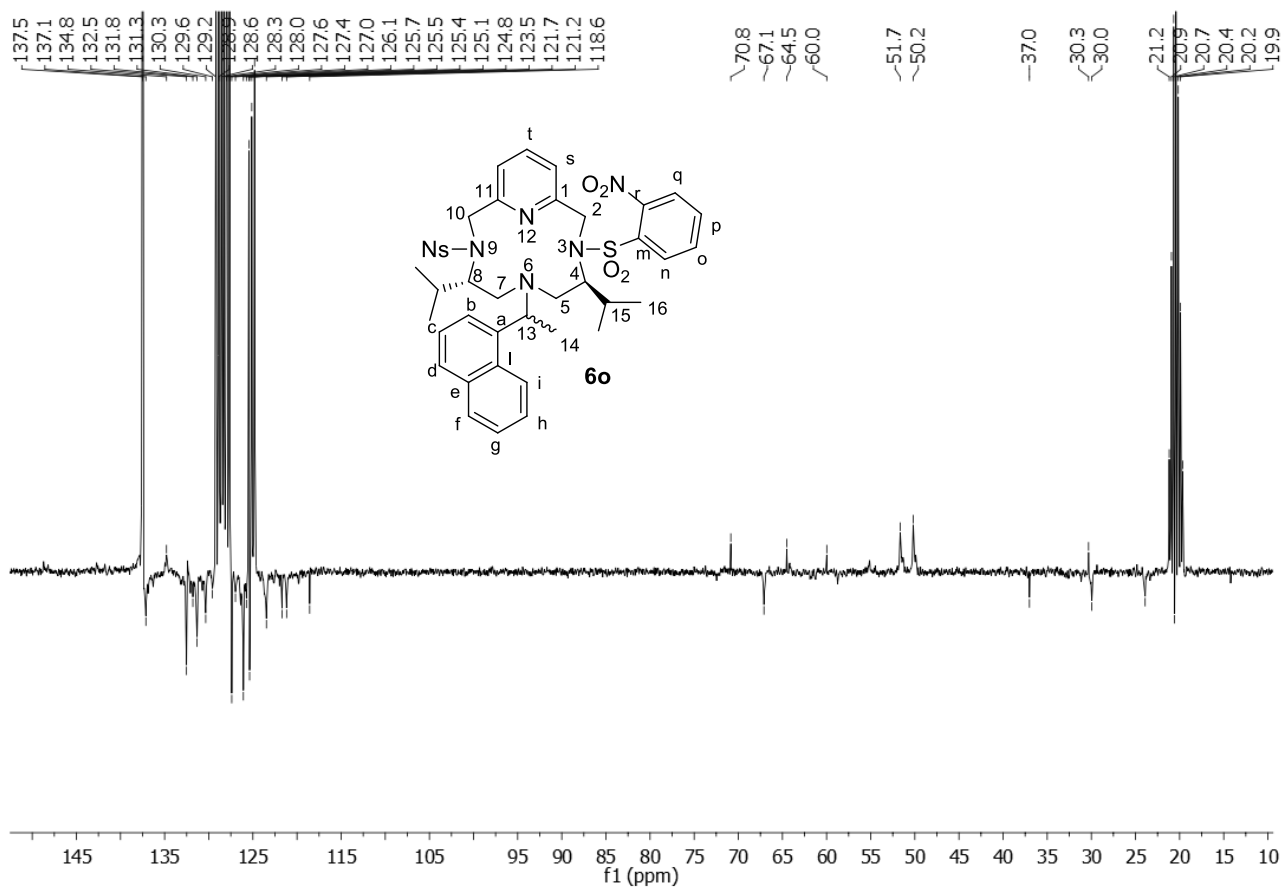
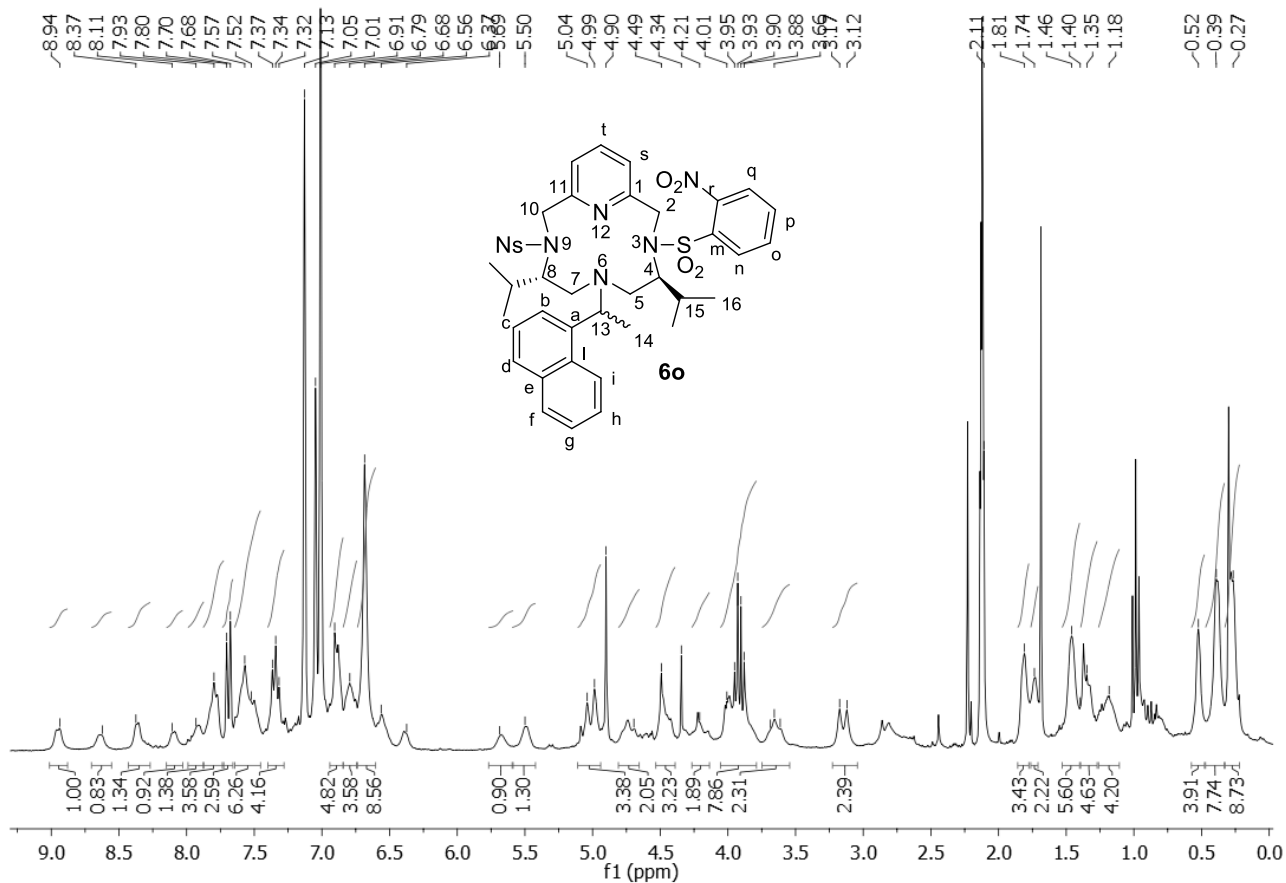


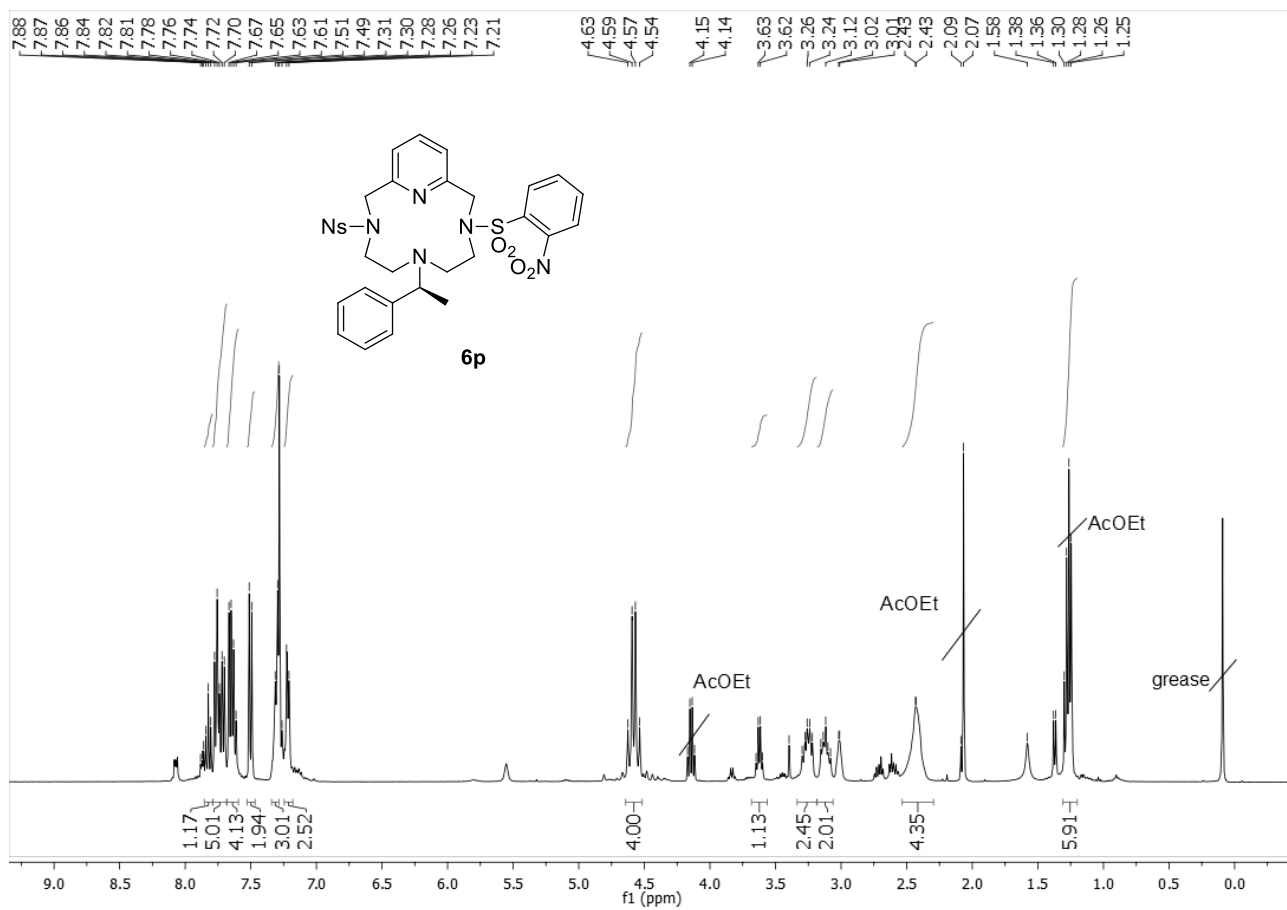


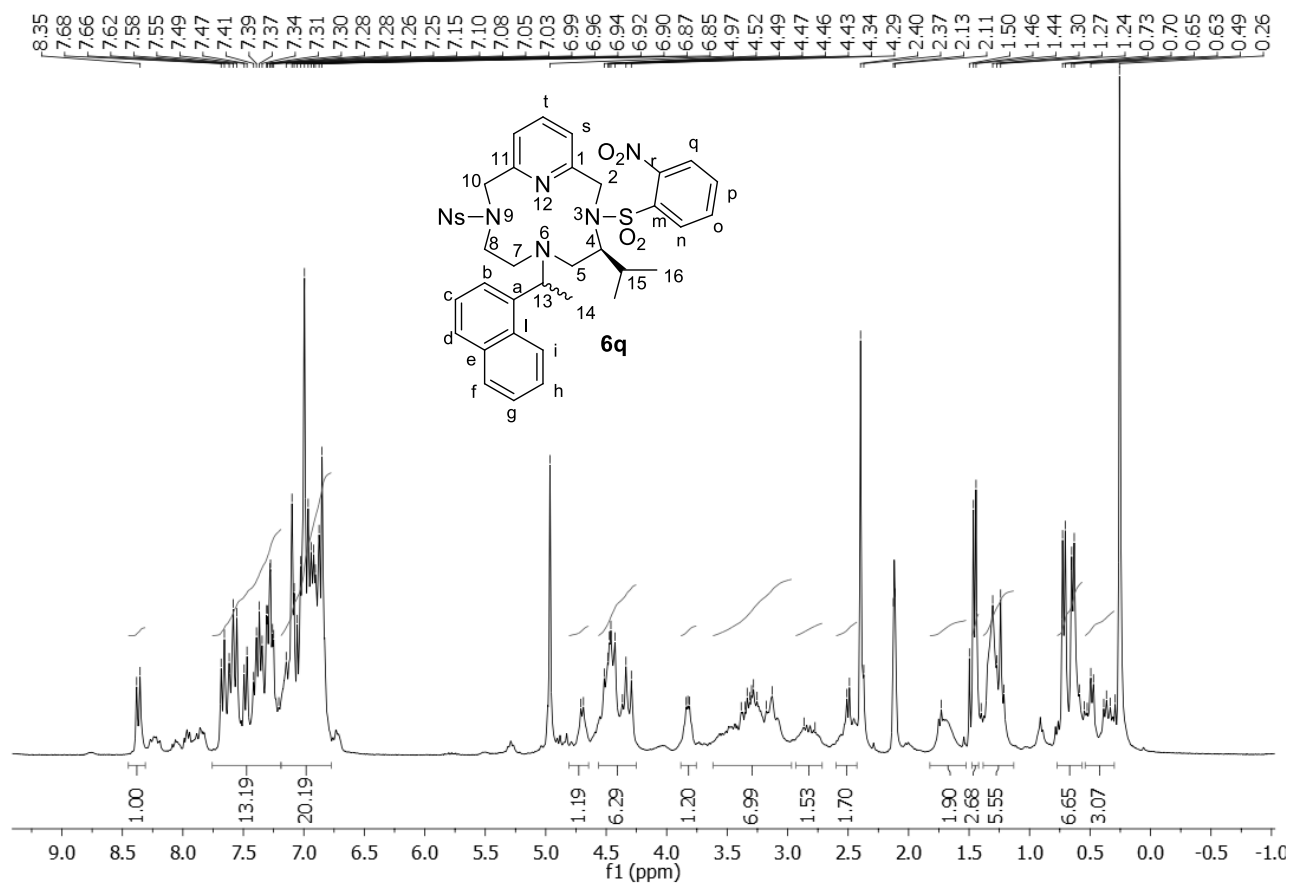












¹H NMR, CDCl₃,
400 MHz

7.74
7.72
7.35
7.33
7.31
7.26

4.32

3.64

3.12

3.10

3.08

2.65

2.44

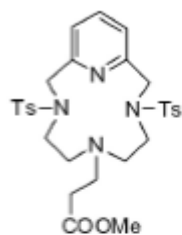
2.33

2.29

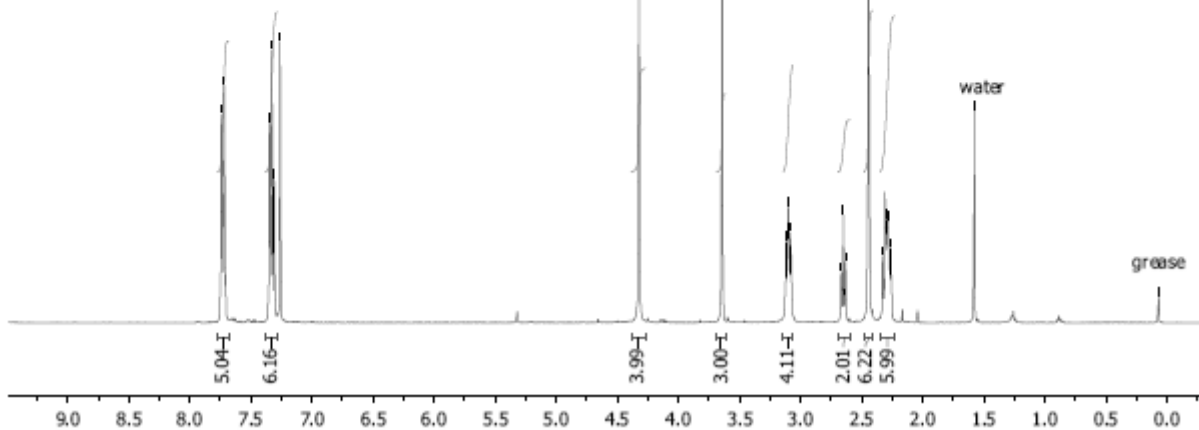
2.28

1.98

0.07



6r



¹³C NMR, CDCl₃,
100 MHz

172.8

155.2

143.7

138.9

136.2

130.0

127.3

124.2

77.2

54.7

52.5

51.7

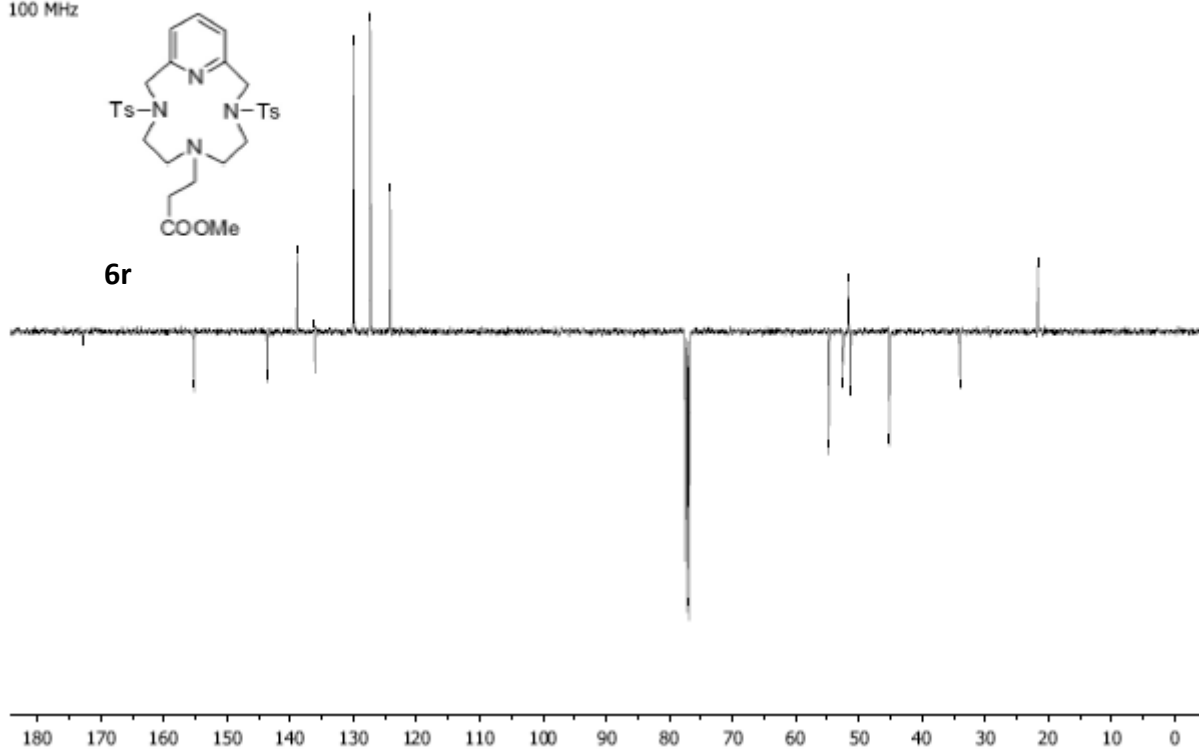
51.3

45.2

34.0

21.7

6r



¹H NMR, CDCl₃
300 MHz

7.74
7.71
7.69
7.35
7.32
7.31
7.28
7.26

5.30
5.28
5.11

4.33

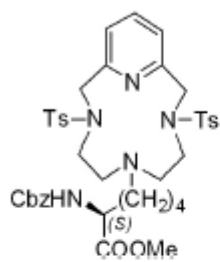
3.74

3.12
3.10
3.07

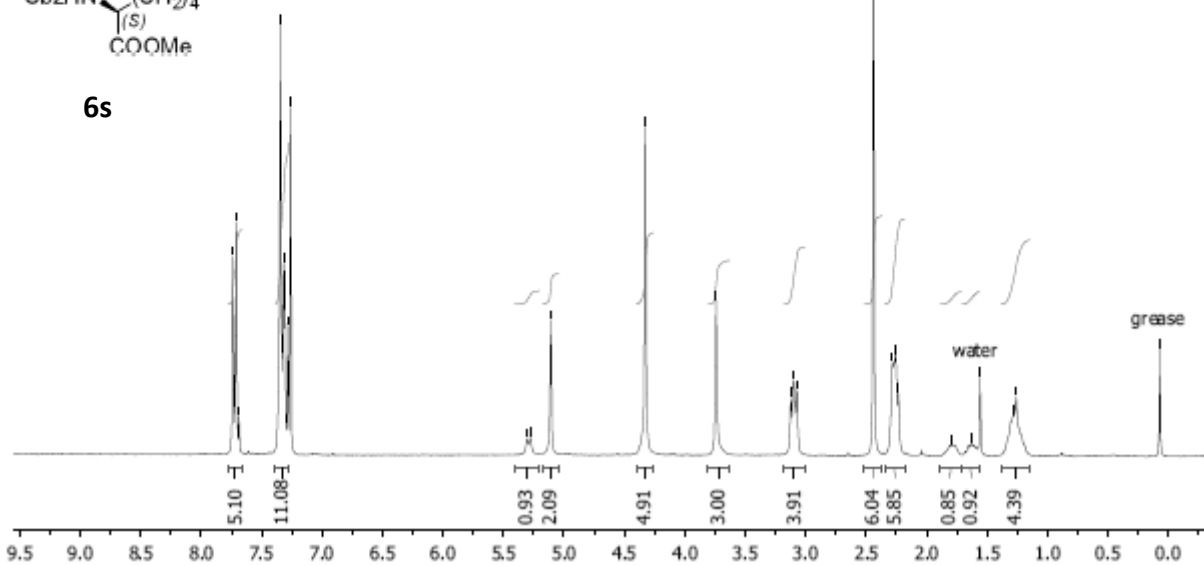
2.44
2.28
2.25
2.23

1.79
1.63
1.56
1.28
1.26

0.07



6s



¹³C NMR, CDCl₃
75 MHz

173.1

155.1

143.7

138.9

136.2

130.0

128.7

128.3

127.3

124.2

77.2

67.1

55.2

54.6

54.0

52.5

51.8

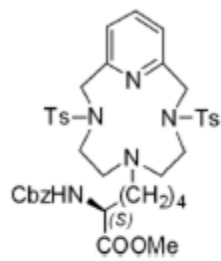
44.8

32.6

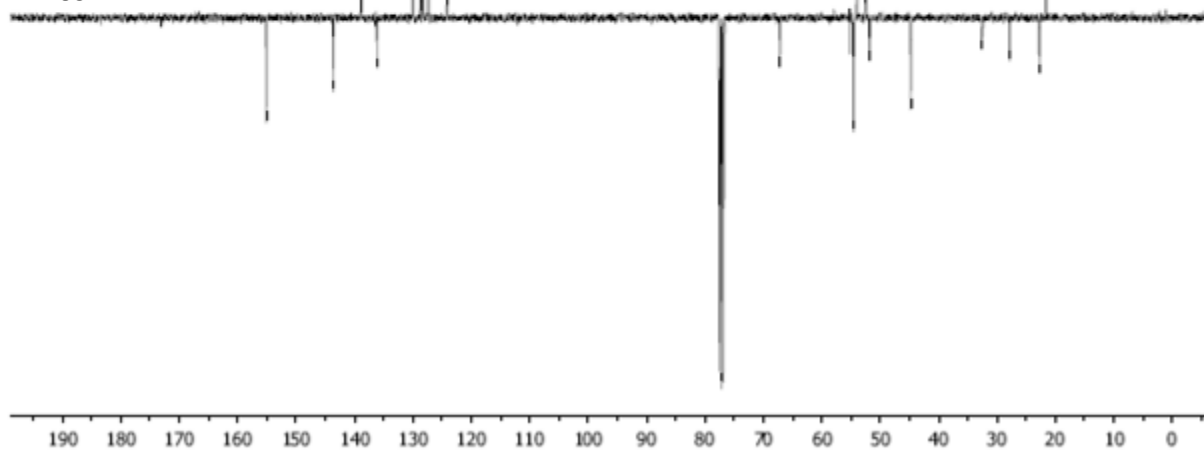
27.9

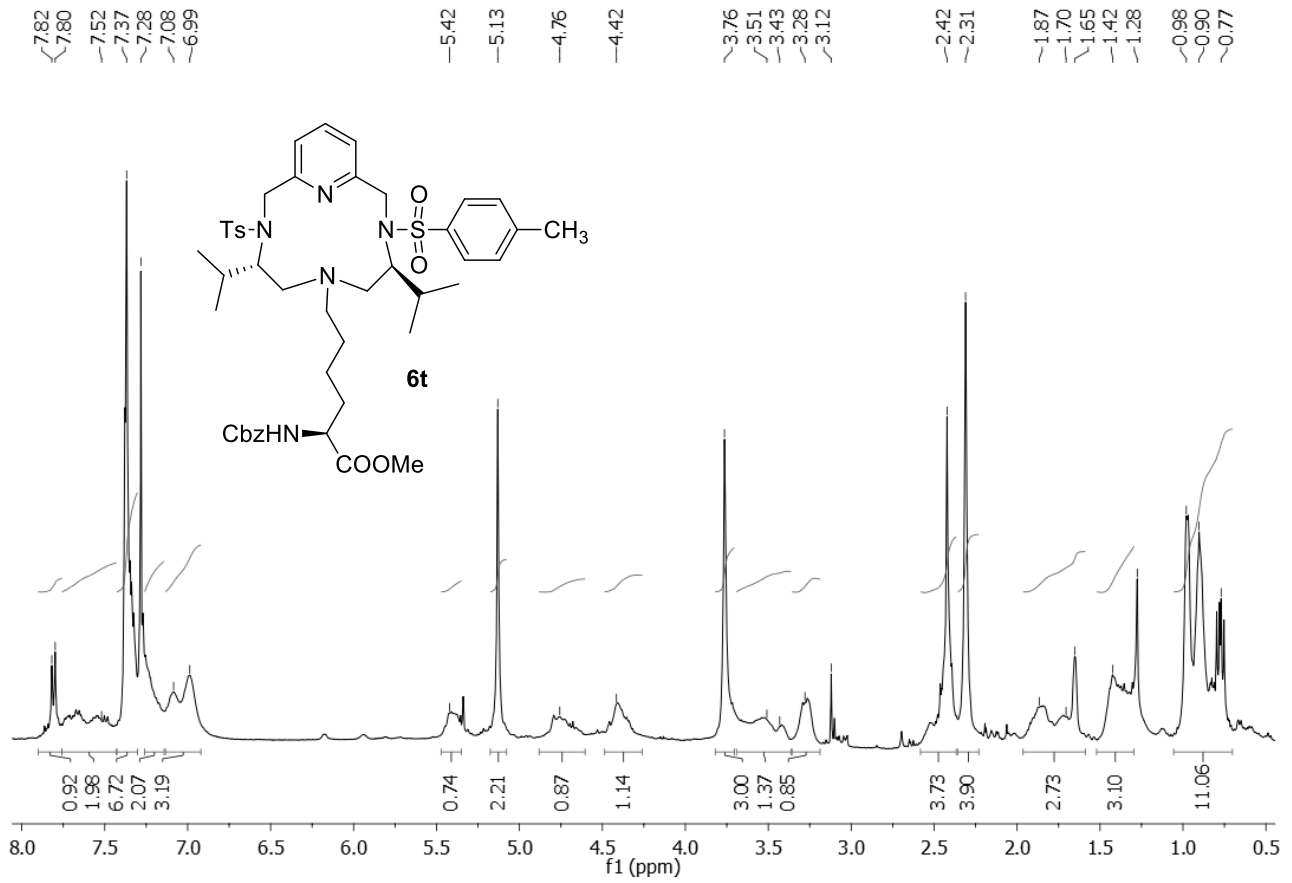
22.8

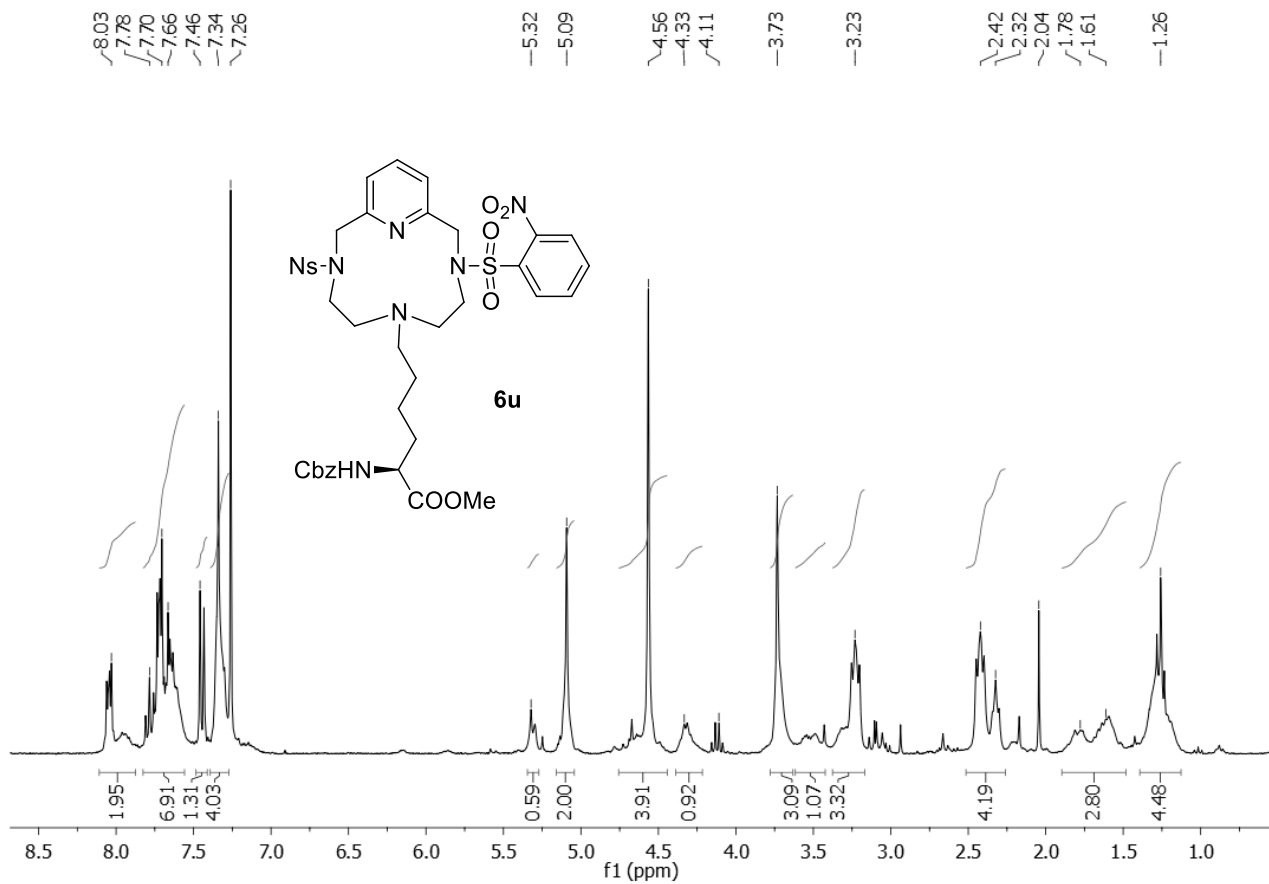
21.7

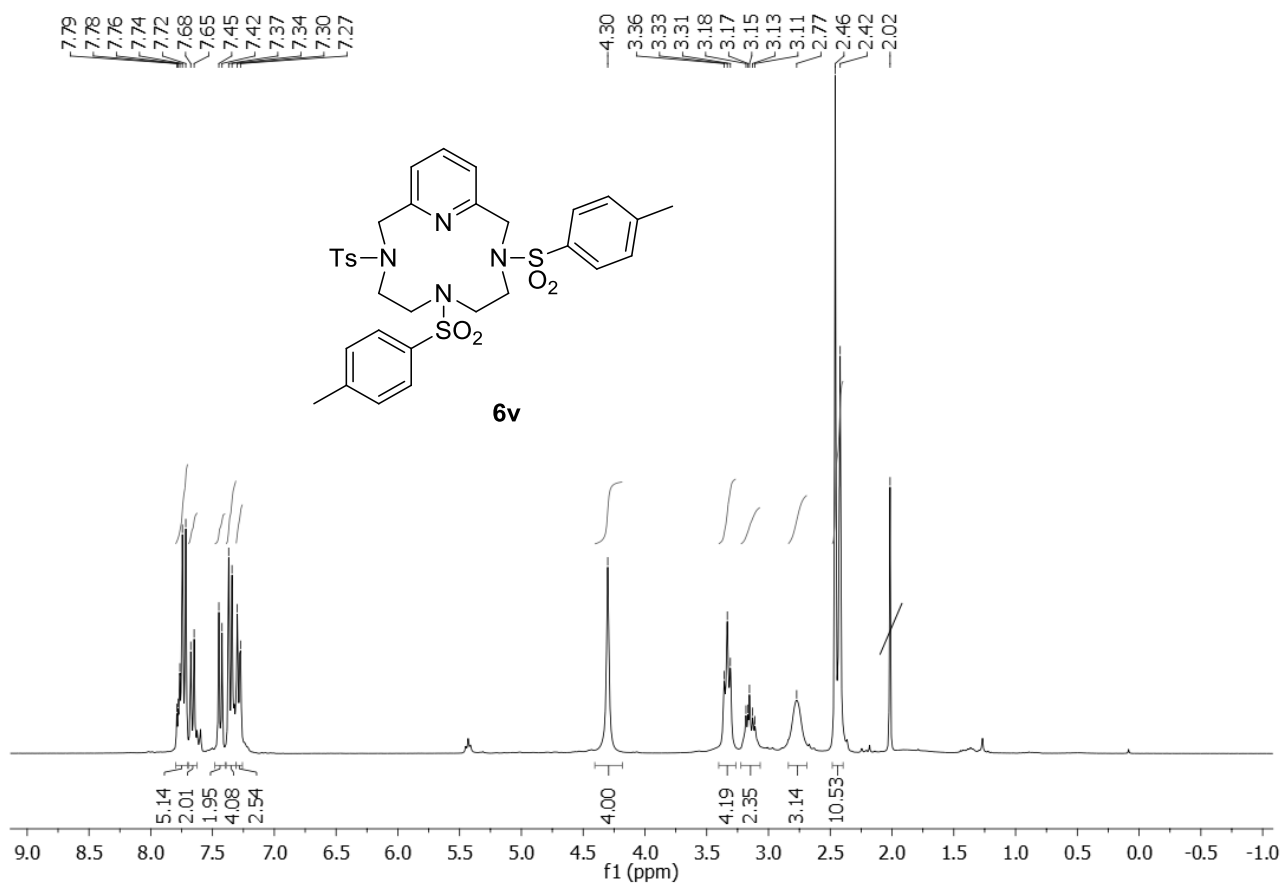


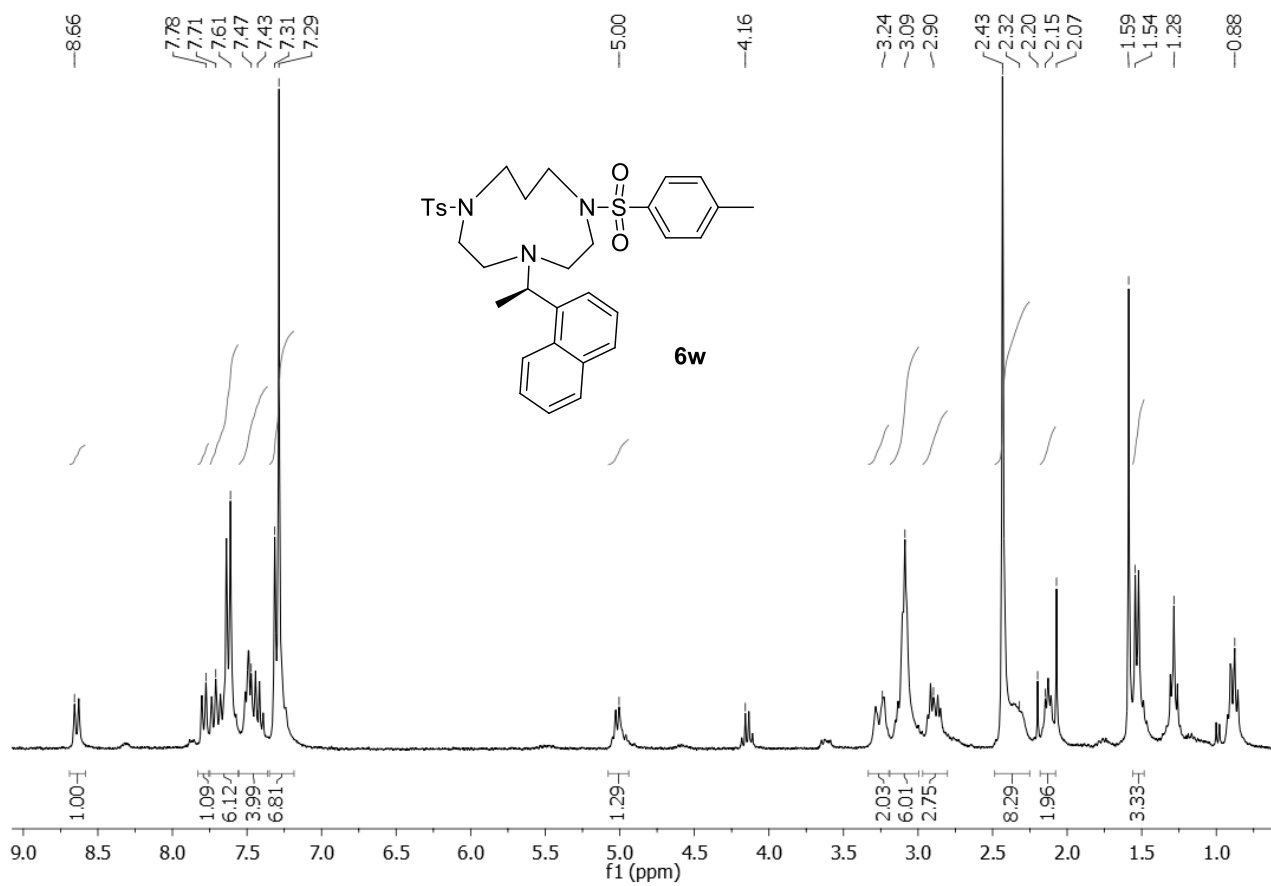
6s

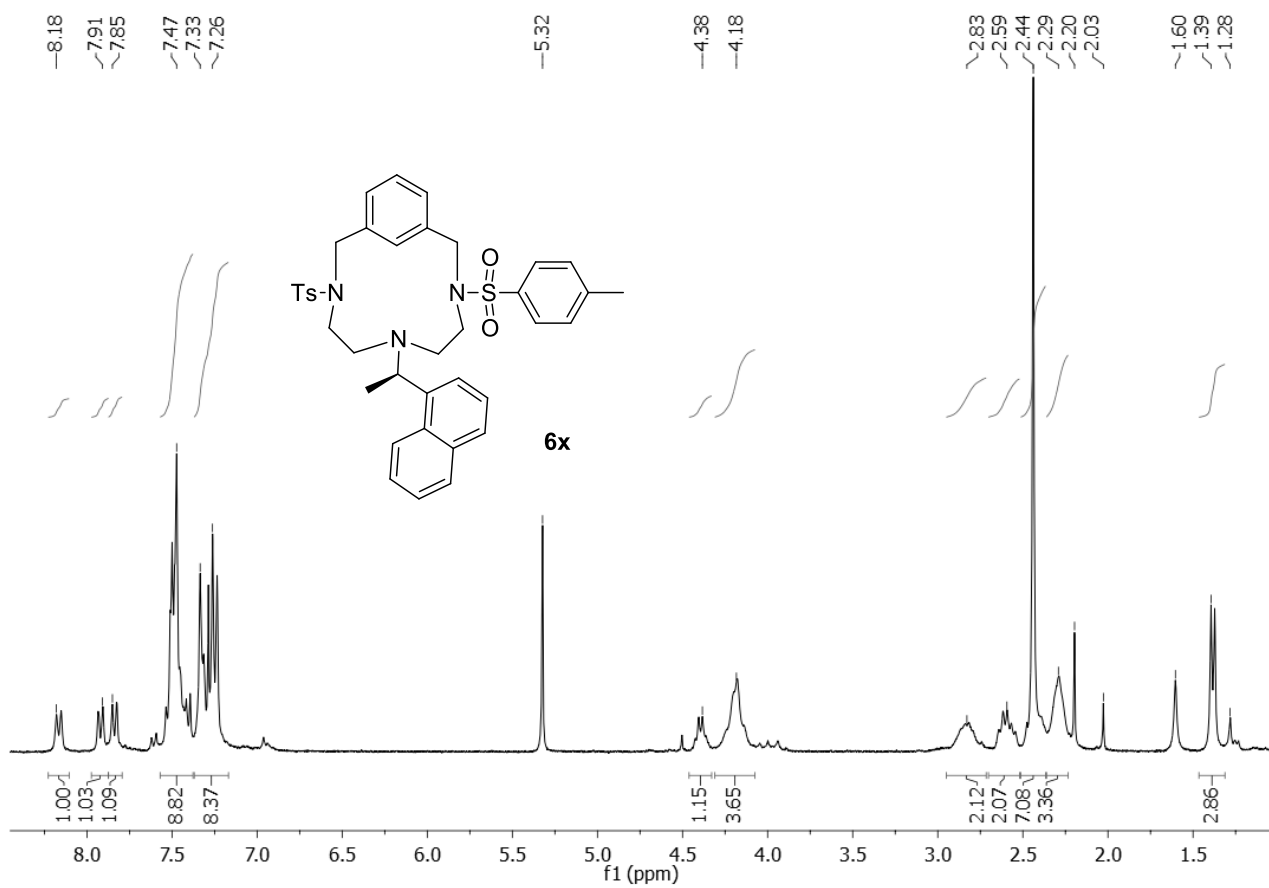


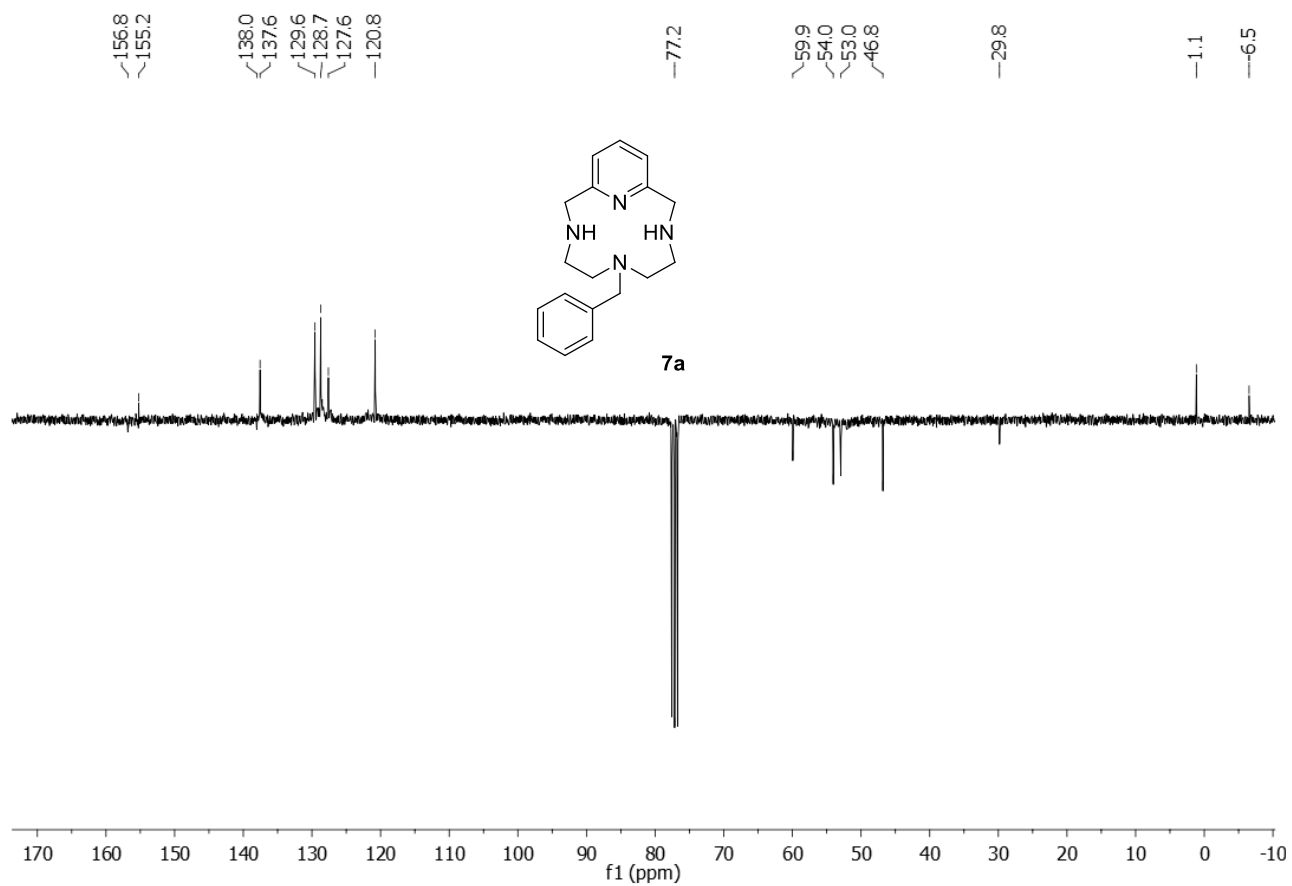
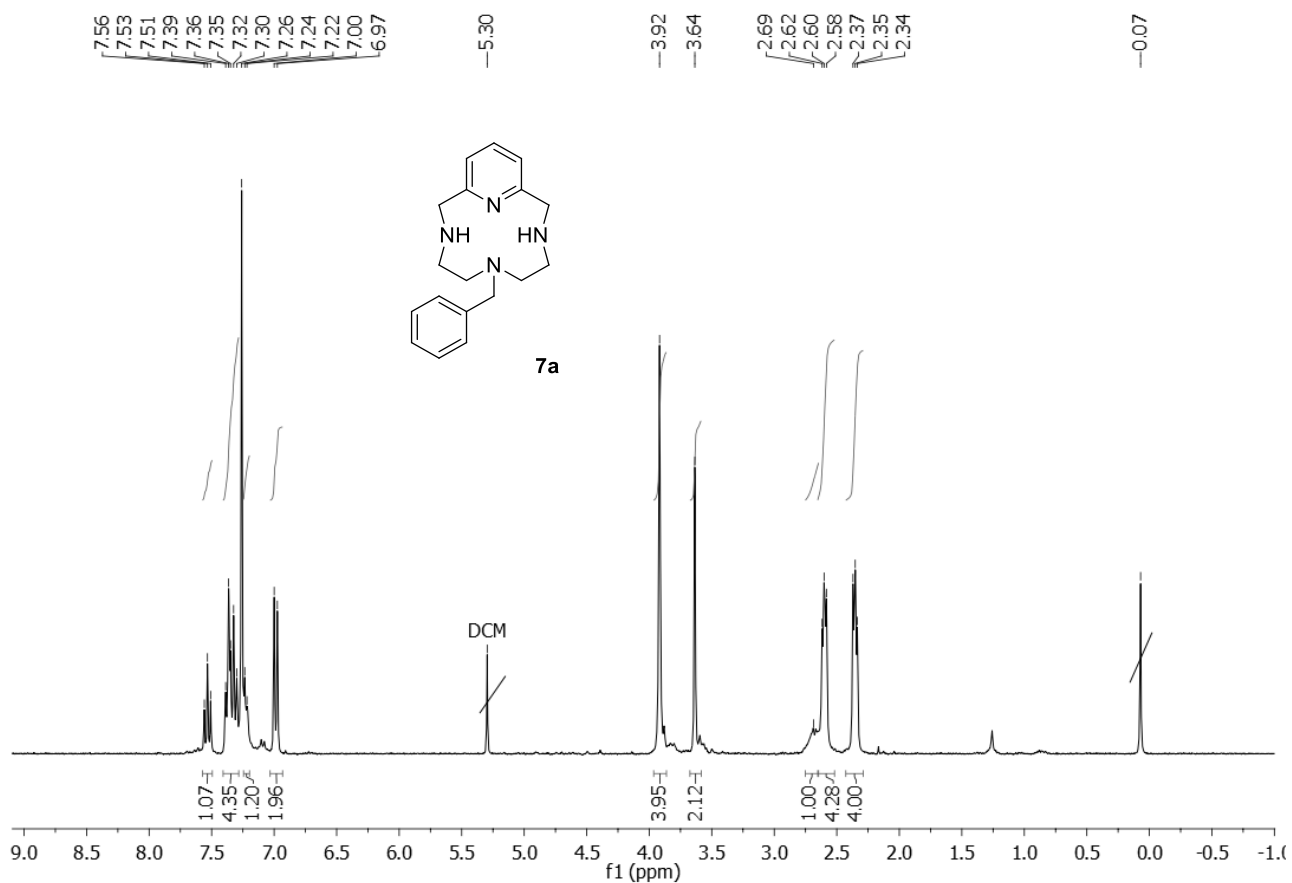


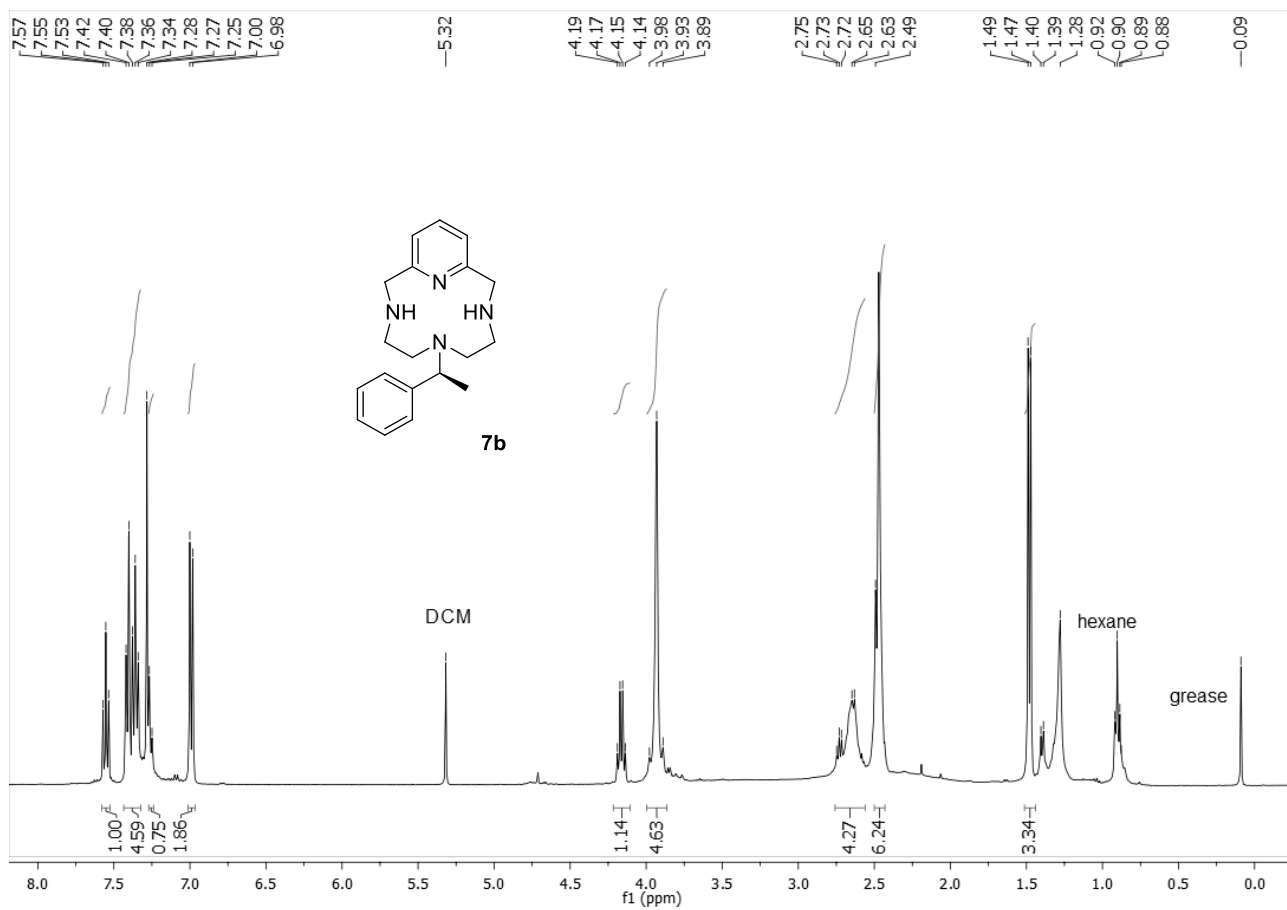


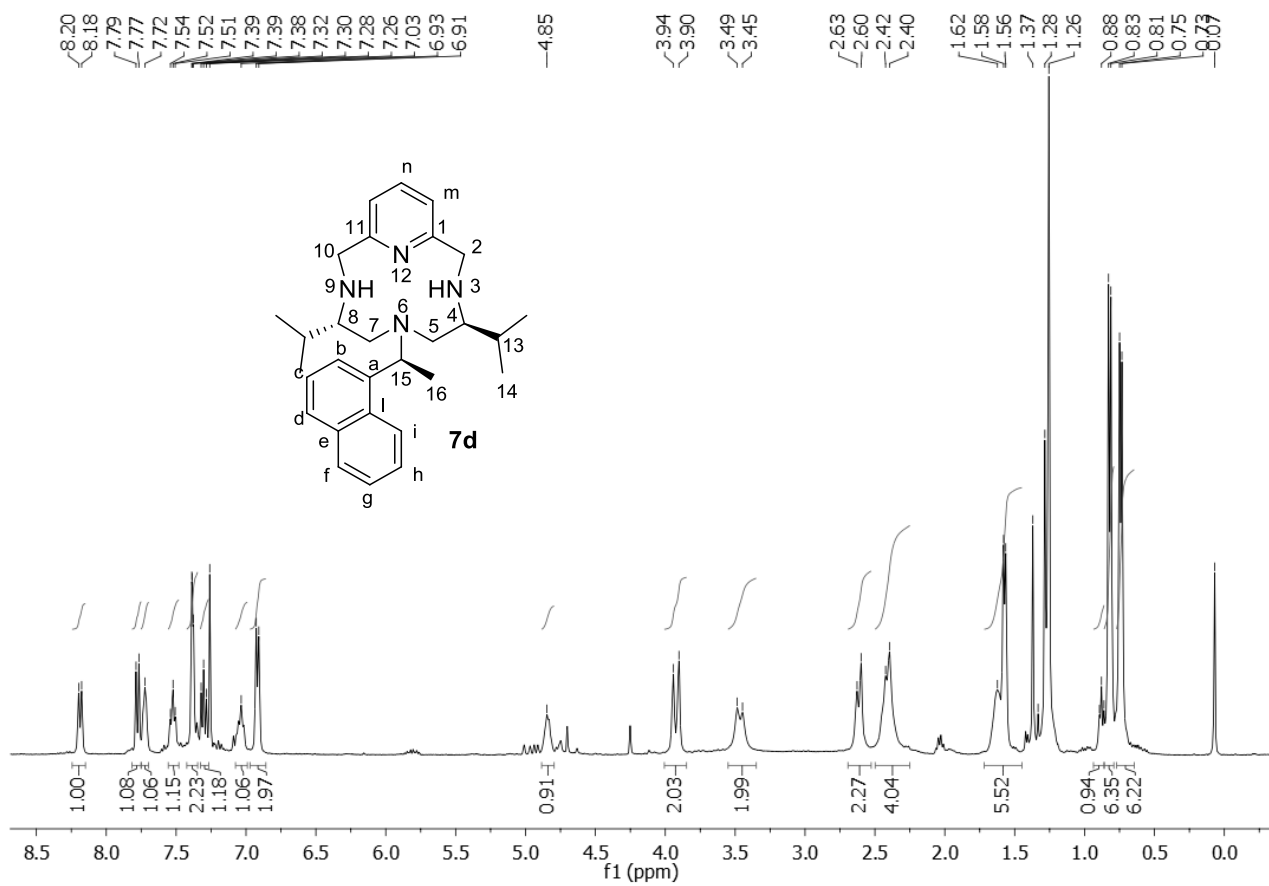


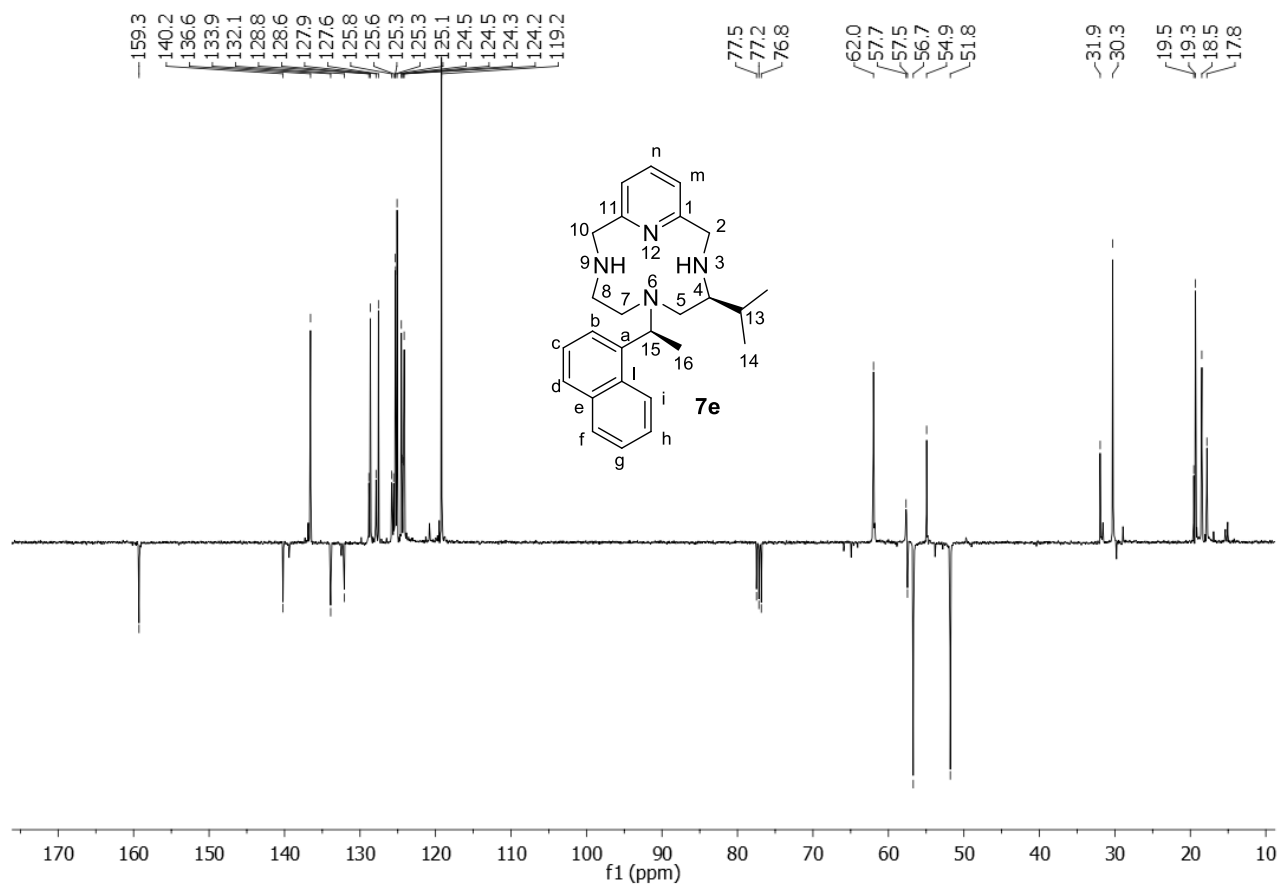
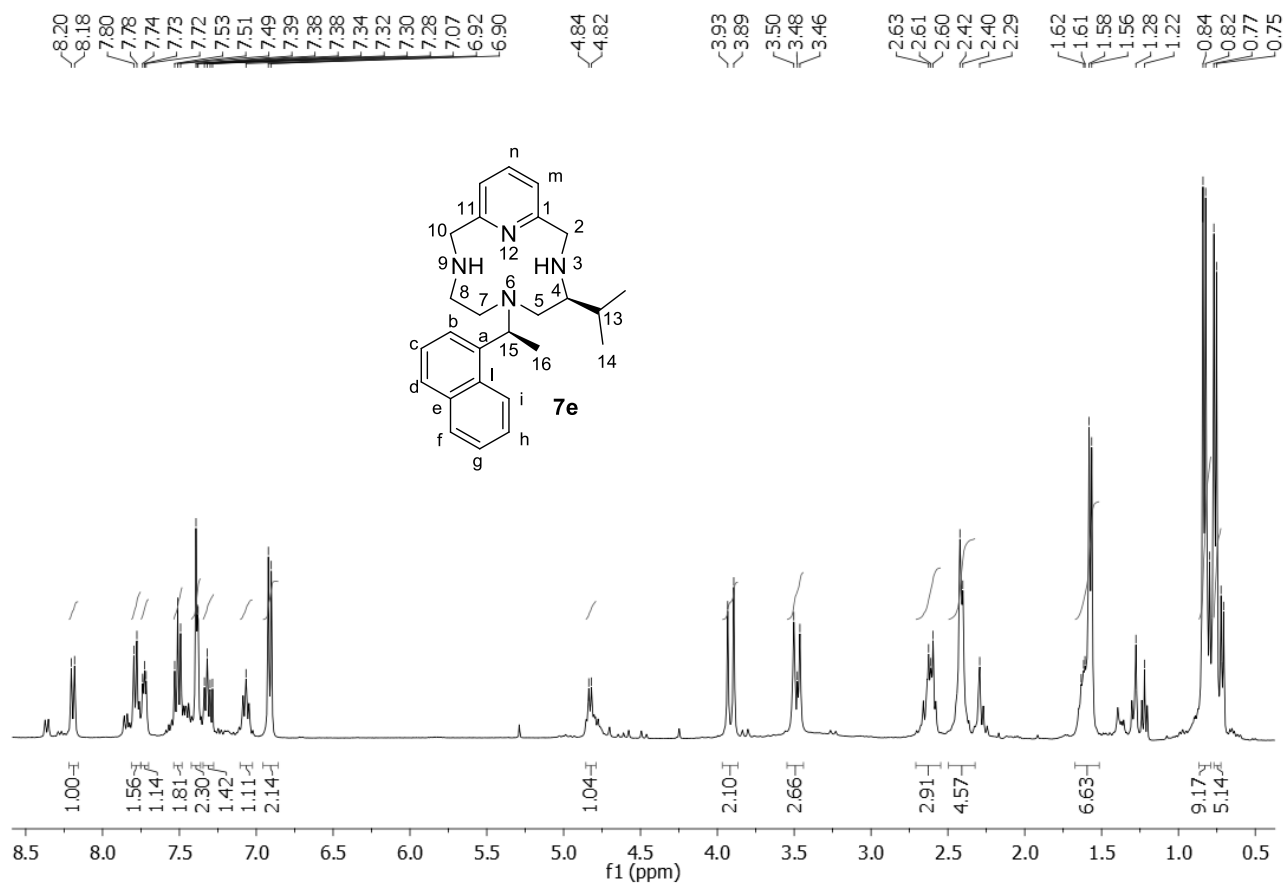


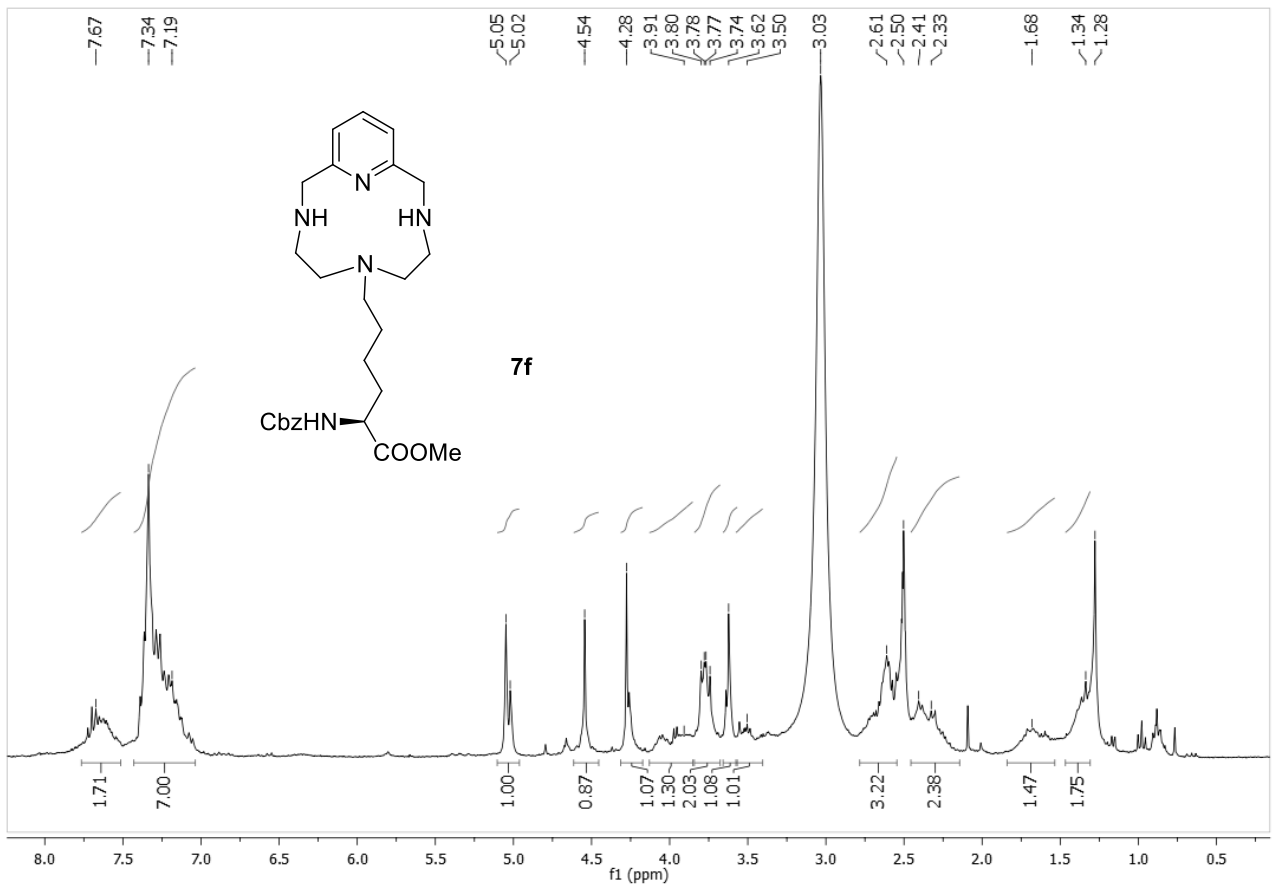


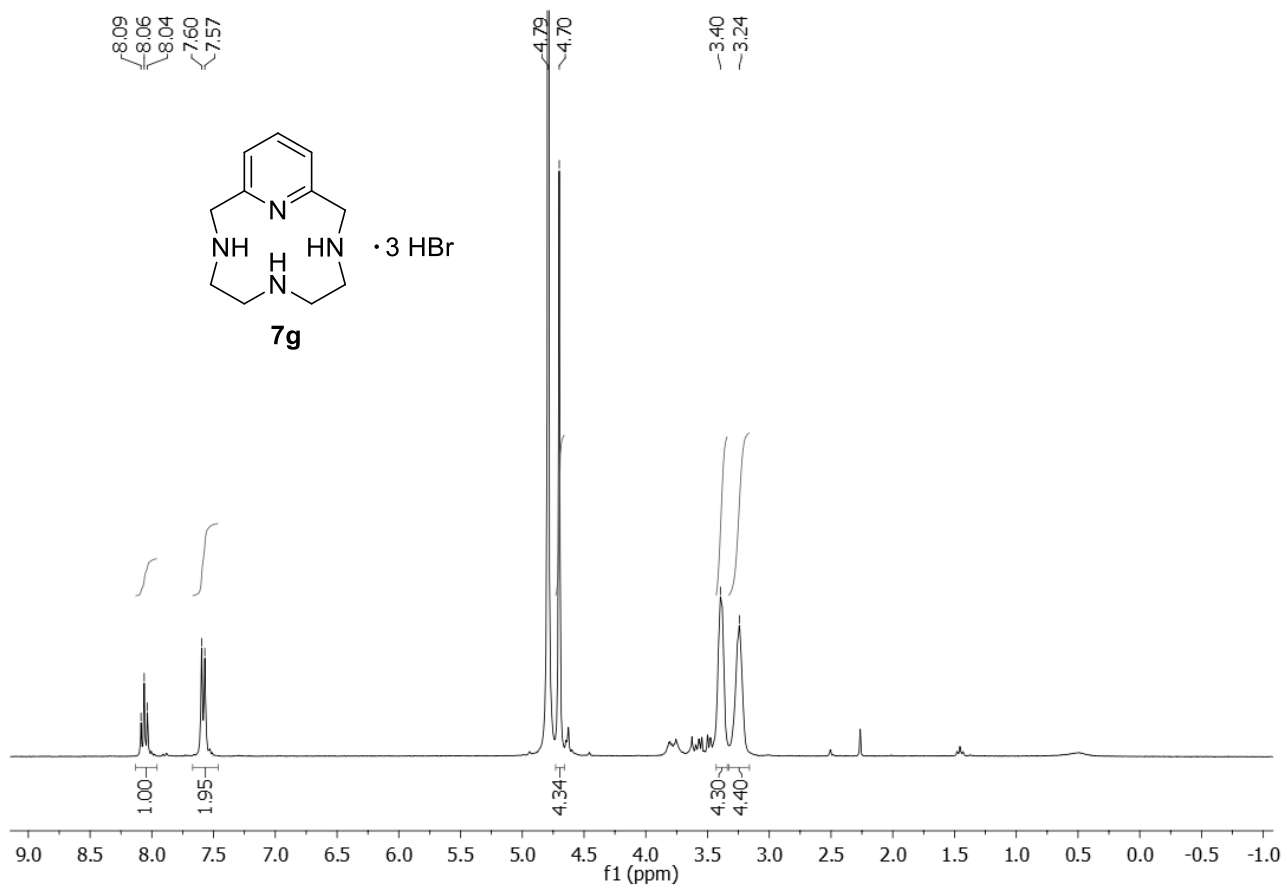


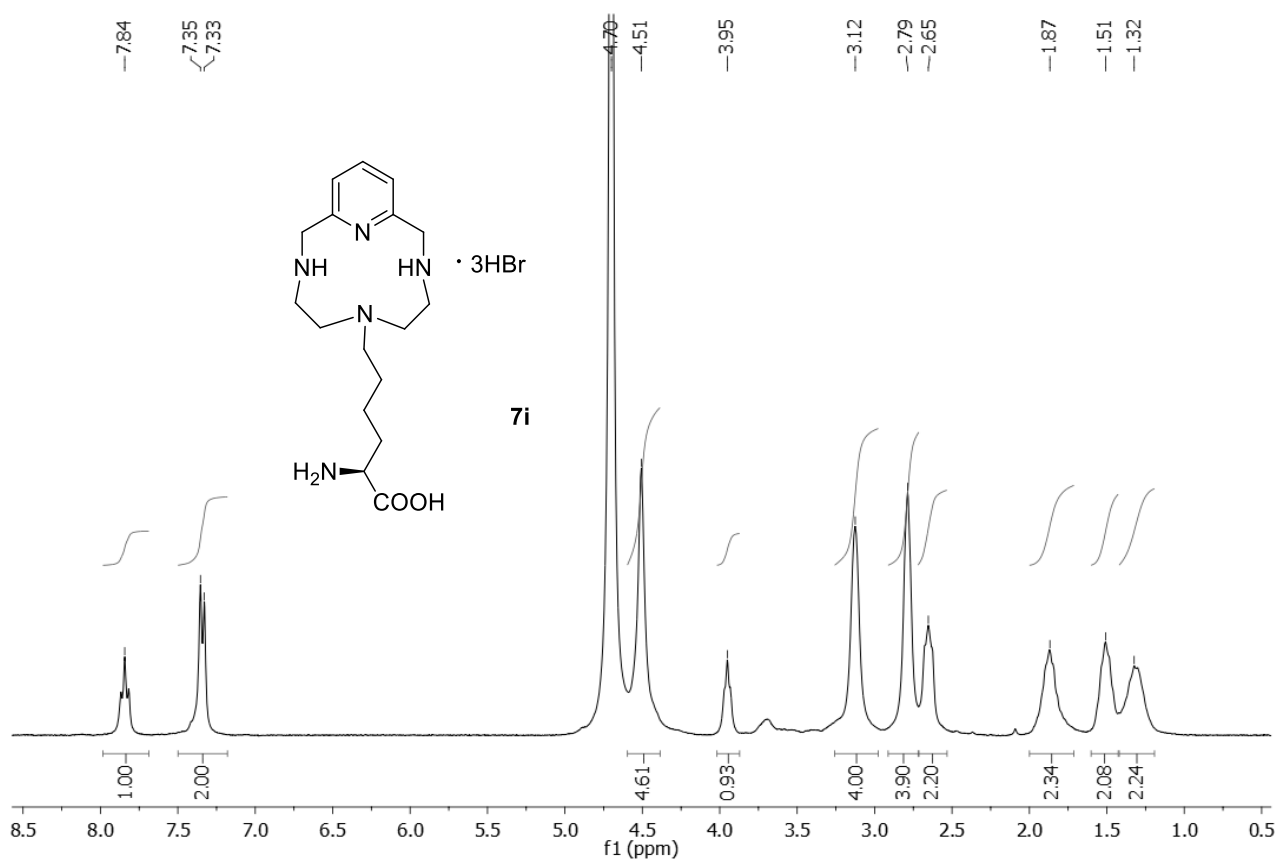


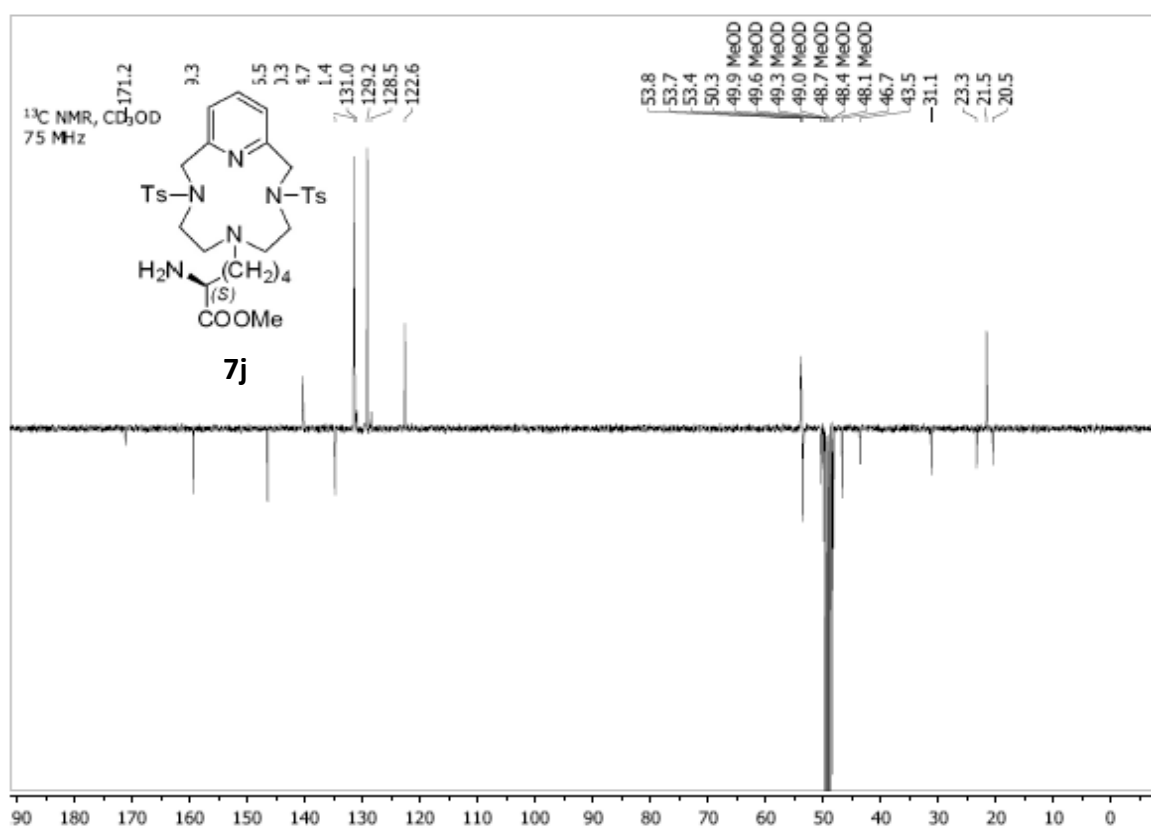
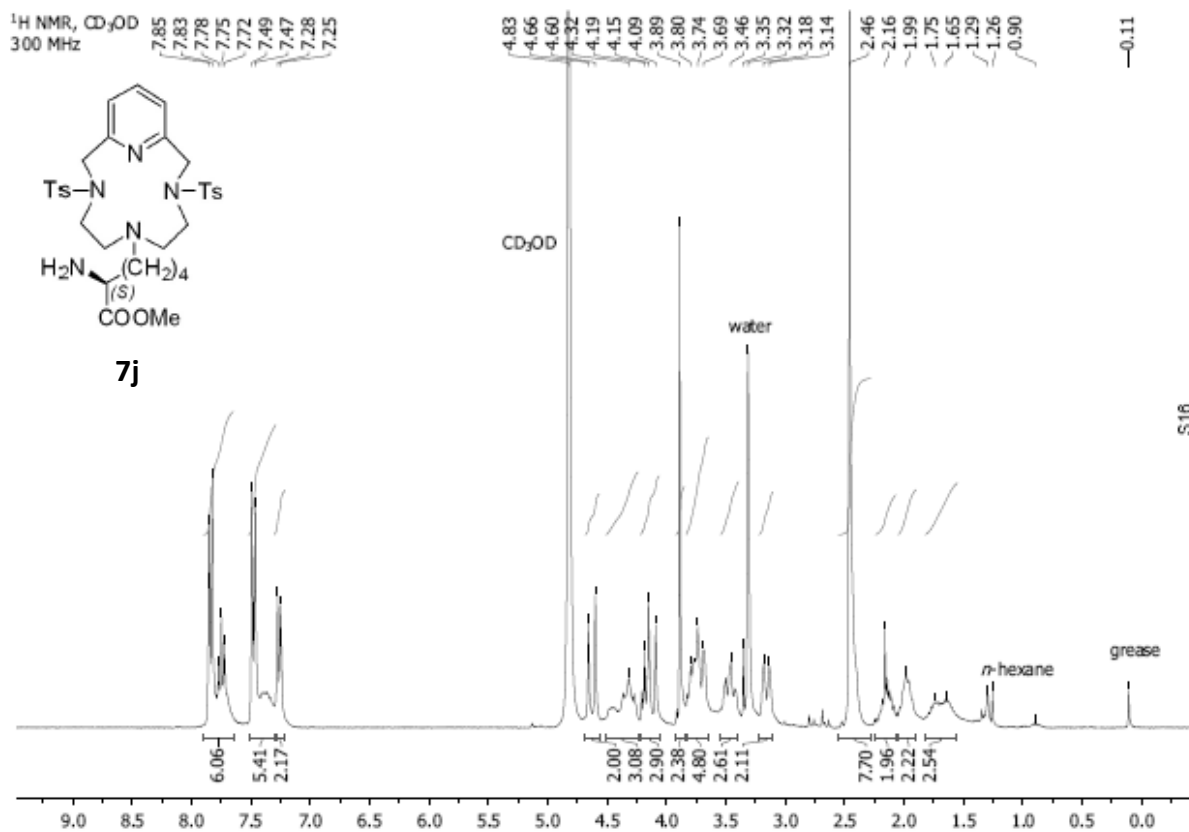


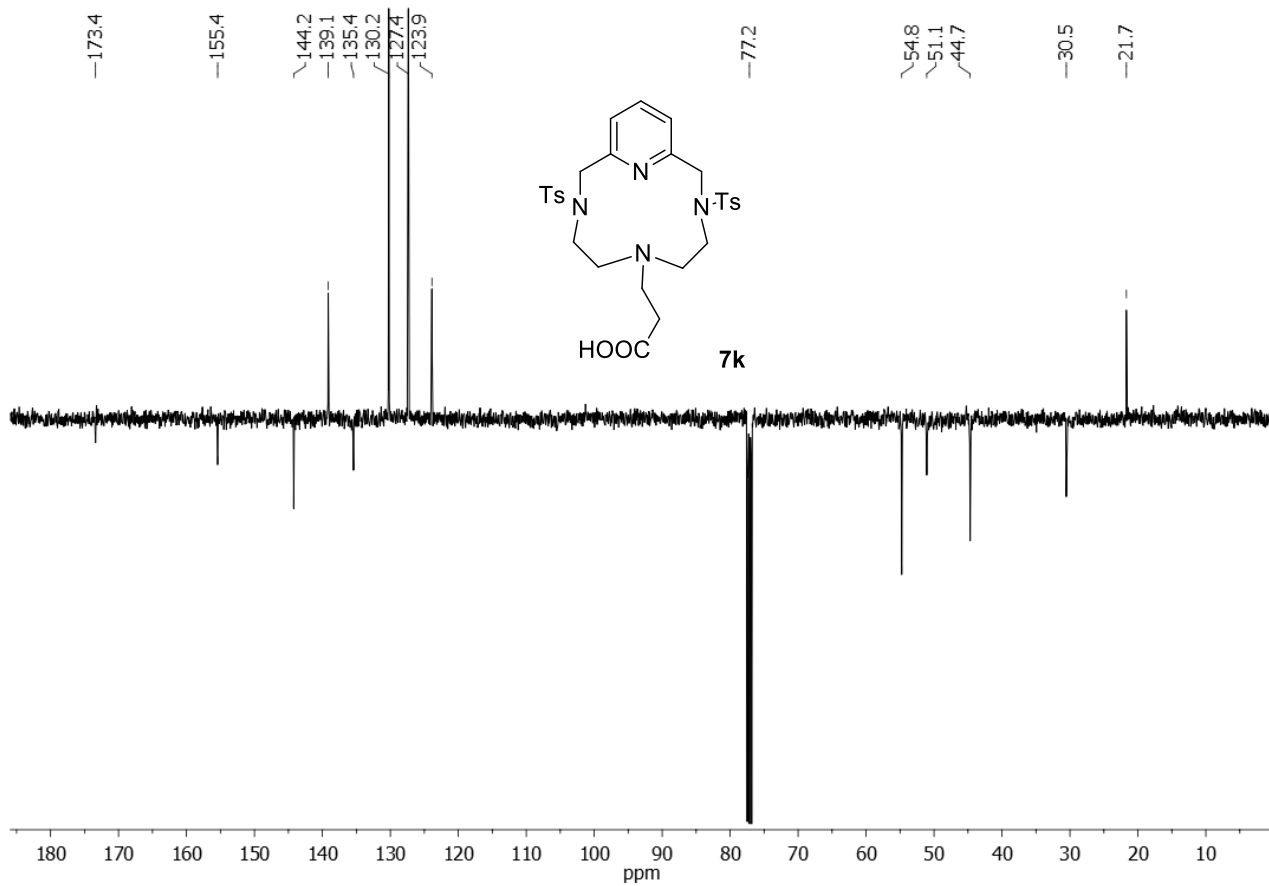
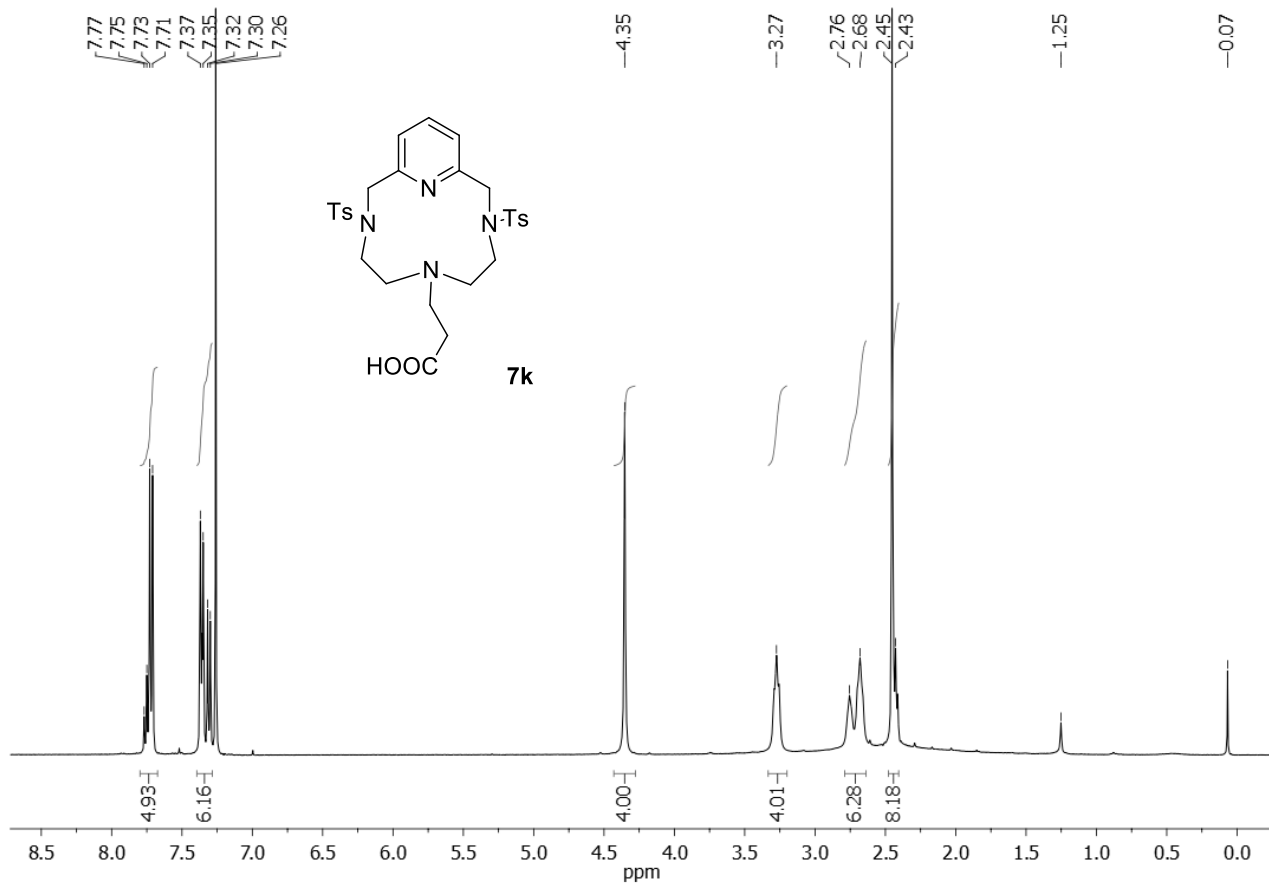


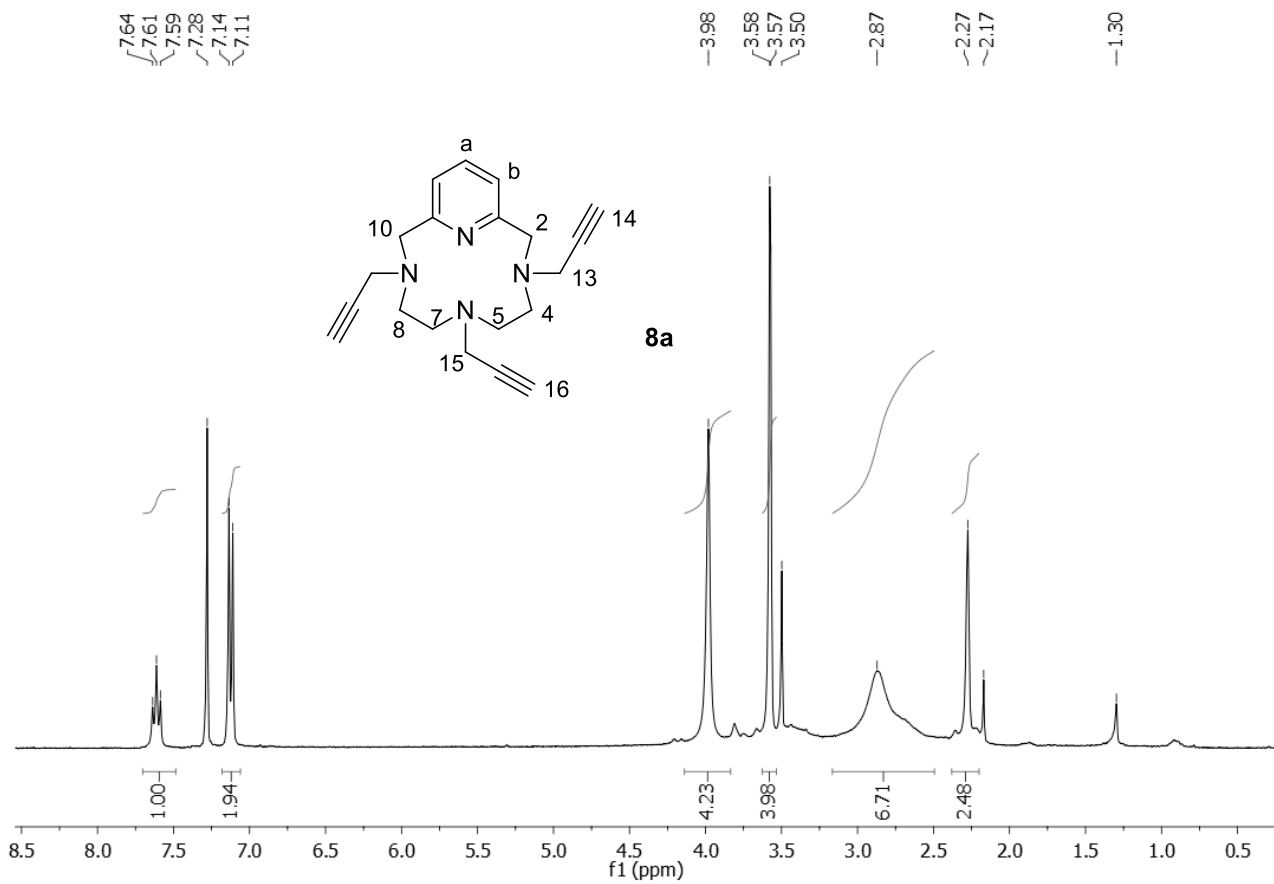


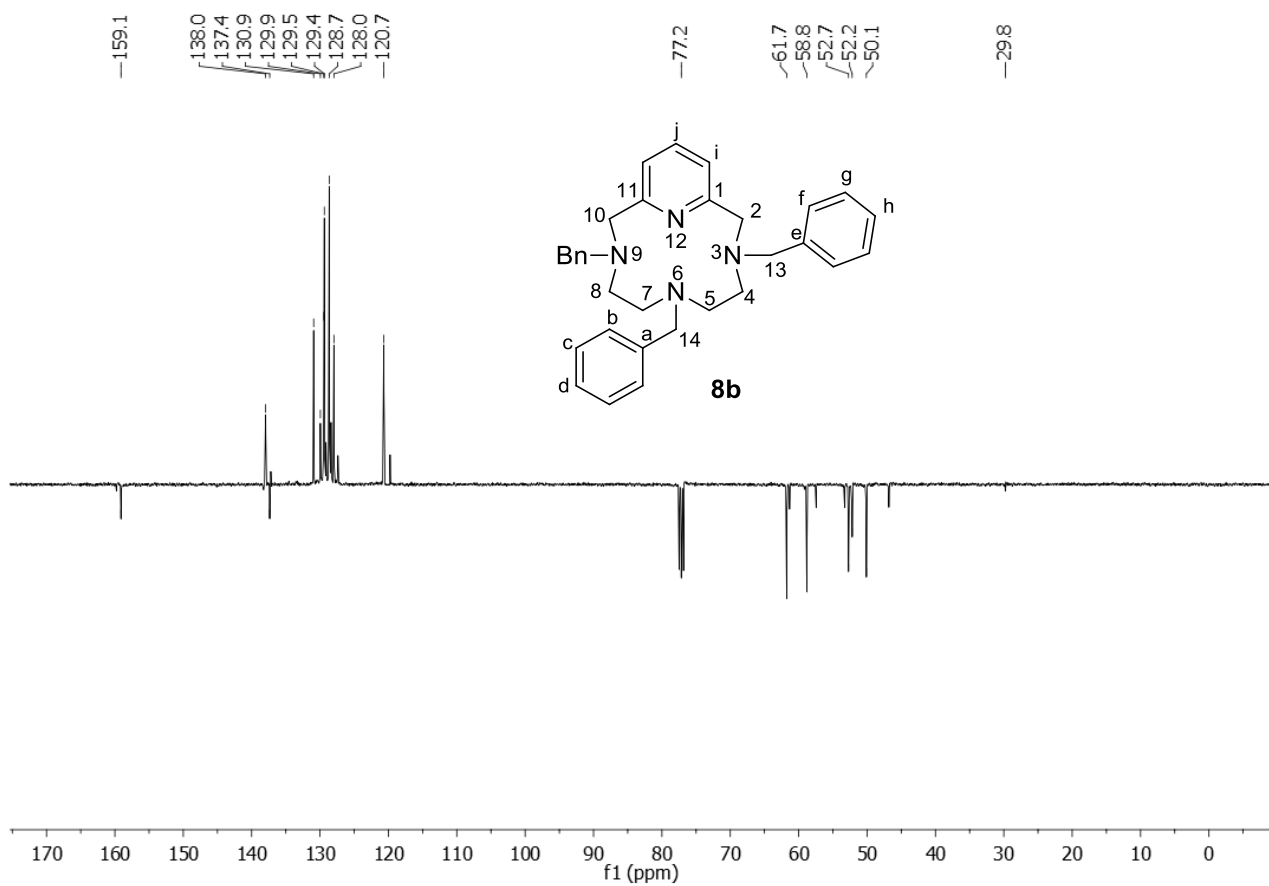
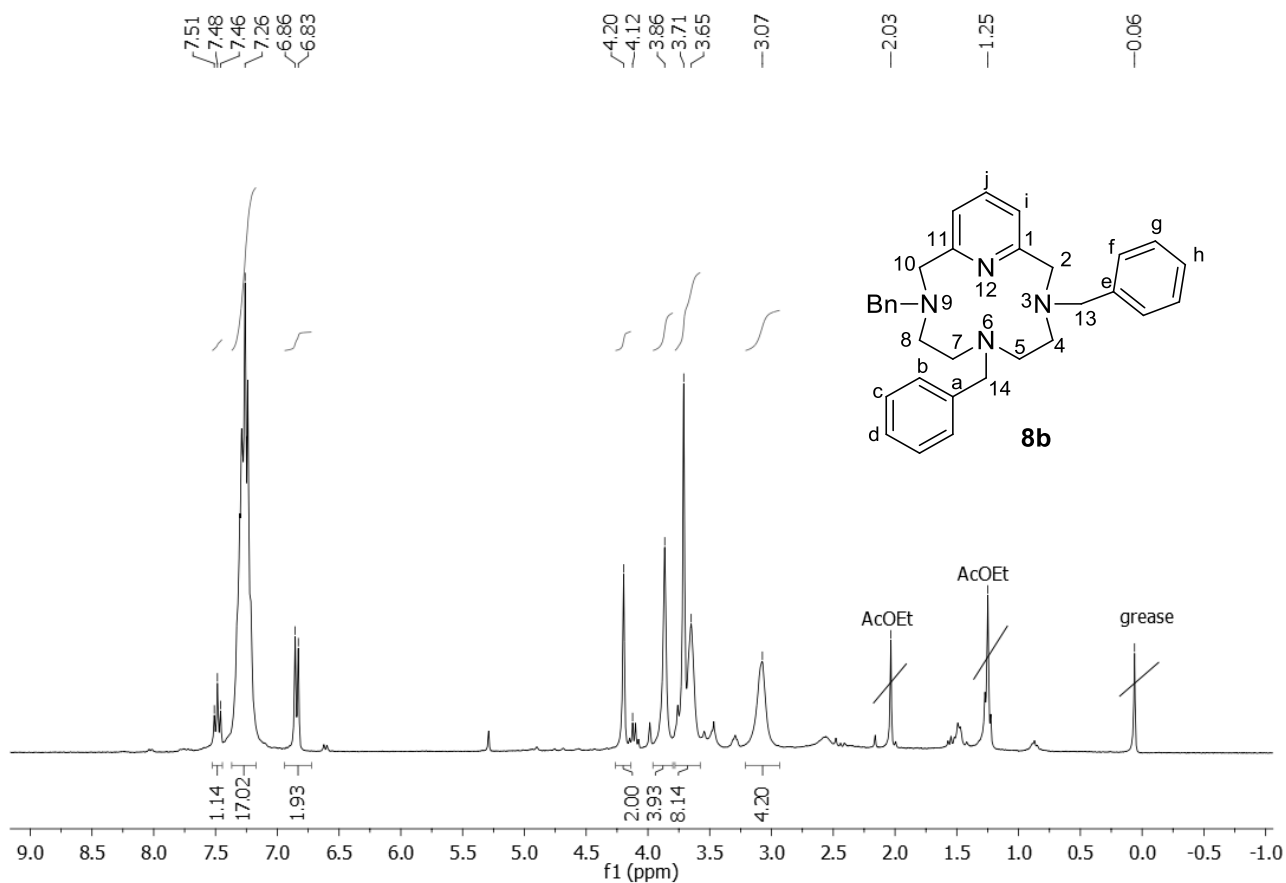








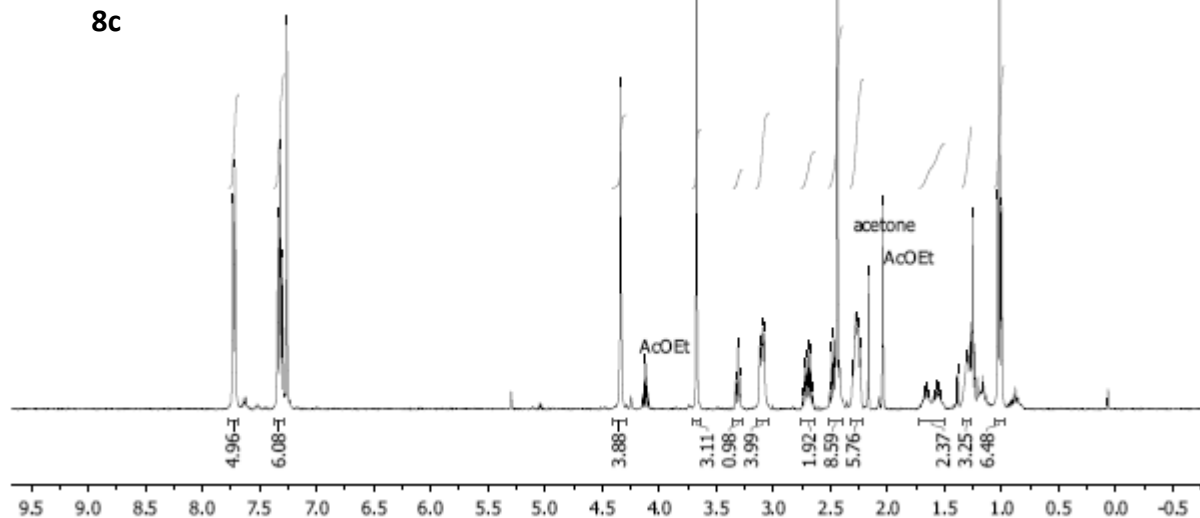
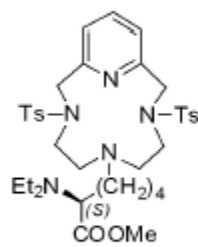




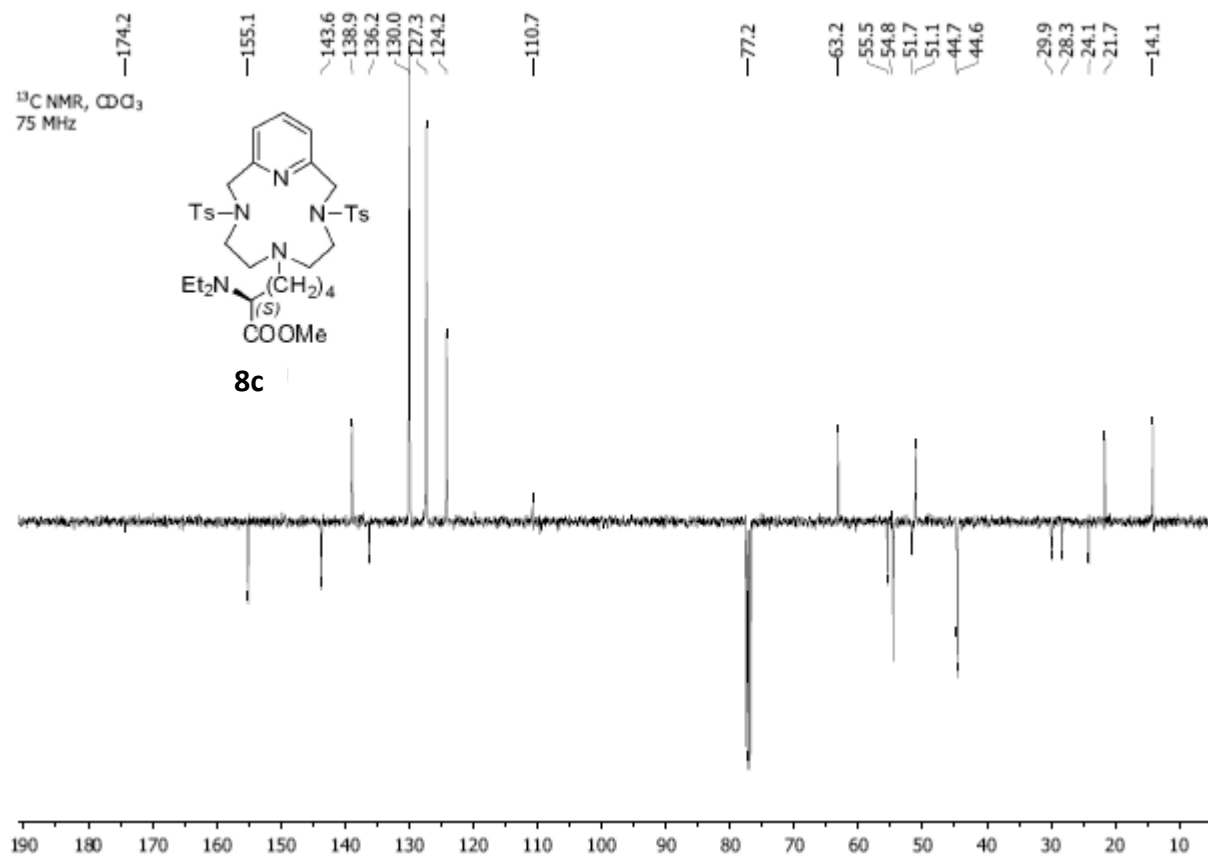
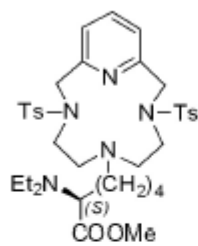
¹H NMR, CDCl₃
400 MHz

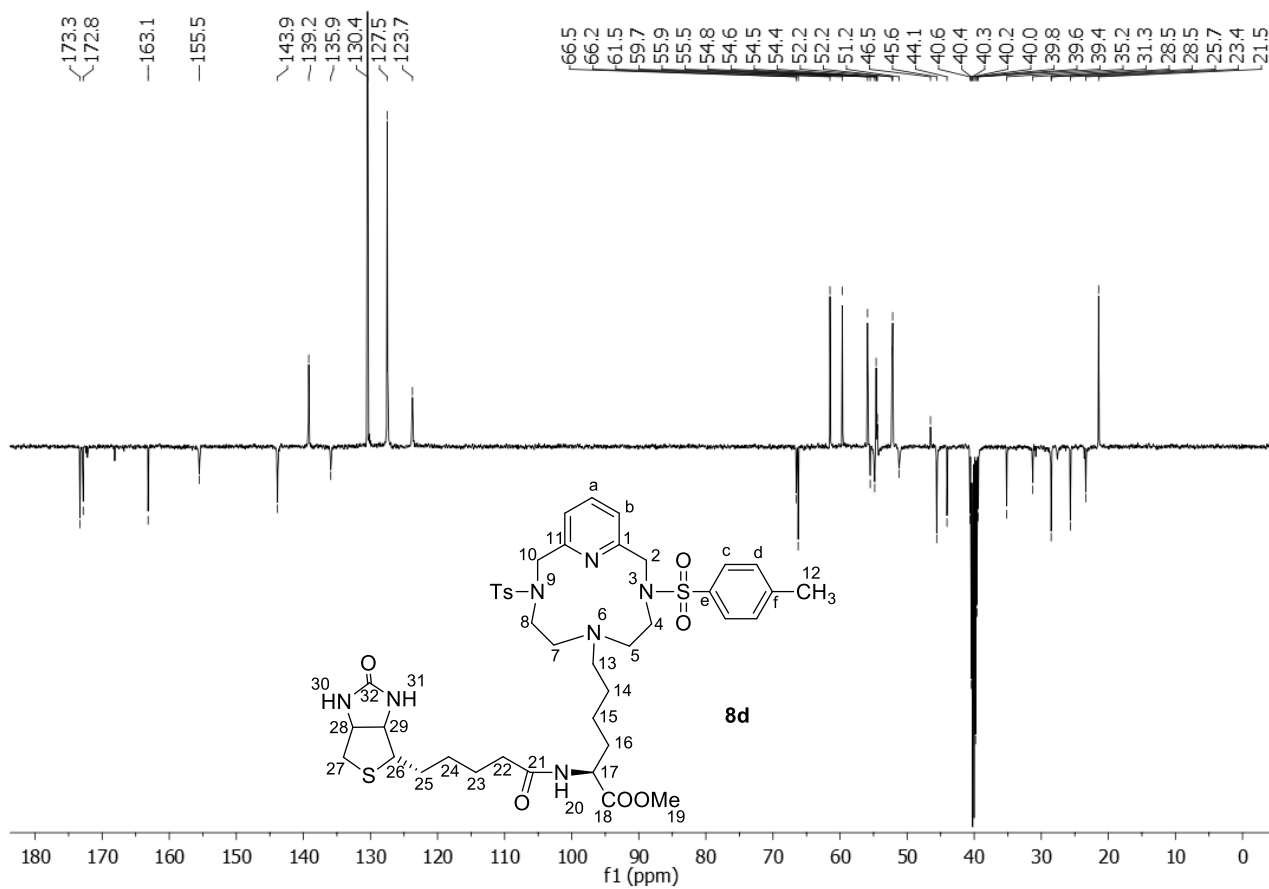
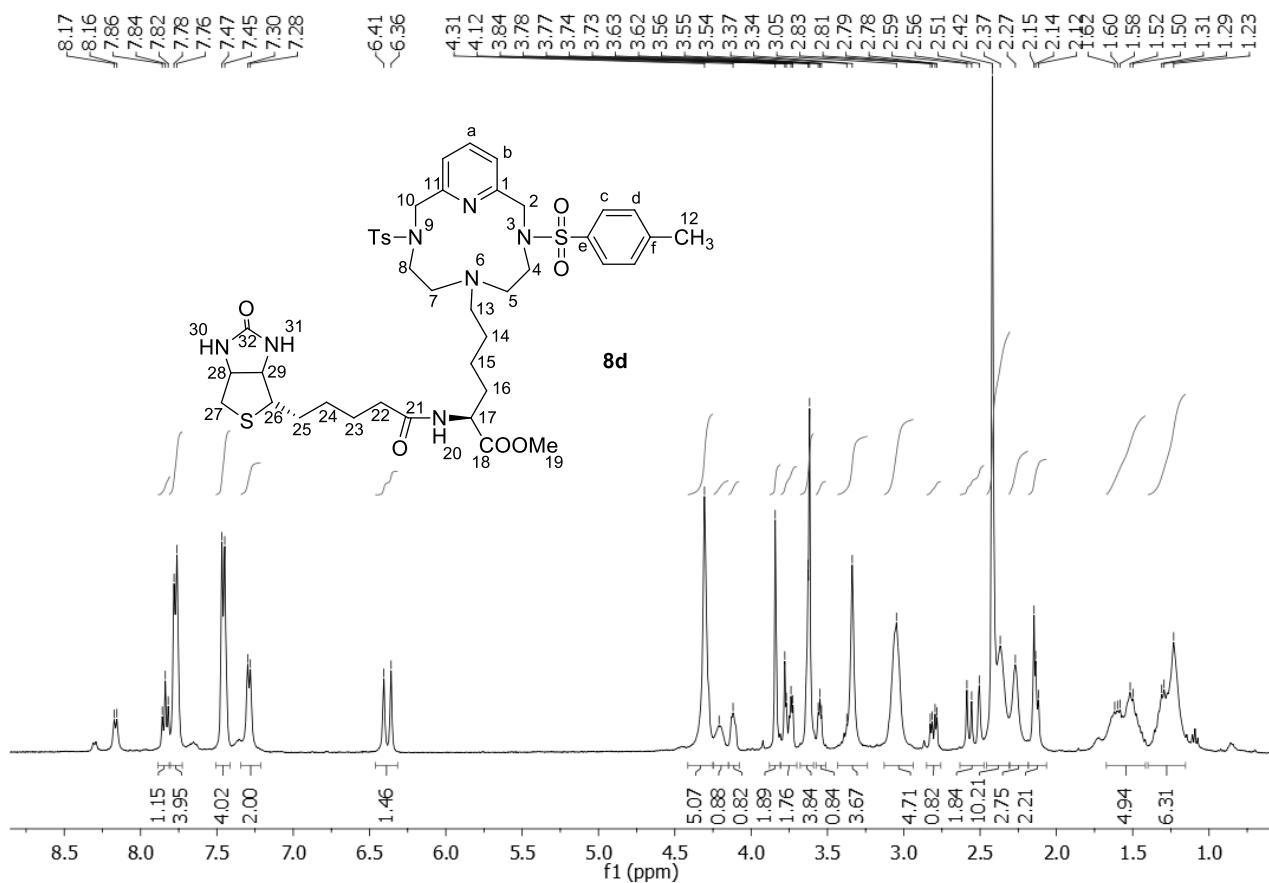
7.73
7.71
7.34
7.32
7.30
7.26

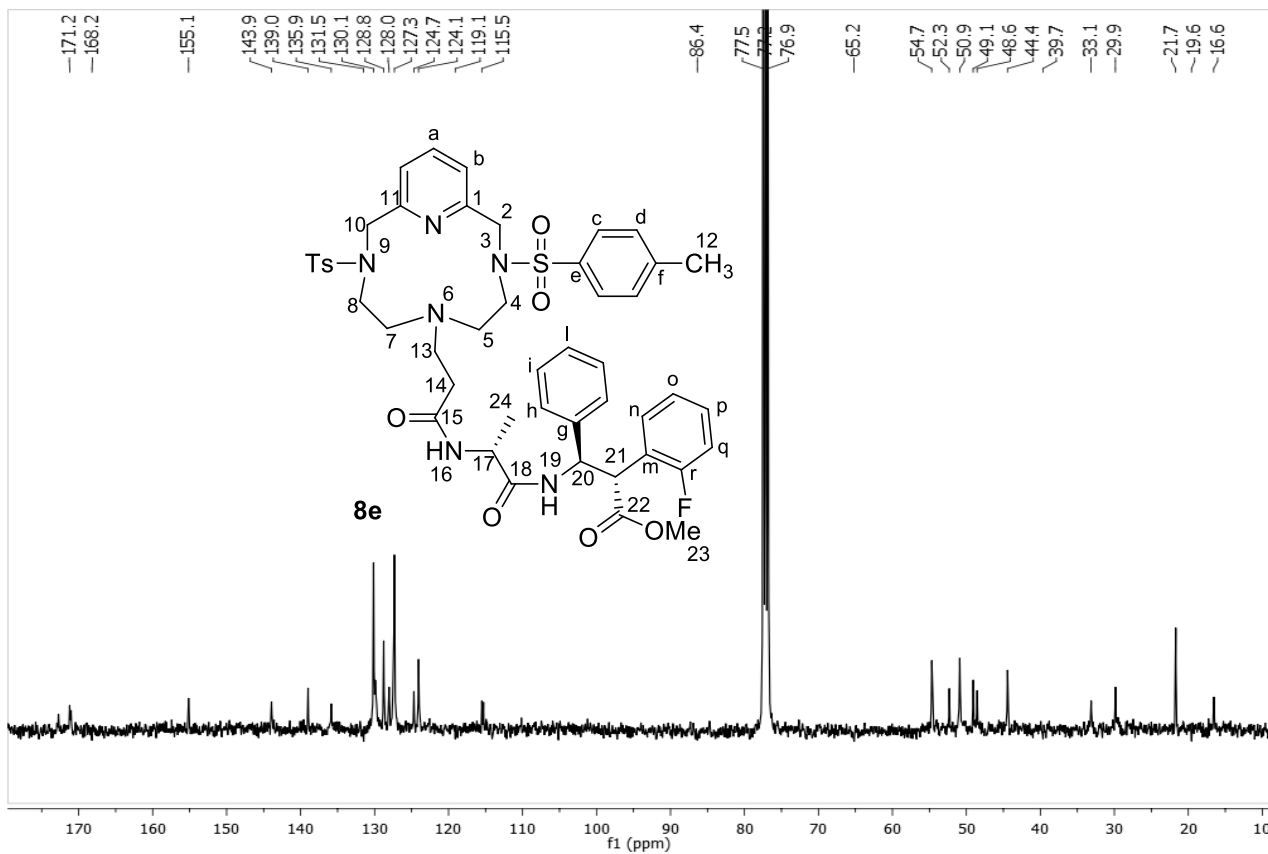
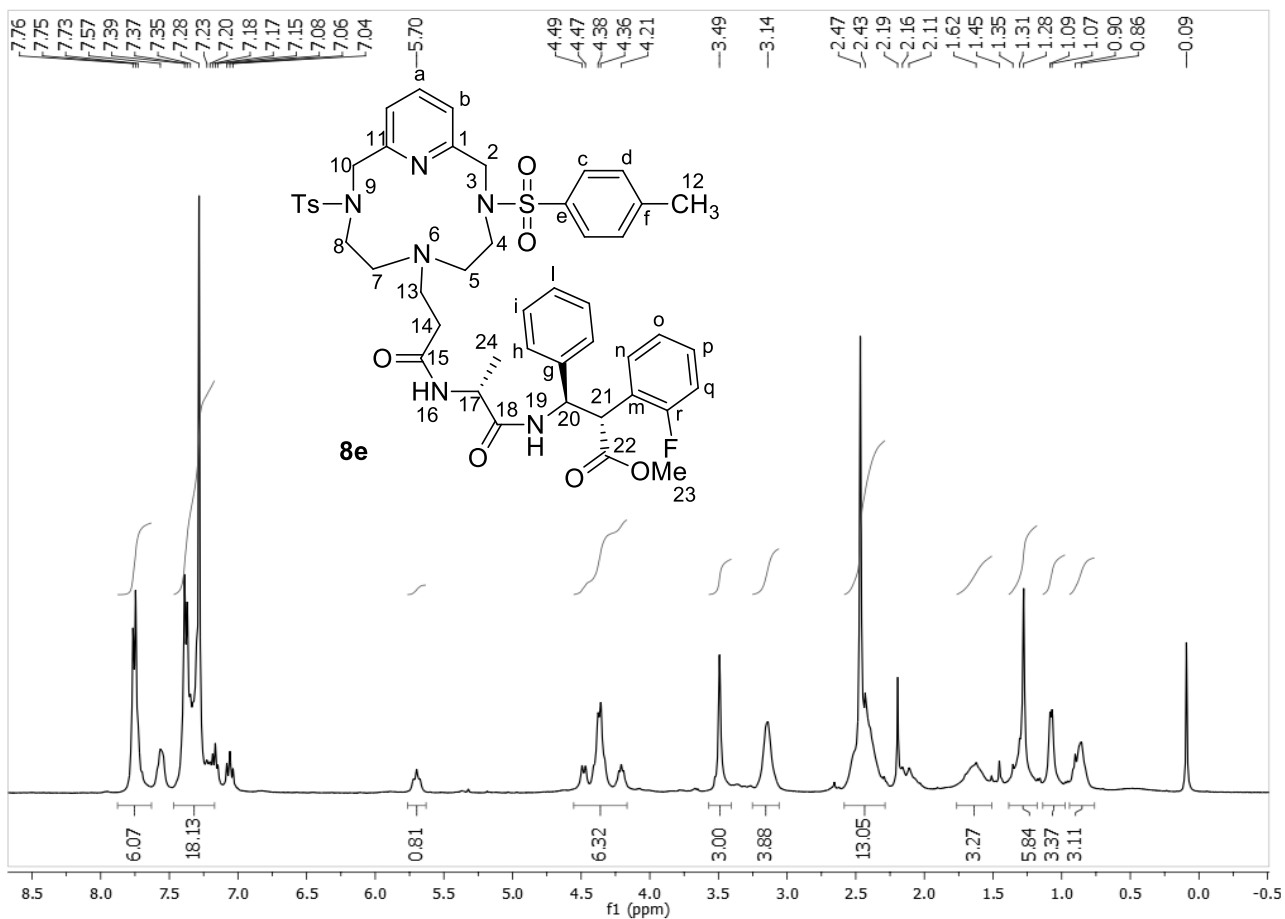
4.34
4.13
3.67
3.31
3.12
3.10
3.08
2.69
2.67
2.49
2.47
2.44
2.44
2.27
2.26
2.24
2.17
2.04
1.26
1.04
1.02
1.00



¹³C NMR, CDCl₃
75 MHz







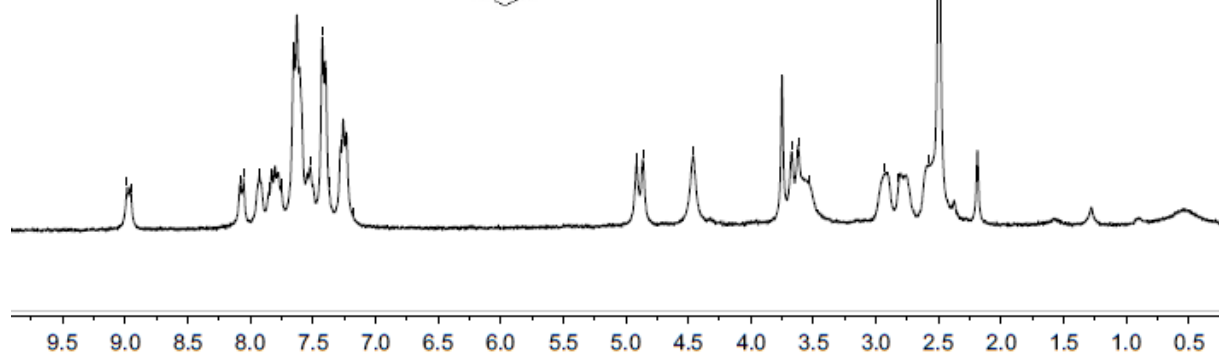
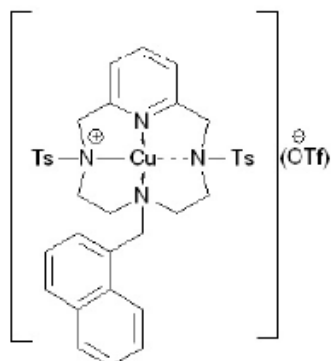
8.99
8.95
8.08
8.05
7.92
7.85
7.75
7.65
7.52
7.42
7.37
7.27
7.17

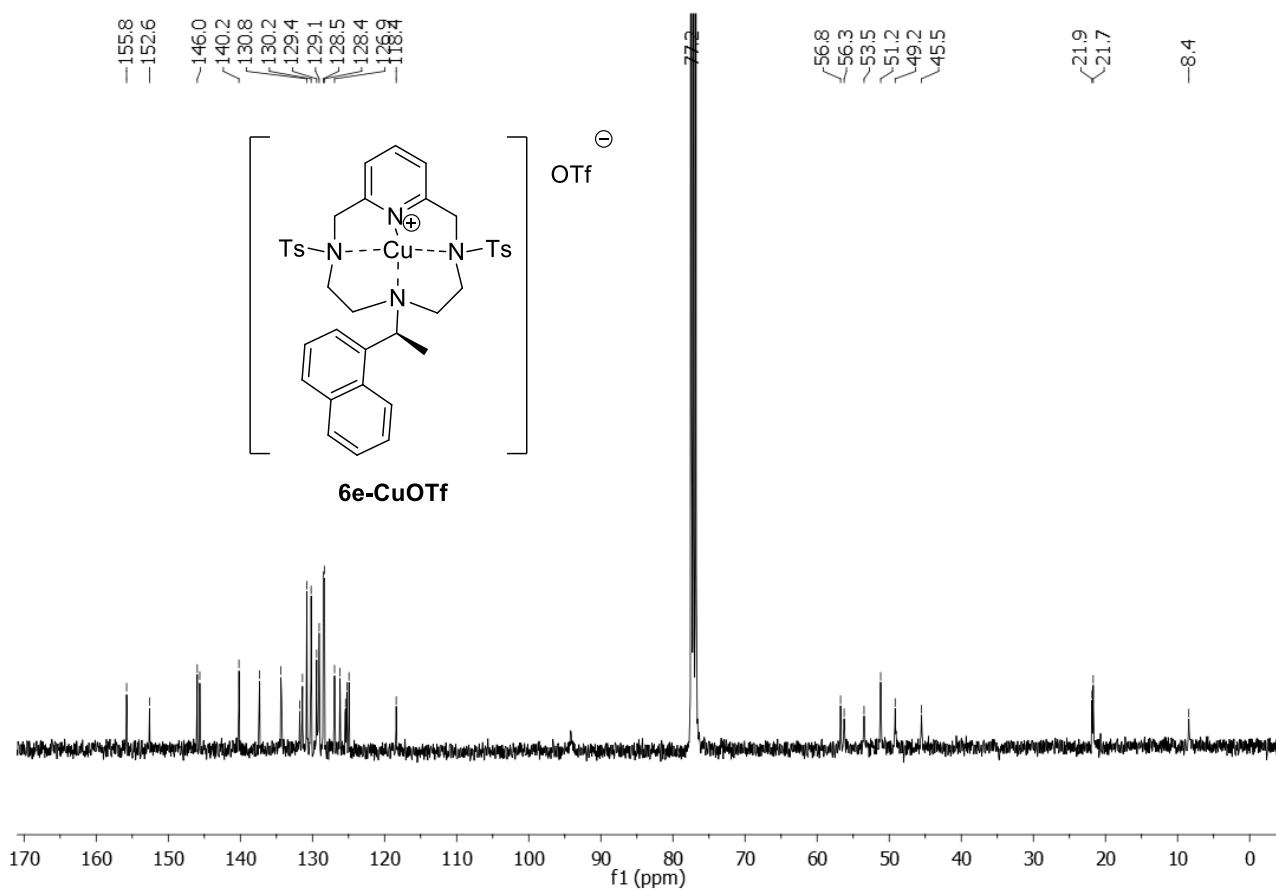
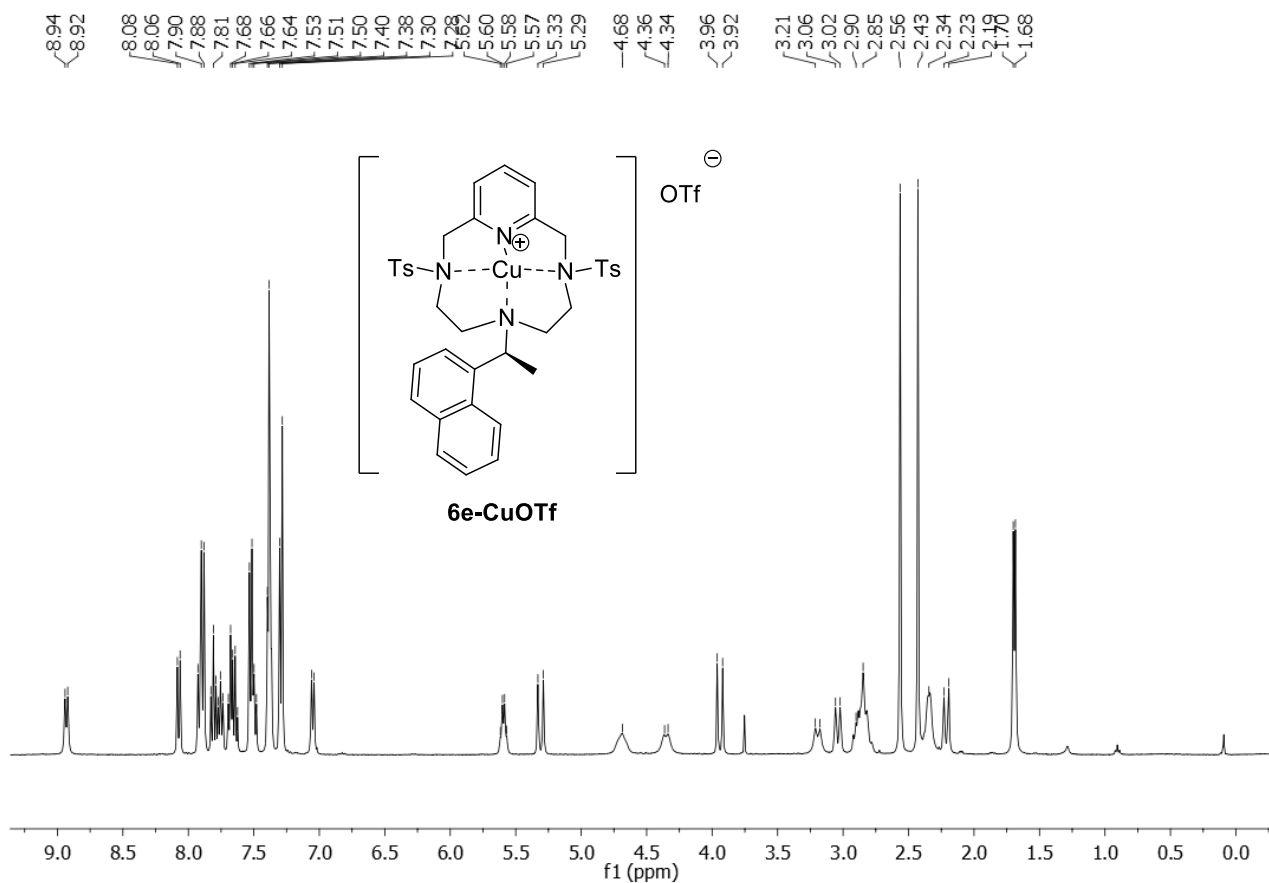
4.91
4.86
4.46

3.68
3.62
3.53

2.93
2.82
2.58
2.50

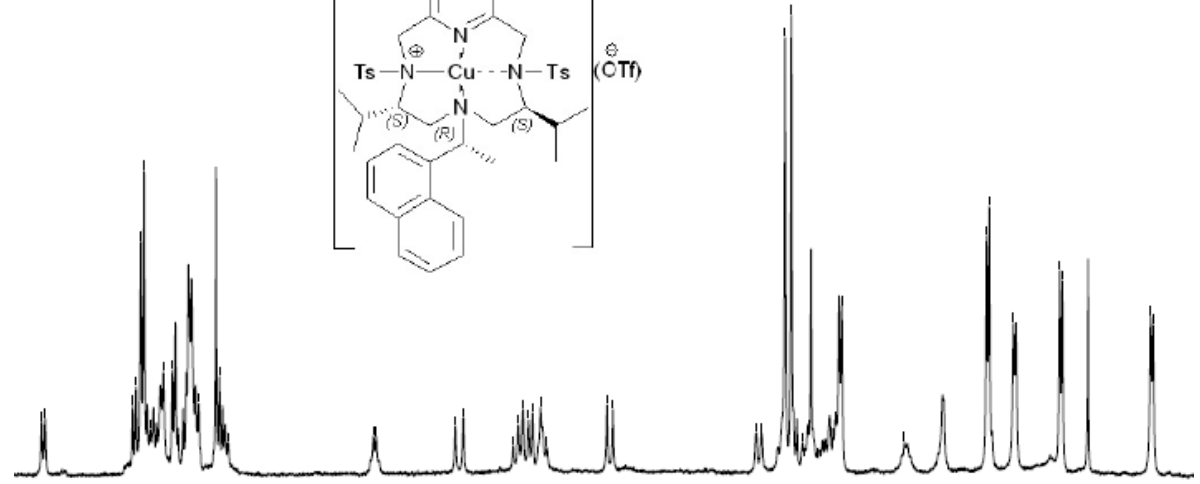
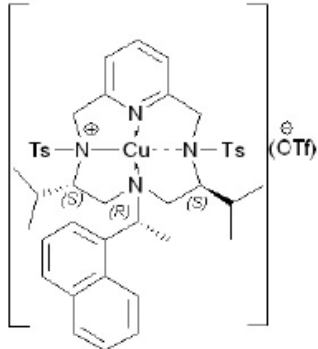
6d-CuOTf





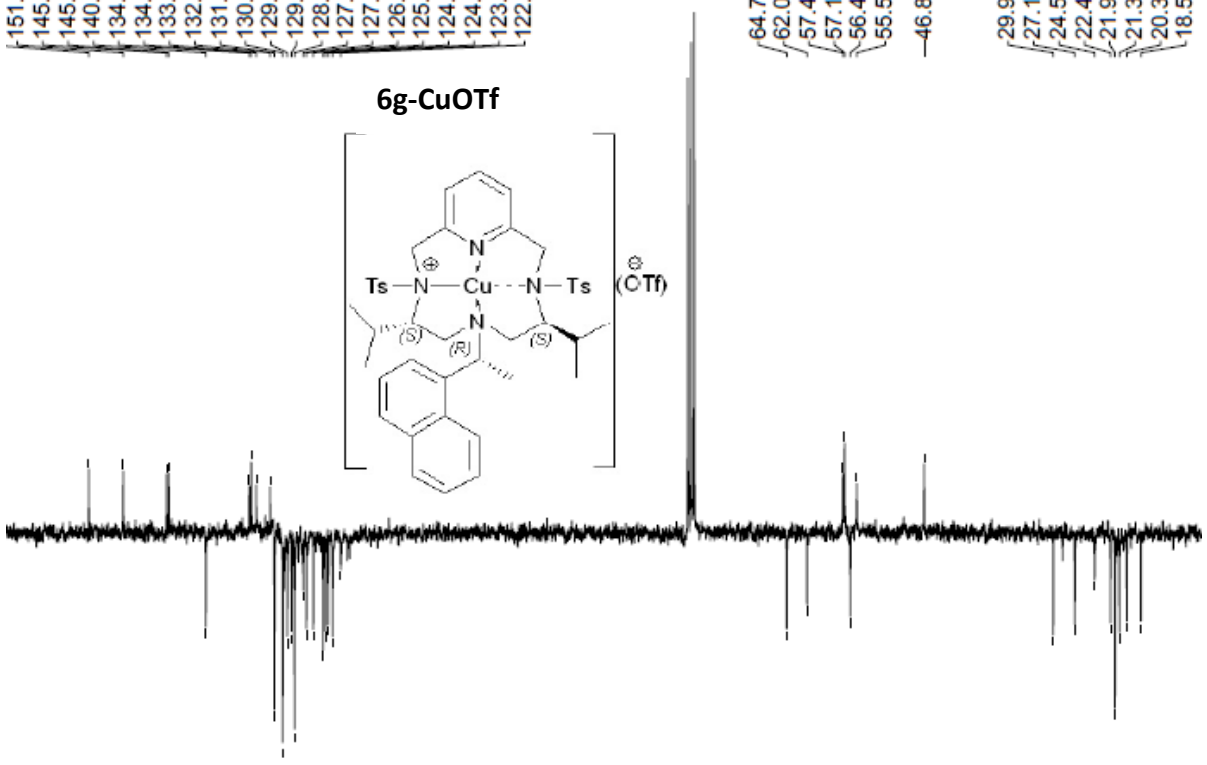
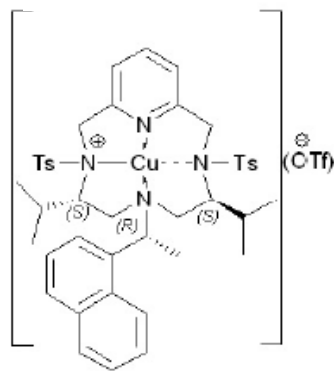
8.70 8.67 7.95 7.92 7.88 7.85 7.80 7.69 7.62 7.40 7.23 7.16
 5.96 5.94 5.29 5.22 4.73 4.68 4.65 4.58 4.54 3.99
 2.81 2.76 2.57 2.52 2.42 2.37 2.30 2.15 2.10 -1.59
 -0.91 -0.88 -0.69 -0.66 -0.30 -0.28
 -0.45 -0.47

6g-CuOTf

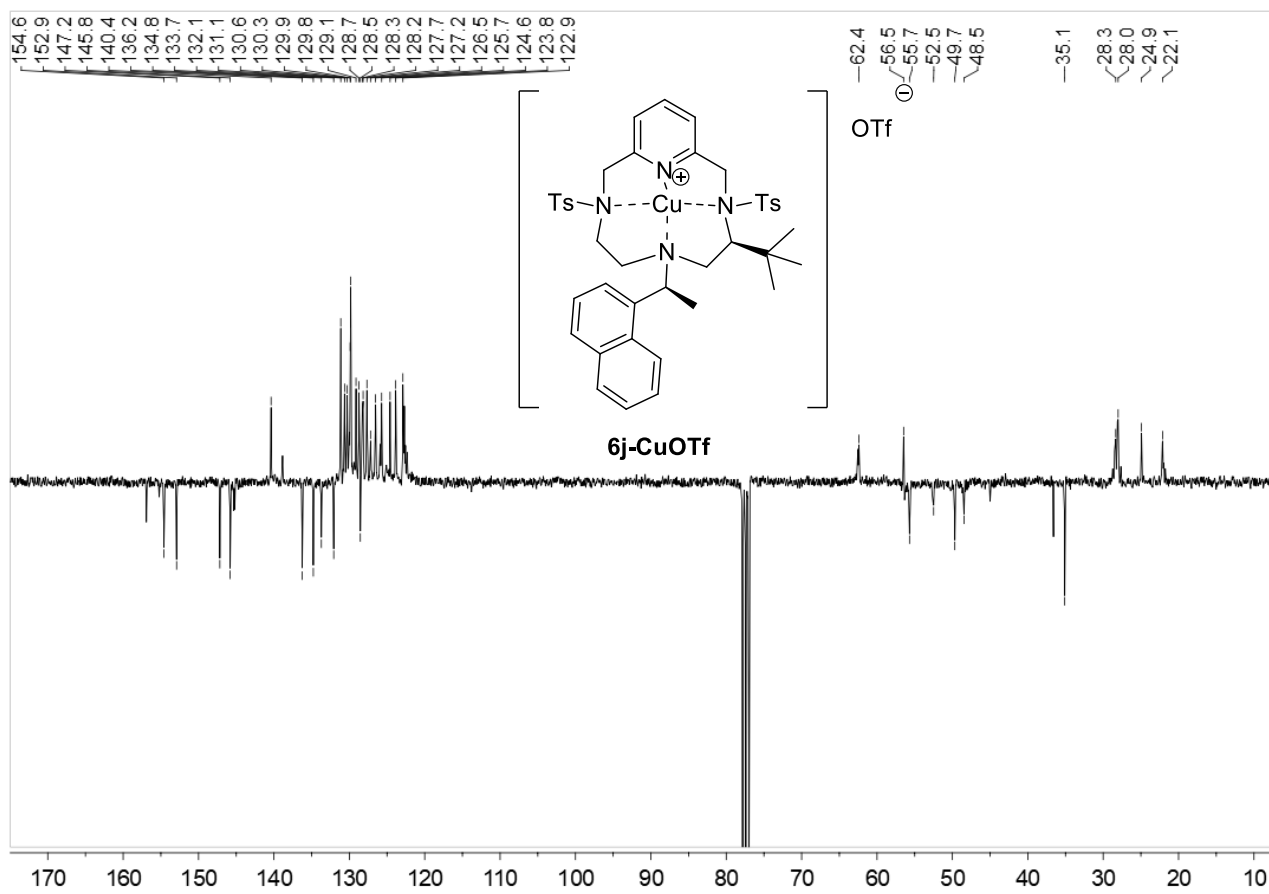
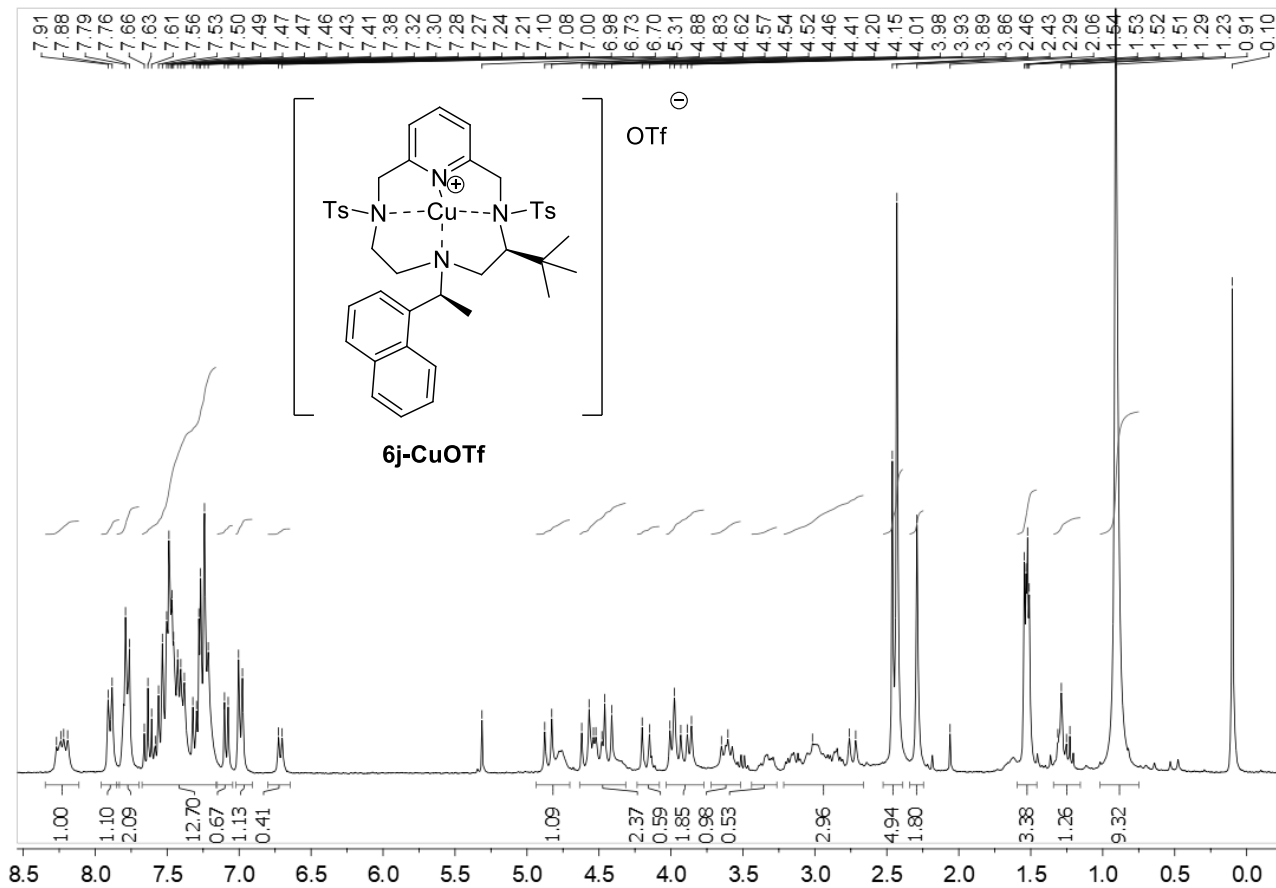


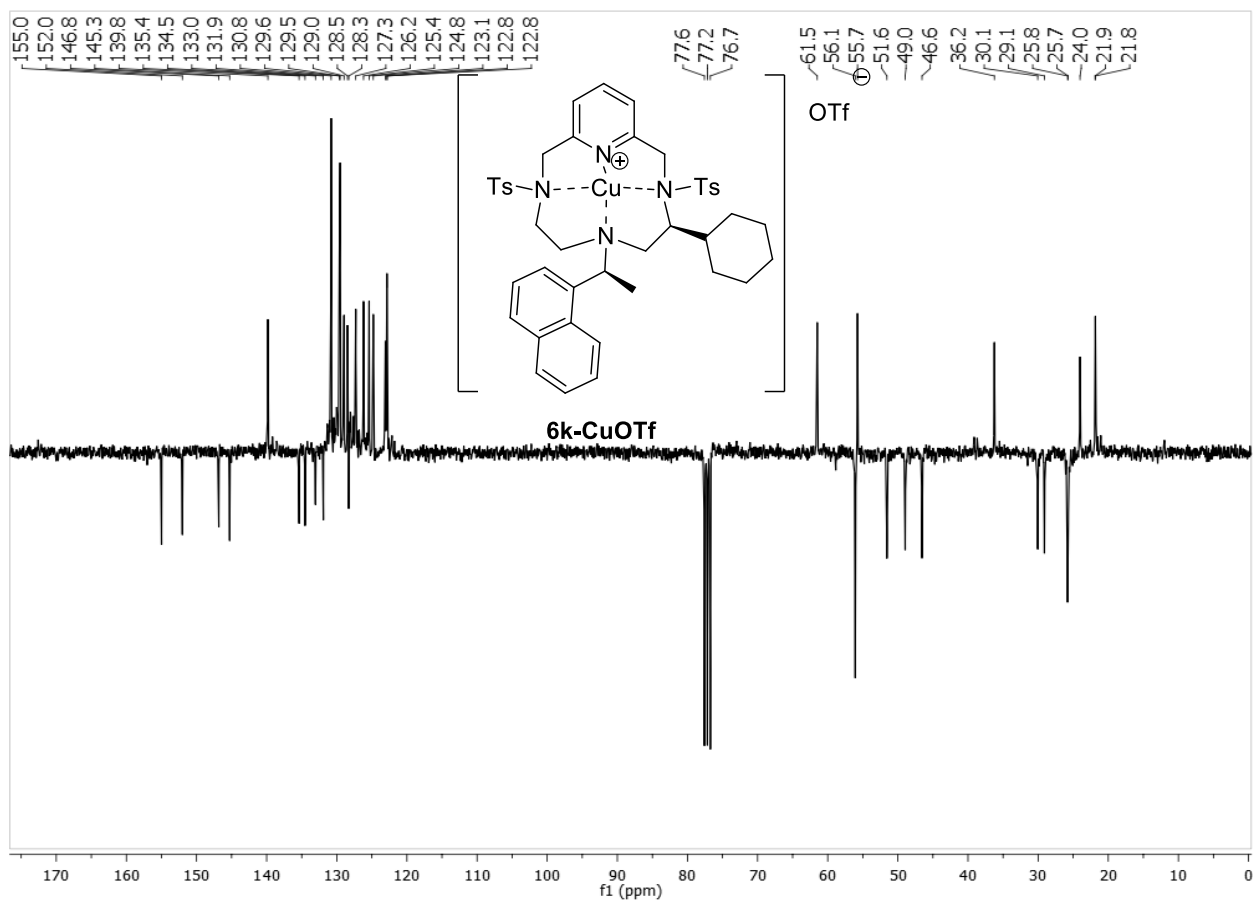
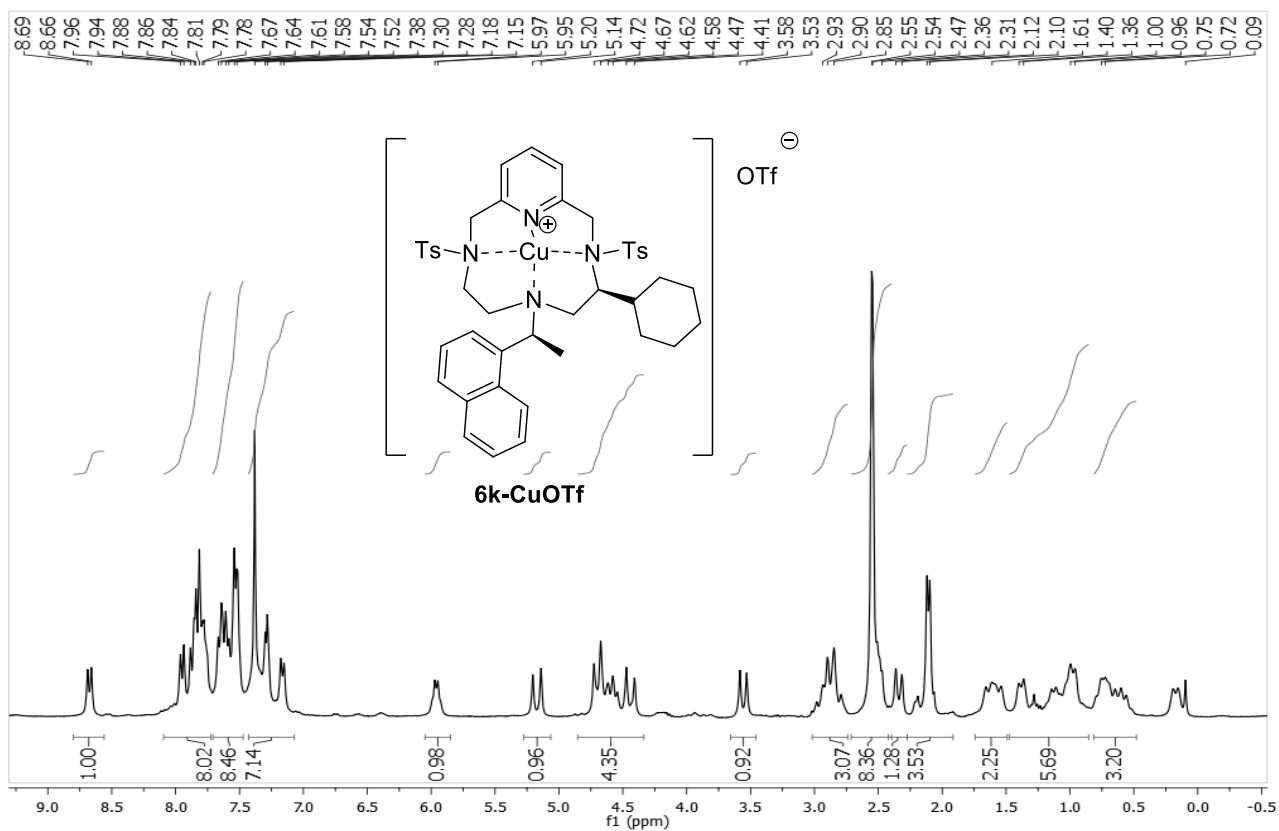
151.2 145.6 145.3 140.4 134.8 134.5 133.9 132.1 131.5 130.4 129.8 129.3 128.9 127.7 127.3 126.4 125.2 124.8 124.5 123.9 122.8
 64.7 62.0 57.4 57.1 56.4 55.5 46.8 29.9 27.1 24.5 22.4 21.9 21.3 20.3 18.5

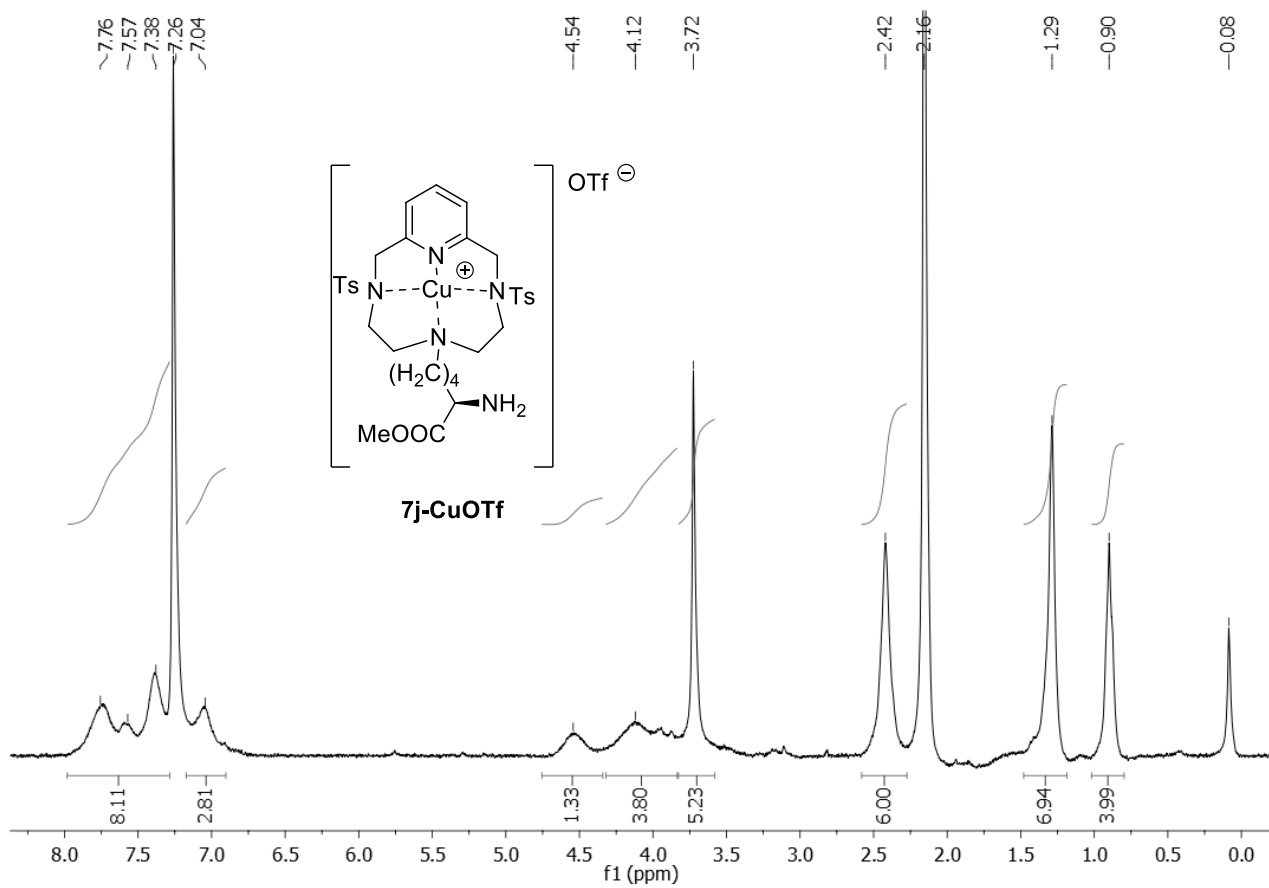
6g-CuOTf

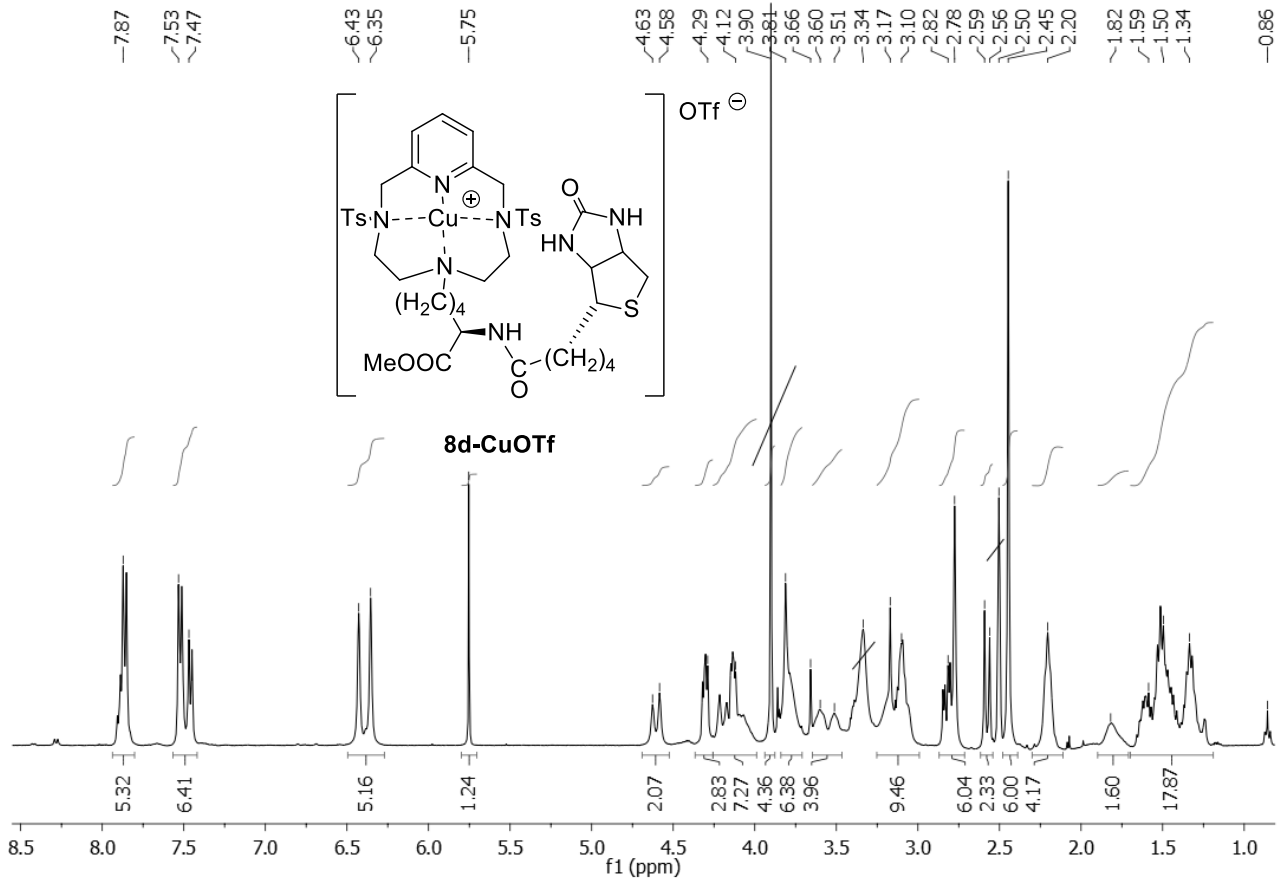


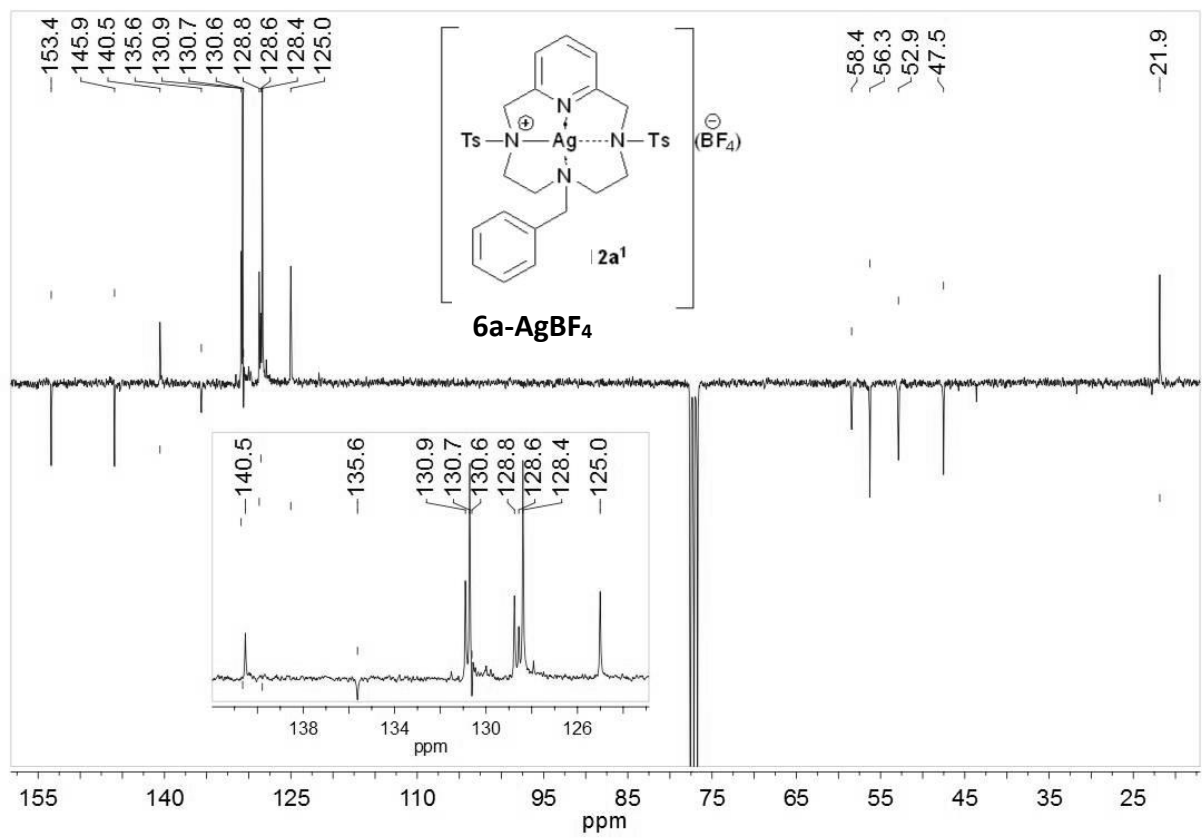
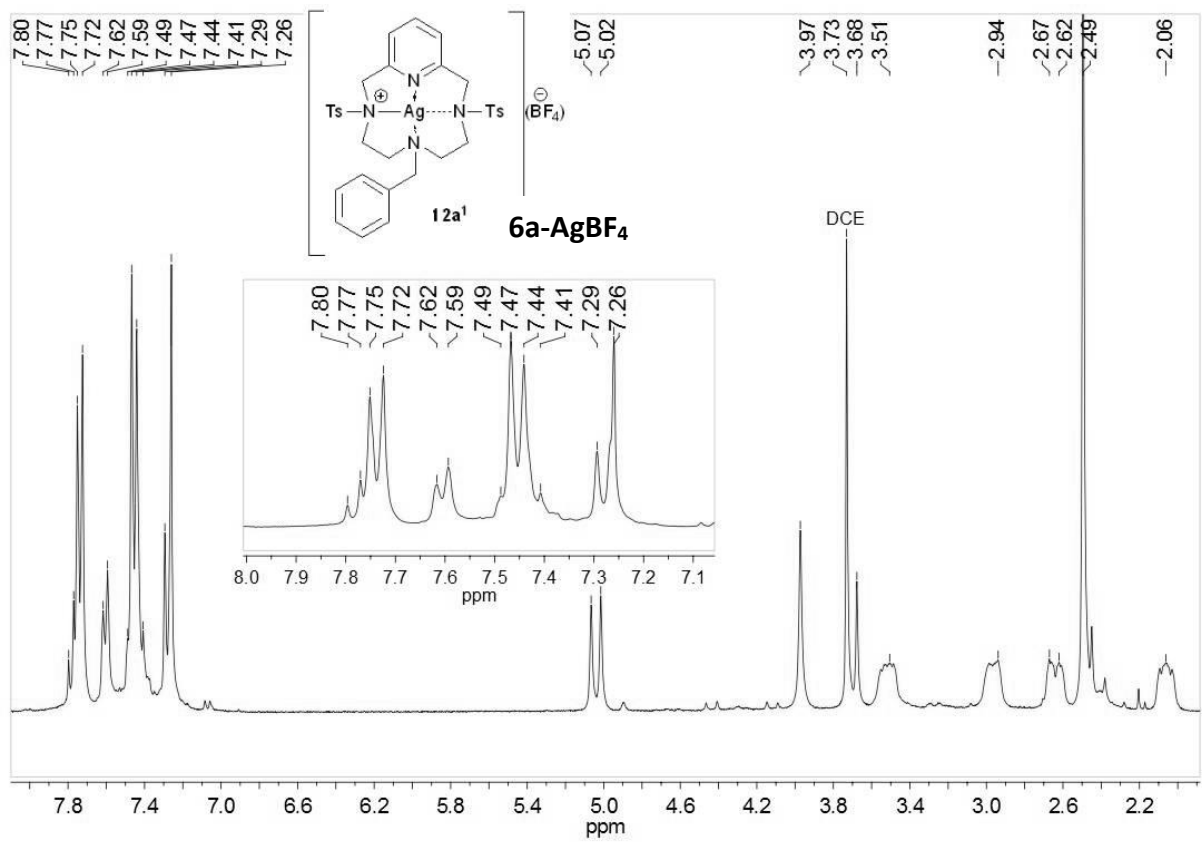
160 150 140 130 120 110 100 90 80 70 60 50 40 30 20 1

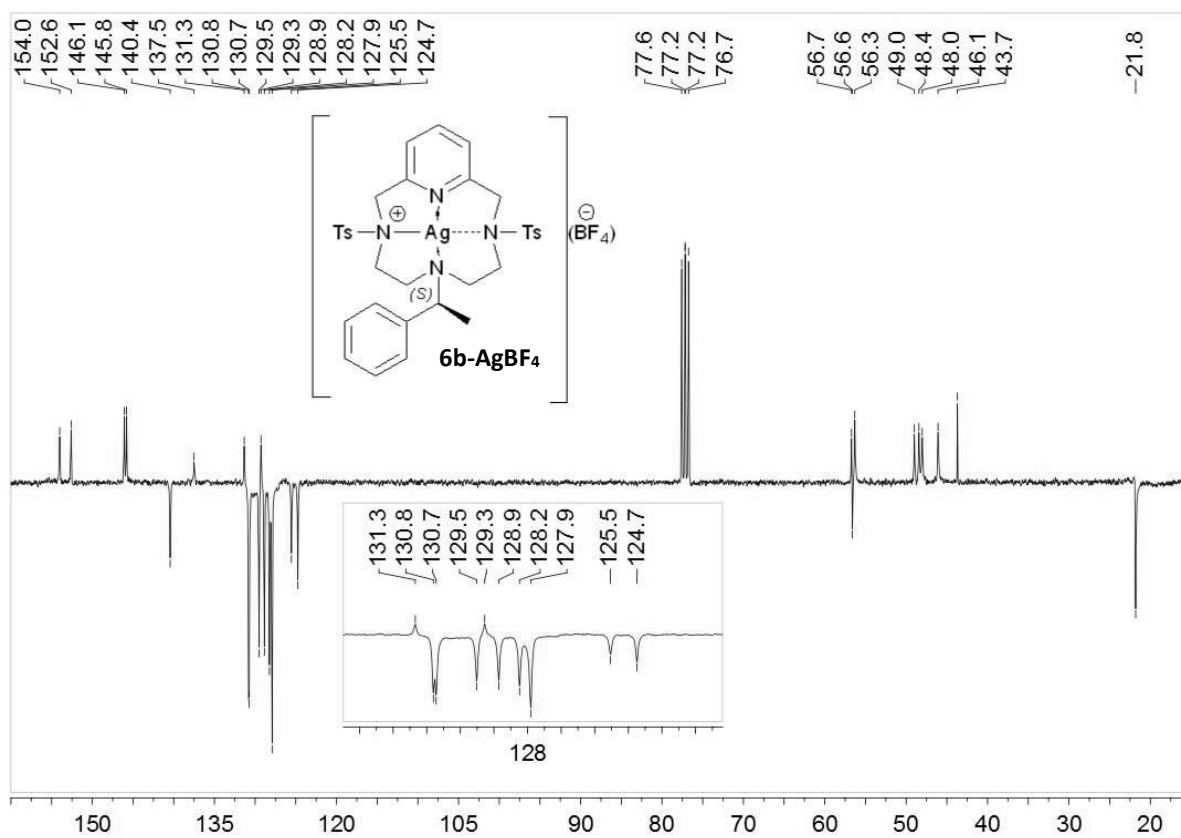
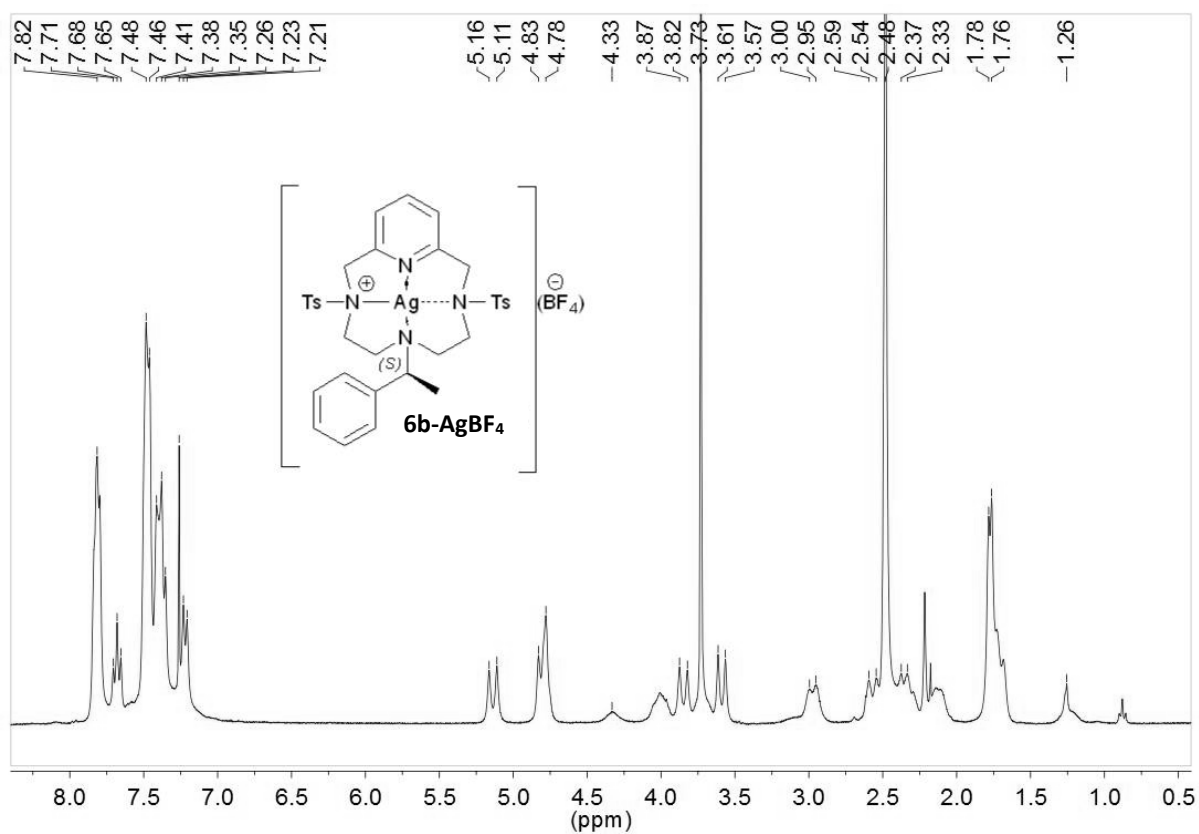


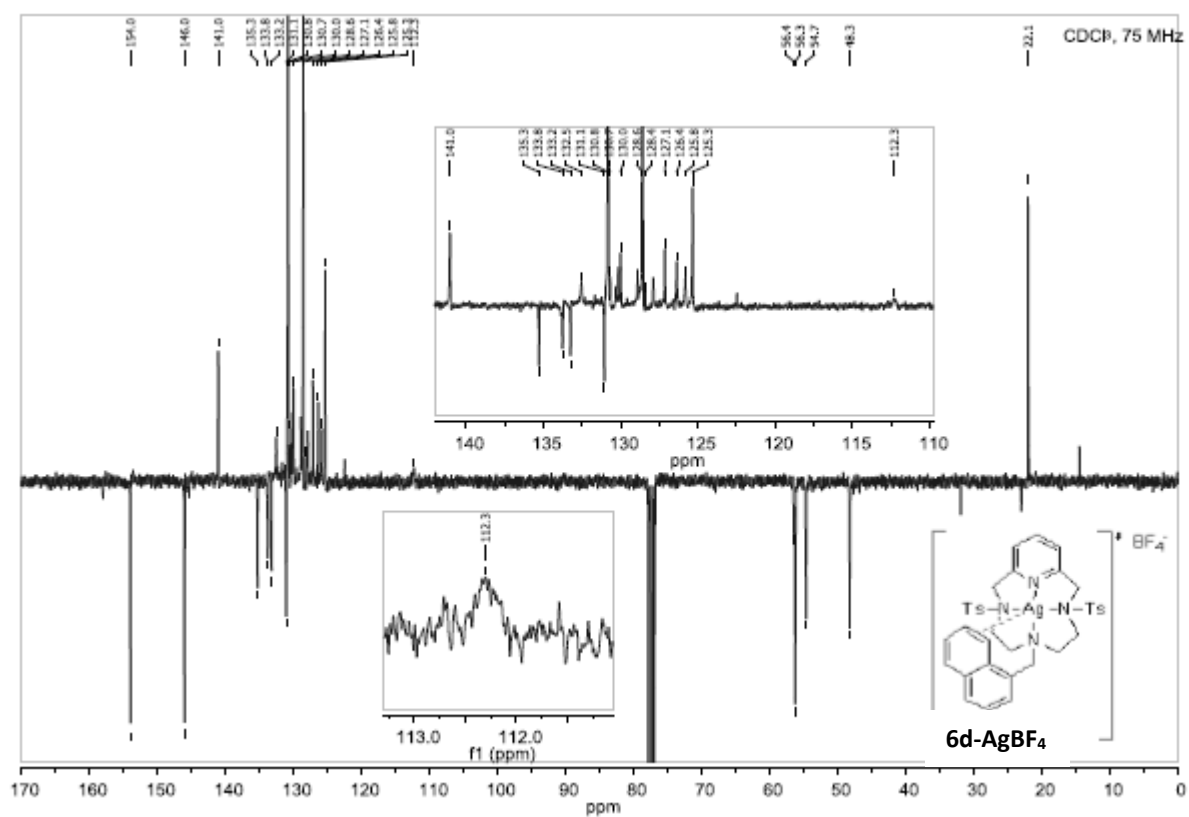
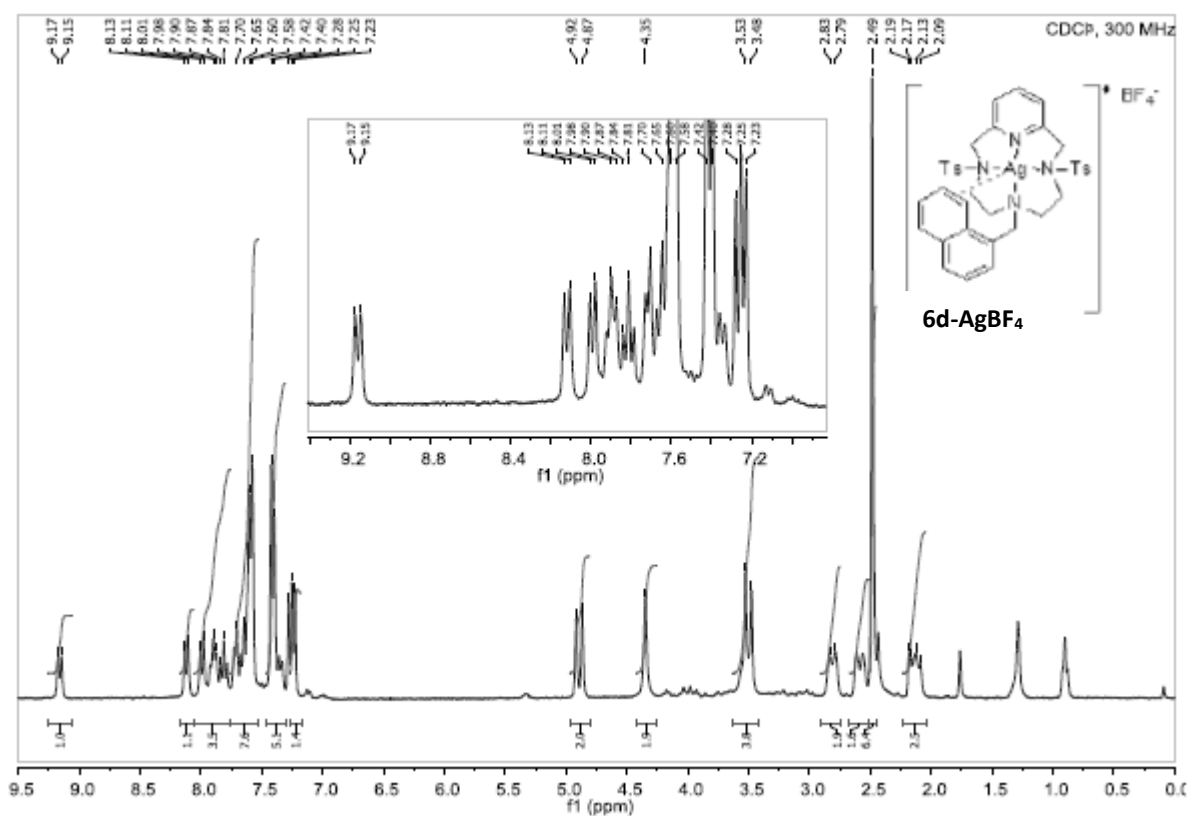


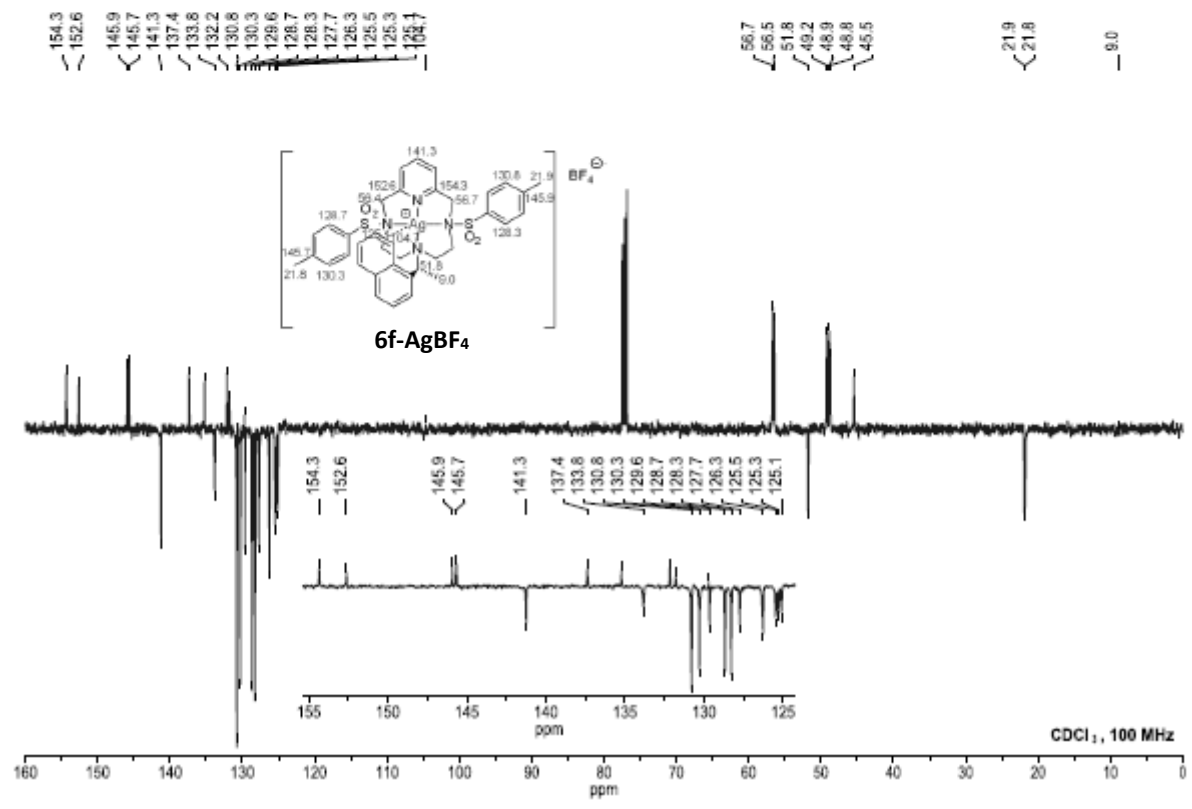
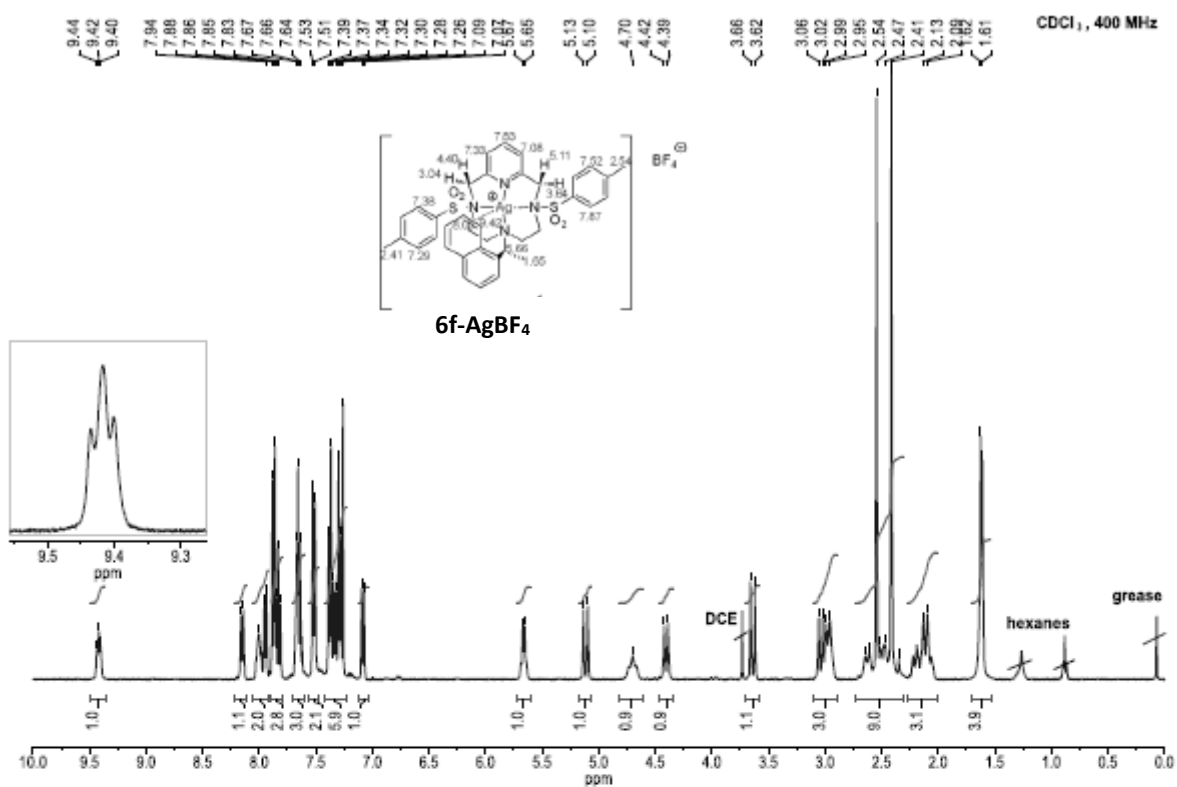


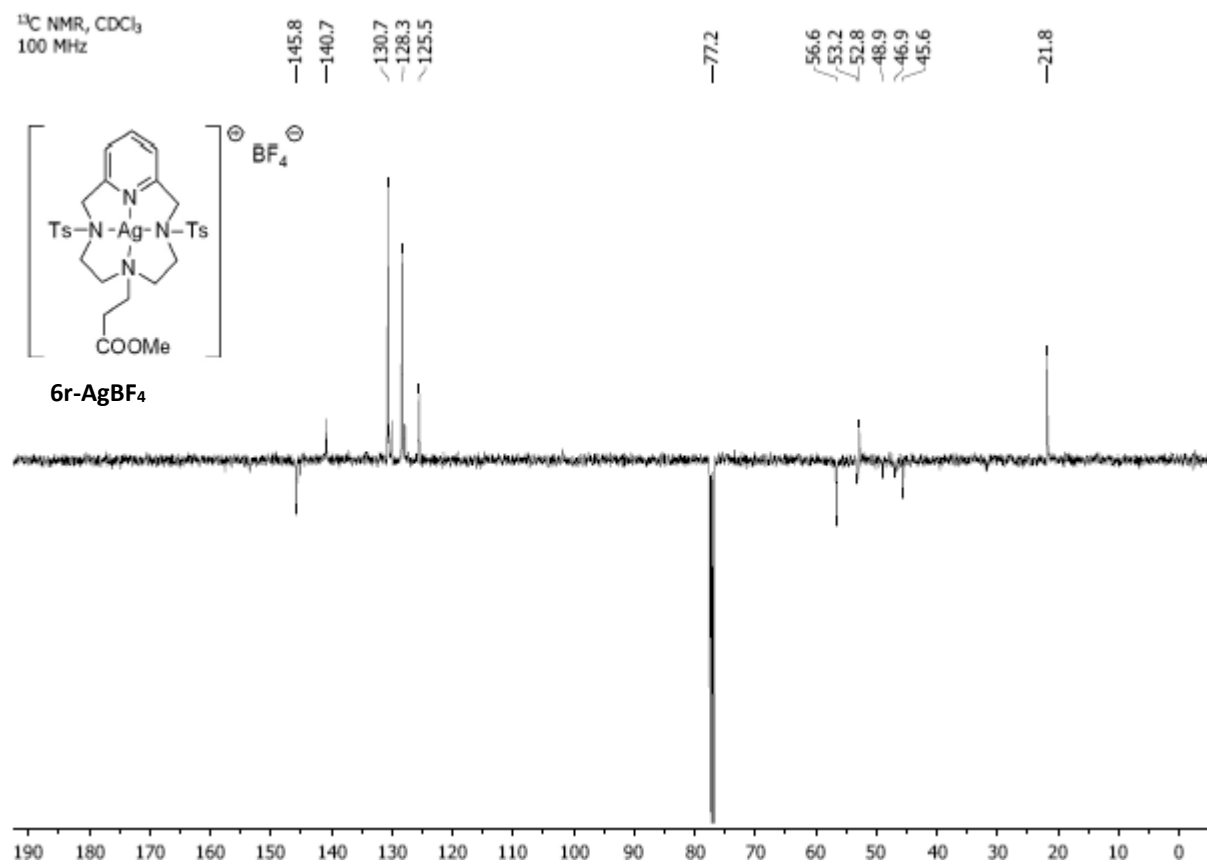
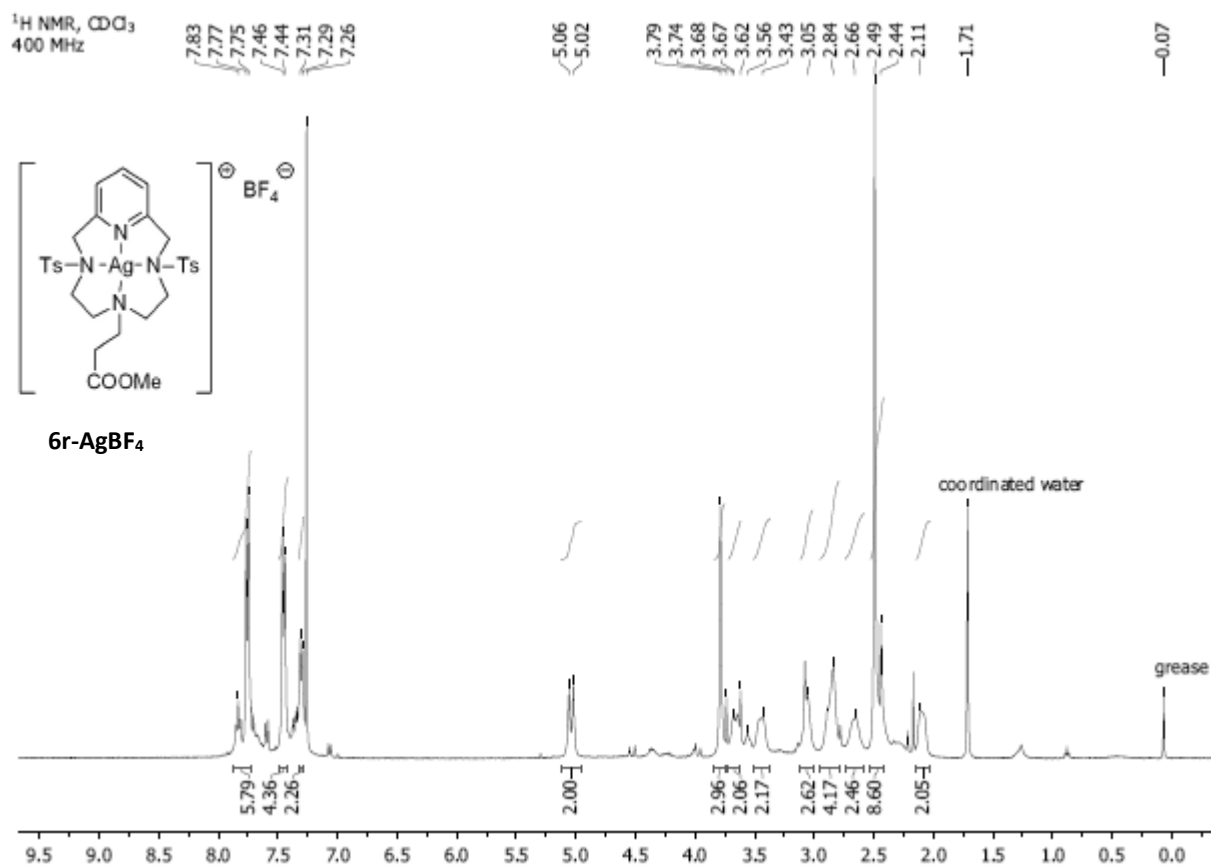


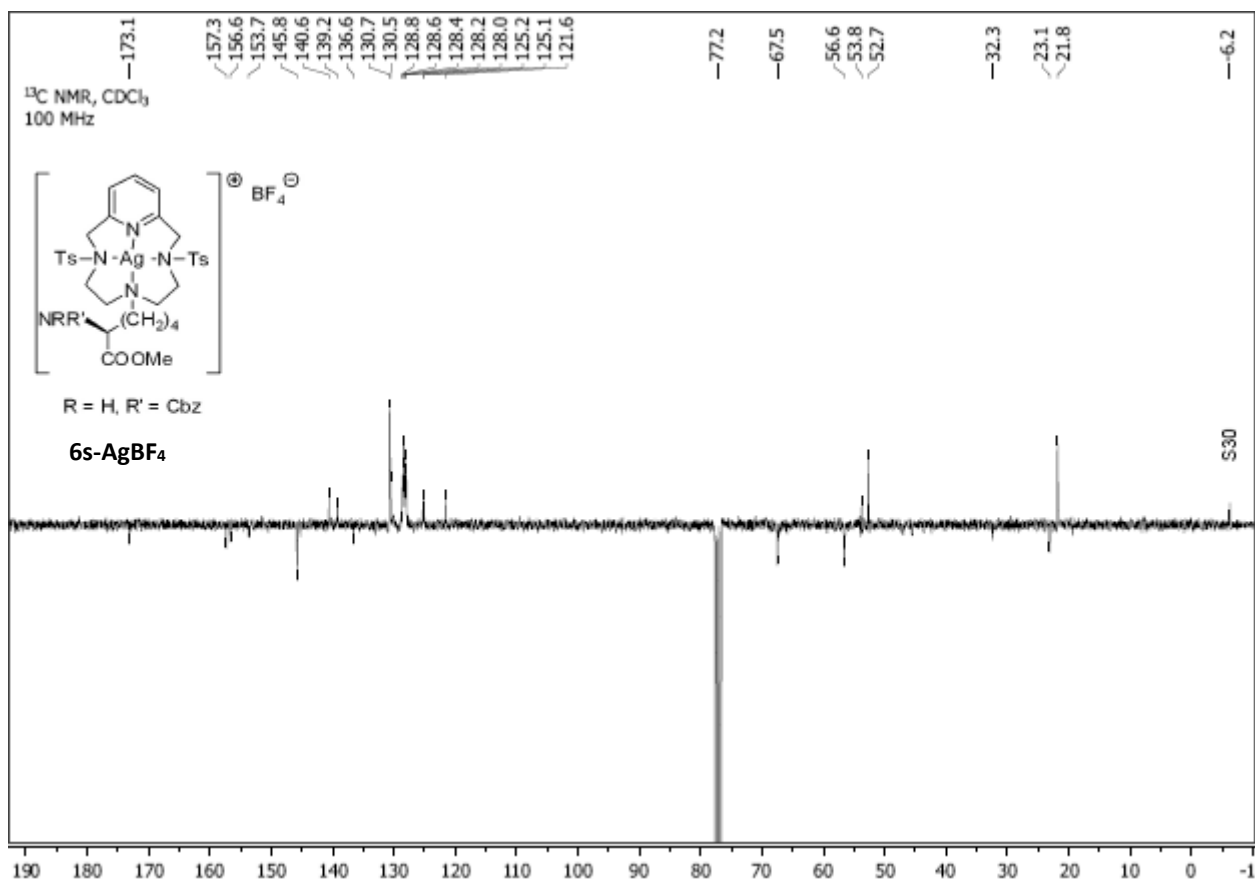
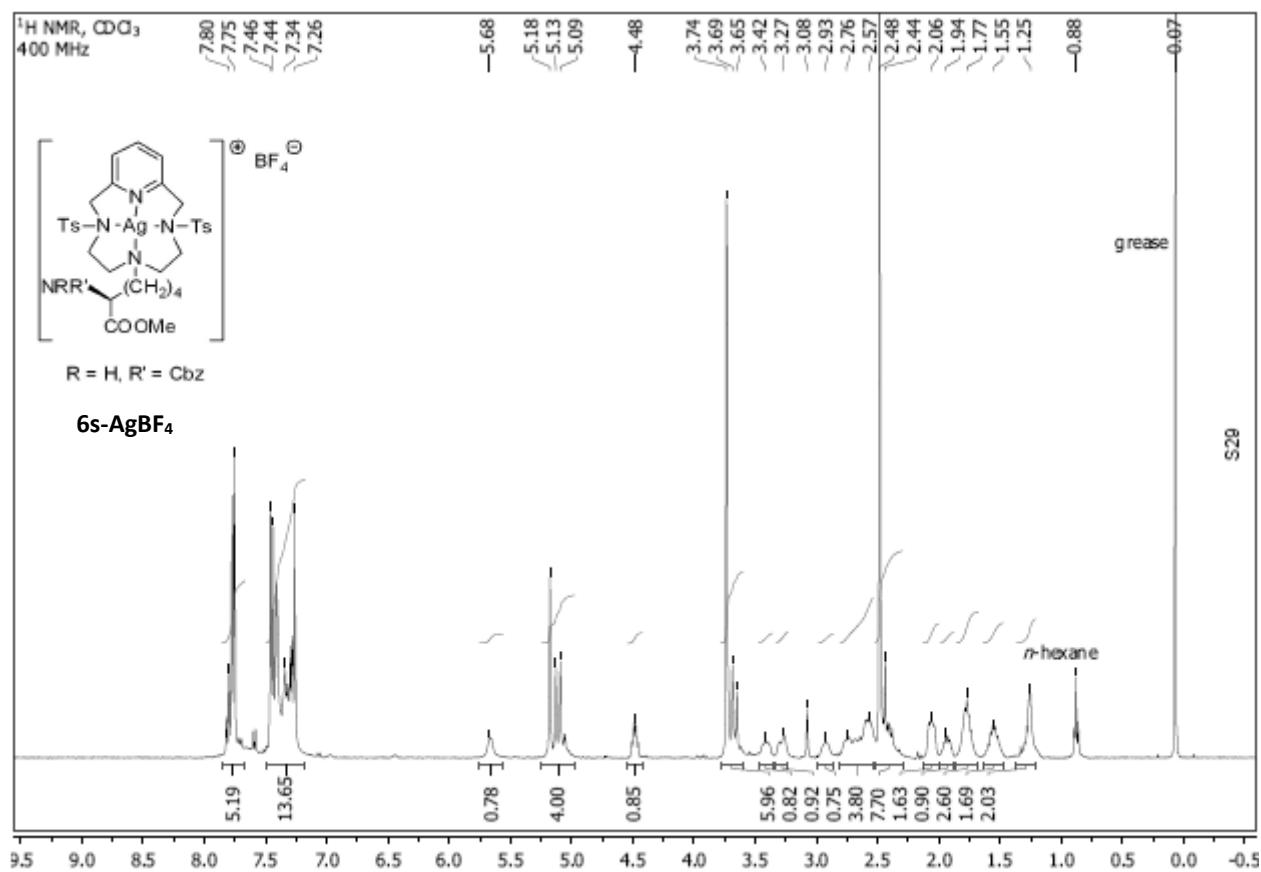


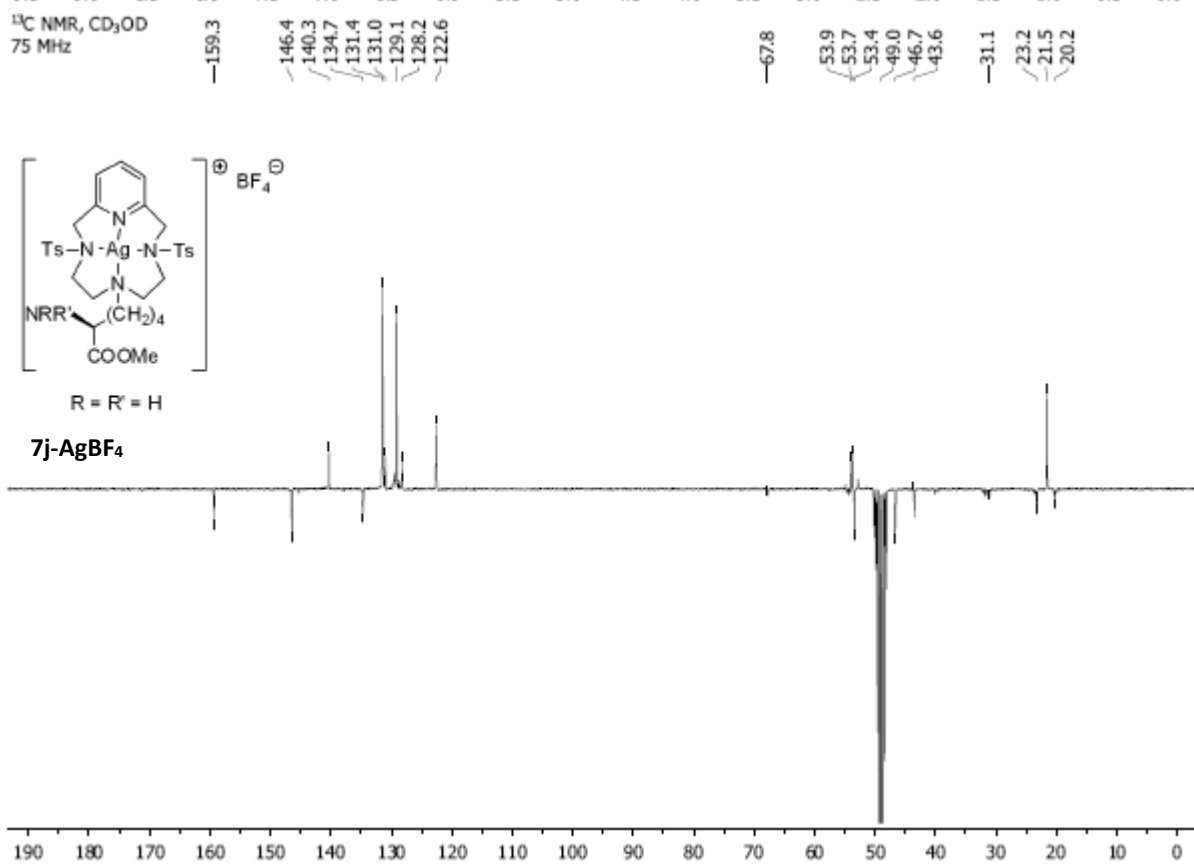
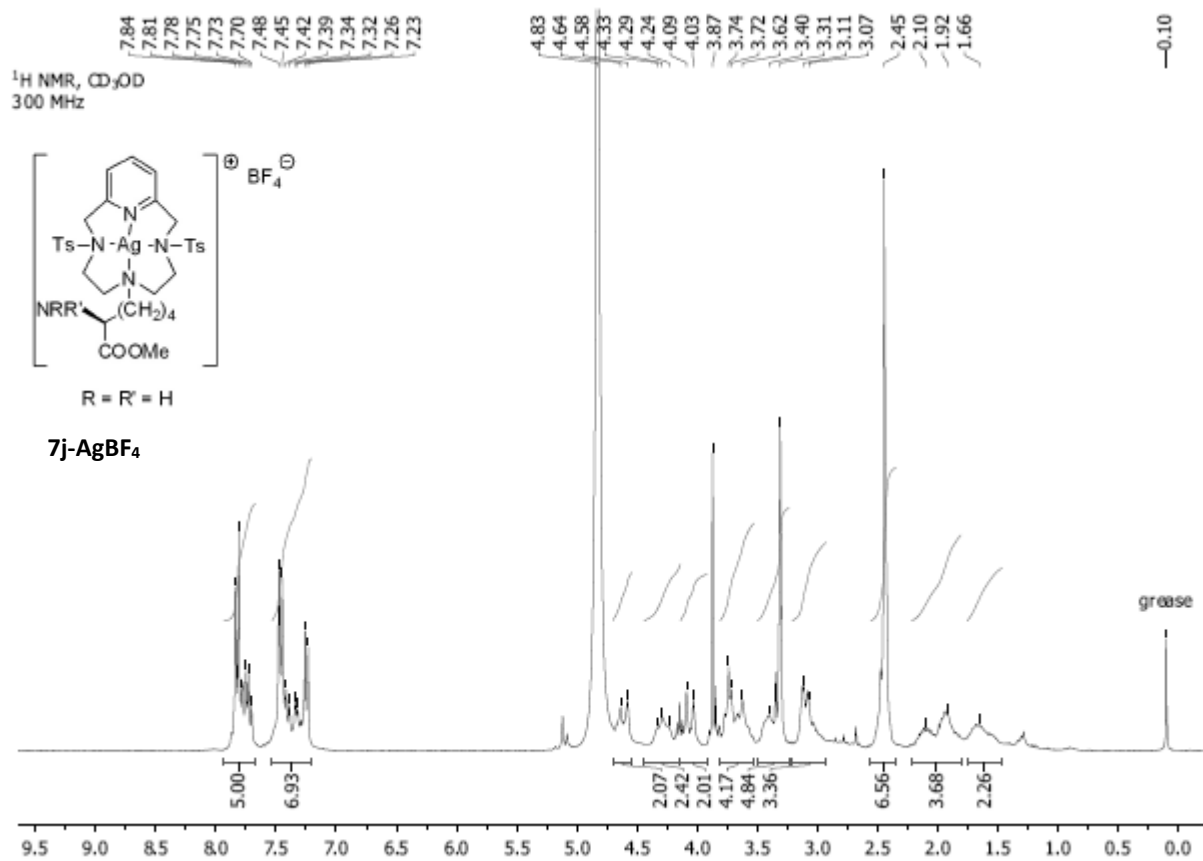


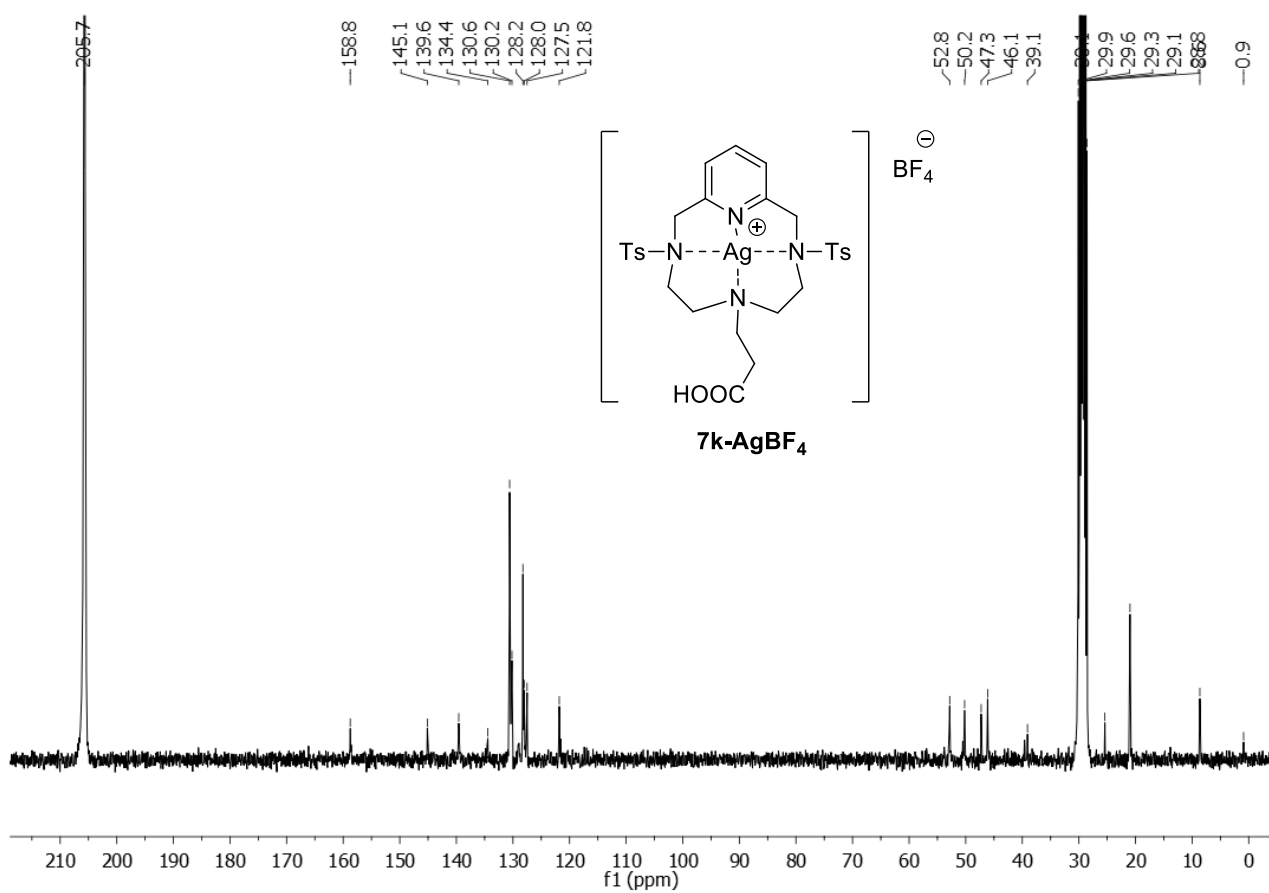
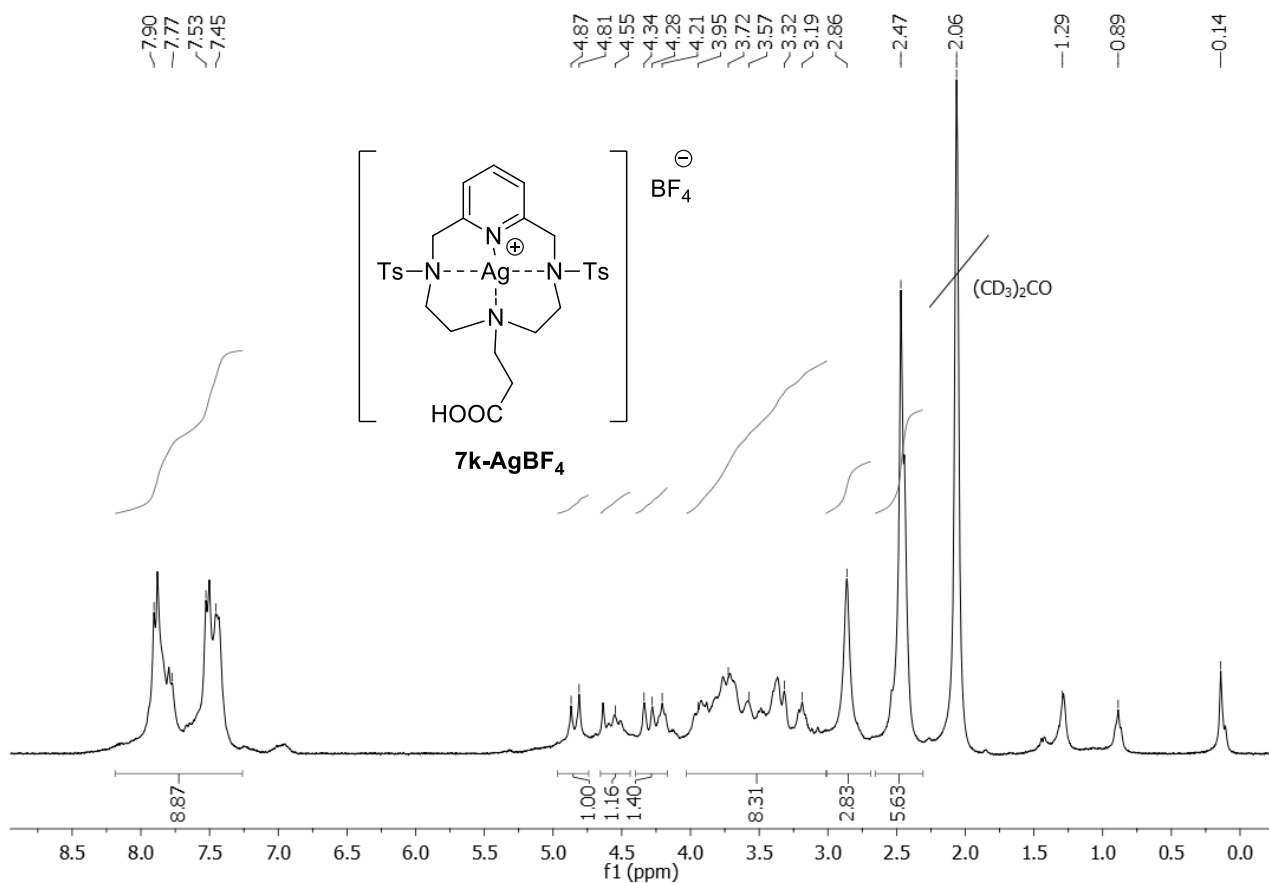




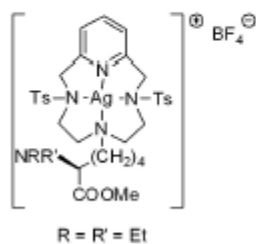




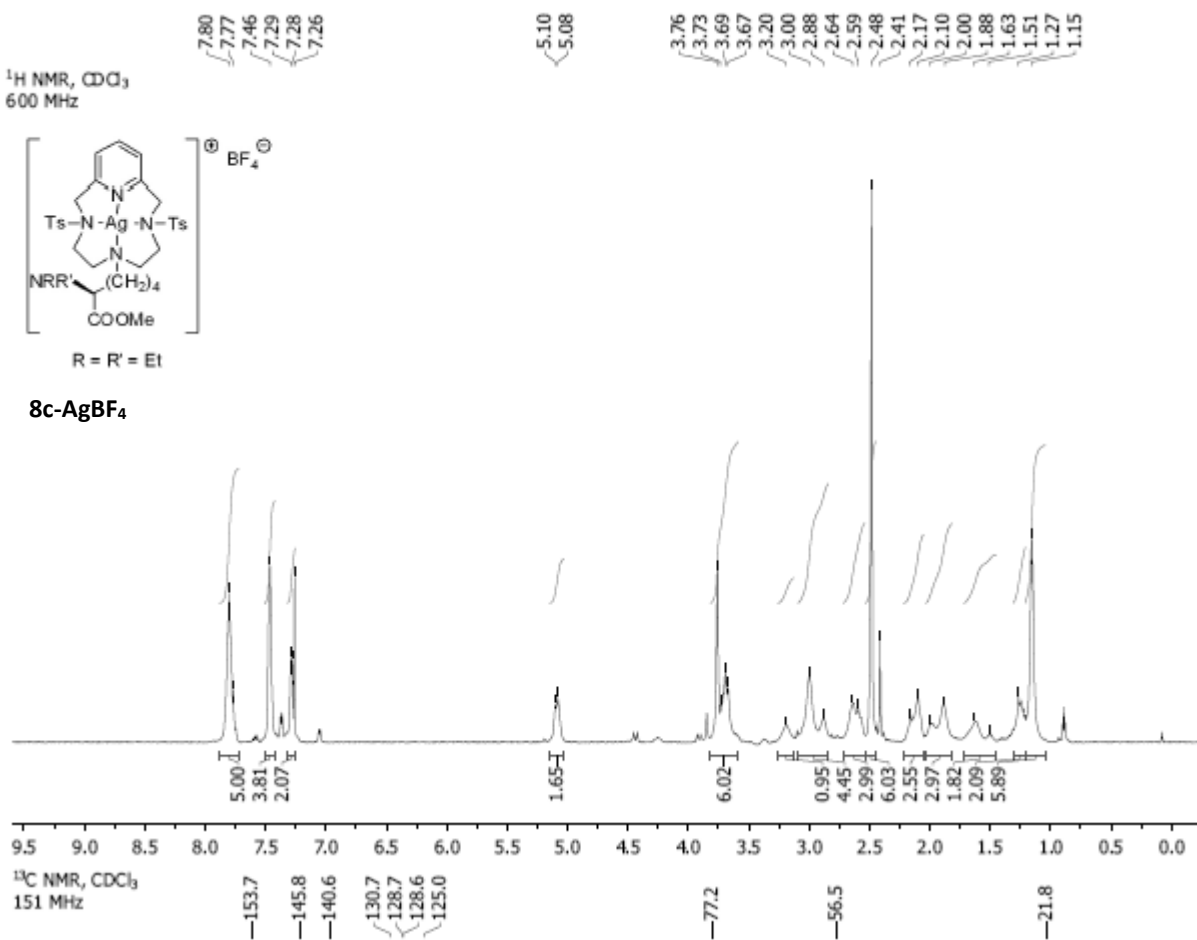




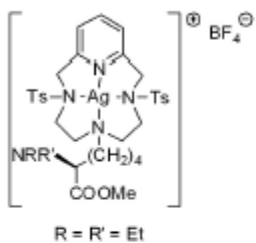
$^1\text{H NMR}$, CDCl_3
600 MHz



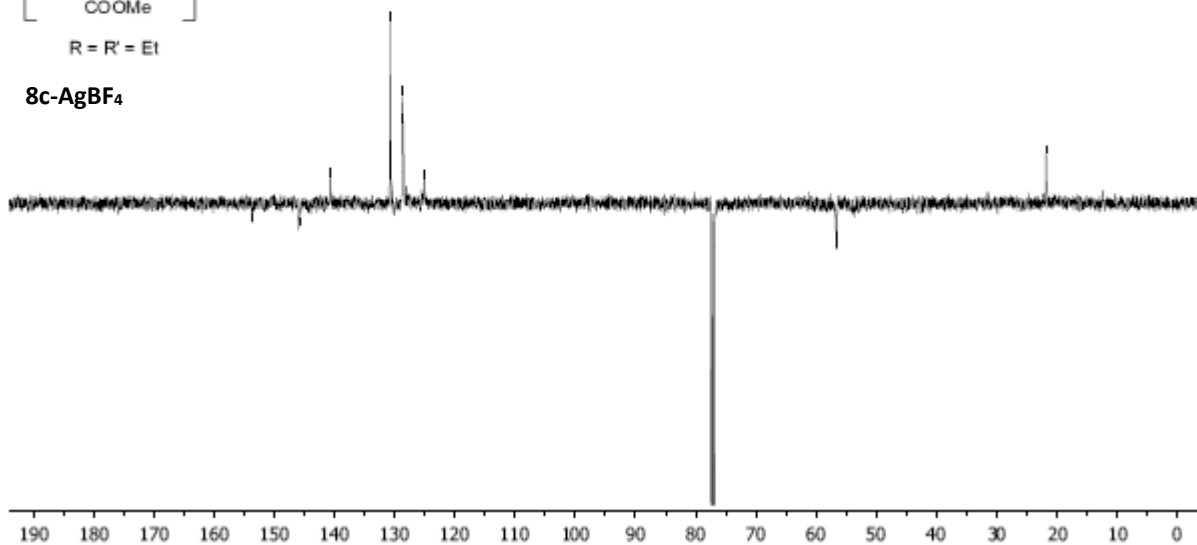
8c-AgBF₄

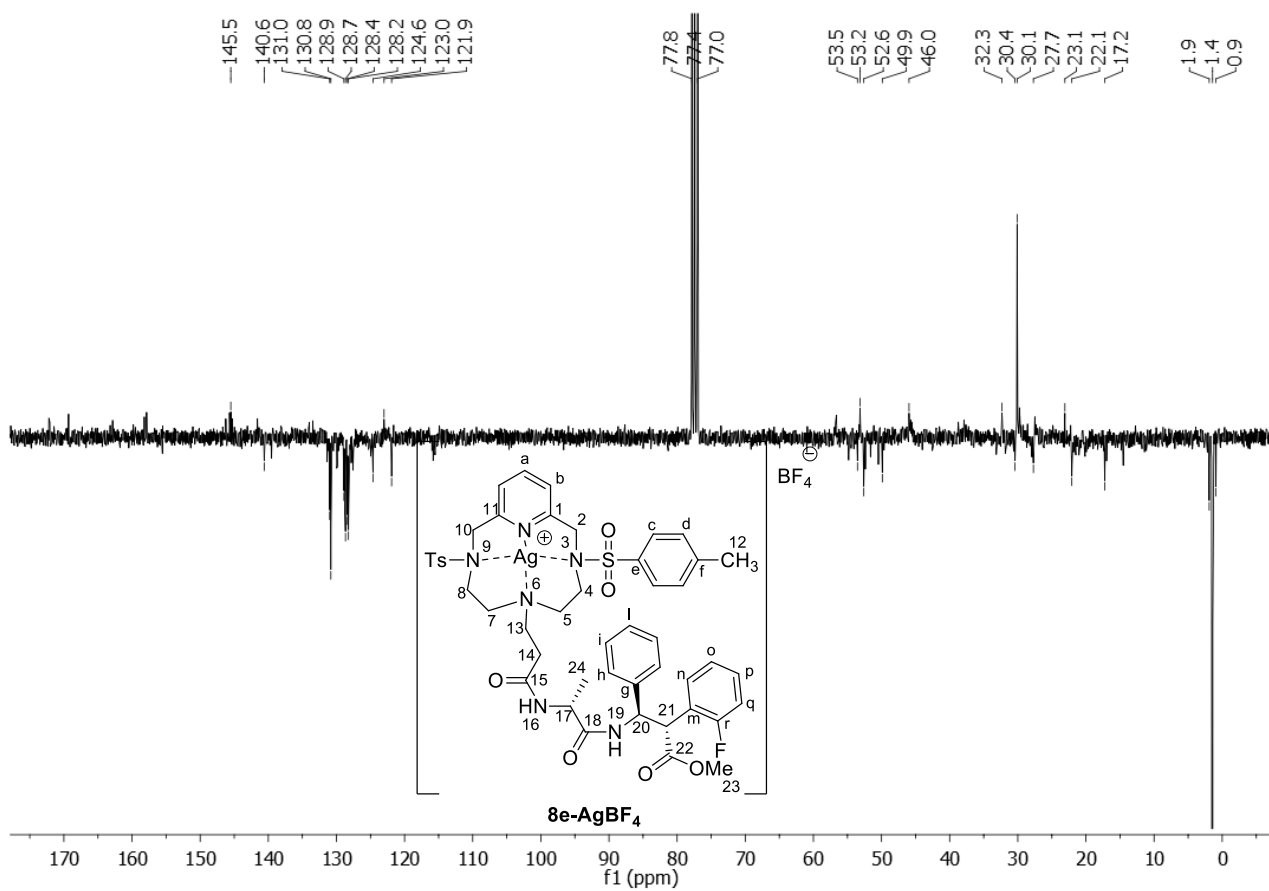
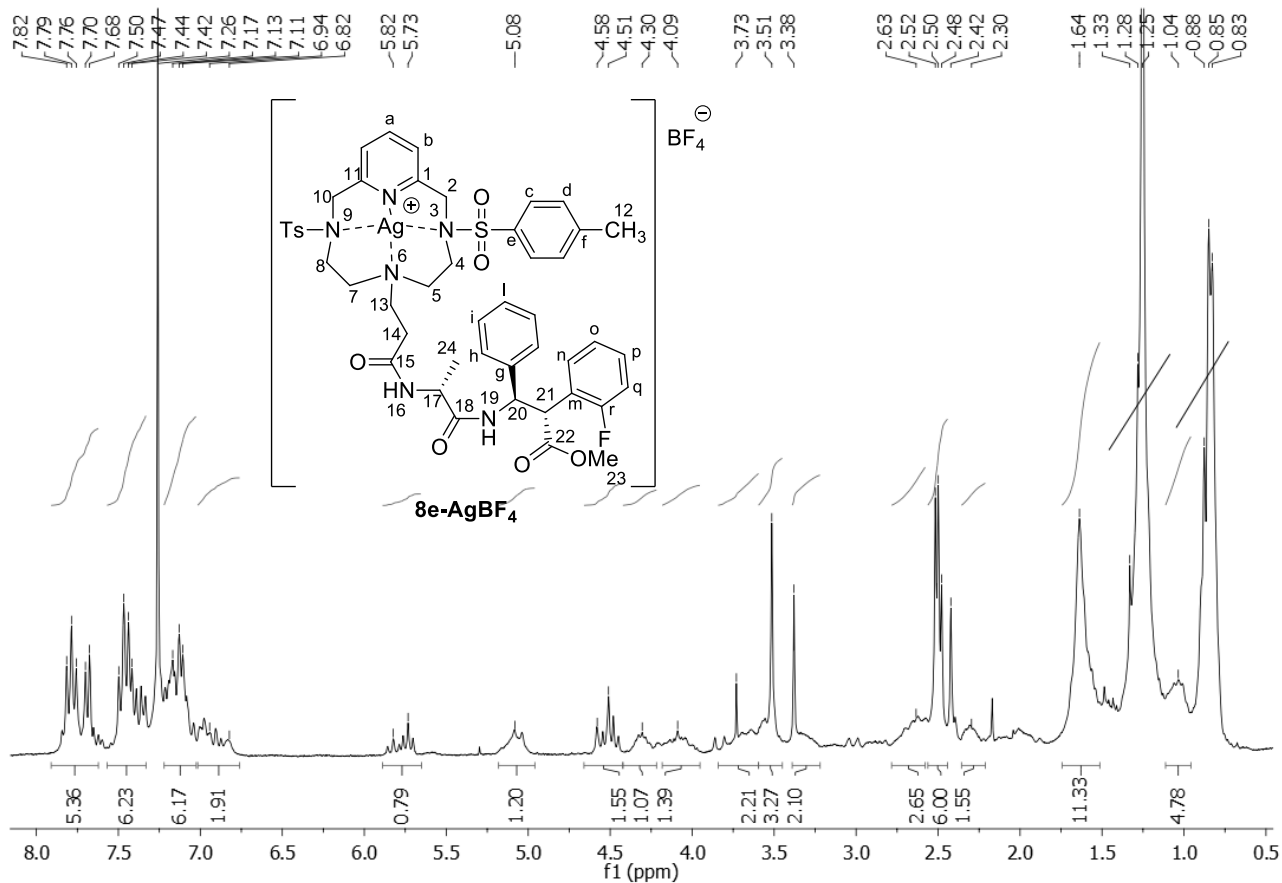


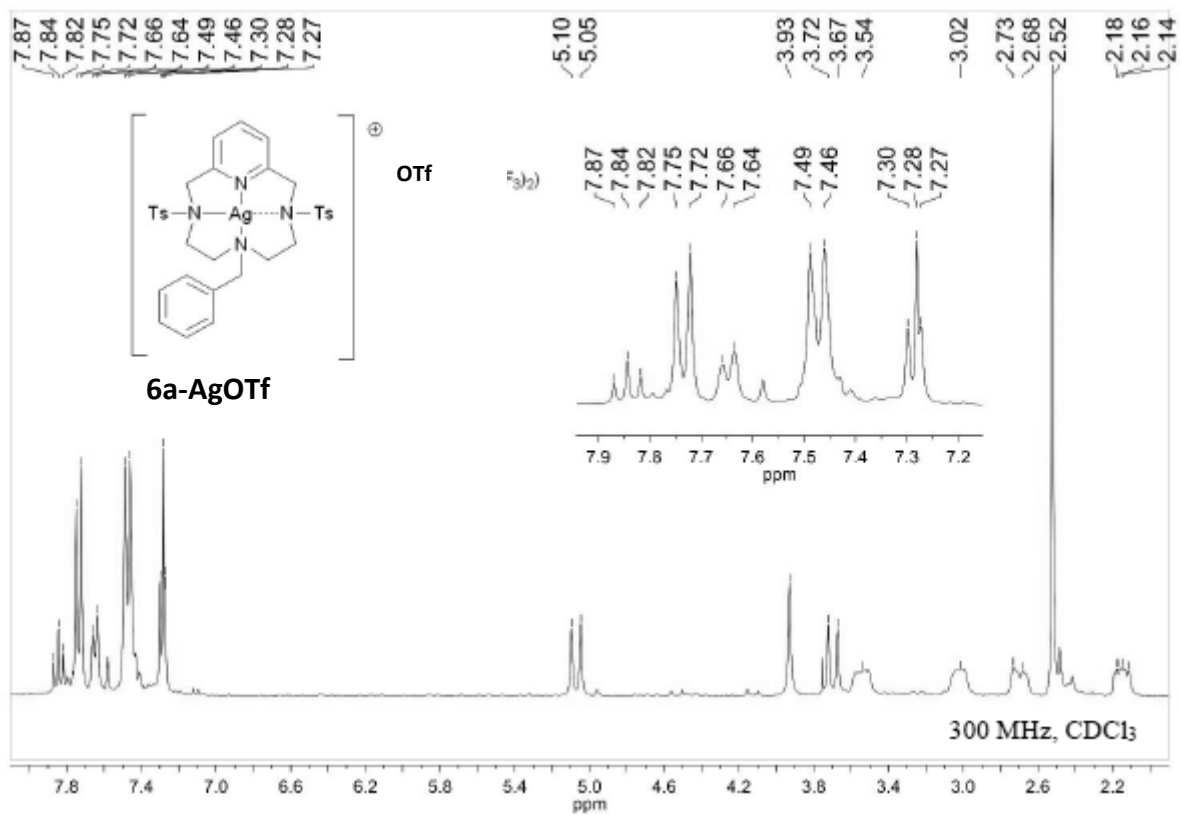
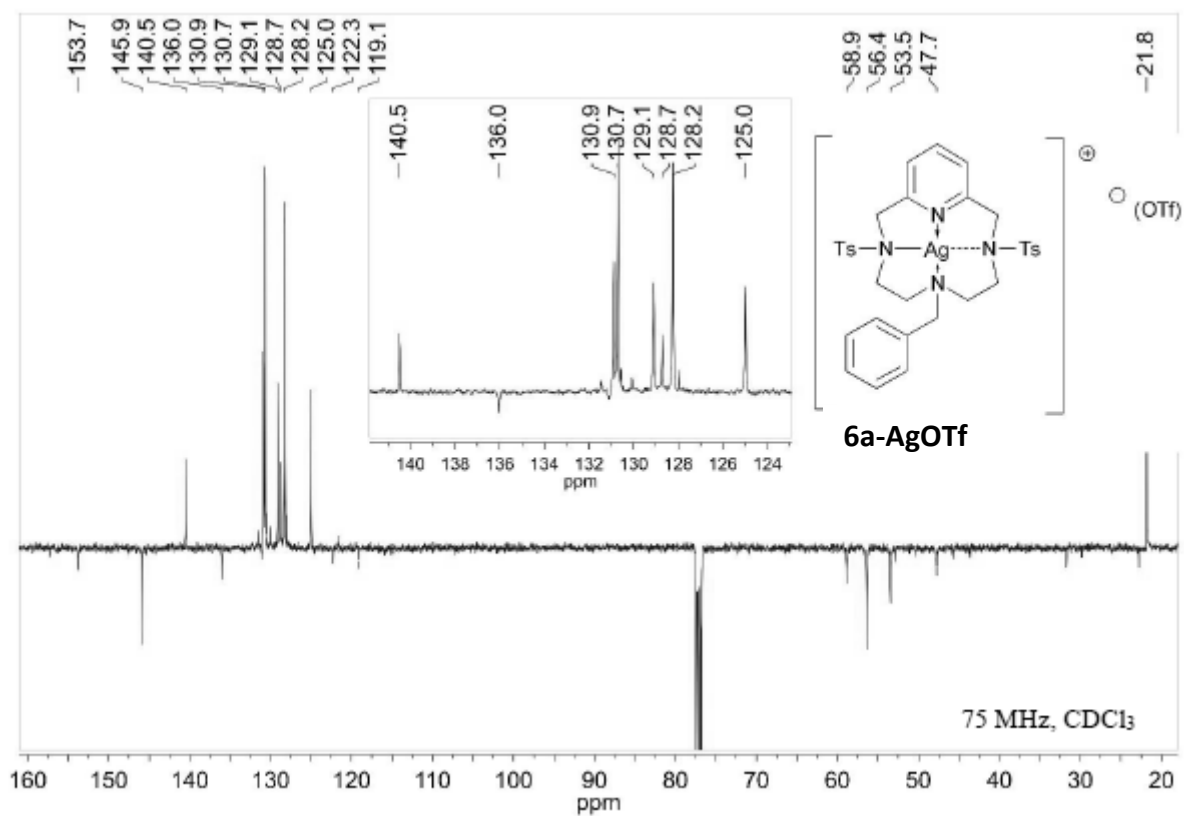
$^{13}\text{C NMR}$, CDCl_3
151 MHz

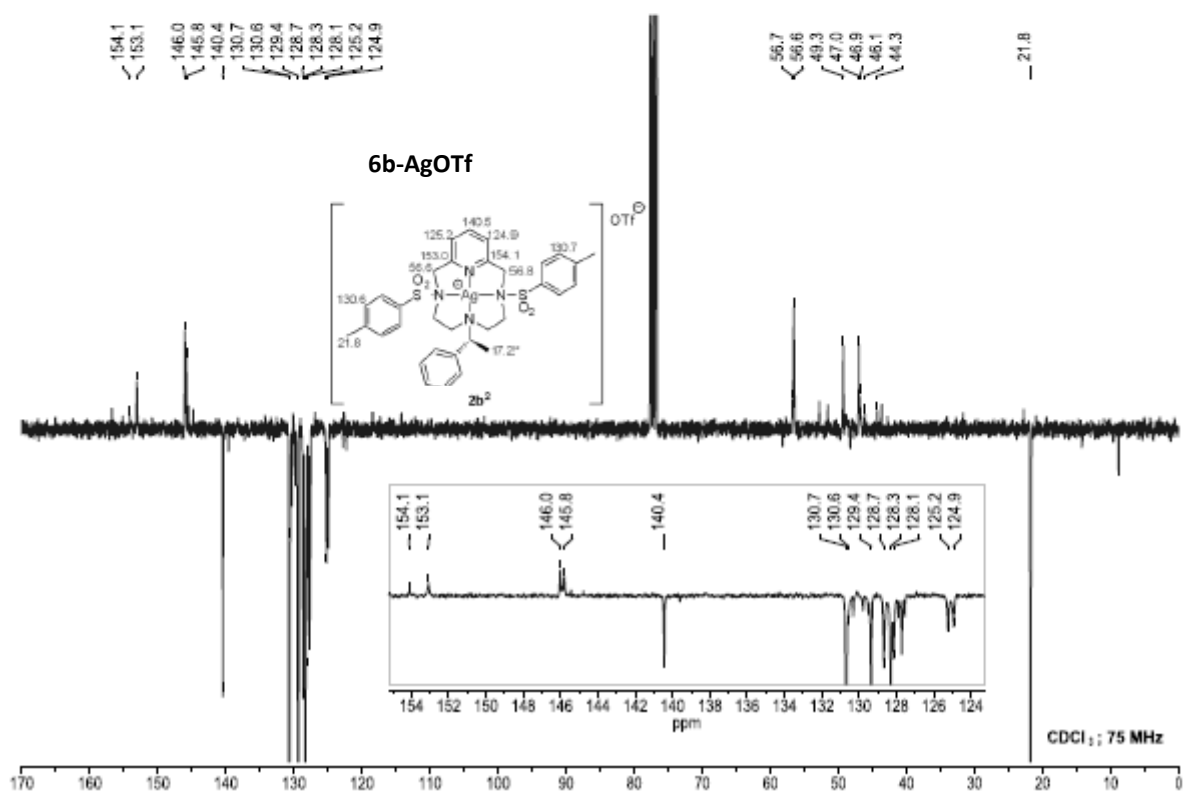
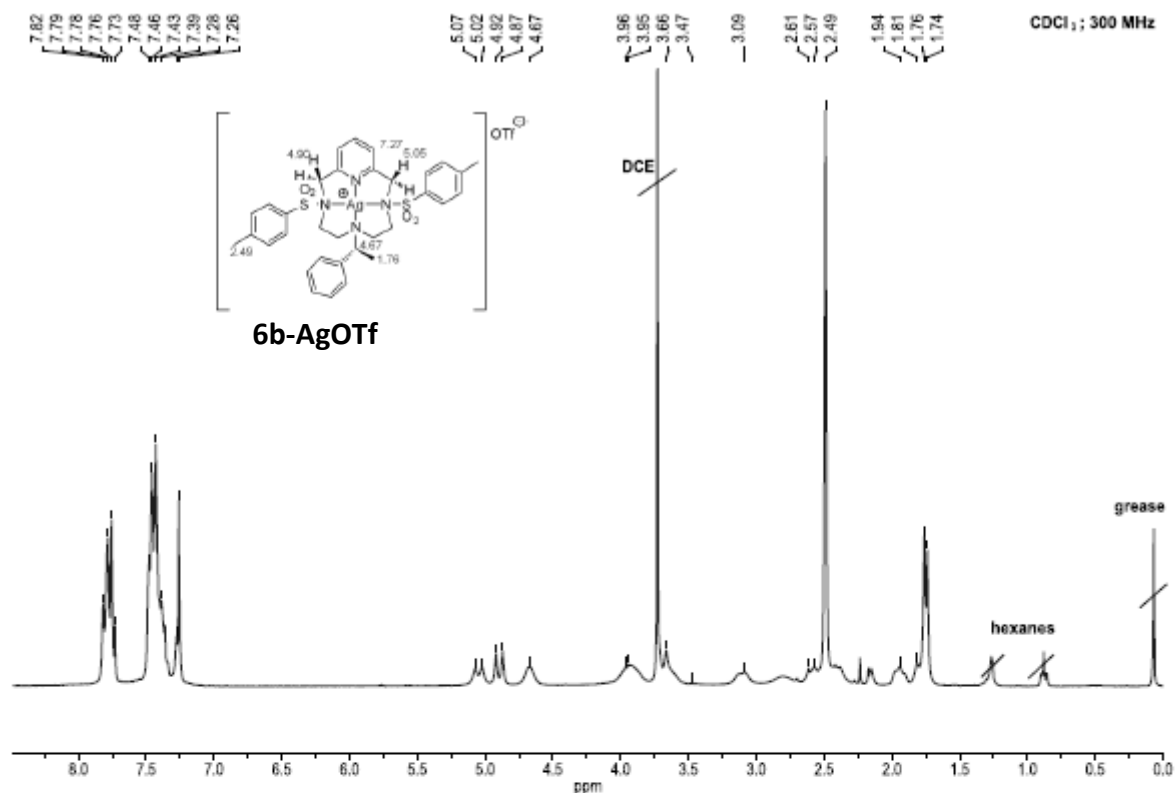


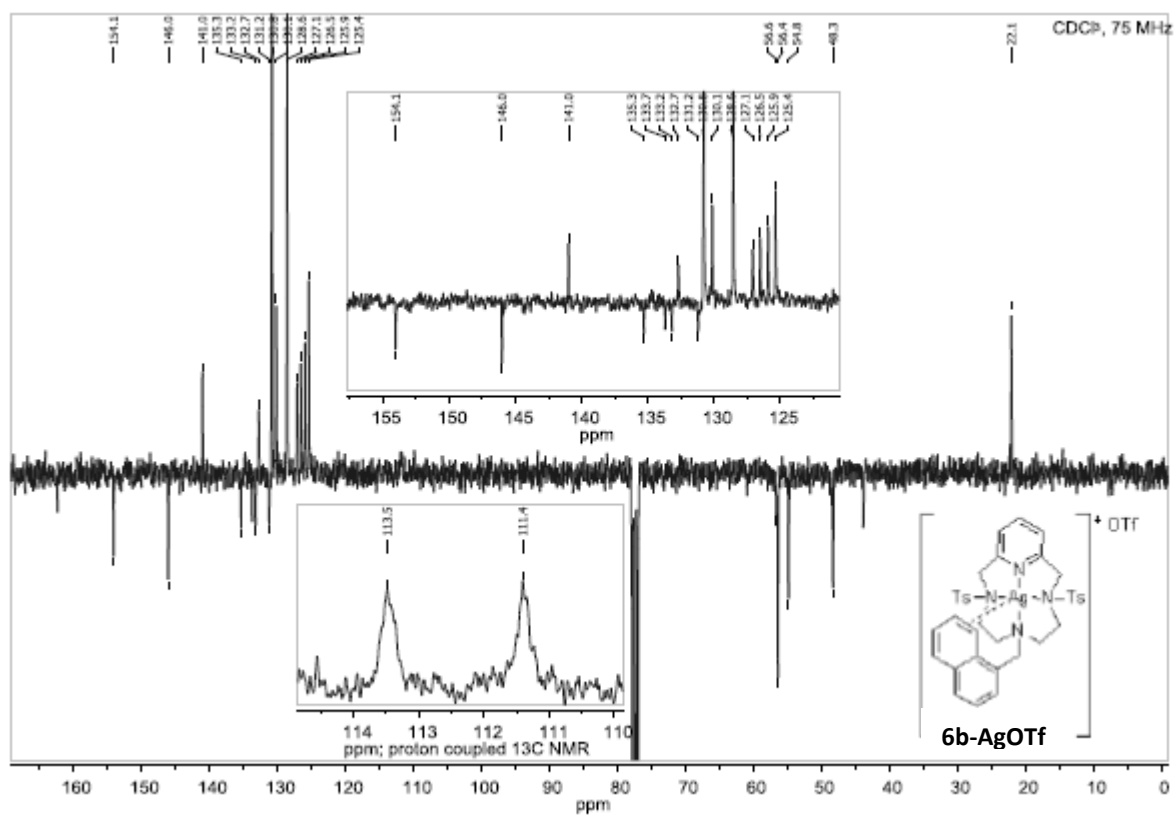
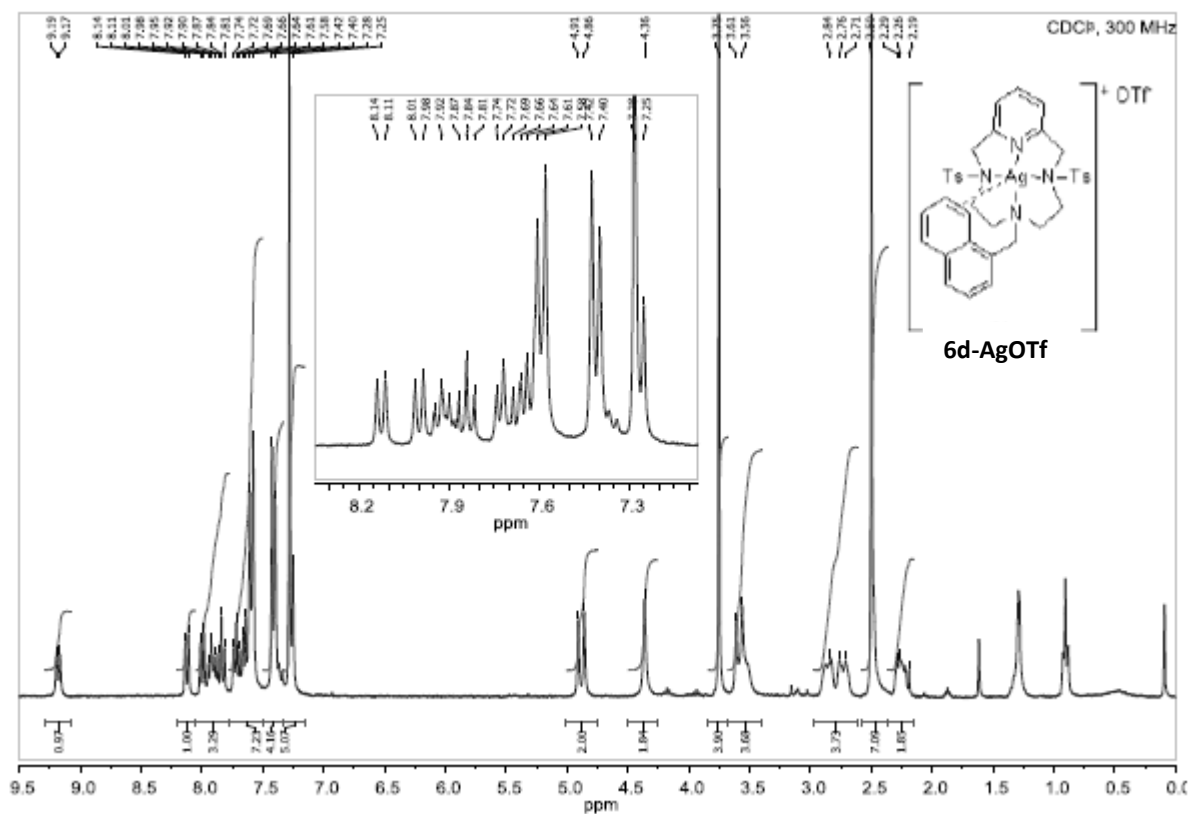
8c-AgBF₄











$^1\text{H NMR}$, CDCl_3
300 MHz

7.89
7.86
7.84
7.77
7.75
7.47
7.44
7.33
7.30
7.26

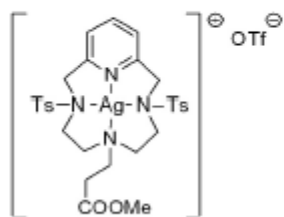
5.30
5.06
5.01

3.81
3.72
3.67
3.49
3.43

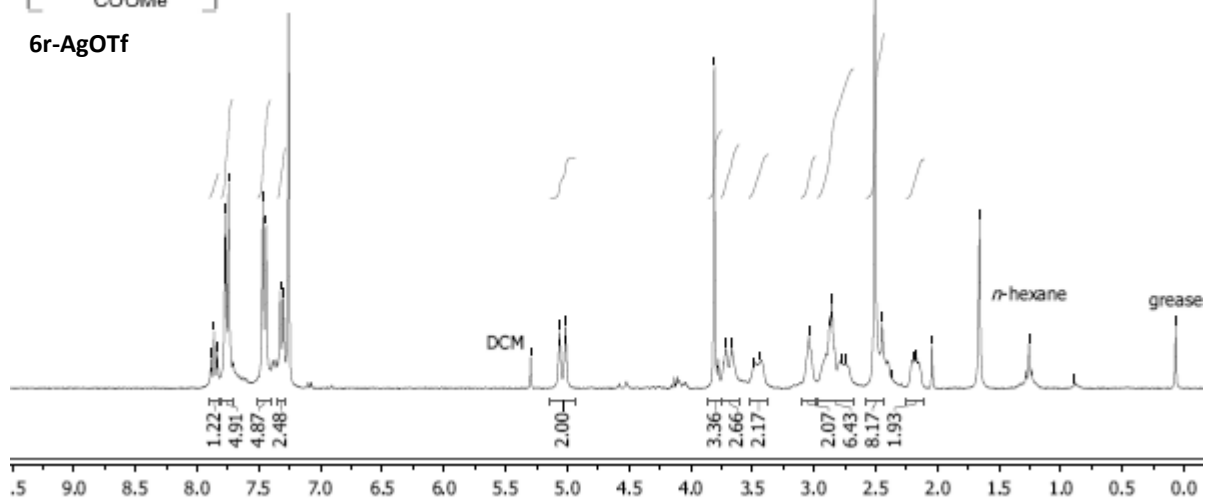
3.04
2.85
2.77
2.51
2.45
2.19
2.18
2.06

1.26
0.89

0.07



6r-AgOTf



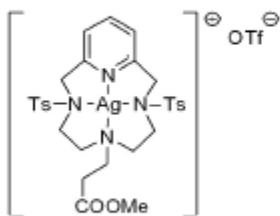
$^{13}\text{C NMR}$, CDCl_3
75 MHz

153.5
145.8
140.9
130.7
128.3
125.5

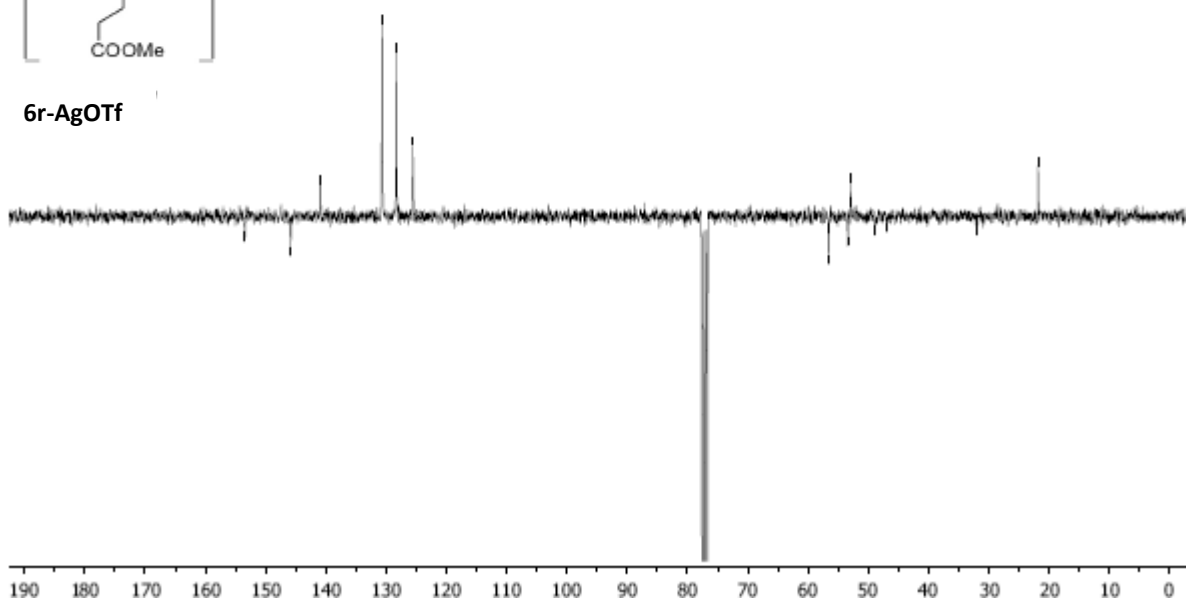
77.2

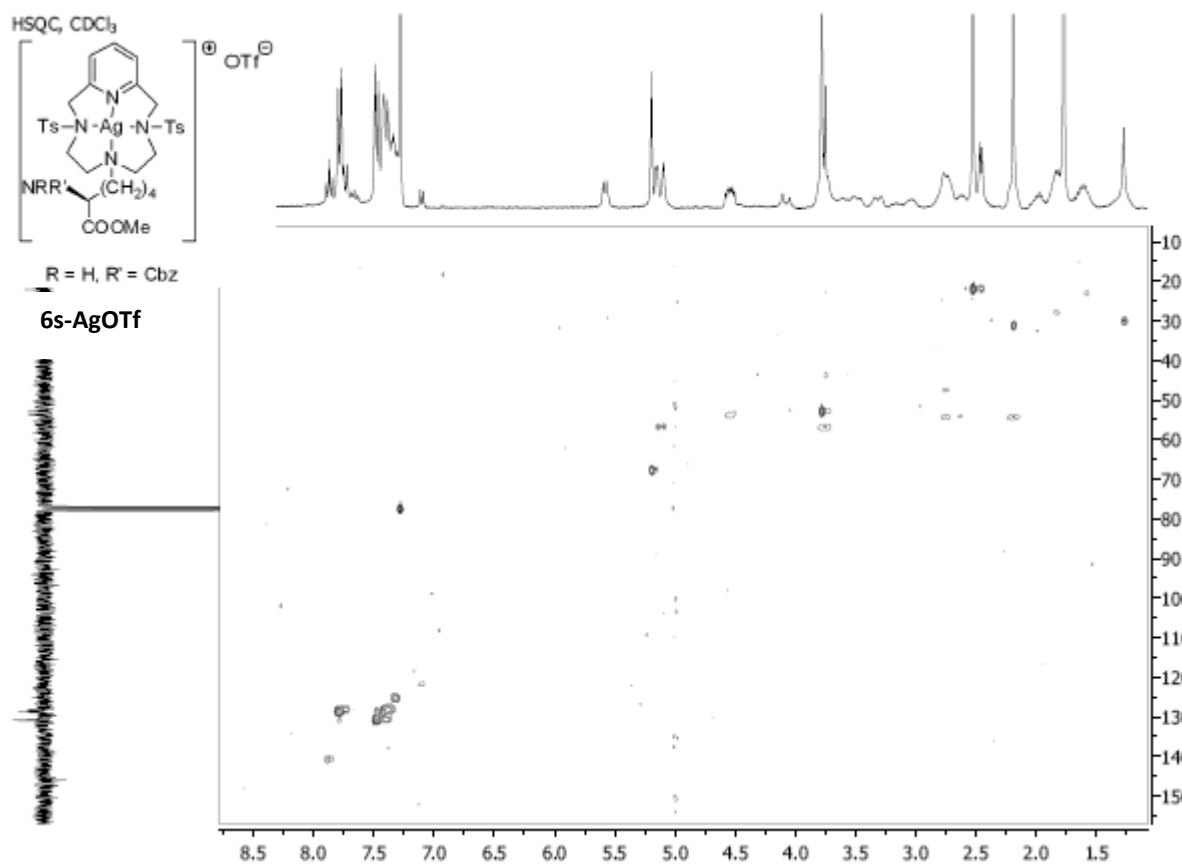
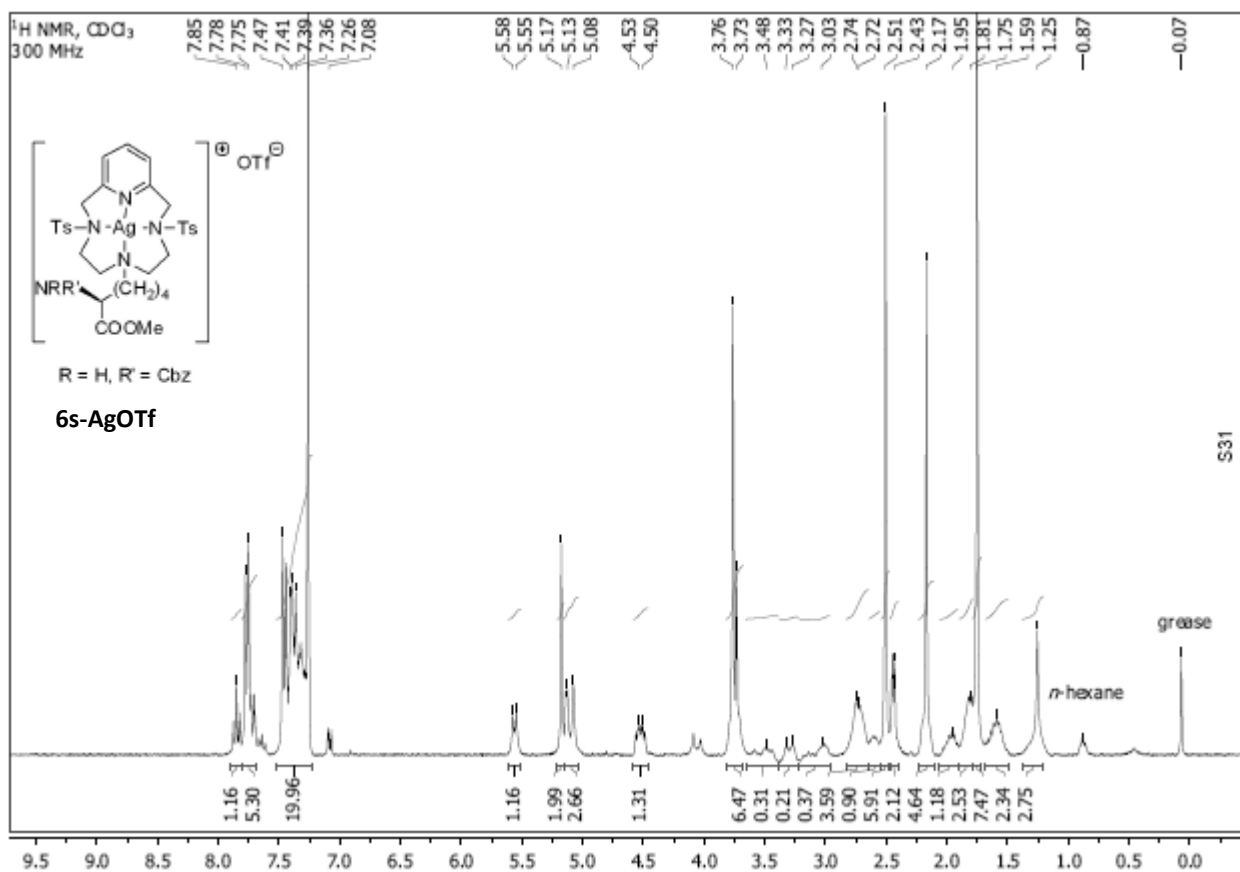
56.6
53.4
52.9
48.9
47.0

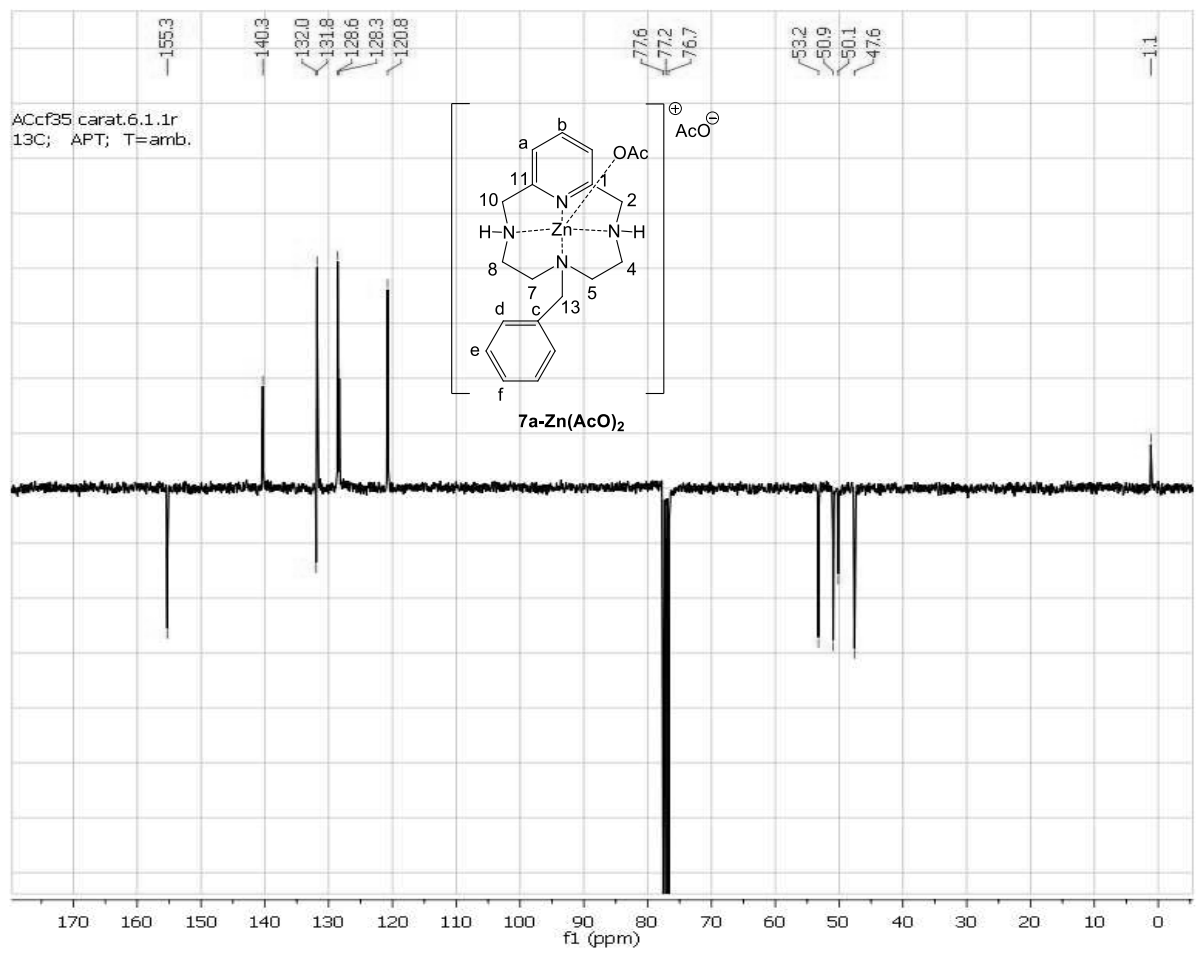
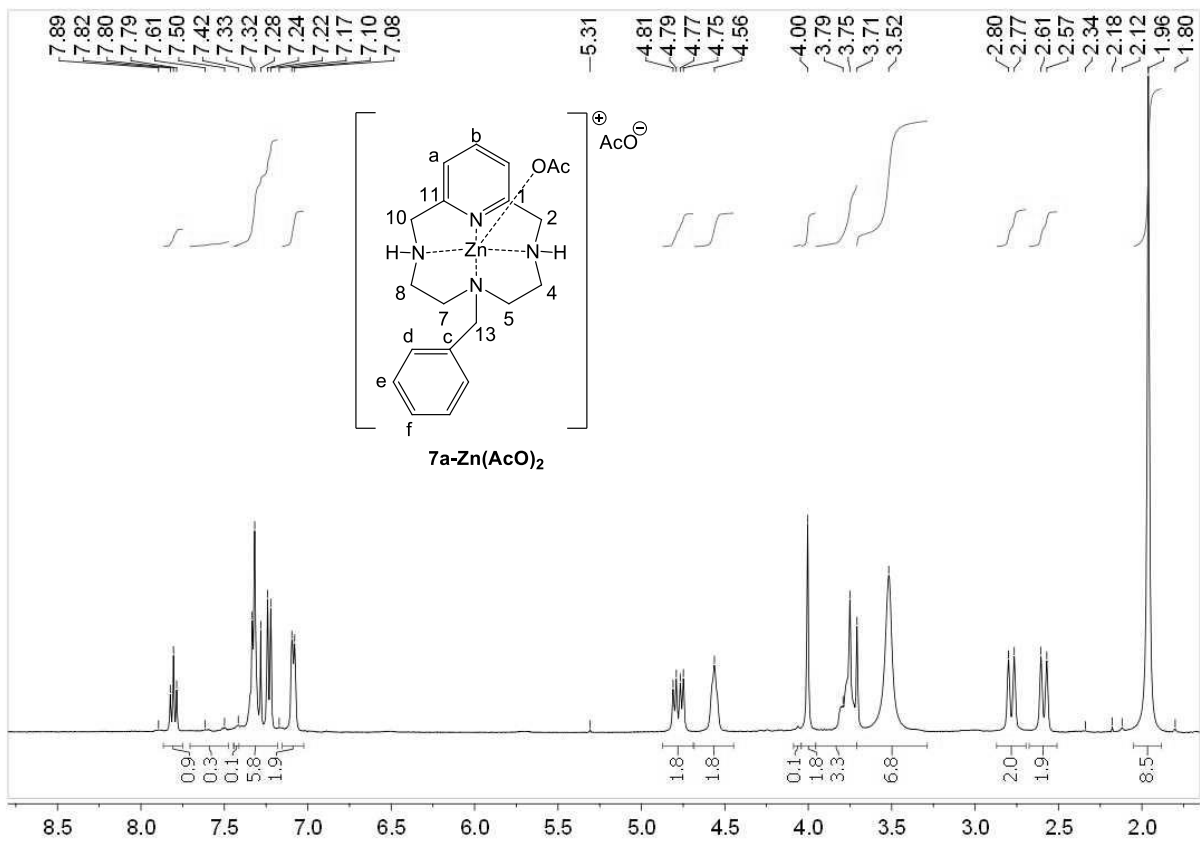
31.9
21.8

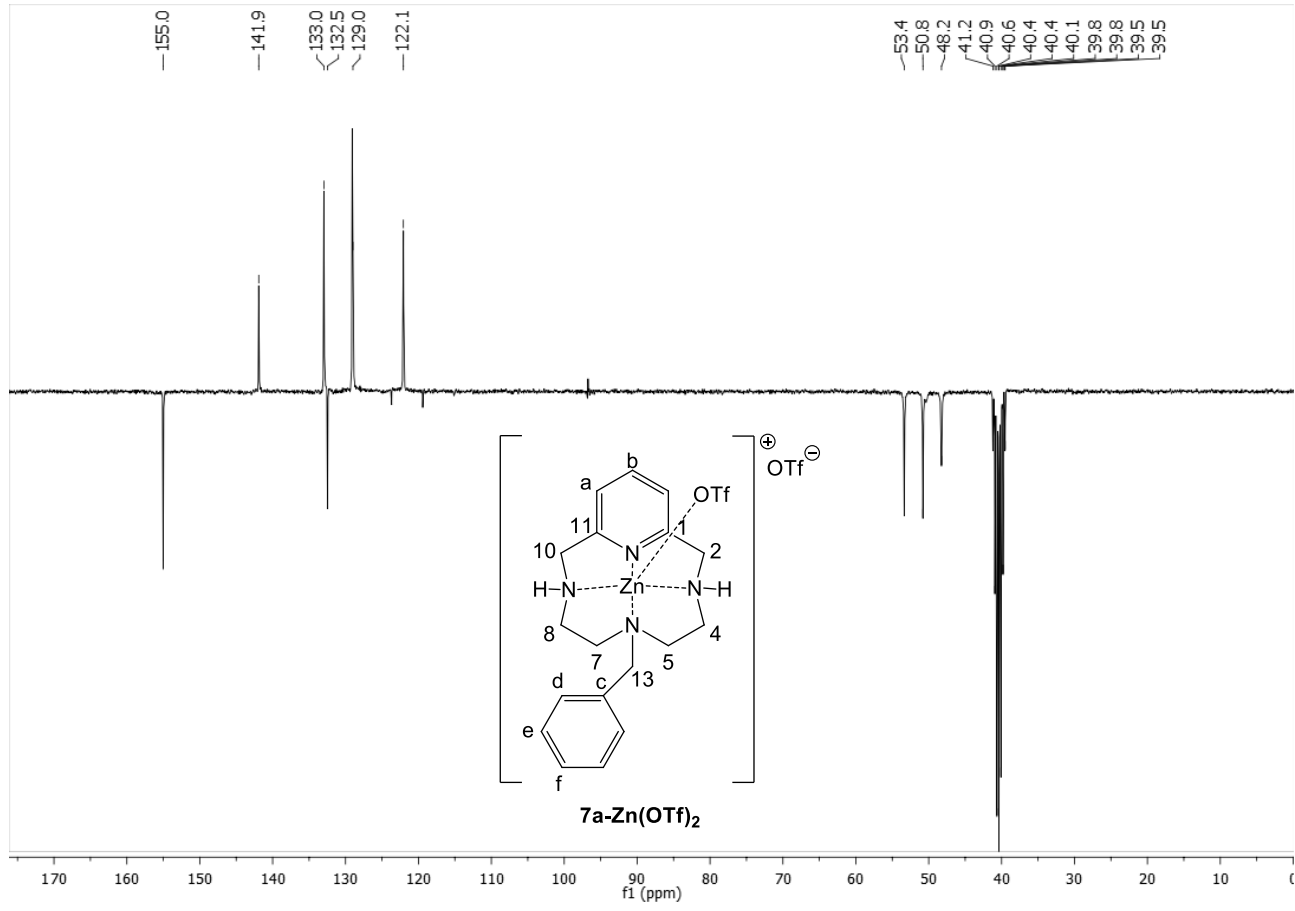
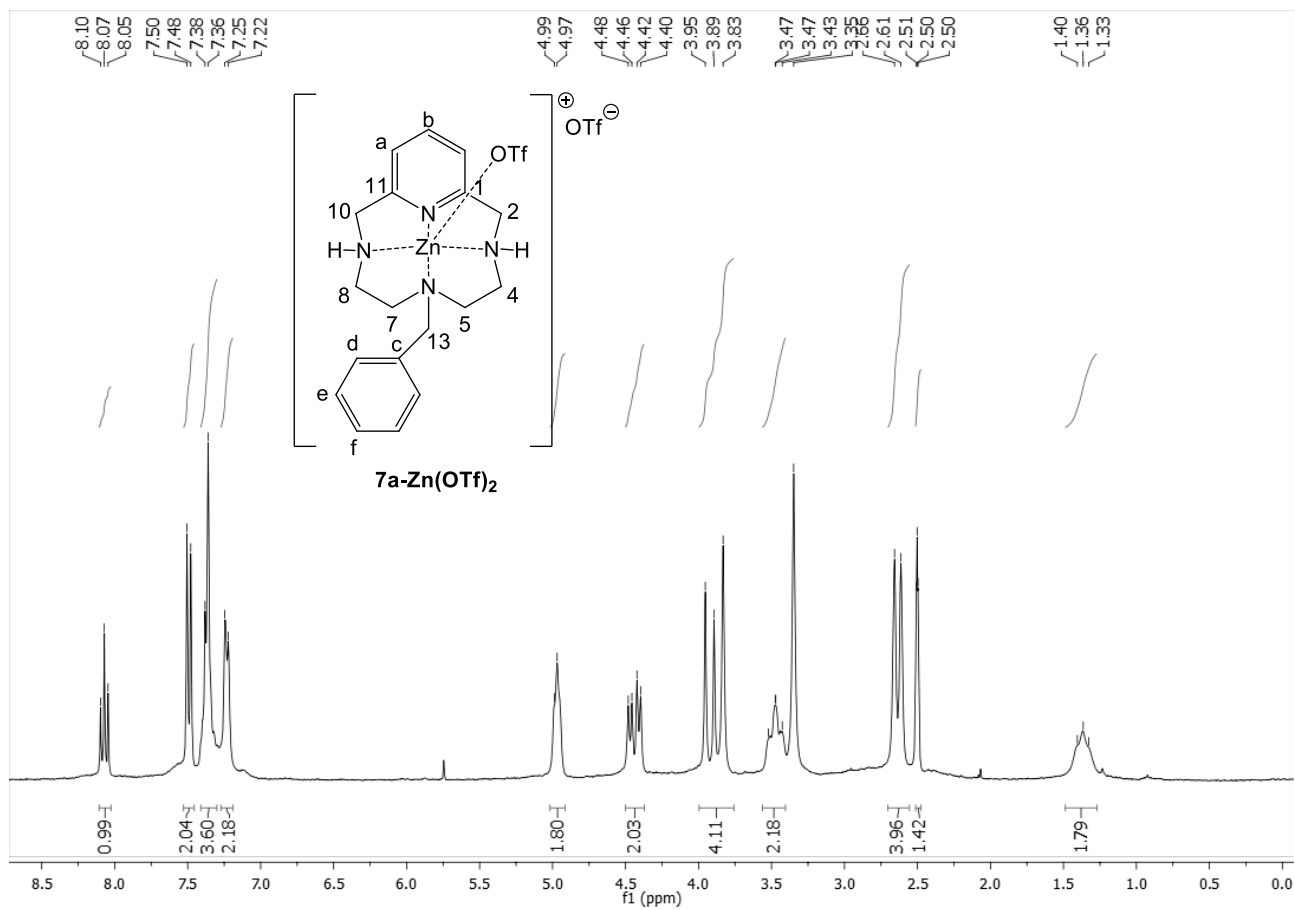


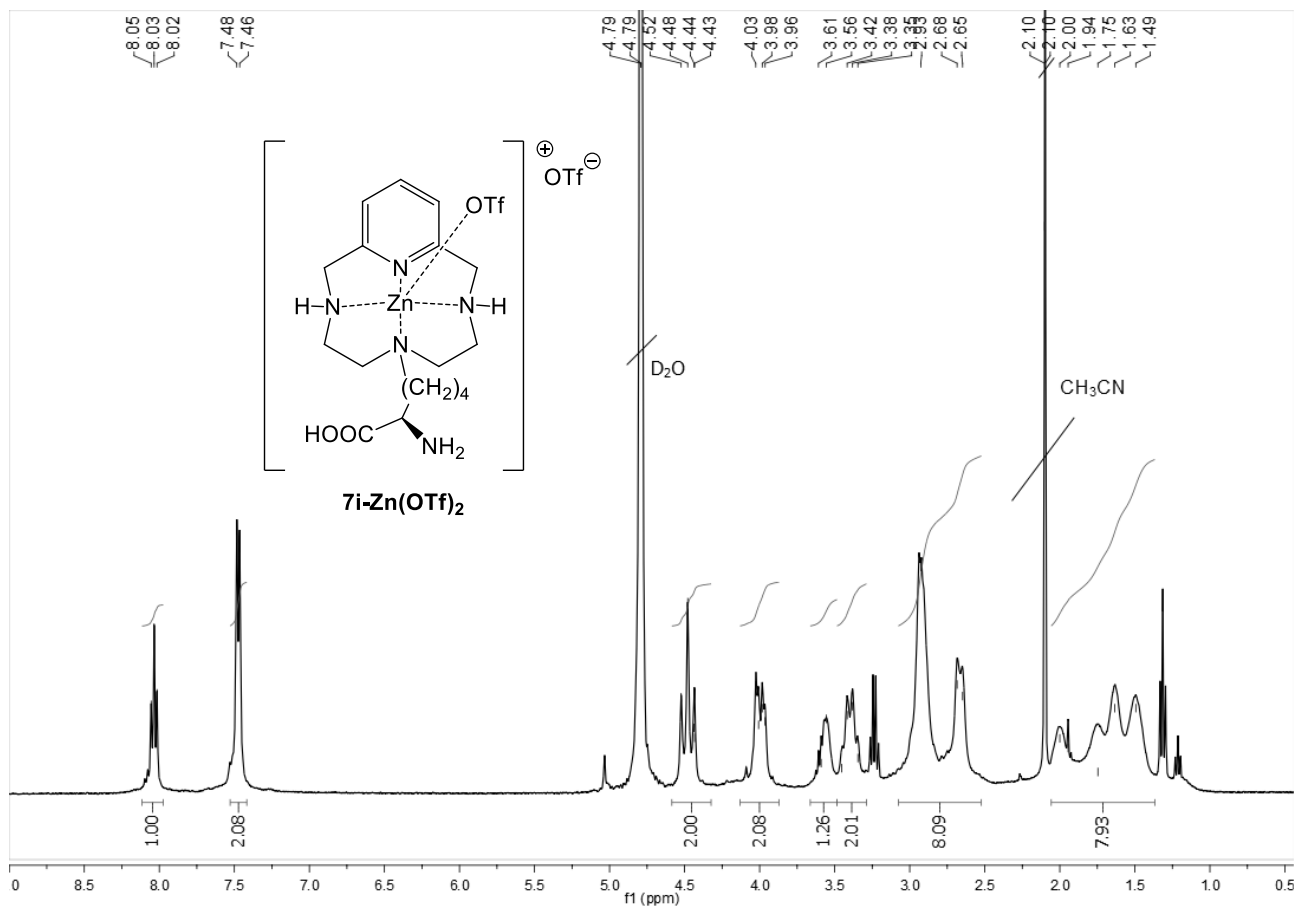
6r-AgOTf

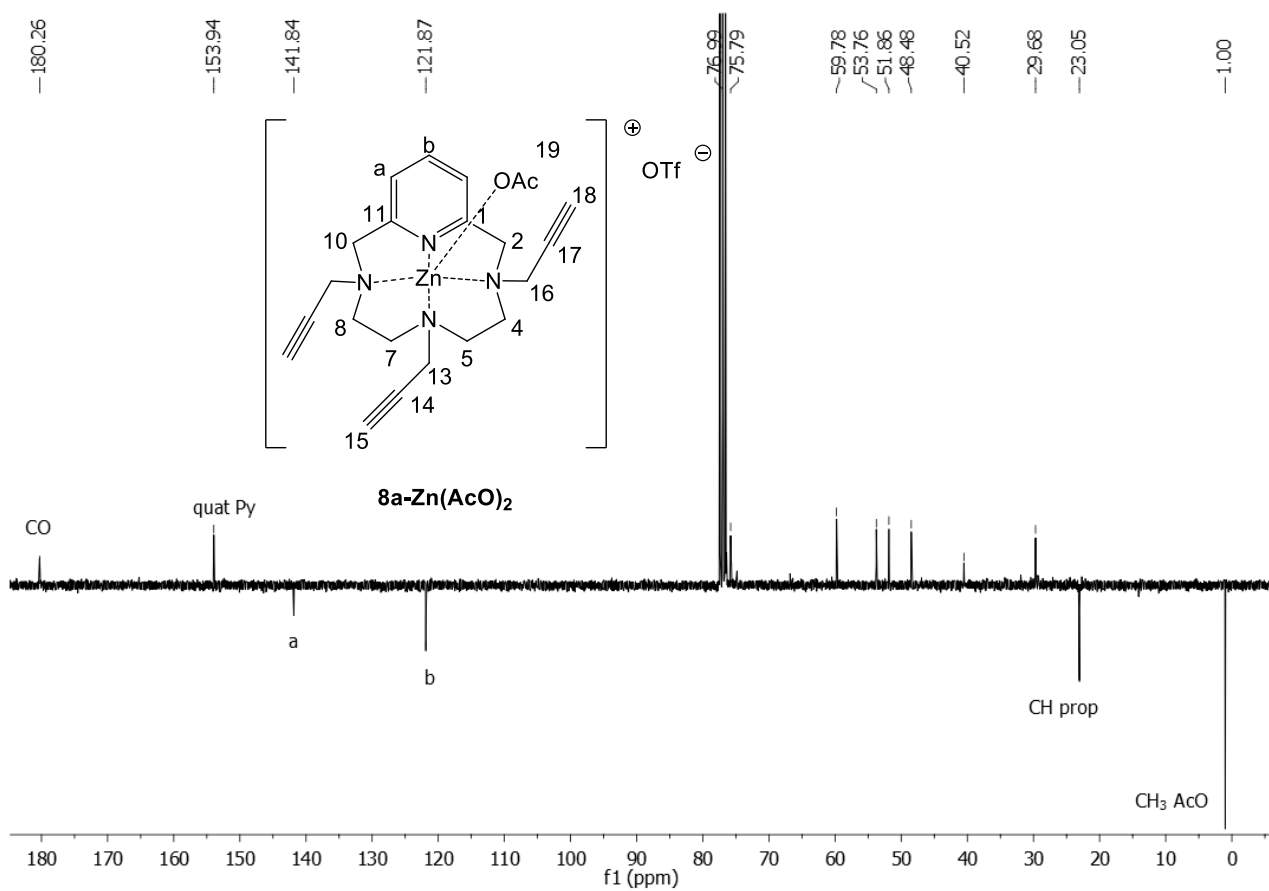
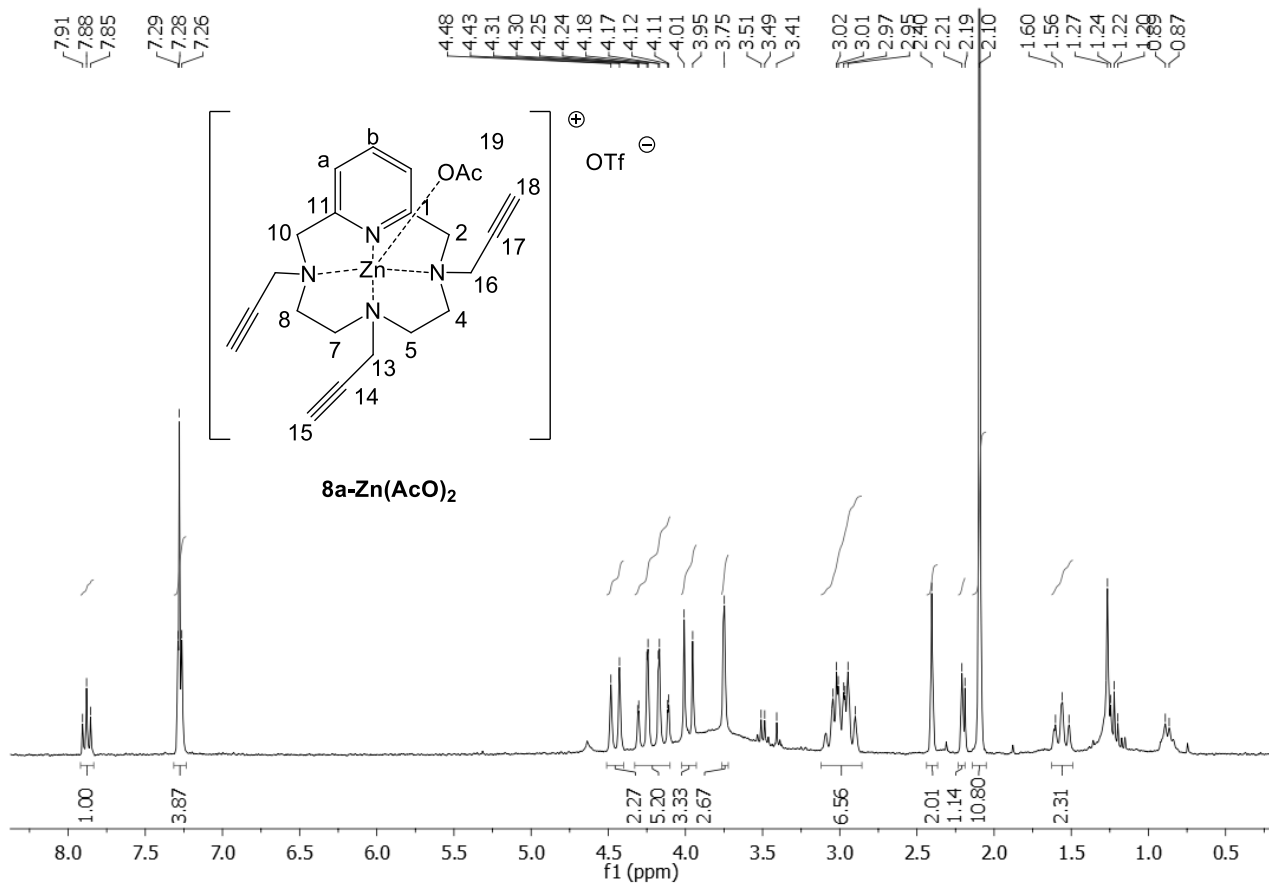


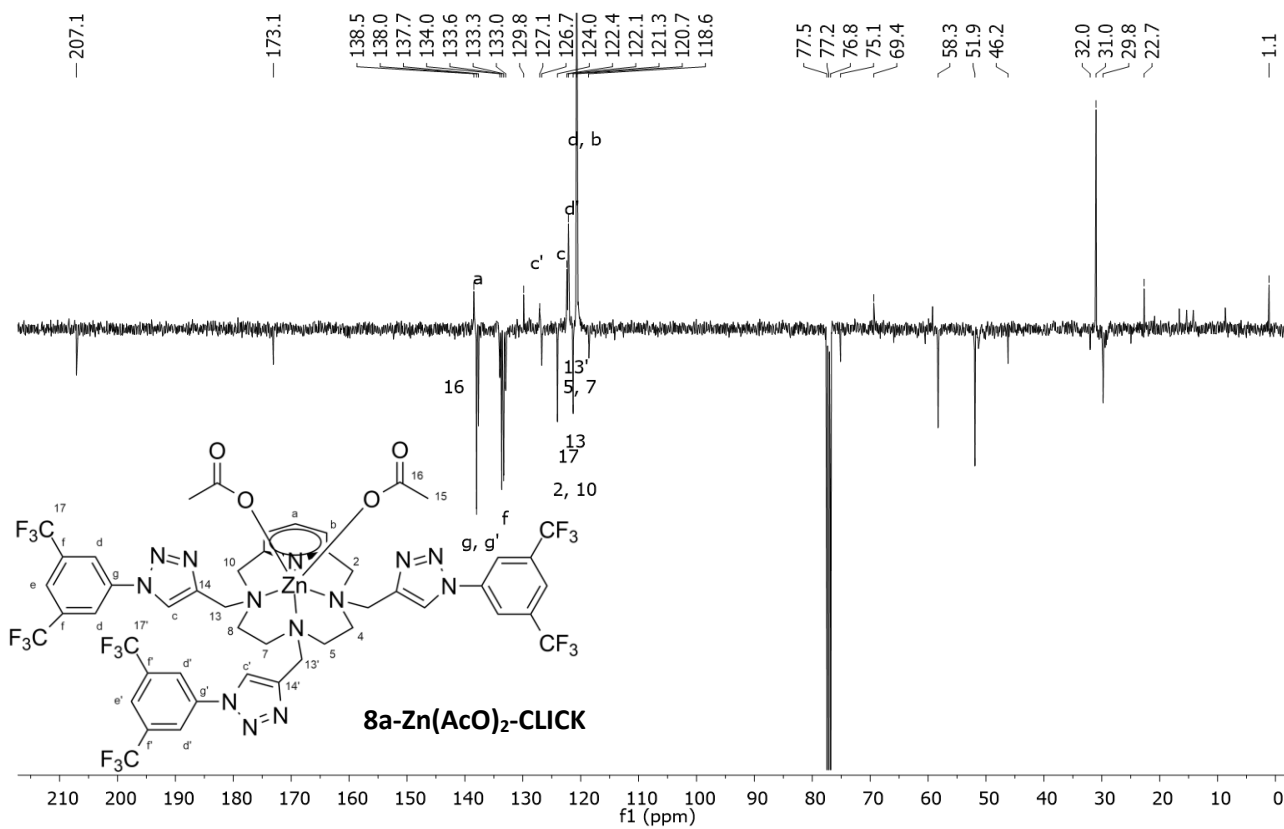
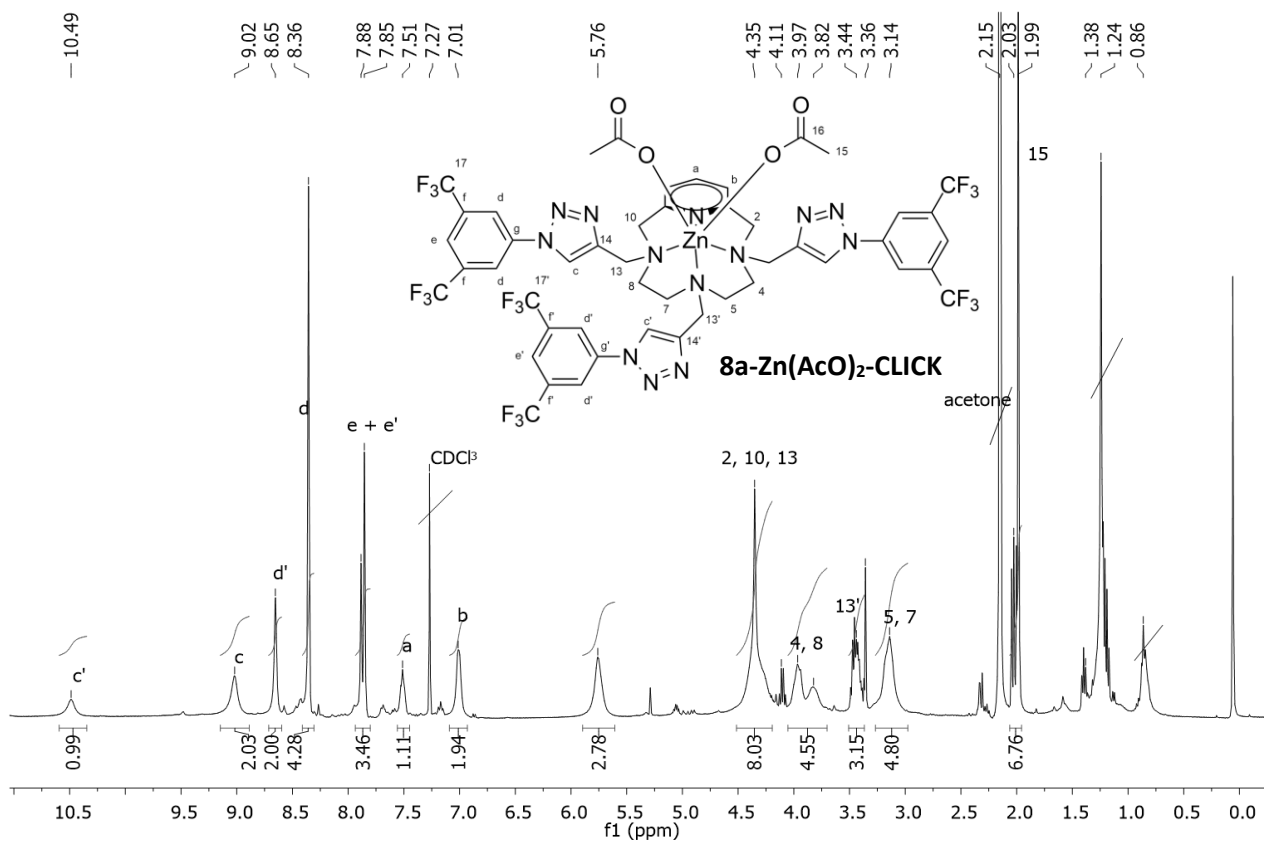


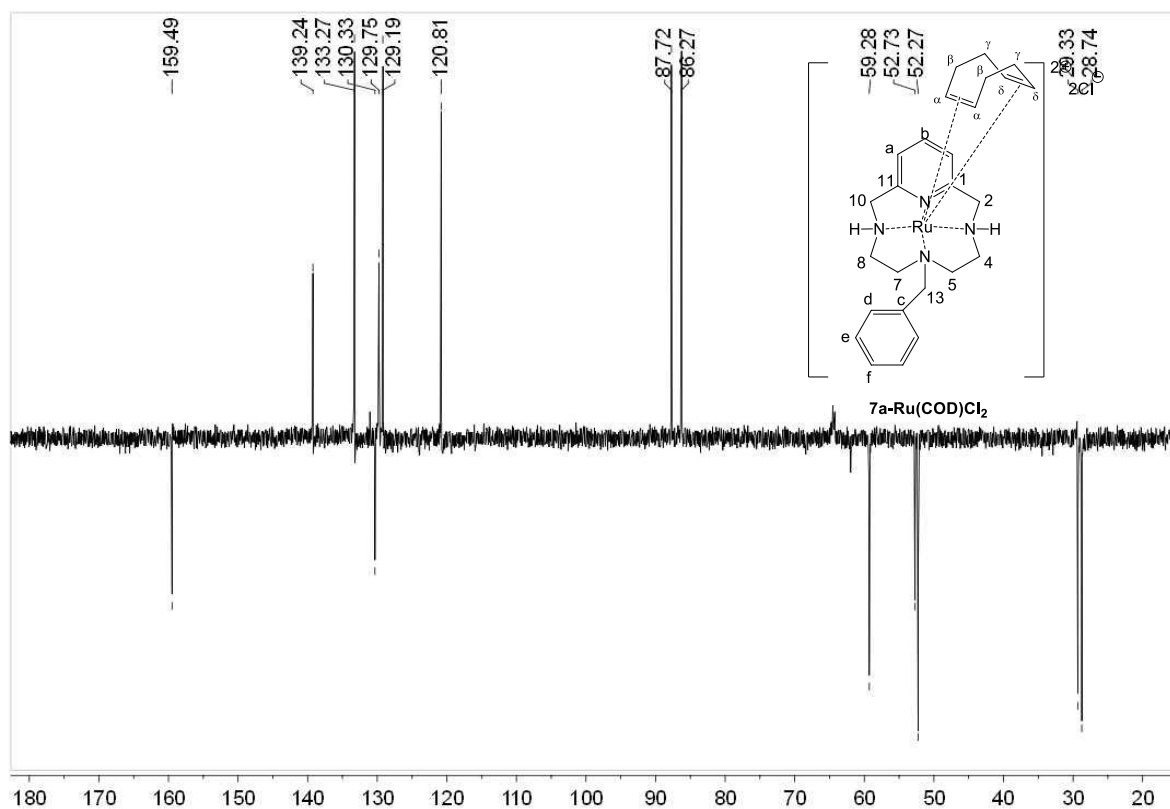
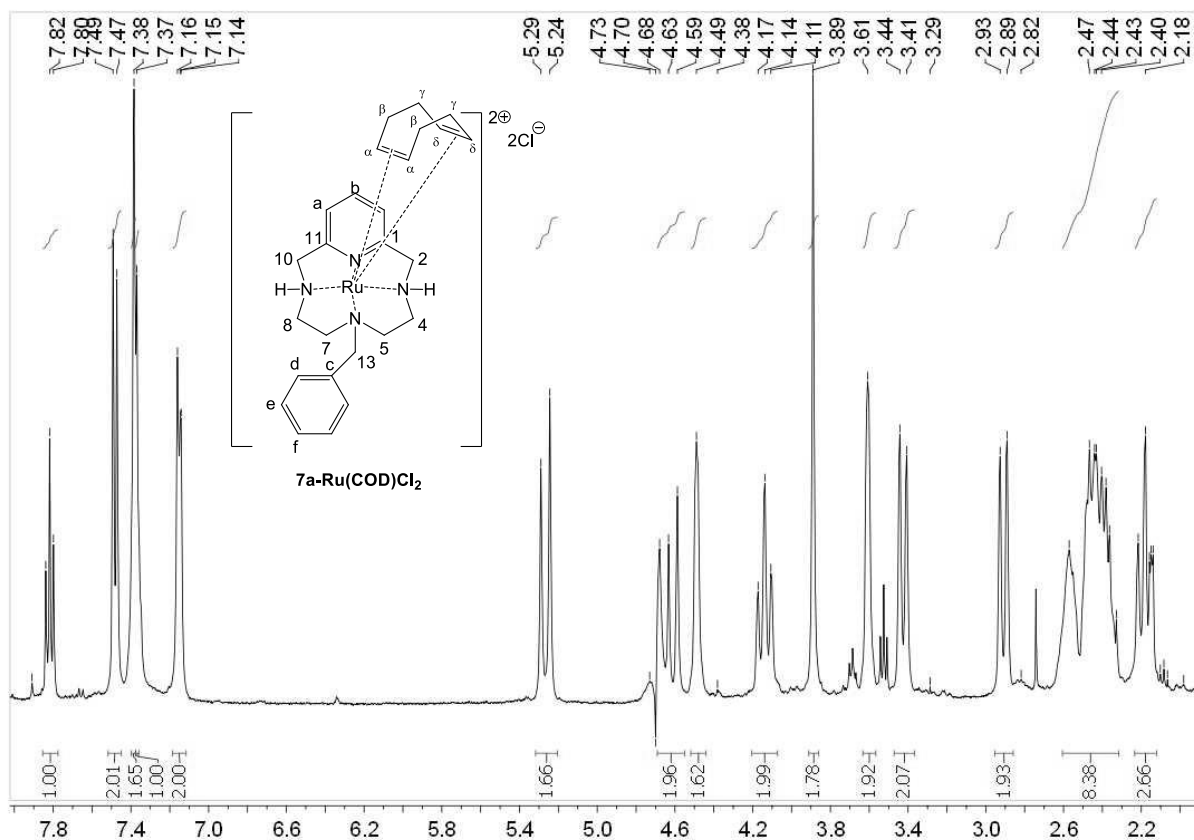












5. References

1. Fischer, H.; Walach, B., Synthesis of porphyrins. VI. Synthesis of octamethylporphin, the methyl analog of etioporphyrin. *Justus Liebigs Ann. Chem.* **1926**, *450*, 164-81.
2. Curtis, N. F., 855. Transition-metal complexes with aliphatic Schiff bases. Part I. Nickel(II) complexes with N-isopropylidene-ethylenediamine schiff bases. *J. Chem. Soc.* **1960**, (0), 4409-4413.
3. Cabiness, D. K.; Margerum, D. W., Macrocyclic effect on the stability of copper(II) tetramine complexes. *J. Am. Chem. Soc.* **1969**, *91* (23), 6540-6541.
4. Hancock, R. D., Chelate ring size and metal ion selection: the basis of selectivity for metal ions in open-chain ligands and macrocycles. *J. Chem. Educ.* **1992**, *69* (Copyright (C) 2014 American Chemical Society (ACS). All Rights Reserved.), 615-21.
5. Jackson, T. A.; Rohde, J.-U.; Seo, M. S.; Sastri, C. V.; DeHont, R.; Stubna, A.; Ohta, T.; Kitagawa, T.; Münck, E.; Nam, W.; Que, L., Axial Ligand Effects on the Geometric and Electronic Structures of Nonheme Oxoiron(IV) Complexes. *J. Am. Chem. Soc.* **2008**, *130* (37), 12394-12407.
6. Lima, L. M. P.; Esteban-Gomez, D.; Delgado, R.; Platas-Iglesias, C.; Tripier, R., Monopicolinate Cyclen and Cyclam Derivatives for Stable Copper(II) Complexation. *Inorg. Chem.* **2012**, *51* (Copyright (C) 2014 American Chemical Society (ACS). All Rights Reserved.), 6916-6927.
7. Liu, W.-M.; Keizers, P. H. J.; Hass, M. A. S.; Blok, A.; Timmer, M.; Sarris, A. J. C.; Overhand, M.; Ubbink, M., A pH-Sensitive, Colorful, Lanthanide-Chelating Paramagnetic NMR Probe. *J. Am. Chem. Soc.* **2012**, *134* (41), 17306-17313.
8. C. V. Esteves, P. L., R. Delgado, J. Costa, P. Désogère, Y. Rousselin, C. Goze, F. Denat, *Inorg. Chem.* **2013**, *52*, 5138-5153.
9. C. E. Castillo, M. A. M., M. G. Basallote, M. P. Clares, S. Blasco, E. Garcia-Espana, *Dalton Trans.* **2012**, *41*, 5617.
10. Delgado, R.; Felix, V.; Lima, L. M. P.; Price, D. W., Metal complexes of cyclen and cyclam derivatives useful for medical applications: a discussion based on thermodynamic stability constants and structural data. *Dalton Trans.* **2007**, (Copyright (C) 2014 American Chemical Society (ACS). All Rights Reserved.), 2734-2745.
11. (a) M. S. Cooper, M. T. M., K. Sunassee, K. P. Shaw, J. D. Williams, R. L. Paul, P. S. Donnelly, P. J. Blower, *Bioconjugate Chem.* **2012**, *23* (1029); (b) C. L. Ferreira, I. H., C. Bensimon, P. Jurek and G. E. Kiefer, *Mol. Pharmacol.* **2012**, *9*, 2180.
12. Ye, W.; Ho, D. M.; Friedle, S.; Palluccio, T. D.; Rybak-Akimova, E. V., Role of Fe(IV)-Oxo Intermediates in Stoichiometric and Catalytic Oxidations Mediated by Iron Pyridine-Azamacrocycles. *Inorg. Chem.* **2012**, *51* (9), 5006-5021.
13. I. Garcia-Bosch, Z. C., I. Prat, X. Ribas, J. Lloret-Fillol, M. Costas, *Chem.–Eur. J.* **2012**, *18*, 13269.
14. G. Ortiz, S. B., Y. Rousselin, R. Guillard, *Chem.–Eur. J.* **2011**, *17*, 6689.
15. T. D. Sobiesciak, P. Z., *J. Org. Chem.* **2010**, *75*, 2069.
16. Fernandes, A. S.; Cabral, M. F.; Costa, J.; Castro, M.; Delgado, R.; Drew, M. G. B.; Félix, V., Two macrocyclic pentaaza compounds containing pyridine evaluated as novel chelating agents in copper(II) and nickel(II) overload. *Journal of Inorganic Biochemistry* **2011**, *105* (3), 410-419.
17. Rothemund, P.; Menotti, A. R., Porphyrin Studies. IV.1 The Synthesis of $\alpha,\beta,\gamma,\delta$ -Tetraphenylporphine. *J. Am. Chem. Soc.* **1941**, *63* (1), 267-270.
18. Adler, A. D.; Longo, F. R.; Varadi, V., [Preparation of] metalloporphyrins. *Inorg. Synth.* **1976**, *16*, 213-20.
19. Lindsey, J. S.; Schreiman, I. C.; Hsu, H. C.; Kearney, P. C.; Marguerettaz, A. M., Rothemund and Adler-Longo reactions revisited: synthesis of tetraphenylporphyrins under equilibrium conditions. *J. Org. Chem.* **1987**, *52* (5), 827-36.
20. Groves, J. T.; Takahashi, T., Activation and transfer of nitrogen from a nitridomanganese(V) porphyrin complex. Aza analog of epoxidation. *J. Am. Chem. Soc.* **1983**, *105* (7), 2073-4.

21. O'Malley, S.; Kodadek, T., Synthesis and characterization of the \"chiral wall\" porphyrin: a chemically robust ligand for metal-catalyzed asymmetric epoxidations. *J. Am. Chem. Soc.* **1989**, *111* (25), 9116-17.
22. Rose, E.; Andrioletti, B.; Zrig, S.; Quelquejeu-Etheve, M., Enantioselective epoxidation of olefins with chiral metalloporphyrin catalysts. *Chem. Soc. Rev.* **2005**, *34* (7), 573-583.
23. Zhang, R.; Yu, W.-Y.; Sun, H.-Z.; Liu, W.-S.; Che, C.-M., Stereo- and enantioselective alkene epoxidations: a comparative study of D4- and D2-symmetric homochiral trans-dioxoruthenium(VI) porphyrins. *Chem. Eur. J.* **2002**, *8* (11), 2495-2507.
24. Berkessel, A.; Kaiser, P.; Lex, J., Electronically tuned chiral ruthenium porphyrins: Extremely stable and selective catalysts for asymmetric epoxidation and cyclopropanation. *Chem. Eur. J.* **2003**, *9* (19), 4746-4756.
25. Lai, T.-S.; Kwong, H.-L.; Che, C.-M.; Peng, S.-M., Catalytic and asymmetric aziridination of alkenes catalyzed by a chiral manganese porphyrin complex. *Chem. Commun.* **1997**, (24), 2373-2374.
26. Rose, E.; Ren, Q.-z.; Andrioletti, B., A unique binaphthyl strapped iron-porphyrin catalyst for the enantioselective epoxidation of terminal olefins. *Chem. Eur. J.* **2004**, *10* (1), 224-230.
27. Ragaini, F.; Penoni, A.; Gallo, E.; Tollari, S.; Li Gotti, C.; Lapadula, M.; Mangioni, E.; Cenini, S., Amination of benzylic C-H bonds by arylazides catalyzed by CoII-porphyrin complexes: A synthetic and mechanistic study. *Chem. Eur. J.* **2003**, *9* (1), 249-259.
28. Penoni, A.; Wanke, R.; Tollari, S.; Gallo, E.; Musella, D.; Ragaini, F.; Demartin, F.; Cenini, S., Cyclopropanation of olefins with diazoalkanes, catalyzed by CoII(porphyrin) complexes - a synthetic and mechanistic investigation and the molecular structure of CoIII(TPP)(CH₂CO₂Et) (TPP = dianion of meso-tetraphenylporphyrin). *Eur. J. Inorg. Chem.* **2003**, (7), 1452-1460.
29. Zardi, P.; Intriери, D.; Caselli, A.; Gallo, E., Co(porphyrin)-catalysed amination of 1,2-dihydronaphthalene derivatives by aryl azides. *J. Organomet. Chem.* **2012**, *716*, 269-274.
30. Fantauzzi, S.; Gallo, E.; Caselli, A.; Piangiolino, C.; Ragaini, F.; Cenini, S., The (porphyrin)ruthenium-catalyzed aziridination of olefins using aryl azides as nitrogen sources. *Eur. J. Org. Chem.* **2007**, (36), 6053-6059.
31. Piangiolino, C.; Gallo, E.; Caselli, A.; Fantauzzi, S.; Ragaini, F.; Cenini, S., The [Ru(CO)(porphyrin)]-catalyzed synthesis of N-aryl-2-vinylaziridines. *Eur. J. Org. Chem.* **2007**, (5), 743-750.
32. Intriери, D.; Caselli, A.; Ragaini, F.; Cenini, S.; Gallo, E., Ruthenium porphyrins-catalyzed atom-efficient amination of C-H bonds by arylazides. *J. Porphyrins Phthalocyanines* **2010**, *14* (8), 732-740.
33. Intriери, D.; Zardi, P.; Caselli, A.; Gallo, E., Organic azides: \"energetic reagents\" for the intermolecular amination of C-H bonds. *Chem. Commun.* **2014**, *50* (78), 11440-11453.
34. Fantauzzi, S.; Gallo, E.; Rose, E.; Raoul, N.; Caselli, A.; Issa, S.; Ragaini, F.; Cenini, S., Asymmetric Cyclopropanation of Olefins Catalyzed by Chiral Cobalt(II)-Binaphthyl Porphyrins. *Organometallics* **2008**, *27* (23), 6143-6151.
35. Caselli, A.; Gallo, E.; Ragaini, F.; Ricatto, F.; Abbiati, G.; Cenini, S., Chiral porphyrin complexes of cobalt(II) and ruthenium(II) in catalytic cyclopropanation and amination reactions. *Inorg. Chim. Acta* **2006**, *359* (9), 2924-2932.
36. Aime, S.; Gianolio, E.; Corpillo, D.; Cavallotti, C.; Palmisano, G.; Sisti, M.; Giovenzana, G. B.; Pagliarin, R., Designing novel contrast agents for magnetic resonance imaging. Synthesis and relaxometric characterization of three gadolinium(III) complexes based on functionalized pyridine-containing macrocyclic ligands. *Helv. Chim. Acta* **2003**, *86* (3), 615-632.
37. Caselli, A.; Cesana, F.; Gallo, E.; Casati, N.; Macchi, P.; Sisti, M.; Celentano, G.; Cenini, S., Designing new ligands: asymmetric cyclopropanation by Cu(I) complexes based on functionalised pyridine-containing macrocyclic ligands. *Dalton Trans.* **2008**, (32), 4202-4205.
38. C. Martín, J. M. a. M. o.-M., A. Locati, E. Alvarez, F. Maseras, T. s. R. Belderrain, P. J. Pérez, *Organometallics* **2010**, *29*, 3481-3489.
39. Licini, G. S., P., *Angew. Chem. Int. Ed.* **2003**, *42*, 4572.
40. Ringenberg, M. R. W., T.R., *Chem. Commun.* **2011**, *47*, 8470.

41. (a) Friel, D. K. S., M.L.; Hoveyda, A.H. , *J. Am. Chem. Soc.* **2008**, *130*, 9942; (b) Agarkov, A. G., S.; Xie, D.; Pawlick, R.; Starkey, G.; Gilbertson, S.R. , *Peptide Science* **2006**, *84*, 48.
42. (a) Muñoz Robles, V. O.-C., E.; Alonso-Cotchico, L.; Rodriguez-Guerra, J.; Lledos, A.; Marechal, J.D. , *ACS Catal.* **2015**, *5*, 2469; (b) Pamies, O. D., M.; Backvall, J.E. , *Adv. Synth. Catal.* **2015**, *357*, 1567.
43. (a) Heinisch, T.; Ward, T. R., Artificial Metalloenzymes Based on the Biotin–Streptavidin Technology: Challenges and Opportunities. *Acc. Chem. Res.* **2016**, *49* (9), 1711-1721; (b) Mallin, H.; Hesticova, M.; Reuter, R.; Ward, T. R., Library design and screening protocol for artificial metalloenzymes based on the biotin-streptavidin technology. *Nat. Protocols* **2016**, *11* (5), 835-852.
44. Suckling, C. J., *Angew. Chem. Int. Ed. Engl.* **1998**, *27*, 537.
45. D. Arlt, M. J., R. Lantsch, *Angew. Chem. Int. Ed.* **1981**, *20*, 703.
46. Kirk-Othmer, *Encyclopedia of Chem Tech. Insecticides* **1965**, *2*, 685.
47. K. V. Toraskar MP, K. V., *Int J Pharm and Pharma Sci* **2**, 132-133.
48. R. Csuk, M. J. S., Y. Von Scholz, *Tetrahedron: Asymm* **1996**, *7*, 3505.
49. Blaser, H. U.; Schmidt, E., *Asymmetric Catalysis on Industrial Scale: Challenges, Approaches and Solutions*. 2004; p 454 pp.
50. Emschwiller, G., *Compt. Rend.* **1929**, *188*, 1555.
51. H. E. Simmons, R. D. S., *J. Am. Chem. Soc.* **1959**, *81*, 4256.
52. G. Wittig, K. S., *Angew. Chem.* **1959**, *71*, 652.
53. J. Furukawa, N. K., J. Nishimura, , *Tetrahedron Lett.* **1966**, *7*, 3353.
54. C. Zhu, A. Y., L. Ji, Y. Wei, V. N. Nemykin, V. V. Zhdankin, , *Org. Lett.* **2012**, *14*, 3170-3173.
55. Nozaki, H.; Moriuti, S.; Takaya, H.; Noyori, R., Asymmetric induction in carbenoid reactions by means of a dissymmetric copper chelate. *Tetrahedron Lett.* **1966**, (43), 5239-44.
56. (a) Pellissier, H., Recent developments in asymmetric cyclopropanation. *Tetrahedron* **2008**, *64* (30-31), 7041-7095; (b) T. Sawada, M. N., *Tetrahedron: Asymmetry* **2012**, *23*(5), 350-356.
57. R. Silva, V. G., L. Carneiro, N. Nunes, S. Borges, J. Pires, Â. Martins, A. P. Carvalho, *Microporous and Mesoporous Materials* **2013**, *179*, 231-241.
58. D. Kellehan, F. K., D. Frain, A. M. Rodríguez-García, J. I. García, P. O’Leary, *Tetrahedron: Asymmetry* **2013**, *24*, 750-757.
59. Intrieri, D.; Caselli, A.; Gallo, E., Cyclopropanation Reactions Mediated by Group 9 Metal Porphyrin Complexes. *Eur. J. Inorg. Chem.* **2011**, (33), 5071-5081.
60. S. Gharaati, M. M., S. Tangestaninejad, V. Mirkhani, I. Mohammadpoor-Baltork, B. Barati, F. Sadegh,, *J. Organomet. Chem.* **2013**, *741-742*, 78-82.
61. Bartoli, G.; Bencivenni, G.; Dalpozzo, R., Asymmetric Cyclopropanation Reactions. *Synthesis* **2014**, *46* (EFirst), 979-1029.
62. Castano, B.; Guidone, S.; Gallo, E.; Ragaini, F.; Casati, N.; Macchi, P.; Sisti, M.; Caselli, A., Asymmetric cyclopropanation of olefins catalysed by Cu(i) complexes of chiral pyridine-containing macrocyclic ligands (Pc-L*). *Dalton Trans.* **2013**, *42* (Copyright (C) 2013 American Chemical Society (ACS). All Rights Reserved.), 2451-2462.
63. Castano, B.; Gallo, E.; Cole-Hamilton, D. J.; Dal Santo, V.; Psaro, R.; Caselli, A., Continuous flow asymmetric cyclopropanation reactions using Cu(i) complexes of Pc-L* ligands supported on silica as catalysts with carbon dioxide as a carrier. *Green Chem.* **2014**, *16* (6), 3202-3209.
64. (a) Gillingham, D.; Fei, N., Catalytic X-H insertion reactions based on carbenoids. *Chem Soc Rev* **2013**, *42* (12), 4918-31; (b) Zhu, S. F.; Zhou, Q. L., Transition-metal-catalyzed enantioselective heteroatom-hydrogen bond insertion reactions. *Acc Chem Res* **2012**, *45* (8), 1365-77.
65. (a) Rappoport, Z.; Apeloig, Y.; Editors, *The Chemistry of Organic Silicon Compounds, Volume 3*. John Wiley & Sons Ltd.: 2001; p 1148 pp; (b) Brook, M. A., *Silicon in Organic Organometallic, and Polymer Chemistry*. Wiley-VCH Verlag: 2000; p No pp. given.
66. Corey, J. Y., Reactions of hydrosilanes with transition metal complexes and characterization of the products. *Chem. Rev.* **2011**, *111* (2), 863-1071.

67. (a) Ma, J.; Zhang, L.; Zhu, S., Enynal/Enynone: A Safe and Practical Carbenoid Precursor. *Curr. Org. Chem.* **2016**, *20* (1), 102-118; (b) Mata, S.; López, L. A.; Vicente, R., Zinc-Catalyzed Functionalization of Si-H Bonds with 2-Furyl Carbenoids through Three-Component Coupling. *Chem. Eur. J.* **2015**, *21* (25), 8998-9002; (c) Vicente, R.; González, J.; Riesgo, L.; González, J.; López, L. A., Catalytic Generation of Zinc Carbenes from Alkynes: Zinc-Catalyzed Cyclopropanation and Si-H Bond Insertion Reactions. *Angew. Chem. Int. Ed.* **2012**, *51* (32), 8063-8067.
68. (a) Cassani, C.; Bergonzini, G.; Wallentin, C.-J., Active Species and Mechanistic Pathways in Iron-Catalyzed C-C Bond-Forming Cross-Coupling Reactions. *ACS Catal.* **2016**, *6* (3), 1640-1648; (b) Narayan, R.; Matcha, K.; Antonchick, A. P., Metal-Free Oxidative C-C Bond Formation through C-H Bond Functionalization. *Chem. Eur. J.* **2015**, *21* (42), 14678-14693.
69. (a) Roberto, B.; Serena, G.; Alessandro, P., Aliphatic Nitrocompounds as Versatile Building Blocks for the One-Pot Processes. In *Green Chemistry for Environmental Sustainability*, CRC Press: 2010; pp 53-78; (b) Ono, N.; Editor, *The Nitro Group in Organic Synthesis*. John Wiley & Sons, Inc.: 2001; p 392 pp.
70. Henry, L., Nitro-alcohols. *Compt. rend.* **1895**, *120*, 1265-8.
71. (a) Ballini, R.; Barboni, L.; Fringuelli, F.; Palmieri, A.; Pizzo, F.; Vaccaro, L., Recent developments on the chemistry of aliphatic nitro compounds under aqueous medium. *Green Chem.* **2007**, *9* (8), 823-838; (b) Luzzio, F. A., The Henry reaction: recent examples. *Tetrahedron* **2001**, *57* (6), 915-945.
72. (a) Chinnaraja, E.; Arunachalam, R.; Choudhary, M. K.; Kureshy, R. I.; Subramanian, P. S., Binuclear Cu(II) chiral complexes: Synthesis, characterization and application in enantioselective nitroaldol (Henry) reaction. *Appl. Organomet. Chem.* **2016**, *30* (2), 95-101; (b) Shixaliyev, N. Q.; Maharramov, A. M.; Gurbanov, A. V.; Nenajdenko, V. G.; Muzalevskiy, V. M.; Mahmudov, K. T.; Kopylovich, M. N., Zinc(II)-1,3,5-triazapentadienate complex as effective catalyst in Henry reaction. *Catal. Today* **2013**, *217*, 76-79; (c) Pettinari, C.; Marchetti, F.; Cerquetella, A.; Pettinari, R.; Monari, M.; MacLeod, T. C. O.; Martins, L.; Pombeiro, A. J. L., Coordination Chemistry of the (eta(6)-p-Cymene)ruthenium(II) Fragment with Bis-, Tris-, and Tetrakis(pyrazol-1-yl)borate Ligands: Synthesis, Structural, Electrochemical, and Catalytic Diastereoselective Nitroaldol Reaction Studies. *Organometallics* **2011**, *30* (6), 1616-1626.
73. (a) Yu, X.; Perez, B.; Zhang, Z.; Gao, R.; Guo, Z., Mining catalytic promiscuity from Thermophilic archaea: an acyl-peptide releasing enzyme from *Sulfolobus tokodaii* (ST0779) for nitroaldol reactions. *Green Chem.* **2016**, *18* (9), 2753-2761; (b) Milner, S. E.; Moody, T. S.; Maguire, A. R., Biocatalytic Approaches to the Henry (Nitroaldol) Reaction. *Eur. J. Org. Chem.* **2012**, *2012* (16), 3059-3067.
74. (a) Collier, V. E.; Ellebracht, N. C.; Lindy, G. I.; Moschetta, E. G.; Jones, C. W., Kinetic and Mechanistic Examination of Acid-Base Bifunctional Aminosilica Catalysts in Aldol and Nitroaldol Condensations. *ACS Catal.* **2016**, *6* (1), 460-468; (b) Brunelli, N. A.; Jones, C. W., Tuning acid-base cooperativity to create next generation silica-supported organocatalysts. *J. Catal.* **2013**, *308*, 60-72.
75. (a) Xu, F.; Yan, L.; Lei, C.; Zhao, H.; Li, G., Asymmetric Cu-catalyzed Henry reaction promoted by chiral camphor-derived β -amino alcohols with a thiophene moiety. *Tetrahedron: Asymmetry* **2015**, *26* (7), 338-343; (b) Castano, B.; Pedrazzini, T.; Sisti, M.; Gallo, E.; Ragaini, F.; Casati, N.; Caselli, A., Henry reaction catalyzed by copper(I) complexes of a new pyridine-containing macrocyclic ligand. *Appl. Organomet. Chem.* **2011**, *25* (11), 824-829; (c) Jin, W.; Li, X.; Wan, B., A Highly Diastereo- and Enantioselective Copper(I)-Catalyzed Henry Reaction Using a Bis(sulfonamide)-Diamine Ligand. *J. Org. Chem.* **2011**, *76* (2), 484-491.
76. (a) Tang, L.-W.; Dong, X.; Zhou, Z.-M.; Liu, Y.-Q.; Dai, L.; Zhang, M., The first 4,4'-imidazolium-tagged C₂-symmetric bis(oxazolines): application in the asymmetric Henry reaction. *RSC Adv.* **2015**, *5* (7), 4758-4765; (b) Wang, X.; Zhao, W.; Li, G.; Wang, J.; Liu, G.; Liu, L.; Zhao, R.; Wang, M., Enantioselective copper(II)-catalyzed Henry reaction utilizing chiral aziridinyl alcohols. *Appl. Organomet. Chem.* **2014**, *28* (12), 892-899; (c) Solinas, M.; Sechi, B.; Baldino, S.; Chelucci, G., Synthesis and application of new iminopyridine ligands to enantioselective copper(II)-catalyzed Henry reaction. *J. Mol. Catal. A: Chem.* **2013**, *378*, 206-212.

77. Pedrazzini, T.; Pirovano, P.; Dell'Acqua, M.; Ragaini, F.; Illiano, P.; Macchi, P.; Abbiati, G.; Caselli, A., Organometallic Reactivity of [Silver(I)(Pyridine-Containing Ligand)] Complexes Relevant to Catalysis. *Eur. J. Inorg. Chem.* **2015**, *2015* (30), 5089-5098.
78. Dell'Acqua, M.; Castano, B.; Cecchini, C.; Pedrazzini, T.; Pirovano, V.; Rossi, E.; Caselli, A.; Abbiati, G., Mild Regiospecific Synthesis of 1-Alkoxy-isochromenes Catalyzed by Well-Defined [Silver(I)(Pyridine-Containing Ligand)] Complexes. *J. Org. Chem.* **2014**, *79* (8), 3494-3505.
79. Trose, M.; Dell'Acqua, M.; Pedrazzini, T.; Pirovano, V.; Gallo, E.; Rossi, E.; Caselli, A.; Abbiati, G., [Silver(I)(Pyridine-Containing Ligand)] Complexes As Unusual Catalysts for A3-Coupling Reactions. *J. Org. Chem.* **2014**, *79* (16), 7311-7320.
80. Tseberlidis, G.; Dell'Acqua, M.; Valcarenghi, D.; Gallo, E.; Rossi, E.; Abbiati, G.; Caselli, A., Silver comes into play: Henry reaction and domino cycloisomerisation sequence catalysed by [Ag(i)(Pc-L)] complexes. *RSC Adv.* **2016**, *6* (99), 97404-97419.
81. Hashmi, A. S. K., Gold-Catalyzed Organic Reactions. *Chem. Rev.* **2007**, *107* (7), 3180-3211.
82. Lu, D.; Zhou, Y.; Li, Y.; Yan, S.; Gong, Y., Copper(II)-Catalyzed Asymmetric Henry Reaction of o-Alkynylbenzaldehydes Followed by Gold(I)-Mediated Cycloisomerization: An Enantioselective Route to Chiral 1H-Ischromenes and 1,3-Dihydroisobenzofurans. *J. Org. Chem.* **2011**, *76* (21), 8869-8878.
83. (a) Parales, R. E.; Haddock, J. D., Biocatalytic degradation of pollutants. *Current Opinion in Biotechnology* **2004**, *15* (4), 374-379; (b) Fernandes, T. A. R.; da Silveira, W. B.; Passos, F. M. L.; Zucchi, T. D., Laccases from Actinobacteria-what we have and what to expect. *Adv. Microbiol.* **2014**, *4* (6), 285-296, 12; (c) Liang, H.-C.; Dahan, M.; Karlin, K. D., Dioxygen-activating bio-inorganic model complexes. *Current Opinion in Chemical Biology* **1999**, *3* (2), 168-175.
84. Oloo, W. N.; Que, L., Bioinspired Nonheme Iron Catalysts for C-H and C=C Bond Oxidation: Insights into the Nature of the Metal-Based Oxidants. *Acc. Chem. Res.* **2015**, *48* (9), 2612-2621.
85. Kryatov, S. V.; Rybak-Akimova, E. V.; Schindler, S., Kinetics and Mechanisms of Formation and Reactivity of Non-heme Iron Oxygen Intermediates. *Chem. Rev.* **2005**, *105* (6), 2175-2226.
86. Kimura, E.; Kodama, M.; Machida, R.; Ishizu, K., A new pyridyl-containing pentaaza macrocyclic ligand. Stabilization in aqueous solutions of the iron (II) complex and its dioxygen adduct. *Inorg. Chem.* **1982**, *21* (2), 595-602.
87. Koch, W. O.; Schünemann, V.; Gerdan, M.; Trautwein, A. X.; Krüger, H.-J., Structural, Spectroscopic, and Chemical Properties of the First Low-Spin Iron(III) Semiquinonate Complexes in the Solid State and in Solution. *Chem. Eur. J.* **1998**, *4* (7), 1255-1265.
88. (a) Herrera, A. M.; Staples, R. J.; Kryatov, S. V.; Nazarenko, A. Y.; Rybak-Akimova, E. V., Nickel(ii) and copper(ii) complexes with pyridine-containing macrocycles bearing an aminopropyl pendant arm: synthesis, characterization, and modifications of the pendant amino group. *Dalton Trans.* **2003**, (5), 846-856; (b) Verdejo, B.; Ferrer, A.; Blasco, S.; Castillo, C. E.; Gonzalez, J.; Latorre, J.; Manez, M. A.; Basallote, M. G.; Soriano, C.; Garcia-Espana, E., Hydrogen and Copper Ion-Induced Molecular Reorganizations in Scorpionand-like Ligands. A Potentiometric, Mechanistic, and Solid-State Study. *Inorg. Chem.* **2007**, *46* (14), 5707-5719.
89. Richman, J. E.; Atkins, T. J., Nitrogen analogs of crown ethers. *J. Am. Chem. Soc.* **1974**, *96* (7), 2268-2270.
90. Aime, S.; Botta, M.; Crich, S. G.; Giovenzana, G. B.; Jommi, G.; Pagliarin, R.; Sisti, M., Synthesis and NMR Studies of Three Pyridine-Containing Triaza Macrocyclic Triacetate Ligands and Their Complexes with Lanthanide Ions. *Inorg. Chem.* **1997**, *36* (14), 2992-3000.
91. Serrano-Plana, J.; Oloo, W. N.; Acosta-Rueda, L.; Meier, K. K.; Verdejo, B.; García-España, E.; Basallote, M. G.; Münck, E.; Que, L.; Company, A.; Costas, M., Trapping a Highly Reactive Nonheme Iron Intermediate That Oxygenates Strong C-H Bonds with Stereoretention. *J. Am. Chem. Soc.* **2015**, *137* (50), 15833-15842.
92. Ye, W.; Leow, D.; Goh, S. L. M.; Tan, C.-T.; Chian, C.-H.; Tan, C.-H., Chiral bicyclic guanidines: a concise and efficient aziridine-based synthesis. *Tetrahedron Lett.* **2006**, *47* (6), 1007-1010.

93. J. Farràs, X. G., P. W. Sutton, J. Taltavull, F. Egeler, P. Romea, F. Urpì, J. Vilarrasa, *Tetrahedron* **2001**, *57*, 7665-7674.
94. Meth-Cohn, O.; Jiang, H., Ligands containing alternating 2,6-linked pyridine and 2,5-linked thiophene units 1. *J. Chem. Soc., Perkin Trans. 1* **1998**, (22), 3737-3746.
95. H. Rubin, J. C., J. B. Morgan, *J. Org. Chem.* **2013**, 130827114305001.
96. Aime, S.; Botta, M.; Frullano, L.; Crich, S. G.; Giovenzana, G.; Pagliarin, R.; Palmisano, G.; Sirtori, F. R.; Sisti, M., GdPCP2A(H₂O)(2) (-): A paramagnetic contrast agent designed for improved applications in magnetic resonance imaging. *J. Med. Chem.* **2000**, *43* (21), 4017-4024.
97. Ankner, T.; Hilmersson, G. r., Instantaneous Deprotection of Tosylamides and Esters with SmI₂/Amine/Water. *Org. Lett.* **2009**, *11* (3), 503-506.
98. Fukuyama, T.; Jow, C.-K.; Cheung, M., 2- and 4-Nitrobenzenesulfonamides: Exceptionally versatile means for preparation of secondary amines and protection of amines. *Tetrahedron Lett.* **1995**, *36* (36), 6373-6374.
99. Eftink, T. T. R. M. R., *Synth. Commun.* **1998**, *28*, 3787.
100. G. Oezueduru, T. S., M. M. K. Boysen, *Org. Lett.* **2012**, *14*, 4990.
101. P. J. Gritsch, E. S., T. Gaich, *Org. Lett.* **2013**, *15*, 5272.
102. Belmont, P., Silver-Catalyzed Cycloisomerization Reactions. In *Silver in Organic Chemistry*, 2010; pp 143-165.
103. Bellina, F.; Ciucci, D.; Vergamini, P.; Rossi, R., Regioselective Synthesis of Natural and Unnatural (Z)-3-(1-Alkylidene)phthalides and 3-Substituted Isocoumarins Starting from Methyl 2-Hydroxybenzoates. *Tetrahedron* **2000**, *56* (16), 2533-2545.
104. de Visser, S. P.; Rohde, J.-U.; Lee, Y.-M.; Cho, J.; Nam, W., Intrinsic properties and reactivities of mononuclear nonheme iron–oxygen complexes bearing the tetramethylcyclam ligand. *Coord. Chem. Rev.* **2013**, *257* (2), 381-393.
105. Serrano-Plana, J.; Aguinaco, A.; Belda, R.; García-España, E.; Basallote, M. G.; Company, A.; Costas, M., Exceedingly Fast Oxygen Atom Transfer to Olefins via a Catalytically Competent Nonheme Iron Species. *Angew. Chem. Int. Ed.* **2016**, *55* (21), 6310-6314.
106. Tseberlidis, G.; Caselli, A.; Vicente, R., Carbene XH bond insertions catalyzed by copper(I) macrocyclic pyridine-containing ligand (PcL) complexes. *J. Organomet. Chem.* **2017**, *835*, 1-5.